Handbook of Experimental Pharmacology 221

Peter C. Ruben *Editor*

Voltage Gated Sodium Channels

Springer

Handbook of Experimental Pharmacology

Volume 221

For further volumes:
http://www.springer.com/series/164

Peter C. Ruben
Editor

Voltage Gated Sodium Channels

Springer

Editor
Peter C. Ruben
Biomedical Physiology & Kinesiology
Simon Fraser University
Burnaby
British Columbia
Canada

ISSN 0171-2004 ISSN 1865-0325 (electronic)
ISBN 978-3-642-41587-6 ISBN 978-3-642-41588-3 (eBook)
DOI 10.1007/978-3-642-41588-3
Springer Heidelberg New York Dordrecht London

Library of Congress Control Number: 2014935987

Printed on acid-free paper

Springer is part of Springer Science+Business Media (www.springer.com)

Preface

Just over 60 years ago, Hodgkin and Huxley first proposed the ionic basis of the action potential in neurons. Their insightful—and foresighted—work, based on experiments performed in squid giant axons, laid the groundwork for a new research field: ion channel biophysics. The elegance and importance of their work earned them a Nobel Prize 11 years after their groundbreaking work was first published and set the stage for other ion channel biophysicists to follow in their footsteps: Sakmann and Neher (1991) and MacKinnon (2003). Many others, however, substantively contributed to a rich research field, achievements, and advances which are celebrated each year at the Annual Meeting of the Biophysical Society. The study of ion channel biophysics has far-reaching implications in medicine, animal behavior, and evolution. Ion channels are targets for a vast and impressive array of naturally occurring and artificial compounds, including toxins and pharmaceutical agents. Their presence in the membrane of all cells makes them particularly vulnerable (in the case of toxins) and attractively accessible (in the case of drugs, some of which are modeled after toxins).

Voltage-gated sodium channels, the focus of this Handbook, are—in a sense—the first in a physiological lineage of ion channels, and the classic opening line of many publications about sodium channels exemplifies their importance; sodium channels are the basis of the rising phase of action potentials in nerve and muscle. That simple understatement characterizes the critical importance of sodium channels in the electrical activity of neurons and muscle cells. Sodium channels are responsible for the generation and propagation of action potentials along the cell membrane and are, therefore, the lynchpin in the processes of information transmission within the nervous system and muscle contraction.

Mutations in voltage-gated sodium channels impart changes in their structure and function. Some of these changes underlie diseases that span the spectrum from relatively benign to fatal. For clinical reasons, then, the study of mutations in sodium channels hold great potential for understanding the molecular basis of disease. Many mutations impart changes in the biophysical properties of sodium channels, particularly those associated with gating, and are thus of great interest in terms of understanding the structure/function relationship of channels. Indeed, site-directed mutagenesis has been, for nearly a quarter century, since Stuhmer et al. (1989),

the technique of choice to understand the structural basis of sodium channel function. The involvement of sodium channel mutations in disease is the subject of Chapters "The Voltage Sensor Module in Sodium Channels," "Slow Inactivation of Na^+ Channels," "The Role of Non-Pore-Forming β Subunits in Physiology and Pathophysiology of Voltage-Gated Sodium Channels," "Altered Sodium Channel Gating as Molecular Basis for Pain: Contribution of Activation, Inactivation, and Resurgent Currents," Regulation/Modulation of Sensory Neuron Sodium Channels," and "The Role of Late I_{Na} in Development of Cardiac Arrhythmias" of this Handbook.

By virtue of their critical importance in cellular excitability and their vulnerable position in the cell membrane, including an extensive exposure to the extracellular milieu, sodium channels are attractive targets for toxins, venoms, and drugs. In addition, sodium channel activity is modulated by a host of intracellular messengers. Studies of the interactions between sodium channels and agents that bind to them have revealed a wealth of information about their structure and function, and many biophysical properties of sodium channels have been revealed by these interactions. We have also learned much about evolution, predator–prey interactions, and discovered many agents to treat a wide range of diseases of excitability. The interaction between sodium channels and both naturally occurring and manufactured agents continues to be a vibrant and important line of research with implications for the treatment of diseases underlying the highest morbidity and mortality: cancer and heart disease. Chapters "Proton Modulation of Cardiac I_{Na}: A Potential Arrhythmogenic Trigger," "Probing Gating Mechanisms of Sodium Channels Using Pore Blockers," "Animal Toxins Influence Voltage-Gated Sodium Channel Function," "Ubiquitylation of Voltage-Gated Sodium Channels," and "Pharmacological Insights and Quirks of Bacterial Sodium Channels" in this Handbook deal with various aspects of sodium channel modulation by intrinsic and extrinsic agents.

Bacterial sodium channels have finally provided a way to visualize the structure of voltage-gated sodium channels through crystallography. This relatively recent breakthrough has allowed researchers in the field to "put it all together" through homology modeling. Soon, someone will crystallize a mammalian sodium channel and bring us one step closer to an even more complete understanding of how structure and function relate to one another, how drugs and toxins interact with the channel, and how changes in channel structure result in debilitating diseases. The authors and editor of this volume of the Handbook of Pharmacology hope that the chapters contained herein will inspire present and future sodium channel devotees to pursue the unanswered questions and resolve the structure and function of this complicated, fascinating, and physiologically pivotal protein.

September, 2013 Peter C. Ruben
Burnaby, BC, Canada

Contents

Introduction to Sodium Channels

Colin H. Peters and Peter C. Ruben

Contents

Abstract

Voltage-gated sodium channels (VGSCs) are present in many tissue types within the human body including both cardiac and neuronal tissues. Like other channels, VGSCs activate, deactivate, and inactivate in response to changes in membrane potential. VGSCs also have a similar structure to other channels: 24 transmembrane segments arranged into four domains that surround a central pore. The structure and electrical activity of these channels allows them to create and respond to electrical signals in the body. Because of their distribution throughout the body, VGSCs are implicated in a variety of diseases including epilepsy, cardiac arrhythmias, and neuropathic pain. As such the study of these channels is essential. This brief review will introduce sodium channel structure, physiology, and pathophysiology.

Keywords

Sodium • Channels • Structure • Physiology • Disease

C.H. Peters (✉) • P.C. Ruben
Department of Biomedical Physiology and Kinesiology, Simon Fraser University, Burnaby, BC, Canada
e-mail: chpeters@sfu.ca; pruben@sfu.ca

P.C. Ruben (ed.), *Voltage Gated Sodium Channels*, Handbook of Experimental Pharmacology 221, DOI 10.1007/978-3-642-41588-3_1,

1 Overview

Voltage-gated ion channels are proteins that allow movement of ions across cellular membranes. As suggested by their name, the activity of these channels is regulated by the voltage difference across the membrane they span. The movement of charged ions, such as sodium, potassium, calcium, and chloride, as well as the voltage dependence of these channels allows them to produce and respond to electrical signals within the body.

One class of voltage-gated ion channels is the voltage-gated sodium (Na_V) channel. The kinetics of Na_V channels were studied by Hodgkin and Huxley in squid axon in 1952 and were part of their subsequent model (Hodgkin and Huxley 1952). Na_V channels have since been discovered to comprise a family consisting of $Na_V1.1$ through $Na_V1.9$ and a lesser studied group of Na_V2 channels (Catterall et al. 2005; Goldin 1999; Watanabe et al. 2000). Na_V channels are present in many electrically active tissues including neurons and both cardiac and skeletal muscle cells (Goldin 1999). In these cells voltage-gated sodium channels allow sodium to flow from the extracellular solution into the cytosol thus causing a depolarization of the cell. Different types of tissue express different sodium channel isoforms. $Na_V1.1$, $Na_V1.2$, $Na_V1.3$, and $Na_V1.6$ are primarily expressed within the central nervous system; $Na_V1.4$ is found predominantly in skeletal muscle; $Na_V1.5$ is the primary variants in cardiac muscle; and $Na_V1.7$, $Na_V1.8$, and $Na_V1.9$ are found in the peripheral nervous system (Catterall et al. 2005; Goldin 1999).

2 Structure and Function

All the voltage-gated sodium channel variants share a common structure (Goldin 1999). The largest subunit of the sodium channel is the alpha-subunit. Smaller beta-subunits are associated with and modulate the channel, but the alpha-subunit alone is sufficient to conduct sodium (Egri et al. 2012). Similar to voltage-gated potassium (K_V) channels, the alpha-subunit of the voltage-gated sodium channel is made up of 24 alpha-helical transmembrane segments arranged into four domains (Fig. 1) (Catterall et al. 2005). Unlike K_V channels which are made of four identical subunits, in Na_V channels the four domains are not identical and are formed by a single protein, approximately 2,000 amino acids in length (Ahmed et al. 1992). Each of the four domains of the Na_V channel consists of a voltage-sensing domain formed by the first four transmembrane segments and a pore domain consisting transmembrane segments five and six as well as the extracellular linker between these two segments (the p-loop) (Payandeh et al. 2011). Recently multiple bacterial Na_V channel crystal structures were solved (McCusker et al. 2012; Payandeh et al. 2011, 2012). These structures show that the four voltage-sensing domains are arranged around a central aqueous channel formed by the pore domain (Fig. 2).

The selectivity filter for the channel is formed by residues in the p-loop segments. Sodium channels are highly selective for sodium entry into the cell with a potassium permeability to sodium permeability ratio of less than 0.10

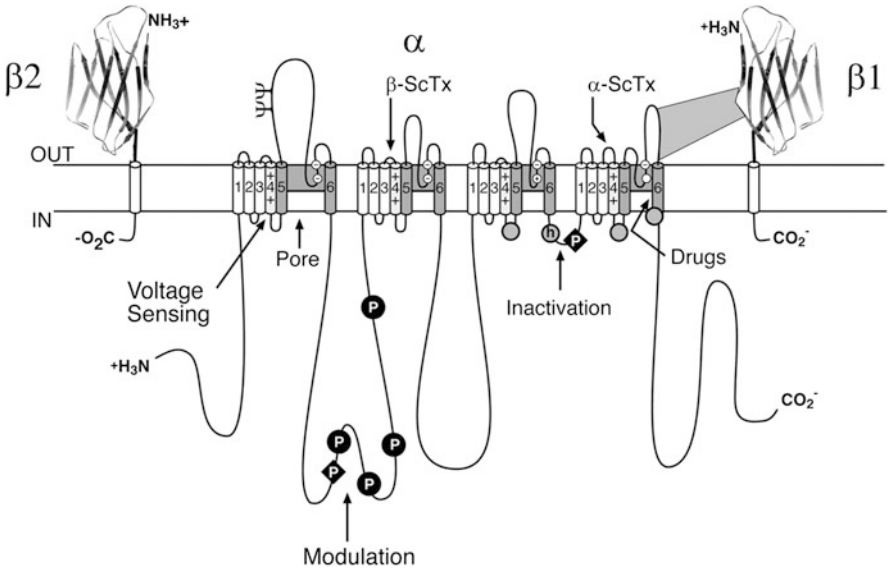

Fig. 1 The primary sequence of the voltage-gated sodium channel. The alpha-subunit is a single protein with 24 transmembrane segments arranged in four domains. The S5 and S6 segments of each domain as well as the S5–S6 linkers form the pore of the channel. The alpha-subunit is also associated with beta-subunits (Catterall et al. 2005)

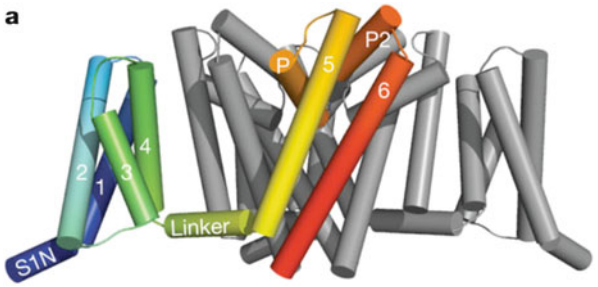

Fig. 2 Tertiary structure of a bacterial voltage-gated sodium channel. A single domain is highlighted in color. The voltage-sensing regions of each domain are arranged around the pore regions and are connected by the S4–S5 linkers (Payandeh et al. 2011)

(Favre et al. 1996; Lipkind and Fozzard 2008). The selectivity filter is formed by a ring of four residues: aspartate in domain I, glutamic acid in domain II, lysine in domain III, and alanine in domain IV (Heinemann et al. 1992; Lipkind and Fozzard 2008). Hydrated sodium passing through the selectivity filter interacts mainly with the two oxygen groups of the glutamate as it passes through the selectivity filter. In this process the DEKA residues shift to form both hydrogen bonds and van der waals interactions. Potassium does not pass through the channel easily as it forms a weaker interaction with the glutamate and is repelled more strongly by the lysine

then is sodium (Lipkind and Fozzard 2008). Previous researchers have shown that by replacing the lysine at position 1,237 the sodium selectivity of the channel is abolished and both potassium and calcium are allowed to move through the channel (Favre et al. 1996; Heinemann et al. 1992).

The voltage-sensing domain is connected to the pore-sensing domain by an intracellular linker between transmembrane segments four and five. Upon depolarization, the positively charged S4 transmembrane segments are believed to move toward the extracellular surface. This motion is transferred to the pore domain via the intracellular linker causing a conformational change resulting in the opening of the sodium channel. Upon repolarization the gate closes and the S4 segments return to their resting positions; this process is called deactivation.

Sodium channel currents in excitable tissues are often of large amplitude; however, the current through the channels lasts only a short period of time as the channel becomes impermeable to ions in a process called fast inactivation. Fast inactivation is a process whereby the channel ceases to conduct current while the voltage sensor is still in an active conformation. Fast inactivation is mediated by four residues in the linker between domains three and four of the sodium channel. This isoleucine, phenylalanine, methionine, and threonine (IFMT) motif is necessary for fast inactivation and mutation causes the abolishment of this process (West et al. 1992). When the cytosol is depolarized, this linker binds to residues on the intracellular side of domains III and IV. The particle, therefore, acts like a hinged lid to occlude the intracellular side of the sodium channel pore preventing sodium from moving through the channel (Goldin 2003). The movement of the fast inactivation gate is not independent from the activation of the channel. Recently Capes et al. showed that the movement of the DIVS4 transmembrane segment is the rate-limiting step in fast inactivation (Capes et al. 2013). After the cell repolarizes, the unbinding of the IFMT particle removes fast inactivation. The recovery from fast inactivation is also rate limited by the movement of the DIVS4 linker (Capes et al. 2013).

Fast inactivation is not the only process by which sodium channels cease to conduct. Sodium channels can also become inactivated in a process called slow inactivation (Richmond et al. 1998). While fast inactivation occurs in the millisecond time range, slow inactivation occurs on the time scale of seconds. Physiologically slow inactivation occurs during repetitive or prolonged depolarizations of sodium channels thereby limiting channel availability over longer time periods (Richmond et al. 1998). The exact process by which slow inactivation occurs is not fully known. Crystal structure data suggest that slow inactivation may be due to continued rearrangement of the channel during prolonged depolarization (Payandeh et al. 2012). This rearrangement can lead to collapse of both the pore and selectivity filter of the sodium channel, thus preventing sodium conduction. As with fast inactivation, the onset of slow inactivation occurs during depolarization and recovery occurs at repolarized potentials.

3 Physiology and Implications in Disease

The general physiological role of sodium channels is to depolarize excitable cells in the initial phase of an action potential. Upon opening, sodium channels pass a large inward sodium current. This influx of positively charged sodium makes the membrane potential more positive. In neuronal cells, depolarization of an axon segment allows the action potential to propagate to the next segment and trigger another action potential. In skeletal and cardiac muscle cells the action potential is used to trigger a contraction. The depolarization from sodium influx activates a calcium signaling cascade that causes cellular contraction. In skeletal muscle this contraction can cause movement of the body, while in cardiac muscle this contraction is used to pump blood.

Different tissues within the human body predominantly express different voltage-gated sodium channel subtypes. Thus mutations in neuronal channels cause neurological disorders such as epilepsy, while mutations in cardiac channels cause cardiac arrhythmias such as Brugada Syndrome or Long QT Syndrome (Meisler and Kearney 2005; Wang et al. 2009). The distribution pattern is also important as different variants show different voltage-dependence and drug-binding affinity. These differences can be exemplified by the difference between $Na_V1.2$ and $Na_V1.5$ which are found predominantly in neuronal and cardiac cells, respectively. Neuronal tissue has a more positive resting membrane potential than does cardiac tissue. Consequently the voltage dependence of activation and inactivation is shifted to more positive potentials in $Na_V1.2$ than in $Na_V1.5$ (Vilin et al. 2012). There are also differences in the degree of drug binding. For example, Tetrodotoxin (TTX), a potent neurotoxin, has an EC50 of approximately 12 nM in $Na_V1.2$ and a much higher EC50 of 1–2 mM in $Na_V1.5$ (Catterall et al. 2005). The differences in the distribution of these channels therefore can have large impacts in reference to the effects of mutations and pharmacological intervention.

Conclusion

From Hodgkin and Huxley's original paper in 1952 to modern crystallography and mutagenesis studies, many aspects of voltage-gated sodium channels have been studied (Capes et al. 2013; Hodgkin and Huxley 1952; Payandeh et al. 2011). This volume presents selected topics on the physiology, pathophysiology, and pharmacology of the voltage-gated sodium channel. Despite this vast body of research, new revelations about its critical structure, function, and role in disease are still being discovered.

References

Ahmed CM, Ware DH, Lee SC, Patten CD, Ferrer-Montiel AV, Schinder AF, McPherson JD, Wagner-McPherson CB, Wasmuth JJ, Evans GA (1992) Primary structure, chromosomal localization, and functional expression of a voltage-gated sodium channel from human brain. Proc Natl Acad Sci U S A 89(17):8220–8224

Capes DL, Goldschen-Ohm MP, Arcisio-Miranda M, Bezanilla F, Chanda B (2013) Domain IV voltage-sensor movement is both sufficient and rate limiting for fast inactivation in sodium channels. J Gen Physiol 142(2):101–112

Catterall WA, Goldin AL, Waxman SG (2005) International Union of Pharmacology. XLVII. Nomenclature and structure-function relationships of voltage-gated sodium channels. Pharmacol Rev 57(4):397–409

Egri C, Vilin YY, Ruben PC (2012) A thermoprotective role of the sodium channel beta1 subunit is lost with the beta1 (C121W) mutation. Epilepsia 53(3):494–505

Favre I, Moczydlowski E, Schild L (1996) On the structural basis for ionic selectivity among Na+, K+, and Ca2+ in the voltage-gated sodium channel. Biophys J 71(6):3110–3125

Goldin AL (1999) Diversity of mammalian voltage-gated sodium channels. Ann N Y Acad Sci 868:38–50

Goldin AL (2003) Mechanisms of sodium channel inactivation. Curr Opin Neurobiol 13(3):284–290

Heinemann SH, Terlau H, Stuhmer W, Imoto K, Numa S (1992) Calcium channel characteristics conferred on the sodium channel by single mutations. Nature 356(6368):441–443

Hodgkin AL, Huxley AF (1952) A quantitative description of membrane current and its application to conduction and excitation in nerve. J Physiol 117(4):500–544

Lipkind GM, Fozzard HA (2008) Voltage-gated Na channel selectivity: the role of the conserved domain III lysine residue. J Gen Physiol 131(6):523–529

McCusker EC, Bagneris C, Naylor CE, Cole AR, D'Avanzo N, Nichols CG, Wallace BA (2012) Structure of a bacterial voltage-gated sodium channel pore reveals mechanisms of opening and closing. Nat Commun 3:1102

Meisler MH, Kearney JA (2005) Sodium channel mutations in epilepsy and other neurological disorders. J Clin Invest 115(8):2010–2017

Payandeh J, Scheuer T, Zheng N, Catterall WA (2011) The crystal structure of a voltage-gated sodium channel. Nature 475(7356):353–358

Payandeh J, Gamal El-Din TM, Scheuer T, Zheng N, Catterall WA (2012) Crystal structure of a voltage-gated sodium channel in two potentially inactivated states. Nature 486(7401):135–139

Richmond JE, Featherstone DE, Hartmann HA, Ruben PC (1998) Slow inactivation in human cardiac sodium channels. Biophys J 74(6):2945–2952

Vilin YY, Peters CH, Ruben PC (2012) Acidosis differentially modulates inactivation in na(v)1.2, na(v)1.4, and na(v)1.5 channels. Front Pharmacol 3:109

Wang K, Yuan Y, Kharche S, Zhang H (2009) The E1784K mutation in SCN5A and phenotypic overlap of type 3 long QT syndrome and Brugada syndrome: a simulation study. Comput Cardiol 36:301

Watanabe E, Fujikawa A, Matsunaga H, Yasoshima Y, Sako N, Yamamoto T, Saegusa C, Noda M (2000) Nav2/NaG channel is involved in control of salt-intake behavior in the CNS. J Neurosci 20(20):7743–7751

West JW, Patton DE, Scheuer T, Wang Y, Goldin AL, Catterall WA (1992) A cluster of hydrophobic amino acid residues required for fast Na(+)-channel inactivation. Proc Natl Acad Sci U S A 89(22):10910–10914

The Voltage Sensor Module in Sodium Channels

James R. Groome

Contents

Abstract

The mechanism by which voltage-gated ion channels respond to changes in membrane polarization during action potential signaling in excitable cells has been the subject of research attention since the original description of voltage-dependent sodium and potassium flux in the squid giant axon. The cloning of ion channel genes and the identification of point mutations associated with channelopathy diseases in muscle and brain has facilitated an electrophysiological approach to the study of ion channels. Experimental approaches to the study of voltage gating have incorporated the use of thiosulfonate reagents to test accessibility, fluorescent probes, and toxins to define domain-specific roles of voltage-sensing S4 segments. Crystallography, structural and homology modeling, and molecular dynamics simulations have added computational

J.R. Groome (✉)
Department of Biological Sciences, Idaho State University, Pocatello, ID 83209, USA
e-mail: groojame@isu.edu

P.C. Ruben (ed.), *Voltage Gated Sodium Channels*, Handbook of Experimental Pharmacology 221, DOI 10.1007/978-3-642-41588-3_2,

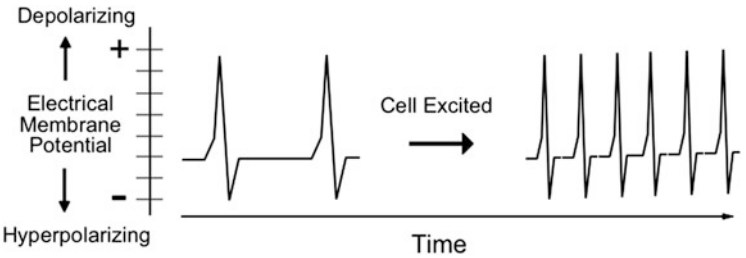

Fig. 1 Action potentials in excitable cells promoted by depolarization

approaches to study the relationship of channel structure to function. These approaches have tested models of voltage sensor translocation in response to membrane depolarization and incorporate the role of negative countercharges in the S1 to S3 segments to define our present understanding of the mechanism by which the voltage sensor module dictates gating particle permissiveness in excitable cells.

Keywords
Patch clamp electrophysiology • Segment four • Sodium channel • Ion channel • Voltage-gated • Voltage sensor module

1 Sodium Channels and the Action Potential

Voltage-gated sodium channels initiate the action potential in excitable tissues such as neurons, cardiac, and skeletal muscle fibers (Armstrong and Hille 1998; Catterall 2012). These channels respond to membrane depolarization by opening, followed rapidly by an inactivating transition that limits the duration of action potentials. Their importance is underscored by the fact that action potential frequency codes for information flow in the nervous system and periphery (Fig. 1).

Cole and Curtis (1938, 1939) exploited preparations afforded by giant axons of *Nitella* and *Loligo* to measure alterations in membrane conductance during action potential generation. The subsequent development of an innovative voltage clamp technique allowed Hodgkin and Huxley (1952) to articulate a description of membrane excitability in which biological gating particles dictate permissiveness of ionic flux across the axonal membrane. Their work provided the requisite biophysical parameters for seminal equations describing voltage sensitivity and action potential propagation. The action potential was now described in mathematical terms, computational neuroscience was born, and the search for the basis of voltage gating in excitable cell membranes was on.

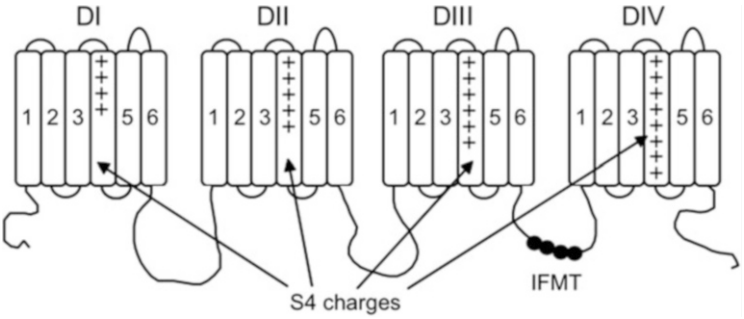

Fig. 2 Structure of the NaV channel, showing the asymmetric distribution of positive charges in the S4 segments in domains I to IV and the inactivation particle (IFMT)

2 S4 Segments as the Voltage Sensor

With the discovery of the genetic code and the subsequent elucidation of gene sequences for ion channels, a molecular approach to understanding bioelectric signaling was added to the growing arsenal of investigation. The first cloned gene for a voltage-gated sodium channel revealed a pattern of regularly spaced arginine and lysine residues in S4 segments (Noda et al. 1984), as for other members of the voltage-gated ion channel superfamily (for reviews see Yu et al. 2005; Bezanilla 2008; Catterall 2010). The hydropathic index of the sodium channel amino acid sequence predicts four domains of six transmembrane segments each. In these channels, S4 segments across the four domains are homologous but contain differing charge content (Fig. 2).

3 S4 Segments as Voltage Sensors: Experimental Approaches

3.1 Mutagenesis Studies

Several decades of research and the results from highly diverse experimental approaches support the premise that S4 segments move outward in response to membrane depolarization. As gene sequences for muscle and neuronal sodium channels were elucidated, classic mutagenesis strategy became possible. Here, the S4 segment was of immediate interest, and mutations of S4 arginine or lysine residues were employed to investigate the functions of these segments (Fig. 3). It was immediately apparent that several aspects of sodium channel gating are perturbed with mutation of positively charged residues, supporting the premise that S4 segments act as voltage sensors to promote activation and initiate fast inactivation (Stuhmer et al. 1989).

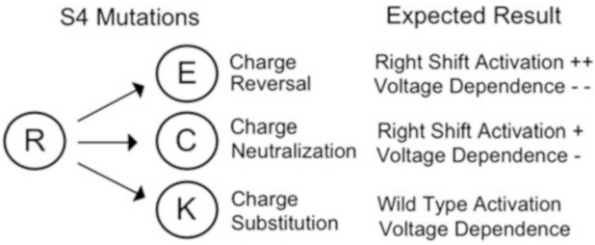

Fig. 3 Mutational strategy for testing the role of charge in S4 segments

3.2 Domain-Specific Roles of S4 Segments in Sodium Channels

While mutations in S4 segments in each of the four domains of the sodium channels affect the probability or kinetics of channel activation and inactivation (Chen et al. 1996; Kontis and Goldin 1997; Kontis et al. 1997; Groome et al. 1999), homologous mutations across these domains are not equivalent. As investigations of sodium and other ion channels progressed, it has become apparent that sodium channel gating is not defined precisely by Hodgkin–Huxley parameters for which activation is due to biological structures that are independent of one another and contribute equally to sodium channel opening (gating particle permissiveness).

3.3 Channelopathy Voltage Sensor Mutations

The identification of point mutations in sodium channel genes sequenced from patients with skeletal muscle disorders has provided an area of research attention on structural determinants of voltage-dependent gating. For example, investigations of sodium channelopathies provide support for the hypothesis that the S4 segment in domain IV functions as the inactivation gate voltage sensor. Sodium channels enter into fast inactivation during the action potential (open-state) or during closed-state transitions (Armstrong 2006; and Fig. 4). Transition into, or recovery from, the fast-inactivated state is typically defective in channelopathy mutations.

For example, the outer arginine in DIVS4 is mutant in the skeletal muscle disorder paramyotonia congenita (PC, Jurkat-Rott et al. 2010). Sodium channel open-state fast inactivation is slowed by PC mutations at this locus including R1448P (Lerche et al. 1996), R1448C (Richmond et al. 1997), R1448H (Yang et al. 1994), and R1448S (Bendahhou et al. 1999). An example of the effect of a charge-neutralizing PC mutation is shown in Fig. 5 for sodium channels recorded with the macropatch configuration. Channel activation is unaffected, while entry into the fast-inactivated state is prolonged, and exhibits shallow voltage dependence. Other studies of paramyotonia mutations at this locus support the premise that DIVS4 couples the voltage-dependent process of channel activation to fast inactivation (Chahine et al. 1994). Structure–function analyses of the domain IV segment in other sodium channels support a prominent role of DIVS4 in fast inactivation (Chen et al. 1996; Kontis and Goldin 1997; Sheets et al. 1999).

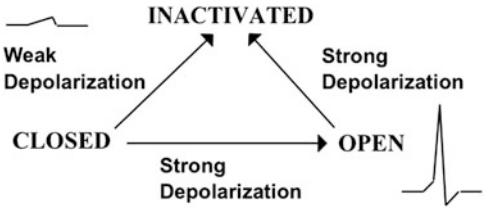

Fig. 4 Sodium channel fast inactivation from closed or open states

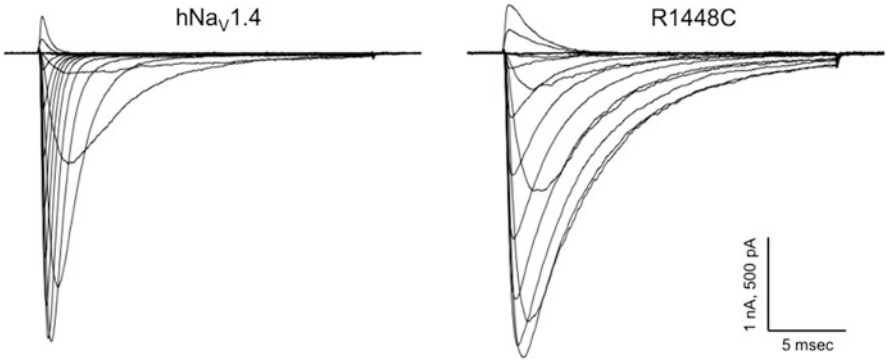

Fig. 5 PC mutant R1448C slows the entry of sodium channels into the fast-inactivated state. Groome and Ruben, unpublished

Channelopathy mutations in DIVS4 affect both routes into fast inactivation. For instance, PC mutations enhance closed-state transitions (Mohammadi et al. 2003, 2005). Mutation at the homologous locus in the cardiac sodium channel hNa$_V$1.5 (R1623Q) is associated with long QT syndrome 3 (Kambouris et al. 1998). Like PC mutations at DIVS4 R1, R1623Q slows channel inactivation from the open state but accelerates closed-state fast inactivation (Kambouris et al. 2000). These findings are consistent with those from cysteine-scanning mutagenesis of the DIV voltage sensor in cardiac channels (Sheets et al. 1999) indicating that the outermost arginine carries the predominant gating charge associated with fast inactivation.

In domains I to III, sodium channel voltage sensor mutations are often associated with periodic paralysis in skeletal muscle (for reviews see Cannon 2006; Jurkat-Rott et al. 2010). Gating defects for hypokalemic periodic paralysis (HypoPP) mutations in DIS4 (R222G; Holzherr et al. 2010), DIIS4 (Jurkat-Rott et al. 2000; Struyk et al. 2000; Kuzmenkin et al. 2002), and DIIIS4 (Carle et al. 2006) generally stabilize the fast-inactivated state, but do not explain the depolarization (and thus weakness) observed in patient muscle fibers in response to depressed serum potassium levels.

One interesting development in the search for the link between sodium channel mutations in HypoPP patients and the cellular phenotype has been the discovery of "omega" or gating pore currents associated with HypoPP mutations in S4 segments in the first three domains of Na$_V$1.4. First identified as a proton current in

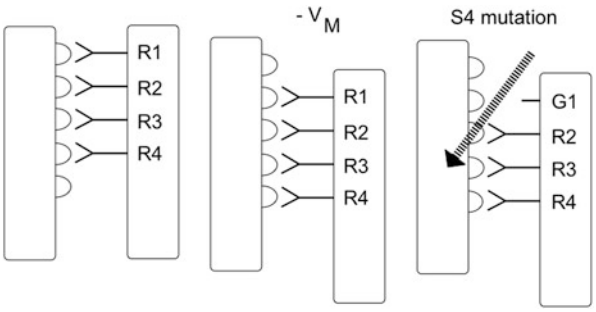

Fig. 6 Diagram of hyperpolarization-activated omega current produced by S4 mutation. In wild-type channels, side chains of S4 arginine residues maintain close contact with residues in the gating pore. With glycine substitution, ionic flow (*arrow*) through the gating pore is permitted as the voltage sensor moves downward

histidine-scanning mutagenesis of the *Shaker* K + channel (Starace and Bezanilla 2004), cationic omega currents are now hypothesized as an integral part of the pathogenesis of periodic paralysis for channelopathies of $Ca_V1.1$ and $Na_V1.4$ (for reviews see Cannon 2010; George 2012; Jurkat-Rott et al. 2012). The noncanonical currents that flow through the voltage sensor module with mutation of R1 or R2 in the voltage sensors of the first three domains are profoundly rectifying at hyperpolarized potentials (Fig. 6).

Channelopathy-associated omega currents identified in HypoPP include proton current observed with histidine mutation and cationic current observed in glycine, cysteine, or glutamine mutations (Struyk and Cannon 2007; Struyk et al. 2008; Sokolov et al. 2010; Francis et al. 2011). Omega currents have been detected in brain sodium channels (Sokolov et al. 2005) and recently in a cardiac sodium channelopathy mutation (Gosselin-Badaroudine et al. 2012a).

The pattern of voltage sensor mutations that produces the omega current has advanced our understanding of the structural basis of S4 translocation through the transmembrane electric field. Motivation for these studies, in part, was to test whether or not S4 traversed a lipid environment across the width of the membrane ("paddle hypothesis") or traversed a polar environment through a narrow gating pore comprising a focused electric field ("sliding helix or screw helical hypotheses"). Studies of *Shaker* K + channels demonstrating proton-selective (Starace and Bezanilla 2004) or cation-selective (Tombola et al. 2005) leak currents favored the sliding helix or screw helical models of S4 translocation. One of the interpretations of a voltage-dependent omega current is that in wild-type channels, positively charged residues traverse a short distance to comprise the gating charge moved in response to depolarization and channel opening (for review, see Chanda and Bezanilla 2008).

The highly conserved nature of the S1–S4 voltage sensor module in voltage-gated ion channels predicts that voltage-dependent gating charge transfer mechanisms are similar in these channels. In neuronal sodium channels, DIIS4 R1Q/R2Q mutations produce an inwardly directed current at hyperpolarized

potentials, whereas R2Q/R3Q mutations produce an outwardly directed current at depolarized potentials (Sokolov et al. 2005). The differential rectification for these mutations suggests the positioning of individual S4 arginine residues above (R1, R2) or below (R3) the gating pore for the resting state of the channel. Subsequent investigations of periodic paralysis mutations further clarified positions of R1 to R3 in resting and activated states of the channel. HypoPP mutations at R1 or R2 in domains I to III produce an inwardly rectifying cationic current (Struyk and Cannon 2007; Struyk et al. 2008; Sokolov et al. 2010; Francis et al. 2011), whereas normokalemic periodic paralysis mutations in DII (R3Q/G/W) produce an outwardly rectifying cationic current (Sokolov et al. 2008a). These positions are supported by crystallographic evidence that arginines R1 to R3 are above the gating pore in the closed-activated state of the Na_VAb channel (Payandeh et al. 2011).

3.4 Thiosulfonate Experiments: Voltage Sensor Movement

From the initial amino acid sequence of the sodium channel, the S4 segment pattern of positive charges separated by hydrophobic residues immediately suggested a plausible biological substrate for the voltage sensor, if it could be demonstrated that this segment moved in response to membrane depolarization, and if that movement was the basis for pore opening. Early models predicted a screw-helical translocation of the S4 segment (Guy and Seetharamulu 1986) and investigations focused on identifying this putative movement of the voltage sensor to the extracellular space in response to a depolarizing change in membrane potential. Accessibility of residues to aqueous solutions on either side of the cell membrane has been tested using cysteine mutants of individual voltage sensor residues. Thiosulfonate reagents such as MTSEA or MTSET added to the bath solution test residue-specific access to the extracellular or intracellular compartments. A cysteine-substituted residue that gains access to the extracellular space would, with covalent linkage of reagent through the sulfhydryl group, cause a progressive loss of channel function with repetitive depolarization (Fig. 7). Thiosulfonate reagents may disrupt channel function if applied to the intracellular space when channels are in the resting state. Finally, residues with accessibility to the intracellular space at rest may become "buried" in response to depolarization, as shown by the lack of effect of thiosulfonate agents applied during depolarization.

Several findings from these studies are noteworthy. First, the outer three positive charges in the DIVS4 segment have accessibility to the extracellular space during depolarization, and only two of these charges actually traverse the transmembrane field to reach the extracellular space. These results suggest that a limited number of positively charged residues carry the gating charge during voltage sensor translocation prior to channel opening and fast inactivation (Yang and Horn 1995; Yang et al. 1996), consistent with estimates of 12–14 elemental gating charges crossing the field during activation (Aggarwal and MacKinnon 1996). In NachBac, MTS studies also suggest limited S4 movement, with only slight changes in accessibility

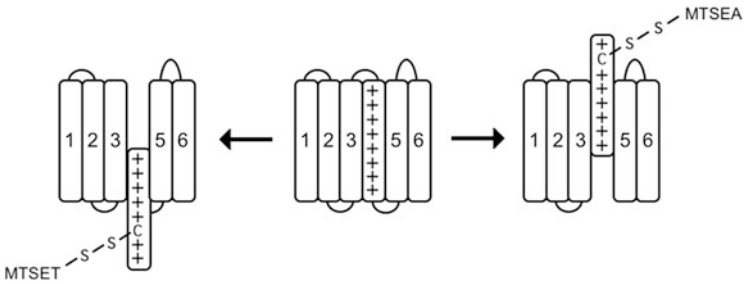

Fig. 7 Application of thiosulfonate to the intracellular compartment (*left*) or extracellular compartment (*right*) as probes for accessibility of voltage sensor charges

from the extracellular or intracellular space during depolarization (Blanchet and Chahine 2007).

3.5 Toxins: Site-Specific Actions on Voltage Sensors

Six pharmacologically distinct regional sites have been described for sodium channel toxins (Catterall 2010). The most widely used toxins in structure to function studies of the voltage sensors of sodium channels are from spiders, scorpions, and anemones (for reviews see Possani et al. 1999; Blumenthal and Seibert 2003; Zuo and Ji 2004; Catterall et al. 2007; Hanck and Sheets 2007; Moran et al. 2009; Bosmans and Swartz 2010). These toxins are differentially potent on insect or mammalian skeletal, cardiac, or neuronal sodium channels. Site-3 toxins include alpha scorpion toxins and anemone toxins, with their most studied actions at overlapping receptor sites in the S3–S4 extracellular loop of domain IV (Catterall and Beress 1978; Rogers et al. 1996). Site-4 toxins include beta scorpion toxins with a primary binding site in the domain II S3–S4 extracellular loop (Jover et al. 1980; Cestele et al. 1998). Site-specific toxins have proven invaluable probes for dissecting the roles of specific voltage sensors in activation and fast inactivation and are often referred to as gating modifier toxins.

Site-3, sea anemone toxins including ATXII and anthopleurin selectively target fast inactivation (El-Sharif et al. 1992; Hanck and Sheets 1995) and inhibit gating charge translocation (Neumcke et al. 1985; Sheets and Hanck 1995). Anthopleurin slows open-state fast inactivation, produces a "plateau" or persistent current, and accelerates recovery of neuronal, cardiac, and skeletal muscle channels with little effect on activation parameters (Hanck and Sheets 1995; Benzinger et al. 1998; Sheets et al. 1999; Groome et al. 2011). An example of the effect of anthopleurin A on brain type IIA sodium channels ($Na_V1.2$) is shown in Fig. 8.

The specific action of anthopleurin to inhibit translocation of DIVS4 (Sheets et al. 1999) has been used to dissect the contribution of individual voltage sensors and residues in gating charge movement during fast inactivation and its recovery. Mutation of the three outer arginine residues in DIVS4 of the cardiac sodium

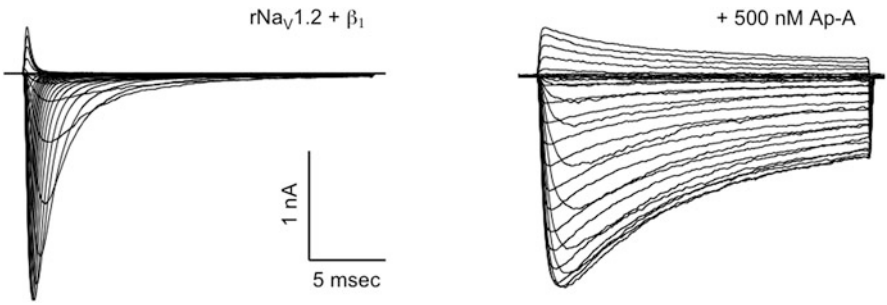

Fig. 8 Patch clamp recordings from *Xenopus* oocyte expressing rNa$_V$1.2 and beta subunit. Anthopleurin slows open-state fast inactivation. Groome, unpublished

channel results in loss of total gating charge (Q_{MAX}) by approximately 1/3, similar to that observed with exposure to anthopleurin. Contributions to gating charge of individual DIVS4 residues could be determined by the relative effect of toxin on Q_{MAX} observed in R to C constructs and show that R1 in DIVS4 carries the most gating charge during fast inactivation, with progressively less charge carried by R2 and R3 (Sheets et al. 1999). The effect of anthopleurin on charge neutralizing mutations in DIIIS4 shows that the outer positive charge there (K1) is outside the electric field (Sheets and Hanck 2002) and that gating charge translocated by DIIIS4 is carried by R2 > R3, with other residues not contributing.

During fast inactivation, a significant fraction of the gating charge becomes immobilized with voltage sensor movement in DIII and DIV (Cha et al. 1999). The respective roles of voltage sensor movement and fast inactivation per se on charge immobilization were determined in two studies (Sheets et al. 2000; Sheets and Hanck 2005). In the first, cysteine substitution in the inactivation particle (IFM–ICM) and exposure to the thiosulfonate reagent MTSET abolished fast inactivation, but did not abolish charge immobilization. In the second, the same ICM mutant was used along with R1C in DIVS4. Wild-type Q_{MAX} and the slow component of charge remobilization were restored by the thiosulfante reagent MTSEA by replacing lost positive charge in R1C, even with abolishment of fast inactivation by intracellular MTSET with the construct ICM/R1C. Thus, while DIVS4 movement is requisite for fast inactivation, the inactivation particle does not itself regulate the mobility of the voltage sensor during recovery.

Groome et al. (2011) found that anthopleurin accelerates charge immobilization during closed-state transitions in skeletal muscle sodium channels. Anthopleurin initially augments charge movement in the hyperpolarized voltage range (closed to closed transitions) with no effect on Q_{MAX}, and with full binding Q_{MAX} is depressed at voltages that drive channel opening. These results suggest that the site-3 toxin promotes DIVS4 toward an intermediate state, first augmenting closed state and then prohibiting open-state fast inactivation. DIVS4 movement promotes fast inactivation presumably by allowing access of the inactivation particle receptor in the distal portion of the DIV S4–S5 linker, as investigated in diverse sodium

channel isoforms (Mitrovic et al. 1996; Tang et al. 1996; Lerche et al. 1997; McPhee et al. 1998; Filatov et al. 1998).

Like anthopleurin, alpha scorpion toxins bind to site-3 and destabilize the fast-inactivated state without affecting activation. Studies with alpha scorpion toxins have uncovered additional features of the domain-specific role of DIVS4 to promote fast inactivation of sodium channels. For example, Ts3 scorpion toxin slows the entry of sodium channels into fast inactivation and accelerates their recovery, but is displaced by strong depolarization (Campos et al. 2004). The interpretation of the effects of toxin is that DIVS4 translocates in two steps; voltage sensor movement in domains I–III (O1) promotes activation, while latter stage DIVS4 translocation (O2) promotes fast inactivation. Subsequent experiments show that this toxin eliminates the voltage dependence of recovery (Campos and Beirao 2006) and decreases the charge immobilized during fast inactivation (Campos et al. 2008), an effect localized to the slow component of both ON and OFF gating currents. Taken together with the results of experiments with anthopleurin, these studies clarify the role of the gating charge comprised by DIVS4 to promote a rapid fast inactivation and to dictate the kinetics of recovery from that absorbing state.

The binding of alpha scorpion toxins from *Leiurus sp*. to the domain IV S3–S4 loop has been studied in some detail, with receptor site comparisons of *Leiuurus* and sea anemone site-3 toxins (Rogers et al. 1996) and structural queries of isoform specificity (Kahn et al. 2009). Extensive investigation using site-directed mutagenesis, chimeric swapping between sodium channels from mammalian and insect sources, and homology modeling have provided atomistic detail of the interaction of alpha scorpion toxin with sodium channels (for review, see Catterall et al. 2007) and that isoform specificity may be localized to sequence disparity in core and NC domains (Kahn et al. 2009). The *Leiurus* toxin core domain acts as a voltage sensor trapper with binding sites at the extracellular ends of domain IV S3 to S4 (part of the voltage sensor module) and the NC domain recognizes the extracellular ends of domain I S5 and S6 (part of the pore module, Gur et al. 2011; Wang et al. 2011). Like other alpha scorpion toxins, *Leiurus* LqhII toxin exhibits high affinity for the closed states of voltage-gated sodium channels. Exploiting this feature, homology models of the sodium channel in the resting state using structural data from $K_V1.2$ channels (Yarov-Yarovoy et al. 2006; Pathak et al. 2007) were subjected to toxin exposure in silico (Wang et al. 2011). The resulting interaction predicts specific interactions of positively charged S4 residues with putative negatively charged counterparts in S2 and S3 segments in the resting state of the channel.

Channel activation is enhanced by spider and beta scorpion site-4 toxins that trap DIIS4 in its activated position. The actions of beta scorpion toxins from *Centruroides sp*. such as CssIV have been studied in some detail. CssIV binds to a receptor complex including IIS1–S2 and IIS3–S4 loops (Zhang et al. 2011). The toxin binds to the channel in its resting state, and with depolarization, the IIS4 segment becomes "trapped" in its outward-favored position, enhancing activation (Cestele et al. 2006, 1998). An interesting finding from scanning mutagenesis of IIS4 is that mutations of hydrophobic residues enhance activation, and several of these residues also contribute to activation trapping. Additionally, mutations of

countercharges in S2 and S3 segments reiterate activation enhancement and toxin trapping phenotypes for mutations of IIS4 positive charge (Montegazza and Cestele 2005). Rescue of wild-type activation and trapping parameters in double charge swapping constructs suggest specific electrostatic interactions in the domain II voltage sensor module. In contrast, the tarantula toxin ProTx II suppresses activation and its gating charge movement, and mutation of the outermost arginines in DIIS4 abolishes the effect of the toxin (Sokolov et al. 2008b). The *Tityus* beta scorpion toxin Tz1 is capable of prohibiting (slowing) activation or deactivation (Leipold et al. 2012), suggesting that toxin binding itself is not dependent on the conformational state of the voltage sensor, but that voltage sensor position during binding dictates the effect of toxin on voltage sensor movement.

Voltage sensor trapping (by Lqh toxin) is also enhanced by domain III charge-reversing mutations (countercharge in S1 or mutations of central charges R4 and R5 in DIIIS4; Song et al. 2011), possibly by allosteric modulation of the DIIS4 voltage sensor trapping effect. In domain III, beta scorpion toxin binding is explored by Zhang et al. (2011). Functional characterization of mutations and modeling of the receptor sites for CssIV in a Na_VAb backbone reveal a third binding site, in the pore module of domain III. This site is shown to be in proximity with the "trappable" voltage sensor module of domain II, supporting the premise of an allosteric, beta scorpion toxin-binding site in domain III.

3.6 Fluorescent Probes of Domain-Specific S4 Functions

Gating charge movement during membrane depolarization has been studied using combined voltage clamp recordings and fluorescence signals, using cysteine residues covalently tagged with sulfhydryl reactive fluorescent dyes (Cha and Bezanilla 1997). For sodium channels, measurements of the combined gating charge transfer, concomitant with changes in fluorescence intensity during channel state transitions, have been utilized for the purposes of investigating the choreography of voltage sensor translocation and its immobilization, nature of elementary charge transfer across the electric field (Chanda and Bezanilla 2008), and domain-specific actions of toxins (Campos et al. 2007, 2008) and anesthetics (Muroi and Chanda 2008; Arcisio-Miranda et al. 2010), to name a few.

The nature of the gating particles that control voltage-dependent (sodium) ion permeability in the squid giant axon was experimentally confirmed by Armstrong and Bezanilla (1973, 1974), who determined that the gating charge moved with channel activation is not recovered instantaneously if channels enter into the fast-inactivated state (Armstrong and Bezanilla 1977). In other words, gating charge becomes "immobilized" during the process of fast inactivation. Cha et al. (1999) used simultaneous fluorescence and gating current measurements to define the roles of the four S4 segments in sodium channels, showing that movement of the voltage sensors in domains III and IV are simultaneous with fast inactivation and that these two segments contain the immobilizable fraction of the gating charge. Channel recovery and remobilization of the gating charge occur with the identical time

course (Armstrong and Bezanilla 1977). Thus, voltage sensor return in domains I and II is rapid, and the slow return of charge (remobilization) in domains III and IV is the primary determinant of sodium channel contribution to the refractory period of the action potential.

The Hodgkin–Huxley parameters describe a process in which three gating particle components m^3, h, and n^4 independently and randomly respond to membrane depolarization to dictate ionic permissiveness. Fluorescence measurements of voltage sensor movements in each domain during state transition have been crucial to our present understanding of the domain-specific and cooperative roles of voltage sensors in domains I to IV.

By correlating the time course of fluorescence intensity change of each S4 (labeled on the N terminal side of the outermost charge) with ionic flux and gating charge development, Chanda and Bezanilla (2002) observed a rapid and simultaneous movement of gating charge during activation in domains I to III, and a slower, delayed movement in domain IV. These results suggest a domain-specific action of voltage sensors in domains I to III for activation (without sequence specificity) and that charge movement in domain IV was not requisite for activation. It should be noted that these authors permitted the possibility of two separate translocations of domain IV, as suggested by the experiments of Horn et al. (2000) in which irradiation-induced immobilization of DIVS4 inhibited both activation and fast inactivation. The second Hodgkin–Huxley postulate of independent gating particles has been addressed by determining the effect of mutation of voltage sensors in one domain on the fluorescence tracking of a voltage sensor in a different domain (Chanda et al. 2004). Perturbation of any one voltage sensor produces a change in the gating charge movement of the other voltage sensors, demonstrating that S4 movement is cooperative. Coupling is strongest for DIS4 and DIVS4, suggesting that coupling of fast inactivation to the activation process has its basis in the cooperative interaction of these two voltage sensors.

4 X Ray Diffraction: Structural Modeling and Molecular Dynamics

The crystal structure of the prokaryotic potassium channel KcSA (Doyle et al. 1988) revealed for the first time interatomic distances within an ion channel that relate specific amino acid residues with the functions of ion permeation and selectivity. X-ray diffraction and electron microscopy data of prokaryotic voltage-gated potassium channel K_VAP (Jiang et al. 2003, 2004; Cuello et al. 2004), and subsequent crystallization and characterization of mammalian *Shaker*-like K_V1.2 (Long et al. 2005a, b; Lee et al. 2005) provided important structural detail into the voltage sensor module in ion channels and sparked a wave of experimental research emphasis to compare the voltage sensor paddle and screw-helical hypotheses. Importantly for this discussion, these efforts initiated a growing trend to incorporate structural detail of ion channels into investigation of their function.

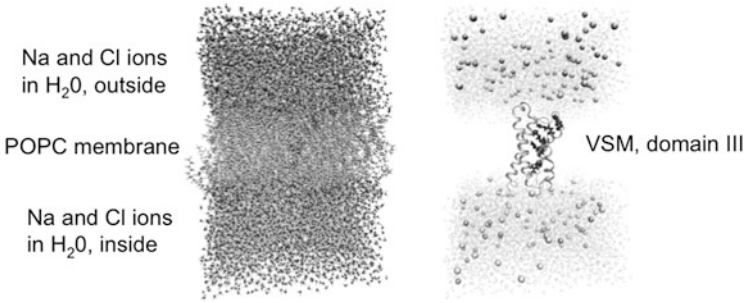

Fig. 9 Voltage sensor module of DIIIS4 of $rNa_V1.4$, embedded in POPC membrane. At *right*, lipid molecules have been removed with S4 charges highlighted. Groome and Winston, unpublished

One avenue of approach to studying the basis of voltage gating in sodium channels is to compare functional data for prokaryotic or eukaryotic channels to structural data inferred from X-ray diffraction data. Structural modeling often employs homology models of the channel of interest, based on the premise that voltage-gated ion channels share considerable sequence homology, especially for regions of voltage gating. Crystal structures are typically determined in a depolarizing environment, yielding data on the activated state in potassium (Long et al. 2005a, b, 2007) and sodium (Payandeh et al. 2011, 2012; Zhang et al. 2012) channels. Closed- or intermediate state models have been built from a comparison of these structures to experimental data on S4 movement using a combination of mutagenesis, fluorescence, spectroscopy, metal ion binding, and/or disulfide locking experiments to establish likely S4 charged residue positions or other interactions within the voltage sensor module (Silverman et al. 2003; Yarov-Yarovoy et al. 2006, 2012; Campos et al. 2007; Baker et al. 1998; Pathak et al. 2007; Broomand and Elinder 2008; Shafrir et al. 2008; DeCaen et al. 2008, 2009, 2011; Chakrapani et al. 2010; Horne et al. 2010; Paldi and Gurevitz 2010; Lin et al. 2011; Henrion et al. 2012). X-ray diffraction data of the S1–S4 region from the crystal structure of the bacterial cyclic nucleotide channel MIotiK1 resolved in the closed state (Clayton et al. 2008) has also proven useful in generating models of voltage-gated channels in the resting conformation. In general, these investigations support a model of voltage gating in which the S4 helix translocates a short distance across a focused electric field, with limited movement of the S1, S2, and S3 helices (studies reviewed in Delemotte et al. 2012; Vargas et al. 2012).

Structural or homology modeling of open and closed states of ion channels has been exploited in computer simulations of voltage sensor movement in molecular dynamics trajectory calculations (reviewed by Sigworth 2007; Dror et al. 2010; Roux 2010; Delemotte et al. 2012; Vargas et al. 2012). An example of a voltage sensor module embedded in a POPC membrane after equilibration and prior to simulation of an applied membrane potential is shown in Fig. 9.

All atom MD simulations for K_V channels have been used to investigate or predict folding events (Gajewski et al. 2011), permeation events or intermediate

states (Jogini and Roux 2007; Treptow et al. 2009; Delemotte et al. 2011; Pan et al. 2011; Lacroix et al. 2012; Jensen et al. 2010, 2012, 2013), the 3–10 helix conformation proposed to provide energetic favoring of aligned S4 and countercharges in gating (Schwaiger et al. 2011), and the omega current defining the position of the gating pore (Delemotte et al. 2010; Jensen et al. 2012; Khalili-Araghi et al. 2012).

Molecular dynamics simulations of sodium channel gating have now been employed in several studies of the voltage sensor module. Incorporation of physical data into the model used for simulations is one method of constraining the protein in its predicted environment or evaluating the equilibration of that protein in the environment in the absence of constraints (Sompornpisut et al. 2008). The activated state of NachBac was predicted in this fashion by running MD simulations of the membrane-bound voltage sensor module after determining constraints for each of the residues in that module with respect to their accessibility to solvent using site-directed spin labeling (Chakrapani et al. 2010). The extensive physical characterization in this study provides a complementary support to MD simulation predictions of NachBac countercharge to S4 interactions. These and other MD simulations of bacterial sodium channels Na_VAb predict countercharge to S4 interactions during activation promoted by dynamic formation of S4 3–10 helical conformation (Amaral et al. 2012).

5 Countercharges in the Sodium Channel VSM: Sliding Helix Model

With the demonstration of S4 segments as voltage sensors, an important goal has been to explain how voltage sensor movement is achieved in the energetically unfavorable environment dictated by a hydrophobic plasma membrane. Energetically favorable intermediate steps in translocation are an important consideration for efficient gating charge transfer across a hydrophobic barrier. Putative negative countercharges might stabilize positively charged voltage sensor residues as they respond to membrane depolarization. This proposed mechanism has evolved from theoretical consideration to an experimentally derived, integral component of the sliding helix model. First studied in potassium channels, negatively charged amino acids in the voltage sensor module influence channel gating (*Shaker*, Papazian et al. 1995; Seoh et al. 1996; HCN2, Chen et al. 2000; BK, Ma et al. 2006; KCNQ, Eldstrom et al. 2010; Pless et al. 2011). Investigations based on potassium crystal structure data support a sliding helix or helical screw model (Yarov-Yarovoy et al. 2006; Pathak et al. 2007; Shafrir et al. 2008). Using this model as the basis for experimentation, recent studies have provided functional characterization of the role of countercharges in sodium channels. It is interesting to note that the earliest models of sodium channel structure posit that negative charges in S1 and S3 provide salt bridge partners for positively charged S4 residues in the helical screw motion of voltage sensor translocation (Guy and Seetharamulu 1986).

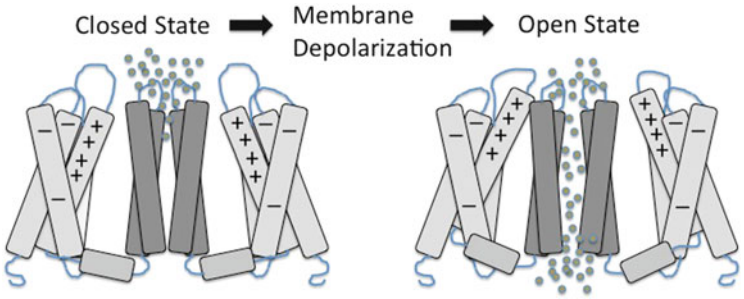

Fig. 10 Model of ion channel activation and pore opening. Countercharges identified in functional investigation of the NacBac channel are shown (−); these form sequential ion pairs with S4 (+) charge to drive that segment outward and via the S4–S5 linker pull open the ion permeation gate of the pore module

5.1 Countercharges in Prokaryotic Sodium Channels

Countercharge interactions with the S4 complement of positive charge have been investigated in prokaryotic sodium channels, with a focus on the bacterial sodium channel NacBac (DeCaen et al. 2008, 2009, 2011; Paldi and Gurevitz 2010; Yarov-Yarovoy et al. 2012). Specific ion pair interactions of negative countercharges in the S1 and S2 segments with S4 positive charges have been identified using disulfide locking experiments with cysteine mutants. The experimental design is based on the fact that the NachBac channel lacks native cysteine residues. By substituting S4 arginine and negative countercharges with cysteine, it is assumed that disulfide locking occurs with proximity of these two residues at 2–3 Å, well within the distance supported by an electrostatic interaction. If the residues lock, channel function is lost, as observed in electrophysiological recording. The sequential nature of these interactions is interpreted from the level of depolarization needed to induce disulfide locking and provide the choreography of salt bridge interactions during intermediate steps towards activation.

These electrophysiological data have been supported by computational methods and structural data to provide the current view of the activation process in sodium channels, in which S1–S4 voltage sensor module (VSM) dictates the opening or closing of S5–S6 segments comprising a pore module (Muroi et al. 2010; Yarov-Yarovoy et al. 2012 and reviewed by Vargas et al. 2012). The proposed mechanism for sodium ion channel activation is shown in Fig. 10. Briefly, sequential electrostatic interactions of countercharge ions with S4 residues are promoted by membrane depolarization. The favorable energetics of ion pairing define intermediate states that drive the S4 segment outwards toward the extracellular space. This movement is transferred through a rigid helix of the S4–S5 linker, providing a mechanical translation of the electrical force of membrane depolarization to open of the pore module gate at the base of S5–S6 segments, promoting ion permeation.

Crystal structures of the prokaryotic sodium channels Na_VAb (Payandeh et al. 2011, 2012) and the NacBac orthologue Na_VRh (Zhang et al. 2012) support

Fig. 11 Models of the voltage sensor module in action. *Left*: Closed-activated Na_VAb (from Payandeh et al. 2011). Inactivated state models from Na_VAb (*middle*, Payandeh et al. 2012) and Na_VRh (*right*, Zhang et al. 2012) show the progressive outward movement of S4 and sequential ion pair formation

the results of functional characterization of the voltage sensor module in prokaryotic sodium channels. The Na_VAb channel has been crystallized in two states of activation, and the Na_VRh channel was crystallized in an even more depolarized state. A comparison of these structures show progressive movement of S4 charges through the gating pore towards potential interacting countercharge partners in the S1 and S2 segments (Fig. 11).

5.2 Countercharges in Eukaryotic Sodium Channels

Investigation of the voltage sensor module in eukaryotic sodium channels has been studied from a theoretical approach using homology models of voltage-gated potassium or sodium channels for which crystal structures have been determined and for several state transitions. Molecular dynamics simulations of the $rNa_V1.4$ (rat skeletal muscle) channel based on homology models of each domain predict a series of interactions of countercharges in S1–S3 segments with voltage sensor residues in each domain (Gosselin-Badaroudine et al. 2012b). Countercharge to S4 interactions define three intermediate states of voltage sensor translocation predicted in these simulations.

Functional characterization of S1–S3 countercharges in eukaryotic sodium channels with disulfide locking experiments has not yet been possible, since these channels contain native cysteine residues, precluding the interpretation of disulfide locking to a specific ion pair. Nevertheless, several studies have investigated the role of S1, S2, and S3 segments in eukaryotic sodium channels using a mutagenesis strategy. For example, charge-neutralizing mutations in S1 of insect channels slow

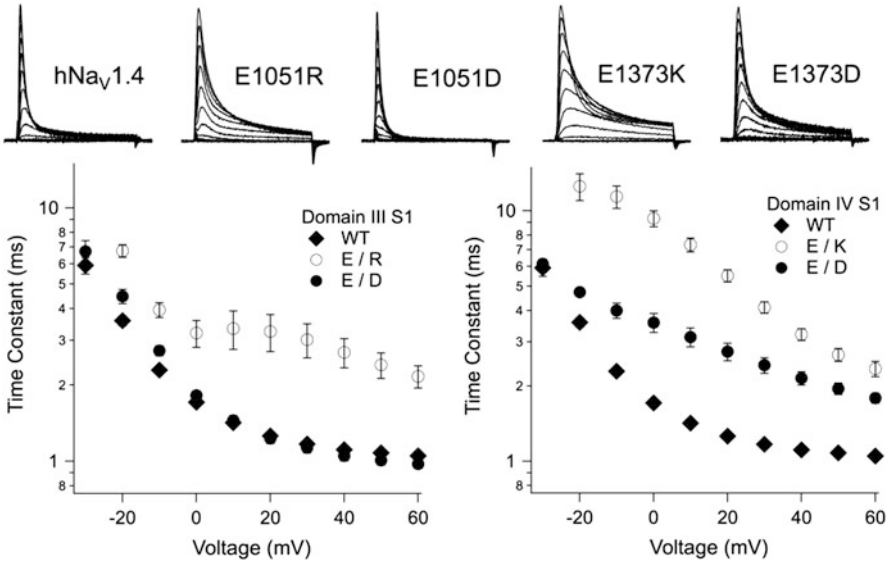

Fig. 12 Negative countercharges in the S1 segment of domains III (E1051) and IV (E1373) promote fast inactivation of the mammalian sodium channel. Plots show kinetics of entry into fast inactivation. Modified from Groome and Winston (2013)

activation and deactivation (Du et al. 2010). In mammalian sodium channels, mutations N1382C and E1392C (DIV S2) slow the entry of channels into fast inactivation (rNa$_V$1.4, Ma et al. 2009). In DIV S3, cysteine substitutions at D1420 or N1417 also slow fast inactivation (hNa$_V$1.4, Nguyen and Horn 2002). Effects of countercharge mutations across the four domains of hNa$_V$1.4 support the premise that domain-specific roles of S4 segments are facilitated by interactions of countercharges in these domains with S4 residues (Groome and Winston 2013). Figure 12 shows the effects of S1 countercharge mutations in domains III and IV on fast inactivation.

It is evident that charge content and structure must be considered to more completely explain the roles of countercharges in sodium channel function. For example, X-ray diffraction data and structural modeling predict networks of hydrogen bond interactions above and below the gating pore that may explain these diverse effects of mutations (Payandeh et al. 2011; Yarov-Yarovoy et al. 2012). Similarly S4 residue structure is important, as charge-conserving mutations of S4 residues often have dramatic effects (Kontis and Goldin 1997; Groome et al. 2002).

Conclusion

Voltage sensitivity of sodium channels is ascribed to movement of gating charge across the transmembrane electric field, as provided by positively charged residues in the S4 segments in each domain. Domain-specific functions of individual voltage sensing S4 segments have been investigated with mutations

including those found in channelopathies of nerve and muscle, chemical modification, and fluorescence. X-ray diffraction data, structural modeling, and molecular dynamics have added a new set of tools to study the interaction of S1 to S3 countercharges with the voltage sensing S4 segments to advance our understanding of the structural basis of channel functions effected by the voltage sensor module in sodium channels.

Acknowledgments This work was supported by NIH 1R15NSO64556-01 to JRG and by NIH P20 RR016454 to Idaho State University. Thanks are given to V Winston (Biology Department, ISU) for contribution of homology models for $hNa_V1.4$ and molecular dynamics simulations. This work is dedicated to the memory of the late Esther Fujimoto.

References

Aggarwal S, MacKinnon R (1996) Contribution of the S4 segment to gating charge in the Shaker K + channel. Neuron 16:1169–1177

Amaral C, Carnevale V, Klein ML, Treptow W (2012) Exploring conformational states of the bacterial sodium channel NaVAb via molecular dynamics simulations. Proc Natl Acad Sci U S A 109:21366–21341

Arcisio-Miranda M, Muroi Y, Chowdhury S, Chanda B (2010) Molecular mechanism of allosteric modification of voltage-dependent sodium channels by local anesthetics. J Gen Physiol 136:541–554

Armstrong CM (2006) Na channel inactivation from open and closed states. Proc Natl Acad Sci U S A 103:17991–17996

Armstrong CM, Bezanilla F (1973) Currents related to movement of the gating particles of the sodium channels. Nature 242:459–461

Armstrong CM, Bezanilla F (1974) Charge movement associated with the opening and closing of the activation gates of the Na channel. J Gen Physiol 65:533–552

Armstrong CM, Bezanilla F (1977) Inactivation of the sodium channel II. Gating current experiments. J Gen Physiol 70:567–590

Armstrong CM, Hille B (1998) Voltage-gated ion channels and electrical excitability. Neuron 20:371–380

Baker OS, Larsson HP, Mannuzzu M, Isacoff EF (1998) Three transmembrane conformations and sequence-dependent displacement of the S4 domain in Shaker K + channel gating. Neuron 20:1283–1294

Bendahhou S, Cummins T, Kwiecinski H, Waxman S, Ptacek L (1999) Characterization of a new sodium channel mutation at arginine 1448 associated with moderate paramyotonia congenita in humans. J Physiol 518:337–344

Benzinger GR, Kyle JW, Blumenthal KM, Hanck DA (1998) A specific interaction between the cardiac sodium channel and site-3 toxin anthopleurin B. J Biol Chem 273:80–84

Bezanilla F (2008) How membrane proteins sense voltage. Nat Rev 9:323–331

Blanchet J, Chahine M (2007) Accessibility of the four arginine residues on the S4 segment of the Bacillus halodurans sodium channel. J Membr Biol 215:169–180

Blumenthal KM, Seibert AL (2003) Voltage-gated sodium channel toxins. Poisons, probes and future promise. Cell Biochem Biophys 38:215–237

Bosmans F, Swartz KJ (2010) Targeting voltage sensors in sodium channels with spider toxins. Trends Pharmacol Sci 31:175–182

Broomand A, Elinder F (2008) Large-scale movement with the voltage-sensor of a potassium channel-support for a helical-screw motion. Neuron 59:770–777

Campos FV, Beirao PSL (2006) Effects of bound Ts3 on voltage dependence of sodium channel transitions to and from inactivation and energetics of its unbinding. Cell Biochem Biophys 44:424–430
Campos FV, Coronas FIV, Beirao PSL (2004) Voltage-dependent displacement of the scorpion toxin Ts3 from sodium channels and its implication on the control of inactivation. Br J Pharamacol 142:1115–1122
Campos FV, Chanda B, Beirao PSL, Bezanilla F (2007) β-scorpion toxin modifies gating transitions in all four voltage sensors of the sodium channel. J Gen Physiol 130:257–268
Campos FV, Chanda B, Beirao PSL, Bezanilla F (2008) α-scorpion toxin impairs a conformational change that leads to fast inactivation of muscle sodium channels. J Gen Phys 132:251–263
Cannon SC (2006) Pathomechanisms in channelopathies of skeletal muscle and brain. Ann Rev Neurol 29:387–415
Cannon SC (2010) Voltage sensor mutations in channelopathies of skeletal muscle. J Physiol 588:1887–1895
Carle T, Lhuillier L, Luce S, Sternberg D, Devust O, Fonataine B, Tabti N (2006) Gating defects of a novel Na + channel mutant causing hypokalemic periodic paralysis. Biochem Biophys Res Comm 348:653–661
Catterall WA (2010) Ion channel voltage sensors: structure, function and pathophysiology. Neuron 67:915–928
Catterall WA (2012) Voltage gated sodium channels at 60: structure, function and pathophysiology. J Physiol 590:2577–2589
Catterall WA, Beress L (1978) Sea anemone toxin and scorpion toxin share a common receptor site associated with the sodium channel ionophore. J Biol Chem 253:7393–7396
Catterall WA, Cestele S, Yarov-Yarovoy V, Konoki K, Scheuer T (2007) Voltage-gated ion channels and gating modifier toxins. Toxicon 49:124–141
Cestele S, Qu Y, Rogers JC, Bochat H, Scheurer T, Catterall WA (1998) Voltage-sensor trapping: enhanced activation of sodium channels by beta-scorpion toxin bound to the S3-S4 loop in domain II. Neuron 1998(21):919–931
Cestele S, Yarov-Yarovoy V, Qu Y, Sampieri F, Scheuer T, Catterall WA (2006) Structure and function of the voltage sensor of sodium channels probed by a b scorpion toxin. J Biol Chem 30:21332–21344
Cha A, Bezanilla F (1997) Characterizing the voltage-dependent conformational changes in the Shaker K + channel with fluorescence. Neuron 19:1127–1140
Cha A, Ruben PC, George AL Jr, Fujimoto E, Bezanilla F (1999) Voltage sensors in domains III and IV, but not I and II, are immobilized by Na + channel fast inactivation. Neuron 22:73–87
Chahine M, George AL Jr, Zhou M, Ji S, Sun W, Barchi RL, Horn R (1994) Sodium channel mutations in paramyotonia congenita uncouple inactivation from activation. Neuron 12:281–294
Chakrapani S, Sompornpisut P, Intharathep P, Roux B, Perozo E (2010) The activated state of a sodium channel voltage sensor in a membrane environment. Proc Natl Acad Sci U S A 107:5435–5440
Chanda B, Bezanilla F (2002) Tracking voltage-dependent conformational changes in skeletal muscle sodium channel during activation. J Gen Physiol 120:629–645
Chanda B, Asamoah OK, Bezanilla F (2004) Coupling interactions between voltage sensors of the sodium channel as revealed by site-specific measurements. J Gen Physiol 123:217–230
Chanda B, Bezanilla F (2008) A common pathway for charge transport through voltage sensing domains. Neuron 57:345–351
Chen J, Mitcheson JS, Lin M, Sanguinetti MC (2000) Functional roles of charged residues in the putative voltage sensor of the HCN2 pacemaker channel. J Biol Chem 275:36465–36471
Chen L-Q, Santarelli V, Horn R, Kallen RG (1996) A unique role for the S4 segment of domain 4 in the inactivation of sodium channels. J Gen Physiol 108:549–556

Clayton GM, Altieri S, Heginbotham L, Unger VM, Morais-Cabral JH (2008) Structure of the transmembrane regions of a bacterial cyclic nucleotide-regulated channel. Proc Natl Acad Sci U S A 105:1511–1515

Cole KS, Curtis HJ (1938) Electrical impedance of Nitella during activity. J Gen Physiol 22:37–64

Cole KS, Curtis HJ (1939) Electrical impedance of the squid giant axon during activity. J Gen Physiol 22:649–670

Cuello LG, Cortes DM, Perozo E (2004) Molecular architecture of the K_VAP voltage-dependent K + channel in a lipid bilayer. Science 306:491–495

DeCaen PG, Yarov-Yarovoy V, Zhao Y, Scheurer T, Catterall WA (2008) Disulfide locking of a sodium channel voltage sensor reveals ion pair formation during activation. Proc Natl Acad Sci U S A 105:15142–15147

DeCaen PG, Yarov-Yarovoy V, Sharp EM, Scheurer T, Catterall WA (2009) Sequential formation of ion pairs during activation of a sodium channel voltage sensor. Proc Natl Acad Sci U S A 106:22498–22503

DeCaen PG, Yarov-Yarovoy V, Scheurer T, Catterall WA (2011) Gating charge interactions with the S1 segment during activation of a Na + channel voltage sensor. Proc Natl Acad Sci U S A 108:18825–18830

Delemotte L, Treptow W, Klein ML, Tarek M (2010) Effect of sensor domain mutations on the properties of voltage-gated ion channels: molecular dynamics studies of the potassium channel K_V1.2. Biophys J 99:L72–L74

Delemotte L, Tarek M, Klein ML, Amaral C, Treptow W (2011) Intermediate states of the K_V1.2 voltage sensor from atomistic molecular dynamics simulations. Proc Natl Acad Sci U S A 108:6109–6114

Delemotte L, Klein ML, Tarek M (2012) Molecular dynamics simulations of voltage-gated cation channels: insights on voltage-sensor domain function and modulation. Front Pharmacol 3:1–15

Du Y, Song W, Groome JR, Nomura Y, Luo N, Dong K (2010) A negative charge in transmembrane segment 1 of domain II of the cockroach sodium channel is critical for channel gating and action of pyrethroid insecticides. Toxicol Appl Pharmacol 247:53–59

Doyle DA, Cabral JM, Pfuetnzner RA, Kuo A, Gulbis JM, Cohen SL, Chait BT, MacKinnon R (1988) The structure of the potassium channel: molecular basis of K + conduction and selectivity. Science 280:69–77

Dror RO, Jensen MO, Borhani DW, Shaw DE (2010) Exploring atomic resolution on a femtosecond to millisecond timescale using molecular dynamics simulations. J Gen Physiol 135:555–562

Eldstrom J, Xu H, Werry D, Kang C, Loewen ME, Degenhardt A, Sanatani S, Tibbits GF, Sanders C, Fedida D (2010) Mechanistic basis for LQT1 caused by S3 mutations in the KCNQ1 subunit of IKs. J Gen Physiol 135:433–438

El-Sharif N, Fozzard HA, Hanck DA (1992) Dose-dependent modulation of the cardiac sodium channel by sea anemone toxin ATXII. Circ Res 70:285–301

Filatov GN, Nguyen TP, Kraner SD, Barchi RL (1998) Inactivation and secondary structure in the D4/S4-5 region of the SkM1 sodium channel. J Gen Physiol 111:703–715

Francis DG, Rybalchenko V, Struyk A, Cannon SC (2011) Leaky sodium channels from voltage sensor mutations in periodic paralysis, but not myotonia. Neurology 76:1–7

Gajewski C, Dagcan A, Roux B, Deutsch C (2011) Biogenesis of the pore architecture of a voltage-gated potassium channel. Proc Natl Acad Sci U S A 108:3240–3245

George AL Jr (2012) Leaky channels make weak muscles. J Clin Invest 122:4333–4326

Gosselin-Badaroudine P, Keller D, Huang H, Pouliot V, Chatelier A, Osswald S, Brink M, Chahine M (2012a) A proton leak current through the cardiac sodium channel is linked to mixed arrhythmia and the dilated cardiomyopathy phenotype. PLoS One 7:1–11

Gosselin-Badaroudine P, Delemotte L, Moreau A, Klein ML, Chahine M (2012b) Gating pore currents and the resting state of Na_V1.4 voltage sensor domains. Proc Natl Acad Sci U S A 109:19250–19255

Groome JR, Winston V (2013) S1-S3 counter charges in the voltage sensor module of a mammalian sodium channel regulate fast inactivation. J Gen Phys 141:601–618
Groome JR, Fujimoto E, George AL Jr, Ruben PC (1999) Differential effects of homologous S4 mutations in human skeletal muscle sodium channels on deactivation gating from open and inactivated states. J Physiol 516:687–698
Groome JR, Fujimoto E, Walter L, Ruben P (2002) Outer and central charged residues in DIVS4 of skeletal muscle sodium channels have differing roles in deactivation. Biophys J 82:1293–1307
Groome JR, Holzherr BD, Lehmann-Horn F (2011) Open- and closed-state fast inactivation in sodium channels. Differential effects of a site-3 anemone toxin. Channels 5:1–14
Gur M, Kahn R, Karbat I, Regev N, Wang J, Catterall WA, Gordon D, Gurevitz M (2011) Elucidation of the molecular basis of selective recognition uncovers the interaction site for the core domain of scorpion α-toxins on sodium channels. J Biol Chem 286:35209–35217
Guy HR, Seetharamulu P (1986) Molecular model of the action potential sodium channel. Proc Natl Acad Sci U S A 83:508–512
Hanck DA, Sheets MF (1995) Modification of inactivation in cardiac sodium channels: ionic current studies with anthopleurin-A toxin. J Gen Physiol 106:601–616
Hanck DA, Sheets MF (2007) Site-3 toxins and cardiac sodium channels. Toxicon 49:181–193
Henrion U, Renhorn J, Borjesson SI, Neslon SI, Nelson EM, Schwaiger CS, Bjelkmar P, Wallner B, Lindhal E, Elinder F (2012) Tracking a complete voltage sensor with metal-ion bridges. Proc Natl Acad Sci U S A 109:8552–8557
Hodgkin AL, Huxley AF (1952) A quantitative description of membrane current and its application to conduction and excitation in nerve. J Physiol 117:500–544
Holzherr, BD, Groome JR, Fauler M, Nied E, Lehmann-Horn F, Jurkat-Rott K (2010) Characterization of a novel h$Na_V1.4$ mutation causing hypokalemic periodic paralysis. Biophys Soc Abstr LB201
Horn R, Ding S, Gruber HJ (2000) Immobilizing the moving parts of voltage-gated ion channels. J Gen Physiol 116:461–475
Horne AJ, Peters CJ, Claydon TW, Fedida D (2010) Fast and slow voltage sensor rearrangements during activation gating in Kv1.2 channels detected using tetramethylrhodamine fluorescence. J Gen Physiol 136:83–99
Jensen MO, Borhani DW, Lindorff-Laren K, Maragakis P, Jogini V, Eastwood MP, Dror RO, Shaw DE (2010) Principles of conduction and hydrophobic gating in K + channels. Proc Natl Acad Sci U S A 107:5833–5838
Jensen MO, Jogini V, Borhani DW, Leffler AE, Dror RO, Shaw DE (2012) Mechanism of voltage gating in potassium channels. Science 336:229–233
Jensen MO, Jogini V, Eastwood MP, Shaw DE (2013) Atomic-level simulation of current-voltage relationships in single-file ion channels. J Gen Physiol 141:619–632
Jiang Y, Lee A, Ruta V, Cadene M, Chait BT, MacKinnon R (2003) X-ray structure of a voltage-dependent K + channel. Nature 423:33–41
Jiang Q-X, Wang D-N, MacKinnon R (2004) Electron microscopic analysis of KVAP voltage-dependent K + channels in an open conformation. Nature 430:806–810
Jogini V, Roux B (2007) Dynamics of the KV1.2 voltage-gated K+ channel in a membrane environment. Biophys J 93:3070–3082
Jover E, Couraud F, Rochat H (1980) Two types of scorpion neurotoxins characterized by their binding to two separate receptor sites on rat brain synaptosomes. Biocim Biophys Res Commun 95:1607–1614
Jurkat-Rott K, Mitrovic N, Hang C, Kouzmekine A, Iaizzo P, Herzog J, Lerche H, Nicole S, Vale-Santos S, Chauveau D, Fontaine B, Lehmann-Horn F (2000) Voltage sensor mutations cause hypokalemic periodic paralysis type 2 by enhanced inactivation and reduced current. Proc Natl Acad Sci U S A 97:9549–9554
Jurkat-Rott K, Holzherr B, Fauler M, Lehmann-Horn F (2010) Sodium channelopaties of skeletal muscle result from gain or loss of function. Plugers Arch 460:239–248

Jurkat-Rott K, Groome JR, Lehmann-Horn F (2012) Pathophysiological role of omega pore current in channelopathies. Front Neuropharmacol 3:1–15

Kahn R, Karbat I, Ilan N, Cohen L, Sokolov S, Catterall WA, Gordon D, Gurevitz M (2009) Molecular requirements for recognition of brain voltage-gated sodium channels by scorpion a-toxins. J Biol Chem 284:20684–20691

Kambouris NG, Nuss HB, Johns DC, Tomaselli GF, Marban E, Balser JR (1998) Phenotypic characterization of a novel long-QT syndrome mutation (R1623Q) in the cardiac sodium channel. Circulation 97:640–644

Kambouris NG, Nuss HB, Johns DC, Marban E, Tomaselli GF, Balser JR (2000) A revised view of cardiac sodium channel "blockade" in the long QT syndrome. J Clin Invest 105:1133–1140

Khalili-Araghi F, Tajkhorsid E, Roux B, Schulten K (2012) Molecular dynamics investigation of the w-current in the $K_V1.2$ voltage sensor domains. Biophys J 102:258–267

Kontis KJ, Goldin AL Jr (1997) Sodium channel inactivation is altered by substitution of voltage sensor positive charges. J Gen Physiol 110:403–413

Kontis KJ, Rounaghi A, Goldin AL Jr (1997) Sodium channel activation gating is affected by substitutions of voltage sensor positive charges in all four domains. J Gen Physiol 110:391–401

Kuzmenkin A, Muncan V, Jurkat-Rott K, Hang C, Lerche H, Lehmann-Horn F, Mitrovic N (2002) Enhanced inactivation and pH sensitivity of Na + channel mutations causing hypokalemic periodic paralysis type II. Brain 125:825–843

Lacroix J, Pless SA, Maragliano L, Campos FV, Galpin JD, Ahern CA, Roux B, Bezanilla F (2012) Intermediate state trapping of a voltage sensor. J Gen Physiol 140:635–652

Lee S-Y, Lee A, Chen J, MacKinnon R (2005) Structure of the KvAP voltage-dependent K+ channel and its dependence on the lipid membrane. Proc Natl Acad Sci USA 102:15441–15446

Leipold E, Borges A, Heinemann SH (2012) Scorpion β-toxin interference with Na_V channel voltage sensor gives rise to excitatory and depressant modes. J Gen Physiol 139:305–319

Lerche H, Mitrovic N, Dubowitz V, Lehmann-Horn F (1996) Paramyotonia congenita: the R1448P Na + channel mutation in adult human skeletal muscle. Ann Neurol 39:599–608

Lerche H, Peter W, Fleischhauer R, Pika-Hartlaub U, Malina T, Mitrovic N, Lehmann-Horn F (1997) Role in fast inactivation of the IV/S4-S5 loop of the human muscle Na + channel probed by cysteine mutagenesis. J Physiol 505:345–352

Lin M-C, Hsieh J-Y, Mock AF, Papapzian DM (2011) R1 in the Shaker S4 occupies the gating charge transfer center in the resting state. J Gen Physiol 138:155–163

Long SB, Campbell EB, MacKinnon R (2005a) Crystal structure of a mammalian voltage-dependent Shaker K + channel. Science 309:897–903

Long SB, Campbell EB, MacKinnon R (2005b) Voltage sensor of $K_V1.2$: structural basis of electromechanical coupling. Science 309:903–908

Long SB, Tao X, Campbell EB, MacKinnon R (2007) Atomic structure of a voltage-dependent K + channel in a lipid membrane-like environment. Nature 450:376–382

Ma Z, Lou XJ, Horrigan FT (2006) Role of charged residues in the S1-S4 voltage sensor of BK channels. J Gen Physiol 127:309–328

McPhee JC, Ragsdale DS, Scheuer T, Catterall WA (1998) A critical role for the S4-S5 intracellular loop in domain IV of the sodium channel a subunit in fast inactivation. J Biol Chem 273:1121–1129

Mitrovic N, Lerche H, Heine R, Fleischhauer R, Pika-Hartlaub U, Hartlaub U, George AL Jr, Lehmann-Horn F (1996) Role in fast inactivation of conserved amino acids in the IV/S4-S5 loop of the human muscle Na + channel. Neurosci Lett 214:9–12

Mohammadi B, Mitrovic N, Lehmann-Horn F, Dengler R, Bufler J (2003) Mechanisms of cold sensitivity of paramyotonia congenita mutation R1448H and overlap syndrome mutation M1360V. J Physiol 547:691–698

Mohammadi B, Jurkat-Rott K, Alekov A, Dengler R, Bufler J, Lehmann-Horn F (2005) Preferred mexiletine block of human sodium channels with IVS4 mutations and its pH dependence. Pharm Genomics 15:235–244

Montegazza M, Cestele S (2005) β-scorpion toxin effects suggest electrostatic interaction in domain II of voltage-dependent sodium channels. J Physiol 568:13–30
Moran Y, Gordon D, Gurevitz M (2009) Sea anemone toxins affecting voltage-gated sodium channels: molecular and evolutionary features. Toxicon 54:1089–1101
Muroi Y, Chanda B (2008) Local anesthetics disrupt energetic coupling between the voltage-sensing segments of a sodium channel. J Gen Physiol 133:1–15
Muroi Y, Arcisio-Miranda M, Chowdhury S, Chanda B (2010) Molecular determinants of coupling between the domain III voltage sensor and pore of a sodium channel. Nat Struct Mol Biol 17:230–237
Neumcke B, Schwarz W, Stampfl R (1985) Comparison of the effects of Anemonia toxin II on sodium and gating currents in frog myelinated nerve. Biochim Biophys Acta 814:111–119
Noda MS, Shizimu S, Tanabe T, Takai T, Kayano T, Ikeda T, Takahashi H, Nakayami Y, Kamaoka N, Minamino N, Kangawa K, Matsuo K, Raferty H, Hirose M, Inayama T, Hayashida H, Miyata T, Numa S (1984) Primary structure of Electrophorus electricus sodium channel deduced from cDNA sequence. Nature 312:121–127
Paldi T, Gurevitz M (2010) Coupling between residues on S4 and S1 defines the voltage-sensor resting conformation in NaChBac. Biophys J 99:456–463
Pan AC, Cuello LG, Perozo E, Roux B (2011) Thermodynamic coupling between activation and inactivation gating in potassium channels reveled by free energy molecular dynamics simulations. J Gen Physiol 138:571–580
Papazian DM, Shao XM, Seoh S-A, Mock AF, Huang Y, Wainstock DH (1995) Electrostatic interactions of S4 voltage sensor in Shaker K+ channel. Neuron 14:1–20
Pathak MM, Yarovy-Yarovy V, Agarwal G, Roux B, Barth P, Kohout S, Tombola F, Iscaof EY (2007) Closing in on the resting state of the Shaker (K+) channel. Neuron 56:124–140
Payandeh J, Scheurer T, Zheng N, Catterall WA (2011) The crystal structure of a voltage-gated sodium channel. Nature 475:353–358
Payandeh J, El-Din G, Scheuer T, Zheng N, Catterall WA (2012) Crystal structure of a voltage-gated sodium channel in two potentially inactivated states. Nature 486:135–140
Pless SA, Galpin JD, Niciforovic AP, Ahern CA (2011) Contributions of countercharge in a potassium channel voltage-sensor domain. Nat Chem Biol 7:617–623
Possani LD, Becerril B, Delepierre M, Tytgat J (1999) Scorpion toxins specific for Na + -channels. Eur Biochem 264:287–300
Richmond JE, Featherstone DE, Ruben PC (1997) Human Na + channel fast and slow inactivation in paramyotonia congenita mutants expressed in Xenopus laevis oocytes. J Physiol 499:589–600
Rogers JC, Qu Y, Tanada TN, Scheuer T, Catterall WA (1996) Molecular determinants of high affinity binding of a-scorpion toxin and sea anemone toxin in the S3-S4 extracellular loop in domain IV of the Na + channel a subunit. J Biol Chem 271:15950–15962
Roux B (2010) Perspectives on: molecular dynamics and computational methods. J Gen Physiol 135:547–548
Schwaiger CS, Bjelkmar P, Hess B, Lindhal E (2011) 3-10 helix conformation facilitates the transition of a voltage sensor S4 segment toward the down state. Biophys J 100:1446–1454
Seoh S-A, Sigg D, Papazian DM, Bezanilla F (1996) Voltage-sensing residues in the S2 and S4 segments of the Shaker K+ channel. Neuron 16:1159–1167
Shafrir Y, Durell SR, Guy HR (2008) Models of voltage-dependent conformational changes in NaChBac channels. Biophys J 95:3663–3676
Sheets MF, Hanck DA (1995) Voltage-dependent open-state inactivation of cardiac sodium channels: gating current studies with anthopleurin-A toxin. J Gen Physiol 106:617–640
Sheets MF, Hanck DA (2002) The outermost lysine of domain III contributes little to the gating charge in sodium channels. Biophys J 82:348–3055
Sheets MF, Hanck DA (2005) Charge immobilization of the voltage sensor in domain IV is independent of sodium current inactivation. J Physiol 563:89–93

Sheets MF, Kyle JW, Kallen RG, Hanck DA (1999) The Na channel voltage sensor associated with fast inactivation is localized to the external charged residues of domain IV, S4. Biophys J 77:747–757

Sheets MF, Kyle JW, Hanck DA (2000) The role of the putative inactivation lid in sodium channel gating. J Gen Physiol 115:609–619

Sigworth F (2007) The last few frames of the voltage-gating movie. Biophys J 93:2981–2983

Silverman WR, Roux B, Papazian DM (2003) Structural basis of two-stage voltage-dependent activation in K + channels. Proc Natl Acad Sci U S A 100:2935–2940

Sokolov S, Scheuer T, Catterall WA (2005) Ion permeation through a voltage-sensitive gating pore in brain sodium channels having voltage sensor mutations. Neuron 47:183–189

Sokolov S, Scheuer T, Catterall WA (2008a) Depolarization-activated gating pore current conducted by mutant sodium channels in potassium-sensitive normokalemic periodic paralysis. Proc Natl Acad Sci 105:19980–19985

Sokolov S, Kraus RL, Scheuer T, Catterall WA (2008b) Inhibition of sodium channel gating by trapping the domain II voltage sensor with protoxin II. Mol Pharmacol 73:1020–1028

Sokolov S, Scheurer T, Catterall WA (2010) Ion permeation and block of the gating pore in the voltage sensor of $Na_V1.4$ channels with hypokalemic periodic paralysis mutations. J Gen Physiol 136:225–236

Sompornpisut P, Roux B, Perozo E (2008) Structural refinement of membrane proteins by restrained molecular dynamics and solvent accessibility data. Biophys J 95:5349–5361

Song W, Du Y, Liu Z, Luo N, Turkov M, Gordon D, Gurevitz M, Goldin A, Dong K (2011) Substitutions in the domain III voltage-sensing module enhance the sensitivity of an insect sodium channel to a scorpion β-toxin. J Biol Chem 286:15781–15788

Starace DM, Bezanilla F (2004) A proton pore in a potassium channel reveals a focused electric field. Nature 427:548–553

Struyk AF, Cannon SC (2007) A Na + channel mutation linked to hypokalemic periodic paralysis exposes a proton-selective gating pore. J Gen Physiol 130:11–20

Struyk AF, Scoggan KA, Bulman DE, Cannon SC (2000) The human skeletal muscle Na channel mutation R669H associated with hypokalemic periodic paralysis enhances slow inactivation. J Neurosci 20:8610–8617

Struyk AF, Markin VS, Francis D, Cannon SC (2008) Gating pore currents in DIIS4 mutations of $Na_V1.4$ associated with periodic paralysis: saturation of ion flux and implications for disease pathogenesis. J Gen Physiol 132:447–464

Stuhmer W, Conti F, Suzuki H, Wang X, Noda N, Yahagi N, Kubo H, Numa S (1989) Structural parts involved in activation and inactivation of the sodium channel. Nature 339:597–604

Tang L, Kallen RG, Horn R (1996) Role of an S4-S5 linker in sodium channel inactivation probed by mutagenesis and a peptide blocker. J Gen Physiol 108:89–104

Tombola F, Pathak MM, Isacoff EY (2005) Voltage-sensing arginines in a potassium channel permeate and occlude cation-selective pores. Neuron 45:379–388

Treptow W, Tarek M, Klein ML (2009) Initial response of the potassium channel voltage sensor to a transmembrane potential. J Am Chem Soc 131:2107–2109

Vargas E, Yarov-Yarovoy V, Khalili-Araghi F, Catterall WA, Klein ML, Tarek M, Lindhal E, Schulten K, Perozo E, Bezanilla F, Roux B (2012) An emerging consensus on voltage-dependent gating from computational modeling and molecular dynamics simulations. J Gen Physiol 140:587–594

Wang J, Yarov-Yarovoy V, Kahn R, Gordon D, Gurevitz M, Scheuer T, Catterall WA (2011) Mapping the receptor site for a-scorpion toxins on an Na + channel voltage sensor. Proc Natl Acad Sci U S A 108:15426–15431

Yang N, Horn R (1995) Evidence for voltage-dependent S4 movement in sodium channels. Neuron 15:213–218

Yang N, Ji S, Zhou M, Ptacek LJ, Barchi RL, Horn R, George AL Jr (1994) Sodium channel mutations in paramyotonia congenita exhibit similar biophysical phenotypes in vitro. Proc Natl Acad Sci U S A 91:12785–12789

Yang N, George AL Jr, Horn R (1996) Molecular basis of charge movement in voltage-gated sodium channels. Neuron 16:113–122

Yarov-Yarovoy V, Baker D, Catterall WA (2006) Voltage sensor conformations in the open and closed states in ROSETTA structural models of K (+) channels. Proc Natl Acad Sci U S A 103:7292–7297

Yarov-Yarovoy V, DeCaen PG, Westenbroek RE, Pan C-Y, Scheuer T, Baker D, Catterall WA (2012) Structural basis for gating charge movement in the voltage sensor of a sodium channel. Proc Natl Acad Sci U S A 109:E93–E102

Yu FH, Yarov-Yarovoy V, Gutman GA, Catterall WA (2005) Overview of molecular relationships in the voltage-gated ion channel superfamily. Phys Rev 57:387–395

Zhang JZ, Yarov-Yarovoy V, Scheuer T, Karbat I, Cohen L, Gordon D, Gurevitz M, Catterall WA (2011) Structure-function map of the receptor site for b-scorpion toxins in domain II of voltage-gated sodium channels. J Biol Chem 286:33641–33651

Zhang X, Ren W, DeCaen P, Yan C, Tao X, Tang L, Wang J, Hasegawa K, Kumasaka T, He J, Wang J, Clapham DE, Yan N (2012) Crystal structure of an orthologue of NachBac voltage-gated sodium channel. Nature 486:130–134

Zuo X-P, Ji Y-H (2004) Molecular mechanism of scorpion neurotoxins acting on sodium channels. Insight into their diverse selectivity. Mol Neurobiol 30:265–278

Slow Inactivation of Na^+ Channels

Jonathan Silva

Contents

Abstract

Prolonged depolarizing pulses that last seconds to minutes cause slow inactivation of Na^+ channels, which regulates neuron and myocyte excitability by reducing availability of inward current. In neurons, slow inactivation has been linked to memory of previous excitation and in skeletal muscle it ensures myocytes are able to contract when K^+ is elevated. The molecular mechanisms underlying slow inactivation are unclear even though it has been studied for 50+ years. This chapter reviews what is known to date regarding the definition, measurement, and mechanisms of voltage-gated Na^+ channel slow inactivation.

Keywords

Inactivation • Fluorometry • Hyperkalemic periodic paralysis

J. Silva (✉)
Department of Biomedical Engineering, Washington University in St. Louis, Campus Box 1097, St. Louis, MO 63116, USA
e-mail: jonsilva@wustl.edu

P.C. Ruben (ed.), *Voltage Gated Sodium Channels*, Handbook of Experimental Pharmacology 221, DOI 10.1007/978-3-642-41588-3_3,

1 Background

1.1 What Is Slow Inactivation?

Slow inactivation of voltage-gated Na^+ channels is a gating phenomenon, distinct from fast inactivation, whereby prolonged depolarizing pulses reduce the number of channels available to provide excitatory inward current.

1.2 Physiological Relevance

In neurons and muscle, initiation of action potentials is regulated by the opening and closing of rapidly gated Na^+ channels that produce inward current and depolarize the membrane. Thus, slow inactivation, which reduces the number of channels that are available to open, regulates excitability.

A hallmark of slow inactivation is that its onset and recovery take place over time domains that span multiple orders of magnitude, such that channels subjected to longer depolarizing pulses require longer times at negative potential for current to be restored (Narahashi 1964; Toib et al. 1998). Consequently, memory of previous excitation can be encoded through the slow inactivation of the Na^+ channels. The lack of a specific time scale over which slow inactivation takes place has been linked to neuronal memory (Toib et al. 1998), which exhibits a similar lack of identifiable time scales (Marom 2010).

In skeletal muscle, slow inactivation prevents contraction when serum K^+ is elevated. Patients with mutations that disrupt slow inactivation in the muscle Na^+ channel suffer from a condition known as hyperkalemic periodic paralysis (HyperPP) (Bendahhou et al. 2002). As a result, when high levels of extracellular K^+ marginally elevate the myocyte membrane potential, Na^+ channels that would normally be slow inactivated produce a persistent inward Na^+ current that further depolarizes the membrane. This additional depolarization causes a large fraction of Na^+ channels to fast inactivate, leading to membrane in-excitability. As a result, when normal neuronal routes of excitation are activated, the muscle is unable to respond (Lengele et al. 2008; Jurkat-Rott et al. 2009; Jurkat-Rott and Lehmann-Horn 2006; George 2005).

Cardiac Na^+ channels exhibit much less slow inactivation in comparison to skeletal muscle and neuronal isoforms, showing incomplete inactivation even after very long pulses (O'Reilly et al. 1999). Physiologically, reduced slow inactivation for these channels would be expected, due to the necessity of maintaining cardiac excitability. However, slow inactivation is still relevant to the cardiac rhythm as it is likely to be regulated via the limited population of channels that do inactivate, because the rate at which the cardiac excitation wavefront propagates, known as conduction velocity, is directly proportional to peak Na^+ current (Shaw and Rudy 1997). Moreover, the ability of the myocardium to sustain an arrhythmia is known to depend on several factors, including the length of the path the arrhythmia can travel, the excitability of the tissue, and the conduction velocity.

Slow inactivation affects two of these parameters, excitability and conduction velocity. Mutations that predispose patients to arrhythmia suggest an antiarrhythmic role for slow inactivation. For example, Vilin et al. showed that a double mutation in the cardiac Na^+ channel not only alters rapid gating events but also significantly reduces slow inactivation, positing that the removal of slow inactivation contributes to the propensity of patients to experience an arrhythmia (Vilin et al. 2001a; Vilin and Ruben 2001).

While most channel research is focused on rapid gating events, the slower transitions also play a key physiological role. Moreover, these movements have a degree of permanence that allow them to modulate phenomena that take place over seconds and minutes, such as the memory of a neuron or the sustenance of an arrhythmia. As such, a large number of therapeutically useful small molecules have been designed to target the slow-inactivated states including anesthetics (Balser et al. 1996a), anticonvulsants (Schauf 1987), antiarrhythmics (Sheets et al. 2010), and insecticides (Song et al. 2011).

The physiological potential of slow gating movements was realized early on in the study of Na^+ channels and is discussed in the next section.

1.3 Early Results

As early as the 1920s, Woronzow (1924) showed that restoration of excitability in neurons depends on the duration of a pulse to negative potentials, indicating a slow state of the neuron, entered at depolarized potentials, that must be exited before subsequent excitation can take place. Several decades later, Na^+ current was found to be responsible for neuronal excitation by Hodgkin and Huxley (1952a), linking it to the Na^+ conducting system. As a result, a critical connection was made between the "availability" of the Na^+ conductance, which is regulated by inactivation, and excitability. This link between Na^+ channel inactivation and excitability was appreciated in some of the first recordings of squid giant axons by Hodgkin and Huxley (1952b) and cardiac Purkinje fibers by Sylvio Weidmann (1955). However, these studies focused on rapid events, such as fast inactivation, that take place over milliseconds. Slow recovery of a refractory neuron is due to another process, slow inactivation, which future results would demonstrate is clearly distinct from fast inactivation.

The detection of multiple inactivation time constants that revealed the existence of slow inactivation was not published until 1964 when Narahashi studied the time dependence of action potential restoration on membrane potential in lobster giant axons, noting different times needed for recovery of inactivation that depended on the magnitude of the depolarizing pulse (Narahashi 1964). Several years later, a study from Adelman and Palti and a series from Chandler and Meves identified time constants of Na^+ current inactivation in squid giant axons ranging from hundreds of milliseconds to hundreds of seconds (Adelman and Palti 1969; Chandler and Meves 1970a, b, c, d). The presence of multiple time constants required to describe slow

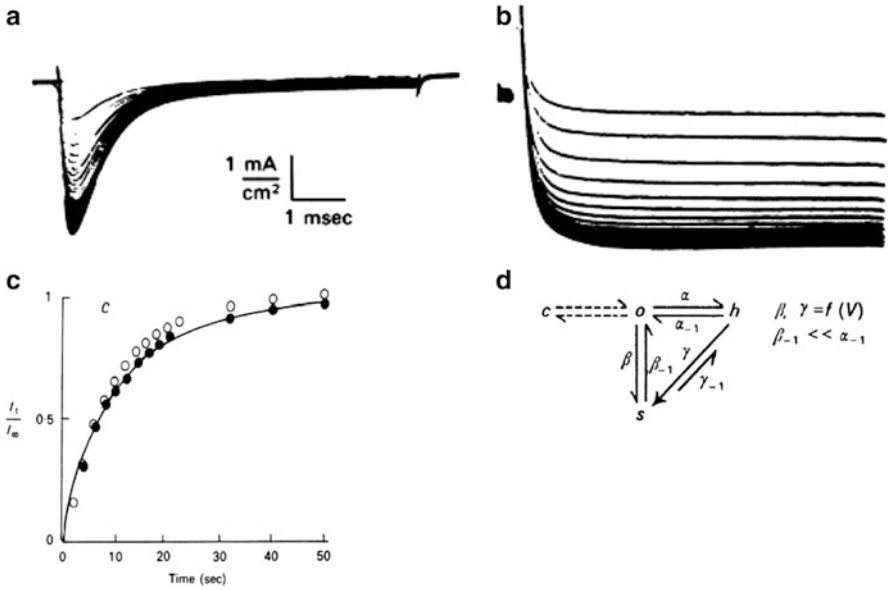

Fig. 1 Early recording of slow inactivation recovery. Measured by Bernardo Rudy in 1978 in *Loligo* squid giant axons maintained at 8°C, modified from Rudy (1978). (**a**) Axons were subjected to depolarization to −8 mV lasting several minutes. Subsequent 5 s pulses to −73 mV allowed the Na^+ current to recover from slow inactivation, while short test pulses to +20 mV were used to quantify availability. The first pulse has the smallest magnitude. (**b**) Same protocol as in panel **a**, but after treatment with pronase to remove fast inactivation, note lack of a rapid decay in the currents. Slow inactivation of the Na^+ conductance still took place, indicating that it is a distinct process. (**c**) Plot of recovery vs. time in seconds. Full recovery of the Na^+ conductance required maintaining negative potentials required 10's of seconds. Recovery with inactivation removed by pronase, *open circles*, was more rapid, having a time constant of 12.7 vs. 14.4 s (*filled circles*) for the untreated axon. (**d**) A putative model to account for the slow transitions. The ability of slow inactivation to take place in the absence and presence of fast inactivation, suggested a unique state (s) of the channel that could be entered when the channel was open (o) or fast inactivated (h)

inactivation, spread over several orders of magnitude, indicated an extraordinarily complex process, not easily described by simple, discrete state transitions.

Subsequently much of the early characterization of slow inactivation was accomplished by Bernardo Rudy, who advocated an important physiological role. The first of this series investigated the resistance of slow inactivation to pronase (Rudy 1978), a protease which had recently been used to show that an intracellular peptide must regulate fast inactivation (Armstrong et al. 1973; Rojas and Rudy 1976). Removal of fast inactivation not only left slow inactivation intact but also apparently facilitated the process, Fig. 1a–c. Thus, the ability of slow inactivation to take place even in the absence of fast inactivation showed that it was a distinct gating process, resulting in a putative model allowed slow inactivation to take place from either the open- or fast-inactivated state (Fig. 1d). Later, Rudy and others showed that slow inactivation of Na^+ channels, a process orders of magnitude

slower than fast inactivation, is responsible for the refractoriness of *Myxicola* giant axons (Rudy 1975, 1981; Schauf et al. 1976) after long depolarizations, indicating a physiological role for slow gating in regulating neuronal activity. In skeletal muscle, slow inactivation was studied by Ruff et al., who proposed that slow Na^+ channel inactivation mediates differences in the excitability of fast and slow twitch skeletal muscle fibers (Ruff et al. 1987, 1988).

In the 1980s, the first Na^+ channel was finally cloned (Tanabe et al. 1984) followed shortly thereafter by mammalian neuronal (Noda et al. 1986a), muscle (Trimmer et al. 1989), and cardiac isoforms (Gellens et al. 1992). The primary structure of the Na^+ channel, which could be formed by monomers, was identified as having four domains (DI–DIV), each with six transmembrane segments (S1–S6). The fourth segment (S4) in each domain carried multiple positively charged residues and was identified as the voltage sensor. Subsequently, methods were developed to express channels heterologously (Noda et al. 1986b), isolating the Na^+ channels from other channels in native cells and allowing systematic study of the structural basis of gating as well as differences between channel isoforms. The results from this new era are described in Sect. 3. However, it is important to first clarify, in the next section, how slow inactivation is quantified and what differences exist between the different channel isoforms.

2 Measurement and Characterization of Slow Inactivation

Several steps are required to accurately quantify slow inactivation in Na^+ channel expressing cells. First, the time course of recovery from fast inactivation must be measured so that it can be isolated and separated from slow inactivation. Typically Na^+ channels recover from fast inactivation after ~30 ms. So, if only fast inactivation is present, the current induced by a second depolarizing pulse after a 30 ms pulse to negative potentials will have the same magnitude as the current from the original pulse. However, if the initial depolarizing pulse is held for longer durations or repeated pulses are applied, the magnitude of the current during the following test pulses will be drastically reduced over time (Fig. 2a), indicating that channels have entered a slow-inactivated state. By applying pulses of different durations or by repeatedly measuring the ionic current after many pulses, the time course of the onset of slow inactivation can be assessed. The recovery kinetics can be measured in analogous fashion by varying the duration of a recovery pulse (Fig. 2b).

The magnitude of slow inactivation is spread over several orders of magnitude. Typically, slow inactivation refers to a process that occurs over seconds to minutes. Channel inactivation that occurs in time domains between that of fast inactivation (several ms) and slow inactivation is called intermediate inactivation and has been linked to the Na^+ channel C-terminus (Cormier et al. 2002; Tateyama et al. 2004; Mantegazza et al. 2001). Ultraslow inactivation occurs at scales longer than that of slow inactivation and requires on the order of 10's of minutes (Szendroedi et al. 2007; Sandtner et al. 2004; Hilber et al. 2002). Still, given the potential for overlap between different types of inactivation, their temperature dependence, and

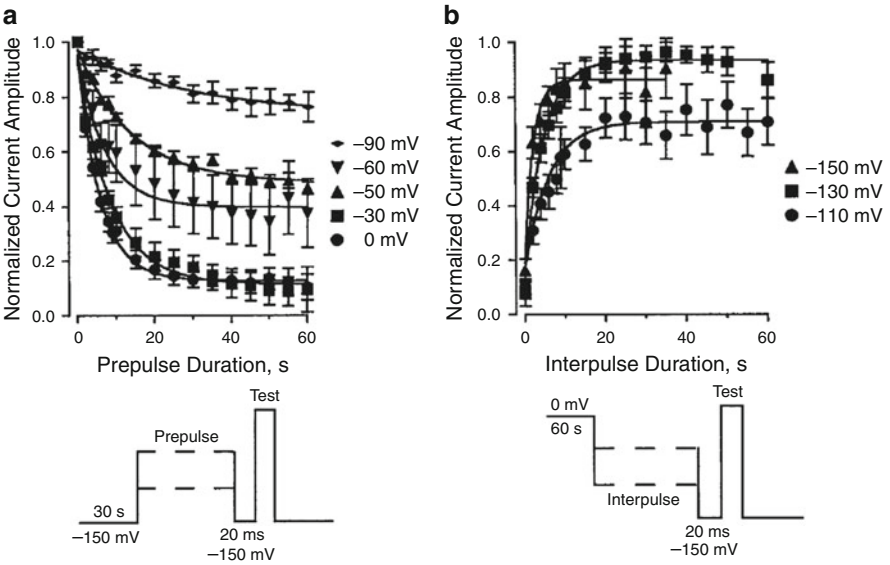

Fig. 2 Measuring the onset of and recovery from slow inactivation. Figures modified from Vilin and Ruben (2001). (**a**) Quantifying onset of inactivation over time at different potentials shown on the left. As in the protocol below, after holding at −150 mV for 30 s, pulses of varying duration were applied to different potentials to induce slow inactivation. After a short pulse of 20 ms to −150 mV that allowed recovery from fast inactivation, a third test pulse was applied to evaluate how much current remained. The peak current from this pulse is plotted above at different voltages and durations for the induction pulse. (**b**) A protocol to measure recovery from slow inactivation is shown below. A pulse to 0 mV for 30 s was used to induce slow inactivation. The interpulse to different potentials with varying durations allowed slow inactivation to recover. Since at some potentials fast inactivation was still present, a short 20 ms pulse to −150 mV was used to remove it. The final test pulse revealed the amount that the slow inactivation had recovered. As in panel **a**, the peak current during this pulse for different voltages and interpulse durations is plotted in the above figure

several orders of magnitude covered by the slow inactivation time domain, assessing which event is being observed from one study to the next can be confounding. Thus, difficulty in isolating a single gating motion associated with slow inactivation is one reason why studies have proven to be quite challenging.

The slow inactivation phenotype varies depending on the channel isoform. In terms of inactivation onset, it abolishes 90 % of Na^+ current after a 60 s pulse in the skeletal muscle isoform in comparison to 40 % in the cardiac isoform (Richmond et al. 1998). The time constant for inactivation onset is also ~6× faster, the voltage dependence steeper, and the recovery slower in the muscle isoform, compared to the cardiac version (O'Reilly et al. 1999). The neuronal isoform (NaV1.2) is similar to the muscle isoform, showing 90 % completeness after 100 s with time constants that resembles the muscle isoform (Toib et al. 1998).

3 Structural Basis of Slow Inactivation

Given the complexity of slow inactivation kinetics, it is unsurprising that many channel locales have been implicated in its generation. These include the channel pore, both intracellular and extracellular facing sides, the channel voltage-sensing domains, and the intracellular loops. Unraveling how all of these different channel motifs interact to cause slow inactivation is a difficult task and there is still much to be done to gain a better understanding of the protein motions that underlie slow Na^+ channel gating. We begin with the role of the channel pore.

3.1 The Role of the Na^+ Channel Pore in Slow Inactivation

Many lines of evidence point to involvement of the channel pore in mediating slow inactivation. Perhaps most directly, decreasing the concentration of Na^+ ions available to flow through the pore impairs slow inactivation on the seconds scale (Townsend and Horn 1997). Additionally, tetrodotoxin (TTX), which blocks the channel pore has been recently shown to inhibit slow inactivation in the time domains of seconds (Capes et al. 2012) and minutes (Silva and Goldstein 2013a). The ability of an extracellular pore blocker to inhibit slow inactivation is consistent with previously published mutations near the outer pore that have also been shown to modulate slow inactivation. These mutations tend to reside near the Na^+ selectivity filter such as DI mutations—W402C (Balser et al. 1996b) and W402A (Kambouris et al. 1998), DII—V787C (O'Reilly et al. 2001), DIII—F1236C (Ong et al. 2000), and DIV—V1583C (Vedantham and Cannon 2000) in the rat skeletal muscle isoform (Fig. 3a). Other residues that are involved with slow inactivation are found directly above the selectivity filter in a ring of four negative charges, one charge per domain, which is thought to draw positively charged Na^+ ions near to the filter. In these experiments, when channels were slow inactivated, double cysteine mutants were not effectively modified by redox catalyst Cu (II) (1,10-phenanthroline)$_3$, implying that slow inactivation renders the sites inaccessible (Xiong et al. 2003).

Additional residues near the outer pore were found by comparing differences between the cardiac and muscle isoforms. The first of these studies swapped entire domains and identified DI and DII as key (O'Reilly et al. 1999). Next, chimeras were created in which the loops between the S5 and S6 segments in each channel domain in the muscle channel were replaced with the cardiac version and conferred the cardiac channel phenotype, consistent with the above results (Vilin et al. 1999). Further study identified a single residue in the DII S5–S6 P-loop that could confer the cardiac phenotype in the muscle channel when replaced with the cardiac residue and conversely impart the muscle phenotype in the cardiac isoform when the muscle residue was transplanted (Vilin et al. 2001b).

The inner side of the pore has also been implicated in slow inactivation with several mutations that cause HyperPP and inhibit slow inactivation colocalized to this location (Fig. 3a). Several of these mutations are found in DII, particular in the

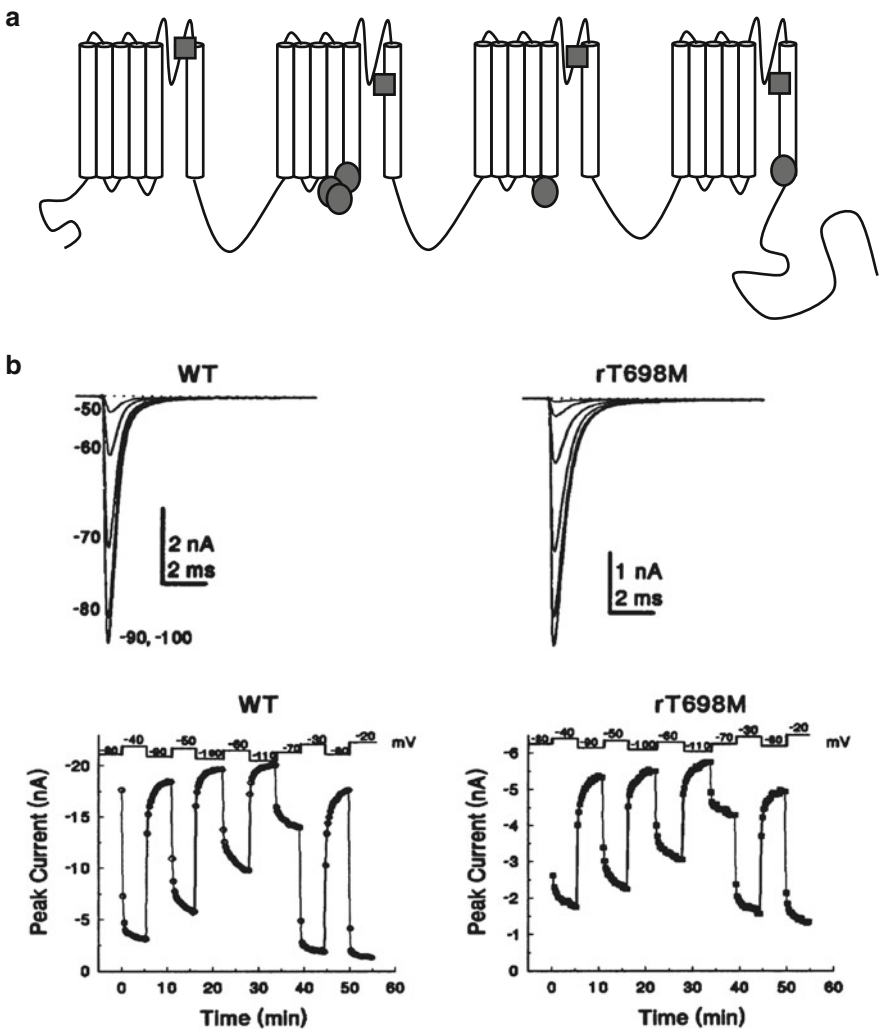

Fig. 3 Mutations proximal to the channel pore modulate slow inactivation. (**a**) Mutations found to affect slow inactivation near the extracellular facing pore are in DI, W402C (Balser et al. 1996b) and W402A (Kambouris et al. 1998); DII, V787C (O'Reilly et al. 2001); DIII, F1236C (Ong et al. 2000); and DIV, V1583C (Vedantham and Cannon 2000) (*Squares*). Several mutations associated with HyperPP, linked to a destabilization of the slow-inactivated state, are localized to the inner pore. In DII, L689I (Bendahhou et al. 2002), I693T (Hayward et al. 1999), and T704M (Cummins and Sigworth 1996; Brancati et al. 2003); DIII, P1158S (Webb and Cannon 2008); and DIV, M1592V (Hayward et al. 1999) (*Circles*). (**a**) An example of a HyperPP mutation, rT689M (homologous to human T704M) that does not significantly affect channel fast kinetics after a single pulse (*top*), but has substantial consequences for slow inactivation (*bottom*), which was measured in response to prolonged depolarization. Figure modified from Cummins and Sigworth (1996)

linker between the charged S4 and the pore-forming S5 segments. Biophysical characterization of these mutants shows insignificant to moderate consequences for the fast gating of the channel, while slow inactivation is measurably impaired (Bendahhou et al. 2002; Cummins and Sigworth 1996; Brancati et al. 2003; Webb and Cannon 2008; Hayward et al. 1999) (Fig. 3b).

3.2 A Link Between Fast Inactivation and Slow Inactivation

While the molecular basis of slow inactivation of sodium channels has remained difficult to pin down, fast inactivation is readily perturbed by intracellular modification of the channel. While early approaches employed pronase to cleave the intracellular sodium channel loops, the availability and identification of the IFM inactivation motif in the loop that connects DIII and DIV, the DIII–DIV linker, allowed researchers to directly target fast inactivation via site-directed mutagenesis without perturbing the rest of the channel (West et al. 1992). One of the first results showed that if IFM is changed to ICM, a construct that still inactivates the modification of the introduced cysteine by methane sulfanilides, which block fast inactivation, is relatively unaffected by slow inactivation (Vedantham and Cannon 1998).

As suggested by Bernardo Rudy after applying pronase to squid axons, slow inactivation is facilitated by the removal of fast inactivation in several Na^+ channel isoforms. Thus, Featherstone et al. showed a greater rate of entry into the slow-inactivated state and a more complete inactivation in the skeletal muscle isoform (Featherstone et al. 1996) when the IFM mutation was mutated to QQQ (Fig. 4a). Similarly, Richmond et al. found enhanced slow inactivation in the cardiac isoform (Richmond et al. 1998) with fast inactivation removed (Fig. 4b). The result in the cardiac isoform is particularly stunning because of the lack of inactivation with fast inactivation present in comparison to the skeletal muscle isoform. More recently, the acidic residues that are adjacent to the IFM motif, which also modulate fast inactivation, were found to interact with slow inactivation (McCollum et al. 2003). Neutralization of acidic residues on either side of the IFM motif altered the voltage dependence of slow inactivation as well as its kinetics.

3.3 Voltage Sensing and Slow Inactivation

Voltage sensing in Na^+ channels arises chiefly from outward displacement of the positively S4 voltage sensors in each domain by depolarization of the membrane potential. Given that slow inactivation is voltage dependent, it would not be surprising if were somehow linked to the voltage sensor motion. The first suggestion of this link came from early studies of the gating current by Bezanilla, Taylor, and Fernandez, which showed that, like the ionic current, it could inactivate. Precisely, after a long pulse to depolarized potentials, less gating current was observed after a test pulse that followed a short pulse to negative potentials (Bezanilla et al. 1982). A further correlation between the gating charge from a

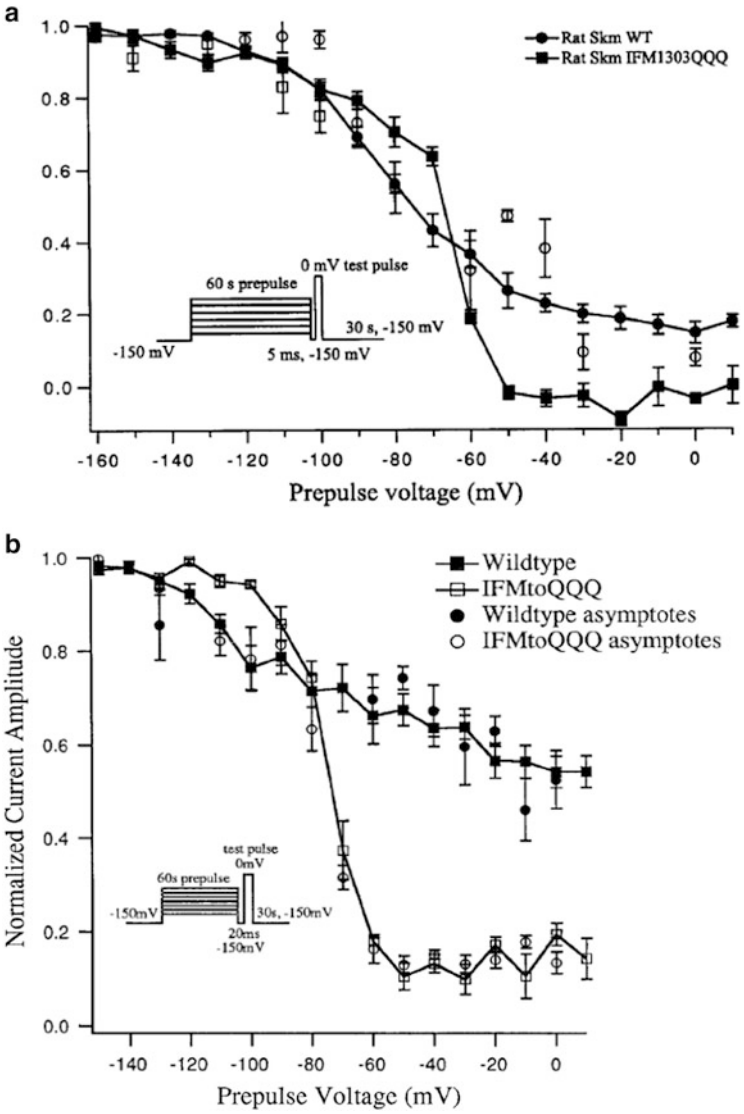

Fig. 4 Removal of fast inactivation potentiates slow inactivation. 60 s pulses to varying potentials are applied, followed by a short pulse to −150 mV and a test pulse as in Fig. 2. Mutations of the IFM motif to QQQ ablate fast inactivation. (**a**) Removing fast inactivation in the skeletal muscle (Skm) isoform allows slow inactivation to occur with a steeper voltage dependence and to a higher degree of completeness. Figure modified from Featherstone et al. (1996). (**b**) The cardiac isoform, which is normally resistant to slow inactivation, shows nearly complete inactivation as well with fast inactivation. Figure modified from Richmond et al. (1998)

depolarizing pulse and slow inactivation was shown by Ruben et al. (1992). Surprisingly, the off-gating charge that resulted from a return to negative potential was not correlated. With the advent of routine site-directed mutagenesis, Kontis and Goldin (1997) neutralized charges on the S4 segments of each of the four Na^+ channel domains to probe the dependence of steady-state inactivation on the voltage sensor. Each sensor contained at least one charge that significantly shifted the voltage dependence of steady-state inactivation.

The recent development of voltage clamp fluorometry has provided a means to assess the structural basis of Na^+ channel gating (Cha et al. 1999; Chanda and Bezanilla 2002). In this method, a fluorophore is conjugated to cysteines that are placed in the extracellular S3–S4 linker in different constructs corresponding to each of the four domains (DI–DIV). Then, when depolarizing pulses are applied, fluorescence changes directly reflect the position of the sensor. Silva and Goldstein applied voltage clamp fluorometry to evaluate which sensors undergo slow immobilization and whether their kinetics correlate to slow inactivation (Silva and Goldstein 2013a) (Fig. 5a). Initial recordings showed that all four sensors are immobilized by long pulses at depolarized potentials (Fig. 5b). However, kinetics of fluorescence immobilization, which should correlate to the inactivation of the gating current, was significantly different. However, the gating current was recorded in the presence of TTX, which may have altered slow inactivation. Additional fluorescence recording with TTX showed that the immobilization of sensors in domains I and II was impaired by the toxin, as was slow inactivation. Recent work by Capes et al. (2012) also showed interaction between block by TTX and the DIV sensor. Thus, the extracellular pore, which was previously shown to interact with the slow-inactivated state, also communicates with the sensors in DI, DII, and DIV.

The identification of disease-linked mutations that impairs slow inactivation suggested a means to perturb both the voltage sensor movements and slow inactivation to test whether there could be a correlation (Silva and Goldstein 2013b). In response, the L689I mutation, which resides on the S4–S5 linker in DII was introduced into each fluorescence construct to evaluate its effect on voltage sensor immobilization. The greatest effects of L689I were observed in DII immobilization, which was nearly abolished, with lesser consequences seen in the immobilization of the DIII and DIV sensors (Fig. 5c). Close examination of the L689I slow inactivation kinetics shows that inactivation that takes place in the 10 s time domain is most affected, which would imply a close link between DII sensor immobilization and this component of slow inactivation.

3.4 Modulation of Slow Inactivation by the β_1 Subunit

In native cells, sodium channels are formed by the co-assembly of α and β subunits, which modify expression and channel gating (Isom et al. 1992). In muscle and cardiac Na^+ channels, the β_1 subunit is present, at least to some extent in native cells (Fozzard and Hanck 1996). Based on frog oocyte experiments, a role for the β_1

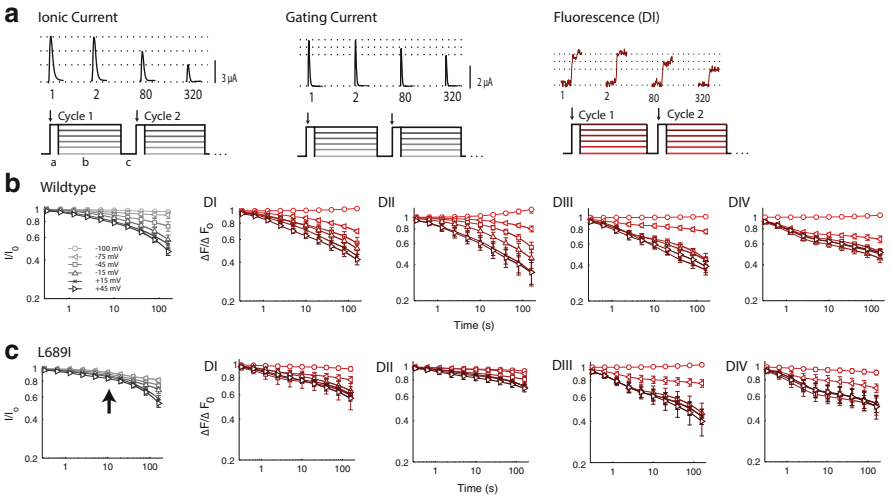

Fig. 5 Potential role for the voltage sensors in slow inactivation. Previously developed constructs used to fluorescently track the position of the S4 segment in each Na^+ channel domain (DI–DIV) were labeled and fluorescence changes were tracked simultaneously with changes in ionic current. Adapted from references Silva and Goldstein (2013a, b) and Cummins and Sigworth (1996). (**a**) *Left*: Applying repetitive pulses to induce slow inactivation of the ionic current, which can be probed by repetitions of a triple pulse protocol from a holding potential of −100 mV: a 5 ms test pulse to +45 mV is used to measure peak current (phase **a**); then slow inactivation is induced by a 500 ms pulse at −100, −75, −45, −15, 15, or 45 mV (phase **b**); and a 30 ms pulse at −100 mV employed (phase **c**) to allow for recovery from fast inactivation before the next test pulse. Sample traces are shown for cycle 1, 2, 80, and 320 and demonstrate progressive decrease in peak current at +45 mV. *Center*: The same protocol can also be used to assess slow kinetics of gating currents in the presence of TTX. *Right*: Tracking the voltage sensor immobilization from a construct with the DI-S4 labeled. (**b**) Voltage dependence of ionic current slow inactivation is shown at the left. On the right fluorescence showing that the S4 segments from all four domains undergo immobilization over a similar voltage range and time domain. (**c**) Introducing the HyperPP mutation L689I caused a loss in a slow component of inactivation that takes place over 10's of seconds (*left*, *arrow*). Immobilization of the sensors in DI and DII was dramatically reduced, with the sensor in DII most impacted. The immobilization of the sensors in DIII and DIV was much less affected

subunit in regulating fast inactivation was assumed for muscle channels (Ji et al. 1994). However, more recent experiments in mammalian cells have shown that fast Na^+ channel kinetics are not dramatically affected, while slow inactivation remains intact (Webb et al. 2009). Quantitatively, the muscle isoform expressed without the β_1 subunit inactivates to 60 % completion, in comparison to when the β_1 subunit is present it inactivates to 90 %. The cardiac isoform is unaffected and consistently shows 40 % inactivation (Vilin et al. 1999).

Conclusions

After many decades of study, myriad questions still remain regarding the molecular underpinnings of slow inactivation. First among these is in regard to the molecular underpinnings. As listed above, many single-point mutations near

the outer channel pore have been found to impair slow inactivation, suggesting strong similarity to C-type inactivation in K^+ channels, which has been linked to pore collapse (Choi et al. 1991; Hoshi et al. 1991; Kiss et al. 1999; Kiss and Korn 1998). Recently, crystal structures of the C-type-inactivated state have provided convincing evidence of its molecular mechanism (Cuello et al. 2010) and within the past 2 years several tetrameric bacterial Na^+ channel structures have been published (Zhang et al. 2012; Payandeh et al. 2011, 2012; McCusker et al. 2012). As it becomes tractable to obtain crystallography data from four-domain monomeric Na^+ channels, we can expect questions regarding the slow-inactivated state of the Na^+ channel to be better resolved.

Even with many mutations identified in the extracellular pore that affect slow inactivation, colocalization of many HyperPP mutations to the inner pore, interaction with the intracellular fast inactivation gate and voltage sensors, suggests that C-type inactivation does fully encapsulate slow inactivation of Na^+ channels. Some argue that the stretching of slow inactivation over many time domains as well as the ability of mutations over the span of the entire channel to perturb the process, make identification of discrete structurally based transitions futile effort. Instead they propose that slow inactivation should thought of as a gating event that is composed of infinitely many small transitions described not as the combination of many single exponentials, but by the more generalized stretch exponential in which discrete structural states of the channel are not defined (Marom 2010; Soudry et al. 2010).

Others may be tempted to speculate as to the structural basis of the different components of slow inactivation based on the time domains over which many interactions with the process occur. Over the fastest domains described by slow inactivation (~1 s), DIV has arisen several times, first in the experiments of Vedantham and Cannon who observed that V1583C modification by methane sulfonimides takes place over milliseconds to seconds (Vedantham and Cannon 2000), then by Mitrovic et al. (2000), who examined slow inactivation over the 5 s time domain, and finally by Silva and Goldstein who showed that DIV immobilization is fastest of all the domains (Silva and Goldstein 2013a) (Fig. 5b).

Over the 10 s time domain, two HyperPP mutations that are localized to DII, L689I (Silva and Goldstein 2013b) (Fig. 5c), and T704M (Melamed-Frank and Marom 1999) remove slow inactivation. Furthermore, skeletal muscle inactivation that takes place over this time domain is impaired by replacing a residue in the DII P-loop with the cardiac residue (Vilin et al. 2001b) or by swapping the entire DI or DII domains (O'Reilly et al. 1999). Finally, limited data observing TTX interaction with slow inactivation shows an inhibition of the 10 s time domain and inhibition of immobilization of DI and DII S4's (Silva and Goldstein 2013a), which is consistent with experiments that localized its binding site to DI and DII (Fozzard and Lipkind 2010).

The longest slow inactivation time domain was not affected by L689I or T704M and persists in the cardiac Na^+ channel. However, this process is enhanced by the removal of fast inactivation, which has been shown to interact

with the fast inactivation gate in the DIII S4–S5 linker in both the cardiac and skeletal muscle isoforms (Goldin 2003; Smith and Goldin 1997). Furthermore, sensor immobilization in DIII, observed via fluorescence, contained a significant slow component (Fig. 5b), suggesting a contribution to this slowest component.

In sum, a compelling working hypothesis arises for those that insist on assigning a structural basis for the different components of slow inactivation. In this hypothesis, DIV accounts for the fastest component (1–5 s), DI and DII are responsible for the intermediate component 10–30 s, and DIII and fast inactivation are linked to the slowest component in the time domain of minutes.

References

Adelman WJ Jr, Palti Y (1969) The effects of external potassium and long duration voltage conditioning on the amplitude of sodium currents in the giant axon of the squid, Loligo pealei. J Gen Physiol 54(5):589–606

Armstrong CM, Bezanilla F, Rojas E (1973) Destruction of sodium conductance inactivation in squid axons perfused with pronase. J Gen Physiol 62(4):375–391

Balser JR et al (1996a) Local anesthetics as effectors of allosteric gating. Lidocaine effects on inactivation-deficient rat skeletal muscle Na channels. J Clin Invest 98(12):2874–2886

Balser JR et al (1996b) External pore residue mediates slow inactivation in mu 1 rat skeletal muscle sodium channels. J Physiol 494(Pt 2):431–442

Bendahhou S et al (2002) Impairment of slow inactivation as a common mechanism for periodic paralysis in DIIS4-S5. Neurology 58(8):1266–1272

Bezanilla F, Taylor RE, Fernandez JM (1982) Distribution and kinetics of membrane dielectric polarization. 1. Long-term inactivation of gating currents. J Gen Physiol 79(1):21–40

Brancati F et al (2003) Severe infantile hyperkalaemic periodic paralysis and paramyotonia congenita: broadening the clinical spectrum associated with the T704M mutation in SCN4A. J Neurol Neurosurg Psychiatry 74(9):1339–1341

Capes DL et al (2012) Gating transitions in the selectivity filter region of a sodium channel are coupled to the domain IV voltage sensor. Proc Natl Acad Sci U S A 109(7):2648–2653

Cha A et al (1999) Voltage sensors in domains III and IV, but not I and II, are immobilized by Na + channel fast inactivation. Neuron 22(1):73–87

Chanda B, Bezanilla F (2002) Tracking voltage-dependent conformational changes in skeletal muscle sodium channel during activation. J Gen Physiol 120(5):629–645

Chandler WK, Meves H (1970a) Slow changes in membrane permeability and long-lasting action potentials in axons perfused with fluoride solutions. J Physiol 211(3):707–728

Chandler WK, Meves H (1970b) Rate constants associated with changes in sodium conductance in axons perfused with sodium fluoride. J Physiol 211(3):679–705

Chandler WK, Meves H (1970c) Evidence for two types of sodium conductance in axons perfused with sodium fluoride solution. J Physiol 211(3):653–678

Chandler WK, Meves H (1970d) Sodium and potassium currents in squid axons perfused with fluoride solutions. J Physiol 211(3):623–652

Choi KL, Aldrich RW, Yellen G (1991) Tetraethylammonium blockade distinguishes two inactivation mechanisms in voltage-activated K + channels. Proc Natl Acad Sci U S A 88(12):5092–5095

Cormier JW et al (2002) Secondary structure of the human cardiac Na + channel C terminus: evidence for a role of helical structures in modulation of channel inactivation. J Biol Chem 277 (11):9233–9241

Cuello LG et al (2010) Structural mechanism of C-type inactivation in K(+) channels. Nature 466 (7303):203–208

Cummins TR, Sigworth FJ (1996) Impaired slow inactivation in mutant sodium channels. Biophys J 71(1):227–236
Featherstone DE, Richmond JE, Ruben PC (1996) Interaction between fast and slow inactivation in Skm1 sodium channels. Biophys J 71(6):3098–3109
Fozzard HA, Hanck DA (1996) Structure and function of voltage-dependent sodium channels: comparison of brain II and cardiac isoforms. Physiol Rev 76(3):887–926
Fozzard HA, Lipkind GM (2010) The tetrodotoxin binding site is within the outer vestibule of the sodium channel. Mar Drugs 8(2):219–234
Gellens ME et al (1992) Primary structure and functional expression of the human cardiac tetrodotoxin-insensitive voltage-dependent sodium channel. Proc Natl Acad Sci U S A 89 (2):554–558
George AL Jr (2005) Inherited disorders of voltage-gated sodium channels. J Clin Invest 115 (8):1990–1999
Goldin AL (2003) Mechanisms of sodium channel inactivation. Curr Opin Neurobiol 13(3):284–290
Hayward LJ, Sandoval GM, Cannon SC (1999) Defective slow inactivation of sodium channels contributes to familial periodic paralysis. Neurology 52(7):1447–1453
Hilber K et al (2002) Interaction between fast and ultra-slow inactivation in the voltage-gated sodium channel. Does the inactivation gate stabilize the channel structure? J Biol Chem 277 (40):37105–37115
Hodgkin AL, Huxley AF (1952a) A quantitative description of membrane current and its application to conduction and excitation in nerve. J Physiol 117(4):500–544
Hodgkin AL, Huxley AF (1952b) The dual effect of membrane potential on sodium conductance in the giant axon of Loligo. J Physiol 116(4):497–506
Hoshi T, Zagotta WN, Aldrich RW (1991) Two types of inactivation in Shaker K + channels: effects of alterations in the carboxy-terminal region. Neuron 7(4):547–556
Isom LL et al (1992) Primary structure and functional expression of the beta 1 subunit of the rat brain sodium channel. Science 256(5058):839–842
Ji S et al (1994) Voltage-dependent regulation of modal gating in the rat SkM1 sodium channel expressed in Xenopus oocytes. J Gen Physiol 104(4):625–643
Jurkat-Rott K, Lehmann-Horn F (2006) Paroxysmal muscle weakness: the familial periodic paralyses. J Neurol 253(11):1391–1398
Jurkat-Rott K et al (2009) K + -dependent paradoxical membrane depolarization and Na + overload, major and reversible contributors to weakness by ion channel leaks. Proc Natl Acad Sci U S A 106(10):4036–4041
Kambouris NG et al (1998) Mechanistic link between lidocaine block and inactivation probed by outer pore mutations in the rat micro1 skeletal muscle sodium channel. J Physiol 512 (Pt 3):693–705
Kiss L, Korn SJ (1998) Modulation of C-type inactivation by K + at the potassium channel selectivity filter. Biophys J 74(4):1840–1849
Kiss L, LoTurco J, Korn SJ (1999) Contribution of the selectivity filter to inactivation in potassium channels. Biophys J 76(1 Pt 1):253–263
Kontis KJ, Goldin AL (1997) Sodium channel inactivation is altered by substitution of voltage sensor positive charges. J Gen Physiol 110(4):403–413
Lengele JP, Belge H, Devuyst O (2008) Periodic paralyses: when channels go wrong. Nephrol Dial Transplant 23(4):1098–1101
Mantegazza M et al (2001) Role of the C-terminal domain in inactivation of brain and cardiac sodium channels. Proc Natl Acad Sci U S A 98(26):15348–15353
Marom S (2010) Neural timescales or lack thereof. Prog Neurobiol 90(1):16–28
McCollum IJ et al (2003) Negatively charged residues adjacent to IFM motif in the DIII-DIV linker of hNa(V)1.4 differentially affect slow inactivation. FEBS Lett 552(2–3):163–169
McCusker EC et al (2012) Structure of a bacterial voltage-gated sodium channel pore reveals mechanisms of opening and closing. Nat Commun 3:1102

Melamed-Frank M, Marom S (1999) A global defect in scaling relationship between electrical activity and availability of muscle sodium channels in hyperkalemic periodic paralysis. Pflugers Arch 438(2):213–217
Mitrovic N, George AL Jr, Horn R (2000) Role of domain 4 in sodium channel slow inactivation. J Gen Physiol 115(6):707–718
Narahashi T (1964) Restoration of action potential by anodal polarization in lobster giant axons. J Cell Physiol 64:73–96
Noda M et al (1986a) Existence of distinct sodium channel messenger RNAs in rat brain. Nature 320(6058):188–192
Noda M et al (1986b) Expression of functional sodium channels from cloned cDNA. Nature 322 (6082):826–828
Ong BH, Tomaselli GF, Balser JR (2000) A structural rearrangement in the sodium channel pore linked to slow inactivation and use dependence. J Gen Physiol 116(5):653–662
O'Reilly JP et al (1999) Comparison of slow inactivation in human heart and rat skeletal muscle Na + channel chimaeras. J Physiol 515(Pt 1):61–73
O'Reilly JP, Wang SY, Wang GK (2001) Residue-specific effects on slow inactivation at V787 in D2-S6 of Na(v)1.4 sodium channels. Biophys J 81(4):2100–2111
Payandeh J et al (2011) The crystal structure of a voltage-gated sodium channel. Nature 475 (7356):353–358
Payandeh J et al (2012) Crystal structure of a voltage-gated sodium channel in two potentially inactivated states. Nature 486(7401):135–139
Richmond JE et al (1998) Slow inactivation in human cardiac sodium channels. Biophys J 74 (6):2945–2952
Rojas E, Rudy B (1976) Destruction of the sodium conductance inactivation by a specific protease in perfused nerve fibres from Loligo. J Physiol 262(2):501–531
Ruben PC, Starkus JG, Rayner MD (1992) Steady-state availability of sodium channels. Interactions between activation and slow inactivation. Biophys J 61(4):941–955
Rudy B (1975) Proceedings: slow recovery of the inactivation of sodium conductance in myxicola giant axons. J Physiol 249(1):22P–24P
Rudy B (1978) Slow inactivation of the sodium conductance in squid giant axons. Pronase resistance J Physiol 283:1–21
Rudy B (1981) Inactivation in myxicola giant axons responsible for slow and accumulative adaptation phenomena. J Physiol 312:531–549
Ruff RL, Simoncini L, Stuhmer W (1987) Comparison between slow sodium channel inactivation in rat slow- and fast-twitch muscle. J Physiol 383:339–348
Ruff RL, Simoncini L, Stuhmer W (1988) Slow sodium channel inactivation in mammalian muscle: a possible role in regulating excitability. Muscle Nerve 11(5):502–510
Sandtner W et al (2004) Lidocaine: a foot in the door of the inner vestibule prevents ultra-slow inactivation of a voltage-gated sodium channel. Mol Pharmacol 66(3):648–657
Schauf CL (1987) Zonisamide enhances slow sodium inactivation in Myxicola. Brain Res 413 (1):185–188
Schauf CL, Pencek TL, Davis FA (1976) Slow sodium inactivation in Myxicola axons. Evidence for a second inactive state. Biophys J 16(7):771–778
Shaw RM, Rudy Y (1997) Ionic mechanisms of propagation in cardiac tissue. Roles of the sodium and L-type calcium currents during reduced excitability and decreased gap junction coupling. Circ Res 81(5):727–741
Sheets MF et al (2010) Sodium channel molecular conformations and antiarrhythmic drug affinity. Trends Cardiovasc Med 20(1):16–21
Silva JR, Goldstein SA (2013a) Voltage-sensor movements describe slow inactivation of voltage-gated sodium channels I: wild-type skeletal muscle Na(V)1.4. J Gen Physiol 141(3):309–321
Silva JR, Goldstein SA (2013b) Voltage-sensor movements describe slow inactivation of voltage-gated sodium channels II: a periodic paralysis mutation in Na(V)1.4 (L689I). J Gen Physiol 141(3):323–334

Smith MR, Goldin AL (1997) Interaction between the sodium channel inactivation linker and domain III S4-S5. Biophys J 73(4):1885–1895
Song W et al (2011) Analysis of the action of lidocaine on insect sodium channels. Insect Biochem Mol Biol 41(1):36–41
Soudry D, Meir R (2010) History-dependent dynamics in a generic model of ion channels—an analytic study. Front Comput Neurosci 4. pii: 3. doi:10.3389/fncom.2010.00003. http://www.ncbi.nlm.nih.gov/pubmed/20725633
Szendroedi J et al (2007) Speeding the recovery from ultraslow inactivation of voltage-gated Na + channels by metal ion binding to the selectivity filter: a foot-on-the-door? Biophys J 93 (12):4209–4224
Tanabe T et al (1984) Primary structure of beta subunit precursor of calf muscle acetylcholine receptor deduced from cDNA sequence. Eur J Biochem 144(1):11–17
Tateyama M et al (2004) Structural effects of an LQT-3 mutation on heart Na + channel gating. Biophys J 86(3):1843–1851
Toib A, Lyakhov V, Marom S (1998) Interaction between duration of activity and time course of recovery from slow inactivation in mammalian brain Na + channels. J Neurosci 18(5):1893–1903
Townsend C, Horn R (1997) Effect of alkali metal cations on slow inactivation of cardiac Na + channels. J Gen Physiol 110(1):23–33
Trimmer JS et al (1989) Primary structure and functional expression of a mammalian skeletal muscle sodium channel. Neuron 3(1):33–49
Vedantham V, Cannon SC (1998) Slow inactivation does not affect movement of the fast inactivation gate in voltage-gated Na + channels. J Gen Physiol 111(1):83–93
Vedantham V, Cannon SC (2000) Rapid and slow voltage-dependent conformational changes in segment IVS6 of voltage-gated Na(+) channels. Biophys J 78(6):2943–2958
Vilin YY, Ruben PC (2001) Slow inactivation in voltage-gated sodium channels: molecular substrates and contributions to channelopathies. Cell Biochem Biophys 35(2):171–190
Vilin YY et al (1999) Structural determinants of slow inactivation in human cardiac and skeletal muscle sodium channels. Biophys J 77(3):1384–1393
Vilin YY, Fujimoto E, Ruben PC (2001a) A novel mechanism associated with idiopathic ventricular fibrillation (IVF) mutations R1232W and T1620M in human cardiac sodium channels. Pflugers Arch 442(2):204–211
Vilin YY, Fujimoto E, Ruben PC (2001b) A single residue differentiates between human cardiac and skeletal muscle Na + channel slow inactivation. Biophys J 80(5):2221–2230
Webb J, Cannon SC (2008) Cold-induced defects of sodium channel gating in atypical periodic paralysis plus myotonia. Neurology 70(10):755–761
Webb J, Wu FF, Cannon SC (2009) Slow inactivation of the NaV1.4 sodium channel in mammalian cells is impeded by co-expression of the beta1 subunit. Pflugers Arch 457(6):1253–1263
Weidmann S (1955) The effect of the cardiac membrane potential on the rapid availability of the sodium-carrying system. J Physiol 127(1):213–224
West JW et al (1992) A cluster of hydrophobic amino acid residues required for fast Na(+)-channel inactivation. Proc Natl Acad Sci U S A 89(22):10910–10914
Woronzow DS (1924) Über die Einwirkung des konstanten Stromes auf den mit Wasser, Zuckerlösung, Alkali- und Erdalkalichloridlösungen behandelten Nerven. Pflüger's Archiv für die gesamte Physiologie des Menschen und der Tiere 203(1):300–318
Xiong W et al (2003) Molecular motions of the outer ring of charge of the sodium channel: do they couple to slow inactivation? J Gen Physiol 122(3):323–332
Zhang X et al (2012) Crystal structure of an orthologue of the NaChBac voltage-gated sodium channel. Nature 486(7401):130–134

The Role of Non-pore-Forming β Subunits in Physiology and Pathophysiology of Voltage-Gated Sodium Channels

Jeffrey D. Calhoun and Lori L. Isom

Contents

J.D. Calhoun • L.L. Isom (✉)
Department of Pharmacology, University of Michigan, Ann Arbor, MI, 48109-5632, USA

Medical School, University of Michigan, Ann Arbor, MI, 48109, USA
e-mail: lisom@umich.edu

P.C. Ruben (ed.), *Voltage Gated Sodium Channels*, Handbook of Experimental Pharmacology 221, DOI 10.1007/978-3-642-41588-3_4,

Abstract

Voltage-gated sodium channel β1 and β2 subunits were discovered as auxiliary proteins that co-purify with pore-forming α subunits in brain. The other family members, β1B, β3, and β4, were identified by homology and shown to modulate sodium current in heterologous systems. Work over the past 2 decades, however, has provided strong evidence that these proteins are not simply ancillary ion channel subunits, but are multifunctional signaling proteins in their own right, playing both conducting (channel modulatory) and nonconducting roles in cell signaling. Here, we discuss evidence that sodium channel β subunits not only regulate sodium channel function and localization but also modulate voltage-gated potassium channels. In their nonconducting roles, VGSC β subunits function as immunoglobulin superfamily cell adhesion molecules that modulate brain development by influencing cell proliferation and migration, axon outgrowth, axonal fasciculation, and neuronal pathfinding. Mutations in genes encoding β subunits are linked to paroxysmal diseases including epilepsy, cardiac arrhythmia, and sudden infant death syndrome. Finally, β subunits may be targets for the future development of novel therapeutics.

Keywords

α subunit • β subunit • Cell adhesion • Neuronal pathfinding • Channelopathy

1 Roles of VGSC β Subunits in Normal Physiology

1.1 Sodium Channel as Signaling Complex

Voltage-gated sodium channel (VGSC) β subunits are multifunctional molecules with conducting and nonconducting roles. β subunits have conducting roles as ion channel regulatory subunits that form a complex with the pore-forming VGSC α subunit. Within this protein complex, β subunits modulate α subunit gating and cell surface expression as well as provide links to other channelome components. VGSC β subunits are unique among ion channel accessory subunits in that they contain an extracellular immunoglobulin (Ig) domain, thus placing them in the Ig superfamily of cell adhesion molecules (CAMs). Emerging evidence suggests that during brain development, β subunits function in nonconducting roles as CAMs in addition to their channel modulatory roles and are subsequently involved in both extracellular and intracellular signaling pathways to help guide neuronal patterning. β subunits, especially those encoded by *SCN1B*, play important roles in cell proliferation and migration, axon outgrowth, pathfinding, and fasciculation in many central nervous system (CNS) areas including the hippocampus, cerebellum, and corticospinal tract. As multifunctional molecules involved in a diverse set of cellular processes and signaling cascades, β subunits are unique, dynamic proteins

that bridge the gap between two distinct signaling paradigms: electrical signaling via action potentials and cell adhesive signaling independent of ion conduction.

There is increasing evidence that β subunits are involved in numerous pathophysiological processes, including but not limited to, epilepsy, cardiac arrhythmia, neuropathic and inflammatory pain, neurodegeneration, and cancer. Mutations in the genes encoding β subunits are linked to human disease. Of particular note, mutation of *SCN1B*, encoding the β1/β1B subunits, is linked to diseases on the Generalized Epilepsy with Febrile Seizures plus (GEFS+) spectrum. Patients that inherit two loss-of-function mutant alleles of *SCN1B* have Dravet syndrome (DS), a severe pediatric epileptic encephalopathy, while patients who inherit one mutant allele of *SCN1B* present with the milder GEFS+ or may not exhibit seizures. Genetic deletion of *Scn1b* in mice recapitulates the hallmark phenotypes associated with DS, suggesting that these mice are a DS model. Given the diverse role of β subunits in normal physiology and in disease processes, β subunits are potential targets for novel therapeutics.

In this review, the conducting (canonical) and nonconducting (noncanonical) roles of VGSC β subunits will be discussed. The structure, expression profile, and regulation of the β subunits will be described. Finally, the impact of β subunits in pathophysiology and potential for novel therapeutics will be examined.

1.2 VGSCs Are αββ Heterotrimers

Heterotrimeric VGSC complexes initiate and propagate action potentials in most electrically excitable mammalian cells including neurons and cardiac myocytes. These heterotrimeric complexes are composed of a single pore-forming α subunit, a non-covalently associated β subunit (β1 or β3), and a covalently associated β subunit (β2 or β4) (Fig. 1). Two distinct gene families encode the 9 α subunit paralogs (*SCNXA*) and the 5 β subunits (*SCNXB*), respectively (Table 1). While there is significant evolutionary conservation and functional similarity within each gene family, each individual gene product is distinct in its properties and expression profile. For example, *SCN5A* is the predominant cardiac sodium channel, as its expression is enriched in cardiac tissue relative to other tissues; however, *SCN1A*, *SCN3A*, and *SCN8A*, commonly considered to be neuronal channels, are also expressed in heart, although at lower levels. Importantly, this diversity allows for different combinations of α and β subunits to be expressed at different levels within a specific cell type and even in specific subcellular domains within a cell, based on the cell's specific job within the overall tissue. An important distinguishing feature of VGSCs is whether they are sensitive or resistant to tetrodotoxin (TTX), a sodium channel-specific pore-blocking toxin from *Fugu* or pufferfish. Most VGSCs (Nav1.1, Nav1.2, Nav1.3, Nav1.4, Nav1.6, and Nav1.7) are blocked by low (nanomolar) concentrations of TTX and are referred to as TTX-sensitive channels (TTX-S). The remainder (Nav1.5, Nav1.8, and Nav1.9) require significantly higher concentrations of TTX (micromolar) for blockade and are referred to as TTX resistant (TTX-R).

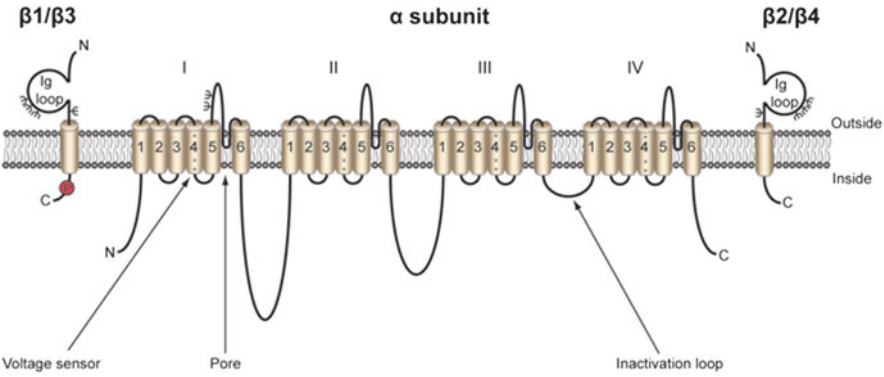

Fig. 1 Topology of the voltage-gated sodium channel α and β subunits. VGSCs contain a pore-forming α subunit consisting of four homologous domains of six transmembrane segments (1–6). Segment 4 contains the voltage sensor (Catterall 2000). VGSCs also contain one or more β subunits. β1, β2, β3, and β4 contain an extracellular immunoglobulin (Ig) loop, transmembrane domain, and an intracellular C-terminal domain (Isom et al. 1994). β1B also contains an Ig loop but lacks a transmembrane domain and is therefore a soluble, secreted protein (Patino et al. 2011). β1 contains a tyrosine phosphorylation site in its C-terminus (Malhotra et al. 2004). ψ denotes glycosylation sites. β1 and β3 are non-covalently linked to α, whereas β2 and β4 are covalently linked through disulfide bonds. Figure reproduced from (Brackenbury and Isom 2011)

Table 1 *SCNXA* genes encode VGSC α subunits and *SCNXB* genes encode VGSC β subunits

VGSC α subunits		VGSC β subunits	
Gene	Protein	Gene	Protein
SCN1A	Nav1.1	*SCN1B*	β1
SCN2A	Nav1.2	*SCN1B*	β1B
SCN3A	Nav1.3	*SCN2B*	β2
SCN4A	Nav1.4	*SCN3B*	β3
SCN5A	Nav1.5	*SCN4B*	β4
SCN8A	Nav1.6		
SCN9A	Nav1.7		
SCN10A	Nav1.8		
SCN11A	Nav1.9		

Given that voltage-dependent sodium current underlies the rising phase of the mammalian action potential, it comes as no surprise that perturbation of sodium channel function due to mutations results in human disease. Additionally, as discussed below, VGSC α subunits are pharmacologic targets for several interventions related to diseases including epilepsy, cardiac arrhythmia, and pain.

1.3 β Subunit Structure

Four genes in the mammalian genome encode five β subunit proteins (Isom et al. 1992, 1995a; Kazen-Gillespie et al. 2000; Morgan et al. 2000; Qin

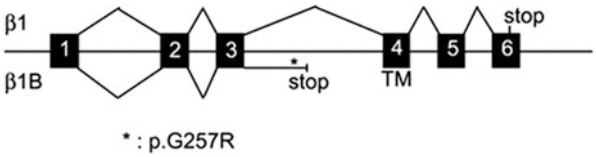

Fig. 2 The genomic structure of *SCN1B*. Exons 1–6 constitute β1. Extension of exon 3 into intron 3 generates the variant, β1B. The novel 3′ end of β1B does not contain a transmembrane domain (TM). The *asterisk* indicates the position of the G257R mutation. (This is not drawn to scale.) Figure reproduced from (Patino et al. 2011)

et al. 2003; Yu et al. 2003). *SCN1B* encodes β1 and the splice variant β1B, *SCN2B* encodes β2, *SCN3B* encodes β3, and *SCN4B* encodes β4. Four of the VGSC β subunits (β1–β4) are transmembrane proteins with type I topology containing an extracellular N-terminus, a single transmembrane segment, and an intracellular C-terminus (Isom 2001). The exception, β1B, contains the same Ig loop domain as in β1, but has an alternate C-terminal region that is the product of a retained intron (Fig. 2) that lacks a transmembrane domain, resulting in a secreted, soluble molecule (Patino et al. 2011; Kazen-Gillespie et al. 2000). Figure 3 provides an overview of the functional architecture of β1/β1B. Structural differences underlie whether a β subunit interacts covalently or non-covalently with pore-forming VGSC α subunits. β2 and β4 interact covalently with α subunits via a single disulfide bond (Messner and Catterall 1985; Chen et al. 2012; Buffington and Rasband 2013; Hartshorne et al. 1982; Hartshorne and Catterall 1984; Yu et al. 2003). Specifically, an N-terminal cysteine residue at position 26 in the extracellular domain of either β subunit forms a disulfide bond with one of multiple candidate cysteine residues in the S5–S6 loops of the α subunit. β1 and β3 associate non-covalently with VGSC α subunits (Messner and Catterall 1985; Hartshorne et al. 1982; Hartshorne and Catterall 1984). Structure–function analysis of β1 suggests the involvement of both N- and C-terminal residues in non-covalent association with α subunits (McCormick et al. 1998; Meadows et al. 2001; Spampanato et al. 2004). The C-terminal domains of β1 and β2 serve as links to the cytoskeleton via interactions with ankyrinG or ankyrinB (Malhotra et al. 2000, 2002). The β1 subunit-intracellular domain contains a single tyrosine residue that can be phosphorylated (Malhotra et al. 2002, 2004). Finally, β subunits are also targets for sequential proteolytic cleavage (Fig. 4), resulting in release of N-terminal and C-terminal fragments (Wong et al. 2005).

Analysis of genes homologous to mammalian sodium channels has yielded valuable information about the evolution of VGSC α and β subunits. NaChBac, an ancestral homolog of the mammalian VGSC α subunits, was discovered in bacteria (Ren et al. 2001). Subsequently, additional prokaryotic VGSCs were discovered, including NavAb, NavB1, NavBp, NavPz, NavRd, NavSHp, and NavSIP (Payandeh et al. 2011; Ren et al. 2001; Koishi et al. 2004; Ito et al. 2004; Irie et al. 2010). Interestingly, the genes coding for bacterial VGSCs generate proteins containing only 6 transmembrane domains rather than the 24 transmembrane domains found in

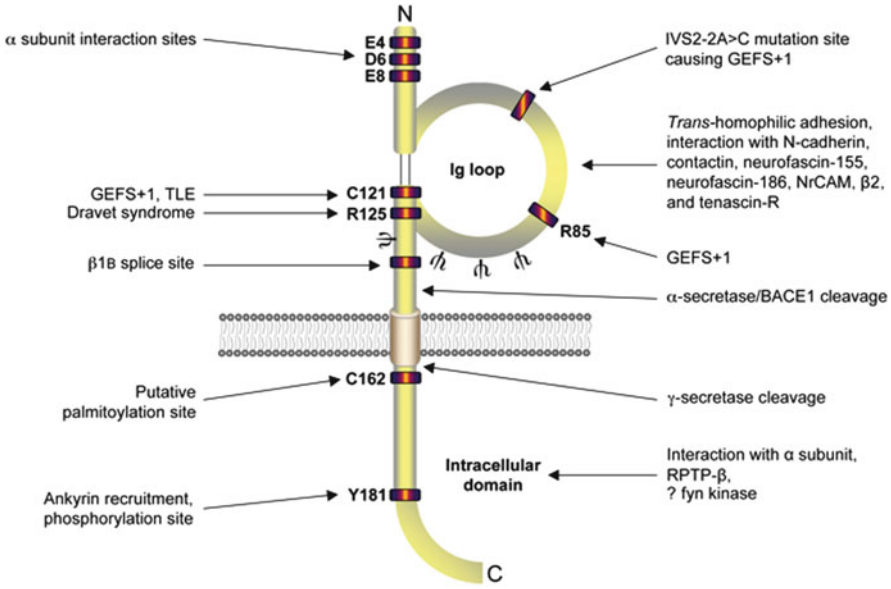

Fig. 3 Functional architecture of β1/β1B. β1 contains residues responsible for interaction with α subunit in its intracellular and extracellular domains (McCormick et al. 1998; Spampanato et al. 2004). Mutation sites responsible for causing epileptic encephalopathy, including Dravet syndrome, are located in the extracellular immunoglobulin loop (Meadows et al. 2002b; Wallace et al. 2002; Audenaert et al. 2003; Scheffer et al. 2007; Patino et al. 2009). Alternative splicing site for β1B (Kazen-Gillespie et al. 2000; Qin et al. 2003; Patino et al. 2011), putative palmitoylation site (McEwen et al. 2004), ankyrin interaction site (Malhotra et al. 2002), tyrosine phosphorylation site (Malhotra et al. 2004), N-glycosylation sites [ψ] (McCormick et al. 1998), α/β/γ-secretase cleavage sites (Wong et al. 2005), receptor protein tyrosine phosphatase β (RPTPβ) interaction (Ratcliffe et al. 2000), and putative fyn kinase interaction (Brackenbury et al. 2008) are also marked. Figure reproduced from (Brackenbury and Isom 2011)

mammalian VGSC α subunits (Charalambous and Wallace 2011). To form a sodium-conducting channel, bacterial sodium channel proteins must form homotetramers, similar to mammalian voltage-gated potassium channels. Mammalian *SCNXA* genes encode full channels (i.e., four tethered channel domains), suggesting the evolution of VGSC genes from encoding homotetrameric channels to encoding monomeric channels. Genes encoding monomeric (24 transmembrane domains) VGSC α subunits have been identified in a diverse set of species, including *Drosophila*, zebrafish, and mammals (Goldin 2002). Genes encoding VGSC β subunits are also present in zebrafish and mammals, but are notably absent in invertebrates (Isom et al. 1992; Fein et al. 2007; Chopra et al. 2007; Patino et al. 2009). This suggests that β subunits evolved later relative to pore-forming α subunits. Notably, sodium channels purified from the electroplax (electric organ) of the South American eel *Electrophorus electricus* contain only α subunits and not β subunits, which provides in vivo evidence that, similar to results obtained in *Xenopus* oocytes and transfected fibroblasts, α subunits are capable of functioning in the

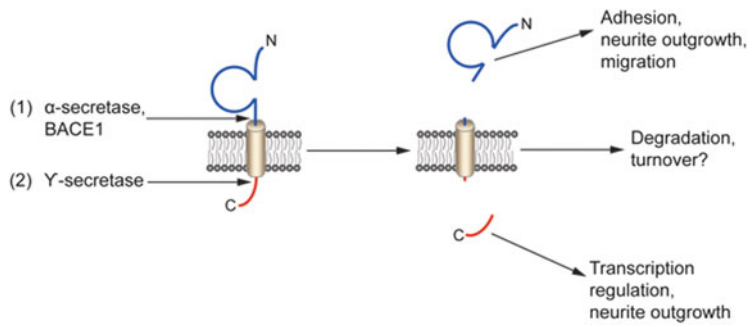

Fig. 4 Sequential cleavage of β subunits by (1) α-secretase and/or β-site amyloid precursor protein-cleaving enzyme (BACE1), followed by (2) γ-secretase yields soluble extracellular N-terminal domains and small intracellular C-terminal domains (Wong et al. 2005; Kim et al. 2005). The soluble immunoglobulin domains are responsible for regulation of adhesion and migration (Davis et al. 2004; Kim et al. 2005). β subunit intracellular domains regulate neurite outgrowth and are putative regulators of voltage-gated sodium channel gene transcription (Kim et al. 2007; Miyazaki et al. 2007). Figure reproduced from (Brackenbury and Isom 2008)

absence of β subunits (Miller et al. 1983; Noda et al. 1986; Goldin et al. 1986; Scheuer et al. 1990; Isom et al. 1995b). Interestingly, while the *Drosophila* genome lacks genes that are homologous to the mammalian VGSC β subunits, it does contain *tipE* which functions as an auxiliary subunit to the pore-forming VGSC α subunit *paralytic* (Li et al. 2011). However, the structure of mammalian VGSC β subunits is distinct from *tipE*.

1.4 VGSC β Subunits Are Ig-CAMs

Each of the mammalian VGSC β subunits contains a single, extracellular Ig domain that is structurally homologous to the V-set of the Ig superfamily of CAMs (Isom et al. 1995a). The Ig loop domain of β1 participates in both homophilic (with itself) and heterophilic (with other CAMs) associations (Malhotra et al. 2000; McEwen and Isom 2004) (Fig. 3). Importantly, the cell adhesive properties of β1 and β2 are independent of α subunit expression in vitro, suggesting that β subunits may have channel-independent functions in vivo. Sequence analysis of the extracellular domains of β1 and β3 reveals homology to the CAM myelin P_0 (Isom et al. 1995a; McCormick et al. 1998; Morgan et al. 2000), which has provided useful guidance for structure–function predictions. While other members of the family of voltage-gated ion channels contain accessory subunits that modulate channel kinetics, cell surface expression, and voltage dependence, only the VGSC β subunits contain extracellular Ig domains. β subunits, particularly β1, function as CAMs. β1 participates in homophilic cell adhesion resulting in cellular aggregation and ankyrin recruitment (Malhotra et al. 2000). Homophilic β1 cell adhesive interactions regulate neurite outgrowth in cerebellar granule neurons (CGNs) (Davis et al. 2004; Brackenbury et al. 2008). Additionally, β1 interacts heterophilically with the neuronal and glial CAMs contactin, VGSC β2,

N-cadherin, neurofascin-155 (NF155), neurofascin-186 (NF186), and NrCAM (McEwen and Isom 2004; Malhotra et al. 2004; Ratcliffe et al. 2001). β1 interactions with contactin and NF186 result in increased VGSC α subunit cell surface expression, suggesting a relationship between CAM function and channel modulation (Kazarinova-Noyes et al. 2001). β1 also participates in cell–matrix adhesion, binding to the extracellular matrix protein tenascin-R to influence cell migration (Xiao et al. 1999). β2, like β1, participates in homophilic interactions, in heterophilic interactions with β1, and in cell–matrix interactions with the extracellular matrix proteins tenascin-R and tenascin-C (Malhotra et al. 2000; Xiao et al. 1999; McEwen and Isom 2004; Srinivasan et al. 1998). While β3 contains an Ig domain, its capacity to engage in CAM interactions is unclear. Unlike β1 and β2, transfection of β3 cDNA into *Drosophila* S2 cells was not sufficient to induce cell aggregation, suggesting it does not engage in homophilic interactions (McEwen et al. 2009). Using soluble recombinant CAM-binding assays, it was observed that heterophilic interactions between β3 and other CAMs are more limited compared to β1 (McEwen and Isom 2004; Ratcliffe et al. 2001). In contrast to (McEwen et al. 2009), Yereddi et al. reported evidence for *trans* β3–β3 homophilic adhesion using coculture of cells expressing differentially epitope-tagged β3 constructs (Yereddi et al. 2013). Evidence for β4 as a CAM is limited, but it does appear to regulate filopodial morphology in transfected cells, suggesting CAM activity (Miyazaki et al. 2007). However, unlike experiments with β1, growth of cerebellar CGNs on β4-expressing monolayers had no effect on the level of CGN neurite outgrowth (Davis et al. 2004). Overall, these observations suggest that VGSC β subunits, particularly β1, are CAMs that provide a link between electrical excitability and extracellular adhesion and/or function independently of ion conduction.

1.5 Regulation of VGSC β Subunits

1.5.1 Glycosylation

Each β subunit Ig domain contains 3 or 4 N-linked glycosylation sites such that glycosylation accounts for approximately one-third of the total molecular weight of the protein (Messner and Catterall 1985; Isom et al. 1992). While the effects of glycosylation on sodium channel α and β subunits in vivo are not known, evidence from heterologous expression suggests these modifications may be important for α subunit cell surface expression and may influence the modulatory effects of β subunits on sodium current. In neuroblastoma cells expressing endogenous VGSCs, tunicamycin was used to study the channel under conditions of glycosylation inhibition (Waechter et al. 1983). Reduced glycosylation resulted in a reduction in the level of mature pore-forming α subunits detectable at the cell surface. The role of glycosylation in the interaction between α, β1, and β2 subunits has been studied in vitro using Chinese hamster ovary (CHO) cells that are either capable (Pro5) or incapable (Lec2) of sialylation, a type of glycosylation that is prevalent in VGSCs (Johnson et al. 2004; Johnson and Bennett 2006). Sialic acids are necessary for the modulation of α subunit (Nav1.2, Nav1.5, and Nav1.7) gating by β1

(Johnson et al. 2004). However, the impact of sialic acid is context dependent. β2 had sialic acid-dependent and -independent effects on α subunit gating, depending on which α subunit gene was co-expressed (Johnson and Bennett 2006). While the importance of glycosylation on the CAM function of β1 has not been tested directly, it is possible that glycosylation may be critical for cell adhesive interactions as well. Homophilic interactions of myelin P_0, a CAM which shares homology with β1 and β3 (Isom et al. 1995a), require glycosylation of the P_0 pair (Filbin and Tennekoon 1993). While more work is needed to fully understand the impact of glycosylation on VGSC α and β subunits, this posttranslational modification is a potential mechanism for fine-tuning of channel function.

1.5.2 Phosphorylation

The β1 C-terminal domain serves as a link between VGSC complexes and the cytoskeleton. This domain contains sites for posttranslational modification, including phosphorylation. An intracellular tyrosine residue (β1Y181) is phosphorylated in vitro and basal tyrosine phosphorylation of β1 is detectable in rat brain membranes (Malhotra et al. 2002) (Fig. 3). A β1 mutant that mimics phosphorylation (β1Y181E) shows normal β1-mediated cell–cell adhesion in a heterologous system, but disrupted β1-mediated ankyrin recruitment normally observed in response to adhesion (Malhotra et al. 2002). Similar to β1, β1Y181E increases cell surface α subunit expression in heterologous systems, but does not modulate sodium current in vitro (McEwen et al. 2004). Finally, tyrosine-phosphorylated β1 (pY-β1) has a distinct subcellular localization in cardiac myocytes. Nav1.5 and pY-β1 colocalize at intercalated disks, whereas non-phosphorylated β1 colocalizes with TTX-S channels at the T-tubules (Malhotra et al. 2004). These data suggest that phosphorylation of β1Y181 regulates its interaction with other proteins as well as its subcellular localization. Recently, a β1 peptide phosphorylated on intracellular threonine residues was reported in a screen for phosphorylated proteins in mouse synaptosomes (Trinidad et al. 2012). It will be interesting to determine the functional significance of this modification.

1.5.3 Proteolytic Processing

All four VGSC β subunits are targets for sequential proteolytic cleavage, at least in vitro (Wong et al. 2005) (Fig. 4). Similar to amyloid precursor protein (APP) (O'Brien and Wong 2011), β subunits are substrates for BACE1 (or β-secretase) and γ-secretase cleavage (Wong et al. 2005). A major gap in our understanding, however, is how β subunit cleavage is regulated in vivo. The initial β-secretase-mediated cleavage results in ectodomain shedding and the release of the Ig loop containing extracellular domain of the β subunit (Wong et al. 2005). Upon release from the cell surface, the β subunit extracellular domain may function as a soluble CAM similar to the proposed function of an engineered soluble β1 extracellular domain construct, β1Fc, or β1B (Patino et al. 2011; Davis et al. 2004; McEwen and Isom 2004). Following ectodomain shedding, subsequent γ-secretase cleavage results in the release of a β subunit-intracellular domain (ICD) into the cytoplasm (Wong et al. 2005). Interestingly, neurite outgrowth induced by homophilic β1 cell

adhesive interactions is abrogated by pharmacological inhibition of γ-secretase, suggesting proteolytic cleavage of the β1 intracellular domain may be critical in this signaling pathway (Brackenbury and Isom 2011). Studies of the role of the β2-ICD suggest that it traffics to the nucleus where it functions to increase *SCN1A* mRNA and subsequent Nav1.1 protein levels without increasing sodium current (Kim et al. 2007). The functions of the other β subunit ICD fragments have not yet been studied. However, *Scn1b* null mice have increased *Scn5a* expression in heart, raising the intriguing possibility that the β1-ICD may normally translocate to the nucleus and negatively regulate *Scn5a* transcription (Lopez-Santiago et al. 2007).

1.6 Expression of VGSC β Subunits

VGSC β subunits are expressed in excitable cells in the CNS, peripheral nervous system (PNS), skeletal muscle, and the heart (Isom et al. 1992, 1995a; Morgan et al. 2000; Yu et al. 2003; Maier et al. 2004; Lopez-Santiago et al. 2006, 2011; Brackenbury et al. 2010). While particular focus has been given to β subunit expressing neurons and myocytes, β subunits are also expressed in non-excitable cells such as astrocytes, radial glia, and Bergmann glia (Aronica et al. 2003; Oh and Waxman 1995; Fein et al. 2008; Davis et al. 2004). For example, *scn1bb*, a zebrafish ortholog of *SCN1B*, was found to be expressed in zrf-1 positive peripheral Schwann cells, supporting non-neuronal cells within olfactory pits and the inner ear, and myelinating glia surrounding the optic nerve (Fein et al. 2008). In contrast, *scn1ba*, another zebrafish ortholog of *SCN1B*, is mostly expressed in excitable cells including neurons and skeletal muscle and may be localized to nodes of Ranvier in optic nerve (Fein et al. 2007). Table 2 summarizes expression data for the β subunits in nervous system and muscle. β subunit expression is developmentally regulated (Sutkowski and Catterall 1990). In general, β1B and β3 are most abundant during fetal development and their expression decreases after birth (Kazen-Gillespie et al. 2000; Patino et al. 2011; Shah et al. 2001). Expression of β1 and β2 increase during the course of postnatal development and dominate during adult life (Kazen-Gillespie et al. 2000; Patino et al. 2011; Isom et al. 1995a). Exceptions to these general rules exist, such as the observation that β1B expression is retained in postnatal and adult heart in contrast to the reduced expression observed in the postnatal brain (Kazen-Gillespie et al. 2000). Additionally, β3 is expressed in adult dorsal root ganglion neurons (DRGs) (Takahashi et al. 2003). β4 is expressed in postnatal tissues, although the developmental time course for β4 expression has not been determined (Yu et al. 2003).

1.6.1 Subcellular Localization of β Subunits

Electrically excitable cells contain specialized substructures that are critical to normal physiology. Immunolocalization studies demonstrate that VGSC β subunits often cluster in specialized, subcellular domains. CNS and PNS neurons develop a specialized subcellular domain at the soma–axon junction called the axon initial segment (AIS). The AIS, devoted to action potential initiation, contains high

Table 2 Expression of VGSC β subunits in the CNS, PNS, and heart

Tissue—cell type	β1	β1B	β2	β3	β4
Central nervous system					
Hippocampal neurons	+ (a)		+ (l)	+ (b,o)	+ (l)
Cortical neurons		+ (j,k)	+ (l)	+ (b,o)	+ (l)
Basal ganglia	− (b)		+ (l)	+ (b,o)	+ (l)
Retinal ganglion cells	+ (c,d)		+ (d)		
Cerebellar Purkinje cells	+ (h)	+ (j,k)	+ (l)	+ (o)	+ (l)
Cerebellar granule neurons	+ (h)			− (b,o)	
Deep cerebellar nuclei		+ (j)	+ (l)		+ (l)
Ventral horn neurons		+ (j)	+ (l)		+ (l)
Astrocytes	+ (e,f)		+ (m)		
Bergmann glia	+ (i)	− (j)	− (i)	− (i)	+ (i)
Radial glia	+ (g)				
Peripheral nervous system					
Dorsal root ganglia	+ (q)	+ (k)	+ (l,n)	+ (p)	+ (l)
Peripheral nerves		+ (k)	+ (n)	+ (p)	
Schwann cells	+ (g)				
Heart					
Ventricular myocytes	+ (r)		+ (r)	+ (r)	+ (r)
Atrial myocytes	+ (s)		+ (s)	+ (s)	+ (s)

+ denotes expression of specific β subunit protein or mRNA was detected. − denotes that expression of specific β subunit protein or mRNA was not detected. (a) Chen et al. (2004), (b) Morgan et al. (2000), (c) Fein et al. (2007), (d) Kaplan et al. (2001), (e) Aronica et al. (2003), (f) Oh and Waxman (1995), (g) Fein et al. 2008, (h) Brackenbury et al. (2010), (i) Davis et al. (2004), (j) Kazen-Gillespie et al. (2000), (k) Qin et al. (2003), (l) Yu et al. (2003), (m) Oh et al. (1997), (n) Pertin et al. (2005), (o) Shah et al. (2001), (p) Casula et al. (2004), (q) Lopez-Santiago et al. (2006), (r) Maier et al. (2004), and (s) Kaufmann et al. (2013). This table is adapted from Patino and Isom (2010)

density molecular complexes ("channelomes") that include the cytoskeletal adaptor protein ankyrinG and VGSC α and β subunits, including Nav1.1, Nav1.2, or Nav1.6, and β1 (Rasband 2010). In some neurons the AIS can be subdivided into two structural units, the proximal segment nearest to the cell soma, and the distal end, which can differ in protein composition (Van Wart et al. 2007). Other CAMs, including the β1 cell adhesive-binding partners NrCAM and NF186, are enriched at the AIS (Rasband 2010). β1 may influence channel gating and channel cell surface expression in this domain. Additionally, β1 plays important roles in stabilizing the subcellular localization of Nav1.6 at the AIS, at least in the cerebellum (Brackenbury et al. 2010). Evidence for this comes from the observation that Nav1.6 localization to the AIS of cerebellar Purkinje neurons is reduced in *Scn1b* null mice (Brackenbury et al. 2010). β1 is predicted to function as a CAM at the AIS, although this possibility has not been tested. In addition to β1, β2 and β4 have been demonstrated to be localized to the AIS in specific neuronal subtypes (Chen et al. 2012; Buffington and Rasband 2013).

Myelinated CNS and PNS neurons contain gaps in the myelin sheath called nodes of Ranvier. These structures are critical for saltatory conduction, the mechanism responsible for rapid electrical communication across long distances (Poliak and Peles 2003). Nodes of Ranvier are composed of a high density of ion channels and CAMs arrayed in protein complexes in specific arrangements that differ somewhat between the CNS and PNS. For example, in the CNS, β1 and β2 subunits are found at optic nerve nodes of Ranvier in vivo (Patino et al. 2009; Kaplan et al. 2001). β4 localizes to a small subset of optic nerve nodes of Ranvier (Buffington and Rasband 2013). Likewise, in the PNS, β1 and β2 subunits localize to nodes of Ranvier in the sciatic nerve in vivo (Chen et al. 2002, 2004). β4 localizes to the majority of nodes of Ranvier in dorsal and ventral spinal cord roots (Buffington and Rasband 2013). What is the role of β subunits at the node of Ranvier? β subunits act as channel modulators and influence cell surface levels of pore-forming VGSC α subunits, which are present at high density in nodes (Chen et al. 2004, 2002). Based on the observation that *Scn1b* null mice have reduced numbers of nodes of Ranvier, dysmyelination, and perturbation of axo–glial cell–cell contacts, β subunits likely play cell adhesive roles in initiating and/or stabilizing nascent axo–glial cell–cell contacts and developing nodes of Ranvier (Chen et al. 2004).

Another important neuronal subcellular structure is the growth cone, which is located at the tip of developing neurites and is responsible for sensing signaling cues to direct the extension or retraction of the neurite (Lowery and Van Vactor 2009). Proteins involved in neurite outgrowth and pathfinding, including β1, localize to this domain (Brackenbury et al. 2010). Localization to the growth cone may be a requirement for the promotion of neurite outgrowth downstream of β1–β1 *trans*-homophilic adhesion (Brackenbury et al. 2008, 2010) (and see below).

β2 localizes to the AIS of mature neurons in culture and to nodes of Ranvier formed in myelinating cocultures as well as in vivo. Interestingly, AIS and nodal localization of β2 require an intact disulfide bond between α and β2 (Chen et al. 2012). A recent report suggests that, like β2, the homologous cysteine residue on β4 allows it to target to the AIS and to nodes (Buffington and Rasband 2013). These data suggest a model whereby the covalently associated VGSC β subunit (β2 or β4) is dependent on its intermolecular disulfide bond to the α subunit for targeting to neuronal subcellular domains. Further experimentation will be needed to study the influence of VGSC β subunits on the subcellular localization of α subunits; however, VGSC α subunits target normally to nodes in *Scn1b* and *Scn2b* null mice (Chen et al. 2002, 2004), suggesting either that b subunits may not be required for trafficking or that b subunits may function interchangeably in terms of nodal targeting.

Two functionally important subcellular structures in ventricular cardiomyocytes are the intercalated disks and transverse (T)-tubules. Intercalated disks form at cell–cell junctions and are critical for mechanical and electrical coupling (Delmar 2004). T-tubules electrically link the plasma membrane to the sarcoplasmic reticulum such that an action potential can efficiently lead to calcium-induced calcium release (Brette and Orchard 2003). β1 localizes to both intercalated disks and T-tubules in the ventricle (Dhar Malhotra et al. 2001; Malhotra et al. 2004; Maier et al. 2004) and to intercalated disks in the atrium (Kaufmann et al. 2013). There is some

disagreement in immunostaining datasets regarding the subcellular localization of β2 subunits. β2 has been reported to localize to the T-tubules or intercalated disks in ventricular myocytes (Dhar Malhotra et al. 2001; Maier et al. 2004) and to the T-tubules in atrial myocardium (Kaufmann et al. 2013). Experiments suggest that β3 localization is limited to T-tubules in ventricular myocytes (Maier et al. 2004) and to intercalated disks and cell surface puncta in atria (Kaufmann et al. 2013). β4 localizes primarily to the intercalated disk in ventricular myocytes (Maier et al. 2004) and to cell surface puncta in atrial myocardium (Kaufmann et al. 2013). What functional roles are the β subunits playing at these critical cardiac structures? β1 likely functions as a channel modulator at T-tubules, but may act solely as a CAM at the intercalated disk, based on the observation that b1 subunits at intercalated disks are tyrosine phosphorylated and heterologous data showing the absence of channel modulation by the tyrosine phosphomimetic construct β1Y181E (McEwen et al. 2004). In contrast, β1B, which regulates Nav1.5 currents in heterologous cells (Watanabe et al. 2008), may function as a channel modulator in this domain. The intercalated disk contains Nav1.5 α subunits as well as both homophilic and heterophilic adhesion partners, supporting the concept of a multifunctional VGSC complex at cardiomyocyte cell–cell junctions.

1.7 Canonical Role of VGSC β Subunits as Modulators of α Subunit Activity and Localization

1.7.1 Modulation of Sodium Current in Heterologous Systems

Soon after the cloning of the first cDNAs encoding VGSC α and β subunits, heterologous expression systems were used to investigate critical questions like channel subunit topology, electrophysiology, and structure–function relationships. While these systems clearly did not mimic what we now understand to be multiprotein sodium channel signaling complexes in native cells, the resulting data were critical to advancing our understanding of these important molecules. Early work expressing VGSC Nav1.2 α subunits in *Xenopus* oocytes demonstrated non-physiological sodium currents that activated and inactivated much more slowly than sodium currents recorded in neurons (Auld et al. 1988; Goldin et al. 1986; Joho et al. 1990). Co-injection of α subunit cRNA with low-molecular weight mRNA isolated from rat brain into oocytes resulted in increased sodium current density, altered voltage dependence of inactivation, and rapidly inactivating currents (Auld et al. 1988; Krafte et al. 1990). These results were more representative of physiological sodium currents and suggested that proteins encoded by the low-molecular weight brain mRNA fraction are important interacting proteins that modulate pore-forming α subunits. β1 and β2, which were known to associate with VGSC α subunits purified to theoretical homogeneity and predicted to be included in the low-molecular weight mRNA fraction, were strong candidates for the functional modulatory proteins in question (Hartshorne et al. 1982; Hartshorne and Catterall 1984). Indeed, after cloning the cDNAs encoding β1 and β2, we found that expression of mRNAs encoding these subunits recapitulated the effects of

low-molecular weight brain mRNA (Isom et al. 1992, 1995a). Specifically, when co-expressed with Nav1.2, β1 increased peak sodium current density, shifted the voltage dependence of inactivation to more negative membrane potentials, and accelerated the rate of inactivation (Isom et al. 1992). Co-expression of β2 and Nav1.2 in oocytes led to increased sodium current density and acceleration of the rate of channel inactivation compared to cells injected with Nav1.2 alone (Isom et al. 1995a). β2-expressing oocytes display increased cell surface area, likely due to an increase in fusion of intracellular vesicles with the plasma membrane and predicting its role as a chaperone protein (Isom et al. 1995a). Importantly, the effects of β1 and β2 on Nav1.2 in oocytes were synergistic: Nav1.2, β1, and β2 expressing oocytes have higher sodium current density than oocytes expressing α subunits alone, α and β1 subunits, or α and β2 subunits (Isom et al. 1995a). Unlike sodium currents from oocytes expressing only VGSC α subunits, currents from oocytes expressing α, β1, and β2 subunits were rapidly inactivating and closely representative of currents recorded from mature neurons (Isom et al. 1995a).

In addition to the oocyte system, much of the work done to characterize how β subunits affect pore-forming α subunits has utilized immortalized mammalian cell lines, with human embryonic kidney (HEK), Chinese hamster lung (CHL), and CHO cells being popular tools. Experiments co-expressing Nav1.2 and β1 in CHL cells confirmed the results in oocytes showing that β1 increases peak sodium current density and induces a negative shift in the voltage dependence of activation and inactivation, although the effects on activation and inactivation were more subtle (Isom et al. 1995b; Patino et al. 2009). In contrast to oocytes, β2 expression in mammalian cells requires co-expression of β1 to exert most of its modulatory effects on α subunits. When β2 is expressed with Nav1.2 α subunits in the absence of β1, sodium current is either unchanged or reduced (Kazarinova-Noyes et al. 2001; McEwen et al. 2004). However, when β2 is expressed with α in the presence of β1, β2 increases cell surface expression of α subunits beyond that observed in the presence of α + β1 (Kazarinova-Noyes et al. 2001).

Work in transfected cell lines identified β1B as a secreted CAM with only subtle effects on sodium current in cells expressing TTX-S channels like Nav1.2 or Nav1.3 (Kazen-Gillespie et al. 2000; Patino et al. 2011). Interestingly, Nav1.5 seems to sequester β1B at the cell surface in vitro and this interaction results in increased channel cell surface expression (Watanabe et al. 2008; Patino et al. 2011). These data suggest that β1B may function as a soluble CAM during brain development and as a sodium channel modulator and cell surface CAM in heart and other cell types that express Nav1.5.

Work investigating β3 and β4 suggests that these subunits, like β1 and β2, act as sodium channel modulators in heterologous systems. β3 induces a negative shift in the voltage dependence of inactivation of Nav1.3 (Meadows et al. 2002a). Modulation of Nav1.3 is likely relevant as neuronal expression of β3 is highest early in development when Nav1.3 expression is also abundant (Shah et al. 2001). β3 also shifts the voltage dependence of inactivation to more negative membrane potentials when co-expressed with Nav1.5 (Ko et al. 2005). When β4 was originally identified, its co-expression with Nav1.2 or Nav1.4 resulted in negative shifts in the voltage

dependence of activation (Yu et al. 2003). Studies on Nav1.1 suggested that, in addition to shifting the voltage dependence of activation to more negative membrane potentials, β4 increased the amount of non-inactivating current in vitro (Aman et al. 2009). β4 appears to affect Nav1.5 channels differently by inducing a negative shift in the voltage dependence of inactivation (Medeiros-Domingo et al. 2007). Finally, β4 modulates resurgent sodium current, as discussed below.

While oocytes and immortalized mammalian cell lines are obviously very different from neurons or myocytes and cannot replicate the situation in native cells, data collected from heterologous overexpression of VGSC α and β subunits made important predictions regarding the roles of β subunits in primary cells and tissues (Ragsdale 2008; Escayg and Goldin 2010). Cell background impacts the effects of β subunits in cell culture, along with the particular VGSC α subunit and specific channel-interacting proteins that are co-expressed (Dib-Hajj and Waxman 2010; Abriel and Kass 2005), accurately predicting that β subunits have context-dependent effects in vivo. Factors contributing to these differences include specific combinations of VGSC α and β subunits expressed, relative expression levels of each VGSC gene product, molecular composition of the VGSC macromolecular complex including non-channel-binding partners, subcellular distribution of VGSC complexes, and developmental maturity (e.g., immature vs. mature neurons).

1.7.2 Modulation of Sodium Current and Excitability In Vivo

The use of genetically engineered mouse models and viral-mediated gene transfer has allowed for the investigation of VGSC α and β subunit function in the whole animal, in acutely isolated primary cells, and in tissue slices. Observations using these methods suggest that β subunit modulation of sodium current in vivo, while cell type specific and more subtle in nature than observed in heterologous systems, is critical for normal electrical excitability in the nervous system and heart.

Sodium current and action potential recordings from *Scn1b* null mice have provided important insights into the role of β1/β1B in modulating electrical excitability in vivo. Recordings from acutely isolated hippocampal pyramidal or bipolar neuronal soma found no measurable differences in sodium current properties in P10-18 *Scn1b* null neurons relative to wild type (Chen et al. 2004; Patino et al. 2009). However, recordings from *Scn1b* null brain slices from the same age range demonstrated hyperexcitability in the CA3 region of the hippocampus as well as epileptiform activity in the hippocampus and cortex (Patino et al. 2009; Brackenbury et al. 2013), suggesting that β1/β1B subunits in neuronal processes may be critical in regulating excitability. These excitability changes are proposed to contribute to the severe seizures observed in *Scn1b* null mice that are a model of DS (Chen et al. 2004; Patino et al. 2009). The observation of altered sodium current and impaired excitability in *Scn1b* null CGNs suggests a role for *Scn1b* in regulating the excitability of the cerebellum (Brackenbury et al. 2010) that may contribute to the ataxic phenotype of *Scn1b* null mice (Chen et al. 2004). In contrast to reduced excitability observed in *Scn1b* null CGNs, *Scn1b* null DRG neurons are hyperexcitable, suggesting that these animals may have allodynia (Lopez-Santiago et al. 2011). Recordings from *Scn1b* null ventricular myocytes demonstrated

increased transient and persistent sodium current relative to wild-type cells, with prolonged QT and RR internals on the electrocardiogram (ECG) (Lopez-Santiago et al. 2007). Clearly, β1/β1B subunits have cell type-specific context-dependent effects on electrical excitability in vivo.

In addition to modulation of sodium current in primary cells, *Scn1b* gene products (β1 and/or β1B) regulate the expression and subcellular distribution of VGSC α subunit proteins in a cell type-specific manner. *Scn1b* null CA3 hippocampal neurons have decreased levels of Nav1.1 and increased levels of Nav1.3 protein compared to wild type, as assessed by immunofluorescence, which may correspond to the overall developmental delay exhibited by these mice (Chen et al. 2004). *Scn1b* is required for localization of Nav1.6 to the AIS in a subpopulation of CGNs and a subpopulation of *Scn1b* null CGNs display increased levels of Nav1.1 channels at the AIS compared to wild type (Brackenbury et al. 2010).

Other members of the VGSC β subunit gene family are involved in modulation of electrical excitability in vivo. Sodium current recordings in *Scn2b* null hippocampal neurons demonstrate a negative shift in the voltage dependence of inactivation relative to cells from WT littermates, resulting in increased channel availability (Chen et al. 2002). In contrast, *Scn2b* null small-fast DRG neurons display decreased TTX-S (Nav1.7) sodium current density and slowed rates of TTX-S sodium current activation and inactivation, with no measurable changes in TTX-R currents (Lopez-Santiago et al. 2006), again demonstrating that β subunit effects in vivo are cell type specific. Experiments using transfection to knockdown or express β4 in primary neurons suggest that this subunit promotes persistent sodium current (Aman et al. 2009; Bant and Raman 2010). Interestingly, β1 and β4 are proposed to play opposite roles in hippocampal neurons, such that β1 promotes channel inactivation, acting as a "brake" on excitability, whereas β4 promotes channel activation, acting as the "accelerator" (Aman et al. 2009). This is consistent with findings that *Scn1b* null mice are spontaneously epileptic (Chen et al. 2004; Brackenbury et al. 2013).

In addition to their roles in the nervous system, β subunits are regulators of electrical excitability in the heart in vivo. Sodium current recordings from *Scn1b* null ventricular cardiomyocytes demonstrated increases in both transient and persistent sodium current density, resulting in prolongation of action potential repolarization and extension of the heart rate-corrected QT interval (Lopez-Santiago et al. 2007). Here, *Scn5a* mRNA, Nav1.5 protein, and ^{3}H-saxitoxin binding were all increased compared to wild type, suggesting increases in both TTX-R and TTX-S VGSC expression in these cells. Mutations in *SCN2B* have been linked to atrial fibrillation (AF) and Brugada syndrome, suggesting a role for β2 in cardiac excitability (Watanabe et al. 2009; Riuro et al. 2013). Cardiac excitability is also abnormal in *Scn3b* null mice, suggesting a role for β3 in the heart (Hakim et al. 2008, 2010). Upon programmed electrical stimulation, ventricular tachycardia occurs in *Scn3b* null, but not wild-type, Langendorff-perfused hearts (Hakim et al. 2008). *Scn3b* null hearts display atrial tachycardia during atrial burst pacing (Hakim et al. 2010). *Scn4b* has been identified as a modifier gene for Long QT Syndrome (LQTS) resulting from a mutant *Scn5a* gene (Remme et al. 2009). While

the 129 OlaHsd mice used in this study are cardiac *Scn4b* hypomorphs, expression in the brain is unaffected (Calhoun and Isom, unpublished observation), suggesting 129 OlaHsd mice harbor a mutation that abolishes a cardiac-specific *cis* regulatory element.

1.7.3 Role of VGSC β Subunits in Resurgent Sodium Current

Resurgent sodium current, defined as the influx of sodium through VGSC α subunits during repolarization (Bean 2005), is an important adaptation for high-frequency firing neurons such as cerebellar Purkinje neurons (Burgess et al. 1995; Raman et al. 1997). The intracellular domain of β4 was proposed to serve as the open-channel blocking particle that allows for resurgent sodium current in neurons in 2005 (Grieco et al. 2005). Here, a β4 C-terminal peptide was shown to prevent the fast inactivation gate from closing, thus allowing for more rapid channel recovery. Subsequent knockdown of β4 expression using siRNA in CGNs resulted in reduced resurgent sodium current and decreased repetitive firing, providing further evidence for β4 as the open-channel blocking particle (Bant and Raman 2010). A peptide corresponding to β4 was sufficient to invoke resurgent sodium current in HEK 293 cells (Theile and Cummins 2011), again strongly suggesting a role for β4 in the generation of resurgent sodium current in vivo. Importantly, however, co-expression of full-length β4 and Nav1.6 subunits was not sufficient to generate resurgent current (Chen et al. 2008), suggesting that key cellular processes, possibly including posttranslational modification, that allow β4 subunits to participate as the open-channel blocking particle may be specific to neurons. In addition to β4, β1 and/or β1B play roles in regulating resurgent current, at least in the cerebellum. *Scn1b* null CGNs have normal transient sodium current but reduced resurgent sodium current and, importantly, β4 protein levels are not reduced (Brackenbury et al. 2010). These observations strongly argue that VGSC β subunits, in particular β4, play a role in regulating resurgent sodium current in vivo.

1.7.4 VGSC β Subunits Modulate Cell Surface Expression of α Subunits

In heterologous systems, β subunits increase the cell surface expression of α subunits. The final step in VGSC biosynthesis in vivo is concomitant α-β2 association and cell surface insertion (Schmidt et al. 1985; Schmidt and Catterall 1986). In vivo observations support this conclusion. Primary *Scn2b* null hippocampal neurons display reduced sodium current density compared to wild type (Chen et al. 2002). In support of this, ^{3}H-saxitoxin binding to cell surface VGSCs is reduced in whole brain neurons isolated from *Scn2b* null mice, while total ^{3}H-saxitoxin binding (intracellular plus cell surface) is unchanged (Chen et al. 2002). Interestingly, this is not the case for all brain areas. Neurons acutely dissociated from wild type and *Scn2b* null dentate gyrus exhibit similar sodium current densities (Uebachs et al. 2010). This result suggests that, similar to β1, the effect of β2 on cell surface α subunit expression may be cell type specific. In addition to being cell type specific, β2 has VGSC-specific effects based on TTX sensitivity. For example, *Scn2b* null small-fast DRG neurons have reduced TTX-S sodium current, but unchanged TTX-R sodium current (Lopez-Santiago et al. 2006).

1.7.5 Novel Role for VGSC β Subunits in Modulation of Potassium Channels

β1 was originally discovered as a subunit of rat brain VGSCs purified to theoretical homogeneity (Hartshorne et al. 1982; Hartshorne and Catterall 1984). In spite of this, β1 is promiscuous in its ability to modify ion channels. For example, when co-expressed with Kv4.3 in *Xenopus* oocytes, β1 modulates potassium current (Deschenes and Tomaselli 2002). Subsequent experiments by this group using siRNA to knock down *Scn1b* expression in neonatal rat ventricular cardiomyocytes resulted in reduced sodium current *and* transient outward potassium current, demonstrating that *Scn1b* modulates multiple channel types in vivo (Deschenes et al. 2008). More recently, β1 has been shown to modulate potassium currents expressed by Kv1.1, Kv1.2, Kv1.3, Kv1.6, or Kv7.2 (but interestingly not Kv3.1) in oocytes (Nguyen et al. 2012). Importantly, immunoprecipitation from mouse brain revealed that β1 subunits associate with Kv4.2 (Marionneau et al. 2012). This provides critical in vivo evidence for association of potassium channels and β1 in a neuronal protein complex. In this same study, shRNA-mediated knockdown of *Scn1b* resulted in a reduction of Kv4-mediated current in neurons (Marionneau et al. 2012). *Scn1b* null mice show prolonged action potentials and increased repetitive firing in cortical pyramidal neurons, supporting not only changes in sodium current, as shown in (Brackenbury et al. 2013) but also a link between VGSC β1/β1B subunits and potassium channel activity (Marionneau et al. 2012). These observations suggest a novel role for VGSC β1/β1B subunits in interacting with and modulating potassium channels, suggesting, perhaps, that these multifunctional proteins should be re-classified independently from the VGSC family.

1.8 Noncanonical Roles of VGSC β Subunits in Brain Development and Cell Signaling

1.8.1 Neurite Outgrowth

VGSC β subunits are multifunctional molecules that do more than modulate channel expression and ionic currents. As CAMs, β subunits, especially β1, participate in neuronal proliferation and migration, neurite outgrowth (Fig. 5), and axonal fasciculation. The first evidence of involvement of β1 in neurite outgrowth came from the observation that CGNs develop longer neurites on β1-expressing fibroblast monolayers compared to mock-transfected monolayers (Davis et al. 2004). To test the effects of other β subunits, CGNs were also plated on β2- or β4-expressing monolayers (Davis et al. 2004). β4-expressing monolayers had no effect, whereas β2-expressing monolayers reduced neurite length. Comparing CGNs isolated from *Scn1b* null mice with those from wild-type littermates demonstrated that β1-mediated neurite outgrowth required *trans*-homophilic adhesion (Davis et al. 2004). This suggests a model where β1–β1 *trans*-homophilic adhesion acts as the initiating event for a signaling cascade that results in neurite outgrowth. β1-mediated neurite outgrowth is abrogated in *Fyn* and *Cntn1* null CGNs, implying that these molecules are key (Brackenbury et al. 2008). *Cntn1* null mice are β1

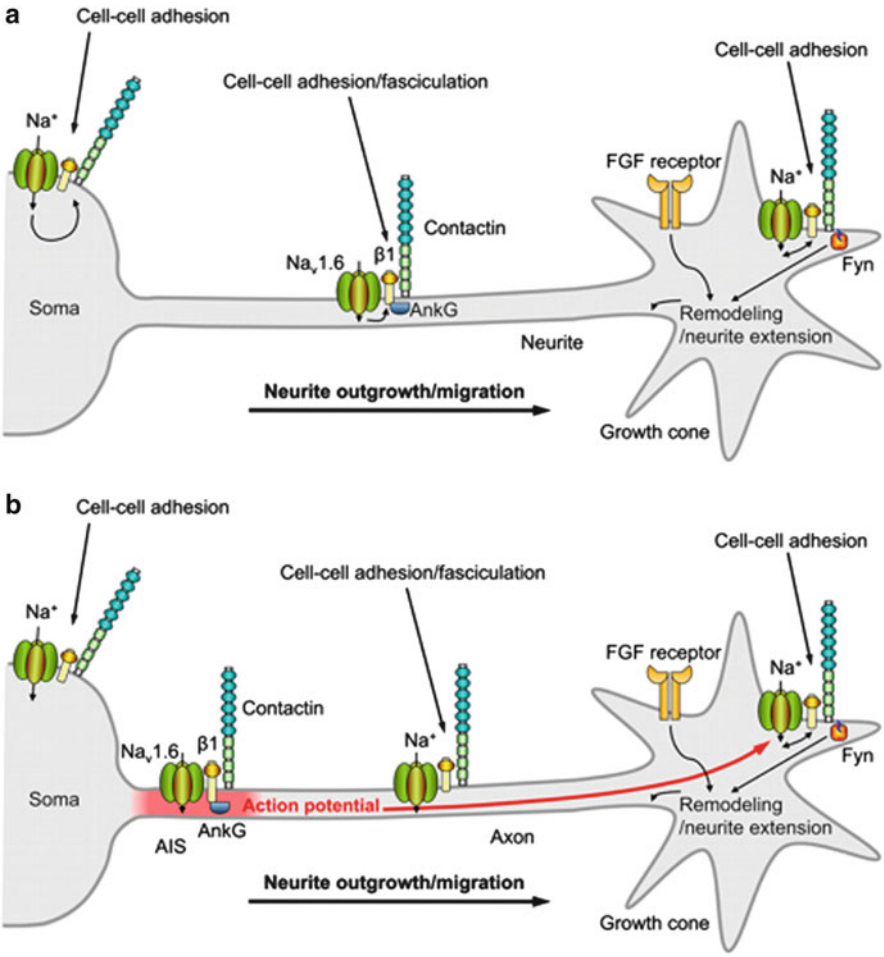

Fig. 5 A model for β1-mediated neurite outgrowth. (**a**) In immature CGNs lacking AIS, complexes containing Nav1.6, β1, and contactin are present throughout the neuronal membrane in the soma, neurite, and growth cone. Localized sodium influx is necessary for β1-mediated neurite extension and migration (Brackenbury et al. 2010). VGSC complexes along the neurite are proposed to participate in cell–cell adhesion and fasciculation (Davis et al. 2004; Brackenbury et al. 2008). (**b**) In 14 DIV CGNs, β1 is also required for Nav1.6 expression at the AIS (Brackenbury et al. 2010) and subsequent high-frequency AP firing through modulation of resurgent sodium current (Van Wart and Matthews 2006; Raman et al. 1997; Raman and Bean 1997). Electrical activity may further promote β1-mediated neurite outgrowth at or near the growth cone in vivo (Van Wart and Matthews 2006; Raman et al. 1997; Raman and Bean 1997). Thus, the developmental functions of β1 and Nav1.6 are complementary, such that sodium influx carried by Nav1.6 is required for β1-mediated neurite outgrowth and β1 is required for normal expression/activity of Nav1.6 at the AIS. Fyn kinase and AnkG also are likely present in all complexes, but they are only shown once in each panel for clarity. The FGF-mediated, β1-independent neurite outgrowth pathway is shown as well. Other CAMs that regulate neurite outgrowth and also may interact with β1 in this system, have been omitted for clarity. Figure reproduced from (Brackenbury et al. 2010)

hypomorphs, suggesting that *Cntn1* and *Scn1b* are linked in some fashion (Brackenbury et al. 2008). β1 expression levels are unchanged in *Fyn* null mice, suggesting that this member of the src family of tyrosine kinases may participate in a signaling cascade downstream of β1–β1-mediated cell–cell adhesion (Brackenbury et al. 2008). A portion of β1 and fyn colocalize in detergent-resistant membrane (DRM) fractions in brain (Brackenbury et al. 2008) and contactin has been identified in this fraction as well (Kramer et al. 1999). These results suggest that β1-mediated neurite outgrowth may occur through a lipid raft signaling mechanism that requires the presence of both fyn and contactin (Brackenbury and Isom 2011). β1-mediated neurite outgrowth in CGNs requires the expression of Nav1.6 and is inhibited by TTX, suggesting that TTX-S sodium current modulates β1-mediated neurite outgrowth (Brackenbury et al. 2010). However, the location of these signaling events in the neuron may differ. It is proposed that sodium current initiated at the AIS (where β1 is also located) signals to β1 subunits at the growth cone which may or may not be associated with α subunits (Brackenbury et al. 2010). Importantly, while TTX inhibits β1-mediated neurite outgrowth, it does not affect FGF-mediated neurite outgrowth (Brackenbury et al. 2010). Conversely, neither FGF nor EGF receptor kinase inhibitors affect β1-mediated neurite extension (Brackenbury et al. 2008). Thus, these signaling cascades appear to involve different players.

1.8.2 Brain Development

The gene products of *Scn1b* are important for neuronal patterning during brain development. Immunohistological examination of wild-type and *Scn1b* null cerebellae demonstrated cerebellar microorganization defects in the null brain (Brackenbury et al. 2008). Specifically, in the cerebellum of *Scn1b* null mice, parallel fiber fascicles were less compact than in wild type. In addition, the external germinal layer (EGL) was expanded in size in null mice relative to wild type, suggesting that a defect in migration may have trapped granule precursors in the EGL, preventing them from migrating to the inner granule layer (IGL). In wild-type cerebellar sections, axon fibers traversing the molecular layer (ML) ran perpendicular to the parallel fibers. However, in *Scn1b* null cerebellar sections, some of the axons traversing the ML deviated from this perpendicular trajectory, suggesting axon outgrowth and pathfinding deficits. In the developing hippocampus, *Scn1b* null mice display a series of developmental defects, including elevated levels of cellular proliferation in the hilus, ectopic *Prox1*-expressing dentate granule neurons in the hilus, decreased neuronal density in the dentate gyrus granule cell layer, increased thickness of the dentate gyrus granule cell layer, and abnormal axon outgrowth and pathfinding (Brackenbury et al. 2013). Spontaneous behavioral seizures begin at approximately postnatal day 10 in *Scn1b* null mice (Chen et al. 2004). Importantly, developmental defects in the *Scn1b* null cerebellum and hippocampus precede the onset of seizures and are detectable at P5 (Brackenbury et al. 2013). Taken together, these observations suggest that β1 and/or β1B function as CAMs in the developing CNS and that perturbation of *Scn1b* results in patterning defects which may set up a substrate for altered excitability.

2 Roles of VGSC β Subunits in Pathophysiology

2.1 Epilepsy

Epilepsy is a common neurological disorder defined by recurrent, unprovoked seizures due to abnormal surges of electrical activity in the brain. While epilepsy can be caused by injury or other disease, as many as 40 % of epilepsy cases are idiopathic and presumed to stem from genetic anomalies. Not surprisingly, mutations in ion channels ("channelopathies") cause epilepsy. Of particular interest is the GEFS+ spectrum of epilepsy disorders which includes GEFS+ and DS. The GEFS+ epilepsy spectrum is a continuum of disease severity and includes pediatric epilepsies wherein febrile seizures persist beyond 6 years of age and are associated with generalized or partial epilepsy (Escayg and Goldin 2010). DS patients exhibit frequent febrile seizures which precede the development of other seizure types and are at risk for status epilepticus, developmental delay, and ataxia. All epilepsy patients, but especially DS patients, have a high risk of Sudden Unexpected Death due to EPilespsy (SUDEP). While multiple mechanisms have been proposed for SUDEP, cardiac arrhythmia is an interesting candidate because ion channel-driven cellular excitability is a shared trait between the brain and the heart (Surges and Sander 2012).

Mutations in the VGSC α subunits *SCN1A* and *SCN2A* are linked to GEFS+ and DS, with mutations in *SCN1A* causing haploinsufficiency being the predominant cause of DS (Meisler and Kearney 2005; Escayg et al. 2000; Claes et al. 2001; Sugawara et al. 2001; Shi et al. 2009). Human *SCN1B* mutations are also linked to epilepsies on the GEFS+ spectrum, including GEFS+ and DS (Wallace et al. 1998, 2002; Patino et al. 2009; Audenaert et al. 2003; Ogiwara et al. 2012). In addition to the GEFS+ spectrum, *SCN1B* mutations are also linked to temporal lobe epilepsy (TLE) and early onset absence epilepsy (EOAE) (Audenaert et al. 2003; Scheffer et al. 2007). To date, most known disease-related *SCN1B* mutations cluster in the Ig loop region of β1/β1B (Brackenbury and Isom 2011). Probands in a number of GEFS+ pedigrees carry rare heterozygous *SCN1B* mutations (Wallace et al. 1998, 2002; Audenaert et al. 2003; Scheffer et al. 2007; Fendri-Kriaa et al. 2011). A homozygous DS mutation in *SCN1B* (p.R125C, Fig. 3) was identified by screening candidate genes after the patient was found to lack mutations in *SCN1A* (Patino et al. 2009). Recently, another homozygous *SCN1B* mutation was discovered in a DS patient (Ogiwara et al. 2012). While the majority of human mutations map to the Ig loop region that is shared by both β1 and β1B splice variants, a β1B-specific mutation was recently identified in two unrelated pedigrees with idiopathic epilepsy (Patino et al. 2011).

Mouse models support the link between *Scn1b* and epilepsy. *Scn1b* null mice display spontaneous generalized seizures and ataxia (a comorbidity of DS), die by P21 (Chen et al. 2004) and are proposed to be a model of DS (Patino et al. 2009). Characterization of *Scn1b* null mice has demonstrated defects in excitability and neuronal development (Patino et al. 2009; Brackenbury et al. 2008, 2013). Importantly, defects in neuronal patterning are observed at P5, prior to seizure onset,

suggesting that this may be a cause, rather than an effect, of neuronal hyperexcitability (Brackenbury et al. 2013). A mouse model of *SCN1B*-related GEFS+, a knock-in of the β1 p.C121W mutation (Fig. 3), recapitulates a number of aspects of the human disease (Wimmer et al. 2010). Both p.C121W heterozygous and homozygous mice are more susceptible to febrile seizures relative to wild-type littermates (Wimmer et al. 2010). Action potential recordings from subicular pyramidal neurons suggested p.C121W knock-in neurons are hyperexcitable (Wimmer et al. 2010). Immunoblots with an anti-β1 antibody suggested no change in β1 expression in C121W knock-in heterozygous or homozygous brains (Wimmer et al. 2010); although the authors make note of a number of nonspecific immunoreactive bands on the Western blot that may complicate interpretation of the data (Wimmer et al. 2010). Data suggest that heterozygous p.C121W knock-in mice, expressing one mutant and one wild-type allele of *Scn1b*, display a GEFS+-like phenotype. At the cellular level, the p.C121W mutation results in hyperexcitability of subicular pyramidal neurons, which may inform the mechanism of febrile seizures resulting from this mutation.

Studies of *SCN1B* mutants have yielded insight into the molecular mechanisms underlying the perturbed functionality of these alleles. β1 p.R125C is a trafficking-deficient mutation which is retained intracellularly, resulting in a functional null phenotype (Patino et al. 2009). Importantly, the β1 p.R125C-trafficking defect can be rescued by incubating cells at lowered temperature, opening the possibility of future development of novel therapeutics similar to those for CFTR and muscular dystrophy (Eckford et al. 2012; Cirak et al. 2011). β1 p.C121W disrupts a conserved intramolecular disulfide bond, a critical feature of the Ig loop structure. β1 p.C121W traffics normally to the cell surface and promotes VGSC α subunit expression in transfected cell lines; however, it does not participate in *trans*-homophilic adhesion and does not modulate sodium current in vitro (Meadows et al. 2002b). The trafficking of β1 p.C121W was studied by viral expression of wild-type or mutant β1-eGFP fusion constructs in neurons. Under these conditions β1 p.C121W was excluded from the AIS, suggesting that the mutation affects β1 trafficking in vivo (Wimmer et al. 2010). Studies of the *SCN1B* GEFS+ mutations p.R85C and p.R85H (Fig. 3) in heterologous systems showed that these mutant β1 subunits fail to modulate VGSC α subunits due to reduced membrane and intracellular β1 expression (Xu et al. 2007). In contrast, we were able to detect p.R85H at the cell surface in transfected CHL cells (Patino et al. 2011). These results present a complex picture of *SCN1B* mutations with differential effects in different expression systems that may include defects in trafficking and/or sodium channel modulation. Importantly, a gap in the literature is in understanding the role of these *SCN1B* mutations in vivo, including their effects on neuronal patterning and/or potassium channel modulation.

Thus far, data on *SCN1B* epilepsy mutations suggest a model in which gene dosage may determine the severity of disease presentation. For example, a single-mutant *SCN1B* allele may result in the development of the milder disease GEFS+. In contrast, expression of two nonfunctional *SCN1B* alleles may result in the very severe disease DS. As more *SCN1B* mutant alleles associated with epilepsy are

identified and studied, the picture will become clearer. The future identification of *SCN1B* modifier genes and gain-of-function or dominant-negative *SCN1B* mutations will certainly revise this model.

2.2 Ataxia

Ataxia, or altered gait, largely resulting from abnormal electrical excitability in the cerebellum, is a comorbidity of DS. *Scn1b* null mice display ataxia (Chen et al. 2004) and the patient carrying two DS mutant *SCN1B* alleles (p.R125C, Fig. 3), predicted to be a functional null, displayed psychomotor deterioration after 5 months of age (Patino et al. 2009). Evidence from studying cerebellar microorganization of *Scn1b* null mice has yielded important information for the understanding of ataxia related to *SCN1B*. As described above, *Scn1b* null CGNs display reduced resurgent sodium current and impaired excitability (Brackenbury et al. 2010). Additionally, the developing *Scn1b* null cerebellum has defasciculated parallel fibers, abnormal migration of CGN precursors, and aberrant axon outgrowth and pathfinding of developing CGNs (Brackenbury et al. 2008). Finally, the expression of β1 subunits in Bergmann glia in the cerebellum raises the possibility that *SCN1B* mutations may result in altered axo–glial interactions (Davis et al. 2004). Thus, the ataxic phenotype of *Scn1b* null mice and possibly of *SCN1B*-linked epilepsy patients likely results from a combination of developmental defects compounded by altered excitability.

2.3 Cardiac Arrhythmia

Channelopathies increase the risk of abnormal heart rhythms, or cardiac arrhythmias, which can be life threatening in the case of ventricular fibrillation (VF). For example, mutations in the predominant cardiac sodium channel gene *SCN5A* are associated with LQTS, Brugada syndrome, and VF (Remme and Bezzina 2010). Mutations in VGSC β subunits *SCN1B*, *SCN2B*, and *SCN3B* are linked to Brugada syndrome, which confers increased risk of sudden cardiac death due to VF (Watanabe et al. 2008; Riuro et al. 2013; Ishikawa et al. 2013). Mutations in *SCN1B*, *SCN2B*, *SCN3B*, and *SCN4B* are linked to AF (Watanabe et al. 2009; Olesen et al. 2011; Li et al. 2013). A mutation in *SCN4B* has been linked to LQTS, in which impaired repolarization of the myocardium provides a substrate for arrhythmia that can result in heart palpitations, syncope, and/or sudden death due to VF (Medeiros-Domingo et al. 2007).

Evidence in transgenic mice suggests an important role for VGSC β subunits in the heart. *Scn1b* null mice have abnormal cardiac action potentials evidenced by an elongated heart rate-corrected QT interval (Lopez-Santiago et al. 2007). Acutely dissociated ventricular cardiomyocytes from *Scn1b* null mice have increased peak and persistent sodium current relative to wild-type cells. Ventricular tachycardia is observed following programmed electrical stimulation in *Scn3b* null, but not

wild-type, Langendorff-perfused hearts (Hakim et al. 2008). In hearts paced using atrial burst pacing, *Scn3b* null hearts were susceptible to atrial tachycardia (Hakim et al. 2010). A genetic modifier screen identified *SCN4B* as a genetic modifier for phenotype severity in a mouse model of an *SCN5A* allele which results in conduction disease and Brugada syndrome with variable severity in patients (Remme et al. 2009).

These results suggest VGSC β subunits are involved in normal cardiac function and that mutation of these genes can result in disease. Given that β subunit mutations are linked to both brain and cardiac disease, one cannot help but consider the possibility of a link between these syndromes. Elucidation of this putative relationship may be an important step toward understanding and preventing SUDEP in the future.

2.4 Sudden Infant Death Syndrome

Sudden Infant Death Syndrome (SIDS) is characterized by the sudden death of an infant with no obvious trauma or identifiable underlying medical condition. Arrhythmia is emerging as one of the potential causes of SIDS (Towbin 2010). In addition to mutations of the predominant cardiac sodium channel gene *SCN5A* in SIDS, rare mutations have been identified in *SCN3B* and *SCN4B* in 3 cases (Tan et al. 2010; Wang et al. 2007; Arnestad et al. 2007). Biochemical characterization of the resulting β3 and β4 mutant proteins suggested that the mutations perturbed the normal function of the proteins. When co-expressed with Nav1.5, the β3 mutant (p.V36M) decreased peak sodium current, while wild-type β3 had no effect (Tan et al. 2010). In contrast, neither wild-type β4 nor the β4 mutant (p.S206L) had an effect on peak current (Tan et al. 2010). Importantly, the β3 and β4 mutants both resulted in increased persistent sodium current (Tan et al. 2010). Expression of β4 p.S206L in adult rat ventricular cardiomyocytes also led to increased persistent sodium current, suggesting the presence of substrates for lethal arrhythmias in these SIDS patients (Tan et al. 2010). These results suggest the possibility of common molecular mechanisms between epilepsy, SUDEP, cardiac arrhythmia, and SIDS.

2.5 Neuropathic Pain

Neuropathic pain can be caused by genetic mutation or nerve injury, resulting in elevated pain sensation, or allodynia, in individuals due to disruptions in nociception, the normal neuronal pathways involved in the sensation of noxious stimuli. VGSC β subunits are expressed in multiple cell types involved in nociception, including DRG neurons and peripheral nerves, and animal studies suggest the involvement of β subunits in nociception. *Scn1b* null DRG neurons are hyperexcitable (Lopez-Santiago et al. 2011). While the early postnatal lethality of *Scn1b* null mice has complicated behavioral pain testing, hyperexcitable DRG neurons in these mice may increase their sensitivity to stimulation and result in

allodynia. The role of *Scn2b* in nociception has also been explored. As described above, β2 modulates TTX-S but not TTX-R VGSC α subunits and currents in small-fast DRG neurons and *Scn2b* null mice are less sensitive than wild-type mice in the late phase of the formalin test, suggesting a role in inflammatory pain (Lopez-Santiago et al. 2006). β2 protein expression increases with nerve injury and this expression is required for the development of mechanical allodynia in a rodent model (Pertin et al. 2005). Finally, β3 is expressed in small-diameter c-fiber DRG neurons and the expression of β3 is upregulated in a chronic constriction rat neuropathic pain model (Shah et al. 2000). These results suggest β subunits play important roles in nociception and are potential therapeutic targets in neuropathic pain.

2.6 Neurodegenerative Disease

Neurodegenerative diseases, including Alzheimer's disease (AD), Parkinson's disease (PD), Multiple sclerosis (MS), and Huntington's disease (HD), are characterized by a progressive loss of neuronal function over time and often involve neuronal cell death. Accumulation of intra-axonal sodium ions resulting in calcium overload is a proposed mechanism for axonal loss and cell death in neurodegenerative disease, suggesting a potential link between VGSCs and neurodegeneration (Waxman 2006). Importantly, pharmacological inhibition of VGSCs is neuroprotective in experimental allergic encephalomyelitis (EAE), a model of MS (Lo et al. 2002, 2003). This result suggested that a reduction in sodium current might be a general mechanism for neuroprotection. *Scn2b* null mice (lacking β2) display reduced sodium current density in CNS and PNS neurons. Thus, it was hypothesized that these mice may display protection from neurodegeneration (Chen et al. 2002; Lopez-Santiago et al. 2006). Using the EAE model, it was demonstrated that *Scn2b* null mice have higher rates of survival and lower rates of symptomatic progression relative to wild-type mice (O'Malley et al. 2009). This finding raised the possibility that in, addition to VGSC α subunits, β2, and possibly other β subunits, may be targets for therapeutic intervention in neurodegenerative disease.

β4 is downregulated in the striatum of HD patients (Oyama et al. 2006). However, whether loss of β4 expression is relevant to the HD disease process or a secondary effect of the disease is unknown. Given the role of β4 in sodium current modulation, resurgent sodium current generation, and potentially as a CAM, it seems plausible that downregulation of β4 could have a significant impact on brain function. A recent report investigating PD identified glycosylated β4 in patient cerebral spinal fluid (CSF) (Zhou et al. 2012), suggesting that the ectodomain of β4 may be released into the CNS during the disease process. However, additional evidence is needed to implicate β4 in the pathogenesis of neurodegenerative disease. At this time, the possibility that altered proteolytic cleavage of β4 is a secondary byproduct of disease

progression cannot be excluded. Even if β4 is not directly involved in the disease mechanism, the potential for its utility as a biomarker may be considered.

2.7 Potential Role of VGSC β Subunits in Cancer

There is increasing evidence that ion channels, including VGSCs, may play a role in carcinogenesis (Prevarskaya et al. 2010). Much of the research on the role of VGSCs in cancer has focused on α subunits as molecules which promote metastatic potential, the ability of a cancer cell to release from the primary tumor and form secondary tumors (Brackenbury 2012). Importantly, pharmacologic inhibition of sodium current inhibits cancer cell invasion in vitro, raising the possibility that VGSCs may be novel targets for treating metastatic cancer (Brackenbury et al. 2007; Yang et al. 2012). Less is known about VGSC β subunits in cancer, though a few studies have been performed which suggest context-specific roles for these molecules. *SCN1B* mRNA transcripts have been detected in prostate cancer and may correlate with high metastatic potential (Diss et al. 2008). In contrast, studies in breast cancer cell lines suggest that β1 expression is high in weakly metastatic cells and low in strongly metastatic cells (Chioni et al. 2009). In cell culture models, β1 acts to limit metastatic potential, suggesting it may be a novel therapeutic target (Chioni et al. 2009). These results may suggest a cell type-specific function for *SCN1B* in cancer; however, they must be interpreted with caution until in vivo evidence emerges. In addition, *SCN3B* may play a novel role as a p53-inducible proapoptotic gene that may partially mediate the tumor suppressor function of p53 (Adachi et al. 2004). However, a putative molecular mechanism for how *SCN3B* functions in apoptosis remains elusive.

2.8 Therapeutic Potential of VGSC β Subunits

As discussed above, VGSC β subunits may be drug targets for a variety of diseases including epilepsy, cardiac arrhythmia, neuropathic pain, multiple sclerosis, and cancer. How to target these molecules remains unknown, although some studies, as discussed below, may provide important insights.

2.8.1 β Subunits Alter VGSC Pharmacology

β subunits affect VGSC pharmacology. In *Xenopus* oocytes, co-expression of β1 or β3 with Nav1.3 abrogates the inhibitory effect of lidocaine, a sodium channel blocker utilized as an antiarrhythmic and local anesthetic (Lenkowski et al. 2003). In addition, in a heterologous system the β1 p.C121W GEFS+ mutation diminishes tonic and use-dependent channel block induced by phenytoin, a sodium channel blocker used as an anticonvulsant (Lucas et al. 2005). The efficacy of the anticonvulsant carbamazepine, a sodium channel blocker, relies on the expression of *Scn1b* in vivo (Uebachs et al. 2010). In contrast, the anticonvulsant lacosamide functions normally in this model (Uebachs et al. 2012). These studies emphasize the

importance of understanding how drugs interact not only with the pore-forming α subunits in isolation but also with relevant VGSC α/β protein complexes. Also, since the expression of VGSC β subunits can be altered by pathophysiology, understanding how sodium channel compounds work in the absence and presence of β subunits is clinically relevant (Ellerkmann et al. 2003).

2.8.2 Rescuing Trafficking-Deficient α Subunits

Some *SCN1A* epilepsy mutations result in trafficking-deficient Nav1.1 channels that can be rescued by modulatory proteins, including VGSC β subunits, and/or by a number of VGSC-targeting compounds (Rusconi et al. 2007, 2009; Thompson et al. 2012). In addition to providing a model for heterogeneity of disease severity in which genetic background may influence the level of mutant Nav1.1 channel proteins trafficked to the cell surface, this may suggest a novel treatment strategy. Utilizing VGSC-targeting drugs or gene therapy to deliver modulatory β subunits may correct channel trafficking in this patient cohort and provide a viable therapeutic intervention. A potential caveat here is that forcing channels with gain-of-function mutations to the neuronal cell surface may exacerbate, rather than ameliorate, disease (Thompson et al. 2012).

2.8.3 Modulation of *SCN2B* Expression in Neurodegenerative Disorders and Neuropathic Pain

Scn2b deletion is neuroprotective in EAE, a model of MS (O'Malley et al. 2009). It is interesting to consider the possibility that reducing the expression of β2 in patients, through small molecules or gene therapy, may be neuroprotective and a potential therapeutic approach to neurodegeneration in MS. Because *Scn2b* null mice are healthy and live normal lifespans, the safety risks of targeting β2 in limited brain areas may be acceptable. In addition, β2 may be a potential therapeutic target in the treatment of neuropathic pain. As discussed above, global *Scn2b* deletion modulates TTX-S VGSC α subunit expression and function in small-fast DRG neurons as well as the animal's response in an inflammatory pain model (although these mice are more sensitive to acute noxious thermal stimuli than wild-type) (Lopez-Santiago et al. 2006). In addition, the expression of β2 increases with nerve injury and β2 upregulation is necessary for the development of mechanical allodynia (Pertin et al. 2005). A small molecule or gene therapy approach to reduce the expression of β2 in neurons within the nociceptive pathway may be a viable strategy to treat neuropathic pain.

3 Concluding Remarks

3.1 *SCN1B*: A Tale of Two Splice Variants

SCN1B encodes both the transmembrane protein β1 and the secreted protein β1B (Patino et al. 2011). Importantly, both splice variants are CAMs (Malhotra et al. 2000; Patino et al. 2011). A critical gap in our knowledge is how each splice

variant contributes to normal development and thus how mutations in only one of the gene products but not the other might contribute to pathophysiology. Most of the disease-related *SCN1B* mutations cluster in or near the extracellular Ig loop, which is common to both β1 and β1B (Brackenbury and Isom 2011). *Scn1b* null mice, which exhibit spontaneous seizures and premature lethality and are a DS model, lack expression of both splice variants and thus imply the importance of both in establishing and maintaining normal physiology (Chen et al. 2004). Further, mutations that affect β1B and not β1 have been identified in a case of Brugada syndrome and two pedigrees of idiopathic epilepsy (Watanabe et al. 2008; Patino et al. 2011), suggesting that both splice variants of *SCN1B* play important roles in normal physiology.

Characterization of *Scn1b* null mice suggests that β1 and/or β1B subunits are critical for normal brain development. But what about adult brain function? It has been demonstrated that proteins involved in tissue development can be co-opted and utilized for adult tissue maintenance. While much of the focus on studying β subunits has focused on early postnatal development, it will be interesting to ask whether β subunit function is critical in the adult. If the β1/β1B subunits play important roles at later time points, this may open up a new avenue to investigate the potential involvement of these proteins in aging, dementia, and/or neurodegeneration, as has been suggested for β2 and β4.

3.2 Functional Redundancy: A Putative Model for Disease Severity

Perturbation of β1/β1B function, either in inherited human disease or by genetic deletion of *Scn1b* in mice, may be more harmful to the organism than perturbation of other VGSC β subunits. While *Scn1b* null mice model DS and SUDEP, *Scn2b* null mice and *Scn3b* null mice do not appear to seize and live normal life spans. Thus, *SCN1B* is essential for life ,while *SCN2B* and *SCN3B* apparently are not. Currently, the lack of a *Scn4b* null mouse model prevents us from understanding the role of β4 in vivo and represents a major gap in our knowledge. A theory that might explain the apparent discrepancy in functional importance of the β subunits, at least in brain, is functional redundancy. It is possible that compensation is poorly achieved with altered *SCN1B* function since β3, the other transmembrane VGSC β subunit that non-covalently associates with α, has a different developmental expression profile and may have altered CAM functions in developing brain compared to β1/β1B. Also, because a secreted splice variant of β3 has not been identified, the loss of secreted β1B, especially during brain development, may be an important factor. *Scn3b* null mice are relatively healthy, thus *Scn1b* may be compensatory in this model. In *Scn2b* null mice, which are also generally healthy, *Scn4b* (encoding the other disulfide-liked β subunit, β4) may provide functional redundancy, for example, serving as a chaperone for the remaining (~50 % of control levels) VGSCs detected at the cell surface of *Scn2b* null neurons. If so, then a double null mouse (*Scn2b*/*Scn4b*) is predicted to have little to no cell surface

VGSCs and result in a lethal phenotype. Interestingly, *Scn2b* may not reciprocally compensate for *Scn4b*, considering the role of β4 as a key player in the generation of resurgent sodium current in high-frequency firing neurons. Loss-of-function *Scn4b* mutations may thus be especially deleterious to neuronal circuits that rely on resurgent sodium current for which *Scn2b* cannot compensate. Development of a *Scn4b* null mouse model will be essential to addressing these questions. Additionally, characterizing mice with multiple null *Scnxb* alleles will shed important light on this ongoing area of investigation. For example, *Scn1b*/*Scn2b* null mice (Aman et al. 2009) have a more severe phenotype and die at a younger age than *Scn1b* null mice (Chen and Isom, unpublished observations). While anecdotal due to a limited sample size, this observation illustrates the potential utility of using such genetic approaches to answer questions about β subunit functional redundancy.

3.3 Modifier Genes: A Model for Disease Heterogeneity

The existence of modifier genes may explain heterogeneity in disease severity within epilepsy, cardiac arrhythmia, and other channelopathies between families and even within the same family. Based on the topics reviewed here about the multifunctional VGSC β subunits, it seems reasonable to predict that β subunit gene variants/mutations may be disease modifying in addition to disease causing. For example, *SCN4B* has been identified as a modifier gene in a mouse model of *SCN5A*-linked LQTS (Remme et al. 2009). Conversely, it is likely that other genes may modify the severity of disease-causing VGSC β subunit gene mutations, for example, genes encoding some of the key β subunit-interacting proteins discussed here. Future discovery of these genetic relationships will not only shed light on disease mechanisms but will provide critical new information regarding the biology of VGSC β subunit-containing protein complexes in normal development and physiology.

3.4 Anything but Auxiliary: The Future of VGSC β Subunits

While originally discovered as ancillary proteins that co-purify with pore-forming VGSC α subunits, there is growing evidence that the β subunits are multifunctional signaling molecules that play VGSC-dependent and -independent roles, including homophilic and heterophilic cell adhesion, regulation of gene transcription, and modulation of potassium currents. Importantly, *SCN1B*-linked channelopathies may be diseases of brain and/or heart development, resulting from impaired β1/β1B-mediated cell adhesion leading to altered neuronal circuitry or cardiac cell–cell junctions. This fascinating VGSC β subunit field now looks forward to the use of tissue- and developmental time-specific null mouse models, knock-in mouse models of human mutations, the identification of modifier genes, the developmental of novel therapeutics, and the use of patient-specific human-induced pluripotent stem cell models to investigate genetic background issues in personalized medicine.

References

Abriel H, Kass RS (2005) Regulation of the voltage-gated cardiac sodium channel Nav1.5 by interacting proteins. Trends Cardiovasc Med 15(1):35–40

Adachi K, Toyota M, Sasaki Y, Yamashita T, Ishida S, Ohe-Toyota M, Maruyama R, Hinoda Y, Saito T, Imai K, Kudo R, Tokino T (2004) Identification of SCN3B as a novel p53-inducible proapoptotic gene. Oncogene 23(47):7791–7798

Aman TK, Grieco-Calub TM, Chen C, Rusconi R, Slat EA, Isom LL, Raman IM (2009) Regulation of persistent Na current by interactions between beta subunits of voltage-gated Na channels. J Neurosci 29(7):2027–2042

Arnestad M, Crotti L, Rognum TO, Insolia R, Pedrazzini M, Ferrandi C, Vege A, Wang DW, Rhodes TE, George AL Jr, Schwartz PJ (2007) Prevalence of long-QT syndrome gene variants in sudden infant death syndrome. Circulation 115(3):361–367

Aronica E, Troost D, Rozemuller AJ, Yankaya B, Jansen GH, Isom LL, Gorter JA (2003) Expression and regulation of voltage-gated sodium channel beta1 subunit protein in human gliosis-associated pathologies. Acta Neuropathol 105(5):515–523

Audenaert D, Claes L, Ceulemans B, Lofgren A, Van Broeckhoven C, De Jonghe P (2003) A deletion in SCN1B is associated with febrile seizures and early-onset absence epilepsy. Neurology 61(6):854–856

Auld VJ, Goldin AL, Krafte DS, Marshall J, Dunn JM, Catterall WA, Lester HA, Davidson N, Dunn RJ (1988) A rat brain Na^+ channel alpha subunit with novel gating properties. Neuron 1 (6):449–461

Bant JS, Raman IM (2010) Control of transient, resurgent, and persistent current by open-channel block by Na channel beta4 in cultured cerebellar granule neurons. Proc Natl Acad Sci U S A 107(27):12357–12362

Bean BP (2005) The molecular machinery of resurgent sodium current revealed. Neuron 45(2): 185–187

Brackenbury WJ (2012) Voltage-gated sodium channels and metastatic disease. Channels 6(5): 352–361

Brackenbury WJ, Calhoun JD, Chen C, Miyazaki H, Nukina N, Oyama F, Ranscht B, Isom LL (2010) Functional reciprocity between Na^+ channel Nav1.6 and beta1 subunits in the coordinated regulation of excitability and neurite outgrowth. Proc Natl Acad Sci U S A 107(5): 2283–2288

Brackenbury WJ, Chioni AM, Diss JK, Djamgoz MB (2007) The neonatal splice variant of Nav1.5 potentiates in vitro invasive behaviour of MDA-MB-231 human breast cancer cells. Breast Cancer Res Treat 101(2):149–160

Brackenbury WJ, Davis TH, Chen C, Slat EA, Detrow MJ, Dickendesher TL, Ranscht B, Isom LL (2008) Voltage-gated Na^+ channel beta1 subunit-mediated neurite outgrowth requires Fyn kinase and contributes to postnatal CNS development in vivo. J Neurosci 28(12):3246–3256

Brackenbury WJ, Isom LL (2008) Voltage-gated Na^+ channels: potential for beta subunits as therapeutic targets. Expert Opin Ther Targets 12(9):1191–1203

Brackenbury WJ, Isom LL (2011) Na channel beta subunits: overachievers of the ion channel family. Front Pharmacol 2:53

Brackenbury WJ, Yuan Y, O'Malley HA, Parent JM, Isom LL (2013) Abnormal neuronal patterning occurs during early postnatal brain development of Scn1b-null mice and precedes hyperexcitability. Proc Natl Acad Sci U S A 110(3):1089–1094

Brette F, Orchard C (2003) T-tubule function in mammalian cardiac myocytes. Circ Res 92(11): 1182–1192

Buffington SA, Rasband MN (2013) Na^+ channel-dependent recruitment of navbeta4 to axon initial segments and nodes of ranvier. J Neurosci 33(14):6191–6202

Burgess DL, Kohrman DC, Galt J, Plummer NW, Jones JM, Spear B, Meisler MH (1995) Mutation of a new sodium channel gene, Scn8a, in the mouse mutant 'motor endplate disease'. Nat Genet 10(4):461–465

Casula MA, Facer P, Powell AJ, Kinghorn IJ, Plumpton C, Tate SN, Bountra C, Birch R, Anand P (2004) Expression of the sodium channel beta3 subunit in injured human sensory neurons. Neuroreport 15(10):1629–1632

Catterall WA (2000) From ionic currents to molecular mechanisms: the structure and function of voltage-gated sodium channels. Neuron 26(1):13–25

Charalambous K, Wallace BA (2011) NaChBac: the long lost sodium channel ancestor. Biochemistry 50(32):6742–6752

Chen C, Bharucha V, Chen Y, Westenbroek RE, Brown A, Malhotra JD, Jones D, Avery C, Gillespie PJ 3rd, Kazen-Gillespie KA, Kazarinova-Noyes K, Shrager P, Saunders TL, Macdonald RL, Ransom BR, Scheuer T, Catterall WA, Isom LL (2002) Reduced sodium channel density, altered voltage dependence of inactivation, and increased susceptibility to seizures in mice lacking sodium channel beta 2-subunits. Proc Natl Acad Sci U S A 99(26): 17072–17077

Chen C, Calhoun JD, Zhang Y, Lopez-Santiago L, Zhou N, Davis TH, Salzer JL, Isom LL (2012) Identification of the cysteine residue responsible for disulfide linkage of Na^+ channel alpha and beta2 Subunits. J Biol Chem 287(46):39061–39069

Chen C, Westenbroek RE, Xu X, Edwards CA, Sorenson DR, Chen Y, McEwen DP, O'Malley HA, Bharucha V, Meadows LS, Knudsen GA, Vilaythong A, Noebels JL, Saunders TL, Scheuer T, Shrager P, Catterall WA, Isom LL (2004) Mice lacking sodium channel beta1 subunits display defects in neuronal excitability, sodium channel expression, and nodal architecture. J Neurosci 24(16):4030–4042

Chen Y, Yu FH, Sharp EM, Beacham D, Scheuer T, Catterall WA (2008) Functional properties and differential neuromodulation of Na(v)1.6 channels. Mol Cell Neurosci 38(4):607–615

Chioni AM, Brackenbury WJ, Calhoun JD, Isom LL, Djamgoz MB (2009) A novel adhesion molecule in human breast cancer cells: voltage-gated Na^+ channel beta1 subunit. Int J Biochem Cell Biol 41(5):1216–1227

Chopra SS, Watanabe H, Zhong TP, Roden DM (2007) Molecular cloning and analysis of zebrafish voltage-gated sodium channel beta subunit genes: implications for the evolution of electrical signaling in vertebrates. BMC Evol Biol 7:113

Cirak S, Arechavala-Gomeza V, Guglieri M, Feng L, Torelli S, Anthony K, Abbs S, Garralda ME, Bourke J, Wells DJ, Dickson G, Wood MJ, Wilton SD, Straub V, Kole R, Shrewsbury SB, Sewry C, Morgan JE, Bushby K, Muntoni F (2011) Exon skipping and dystrophin restoration in patients with Duchenne muscular dystrophy after systemic phosphorodiamidate morpholino oligomer treatment: an open-label, phase 2, dose-escalation study. Lancet 378(9791):595–605

Claes L, Del-Favero J, Ceulemans B, Lagae L, Van Broeckhoven C, De Jonghe P (2001) De novo mutations in the sodium-channel gene SCN1A cause severe myoclonic epilepsy of infancy. Am J Hum Genet 68(6):1327–1332

Davis TH, Chen C, Isom LL (2004) Sodium channel beta1 subunits promote neurite outgrowth in cerebellar granule neurons. J Biol Chem 279(49):51424–51432

Delmar M (2004) The intercalated disk as a single functional unit. Heart Rhythm 1(1):12–13

Deschenes I, Armoundas AA, Jones SP, Tomaselli GF (2008) Post-transcriptional gene silencing of KChIP2 and Navbeta1 in neonatal rat cardiac myocytes reveals a functional association between Na and Ito currents. J Mol Cell Cardiol 45(3):336–346

Deschenes I, Tomaselli GF (2002) Modulation of Kv4.3 current by accessory subunits. FEBS Lett 528(1–3):183–188

Dhar Malhotra J, Chen C, Rivolta I, Abriel H, Malhotra R, Mattei LN, Brosius FC, Kass RS, Isom LL (2001) Characterization of sodium channel alpha- and beta-subunits in rat and mouse cardiac myocytes. Circulation 103(9):1303–1310

Dib-Hajj SD, Waxman SG (2010) Isoform-specific and pan-channel partners regulate trafficking and plasma membrane stability; and alter sodium channel gating properties. Neurosci Lett 486 (2):84–91

Diss JK, Fraser SP, Walker MM, Patel A, Latchman DS, Djamgoz MB (2008) Beta-subunits of voltage-gated sodium channels in human prostate cancer: quantitative in vitro and in vivo analyses of mRNA expression. Prostate Cancer Prostatic Dis 11(4):325–333

Eckford PD, Li C, Ramjeesingh M, Bear CE (2012) Cystic fibrosis transmembrane conductance regulator (CFTR) potentiator VX-770 (ivacaftor) opens the defective channel gate of mutant CFTR in a phosphorylation-dependent but ATP-independent manner. J Biol Chem 287 (44):36639–36649

Ellerkmann RK, Remy S, Chen J, Sochivko D, Elger CE, Urban BW, Becker A, Beck H (2003) Molecular and functional changes in voltage-dependent Na(+) channels following pilocarpine-induced status epilepticus in rat dentate granule cells. Neuroscience 119(2):323–333

Escayg A, Goldin AL (2010) Sodium channel SCN1A and epilepsy: mutations and mechanisms. Epilepsia 51(9):1650–1658

Escayg A, MacDonald BT, Meisler MH, Baulac S, Huberfeld G, An-Gourfinkel I, Brice A, LeGuern E, Moulard B, Chaigne D, Buresi C, Malafosse A (2000) Mutations of SCN1A, encoding a neuronal sodium channel, in two families with GEFS+2. Nat Genet 24(4):343–345

Fein AJ, Meadows LS, Chen C, Slat EA, Isom LL (2007) Cloning and expression of a zebrafish SCN1B ortholog and identification of a species-specific splice variant. BMC Genom 8:226

Fein AJ, Wright MA, Slat EA, Ribera AB, Isom LL (2008) scn1bb, a zebrafish ortholog of SCN1B expressed in excitable and nonexcitable cells, affects motor neuron axon morphology and touch sensitivity. J Neurosci 28(47):12510–12522

Fendri-Kriaa N, Kammoun F, Salem IH, Kifagi C, Mkaouar-Rebai E, Hsairi I, Rebai A, Triki C, Fakhfakh F (2011) New mutation c.374C>T and a putative disease-associated haplotype within SCN1B gene in Tunisian families with febrile seizures. Eur J Neurol 18(5):695–702

Filbin MT, Tennekoon GI (1993) Homophilic adhesion of the myelin P0 protein requires glycosylation of both molecules in the homophilic pair. J Cell Biol 122(2):451–459

Goldin AL (2002) Evolution of voltage-gated Na(+) channels. J Exp Biol 205(Pt 5):575–584

Goldin AL, Snutch T, Lubbert H, Dowsett A, Marshall J, Auld V, Downey W, Fritz LC, Lester HA, Dunn R et al (1986) Messenger RNA coding for only the alpha subunit of the rat brain Na channel is sufficient for expression of functional channels in Xenopus oocytes. Proc Natl Acad Sci U S A 83(19):7503–7507

Grieco TM, Malhotra JD, Chen C, Isom LL, Raman IM (2005) Open-channel block by the cytoplasmic tail of sodium channel beta4 as a mechanism for resurgent sodium current. Neuron 45(2):233–244

Hakim P, Brice N, Thresher R, Lawrence J, Zhang Y, Jackson AP, Grace AA, Huang CL (2010) Scn3b knockout mice exhibit abnormal sino-atrial and cardiac conduction properties. Acta Physiol 198(1):47–59

Hakim P, Gurung IS, Pedersen TH, Thresher R, Brice N, Lawrence J, Grace AA, Huang CL (2008) Scn3b knockout mice exhibit abnormal ventricular electrophysiological properties. Prog Biophys Mol Biol 98(2–3):251–266

Hartshorne RP, Catterall WA (1984) The sodium channel from rat brain. Purification and subunit composition. J Biol Chem 259(3):1667–1675

Hartshorne RP, Messner DJ, Coppersmith JC, Catterall WA (1982) The saxitoxin receptor of the sodium channel from rat brain. Evidence for two nonidentical beta subunits. J Biol Chem 257 (23):13888–13891

Irie K, Kitagawa K, Nagura H, Imai T, Shimomura T, Fujiyoshi Y (2010) Comparative study of the gating motif and C-type inactivation in prokaryotic voltage-gated sodium channels. J Biol Chem 285(6):3685–3694

Ishikawa T, Takahashi N, Ohno S, Sakurada H, Nakamura K, On YK, Park JE, Makiyama T, Horie M, Arimura T, Makita N, Kimura A (2013) Novel SCN3B mutation associated with brugada syndrome affects intracellular trafficking and function of Nav1.5. Circ J 77(4): 959–967

Isom LL (2001) Sodium channel beta subunits: anything but auxiliary. Neuroscientist 7(1):42–54

Isom LL, De Jongh KS, Catterall WA (1994) Auxiliary subunits of voltage-gated ion channels. Neuron 12(6):1183–1194

Isom LL, De Jongh KS, Patton DE, Reber BF, Offord J, Charbonneau H, Walsh K, Goldin AL, Catterall WA (1992) Primary structure and functional expression of the beta 1 subunit of the rat brain sodium channel. Science 256(5058):839–842

Isom LL, Ragsdale DS, De Jongh KS, Westenbroek RE, Reber BF, Scheuer T, Catterall WA (1995a) Structure and function of the beta 2 subunit of brain sodium channels, a transmembrane glycoprotein with a CAM motif. Cell 83(3):433–442

Isom LL, Scheuer T, Brownstein AB, Ragsdale DS, Murphy BJ, Catterall WA (1995b) Functional co-expression of the beta 1 and type IIA alpha subunits of sodium channels in a mammalian cell line. J Biol Chem 270(7):3306–3312

Ito M, Xu H, Guffanti AA, Wei Y, Zvi L, Clapham DE, Krulwich TA (2004) The voltage-gated Na^+ channel NaVBP has a role in motility, chemotaxis, and pH homeostasis of an alkaliphilic Bacillus. Proc Natl Acad Sci U S A 101(29):10566–10571

Johnson D, Bennett ES (2006) Isoform-specific effects of the beta2 subunit on voltage-gated sodium channel gating. J Biol Chem 281(36):25875–25881

Johnson D, Montpetit ML, Stocker PJ, Bennett ES (2004) The sialic acid component of the beta1 subunit modulates voltage-gated sodium channel function. J Biol Chem 279(43):44303–44310

Joho RH, Moorman JR, VanDongen AM, Kirsch GE, Silberberg H, Schuster G, Brown AM (1990) Toxin and kinetic profile of rat brain type III sodium channels expressed in Xenopus oocytes. Brain Res Mol Brain Res 7(2):105–113

Kaplan MR, Cho MH, Ullian EM, Isom LL, Levinson SR, Barres BA (2001) Differential control of clustering of the sodium channels Na(v)1.2 and Na(v)1.6 at developing CNS nodes of Ranvier. Neuron 30(1):105–119

Kaufmann SG, Westenbroek RE, Maass AH, Lange V, Renner A, Wischmeyer E, Bonz A, Muck J, Ertl G, Catterall WA, Scheuer T, Maier SK (2013) Distribution and function of sodium channel subtypes in human atrial myocardium. J Mol Cell Cardiol 61:133–141

Kazarinova-Noyes K, Malhotra JD, McEwen DP, Mattei LN, Berglund EO, Ranscht B, Levinson SR, Schachner M, Shrager P, Isom LL, Xiao ZC (2001) Contactin associates with Na^+ channels and increases their functional expression. J Neurosci 21(19):7517–7525

Kazen-Gillespie KA, Ragsdale DS, D'Andrea MR, Mattei LN, Rogers KE, Isom LL (2000) Cloning, localization, and functional expression of sodium channel beta1A subunits. J Biol Chem 275(2):1079–1088

Kim DY, Carey BW, Wang H, Ingano LA, Binshtok AM, Wertz MH, Pettingell WH, He P, Lee VM, Woolf CJ, Kovacs DM (2007) BACE1 regulates voltage-gated sodium channels and neuronal activity. Nat Cell Biol 9(7):755–764

Kim DY, Ingano LA, Carey BW, Pettingell WH, Kovacs DM (2005) Presenilin/gamma-secretase-mediated cleavage of the voltage-gated sodium channel beta2-subunit regulates cell adhesion and migration. J Biol Chem 280(24):23251–23261

Ko SH, Lenkowski PW, Lee HC, Mounsey JP, Patel MK (2005) Modulation of Na(v)1.5 by beta1– and beta3-subunit co-expression in mammalian cells. Pflugers Arch 449(4):403–412

Koishi R, Xu H, Ren D, Navarro B, Spiller BW, Shi Q, Clapham DE (2004) A superfamily of voltage-gated sodium channels in bacteria. J Biol Chem 279(10):9532–9538

Krafte DS, Goldin AL, Auld VJ, Dunn RJ, Davidson N, Lester HA (1990) Inactivation of cloned Na channels expressed in Xenopus oocytes. J Gen Physiol 96(4):689–706

Kramer EM, Klein C, Koch T, Boytinck M, Trotter J (1999) Compartmentation of Fyn kinase with glycosylphosphatidylinositol-anchored molecules in oligodendrocytes facilitates kinase activation during myelination. J Biol Chem 274(41):29042–29049

Lenkowski PW, Shah BS, Dinn AE, Lee K, Patel MK (2003) Lidocaine block of neonatal Nav1.3 is differentially modulated by co-expression of beta1 and beta3 subunits. Eur J Pharmacol 467 (1–3):23–30

Li RG, Wang Q, Xu YJ, Zhang M, Qu XK, Liu X, Fang WY, Yang YQ (2013) Mutations of the SCN4B-encoded sodium channel beta4 subunit in familial atrial fibrillation. Int J Mol Med 32:144–150

Li J, Waterhouse RM, Zdobnov EM (2011) A remarkably stable TipE gene cluster: evolution of insect para sodium channel auxiliary subunits. BMC Evol Biol 11:337

Lo AC, Black JA, Waxman SG (2002) Neuroprotection of axons with phenytoin in experimental allergic encephalomyelitis. Neuroreport 13(15):1909–1912

Lo AC, Saab CY, Black JA, Waxman SG (2003) Phenytoin protects spinal cord axons and preserves axonal conduction and neurological function in a model of neuroinflammation in vivo. J Neurophysiol 90(5):3566–3571

Lopez-Santiago LF, Brackenbury WJ, Chen C, Isom LL (2011) Na^+ channel Scn1b gene regulates dorsal root ganglion nociceptor excitability in vivo. J Biol Chem 286(26):22913–22923

Lopez-Santiago LF, Meadows LS, Ernst SJ, Chen C, Malhotra JD, McEwen DP, Speelman A, Noebels JL, Maier SK, Lopatin AN, Isom LL (2007) Sodium channel Scn1b null mice exhibit prolonged QT and RR intervals. J Mol Cell Cardiol 43(5):636–647

Lopez-Santiago LF, Pertin M, Morisod X, Chen C, Hong S, Wiley J, Decosterd I, Isom LL (2006) Sodium channel beta2 subunits regulate tetrodotoxin-sensitive sodium channels in small dorsal root ganglion neurons and modulate the response to pain. J Neurosci 26(30):7984–7994

Lowery LA, Van Vactor D (2009) The trip of the tip: understanding the growth cone machinery. Nat Rev Mol Cell Biol 10(5):332–343

Lucas PT, Meadows LS, Nicholls J, Ragsdale DS (2005) An epilepsy mutation in the beta1 subunit of the voltage-gated sodium channel results in reduced channel sensitivity to phenytoin. Epilepsy Res 64(3):77–84

Maier SK, Westenbroek RE, McCormick KA, Curtis R, Scheuer T, Catterall WA (2004) Distinct subcellular localization of different sodium channel alpha and beta subunits in single ventricular myocytes from mouse heart. Circulation 109(11):1421–1427

Malhotra JD, Kazen-Gillespie K, Hortsch M, Isom LL (2000) Sodium channel beta subunits mediate homophilic cell adhesion and recruit ankyrin to points of cell–cell contact. J Biol Chem 275(15):11383–11388

Malhotra JD, Koopmann MC, Kazen-Gillespie KA, Fettman N, Hortsch M, Isom LL (2002) Structural requirements for interaction of sodium channel beta 1 subunits with ankyrin. J Biol Chem 277(29):26681–26688

Malhotra JD, Thyagarajan V, Chen C, Isom LL (2004) Tyrosine-phosphorylated and nonphosphorylated sodium channel beta1 subunits are differentially localized in cardiac myocytes. J Biol Chem 279(39):40748–40754

Marionneau C, Carrasquillo Y, Norris AJ, Townsend RR, Isom LL, Link AJ, Nerbonne JM (2012) The sodium channel accessory subunit Navbeta1 regulates neuronal excitability through modulation of repolarizing voltage-gated K(+) channels. J Neurosci 32(17):5716–5727

McCormick KA, Isom LL, Ragsdale D, Smith D, Scheuer T, Catterall WA (1998) Molecular determinants of Na+ channel function in the extracellular domain of the beta1 subunit. J Biol Chem 273(7):3954–3962

McEwen DP, Chen C, Meadows LS, Lopez-Santiago L, Isom LL (2009) The voltage-gated Na+ channel beta3 subunit does not mediate trans homophilic cell adhesion or associate with the cell adhesion molecule contactin. Neurosci Lett 462(3):272–275

McEwen DP, Isom LL (2004) Heterophilic interactions of sodium channel beta1 subunits with axonal and glial cell adhesion molecules. J Biol Chem 279(50):52744–52752

McEwen DP, Meadows LS, Chen C, Thyagarajan V, Isom LL (2004) Sodium channel beta1 subunit-mediated modulation of Nav1.2 currents and cell surface density is dependent on interactions with contactin and ankyrin. J Biol Chem 279(16):16044–16049

Meadows LS, Chen YH, Powell AJ, Clare JJ, Ragsdale DS (2002a) Functional modulation of human brain Nav1.3 sodium channels, expressed in mammalian cells, by auxiliary beta 1, beta 2 and beta 3 subunits. Neuroscience 114(3):745–753

Meadows LS, Malhotra J, Loukas A, Thyagarajan V, Kazen-Gillespie KA, Koopman MC, Kriegler S, Isom LL, Ragsdale DS (2002b) Functional and biochemical analysis of a sodium channel beta1 subunit mutation responsible for generalized epilepsy with febrile seizures plus type 1. J Neurosci 22(24):10699–10709

Meadows L, Malhotra JD, Stetzer A, Isom LL, Ragsdale DS (2001) The intracellular segment of the sodium channel beta 1 subunit is required for its efficient association with the channel alpha subunit. J Neurochem 76(6):1871–1878

Medeiros-Domingo A, Kaku T, Tester DJ, Iturralde-Torres P, Itty A, Ye B, Valdivia C, Ueda K, Canizales-Quinteros S, Tusie-Luna MT, Makielski JC, Ackerman MJ (2007) SCN4B-encoded sodium channel beta4 subunit in congenital long-QT syndrome. Circulation 116(2):134–142

Meisler MH, Kearney JA (2005) Sodium channel mutations in epilepsy and other neurological disorders. J Clin Investig 115(8):2010–2017

Messner DJ, Catterall WA (1985) The sodium channel from rat brain. Separation and characterization of subunits. J Biol Chem 260(19):10597–10604

Miller JA, Agnew WS, Levinson SR (1983) Principal glycopeptide of the tetrodotoxin/saxitoxin binding protein from electrophorus electricus: isolation and partial chemical and physical characterization. Biochemistry 22(2):462–470

Miyazaki H, Oyama F, Wong HK, Kaneko K, Sakurai T, Tamaoka A, Nukina N (2007) BACE1 modulates filopodia-like protrusions induced by sodium channel beta4 subunit. Biochem Biophys Res Commun 361(1):43–48

Morgan K, Stevens EB, Shah B, Cox PJ, Dixon AK, Lee K, Pinnock RD, Hughes J, Richardson PJ, Mizuguchi K, Jackson AP (2000) beta 3: an additional auxiliary subunit of the voltage-sensitive sodium channel that modulates channel gating with distinct kinetics. Proc Natl Acad Sci U S A 97(5):2308–2313

Nguyen HM, Miyazaki H, Hoshi N, Smith BJ, Nukina N, Goldin AL, Chandy KG (2012) Modulation of voltage-gated K^+ channels by the sodium channel beta1 subunit. Proc Natl Acad Sci U S A 109(45):18577–18582

Noda M, Ikeda T, Suzuki H, Takeshima H, Takahashi T, Kuno M, Numa S (1986) Expression of functional sodium channels from cloned cDNA. Nature 322(6082):826–828

O'Brien RJ, Wong PC (2011) Amyloid precursor protein processing and Alzheimer's disease. Annu Rev Neurosci 34:185–204

O'Malley HA, Shreiner AB, Chen GH, Huffnagle GB, Isom LL (2009) Loss of Na^+ channel beta2 subunits is neuroprotective in a mouse model of multiple sclerosis. Mol Cell Neurosci 40(2): 143–155

Ogiwara I, Nakayama T, Yamagata T, Ohtani H, Mazaki E, Tsuchiya S, Inoue Y, Yamakawa K (2012) A homozygous mutation of voltage-gated sodium channel beta(I) gene SCN1B in a patient with Dravet syndrome. Epilepsia 53(12):e200–203

Oh Y, Lee YJ, Waxman SG (1997) Regulation of Na^+ channel beta 1 and beta 2 subunit mRNA levels in cultured rat astrocytes. Neurosci Lett 234(2–3):107–110

Oh Y, Waxman SG (1995) Differential Na^+ channel beta 1 subunit mRNA expression in stellate and flat astrocytes cultured from rat cortex and cerebellum: a combined in situ hybridization and immunocytochemistry study. Glia 13(3):166–173

Olesen MS, Jespersen T, Nielsen JB, Liang B, Moller DV, Hedley P, Christiansen M, Varro A, Olesen SP, Haunso S, Schmitt N, Svendsen JH (2011) Mutations in sodium channel beta-subunit SCN3B are associated with early-onset lone atrial fibrillation. Cardiovasc Res 89(4): 786–793

Oyama F, Miyazaki H, Sakamoto N, Becquet C, Machida Y, Kaneko K, Uchikawa C, Suzuki T, Kurosawa M, Ikeda T, Tamaoka A, Sakurai T, Nukina N (2006) Sodium channel beta4 subunit: down-regulation and possible involvement in neuritic degeneration in Huntington's disease transgenic mice. J Neurochem 98(2):518–529

Patino GA, Brackenbury WJ, Bao Y, Lopez-Santiago LF, O'Malley HA, Chen C, Calhoun JD, Lafreniere RG, Cossette P, Rouleau GA, Isom LL (2011) Voltage-gated Na^+ channel beta1B: a secreted cell adhesion molecule involved in human epilepsy. J Neurosci 31(41):14577–14591

Patino GA, Claes LR, Lopez-Santiago LF, Slat EA, Dondeti RS, Chen C, O'Malley HA, Gray CB, Miyazaki H, Nukina N, Oyama F, De Jonghe P, Isom LL (2009) A functional null mutation of SCN1B in a patient with Dravet syndrome. J Neurosci 29(34):10764–10778

Patino GA, Isom LL (2010) Electrophysiology and beyond: multiple roles of Na^+ channel beta subunits in development and disease. Neurosci Lett 486(2):53–59

Payandeh J, Scheuer T, Zheng N, Catterall WA (2011) The crystal structure of a voltage-gated sodium channel. Nature 475(7356):353–358

Pertin M, Ji RR, Berta T, Powell AJ, Karchewski L, Tate SN, Isom LL, Woolf CJ, Gilliard N, Spahn DR, Decosterd I (2005) Upregulation of the voltage-gated sodium channel beta2 subunit in neuropathic pain models: characterization of expression in injured and non-injured primary sensory neurons. J Neurosci 25(47):10970–10980

Poliak S, Peles E (2003) The local differentiation of myelinated axons at nodes of Ranvier. Nat Rev Neurosci 4(12):968–980

Prevarskaya N, Skryma R, Shuba Y (2010) Ion channels and the hallmarks of cancer. Trends Mol Med 16(3):107–121

Qin N, D'Andrea MR, Lubin ML, Shafaee N, Codd EE, Correa AM (2003) Molecular cloning and functional expression of the human sodium channel beta1B subunit, a novel splicing variant of the beta1 subunit. Eur J Biochem/FEBS 270(23):4762–4770

Ragsdale DS (2008) How do mutant Nav1.1 sodium channels cause epilepsy? Brain Res Rev 58 (1):149–159

Raman IM, Bean BP (1997) Resurgent sodium current and action potential formation in dissociated cerebellar Purkinje neurons. J Neurosci 17(12):4517–4526

Raman IM, Sprunger LK, Meisler MH, Bean BP (1997) Altered subthreshold sodium currents and disrupted firing patterns in Purkinje neurons of Scn8a mutant mice. Neuron 19(4):881–891

Rasband MN (2010) The axon initial segment and the maintenance of neuronal polarity. Nat Rev Neurosci 11(8):552–562

Ratcliffe CF, Qu Y, McCormick KA, Tibbs VC, Dixon JE, Scheuer T, Catterall WA (2000) A sodium channel signaling complex: modulation by associated receptor protein tyrosine phosphatase beta. Nat Neurosci 3(5):437–444

Ratcliffe CF, Westenbroek RE, Curtis R, Catterall WA (2001) Sodium channel beta1 and beta3 subunits associate with neurofascin through their extracellular immunoglobulin-like domain. J Cell Biol 154(2):427–434

Remme CA, Bezzina CR (2010) Sodium channel (dys)function and cardiac arrhythmias. Cardiovasc Ther 28(5):287–294

Remme CA, Scicluna BP, Verkerk AO, Amin AS, van Brunschot S, Beekman L, Deneer VH, Chevalier C, Oyama F, Miyazaki H, Nukina N, Wilders R, Escande D, Houlgatte R, Wilde AA, Tan HL, Veldkamp MW, de Bakker JM, Bezzina CR (2009) Genetically determined differences in sodium current characteristics modulate conduction disease severity in mice with cardiac sodium channelopathy. Circ Res 104(11):1283–1292

Ren D, Navarro B, Xu H, Yue L, Shi Q, Clapham DE (2001) A prokaryotic voltage-gated sodium channel. Science 294(5550):2372–2375

Riuro H, Beltran-Alvarez P, Tarradas A, Selga E, Campuzano O, Verges M, Pagans S, Iglesias A, Brugada J, Brugada P, Vazquez FM, Perez GJ, Scornik FS, Brugada R (2013) A missense mutation in the sodium channel beta2 subunit reveals SCN2B as a new candidate gene for Brugada syndrome. Hum Mutat 34(7):961–966

Rusconi R, Combi R, Cestele S, Grioni D, Franceschetti S, Dalpra L, Mantegazza M (2009) A rescuable folding defective Nav1.1 (SCN1A) sodium channel mutant causes GEFS+: common mechanism in Nav1.1 related epilepsies? Hum Mutat 30(7):E747–760

Rusconi R, Scalmani P, Cassulini RR, Giunti G, Gambardella A, Franceschetti S, Annesi G, Wanke E, Mantegazza M (2007) Modulatory proteins can rescue a trafficking defective epileptogenic Nav1.1 Na^+ channel mutant. J Neurosci 27(41):11037–11046

Scheffer IE, Harkin LA, Grinton BE, Dibbens LM, Turner SJ, Zielinski MA, Xu R, Jackson G, Adams J, Connellan M, Petrou S, Wellard RM, Briellmann RS, Wallace RH, Mulley JC,

Berkovic SF (2007) Temporal lobe epilepsy and GEFS+ phenotypes associated with SCN1B mutations. Brain 130(Pt 1):100–109

Scheuer T, Auld VJ, Boyd S, Offord J, Dunn R, Catterall WA (1990) Functional properties of rat brain sodium channels expressed in a somatic cell line. Science 247(4944):854–858

Schmidt JW, Catterall WA (1986) Biosynthesis and processing of the alpha subunit of the voltage-sensitive sodium channel in rat brain neurons. Cell 46(3):437–444

Schmidt J, Rossie S, Catterall WA (1985) A large intracellular pool of inactive Na channel alpha subunits in developing rat brain. Proc Natl Acad Sci U S A 82(14):4847–4851

Shah BS, Stevens EB, Gonzalez MI, Bramwell S, Pinnock RD, Lee K, Dixon AK (2000) beta3, a novel auxiliary subunit for the voltage-gated sodium channel, is expressed preferentially in sensory neurons and is upregulated in the chronic constriction injury model of neuropathic pain. Eur J Neurosci 12(11):3985–3990

Shah BS, Stevens EB, Pinnock RD, Dixon AK, Lee K (2001) Developmental expression of the novel voltage-gated sodium channel auxiliary subunit beta3, in rat CNS. J Physiol 534(Pt 3): 763–776

Shi X, Yasumoto S, Nakagawa E, Fukasawa T, Uchiya S, Hirose S (2009) Missense mutation of the sodium channel gene SCN2A causes Dravet syndrome. Brain Dev 31(10):758–762

Spampanato J, Kearney JA, de Haan G, McEwen DP, Escayg A, Aradi I, MacDonald BT, Levin SI, Soltesz I, Benna P, Montalenti E, Isom LL, Goldin AL, Meisler MH (2004) A novel epilepsy mutation in the sodium channel SCN1A identifies a cytoplasmic domain for beta subunit interaction. J Neurosci 24(44):10022–10034

Srinivasan J, Schachner M, Catterall WA (1998) Interaction of voltage-gated sodium channels with the extracellular matrix molecules tenascin-C and tenascin-R. Proc Natl Acad Sci U S A 95(26):15753–15757

Sugawara T, Tsurubuchi Y, Agarwala KL, Ito M, Fukuma G, Mazaki-Miyazaki E, Nagafuji H, Noda M, Imoto K, Wada K, Mitsudome A, Kaneko S, Montal M, Nagata K, Hirose S, Yamakawa K (2001) A missense mutation of the Na^+ channel alpha II subunit gene Na(v) 1.2 in a patient with febrile and afebrile seizures causes channel dysfunction. Proc Natl Acad Sci U S A 98(11):6384–6389

Surges R, Sander JW (2012) Sudden unexpected death in epilepsy: mechanisms, prevalence, and prevention. Curr Opin Neurol 25(2):201–207

Sutkowski EM, Catterall WA (1990) Beta 1 subunits of sodium channels. Studies with subunit-specific antibodies. J Biol Chem 265(21):12393–12399

Takahashi N, Kikuchi S, Dai Y, Kobayashi K, Fukuoka T, Noguchi K (2003) Expression of auxiliary beta subunits of sodium channels in primary afferent neurons and the effect of nerve injury. Neuroscience 121(2):441–450

Tan BH, Pundi KN, Van Norstrand DW, Valdivia CR, Tester DJ, Medeiros-Domingo A, Makielski JC, Ackerman MJ (2010) Sudden infant death syndrome-associated mutations in the sodium channel beta subunits. Heart Rhythm 7(6):771–778

Theile JW, Cummins TR (2011) Inhibition of Navbeta4 peptide-mediated resurgent sodium currents in Nav1.7 channels by carbamazepine, riluzole, and anandamide. Mol Pharmacol 80 (4):724–734

Thompson CH, Porter JC, Kahlig KM, Daniels MA, George AL Jr (2012) Nontruncating SCN1A mutations associated with severe myoclonic epilepsy of infancy impair cell surface expression. J Biol Chem 287(50):42001–42008

Towbin JA (2010) The A, B, Cs of sudden infant death syndrome: an electrical disorder? Heart Rhythm 7(6):779–780

Trinidad JC, Barkan DT, Gulledge BF, Thalhammer A, Sali A, Schoepfer R, Burlingame AL (2012) Global identification and characterization of both O-GlcNAcylation and phosphorylation at the murine synapse. Mol Cell Proteomics 11(8):215–229

Uebachs M, Albus C, Opitz T, Isom L, Niespodziany I, Wolff C, Beck H (2012) Loss of beta1 accessory Na^+ channel subunits causes failure of carbamazepine, but not of lacosamide, in

blocking high-frequency firing via differential effects on persistent Na^+ currents. Epilepsia 53 (11):1959–1967

Uebachs M, Opitz T, Royeck M, Dickhof G, Horstmann MT, Isom LL, Beck H (2010) Efficacy loss of the anticonvulsant carbamazepine in mice lacking sodium channel beta subunits via paradoxical effects on persistent sodium currents. J Neurosci 30(25):8489–8501

Van Wart A, Matthews G (2006) Impaired firing and cell-specific compensation in neurons lacking nav1.6 sodium channels. J Neurosci 26(27):7172–7180

Van Wart A, Trimmer JS, Matthews G (2007) Polarized distribution of ion channels within microdomains of the axon initial segment. J Comp Neurol 500(2):339–352

Waechter CJ, Schmidt JW, Catterall WA (1983) Glycosylation is required for maintenance of functional sodium channels in neuroblastoma cells. J Biol Chem 258(8):5117–5123

Wallace RH, Scheffer IE, Parasivam G, Barnett S, Wallace GB, Sutherland GR, Berkovic SF, Mulley JC (2002) Generalized epilepsy with febrile seizures plus: mutation of the sodium channel subunit SCN1B. Neurology 58(9):1426–1429

Wallace RH, Wang DW, Singh R, Scheffer IE, George AL Jr, Phillips HA, Saar K, Reis A, Johnson EW, Sutherland GR, Berkovic SF, Mulley JC (1998) Febrile seizures and generalized epilepsy associated with a mutation in the Na^+-channel beta1 subunit gene SCN1B. Nat Genet 19(4):366–370

Wang DW, Desai RR, Crotti L, Arnestad M, Insolia R, Pedrazzini M, Ferrandi C, Vege A, Rognum T, Schwartz PJ, George AL Jr (2007) Cardiac sodium channel dysfunction in sudden infant death syndrome. Circulation 115(3):368–376

Watanabe H, Darbar D, Kaiser DW, Jiramongkolchai K, Chopra S, Donahue BS, Kannankeril PJ, Roden DM (2009) Mutations in sodium channel beta1- and beta2-subunits associated with atrial fibrillation. Circ Arrhythm Electrophysiol 2(3):268–275

Watanabe H, Koopmann TT, Le Scouarnec S, Yang T, Ingram CR, Schott JJ, Demolombe S, Probst V, Anselme F, Escande D, Wiesfeld AC, Pfeufer A, Kaab S, Wichmann HE, Hasdemir C, Aizawa Y, Wilde AA, Roden DM, Bezzina CR (2008) Sodium channel beta1 subunit mutations associated with Brugada syndrome and cardiac conduction disease in humans. J Clin Investig 118(6):2260–2268

Waxman SG (2006) Axonal conduction and injury in multiple sclerosis: the role of sodium channels. Nat Rev Neurosci 7(12):932–941

Wimmer VC, Reid CA, Mitchell S, Richards KL, Scaf BB, Leaw BT, Hill EL, Royeck M, Horstmann MT, Cromer BA, Davies PJ, Xu R, Lerche H, Berkovic SF, Beck H, Petrou S (2010) Axon initial segment dysfunction in a mouse model of genetic epilepsy with febrile seizures plus. J Clin Investig 120(8):2661–2671

Wong HK, Sakurai T, Oyama F, Kaneko K, Wada K, Miyazaki H, Kurosawa M, De Strooper B, Saftig P, Nukina N (2005) beta subunits of voltage-gated sodium channels are novel substrates of beta-site amyloid precursor protein-cleaving enzyme (BACE1) and gamma-secretase. J Biol Chem 280(24):23009–23017

Xiao ZC, Ragsdale DS, Malhotra JD, Mattei LN, Braun PE, Schachner M, Isom LL (1999) Tenascin-R is a functional modulator of sodium channel beta subunits. J Biol Chem 274 (37):26511–26517

Xu R, Thomas EA, Gazina EV, Richards KL, Quick M, Wallace RH, Harkin LA, Heron SE, Berkovic SF, Scheffer IE, Mulley JC, Petrou S (2007) Generalized epilepsy with febrile seizures plus-associated sodium channel beta1 subunit mutations severely reduce beta subunit-mediated modulation of sodium channel function. Neuroscience 148(1):164–174

Yang M, Kozminski DJ, Wold LA, Modak R, Calhoun JD, Isom LL, Brackenbury WJ (2012) Therapeutic potential for phenytoin: targeting Na(v)1.5 sodium channels to reduce migration and invasion in metastatic breast cancer. Breast Cancer Res Treat 134(2):603–615

Yereddi NR, Cusdin FS, Namadurai S, Packman LC, Monie TP, Slavny P, Clare JJ, Powell AJ, Jackson AP (2013) The immunoglobulin domain of the sodium channel beta3 subunit contains a surface-localized disulfide bond that is required for homophilic binding. FASEB J 27(2): 568–580

Yu FH, Westenbroek RE, Silos-Santiago I, McCormick KA, Lawson D, Ge P, Ferriera H, Lilly J, DiStefano PS, Catterall WA, Scheuer T, Curtis R (2003) Sodium channel beta4, a new disulfide-linked auxiliary subunit with similarity to beta2. J Neurosci 23(20):7577–7585

Zhou TT, Zhang ZW, Liu J, Zhang JP, Jiao BH (2012) Glycosylation of the sodium channel beta4 subunit is developmentally regulated and involves in neuritic degeneration. Int J Biol Sci 8(5): 630–639

Altered Sodium Channel Gating as Molecular Basis for Pain: Contribution of Activation, Inactivation, and Resurgent Currents

Angelika Lampert, Mirjam Eberhardt, and Stephen G. Waxman

Contents

A. Lampert (✉)
Institute of Physiology, RWTH Aachen University, Pauwelsstrasse 30, 52074 Aachen, Germany
e-mail: alampert@ukaachen.de

M. Eberhardt
Department of Anesthesiology and Intensive Care Medicine, Hannover Medical School, Carl-Neuberg-Strasse 1, 30625, Hannover, Germany
e-mail: eberhardt.mirjam@mh-hannover.de

S.G. Waxman
Center for Neuroscience and Regeneration/Neurorehabilitation Research, Yale University School of Medicine, West Haven, CT, USA

VA Neuroscience Research Center, Bldg. 34, VA Connecticut (127A), 950 Campbell Avenue, West Haven, CT, 06516, USA
e-mail: stephen.waxman@yale.edu

P.C. Ruben (ed.), *Voltage Gated Sodium Channels*, Handbook of Experimental Pharmacology 221, DOI 10.1007/978-3-642-41588-3_5,

Abstract

Mutations in voltage-gated sodium channels, especially Nav1.7, can cause the genetic pain syndromes inherited erythromelalgia, small fiber neuropathy, paroxysmal extreme pain disorder, and chronic insensitivity to pain. Functional analysis of these mutations offers the possibility of understanding the potential pathomechanisms of these disease patterns and also may help to explicate the molecular mechanisms underlying pain in normal conditions. The mutations are distributed over the whole channel protein, but nevertheless induce similar changes for each pain syndrome. In this review we focus on their impact on sodium channel gating, which may be conferred via modulation of (1) conformation (affecting all gating characteristics); (2) the amount of voltage-sensing charges (affecting mainly activation); (3) interaction within the protein (e.g., binding of the inactivation linker); and (4) interaction with other proteins (e.g., for generation of resurgent currents). Understanding the molecular basis for each gating mode and its impact on cellular excitability and nociception in each disease type may provide a basis for development of more specific and effective therapeutic tools.

Keywords

Pain • Nav1.7 • Resurgent current • Hyperexcitability

1 Inherited Pain Syndromes

Some of the most severe chronic pain syndromes, for which treatment is often unsatisfactory, are linked to mutations in the genes of voltage-gated sodium channels (Navs), primarily Nav1.7. Research on those mutations in recent years has fostered our knowledge of the molecular genesis of pain and our understanding of Nav gating and may facilitate the development of new therapeutic strategies targeted against Navs. Some promising drug candidates are already in clinical phase I.

In this chapter we will focus on three main chronic inherited pain syndromes linked to mutations in Navs: inherited Erythromelalgia (IEM), paroxysmal extreme pain disorder (PEPD), and small fiber neuropathy (SFN). All are due to gain-of-function mutations in the SCN9A gene, which codes for Nav1.7. Pain attacks may be initiated by distinct triggers for each of the three syndromes. Onset for patients

suffering from PEPD is in infancy or early childhood, or sometimes even in utero. IEM often begins in early childhood but can manifest in teenagers or adults and SFN usually has onset later in life in adulthood. Humans who have no functional Nav1.7 channel protein due to truncation mutations suffer from chronic insensitivity to pain (CIP): they do not feel any pain and therefore lack protective reflexes. Apart from anosmia, all other sensory functions of these patients are intact.

In the next sections we will begin with the physiological abnormalities observed due to mutations in Nav genes, ask what kind of mutations cause them, and finally what we can learn from it.

2 Activation

IEM patients suffer from attacks triggered by warmth, exercise, or elevated ambient temperature. Extensive research on more than 20 IEM mutations has confirmed that almost all shift the voltage dependence of activation to more hyperpolarized potentials. An overview can be found in Fig. 1 and Table 1, where all IEM mutations published to date are listed.

2.1 A Left Shift of Activation Excites Nociceptors in IEM

What is the effect of the hyperpolarizing shift of channel activation? Voltage-gated channels open when the membrane potential reaches a certain value, the channel-specific threshold potential. Navs open upon depolarization by generator potentials, such as those caused by the activation of warmth sensitive TRP channels. Collective opening of Navs leads to a sodium ion influx and the initiation of an action potential. The electrophysiological readout is the conductance–voltage relation, as shown in Fig. 1b which shows data for WT Nav1.7 and the S241T mutation as a typical example of an IEM mutation (Lampert et al. 2006).

When activation of Nav1.7 is shifted to more hyperpolarized potentials, a smaller generator potential is sufficient to open the channels and to induce action potentials, i.e., the expressing cells turn hyperexcitable. Transfection of several IEM mutations in sensory neurons indeed revealed a lower threshold for action potential firing (Cheng et al. 2010, 2011; Choi et al. 2010; Dib-Hajj et al. 2005; Han et al. 2009; Harty et al. 2006; Hoeijmakers et al. 2012; Yang et al. 2012) and this effect has been modeled in silico (Sheets et al. 2007).

Recently mutations in channels other than Nav1.7 have been reported in patients suffering from familial pain disorders or painful SFN [e.g., Nav1.8, TRPA1 (Faber et al. 2012; Kremeyer et al. 2010)]. Research is now focusing on their potential causative contribution to the disease.

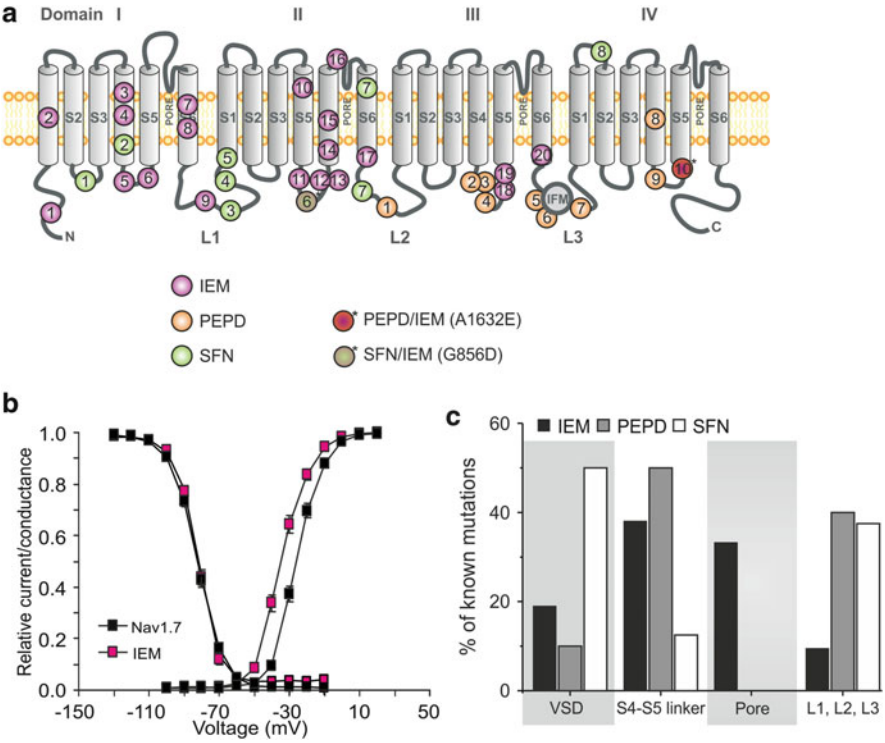

Fig. 1 (**a**) Schematic overview of known IEM, PEPD and SFN mutations in Nav1.7. Number for each disease mutation corresponds to those in the tables. (**b**) Steady-state fast inactivation and conductance–voltage relation of Nav1.7 WT and its S241T mutation as an example for a hyperpolarizing shift of voltage dependence of activation. Currents were recorded from transfected HEK cells (Lampert et al. 2006). (**c**) Relative distribution of gain-of-function mutations in Nav1.7 linked to inherited pain syndromes on the channel protein. IEM mutations, which alter predominantly activation, are mainly situated in the S4–S5 linker, whereas PEPD mutations also largely affect the intracellular linkers that are implicated in fast inactivation. SFN linked mutations which have a less well-defined clinical picture, cluster in the voltage-sensing domains of Nav1.7. VSD: voltage-sensing domain (S1–S4). S4–S5-linker: alpha-helical channel part at the intracellular side connecting the VSD with the pore consisting of S5 and S6. L1, L2, or L3 refer to the large intracellular linkers between the domains. L3 contains the inactivation particle (IFM)

2.2 Molecular Basis of Activation: What Do We Learn from IEM Mutations?

Although almost all IEM mutations affect activation kinetics of Nav1.7, these amino acid substitutions can be found all over the channel protein (see Fig. 1a). This may provide an opportunity to learn about the role of different channel parts during activation and to better understand its structural basis.

Table 1 Mutations in Nav1.7 causing IEM

#	Channel part	Mutation	Charge	Activation			Fast inactivation		Persistent current	Resurgent current	Slow inactivation	Ramp current	DRG/CC Excitability	References
				Vhalf	Deactivation	ttp	Vhalf	Decay						
1	Linker	Q10R	Polar → positive	−5.3	Slower	Faster	n.s.	n.d.	n.d.	n.d.	Enhanced	Same	Enhanced	Han et al. (2009)
2	VSD	I136V	=Hydrophobic	−5.7	Slower	Same	n.s.	Slower	n.d.	n.d.	Enhanced	Larger	n.d.	Cheng et al. (2008), Lee et al. (2007)
				−9.4	n.d.	n.d.	+ 3.7	n.d.	n.d.	n.d.	n.d.	n.d.	n.d.	Wu et al. (2013)
3		S211P	Polar → hydrophobic	−8.2	Slower	Faster	n.s.	Faster	n.d.	n.d.	Enhanced	Larger	n.d.	Estacion et al. (2010)
4		F216S	Hydrophobic → polar	−11.8	Slower	Faster	n.s.	Faster	n.d.	n.d.	Enhanced	Larger	n.d.	Choi et al. (2006), Drenth et al. (2005)
5	S4–S5	I234T	Hydrophobic → polar	−17.9	Slower	Faster	n.s.	Slower	n.d.	n.d.	Enhanced	Larger	n.d.	Ahn et al. (2010)
6		S241T	=Polar	−8.4	Slower	Faster	n.s.	Faster	n.d.	n.d.	Enhanced	Larger	Enhanced	Lampert et al. (2006), Michiels et al. (2005) DRG: Yang et al. (2012)
7	Pore	N395K	Polar → positive	−7.7	Slower	n.d.	n.s.	n.d.	n.d.	n.d.	Reduced	n.d.	n.d.	Drenth et al. (2005), Sheets et al. (2007)
8		V400M	=Hydrophobic	−6.5	Slower	n.d.	+ 7.3	Same	n.d.	n.d.	Same	Larger	n.d.	Fischer et al. (2009), Yang et al. (2012)
9	Linker	G616R[a]	Hydrophobic → positive	n.s.	n.d.	n.d.	+ 5.7	n.d.	n.d.	n.d.	n.d.	n.d.	Enhanced	Choi et al. (2010)
10	VSD	L823R	Hydrophobic → positive	−14.6	Slower	Slower	−9.8	Altered	n.d.	n.d.	n.d.	n.d.	n.d.	Lampert et al. (2009), Takahashi et al. (2007)
11	S4–S5	I848T	Hydrophobic → polar	−13.8	Slower	n.d.	n.s.	Faster	n.d.	n.d.	Reduced	Larger	Enhanced	Cummins et al. (2004), Han et al. (2009), Yang et al. (2004)
				−9.5	n.d.	n.d.	−5.0	Same	n.d.	Same	n.d.	n.d.	n.d.	Theile et al. (2011)
				−4.5	n.d.	n.d.	+ 4.5	n.d.	n.d.	n.d.	n.d.	n.d.	n.d.	Wu et al. (2013)
12		L858H	Hydrophobic → positive	−13.3	Slower	n.d.	−2.5	Faster	n.d.	n.d.	Enhanced	Larger	n.d.	Cummins et al. (2004), Yang et al., (2004)
				−4.0	n.d.	n.d.	−1.5	Faster	n.d.	Same	n.d.	n.d.	n.d.	Theile et al. (2011)

(continued)

Table 1 (continued)

#	Channel part	Mutation	Charge	Activation			Fast inactivation		Persistent current	Resurgent current	Slow inactivation	Ramp current	DRG/CC Excitability	References
				Vhalf	Deactivation	ttp	Vhalf	Decay						
13		L858F	=Hydrophobic	−9.2	Slower	n.d.	+ 3.0	Same	n.d.	n.d.	Same	Larger	Enhanced	Cheng et al. (2011), Drenth et al. (2005), Han et al. (2006))
14	Pore	A863P	=Hydrophobic	−7.7	Slower	n.d.	+ 9.8	Same	n.d.	n.d.	Altered	Larger	Enhanced	Harty et al. (2006)
15		V872G	=Hydrophobic	−9.3	Slower	Faster	n.s.	Faster	n.d.	n.d.	n.d.	Larger	n.d.	Choi et al. (2009)
16		Q875E	Polar → positive	n.d.	n.d.	n.d.	n.d.	n.d.	n.d.	n.d.	n.d.	n.d.	n.d.	Skeik et al. (2012)
17		delL955	Loss of positive charge	−24.2	Slower	n.d.	−2.9	Slower	Increased	n.d.	Enhanced	Larger	Enhanced	Cheng et al. (2011), Yang et al. (2013)
18		F1449V	=Hydrophobic	−7.6	Same	n.d.	+ 4.3	Faster	n.d.	n.d.	Enhanced	Same	Enhanced	Dib-Hajj et al., (2005), Yang et al. (2012)
19	S4–S5	V1316A	=Hydrophobic	−9.4	n.d.	n.d.	n.s.	n.d.	n.d.	n.d.	Enhanced	Larger	n.d.	Estacion et al. (2013)
				−6.8	n.d.	n.d.	+ 3.1	n.d.	n.d.	n.d.	n.d.	n.d.	n.d.	Wu et al. (2013)
20		P1308L	=Hydrophobic	−9.6	Slower	Faster	n.s.	Faster	n.d.	n.d.	Same	Larger	Enhanced	Cheng et al. (2010)

Vhalf half maximal voltage, *ttp* time to peak, *Decay* kinetics of current decay (fast inactivation), *DRG/CC* results of current clamp recordings in DRG neurons, *VSD* voltage-sensing domain, *S4–S5* Linker between the VSD and the pore region, *Linker* intracellular links between the domains or the N-/C-terminus, *Charge* change of charge/hydrophobicity due to the mutation, *n.d.* not determined, *n.s.* change is not significant

[a]Effects were only found in the adult long splice variant

In 1998 Roderick MacKinnon and co-workers published the first crystal structure of a voltage-gated potassium channel, which was used as a template for homology modeling of Navs (Doyle et al. 1998). With the report of the first structure of a bacterial sodium channel [NavAb, (Payandeh et al. 2011)], these structures were refined and some effects of IEM mutations became explicable on the basis of their structural impact. Activation is initiated by an outward movement of the voltage sensor in the electrical field. This movement is conveyed to the pore via the S4–S5 linker, resulting in the opening of the permeation pathway that is formed by S5 and S6.

2.3 Mutations in the Voltage Sensing Domain

Four of the known 20 IEM mutations can be found in the voltage sensor. The L823R mutation adds an additional charge to DII VSD, thereby shifting voltage sensitivity of activation by full −14.6 mV (Lampert et al. 2008). This mutation supports the view that DII may be the domain that is most voltage sensitive (Chanda and Bezanilla 2002), which would predict that the additional charge should have a strong effect on activation. The three remaining mutations in the VSD (I136V, S211P, and F216S; see Table 1) are located in DI and all change activation kinetics most probably via conformational changes, as none of them adds or removes charge. It may be that the gating charges move more favorably in the altered VSD, thereby alleviating voltage-sensing.

2.4 Mutations in the S4–S5 Linker

The movement of the voltage sensor is related to the pore via the S4–S5 linker of each domain, and most IEM mutations can be found in this region (38 %, Fig. 1c), strengthening its potential role in channel activation. Remarkably, all except for one mutation replace a hydrophobic residue, mostly with either a polar or a charged residue (I234T, I848T, G856D, L858H, L858F, V1316A, and P1308L; exception: S241T replacing a polar residue with a polar one). This suggests that a lipophilic interaction either with the cell membrane or within the channel protein may be disturbed. Two mutations occur at the same position: L858H and L858F. Both replace the hydrophobic leucine with a significantly larger residue and each contains a ring structure. We suggest that a small increase in size of a side chain on the S4–S5 linker in position of S241 may lead to a better positioning of the VSD, and therefore potentially less force/voltage change is needed in order to move it as seen in the IEM mutation S241T. The same may happen, if a charged or polar aminoacid is introduced in a position where it would disrupt a potential hydrophobic interaction. This may result in a lowered voltage sensitivity for activation, emphasizing that the S4–S5 linker is a very sensitive part of the channel protein for the coupling of voltage changes to pore opening.

2.5 Mutations in the Pore Region

Homology modeling provided an important source of hypothesis in the discovery of the potential activation gate of Nav1.7: the IEM mutation F1449V is located at the cytosolic end of the S6 segment in domain III. It is known from several potassium channels that a hydrophobic interaction of a ring of amino acids at the inner end of the permeation pathway needs to be de-stabilized in order for the channel to open (Clayton et al. 2008; Kuo et al. 2003). The phenylalanine in position 1449 may constitute part of such a hydrophobic ring, as it may interact with DI/Y450, DII/F960, and DIV/F1752. The smaller valine that is introduced by the IEM mutation DIII/F1449V may disrupt such an interaction. In order to test this hypothesis, we mutated the corresponding hydrophobic residues in DI, DII and DIV. Both mutations DII and DIII similarly shifted activation to the right (Lampert et al. 2008), and subsequent modeling studies on the basis of NavAb further supported our hypothesis (Yang et al. 2013). Thus, investigation of the structural changes induced by a naturally occurring IEM mutation helped us understand the activation mechanism of Nav channels.

In some amino acids more N-terminal to the activation gate in S6 the deletion mutation del-L955 was identified, inducing structural changes in the pore leading to a dramatic left shift of activation (Cheng et al. 2011). In-depth homology modeling based on the bacterial sodium channels NavAb and NavRh revealed that due to the loss of L955, the S6 twists, and the phenylalanine in position 960 can no longer serve as part of the activation gate (Yang et al. 2013). Instead, a serine in position 961 now faces the hydrophobic residues of the other domains. Substitution of this residue with a proline, S961P, combined with a reduction in size of the displaced phenylalanine of that domain (F960A/S), shifted activation properties toward WT characteristics.

2.6 Mutation-Specific Therapeutic Efforts

Therapeutic efforts for IEM mutations that hyperpolarize activation should focus on normalizing activation properties, by shifting it to more depolarized potentials. Studies with the toxin ProTx-II have shown some promising effects, as it relatively selectively depolarizes voltage dependence of Nav1.7 activation (Schmalhofer et al. 2008). However, therapeutic application of this toxin is, at present, not feasible.

Some IEM patients have been treated with some, albeit often transient, success via known Nav blockers such as the local anesthetics lidocaine, mexiletine, or carbamazepine (CBZ) [G616R, (Choi et al. 2010); I848T, (Wu et al. 2013); A863P, (Harty et al. 2006); V1316A, (Estacion et al. 2013; Wu et al. 2013)]. Tonic block, but not use-dependent block by mexiletine is slightly enhanced by the mutation I848T (Wu et al. 2013). Local anesthetics are known to bind within the pore on a specific, well-defined binding site formed by the S6 of DIII and DIV (Catterall 2000; Nau and Wang 2004; Wang and Strichartz 2012). As IEM mutations can be

found in this region (Fig. 1), it is no surprise that the effect of local anesthetics may be altered in some cases. The N395K mutation, located directly within this binding site, exhibits dramatically increased IC50 for block of inactivated channels [from 500 μM for WT to 2.8 mM for N395K mutated Nav1.7; (Sheets et al. 2007)].

The IEM mutation V400M is notable in showing increased sensitivity to CBZ compared to WT, allowing successful treatment of the mutation carriers (Fischer et al. 2009). In this mutation, CBZ surprisingly shifts activation back toward WT values, whereas it leaves inactivation properties unchanged. Interestingly, structural modeling studies showed that the S241T mutation on the S4–S5 segment seems to be thermodynamically coupled to the V400M mutation during activation, suggesting that both mutations impose their effects via a common mechanism on the channel (Yang et al. 2012). Consequent testing of the S241T mutation for its CBZ sensitivity revealed a similar effect as in V400M: in both mutations CBZ shifts activation to more depolarized potentials, opposing the IEM effects. V400 is not part of the local anesthetic binding site, but it was suggested that drug binding to S6 in DIII and DIV leads to allosteric coupling to the voltage sensors, inhibiting its movement (Sheets and Hanck 2003). It is possible that CBZ leads to a stabilization of the WT configuration in the S241T and V400M mutated Nav1.7, thereby supporting normal channel function.

3 Fast Inactivation

Paroxysmal extreme pain disorder (PEPD) is characterized by attacks of severe pain in proximal parts of the body including the face, the genital region, or the torso. The attacks may be triggered by cold, mechanical stimulation, bowel movements, or startling of the child and can be accompanied by a harlequin-type reddening of the skin and also symptoms of the autonomous nervous system. The debilitating symptoms often begin in early infancy and can be combined with autonomic dysfunction (Fertleman et al. 2007). Their frequency declines with age and treatment with CBZ often attenuates the intensity or rate of the attacks.

3.1 Right Shift of Inactivation Keeps the Nociceptor Excited

All of the ten known PEPD mutations in Nav1.7 induce a depolarizing shift of steady-state fast inactivation and slow fast inactivation kinetics, thereby enhancing persistent currents and hampering channel closure during an action potential (Table 2). This impairment of fast inactivation enhances excitability in transfected sensory neurons (Cheng et al. 2010; Dib-Hajj et al. 2008; Estacion et al. 2008), which is likely to underlie the pain symptoms experienced by the patients.

Table 2 Mutations in Nav1.7 causing PEPD

#	Channel part	Mutation	Charge	Activation			Fast inactivation		Persistent current	Resurgent current	Slow inactivation	Ramp current	DRG/CC	References
				Vhalf	Deactivation	ttp	Vhalf	Decay					Excitability	
1	Linker	R996C	Positive → polar	n.d.	n.d.	n.d.	n.d.	n.d.	n.d.	n.d.	n.d.	n.d.	n.d.	Fertleman et al. (2006)
2	S4–S5	V1298D	Hydrophobic → negative	n.d.	n.d.	n.d.	n.d.	n.d.	n.d.	n.d.	n.d.	n.d.	n.d.	Fertleman et al. (2006)
3		V1298F	=Hydrophobic	n.s.	Same	Slower	+ 16.1	Slower	n.d.	n.d.	Reduced	Larger	Enhanced	Cheng et al. (2010) Fertleman et al. (2006)
				+ 6.3	Same	n.d.	+ 19.8	Slower	Increased	n.d.	Altered	Larger	n.d.	Jarecki et al. (2008)
4		V1299F	=Hydrophobic	n.s.	n.d.	n.d.	+ 13.1	Same	Increased	Increased	n.d.	n.d.	n.d.	Fertleman et al. (2006), Theile et al. (2011))
				+ 4.5	Same	n.d.	+ 21.0	Slower	Increased	n.d.	Altered	Larger	n.d.	Jarecki et al. (2008)
5	Linker	I1461T	Hydrophobic → polar	n.d.	Same	n.d.	Depol.	n.d.	Increased	n.d.	n.d.	n.d.	n.d.	Fertleman et al. (2006)
				n.s.	Same	n.d.	+ 18.8	Slower	Increased	Increased	Altered	Larger	n.d.	Jarecki et al. (2008, 2010)
6		F1462V	=Hydrophobic	n.d.	n.d.	n.d.	n.d.	n.d.	n.d.	n.d.	n.d.	n.d.	n.d.	Fertleman et al. (2006)
7		T1464I	Polar → hydrophobic	+ 6.8	n.d.	n.d.	Depol.	Altered	Increased	n.d.	n.d.	n.d.	n.d.	Fertleman et al. (2006)
				n.s.	n.d.	n.d.	+ 20.2	Slower	n.d..	Increased	n.d.	n.d.	n.d.	Theile et al. (2011)
				n.s.	n.d.	n.d.	+ 9.8	Slower	Increased	Increased	n.d.	n.d.	n.d.	Theile and Cummins (2011)
8	VSD	G1607R	=Positive	+ 4.3	n.d.	n.d.	+31.5	n.d.	Increased	n.d.	n.d.	Larger	n.d.	Choi et al. (2011)
9	S4–S5	M1627K	Hydrophobic → positive	n.d.	Same	n.d.	+ 22.2	n.d.	Increased	n.d.	n.d.	n.d.	n.d.	Fertleman et al. (2006)
				n.s.	Same	n.d.	+ 19.8	Slower	n.d.	n.d.	Altered	Larger	Enhanced	Dib-Hajj et al. (2008)
				n.s.	n.d.	n.d.	+ 20.2	Slower	n.d.	Increased	n.d.	n.d.	n.d.	Theile et al. (2011)
				n.s.	n.d.	n.d.	+ 21.7	Slower	Increased	Increased	n.d.	n.d.	n.d.	Theile and Cummins (2011)
10		A1632E[a]	Hydrophobic → negative	−7.1	Slower	Slower	+ 17.0	Slower	Increased	n.d.	Impaired	Larger	Enhanced	Estacion et al. (2008)

Vhalf half maximal voltage, *ttp* time to peak, *Decay* kinetics of current decay (fast inactivation), *DRG/CC* results of current clamp recordings in DRG neurons, *VSD* voltage-sensing domain, *S4–S5* linker between the VSD and the pore region, *Linker* intracellular links between the domains or the N-terminus, *Charge* change of charge/hydrophobicity due to the mutation, *n.d.* not determined, *n.s.* change is not significant

[a]Mixed phenotype PEPD/IEM

3.2 PEPD Mutations Affect Channel Areas Involved in Fast Inactivation

Fast inactivation of Navs is mediated by obliteration of the channel pore with the inactivation particle, which is formed by the IFM motif on the linker L3 between DIII and DIV. Parts of the S4–S5 segments serve as inactivation particle receptor sites. Not surprisingly, most PEPD mutations can be found in areas of the channel involved in fast inactivation: L3 and the S4–S5 linkers (Fig. 1). Most likely, the mutations disturb the interaction of the IFM motif with the intracellular channel parts that act as its receptor, thereby impairing normal inactivation.

The PEPD mutation G1607R is located in the VSD of DIV, adding a positive charge (Choi et al. 2011). Like in the IEM mutation L823R, which also increases the positive charges of the VSD, activation is affected, but surprisingly the shift in activation of G1607R is directed to more positive potentials, which would result, if at all, in a reduced excitability. Steady-state fast inactivation, on the other hand, is shifted by 31.5 mV to more depolarized potentials: this is the largest shift observed in any pain-causing Nav mutation so far. As fast inactivation is impaired, persistent and ramp currents occur, and these persisting depolarizing currents are likely to enhance repetitive firing in nociceptive neurons.

4 Resurgent Currents

Impaired inactivation leads to prolonged openings of the pore and thus not only ions may enter it but also small intracellular peptides, such as open channel blockers. Navs that have undergone open channel block may give rise to resurgent currents upon repolarization. On a molecular level the IFM motif binding is hampered by an intracellular blocking particle occluding the pore before fast inactivation can occur (Fig. 2). Due to its positive charge this blocking particle is expelled upon slight repolarization giving rise to resurgent currents (Raman and Bean 1997). They were first described in Purkinje neurons of the cerebellum, where they are generated mainly by Nav1.6 (Raman et al. 1997). As resurgent currents occur during the falling phase of the action potential, they depolarize the membrane potential and hold it closer to threshold. Hyperexcitability due to resurgent currents may be conveyed by two mechanisms: (1) flow of a depolarizing Na^+ inward current during repolarization with their peak between −20 and −50 mV exceeds the threshold for following action potentials and (2) shortened refractory period due to open channel block without channel inactivation increases the availability of Navs for subsequent action potentials (Cruz et al. 2011; Raman and Bean 2001).

Research on resurgent currents has been complicated by the fact that they normally cannot be detected in heterologously expressed Navs (Smith et al. 1998). Early experiments on resurgent currents also showed that their generation was critically dependent on the cell background and they cannot be detected, e.g., in CA3 neurons (Raman and Bean 1997). Beta subunits interact closely with the channels and are therefore candidates that could provide the open channel blocker. The ß4 subunit is

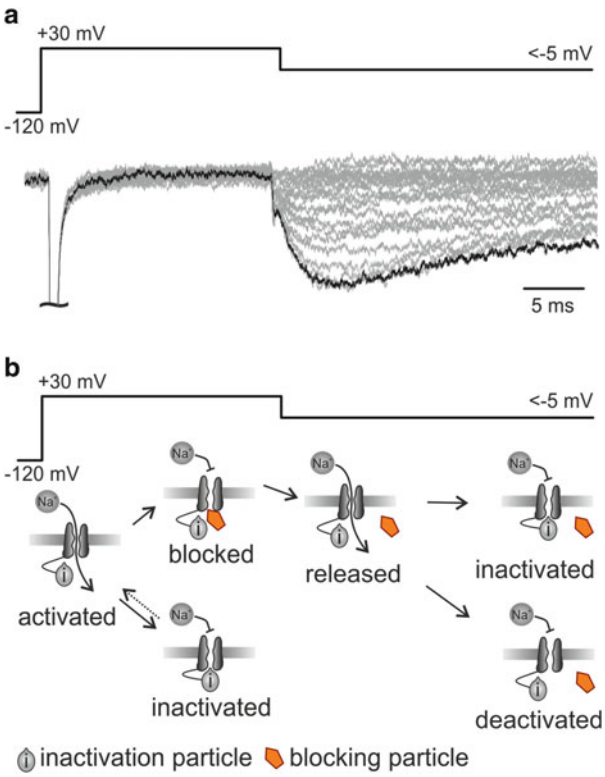

Fig. 2 (**a**) Resurgent currents evoked in a large diameter DRG neuron with the appropriate protocol. Transient peak inward currents were truncated. (**b**) Schematic view of the molecular mechanisms that are likely to underlie the emergence of resurgent currents

especially interesting in this regard since it displays several charged residues in its intracellular part and its expression pattern in certain neuronal cells matched reasonably well with those cells displaying resurgent currents (Yu et al. 2003). Grieco et al. identified the sequence "KKLITFILKKTREK" in the cytoplasmic domain of the β4 subunit as one responsible region for open channel block (Grieco et al. 2005). Addition of this peptide to the recording pipette enables the detection of resurgent currents even in heterologously expressed Navs (Wang et al. 2006). It is still puzzling that cotransfection of ß4 itself is not sufficient to induce resurgent currents. It is possible that in native neuronal cells the cytoplasmic tail of the ß4 subunit needs to be processed (Huth et al. 2011) prior to serving as open channel blocker. ß4 is not necessarily the exclusive candidate to function as an open channel blocker, but so far the most likely one.

4.1 PEPD Mutations Enhance Resurgent Currents

Resurgent currents in cerebellar Purkinje neurons promote high frequency action potential discharges (Raman et al. 1997). Nav1.6 is the major contributor to resurgent currents in these cells under physiological conditions. When transfected into dorsal root ganglion (DRG) neurons, heterologous Nav1.6 generates resurgent currents (Cummins et al. 2005), whereas those produced by WT Nav1.7 are very small. DRG neurons transfected with mutations in Nav1.7 being causative for PEPD, on the other hand, yield robust resurgent currents, suggesting a contribution to hyperexcitability (Jarecki et al. 2010). Computer simulations of a PEPD-causing mutation showed high frequency firing due to addition of resurgent currents to the model consistent with the pathophysiology of episodic neuropathic pain associated with this channelopathy.

While Nav1.6 is prone to inactivate more slowly than other Navs and can produce resurgent currents, other neuronal Navs can conduct resurgent currents if inactivation is slowed, e.g., by toxins (Grieco and Raman 2004; Klinger et al. 2012). Interestingly, all PEPD mutations tested slowed current decay of Nav1.7 (see Table 2), suggesting that an endogenous blocking particle may have more time to bind to the channel thereby promoting resurgent currents. Indeed, heterologous expression of two PEPD mutations (M1627K, T1464I, and V1299V) and recordings with the β4 peptide in the pipette showed resurgent currents, whereas measurements with IEM mutations did not (Theile et al. 2011). The amplitudes of the detected resurgent currents correlate with slowed decay time constants of fast inactivation, suggesting that the PEPD mutation-induced slowed inactivation kinetics support resurgent current formation and that these currents contribute to the pathology of PEPD.

4.2 Pathologically Enhanced Resurgent Currents Alter Nociceptive Sensations in Humans

ATX-II, a toxin from the sea anemone *Anemonia sulcata*, has been shown to slow fast inactivation. At very low concentrations it mainly modifies the neuronal Navs Nav1.1, Nav1.2, and Nav1.6 (Lewis and Raman 2011; Oliveira et al. 2004; Rathmayer 1979). This predestines the occurrence of resurgent currents, as slowing of current decay increases the probability of the blocking particle to bind to the open channel. Indeed, ATX-II enhances resurgent currents of heterologously expressed Nav1.6 (Schiavon et al. 2006) and in large diameter DRG neurons, but fails to do so in small DRG neurons (Klinger et al. 2012; Sittl et al. 2012). This may be due to differential expression of Nav subunits, as small DRG neurons express less Nav1.6 and ß4 compared to larger ones, so that the physiological ingredients for resurgent currents may not be available in these cells (Felts et al. 1997; Ho and O'Leary 2011; Klinger et al. 2012). Nav1.7 on the other hand can be found at similar expression levels in both cell sizes. A PEPD mutation may render Nav1.7 prone to produce resurgent currents, as it slows current decay. This may preferentially affect small DRG neurons, in which Nav1.7 is expressed at a relatively higher

level. As small DRG neurons are linked to C-fibers (Fang et al. 2006; Harper and Lawson 1985), this may result in the pain symptoms observed in PEPD patients.

Evidence that enhanced resurgent currents are likely to alter human perception can be derived from psychophysical experiments with very low concentrations of ATX-II. When only a few nanomolar ATX-II are applied, resurgent currents are selectively enhanced in large diameter DRG neurons and therefore most likely also in A-fibers. Humans exposed to very low concentrations of ATX-II in the skin report pain and a mechanical missensation that some referred to as "itch-like" (Klinger et al. 2012). Recently, the chemotherapeutic oxaliplatin was shown to enhance resurgent currents in large diameter DRG neurons in a temperature-dependent manner (Sittl et al. 2012). Patients receiving treatment with this anticancer drug often suffer from a cold-sensitive peripheral neuropathy, which is likely due to increased persistent and resurgent currents in large diameter DRG neurons. PEPD attacks may also be triggered by cold, and it is possible that the mechanism of the oxaliplatin-induced neuropathy presents a general mechanism of cold-induced pathologically enhanced resurgent currents in peripheral neurons.

5 Slow Inactivation

5.1 Some IEM Mutations Enhance Slow Inactivation

In contrast to fast inactivation which occurs within a few milliseconds following channel activation, slow inactivation develops over a period of seconds and therefore reflects long-term changes in resting membrane potentials. Nevertheless, channels may enter the slow-inactivated state from the open state as also repetitive firing leads to a reduction of available channels due to slow inactivation. The majority of IEM mutations enhance slow inactivation of Nav1.7 (71 % of those tested, see Table 1). This finding seems counterintuitive, as IEM causes hyperexcitability and pain, whereas a stronger slow inactivation is likely to reduce firing. Computer simulations revealed that slow inactivation may modulate the overall impact of gain-of-function mutations and its enhancement may alleviate the pain symptoms, thereby protecting the patients from even further pain (Sheets et al. 2007). The deletion mutation delL955 induces a shift of slow inactivation as large as ~−39 mV, suggesting that it may alleviate the pain the patient is suffering from due to the prominent shift of activation to more negative potentials (Cheng et al. 2011).

5.2 PEPD and SFN Mutations Impair Slow Inactivation or Render Its Voltage Dependence Steeper

Patients diagnosed with SFN suffer from neuropathic pain often with burning character combined with autonomic symptoms. This disorder affects small thinly or unmyelinated nerve fibers and the patients' skin biopsies typically display a reduction of interepidermal nerve fiber density. Patients are affected in adulthood

Table 3 Mutations in Nav1.7 causing SFN

#	Channel part	Mutation	Charge	Activation			Fast inactivation		Persistent current	Resurgent current	Slow inactivation	Ramp current	DRG/CC Excitability	References
				vhalf	Deactivation	ttp	Vhalf	Decay						
1	VSD	R185H	=Positive	Same	n.d.	n.d.	n.d.	n.d.	n.d.	Increased	n.d.	Same	Enhanced	Faber et al. (2012)
2		I228M	=Hydrophobic	n.s.	Same	n.d.	n.s.	Same	Same	n.d.	Reduced	Same	Enhanced	Estacion et al. (2011), Faber et al. (2012)
3	Linker	D623N	Negative → polar	n.s.	n.d.	n.d.	+ 4.5	n.d.	n.d.	n.d.	Reduced	Same	Enhanced	Faber et al. (2012)
4		I720K	Hydrophobic → positive	n.s.	n.d.	n.d.	n.s.	n.d.	n.d.	n.d.	Reduced	Same	Enhanced	Faber et al. (2012)
5	VSD	I739V	=Hydrophobic	n.s.	Same	n.d.	n.s.	n.d.	n.d.	n.d.	Reduced	Same	Enhanced	Faber et al. 2012, Han et al. 2012
6	S4–S5	G856D[a]	Hydrophobic → negative	−9.3	Slower	n.d.	+ 6.2	Slower	Increased	Increased	Enhanced	Larger	Enhanced	Hoeijmakers et al. (2012)
7	Linker	M932L/ V991L	Both = hydrophobic	n.s.	Same	n.d.	n.s.	n.d.	n.d.	Increased	Same	Same	Enhanced	Faber et al. (2012)
8	VSD	M1532I	=Hydrophobic	Same	n.d.	n.d.	n.d.	n.d.	n.d.	n.d.	Reduced	Same	Enhanced	Faber et al. (2012)

Vhalf half maximal voltage, *ttp* time to peak, *Decay* kinetics of current decay (fast inactivation), *DRG/CC* results of current clamp recordings in DRG neurons, *VSD* voltage-sensing domain, *S4–S5* linker between the VSD and the pore region, *Linker* intracellular links between the domains or the N-terminus, *Charge* change of charge/hydrophobicity due to the mutation. *n.d.* not determined, *n.s.* change is not significant

[a]Mixed phenotype SFN/IEM also associated with acromesomelia

and treatment is often difficult. Recently mutations in Nav1.7 were identified in 28 % of idiopathic SFN patients, and those characterized showed a gain-of-function (Faber et al. 2012). The electrophysiological alterations are more subtle or selective than those for IEM or PEPD, e.g., the M932L/V991L mutation leads to a selective enhancement of resurgent currents, leaving activation and fast or slow inactivation kinetics unchanged (see Table 3). The most common change in Nav1.7 gating due to SFN mutations is an impaired slow inactivation. In three characterized mutations this is the only detected change [I739V (Han et al. 2012), I720K (Faber et al. 2012), I228M (Estacion et al. 2011)], and one displays additionally a small shift of steady-state fast inactivation [D623N, (Faber et al. 2012)]. Expression in DRG neurons led to hyperexcitability, suggesting that impaired slow inactivation indeed may be disease causing by itself.

PEPD as well as SFN alter slow inactivation in an almost opposite manner compared to IEM. In all PEPD mutations tested so far slow inactivation was reduced or the voltage dependence became steeper: at lower potentials slow inactivation is reduced but at higher potentials enhanced. As such its effect may vary with cell activity and changes in resting membrane potential. The discrepancy—enhanced slow inactivation in IEM, reduced in SFN and PEPD—may hint toward a role of slow inactivation in generation of autonomic symptoms, which are more prominent in the latter two pain syndromes.

5.3 What Do We Learn from Alterations of Slow Inactivation?

Mutations affecting slow inactivation do not cluster in certain parts of the channel proteins; they are almost equally distributed, suggesting that they are affecting a complex structural process that may be assessed and influenced from many parts of the channel. Artificial mutations in the pore of Nav1.4, Nav1.6, or Nav1.2 have identified residues that almost exclusively alter slow inactivation (Chen et al. 2006; O'Reilly et al. 2001), suggesting that the pore or its collapse play an important role. More detailed work needs to be done in order to understand the molecular basis of slow inactivation, which would put us in a better position to therapeutically target this channel gating characteristic. Lacosamide is a known enhancer of Nav slow inactivation and in clinical use for treatment of diabetes-induced neuropathic pain. By enhancing slow inactivation it may alleviate pain and other SFN symptoms. Whether lacosamide, or other Nav blocker, may also inhibit small fiber loss, is not yet known.

Conclusion/Outlook

Although we have gained substantial knowledge on pain syndromes due to mutations in Nav1.7, therapeutic options are still sparse and research on potential drugs is in progress. These mutations affect different gating modes in different diseases, thus providing an opportunity to understand the importance of each of the channel's functions in a physiological and pathophysiological context. This may help us develop more specific treatment for each condition—via subtype specificity, gating specificity, or local targeting of nociceptors.

References

Ahn HS, Dib-Hajj SD, Cox JJ, Tyrrell L, Elmslie FV, Clarke AA et al (2010) A new Nav1.7 sodium channel mutation I234T in a child with severe pain. Eur J Pain 14(9):944–950

Catterall WA (2000) From ionic currents to molecular mechanisms: the structure and function of voltage-gated sodium channels. Neuron 26(1):13–25

Chanda B, Bezanilla F (2002) Tracking voltage-dependent conformational changes in skeletal muscle sodium channel during activation. J Gen Physiol 120(5):629–645

Chen Y, Yu FH, Surmeier DJ, Scheuer T, Catterall WA (2006) Neuromodulation of Na^+ channel slow inactivation via cAMP-dependent protein kinase and protein kinase C. Neuron 49(3):409–420

Cheng X, Dib-Hajj S, Tyrrell L, Waxman S (2008) Mutation I136V alters electrophysiological properties of the $Na_V1.7$ channel in a family with onset of erythromelalgia in the second decade. Mol Pain 4(1):1

Cheng X, Dib-Hajj SD, Tyrrell L, Wright DA, Fischer TZ, Waxman SG (2010) Mutations at opposite ends of the DIII/S4-S5 linker of sodium channel $Na_V1.7$ produce distinct pain disorders. Mol Pain 6:24

Cheng X, Dib-Hajj SD, Tyrrell L, Te Morsche RH, Drenth JP, Waxman SG (2011) Deletion mutation of sodium channel Na(V)1.7 in inherited erythromelalgia: enhanced slow inactivation modulates dorsal root ganglion neuron hyperexcitability. Brain 134(Pt 7):1972–1986

Choi JS, Dib-Hajj SD, Waxman SG (2006) Inherited erythermalgia: limb pain from an S4 charge-neutral Na channelopathy. Neurology 67(9):1563–1567

Choi J-S, Zhang L, Dib-Hajj SD, Han C, Tyrrell L, Lin Z et al (2009) Mexiletine-responsive erythromelalgia due to a new Nav1.7 mutation showing use-dependent current fall-off. Exp Neurol 216(2):383

Choi J-S, Cheng X, Foster E, Leffler A, Tyrrell L, te Morsche RHM et al (2010) Alternative splicing may contribute to time-dependent manifestation of inherited erythromelalgia. Brain 133(6):1823–1835

Choi JS, Boralevi F, Brissaud O, Sanchez-Martin J, Te Morsche RH, Dib-Hajj SD et al (2011) Paroxysmal extreme pain disorder: a molecular lesion of peripheral neurons. Nat Rev Neurol 7 (1):51–55

Clayton GM, Altieri S, Heginbotham L, Unger VM, Morais-Cabral JH (2008) Structure of the transmembrane regions of a bacterial cyclic nucleotide-regulated channel. Proc Natl Acad Sci 105(5):1511–1515

Cruz JS, Silva DF, Ribeiro LA, Araujo IG, Magalhaes N, Medeiros A et al (2011) Resurgent Na^+ current: a new avenue to neuronal excitability control. Life Sci 89(15–16):564–569

Cummins TR, Dib-Hajj SD, Waxman SG (2004) Electrophysiological properties of mutant Nav1.7 sodium channels in a painful inherited neuropathy. J Neurosci 24(38):8232–8236

Cummins TR, Dib-Hajj SD, Herzog RI, Waxman SG (2005) Nav1.6 channels generate resurgent sodium currents in spinal sensory neurons. FEBS Lett 579(10):2166

Dib-Hajj SD, Rush AM, Cummins TR, Hisama FM, Novella S, Tyrrell L et al (2005) Gain-of-function mutation in Nav1.7 in familial erythromelalgia induces bursting of sensory neurons. Brain 128(Pt 8):1847–1854

Dib-Hajj S, Estacion M, Jarecki B, Tyrrell L, Fischer T, Lawden M et al (2008) Paroxysmal extreme pain disorder M1627K mutation in human Nav1.7 renders DRG neurons hyperexcitable. Mol Pain 4(1):37

Doyle DA, Morais Cabral J, Pfuetzner RA, Kuo A, Gulbis JM, Cohen SL et al (1998) The structure of the potassium channel: molecular basis of K^+ conduction and selectivity. Science 280 (5360):69–77

Drenth JP, te Morsche RH, Guillet G, Taieb A, Kirby RL, Jansen JB (2005) SCN9A mutations define primary erythermalgia as a neuropathic disorder of voltage gated sodium channels. J Invest Dermatol 124(6):1333–1338

Estacion M, Dib-Hajj SD, Benke PJ, te Morsche RHM, Eastman EM, Macala LJ et al (2008) NaV1.7 gain-of-function mutations as a continuum: A1632E displays physiological changes associated with erythromelalgia and paroxysmal extreme pain disorder mutations and produces symptoms of both disorders. J Neurosci 28(43):11079–11088

Estacion M, Choi JS, Eastman EM, Lin Z, Li Y, Tyrrell L et al (2010) Can robots patch-clamp as well as humans? Characterization of a novel sodium channel mutation. J Physiol 588(Pt 11): 1915–1927

Estacion M, Han C, Choi JS, Hoeijmakers JG, Lauria G, Drenth JP et al (2011) Intra- and interfamily phenotypic diversity in pain syndromes associated with a gain-of-function variant of $Na_V1.7$ Mol Pain 7:92

Estacion M, Yang Y, Dib-Hajj SD, Tyrrell L, Lin Z, Yang Y et al (2013) A new Nav1.7 mutation in an erythromelalgia patient. Biochem Biophys Res Commun 432(1):99–104

Faber CG, Hoeijmakers JG, Ahn HS, Cheng X, Han C, Choi JS et al (2012) Gain of function $Na_V1.7$ mutations in idiopathic small fiber neuropathy. Ann Neurol 71(1):26–39

Fang X, Djouhri L, McMullan S, Berry C, Waxman SG, Okuse K et al (2006) Intense isolectin-B4 binding in rat dorsal root ganglion neurons distinguishes c-fiber nociceptors with broad action potentials and high Nav1.9 expression. J Neurosci 26(27):7281–7292

Felts PA, Yokoyama S, Dib-Hajj S, Black JA, Waxman SG (1997) Sodium channel alpha-subunit mRNAs I, II, III, NaG, Na6 and hNE (PN1): different expression patterns in developing rat nervous system. Brain Res Mol Brain Res 45(1):71–82

Fertleman CR, Baker MD, Parker KA, Moffatt S, Elmslie FV, Abrahamsen B et al (2006) SCN9A mutations in paroxysmal extreme pain disorder: allelic variants underlie distinct channel defects and phenotypes. Neuron 52:767–774

Fertleman CR, Ferrie CD, Aicardi J, Bednarek NA, Eeg-Olofsson O, Elmslie FV et al (2007) Paroxysmal extreme pain disorder (previously familial rectal pain syndrome). Neurology 69 (6):586–595

Fischer TZ, Gilmore ES, Estacion M, Eastman E, Taylor S, Melanson M et al (2009) A novel Nav1.7 mutation producing carbamazepine-responsive erythromelalgia. Ann Neurol 65(6): 733–741

Grieco TM, Raman IM (2004) Production of resurgent current in NaV1.6-null Purkinje neurons by slowing sodium channel inactivation with β-pompilidotoxin. J Neurosci 24(1):35–42

Grieco TM, Malhotra JD, Chen C, Isom LL, Raman IM (2005) Open-channel block by the cytoplasmic tail of sodium channel [β]4 as a mechanism for resurgent sodium current. Neuron 45(2):233–244

Han C, Rush AM, Dib-Hajj SD, Li S, Xu Z, Wang Y et al (2006) Sporadic onset of erythermalgia: a gain-of-function mutation in Nav1.7. Ann Neurol 59(3):553–558

Han C, Dib-Hajj SD, Lin Z, Li Y, Eastman EM, Tyrrell L et al (2009) Early- and late-onset inherited erythromelalgia: genotype-phenotype correlation. Brain 132:awp078

Han C, Hoeijmakers JGJ, Ahn H-S, Zhao P, Shah P, Lauria G et al (2012) Nav1.7-related small fiber neuropathy. Neurology 78:1635–43

Harper AA, Lawson SN (1985) Conduction velocity is related to morphological cell type in rat dorsal root ganglion neurones. J Physiol 359:31–46

Harty TP, Dib-Hajj SD, Tyrrell L, Blackman R, Hisama FM, Rose JB et al (2006) Na(V)1.7 mutant A863P in erythromelalgia: effects of altered activation and steady-state inactivation on excitability of nociceptive dorsal root ganglion neurons. J Neurosci 26(48):12566–12575

Ho C, O'Leary ME (2011) Single-cell analysis of sodium channel expression in dorsal root ganglion neurons. Mol Cell Neurosci 46(1):159–166

Hoeijmakers JG, Han C, Merkies IS, Macala LJ, Lauria G, Gerrits MM et al (2012) Small nerve fibres, small hands and small feet: a new syndrome of pain, dysautonomia and acromesomelia in a kindred with a novel NaV1.7 mutation. Brain 135(Pt 2):345–358

Huth T, Rittger A, Saftig P, Alzheimer C (2011) Beta-site APP-cleaving enzyme 1 (BACE1) cleaves cerebellar Na^+ channel beta4-subunit and promotes Purkinje cell firing by slowing the decay of resurgent Na^+ current. Pflugers Arch 461:355–371

Jarecki BW, Sheets PL, Jackson IIJO, Cummins TR (2008) Paroxysmal extreme pain disorder mutations within the D3/S4-S5 linker of Nav1.7 cause moderate destabilization of fast-inactivation. J Physiol 586:4137–53

Jarecki BW, Piekarz AD, Jackson JO 2nd, Cummins TR (2010) Human voltage-gated sodium channel mutations that cause inherited neuronal and muscle channelopathies increase resurgent sodium currents. J Clin Invest 120(1):369–378

Klinger AB, Eberhardt M, Link AS, Namer B, Schuy ET, Sittl R et al (2012) Sea-anemone toxin ATX-II elicits A-fiber-dependent pain and enhances resurgent and persistent sodium currents in large sensory neurons. Mol Pain 8(1):69

Kremeyer B, Lopera F, Cox JJ, Momin A, Rugiero F, Marsh S et al (2010) A gain-of-function mutation in TRPA1 causes familial episodic pain syndrome. Neuron 66(5):671–680

Kuo A, Gulbis JM, Antcliff JF, Rahman T, Lowe ED, Zimmer J et al (2003) Crystal structure of the potassium channel KirBac1.1 in the closed state. Science 300(5627):1922–1926

Lampert A, Dib-Hajj SD, Tyrrell L, Waxman SG (2006) Size matters: erythromelalgia mutation S241T in Nav1.7 alters channel gating. J Biol Chem 281(47):36029–36035

Lampert A, O'Reilly AO, Dib-Hajj SD, Tyrrell L, Wallace BA, Waxman SG (2008) A pore-blocking hydrophobic motif at the cytoplasmic aperture of the closed-state Nav1.7 channel is disrupted by the erythromelalgia-associated F1449V mutation. J Biol Chem 283(35): 24118–24127

Lampert A, Dib-Hajj S, Eastman E, Tyrrell L, Lin Z, Yang Y et al (2009) Erythromelalgia mutation L823R shifts activation and inactivation of threshold sodium channel Nav1.7 to hyperpolarized potentials. Biochem Biophys Res Commun 390(2):319–324

Lee MJ, Yu HS, Hsieh ST, Stephenson DA, Lu CJ, Yang CC (2007) Characterization of a familial case with primary erythromelalgia from Taiwan. J Neurol 254:210–214

Lewis AH, Raman IM (2011) Cross-species conservation of open-channel block by Na channel β4 peptides reveals structural features required for resurgent Na current. J Neurosci 31(32): 11527–11536

Michiels JJ, te Morsche RH, Jansen JB, Drenth JP (2005) Autosomal dominant erythermalgia associated with a novel mutation in the voltage-gated sodium channel alpha subunit Nav1.7. Arch Neurol 62(10):1587–1590

Nau C, Wang GK (2004) Interactions of local anesthetics with voltage-gated Na + channels. J Membr Biol 201(1):1–8

Oliveira JS, Redaelli E, Zaharenko AJ, Cassulini RR, Konno K, Pimenta DC et al (2004) Binding specificity of sea anemone toxins to Nav 1.1-1.6 sodium channels: unexpected contributions from differences in the IV/S3-S4 outer loop. J Biol Chem 279(32):33323–33335

O'Reilly JP, Wang S-Y, Wang GK (2001) Residue-specific effects on slow inactivation at V787 in D2-S6 of Nav1.4 sodium channels. J Biophys 81(4):2100–2111

Payandeh J, Scheuer T, Zheng N, Catterall WA (2011) The crystal structure of a voltage-gated sodium channel. Nature 475(7356):353–358

Raman IM, Bean BP (1997) Resurgent sodium current and action potential formation in dissociated cerebellar Purkinje neurons. J Neurosci 17(12):4517–4526

Raman IM, Bean BP (2001) Inactivation and recovery of sodium currents in cerebellar purkinje neurons: evidence for two mechanisms. Biophys J 80(2):729–737

Raman IM, Sprunger LK, Meisler MH, Bean BP (1997) Altered subthreshold sodium currents and disrupted firing patterns in Purkinje neurons of Scn8a mutant mice. Neuron 19(4):881–891

Rathmayer W (1979) Anemone toxin discriminates between ionic channels for receptor potential and for action potential production in a sensory neuron. Neurosci Lett 13(3):313–318

Schiavon E, Sacco T, Cassulini RR, Gurrola G, Tempia F, Possani LD et al (2006) Resurgent current and voltage sensor trapping enhanced activation by a β-scorpion toxin solely in Nav1.6 channel: significance in mice purkinje neurons. J Biol Chem 281(29):20326–20337

Schmalhofer W, Calhoun J, Burrows R, Bailey T, Kohler MG, Weinglass AB, et al. (2008). ProTx-II, a selective inhibitor of NaV1.7 sodium channels, blocks action potential propagation in nociceptors. *Mol Pharmacol*: mol.108.047670.

Sheets MF, Hanck DA (2003) Molecular action of lidocaine on the voltage sensors of sodium channels. J Gen Physiol 121(2):163–175

Sheets PL, Jackson JO 2nd, Waxman SG, Dib-Hajj SD, Cummins TR (2007) A Nav1.7 channel mutation associated with hereditary erythromelalgia contributes to neuronal hyperexcitability and displays reduced lidocaine sensitivity. J Physiol 581(Pt 3):1019–1031

Sittl R, Lampert A, Huth T, Schuy ET, Link AS, Fleckenstein J et al (2012) Anticancer drug oxaliplatin induces acute cooling-aggravated neuropathy via sodium channel subtype $Na_V1.6$-resurgent and persistent current. Proc Natl Acad Sci 109(17):6704–6709

Skeik N, Rooke TW, Davis MD, Davis DM, Kalsi H, Kurth I et al (2012) Severe case and literature review of primary erythromelalgia: novel SCN9A gene mutation. Vascular Med 17(1):44–49

Smith MR, Smith RD, Plummer NW, Meisler MH, Goldin AL (1998) Functional analysis of the mouse Scn8a sodium channel. J Neurosci 18(16):6093

Takahashi K, Saitoh M, Hoshino H, Mimaki M, Yokoyama Y, Takamizawa M et al (2007) A case of primary erythermalgia, wintry hypothermia and encephalopathy. Neuropediatrics 38(03): 157

Theile JW, Cummins TR (2011) Inhibition of Nav{β}4 peptide-mediated resurgent sodium currents in Nav1.7 channels by carbamazepine, riluzole and anandamide. Mol Pharmacol 80 (4):724–34

Theile JW, Jarecki BW, Piekarz AD, Cummins TR (2011) Nav1.7 mutations associated with paroxysmal extreme pain disorder, but not erythromelalgia, enhance Navβ4 peptide-mediated resurgent sodium currents. J Physiol 589(Pt 3):597–608

Wang GK, Strichartz GR (2012) State-dependent inhibition of sodium channels by local anesthetics: a 40-year evolution. Biochem (Mosc) Suppl Ser A Membr Cell Biol 6(2):120–127

Wang GK, Edrich T, Wang SY (2006) Time-dependent block and resurgent tail currents induced by mouse β4(154–167) peptide in cardiac Na^+ channels. J Gen Physiol 127(3):277–289

Wu MT, Huang PY, Yen CT, Chen CC, Lee MJ (2013) A novel SCN9A mutation responsible for primary erythromelalgia and is resistant to the treatment of sodium channel blockers. PLoS One 8(1):e55212

Yang Y, Wang Y, Li S, Xu Z, Li H, Ma L et al (2004) Mutations in SCN9A, encoding a sodium channel alpha subunit, in patients with primary erythermalgia. J Med Genet 41(3):171–174

Yang Y, Dib-Hajj SD, Zhang J, Zhang Y, Tyrrell L, Estacion M et al (2012) Structural modelling and mutant cycle analysis predict pharmacoresponsiveness of a Na(v)1.7 mutant channel. Nat Commun 3:1186

Yang Y, Estacion M, Dib-Hajj SD, Waxman SG (2013) Molecular architecture of a sodium channel S6 helix: radial tuning of the voltage-gated sodium channel 1.7 activation gate. J Biol Chem 288(19):13741–13747

Yu FH, Westenbroek RE, Silos-Santiago I, McCormick KA, Lawson D, Ge P et al (2003) Sodium channel β4, a new disulfide-linked auxiliary subunit with similarity to β2. J Neurosci 23 (20):7577

Regulation/Modulation of Sensory Neuron Sodium Channels

Mohamed Chahine and Michael E. O'Leary

Contents

Abstract

The pseudounipolar sensory neurons of the dorsal root ganglia (DRG) give rise to peripheral branches that convert thermal, mechanical, and chemical stimuli into electrical signals that are transmitted via central branches to the spinal cord. These neurons express unique combinations of tetrodotoxin-sensitive (TTX-S) and tetrodotoxin-resistant (TTX-R) Na^+ channels that contribute to the resting membrane potential, action potential threshold, and regulate neuronal firing frequency. The small-diameter neurons (<25 μm) isolated from the DRG

M. Chahine (✉)
Centre de recherche, Institut en santé mentale de Québec, Local F-6539, 2601, chemin de la Canardière, QC City, QC, Canada G1J 2G3

Department of Medicine, Université Laval, Quebec City, QC, Canada G1K 7P4
e-mail: mohamed.chahine@phc.ulaval.ca

M.E. O'Leary
Cooper Medical School of Rowan University, Camden, NJ, USA

P.C. Ruben (ed.), *Voltage Gated Sodium Channels*, Handbook of Experimental Pharmacology 221, DOI 10.1007/978-3-642-41588-3_6,

represent the cell bodies of C-fiber nociceptors that express both TTX-S and TTX-R Na^+ currents. The large-diameter neurons (>35 μm) are typically low-threshold A-fibers that predominately express TTX-S Na^+ currents. Peripheral nerve damage, inflammation, and metabolic diseases alter the expression and function of these Na^+ channels leading to increases in neuronal excitability and pain. The Na^+ channels expressed in these neurons are the target of intracellular signaling cascades that regulate the trafficking, cell surface expression, and gating properties of these channels. Post-translational regulation of Na^+ channels by protein kinases (PKA, PKC, MAPK) alter the expression and function of the channels. Injury-induced changes in these signaling pathways have been linked to sensory neuron hyperexcitability and pain. This review examines the signaling pathways and regulatory mechanisms that modulate the voltage-gated Na^+ channels of sensory neurons.

Keywords
Pain • Dorsal root ganglion • Na_V • Protein kinase • Nociception

1 Sensory Neuron Physiology

Primary sensory neurons play an essential role in the detection of external stimuli and the transmission of information regarding the modality, location, and intensity of the stimuli to the central nervous system. The cell bodies of these afferent nerve fibers are located just outside of the spinal cord in the dorsal root ganglion (DRG). Branches of these neurons innervate peripheral and visceral tissues and are invested with specialized transducing channels that convert thermal, mechanical, and chemical stimuli into electrotonic receptor potentials capable of triggering action potentials in sensory neurons. Action potentials elicited in peripheral branches are transmitted through the DRG to the central processes of these neurons where they synapse on second-order sensory neurons located in the dorsal horn of the spinal cord. The pseudounipolar morphology and electrophysiology of sensory neurons are ideally suited to detect peripheral stimuli and transmit impulses to the spinal cord.

Afferent nerve fibers have been classified based on morphology, sensory modality, stimulation threshold, and conduction velocity (Fornaro et al. 2008; Goldstein et al. 1991; Harper and Lawson 1985a; Lawson et al. 1993; Lee et al. 1986; Yoshida and Matsuda 1979; Lawson 2002). Unmyelinated C fibers and thinly myelinated Aδ fibers have narrow axonal diameters (0.5–4 μm) and conduct impulses at a slow rate (1–30 m/s). The peripheral branches of nociceptors terminate as free nerve endings in muscle, skin, and viscera (Kruger et al. 2003). The majority of cutaneous C and Aδ fibers preferentially respond to noxious stimulation (≈90 %) and convey information about potential tissue-damaging conditions. The inverse relationship between afferent conduction velocity and the threshold for noxious stimulation are

consistent with an important role for unmyelinated C and thinly myelinated Aδ fibers in nociception (Burgess and Perl 1967). Myelinated A fibers have large-diameter axons (12–20 μm) and fast rates of impulse conduction (70–120 m/s). The peripheral branches of cutaneous Aβ fibers are frequently encapsulated by accessory structures that modify sensory transduction (i.e., Pacinian corpuscles, Ruffini endings, Merkle discs). These low-threshold mechanoreceptors are tuned to respond to non-noxious tactile stimulation and vibration.

Afferent nerve fibers can be further distinguished based on the expression of cytoskeletal proteins and cell adhesion molecules. Neurofilaments contribute to the cytoskeletal structure of sensory neurons and are important determinants of axonal diameter and conduction velocity (Hoffman et al. 1985; Fuchs and Cleveland 1998). The neurofilaments NF200 (200 kDa) and peripherin (57 kDa) are differentially expressed in large- and small-diameter DRG neurons, respectively (Goldstein et al. 1991; Fornaro et al. 2008). Antibodies directed against NF200 preferentially label large-diameter neurons and are widely used as markers for myelinated nerve fibers. Necls are a family of cell adhesion molecules expressed in peripheral neurons (Necl-1) where they contribute to myelination (Spiegel et al. 2007; Maurel et al. 2007). The preferential expression of NF200 and Necl-1 in large-diameter neurons have proved to be useful for identifying myelinated A fibers (Ho and O'Leary 2011). This contrasts with small-diameter DRG neurons that express peripherin but low levels of NF200 and Necl-1, a pattern that is more consistent with unmyelinated C-fibers. The expression of Necls is differentially regulated in models of nerve injury and is believed to play a role in axonal remyelination (Zelano et al. 2009).

C-fiber nociceptors are further subdivided based on differences in the expression of sensory receptors, projections within the dorsal horn, and the binding of the isolectin B4 (IB_4) (Snider and McMahon 1998; Stucky and Lewin 1999; Ringkamp 2009). IB_4 is a marker of non-peptidergic nociceptors that express the purinergic P2X3 channel, receptors for glial-derived neurotrophic factor (c-ret, GDNFRα1-4), and mas-related G protein-coupled receptors (MrgprD) (Bradbury et al. 1998; Dong et al. 2001; Priestley et al. 2002; Albrecht and Rice 2010). Non-peptidergic C-fibers account for the majority (≈70 %) of epidermal innervation and terminate in lamina II of the dorsal horn (Zylka et al. 2005; Liu et al. 2007). This contrasts with the peptidergic nociceptors that preferentially express Substance P, calcitonin gene-related peptide (CGRP), and the TrkA neurotrophin receptor (Priestley et al. 2002; Albrecht and Rice 2010). Peptidergic C-fibers terminate in lamina I and the outer portion of lamina II_o of the dorsal horn (Zylka et al. 2005). Although TPRV1 is broadly expressed in small-diameter neurons, immunocytochemistry and capsaicin sensitivity suggest that these channels may be preferentially expressed in non-peptidergic nociceptors (Caterina et al. 1997; Guo et al. 1999; Michael and Priestley 1999; Petruska et al. 2000, 2002; Liu et al. 2004). While these broad classifications of peptidergic and non-peptidergic neurons are generally useful, the expression patterns of sensory receptors display considerable overlap and vary with species (Ringkamp 2009; Price and Flores 2007). Species-specific difference in expression has been clearly shown for TRPV1, which is found to be primarily

localized in peptidergic afferents of mice and non-peptidergic fibers in rats (Zwick et al. 2002).

2 DRG Sensory Neurons Express Multiple Isoforms of Voltage-gated Na^+ Channels

Small- and large-diameter DRG neurons express distinct populations of voltage-gated Na^+ currents that contribute to the unique electrophysiology of these neurons (Cummins et al. 2007; Dib-Hajj et al. 2009; Rush et al. 2007). These Na^+ currents have been broadly classified based on voltage dependence, kinetics, and pharmacology into rapid tetrodotoxin-sensitive (TTX-S), slowly gating TTX-resistant (TTX-R), and persistent TTX-R components (Caffrey et al. 1992; Elliott and Elliott 1993; Kostyuk et al. 1981; Roy and Narahashi 1992). Four distinct TTX-S isoforms ($Na_v1.1$, $Na_v1.2$, $Na_v1.6$, $Na_v1.7$) and two TTX-R isoforms ($Na_v1.8$, $Na_v1.9$) are known to be differentially expressed in subpopulations of DRG neurons (Black et al. 1996; Amaya et al. 2000; Dib-Hajj et al. 1998b; Ho and O'Leary 2011). Small-diameter neurons (<25 μm) express a combination of rapid TTX-S ($Na_v1.7$), slow TTX-R ($Na_v1.8$), and persistent TTX-R ($Na_v1.9$) Na^+ currents. This contrasts with medium- and large-diameter DRG neurons (>30 μm) that preferentially express high-threshold rapidly inactivating TTX-S isoforms ($Na_v1.1$, $Na_v1.6$, and $Na_v1.7$). Intrinsic differences in the kinetics and voltage dependence of the TTX-S and TTX-R Na^+ channels coupled with the differential expression of these channels in subpopulations of DRG neurons determine the unique action potential thresholds and firing patterns of nociceptors and low-threshold sensory neurons.

While the diameter of the cell body is widely used to infer nociceptive and non-nociceptive function, there is substantial overlap in the Na^+ channel isoforms expressed in these neuronal populations. Analysis of Na^+ channel transcript and protein expression showed that in addition to TTX-S isoforms some 10–30 % of large DRG neurons also express TTX-R Na^+ current and $Na_v1.8$ channels (Amaya et al. 2000; Djouhri et al. 2003; Black et al. 2004; Sangameswaran et al. 1996; Novakovic et al. 1998; Tate et al. 1998; Renganathan et al. 2000; Ho and O'Leary 2011). While it is tempting to speculate that these large neurons displaying TTX-R Na^+ currents are Aδ neurons, this has not been clearly established.

3 Voltage-gated Na^+ Channels Are Important Determinants of Neuronal Excitability

$Na_v1.7$ produces a rapidly gating TTX-S Na^+ current and is the predominant TTX-S Na^+ channel expressed in nociceptors (Toledo-Aral et al. 1997; Black et al. 1996; Sangameswaran et al. 1997; Ho et al. 2012). The endogenous TTX-S current of small DRG neurons and heterologously expressed $Na_v1.7$ channels display a similar low threshold for activation (≈−50 mV) and display rapid gating kinetics

by comparison to the co-expressed TTX-R Na^+ current (Caffrey et al. 1992; Cummins and Waxman 1997; Cummins et al. 1998; Elliott and Elliott 1993; Ho and O'Leary 2011; Roy and Narahashi 1992; Vijayaragavan et al. 2001; Zhao et al. 2011). Because of the hyperpolarized range of voltages where $Na_v1.7$ activates, these channels are important determinants of the action potential threshold (Schild and Kunze 1997; Blair and Bean 2002). The resting membrane potential of a typical DRG neuron (≈ -65 mV) is close to the midpoint of $Na_v1.7$ steady-state inactivation ($V_{0.5} = -65$ mV) suggesting that under resting conditions, approximately 50 % of these channels will be inactivated and therefore unavailable to open in response to depolarization (Ogata and Tatebayashi 1993). Because of the steep voltage dependence of $Na_v1.7$ inactivation even small shifts in the resting membrane potential substantially alter the steady-state availability of these channels and consequently the action potential threshold. Although $Na_v1.7$ channels rapidly activate and inactivate at depolarized voltages, they display unusually slow-gating kinetics at hyperpolarized voltages. At -80 mV the endogenous TTX-S and $Na_v1.7$ Na^+ currents slowly recover from inactivation ($\tau \approx 100$ ms), which may contribute to the intrinsic slow firing frequency of nociceptors (Elliott and Elliott 1993; Cummins et al. 1998; Vijayaragavan et al. 2001; Ho et al. 2012). Another important feature of $Na_v1.7$ is its slow rate of inactivation from closed states, which makes these channels comparatively resistant to subthreshold depolarizations (Cummins et al. 1998). Slow closed-state inactivation appears to enable $Na_v1.7$ channels to amplify subthreshold depolarization such as those evoked by stimulus-transducing channels (Cummins et al. 2007). Physiologically, $Na_v1.7$ appears to play a critical role by spanning the gap between subthreshold receptor potentials and the activation of high-threshold $Na_v1.8$ channels that drive the rapid depolarizing phase of nociceptor action potential (Blair and Bean 2002). The biophysical properties of $Na_v1.7$ indicate these channels contribute to the action potential threshold and are important determinants of nociceptor firing frequency.

Two components of TTX-R Na^+ current have been identified in small DRG neurons. The predominant TTX-R Na^+ current of DRG neurons displays slow-gating properties and activate (≈ -15 mV) and inactivate (≈ -30 mV) at voltages 20–30 mV more depolarized than the endogenous TTX-S currents (Caffrey et al. 1992; Elliott and Elliott 1993; Kostyuk et al. 1981; Ogata and Tatebayashi 1993; Roy and Narahashi 1992). This TTX-R current is observed in the majority of nociceptors and a subpopulation of large myelinated sensory neurons (Akopian et al. 1996; Amaya et al. 2000; Djouhri et al. 2003; Sangameswaran et al. 1996). Studies of null mice determined that the $Na_v1.8$ channel underlie the predominant TTX-R Na^+ current in small DRG neurons (Akopian et al. 1999) and contributes to the shoulder observed on the falling phase of nociceptor action potentials (Gold et al. 1996a; Harper and Lawson 1985b; Waddell and Lawson 1990). While the gating of $Na_v1.8$ at depolarized voltages is sluggish by comparison to $Na_v1.7$, $Na_v1.8$ channels display faster recovery from inactivation at hyperpolarized voltages (Cummins and Waxman 1997; Elliott and Elliott 1993). The biophysical

properties of the heterologously expressed $Na_v1.8$ channels are similar to those of the endogenous TTX-R Na^+ current of DRG neurons (Akopian et al. 1996; Sangameswaran et al. 1996; Vijayaragavan et al. 2001; Zhao et al. 2011). The combination of rapid recovery and depolarized threshold for steady-state inactivation of $Na_v1.8$ channels enables nociceptors to maintain high rates of action potential firing after nerve damage or under depolarizing conditions where TTX-S Na^+ channels are inactivated (Renganathan et al. 2001). Another important feature of $Na_v1.8$ is its usually rapid entry into slow-inactivated states that accounts the frequency-dependent reduction of TTX-R Na^+ current observed during repetitive stimulation (Blair and Bean 2003; Rush et al. 1998; Vijayaragavan et al. 2001; d'Alcantara et al. 2002; Tripathi et al. 2006). Despite their slow kinetics and high threshold for activation, $Na_v1.8$ channels account for the majority of the inward current during the rapid rising phase of nociceptor action potentials and make a small but significant contribution to setting the action potential threshold (Renganathan et al. 2001; Blair and Bean 2002).

Electrophysiology identified a small persistent TTX-R Na^+ current in many small DRG neurons (Cummins and Waxman 1997). Unlike the TTX-R current of $Na_v1.8$ channels, these currents activate over a relatively hyperpolarized range of voltages and display comparatively slow-gating kinetics. Subsequent work demonstrated that $Na_v1.9$ channels produced slowly inactivating currents that are exclusively expressed in small DRG neurons (Dib-Hajj et al. 1998b, 1999; Fang et al. 2002, 2006). This was confirmed by studies showing that the persistent TTX-R component of Na^+ current of small DRG neurons was absent in $Na_v1.9$ null mice and reconstituted when $Na_v1.9$ was heterologously expressed in the null background (Amaya et al. 2000; Priest et al. 2005). Unfortunately, detailed studies of these persistent Na^+ currents were hampered by the overlapping expression of $Na_v1.9$ and $Na_v1.8$ currents in DRG neurons and the poor heterologous expression profile of $Na_v1.9$ channels in cultured cell lines (Dib-Hajj et al. 2002). Utilizing $Na_v1.8$ null mice, the TTX-R currents produced by $Na_v1.9$ channels were found to display slow-gating kinetics and activated (-47 mV) and inactivated (-44 mV) over a relatively hyperpolarized range of voltages (Cummins et al. 1999). Despite the extensive overlap of activation and steady-state inactivation and high current density, $Na_v1.9$ channels are largely slow inactivated (>95 %) at voltages near the resting membrane potential of DRG neurons (-65 mV) (Cummins et al. 1999). Recent studies of heterologously expressed $Na_v1.9$ channels confirmed that these channels activate and inactivate over a relatively hyperpolarized range of voltages (Vanoye et al. 2013). Importantly, the activation and inactivation of $Na_v1.9$ channels display substantial overlap raising the possibility of persistently activated TTX-R Na^+ currents at voltages near the resting membrane potential. Despite the low probability of activation, persistent opening of a small fraction of these channels could substantially alter the resting membrane potential or alter the neurons response to subthreshold stimulation (Herzog et al. 2001).

4 Peripheral Nerve Injury and Sensory Neuron Plasticity

Pain is a physiologically important sensation that signals the presence of noxious stimuli and serves as a defense mechanism for preventing tissue damage. An important feature of nociceptive pain is that it generally subsides after the removal of tissue stimulation. However, nerve injury, inflammation, metabolic diseases, and genetic disorders can trigger persistent changes in somatosensory systems resulting in hyperalgesia and chronic pain in the apparent absence of tissue damage or inflammation. Unlike nociceptive pain, this neuropathic pain is maladaptive in that it neither accurately reflects tissue damage nor aids in wound healing. Although the underlying mechanisms are not known, plasticity in both the peripheral and central nervous systems are known to contribute to development and maintenance of neuropathic pain (Campbell and Meyer 2006; Costigan et al. 2009).

Primary afferents (C, Aδ fibers) are the initial link in the nociceptive pathway and play a central role in the development and maintenance of neuropathic pain. The peripheral terminals of these nociceptors express a wide variety of receptors and transducers that respond to high-threshold noxious stimuli (McCleskey and Gold 1999; Dubin and Patapoutian 2010). Sensitization of peripheral nerve fibers due to increased expression or decreased threshold of these receptors/transducers contribute to chronic pain, hyperalgesia, and allodynia observed after nerve and tissue damage(Julius and Basbaum 2001; Bhave and Gereau 2004; Hucho and Levine 2007; Woolf and Ma 2007; Cheng and Ji 2008). In addition to these receptor-mediated mechanisms, decreased action potential thresholds and increased firing frequency also contribute to the development of neuropathic pain and numerous studies have linked such injury-induced hyperexcitability to changes in voltage-gated ion channels (Cummins et al. 2007; Dang and McCleskey 1998; Lai et al. 2004). $Na_v1.7$, $Na_v1.8$, and $Na_v1.9$ channels regulate the resting membrane potential and action potential threshold and produce the depolarizing phase of nociceptor action potentials. Although the voltage dependence and gating of Na^+ channels are principally determined by the intrinsic properties of the pore-forming subunit, these processes are modulated by intracellular signaling and posttranslational modification. Activation of Ca^{2+}-dependent protein kinases (PKC) and cAMP-dependent protein kinases (PKA) alter the biophysical properties, cell surface expression, and trafficking of neuronal Na^+ channels. Figure 1 illustrates the putative signal transduction pathway in a DRG neuron. This is a schematic representation of the Na^+ channel and all the known sites of PKA and PKC regulation. The following sections will review the modulation of neuronal Na^+ channels by signaling pathways and protein phosphorylation.

5 Na^+ Channel Modulation by PKC

Activation of PKC by phorbol esters causes a reduction in the Na^+ currents of channels heterologously expressed in *Xenopus* oocytes including $Na_v1.2$, $Na_v1.4$, $Na_v1.5$, $Na_v1.7$, and $Na_v1.8$ (Schreibmayer et al. 1991; Murray et al. 1997;

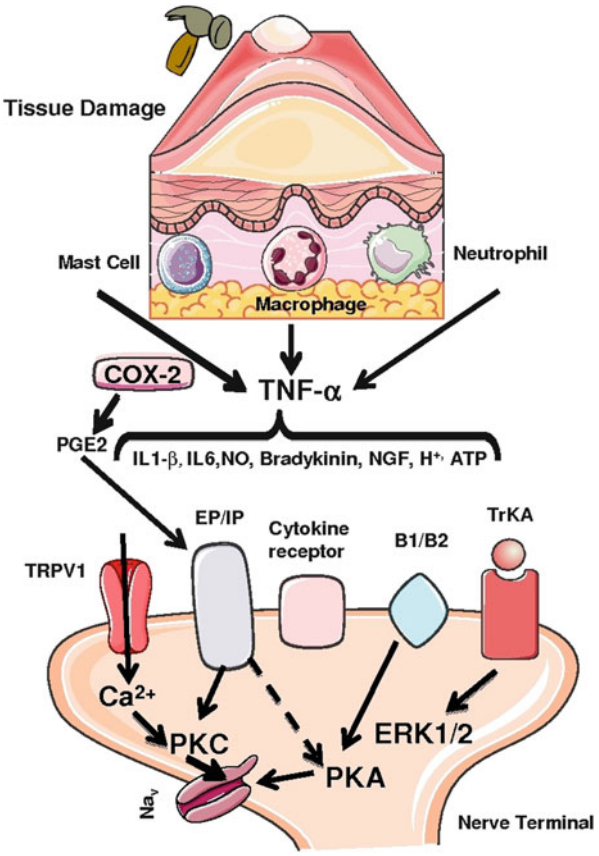

Fig. 1 Tissue damage cause nociceptive, inflammatory and neuropathic pain. Schematic representation of a mammalian sensory signaling relay, following tissue damage and inflammation. The inflammatory cells release several chemical mediators creating an inflammatory soup that activates or alters the stimulus response properties of nociceptor afferents. Activation of Ca^{2+} dependent protein kinases (PKC) and cAMP-dependent protein kinases (PKA), ERK1/2 affect the biophysical properties of several sensory neuron channels in particular Na_v channels

Bendahhou et al. 1995; Vijayaragavan et al. 2004). Similar PKC-dependent reductions in current amplitudes are observed for Na^+ channels expressed in Chinese hamster lung 1,610 cells (CHO) and neuroblastoma indicating that the observed inhibition is independent of the cells used for expression (Numann et al. 1991; Qu et al. 1994; Godoy and Cukierman 1994). The PKC inhibition of $Na_v1.2$ channels has been attributed to a slow time constant of inactivation and reduced availability of channels due to a negative shift in steady-state inactivation (Godoy and Cukierman 1994; Qu et al. 1994). Consistent with these observations, single channel data showed no change in unitary conductance, prolonged open times, and reduced probability of opening after PKC activation (Numann et al. 1991). Related studies showed that activation of PKC-linked muscarinic receptors reduced the endogenous Na^+ currents of embryonic brain, hippocampal, pyramidal, medium spiny, and cortical neurons (Cantrell et al. 1996; Numann et al. 1991; Mittmann and Alzheimer 1998). Phosphopeptide analysis revealed that the PKC-induced reduction in $Na_v1.2$ currents required phosphorylation of

serine residues in the interdomain DIII–DIV linker (*S1506*) and in the DI–II cytoplasmic loop (*S554* and *S573*) (West et al. 1991; Cantrell et al. 2002a). These phosphorylation sites are highly conserved in neuronal Na^+ channels suggesting a common mechanism may underlie the PKC-dependent reduction in Na^+ current amplitude in these channels. By comparison these DI–DII phosphorylation sites are absent in skeletal muscle $Na_v1.4$ channels resulting in Na^+ currents that fail to respond to PKA activation (Smith and Goldin 1996).

Although PKC reduces the amplitude of many endogenous neuronal Na^+ currents and inhibits heterologously expressed Na^+ channels, application of inflammatory mediators that activate these kinases (PGE_2) potentiate the TTX-R Na^+ currents of primary sensory neurons (Gold et al. 1996a, 1998). Phorbol ester activators (PMA, PDBu) produced a 30 % increase in the amplitude of the TTX-R Na^+ current with no change in the conductance–voltage relationship or current kinetics (Gold et al. 1998). The observed increases in the TTX-R Na^+ current of sensory neurons induced by PDBu and PGE_2 were antagonized by PKC inhibitors (staurosporine, $PKC_{19–36}$ peptide). Similar studies reported 12–19 % increases in TTX-R peak current and slight hyperpolarizing shifts in activation and inactivation (2–5 mV) after PMA application (Ikeda et al. 2005; Cang et al. 2009). These data suggest that PKC-mediated upregulation of TTX-R Na^+ current contributes to the sensitization of sensory neurons by inflammatory agents (Gold et al. 1996b, 1998).

The PKC family of kinases is composed of 12 isozymes that are classified as conventional, novel, and atypical (Dempsey et al. 2000; Battaini 2001). Specific PKC isozymes of the conventional and novel families appear to be involved in nociceptor hyperexcitability (Aley et al. 2000; Igwe and Chronwall 2001; Martin et al. 1999; Khasar et al. 1999; Cesare et al. 1999). Inflammatory mediators promote the translocation of PKC-ε to the plasma membrane where it contributes to peripheral sensitization and pain (Khasar et al. 1999; Zhang et al. 2007). This is supported by studies showing that increased activity of the nPKCε and cPKCβII isozymes is linked to inflammatory hyperalgesia (Aley et al. 2000; Igwe and Chronwall 2001; Martin et al. 1999; Khasar et al. 1999; Cesare et al. 1999). nPKCε and cPKCβII have been shown to downregulate heterologously expressed $Na_v1.7$ channels, while the nPKCε isoform preferentially reduces $Na_v1.8$ current (Vijayaragavan et al. 2004). These findings suggest that the TTX-S and TTX-R Na^+ channels expressed in sensory neurons may be targeted by distinct PKC isoforms. Furthermore, the nPKCε downregulation of $Na_v1.8$ channels heterologously expressed in oocytes (Vijayaragavan et al. 2004) sharply contrasts with the PMA-induced potentiation of TTX-R Na^+ current observed in native DRG neurons (Cang et al. 2009). Although the causes of this discrepancy are not known, PKC isozymes may be differentially expressed or differentially regulate the $Na_v1.8$ channels expressed in native neuronal and non-neuronal cell lines.

Hyperalgesic priming is a long-lasting latent state of nociceptor hyperresponsiveness to the inflammatory state following an inflammatory or neuropathic upset (Reichling and Levine 2009). Further studies in DRG neurons concluded that hyperalgesic priming occurs only in IB4(+) nociceptors (Joseph and Levine 2010).

Recent study showed that hyperalgesic priming could be induced by ψεRACK pseudo-receptor octapeptide for activated PKCε at low doses that fail to induce hyperalgesia (Parada et al. 2003).

6 Modulation of Na^+ Channels by PKA

Tissue injury and inflammation produces hyperalgesia and pain that is in part results from an increase in the excitability of primary afferents (Julius and Basbaum 2001; Woolf and Ma 2007; Bhave and Gereau 2004; Ji and Strichartz 2004; Woolf and Costigan 1999). These effects are mediated by a variety of inflammatory mediators that are released in response to tissue damage including nerve growth factors, prostaglandins, bradykinin, and tissue necrosis factor. The peripheral sensitization produced by these factors is characterized by increased spontaneous and evoked firing, enhanced responses to noxious stimuli, and mechanical/thermal hyperalgesia. These inflammatory reactions occur within minutes of tissue damage suggesting that these effects are locally mediated within nerve terminals situated near the site of injury (Gold 1999). Studies indicate that the observed changes in excitability results from the activation of G-protein-coupled receptors and intracellular signaling pathways that modulate the sensory transducers and voltage-gated ion channels present on the peripheral terminals of these neurons (Gold 1999; Woolf and Costigan 1999; Ji and Strichartz 2004; Cheng and Ji 2008).

The PKA activators forskolin and 8-bromo cAMP reduce the Na^+ currents of heterologously expressed $Na_v1.2$ without significantly altering channel gating properties (Smith and Goldin 1996; Li et al. 1992). The underlying mechanism was determined using single-channel measurements demonstrating that PKA activation shifted the channels to a null gating mode that reduced the open probability and peak current amplitude (Li et al. 1992). PKA activation produced a similar reduction in the currents of heterologously expressed $Na_v1.1$, $Na_v1.6$, and $Na_v1.8$ channels (Smith and Goldin 1992; Zhou et al. 2000; Fitzgerald et al. 1999; Schreibmayer et al. 1994; Vijayaragavan et al. 2004). This contrasts with the endogenous Na^+ currents of sensory neurons, where PKA activation (cAMP, forskolin) increased TTX-R Na^+ currents (13–35 %), produced hyperpolarizing shifts in activation and steady-state inactivation (4–7 mV), and increased the rates of activation and deactivation (Gold et al. 1996b, 1998; England et al. 1996). A similar forskolin-induced increase in TTX-R Na^+ current was observed for $Na_v1.8$ channels heterologously expressed ion COS-7 cells (Fitzgerald et al. 1999). Eliminating the DI–DII linker consensus phosphorylation sites substantially weakened the PKA regulation of $Na_v1.8$ channels (Fitzgerald et al. 1999). Studies of $Na_v1.2$ channels found that the length of the DI–DII linker upstream from the conserved PKA phosphorylation sites is an important determinant of Na^+ channel potentiation (Smith and Goldin 2000). The DI–DII linker also interacts with synaptotagamin, a synaptic protein that may modulate the effects of PKA on Na^+ channels (Sampo et al. 2000).

Alternative splicing is a mechanism that permits the production of functionally distinct Na^+ channels from a single gene, thereby increasing the diversity of voltage-gated Na^+ currents. Previous studies have shown that sodium channel splice variants contribute to the development of neuropathic pain in animal models of nerve injury (Raymond et al. 2004). Variants of $Na_v1.7$ channels include alternative splicing in exon 11 that encodes for a portion of the cytoplasmic DI–DII linker (Raymond et al. 2004). The 11 L variant includes an 11 amino acid insertion into the D1-day linker that does not substantially alter $Na_v1.7$-gating properties but reduces the sensitivity of the channels to PKA regulation (Chatelier et al. 2008). Application of cAMP produced a significant hyperpolarizing shift in the activation (−8 mV) of the $Na_v1.7$-11S but not the $Na_v1.7$-11 L variant. The upregulation of $Na_v1.7$-11S in injured neurons, along with the increased sensitivity to cAMP and hyperpolarizing shift in activation may contribute nociceptor hyperexcitability and the development of neuropathic pain after nerve injury.

In addition to acute modulation of Na^+ channel function, PKA activators have been shown to increase cell surface expression and Na^+ currents by promoting the trafficking of TTX-R $Na_v1.8$ channels to the plasma membrane (Vijayaragavan et al. 2004). In *Aplysia* neurons, PKA activation enhances the rate of microtubule-dependent organelle transport by two to threefold (Azhderian et al. 1994). The PKA potentiation of $Na_v1.5$ channels results from a combination of phosphorylation of DI–DII linker serines and PKA-dependent interaction with as yet unidentified proteins involved in channel trafficking (Zhou et al. 2002). The interdomain DI–DII linker of Na^+ channels is multifunctional contributing to both the posttranslational regulation of Na^+ channel function and cell-surface expression. Isoform-specific differences in trafficking may explain why PKA activators potentiate the Na^+ currents of some ($Na_v1.5$, $Na_v1.8$, TTX-R) but not all ($Na_v1.2$, $Na_v1.7$, TTX-S) voltage-gated Na^+ channels.

Intracellular GTPγS induced an upregulation of the persistent TTX-R Na^+ currents of DRG neurons that was linked to reduced action potential thresholds and spontaneous firing (Ostman et al. 2008). Recent work demonstrated that this GTPγS upregulation of the persistent $Na_v1.9$ current resulted from an increase in the open probability and prolonged opening of the channel (Vanoye et al. 2013). Because the persistent TTX-R current activates at relatively hyperpolarized voltages ($V_{0.5} \approx -45$ mV) by comparison to the rapidly inactivating TTX-R ($V_{0.5} \approx -15$ mV) and TTX-S ($V_{0.5} \approx -25$ mV) currents, this predicts that selectivity increasing persistent TTX-R may be effective in reducing the action potential threshold. Neurons of $Na_v1.9$ null mice reversed many of the effects of internal GTP on the persistent TTX-R current and neuronal excitability (Ostman et al. 2008). $Na_v1.9$ channels are upregulated by inflammatory mediators consistent with a role for these channels in peripheral inflammation (Maingret et al. 2008). Inflammatory mediators produce a similar upregulation of TTX-R $Na_v1.8$ channels that is in part mediated by activation of PKA (Gold et al. 1998). G protein-dependent activation of the adenylate cyclase/cAMP/PKA cascade may also contribute to the upregulation of $Na_v1.9$ channels.

7 Convergent Regulation of Na^+ Channels by the PKA and PKC Pathways

The PKC and PKA regulation of neuronal Na^+ currents involves the phosphorylation of multiple sites on the channel. Phosphopeptide mapping, mutational analyses, and functional measurements of Na^+ currents identified four conserved serine residues located on the DI–II (S554, S573, S576) and DIII–DIV (S1506) linkers of $Na_v1.2$ channels that are targets of PKA and PKC protein phosphorylation (Cantrell et al. 2002a). S573 appears to play a predominant role in the PKA regulation of $Na_v1.2$ channels (Smith and Goldin 1997). Activation of PKC results in the phosphorylation of three serines including two in the DI–DII (S554, S573) and one in the DIII–DIV (S1506) linkers. S1506 is situated on the Na^+ channel inactivation gate and phosphorylation at this site is required for PKC inhibition of peak current and slowing of inactivation (West et al. 1991). Replacement of S1506 with a negatively charged residue partially mimics the effect of phosphorylation at this site and promotes PKA-dependent phosphorylation (Cantrell et al. 2002b; Murphy et al. 1993). S573 appears to be a substrate for both the PKA and PKC kinases and is required for Na^+ current inhibition (Murphy and Catterall 1992). Maximal reduction of $Na_v1.2$ conductance requires PKC phosphorylation on the DIII–IV (S1506) and DI–II linkers (S554, S573) (Cantrell et al. 2002b). Phosphorylation of S576 and S1506 by PKC appears to facilitate phosphorylation of the DI–II loop by PKA (S554, S573). In this way the PKA and PKC pathways produce convergent regulation at the level of individual Na^+ channels. Reductions in the peak Na^+ current and slower inactivation kinetics mediated by convergent PKA/PKC regulation could have important implications for the action potential threshold and firing frequency of neurons.

Convergent PKA/PKC regulation is observed when $Na_v1.2$ channels are heterologously expressed in the CHO cells but not the HEK293-derived tsA201 cell line. This discrepancy has been attributed to the voltage-dependent modulation of these channels by PKA (Kondratyuk and Rossie 1997; Cantrell et al. 1999). At hyperpolarized holding potentials (−110 mV), the PKA modulation of $Na_v1.2$ is highly dependent on concurrent activity of PKC. Holding at a more depolarized voltage (−75 mV) reduces this dependence permitting PKA modulation in the absence of PKC activation (Cantrell et al. 1999, 2002b; Kondratyuk and Rossie 1997). Although the underlying mechanism is not known, it has been speculated that depolarization may induce a conformational change in $Na_v1.2$ channels that facilitates PKA phosphorylation (Cantrell et al. 1999). Alternatively, depolarization may promote phosphorylation by recruiting PKA to the DI–DII linker (Kondratyuk and Rossie 1997).

The rapidly inactivating component of TTX-R Na^+ current of DRG neurons displays similar PKA/PKC convergent regulation (Gold et al. 1998). Inhibitors of PKC attenuate the forskolin-induced modulation of TTX-R. This contrasts with PKA inhibitors, which have little if any impact on PKC modulation. These findings are in agreement with studies of $Na_v1.2$ where phosphorylation of the DIII–DIV

linker potentiates PKA modulation, presumably by facilitating phosphorylation of the DI–DII linker (Li et al. 1993).

In addition to kinases, $Na_v1.2$ channels are substrates of phosphatases that are important determinants of modulation by signaling pathways (Murphy et al. 1993; Chen et al. 1995). The calcium-regulated phosphatase calcineurin reduces phosphorylation at four sites within the DI–DII linker (S623, S573, S610, S687), while phosphatase 2A selectively dephosphorylates S610. These data indicate that the PKA modulation of $Na_v1.2$ channels reflects a balance of PKA phosphorylation and dephosphorylation at multiple sites within the DI–DII linker.

8 Mitogen-Activated Protein Kinases

The mitogen-activated family of protein kinases (MAPKs) are group of serine/threonine-specific kinases that couple activation of membrane-bound receptors to intracellular signal cascades (Lewis et al. 1998; Seger and Krebs 1995; Widmann et al. 1999). Dysfunction of the mitogen-activated protein kinases (MAPK) signaling is observed during stress and tissue injury and has been implicated in a number of neuronal disorders (Kim and Choi 2010). Activation of upstream regulatory pathways phosphorylate MAPKs inducing a conformational change in the substrate-binding site. The inactivate (non-phosphorylated) forms of MAPKs (ERK, p38, JNK) predominant in naive DRG neurons but increase after inflammation, axotomy, and spinal nerve ligation (Kim et al. 2002; Jin et al. 2003). In sensory neurons, MAPKs directly phosphorylate cellular proteins, activate downstream regulatory pathways, and increase the transcription of pain-related genes (Obata and Noguchi 2004).

An important role for MAPKs in sensory neuron excitability is supported by studies showing that MAPKs (ERK1/2, p38) and voltage-gated Na^+ channels ($Na_v1.7$, $Na_v1.8$) are upregulated in painful human neuromas (Black et al. 2008). The expression of p38 increases in animal models of nerve injury where it upregulates both TTX-R current and the TTX-S currents of DRG neurons (Obata and Noguchi 2004; Obata et al. 2004; Xu et al. 2007; Jin and Gereau 2006; Chattopadhyay et al. 2008). Activation of p38 produced changes in the current densities of $Na_v1.8$ and $Na_v1.6$ but no change in the gating properties of these channels (Hudmon et al. 2008; Wittmack et al. 2005). The p38 modulation of $Na_v1.6$ was eliminated by replacing a serine of the DI–DII linker region with alanine (S533A) suggesting a direct phosphorylation of the channel. This contrasts with the extracellular signal-related kinase (ERK1/2), which induces hyperpolarizing shifts in $Na_v1.7$ activation and inactivation with no change in current density and increases the action potential firing frequency of DRG neurons (Stamboulian et al. 2010). MAPKs appear to preferentially target distinct Na^+ channel isoforms and differentially regulate the conductance and gating of the channels.

9 Physiological Regulation of Sodium Channels

Prostaglandins (PGE_2, PGI_2) are metabolites of arachidonic acid that bind to G protein-coupled EP or IP prostinoid receptors and activate intracellular signaling cascades (Kawabata 2011). In situ hybridization has verified the expression of EP receptors in sensory neurons and in particular small-diameter nociceptors (Sugimoto et al. 1994; Oida et al. 1995; Perl 1996). PGE_2 plays a key role in the development of inflammatory pain through the activation of both cyclic AMP-dependent (PKA) and calcium-activated (PKC) protein kinases (Petho and Reeh 2012). Intraplantar injection of PGE_2 produces mechanical and thermal hyperalgesia that has been linked to the activation of PKA and PKC in nociceptors (Moriyama et al. 2005; Sachs et al. 2009). Exposure to PGE_2 in vitro reduces action potential thresholds, promotes repetitive firing, and increases the evoked release of neuropeptides (Nicol and Cui 1994; Lopshire and Nicol 1998; Vasko et al. 1994; Andreeva and Rang 1993). Both the $Na_v1.8$ and $Na_v1.9$ Na^+ channels are targets of these kinases and contribute to the thermal and mechanical hyperalgesia associated with intraplantar injection of PGE_2 (Amaya et al. 2006; Villarreal et al. 2005). In rats, $Na_v1.8$ knockdown by intrathecal administrations of antisense oligonucleotides (ODN) reduced both acute and prolonged hyperalgesia (Villarreal et al. 2005). In DRG neurons, PGE_2 caused a twofold increase in Nav1.9 current amplitude and shifted the activation and inactivation curves toward more hyperpolarized voltages (Rush and Waxman 2004). However, similar studies failed to observe changes in the rapidly inactivating ($Na_v1.8$) or persistent ($Na_v1.9$) components of TTX-R Na^+ current after acute administration of PGE_2 (Zheng et al. 2007). Despite this discrepancy, the inflammatory pain elicited by intraplantar injection of PGE_2 or carrageenan was reduced in Nav1.9 null mice (Priest et al. 2005; Amaya et al. 2006). Conditional knockout of the $Na_v1.7$ channel eliminated the mechanical and thermal hyperalgesia in mice treated with a variety of pro-inflammatory agents (formalin, carrageenan, complete Freund's adjuvant, NGF) (Nassar et al. 2004). Overall, these data are consistent with important roles for TTX-S ($Na_v1.7$) and TTX-R ($Na_v1.8$, $Na_v1.9$) Na^+ channels in the development of inflammatory pain.

10 Modulating the Expression Levels of Peripheral Sodium Channels

The expression of Na^+ channels in sensory neurons is developmentally regulated by neurotrophic factors including nerve growth factor (NGF) and glial-derived neurotrophic factor (GDNF). NGF- and GDNF-dependent regulation of $Na_v1.8$ and $Na_v1.9$ channels occurs in developing primary somatosensory neurons (Dib-Hajj et al. 1998a; Cummins et al. 2000). $Na_v1.8$ expression at embryonic stage E15 coincides with the beginning of A- and C-fiber innervation of the skin and is coupled to NGF expression (Benn et al. 2001; Elkabes et al. 1994). This contrast with the expression of $Na_v1.9$, which appears to correlate with the release of GDNF

from Schwann cells at embryonic stages E14–16 (Wright and Snider 1996; Benn et al. 2001). This upregulation of $Na_v1.9$ coincides with the downregulation of embryonic $Na_v1.3$ channels (Waxman et al. 1994). An apparent reversal of this expression pattern is observed after peripheral injury where downregulation of $Na_v1.9$ is accompanied by an upregulation of $Na_v1.3$ (Rizzo et al. 1995; Black et al. 1999). NGF is believed to act through as yet unidentified transcription factors. One potential candidate is Tumor Necrosis Factor alpha (TNF-α), which appears to regulate the expression of $Na_v1.3$ and $Na_v1.8$ sodium channels after nerve injury (He et al. 2010).

The transcription repressor, Repressor element-1 silencing transcription/neuronal-restrictive silencing factor (REST/NRSF), is expressed in non-neuronal and undifferentiated neuronal cells (Chong et al. 1995). REST/NRSF interacts with a complex of proteins (Co-REST/MeCP2/SUV39H1/K^m9H3/HP1) involved in gene silencing that downregulates the expression of $Na_v1.2$ and $Na_v1.3$ in non-neuronal cells and controls the expression of these channels during neuronal development (Lunyak et al. 2002).

11 Modulation of Sodium Channels by Glycosylation

Na^+ channels are heavily glycosylated membrane-bound proteins. The carbohydrate moiety accounts for 5–30 % of the mass of most channels (Schmidt and Catterall 1986; Tyrrell et al. 2001). Glycosylation is essential for proper folding, maintenance of cell surface expression, and interactions with auxiliary subunits in the neurons (Schmidt and Catterall 1986). The degree of sialidation has also been shown to affect the gating properties of skeletal and cardiac Na^+ channels (Bennett et al. 1997). The heavily glycosylated neonatal form of $Na_v1.9$ channel inactivates at more hyperpolarized potentials relative to the lightly glycosylated adult-type channel (Tyrrell et al. 2001). The observed differences in $Na_v1.9$-gating properties may cause the sensory neurons of neonatal and adult animals to respond differently to identical stimuli (Tyrrell et al. 2001).

12 Summary

Peripheral nerve damage, inflammation, and metabolic diseases alter the expression and function of voltage-gated Na^+ channels leading to neuronal hyperexcitability and pain. Increased Na^+ channel expression, enhanced trafficking to the plasma membrane, and altered gating all serve to increase the excitability of primary sensory neurons. The Na^+ channels expressed in these neurons are substrates of protein kinases (PKA, PKC, MAPK) that regulate the expression and function of the channels. Injury-induced changes in both Na^+ channels and intracellular signaling pathways have been linked to sensory neuron hyperexcitability and pain. Convergent regulation of Na^+ channels by the PKA and PKC pathways enables the integration of multiple signals at the level of individual Na^+ channels and

directly alters the excitability of sensory neurons. Injury-induced changes in the expression of Na^+ channel splice variants further modulates channel regulation by these signaling pathways. A thorough understanding of the mechanisms of Na^+ channel regulation could lead to development of novel therapeutics for the treatment of acute and chronic pain.

Acknowledgments Mohamed Chahine's studies are supported by grants from the Heart and Stroke Foundation of Quebec (HSFQ) and the Canadian Institutes of Health Research (CIHR, MT-13181).

References

Akopian AN, Sivilotti L, Wood JN (1996) A tetrodotoxin-resistant voltage-gated sodium channel expressed by sensory neurons. Nature 379:257–262

Akopian AN, Souslova V, England S, Okuse K, Ogata N, Ure J, Smith A, Kerr BJ, McMahon SB, Boyce S, Hill R, Stanfa LC, Dickenson AH, Wood JN (1999) The tetrodotoxin-resistant sodium channel SNS has a specialized function in pain pathways. Nat Neurosci 2:541–548

Albrecht PJ, Rice FL (2010) Role of small-fiber afferents in pain mechanisms with implications on diagnosis and treatment. Curr Pain Headache Rep 14:179–188

Aley KO, Messing RO, Mochly-Rosen D, Levine JD (2000) Chronic hypersensitivity for inflammatory nociceptor sensitization mediated by the epsilon isozyme of protein kinase C. J Neurosci 20:4680–4685

Amaya F, Decosterd I, Samad TA, Plumpton C, Tate S, Mannion RJ, Costigan M, Woolf CJ (2000) Diversity of expression of the sensory neuron-specific TTX-resistant voltage-gated sodium ion channels SNS and SNS2. Mol Cell Neurosci 15(4):331–342

Amaya F, Wang H, Costigan M, Allchorne AJ, Hatcher JP, Egerton J, Stean T, Morisset V, Grose D, Gunthorpe MJ, Chessell IP, Tate S, Green PJ, Woolf CJ (2006) The voltage-gated sodium channel Na(v)1.9 is an effector of peripheral inflammatory pain hypersensitivity. J Neurosci 26:12852–12860

Andreeva L, Rang HP (1993) Effect of bradykinin and prostaglandins on the release of calcitonin gene-related peptide-like immunoreactivity from the rat spinal cord in vitro. Br J Pharmacol 108:185–190

Azhderian EM, Hefner D, Lin CH, Kaczmarek LK, Forscher P (1994) Cyclic AMP modulates fast axonal transport in Aplysia bag cell neurons by increasing the probability of single organelle movement. Neuron 12:1223–1233

Battaini F (2001) Protein kinase C isoforms as therapeutic targets in nervous system disease states. Pharmacol Res 44:353–361

Bendahhou S, Cummins TR, Potts JF, Tong J, Agnew WS (1995) Serine-1321-independent regulation of the μ_1 adult skeletal muscle Na^+ channel by protein kinase C. Proc Natl Acad Sci U S A 92:12003–12007

Benn SC, Costigan M, Tate S, Fitzgerald M, Woolf CJ (2001) Developmental expression of the TTX-resistant voltage-gated sodium channels $Na_v1.8$ (SNS) and $Na_v1.9$ (SNS2) in primary sensory neurons. J Neurosci 21:6077–6085

Bennett E, Urcan MS, Tinkle SS, Koszowski AG, Levinson SR (1997) Contribution of sialic acid to the voltage dependence of sodium channel gating. A possible electrostatic mechanism. J Gen Physiol 109:327–343

Bhave G, Gereau RW (2004) Posttranslational mechanisms of peripheral sensitization. J Neurobiol 61:88–106

Black JA, Dib-Hajj S, McNabola K, Jeste S, Rizzo MA, Kocsis JD, Waxman SG (1996) Spinal sensory neurons express multiple sodium channel alpha-subunit mRNAs. Brain Res Mol Brain Res 43:117–131

Black JA, Cummins TR, Plumpton C, Chen YH, Hormuzdiar W, Clare JJ, Waxman SG (1999) Upregulation of a silent sodium channel after peripheral, but not central, nerve injury in DRG neurons. J Neurophysiol 82:2776–2785

Black JA, Liu S, Tanaka M, Cummins TR, Waxman SG (2004) Changes in the expression of tetrodotoxin-sensitive sodium channels within dorsal root ganglia neurons in inflammatory pain. Pain 108:237–247

Black JA, Nikolajsen L, Kroner K, Jensen TS, Waxman SG (2008) Multiple sodium channel isoforms and mitogen-activated protein kinases are present in painful human neuromas. Ann Neurol 64:644–653

Blair NT, Bean BP (2002) Roles of tetrodotoxin (TTX)-sensitive Na^+ current, TTX-resistant Na^+ current, and Ca^{2+} current in the action potentials of nociceptive sensory neurons. J Neurosci 22:10277–10290

Blair NT, Bean BP (2003) Role of tetrodotoxin-resistant Na^+ current slow inactivation in adaptation of action potential firing in small-diameter dorsal root ganglion neurons. J Neurosci 23:10338–10350

Bradbury EJ, Burnstock G, McMahon SB (1998) The expression of P2X3 purinoreceptors in sensory neurons: effects of axotomy and glial-derived neurotrophic factor. Mol Cell Neurosci 12:256–268

Burgess PR, Perl ER (1967) Myelinated afferent fibres responding specifically to noxious stimulation of the skin. J Physiol 190:541–562

Caffrey JM, Eng DL, Black JA, Waxman SG, Kocsis JD (1992) Three types of sodium channels in adult rat dorsal root ganglion neurons. Brain Res 592:283–297

Campbell JN, Meyer RA (2006) Mechanisms of neuropathic pain. Neuron 52:77–92

Cang CL, Zhang H, Zhang YQ, Zhao ZQ (2009) PKCepsilon-dependent potentiation of TTX-resistant Nav1.8 current by neurokinin-1 receptor activation in rat dorsal root ganglion neurons. Mol Pain 5:33

Cantrell AR, Ma JY, Scheuer T, Catterall WA (1996) Muscarinic modulation of sodium current by activation of protein kinase C in rat hippocampal neurons. Neuron 16:1019–1026

Cantrell AR, Scheuer T, Catterall WA (1999) Voltage-dependent neuromodulation of Na^+ channels by D1-like dopamine receptors in rat hippocampal neurons. J Neurosci 19:5301–5310

Cantrell AR, Tibbs VC, Yu FH, Murphy BJ, Sharp EM, Qu Y, Catterall WA, Scheuer T (2002a) Molecular mechanism of convergent regulation of brain Na^+ channels by protein kinase C and protein kinase A anchored to AKAP-15. Mol Cell Neurosci 21:63–80

Cantrell AR, Yu F, Sharp EM, Qu Y, Murphy BJ, Scheuer T, Catterall WA (2002b) Molecular mechanisms underlying convergent regulation of brain Na^+ channels by protein kinase A and protein kinase C. J Neurosci, 713.17 [Ref type: Abstract]

Caterina MJ, Schumacher MA, Tominaga M, Rosen TA, Levine JD, Julius D (1997) The capsaicin receptor: a heat-activated ion channel in the pain pathway. Nature 389:816–824

Cesare P, Dekker LV, Sardini A, Parker PJ, McNaughton PA (1999) Specific involvement of PKC-ε in sensitization of the neuronal response to painful heat. Neuron 23:617–624

Chatelier A, Dahllund L, Eriksson A, Krupp J, Chahine M (2008) Biophysical properties of human Na v1.7 splice variants and their regulation by protein kinase A. J Neurophysiol 99:2241–2250

Chattopadhyay M, Mata M, Fink DJ (2008) Continuous delta-opioid receptor activation reduces neuronal voltage-gated sodium channel (NaV1.7) levels through activation of protein kinase C in painful diabetic neuropathy. J Neurosci 28:6652–6658

Chen TC, Law B, Kondratyuk T, Rossie S (1995) Identification of soluble protein phosphatases that dephosphorylate voltage-sensitive sodium channels in rat brain. J Biol Chem 270:7750–7756

Cheng JK, Ji RR (2008) Intracellular signaling in primary sensory neurons and persistent pain. Neurochem Res 33:1970–1978

Chong JA, Tapia-Ramirez J, Kim S, Toledo-Aral JJ, Zheng Y, Boutros MC, Altshuller YM, Frohman MA, Kraner SD, Mandel G (1995) REST: a mammalian silencer protein that restricts sodium channel gene expression to neurons. Cell 80:949–957

Costigan M, Scholz J, Woolf CJ (2009) Neuropathic pain: a maladaptive response of the nervous system to damage. Annu Rev Neurosci 32:1–32

Cummins TR, Waxman SG (1997) Downregulation of tetrodotoxin-resistant sodium currents and upregulation of a rapidly repriming tetrodotoxin-sensitive sodium current in small spinal sensory neurons after nerve injury. J Neurosci 17:3503–3514

Cummins TR, Howe JR, Waxman SG (1998) Slow closed-state inactivation: a novel mechanism underlying ramp currents in cells expressing the hNE/PN1 sodium channel. J Neurosci 18:9607–9619

Cummins TR, Dib-Hajj SD, Black JA, Akopian AN, Wood JN, Waxman SG (1999) A novel persistent tetrodotoxin-resistant sodium current in SNS-null and wild-type small primary sensory neurons. J Neurosci 19:43

Cummins TR, Black JA, Dib-Hajj SD, Waxman SG (2000) Glial-derived neurotrophic factor upregulates expression of functional SNS and NaN sodium channels and their currents in axotomized dorsal root ganglion neurons. J Neurosci 20:8754–8761

Cummins TR, Sheets PL, Waxman SG (2007) The roles of sodium channels in nociception: implications for mechanisms of pain. Pain 131:243–257

d'Alcantara P, Cardenas LM, Swillens S, Scroggs RS (2002) Reduced transition between open and inactivated channel states underlies 5HT increased I(Na+) in rat nociceptors. Biophys J 83:5–21

Dang TX, McCleskey EW (1998) Ion channel selectivity through stepwise changes in binding affinity. J Gen Physiol 111:185–193

Dempsey EC, Newton AC, Mochly-Rosen D, Fields AP, Reyland ME, Insel PA, Messing RO (2000) Protein kinase C isozymes and the regulation of diverse cell responses. Am J Physiol 279:L429–L438

Dib-Hajj SD, Black JA, Cummins TR, Kenney AM, Kocsis JD, Waxman SG (1998a) Rescue of α-SNS sodium channel expression in small dorsal root ganglion neurons after axotomy by nerve growth factor in vivo. J Neurophysiol 79:2668–2676

Dib-Hajj SD, Tyrrell L, Black JA, Waxman SG (1998b) NaN, a novel voltage-gated Na channel, is expressed preferentially in peripheral sensory neurons and down-regulated after axotomy. Proc Natl Acad Sci 95:8963–8968

Dib-Hajj SD, Tyrrell L, Cummins TR, Black JA, Wood PM, Waxman SG (1999) Two tetrodotoxin-resistant sodium channels in human dorsal root ganglion neurons. FEBS Lett 462:117–120

Dib-Hajj S, Black JA, Cummins TR, Waxman SG (2002) NaN/Nav1.9: a sodium channel with unique properties. Trends Neurosci 25:253–259

Dib-Hajj SD, Binshtok AM, Cummins TR, Jarvis MF, Samad T, Zimmermann K (2009) Voltage-gated sodium channels in pain states: role in pathophysiology and targets for treatment. Brain Res Rev 60:65–83

Djouhri L, Fang X, Okuse K, Wood JN, Berry CM, Lawson SN (2003) The TTX-resistant sodium channel Nav1.8 (SNS/PN3): expression and correlation with membrane properties in rat nociceptive primary afferent neurons. J Physiol 550:739–752

Dong X, Han S, Zylka MJ, Simon MI, Anderson DJ (2001) A diverse family of GPCRs expressed in specific subsets of nociceptive sensory neurons. Cell 106:619–632

Dubin AE, Patapoutian A (2010) Nociceptors: the sensors of the pain pathway. J Clin Invest 120:3760–3772

Elkabes S, Dreyfus CF, Schaar DG, Black IB (1994) Embryonic sensory development: local expression of neurotrophin-3 and target expression of nerve growth factor. J Comp Neurol 341:204–213

Elliott AA, Elliott JR (1993) Characterization of TTX-sensitive and TTX-resistant sodium currents in small cells from adult rat dorsal root ganglia. J Physiol 463:39–56

England S, Bevan S, Docherty RJ (1996) PGE_2 modulates the tetrodotoxin-resistant sodium current in neonatal rat dorsal root ganglion neurones via the cyclic AMP-protein kinase A cascade. J Physiol 495:429–440

Fang X, Djouhri L, Black JA, Dib-Hajj SD, Waxman SG, Lawson SN (2002) The presence and role of the tetrodotoxin-resistant sodium channel Na(v)1.9 (NaN) in nociceptive primary afferent neurons. J Neurosci 22:7425–7433

Fang X, Djouhri L, McMullan S, Berry C, Waxman SG, Okuse K, Lawson SN (2006) Intense isolectin-B4 binding in rat dorsal root ganglion neurons distinguishes C-fiber nociceptors with broad action potentials and high Nav1.9 expression. J Neurosci 26:7281–7292

Fitzgerald EM, Okuse K, Wood JN, Dolphin AC, Moss SJ (1999) cAMP-dependent phosphorylation of the tetrodotoxin-resistant voltage-dependent sodium channel SNS. J Physiol 516:433–446

Fornaro M, Lee JM, Raimondo S, Nicolino S, Geuna S, Giacobini-Robecchi M (2008) Neuronal intermediate filament expression in rat dorsal root ganglia sensory neurons: an in vivo and in vitro study. Neuroscience 153:1153–1163

Fuchs E, Cleveland DW (1998) A structural scaffolding of intermediate filaments in health and disease. Science 279:514–519

Godoy CMG, Cukierman S (1994) Diacylglycerol-induced activation of protein kinase C attenuates Na^+ currents by enhancing inactivation from the closed state. Pflugers Arch 429:245–252

Gold MS (1999) Tetrodotoxin-resistant Na^+ currents and inflammatory hyperalgesia. Proc Natl Acad Sci U S A 96:7645–7649

Gold MS, Dastmalchi S, Levine JD (1996a) Co-expression of nociceptor properties in dorsal root ganglion neurons from the adult rat in vitro. Neuroscience 71:265–275

Gold MS, Reichling DB, Shuster MJ, Levine JD (1996b) Hyperalgesic agents increase a tetrodotoxin-resistant Na^+ current in nociceptors. Proc Natl Acad Sci U S A 93:1108–1112

Gold MS, Levine JD, Correa AM (1998) Modulation of TTX-R I_{Na} by PKC and PKA and their role in PGE_2-induced sensitization of rat sensory neurons in vitro. J Neurosci 18:10345–10355

Goldstein ME, House SB, Gainer H (1991) NF-L and peripherin immunoreactivities define distinct classes of rat sensory ganglion cells. J Neurosci Res 30:92–104

Guo A, Vulchanova L, Wang J, Li X, Elde R (1999) Immunocytochemical localization of the vanilloid receptor 1 (VR1): relationship to neuropeptides, the P2X3 purinoceptor and IB4 binding sites. Eur J Neurosci 11:946–958

Harper AA, Lawson SN (1985a) Conduction velocity is related to morphological cell type in rat dorsal root ganglion neurones. J Physiol 359:31–46

Harper AA, Lawson SN (1985b) Electrical properties of rat dorsal root ganglion neurones with different peripheral nerve conduction velocities. J Physiol 359(47–63):47–63

He XH, Zang Y, Chen X, Pang RP, Xu JT, Zhou X, Wei XH, Li YY, Xin WJ, Qin ZH, Liu XG (2010) TNF-alpha contributes to up-regulation of Nav1.3 and Nav1.8 in DRG neurons following motor fiber injury. Pain 151:266–279

Herzog RI, Cummins TR, Waxman SG (2001) Persistent TTX-resistant Na^+ current affects resting potential and response to depolarization in simulated spinal sensory neurons. J Neurophysiol 86:1351–1364

Ho C, O'Leary ME (2011) Single-cell analysis of sodium channel expression in dorsal root ganglion neurons. Mol Cell Neurosci 46:159–166

Ho C, Zhao J, Malinowski S, Chahine M, O'Leary ME (2012) Differential expression of sodium channel beta subunits in dorsal root ganglion sensory neurons. J Biol Chem 287:15044–15053

Hoffman PN, Thompson GW, Griffin JW, Price DL (1985) Changes in neurofilament transport coincide temporally with alterations in the caliber of axons in regenerating motor fibers. J Cell Biol 101:1332–1340

Hucho T, Levine JD (2007) Signaling pathways in sensitization: toward a nociceptor cell biology. Neuron 55:365–376

Hudmon A, Choi JS, Tyrrell L, Black JA, Rush AM, Waxman SG, Dib-Hajj SD (2008) Phosphorylation of sodium channel Na(v)1.8 by p38 mitogen-activated protein kinase increases current density in dorsal root ganglion neurons. J Neurosci 28:3190–3201

Igwe OJ, Chronwall BM (2001) Hyperalgesia induced by peripheral inflammation is mediated by protein kinase C βII isozyme in the rat spinal cord. Neuroscience 104:875–890

Ikeda M, Yoshida S, Kadoi J, Nakano Y, Mastumoto S (2005) The effect of PKC activity on the TTX-R sodium currents from rat nodose ganglion neurons. Life Sci 78:47–53

Ji RR, Strichartz G (2004) Cell signaling and the genesis of neuropathic pain. Sci STKE 2004: reE14

Jin X, Gereau RW IV (2006) Acute p38-mediated modulation of tetrodotoxin-resistant sodium channels in mouse sensory neurons by tumor necrosis factor-α. J Neurosci 26:246–255

Jin SX, Zhuang ZY, Woolf CJ, Ji RR (2003) p38 mitogen-activated protein kinase is activated after a spinal nerve ligation in spinal cord microglia and dorsal root ganglion neurons and contributes to the generation of neuropathic pain. J Neurosci 23:4017–4022

Joseph EK, Levine JD (2010) Hyperalgesic priming is restricted to isolectin B4-positive nociceptors. Neuroscience 169:431–435

Julius D, Basbaum AI (2001) Molecular mechanisms of nociception. Nature 413:203–210

Kawabata A (2011) Prostaglandin E2 and pain–an update. Biol Pharm Bull 34:1170–1173

Khasar SG, Lin YH, Martin A, Dadgar J, McMahon T, Wang D, Hundle B, Aley KO, Isenberg W, McCarter G, Green PG, Hodge CW, Levine JD, Messing RO (1999) A novel nociceptor signaling pathway revealed in protein kinase C ε mutant mice. Neuron 24:253–260

Kim EK, Choi EJ (2010) Pathological roles of MAPK signaling pathways in human diseases. Biochim Biophys Acta 1802:396–405

Kim CH, Oh Y, Chung JM, Chung K (2002) Changes in three subtypes of tetrodotoxin sensitive sodium channel expression in the axotomized dorsal root ganglion in the rat. Neurosci Lett 323:125–128

Kondratyuk T, Rossie S (1997) Depolarization of rat brain synaptosomes increases phosphorylation of voltage-sensitive sodium channels. J Biol Chem 272:16978–16983

Kostyuk PG, Veselovsky NS, Tsyndrenko AY (1981) Ionic currents in the somatic membrane of rat dorsal root ganglion neurons-I. Sodium currents. Neuroscience 6:2423–2430

Kruger L, Light AR, Schweizer FE (2003) Axonal terminals of sensory neurons and their morphological diversity. J Neurocytol 32:205–216

Lai J, Porreca F, Hunter JC, Gold MS (2004) Voltage-gated sodium channels and hyperalgesia. Annu Rev Pharmacol Toxicol 44:371–397

Lawson SN (2002) Phenotype and function of somatic primary afferent nociceptive neurones with C-, Adelta- or Aalpha/beta-fibres. Exp Physiol 87:239–244

Lawson SN, Perry MJ, Prabhakar E, McCarthy PW (1993) Primary sensory neurones: neurofilament, neuropeptides, and conduction velocity. Brain Res Bull 30:239–243

Lee KH, Chung K, Chung JM, Coggeshall RE (1986) Correlation of cell body size, axon size, and signal conduction velocity for individually labelled dorsal root ganglion cells in the cat. J Comp Neurol 243:335–346

Lewis TS, Shapiro PS, Ahn NG (1998) Signal transduction through MAP kinase cascades. Adv Cancer Res 74:49–139

Li M, West JW, Lai Y, Scheuer T, Catterall WA (1992) Functional modulation of brain sodium channels by cAMP-dependent phosphorylation. Neuron 8:1151–1159

Li M, West JW, Numann R, Murphy BJ, Scheuer T, Catterall WA (1993) Convergent regulation of sodium channels by protein kinase C and cAMP-dependent protein kinase. Science 261:1439–1442

Liu M, Willmott NJ, Michael GJ, Priestley JV (2004) Differential pH and capsaicin responses of Griffonia simplicifolia IB4 (IB4)-positive and IB4-negative small sensory neurons. Neuroscience 127:659–672

Liu Q, Vrontou S, Rice FL, Zylka MJ, Dong X, Anderson DJ (2007) Molecular genetic visualization of a rare subset of unmyelinated sensory neurons that may detect gentle touch. Nat Neurosci 10:946–948

Lopshire JC, Nicol GD (1998) The cAMP transduction cascade mediates the prostaglandin E2 enhancement of the capsaicin-elicited current in rat sensory neurons: whole-cell and single-channel studies. J Neurosci 18:6081–6092

Lunyak VV, Burgess R, Prefontaine GG, Nelson C, Sze S-H, Chenoweth J, Schwartz P, Pevzner PA, Glass C, Mandel G, Rosenfeld MG (2002) Corepressor-dependent silencing of chromosomal regions encoding neuronal genes. Science 298:1747–1752

Maingret F, Coste B, Padilla F, Clerc N, Crest M, Korogod SM, Delmas P (2008) Inflammatory mediators increase Nav1.9 current and excitability in nociceptors through a coincident detection mechanism. J Gen Physiol 131:211–225

Martin WJ, Liu H, Wang H, Malmberg AB, Basbaum AI (1999) Inflammation-induced up-regulation of protein kinase Cγ immunoreactivity in rat spinal cord correlates with enhanced nociceptive processing. Neuroscience 88:1267–1274

Maurel P, Einheber S, Galinska J, Thaker P, Lam I, Rubin MB, Scherer SS, Murakami Y, Gutmann DH, Salzer JL (2007) Nectin-like proteins mediate axon Schwann cell interactions along the internode and are essential for myelination. J Cell Biol 178:861–874

McCleskey EW, Gold MS (1999) Ion channels of nociception. Annu Rev Physiol 61:835–856

Michael GJ, Priestley JV (1999) Differential expression of the mRNA for the vanilloid receptor subtype 1 in cells of the adult rat dorsal root and nodose ganglia and its downregulation by axotomy. J Neurosci 19:1844–1854

Mittmann T, Alzheimer C (1998) Muscarinic inhibition of persistent Na^+ current in rat neocortical pyramidal neurons. J Neurophysiol 79:1579–1582

Moriyama T, Higashi T, Togashi K, Iida T, Segi E, Sugimoto Y, Tominaga T, Narumiya S, Tominaga M (2005) Sensitization of TRPV1 by EP1 and IP reveals peripheral nociceptive mechanism of prostaglandins. Mol Pain 1:3

Murphy BJ, Catterall WA (1992) Phosphorylation of purified rat brain Na^+ channel reconstituted into phospholipid vesicles by protein kinase C. J Biol Chem 267:16129–16134

Murphy BJ, Rossie S, De Jongh KS, Catterall WA (1993) Identification of the sites of selective phosphorylation and dephosphorylation of the rat brain Na^+ channel α subunit by cAMP-dependent protein kinase and phosphoprotein phosphatases. J Biol Chem 268:27355–27362

Murray KT, Hu NN, Daw JR, Shin HG, Watson MT, Mashburn AB, George AL Jr (1997) Functional effects of protein kinase C activation on the human cardiac Na^+ channel. Circ Res 80:370–376

Nassar MA, Stirling LC, Forlani G, Baker MD, Matthews EA, Dickenson AH, Wood JN (2004) Nociceptor-specific gene deletion reveals a major role for Nav1.7 (PN1) in acute and inflammatory pain. Proc Natl Acad Sci U S A 101:12706–12711

Nicol GD, Cui M (1994) Enhancement by prostaglandin E2 of bradykinin activation of embryonic rat sensory neurones. J Physiol 480(Pt 3):485–492

Novakovic SD, Tzoumaka E, McGivern JG, Haraguchi M, Sangameswaran L, Gogas KR, Eglen RM, Hunter JC (1998) Distribution of the tetrodotoxin-resistant sodium channel PN3 in rat sensory neurons in normal and neuropathic conditions. J Neurosci 18:2174–2187

Numann R, Catterall WA, Scheuer T (1991) Functional modulation of brain sodium channels by protein kinase C phosphorylation. Science 254:115–118

Obata K, Noguchi K (2004) MAPK activation in nociceptive neurons and pain hypersensitivity. Life Sci 74:2643–2653

Obata K, Yamanaka H, Kobayashi K, Dai Y, Mizushima T, Katsura H, Fukuoka T, Tokunaga A, Noguchi K (2004) Role of mitogen-activated protein kinase activation in injured and intact primary afferent neurons for mechanical and heat hypersensitivity after spinal nerve ligation. J Neurosci 24:10211–10222

Ogata N, Tatebayashi H (1993) Kinetic analysis of two types of Na^+ channels in rat dorsal root ganglia. J Physiol 466:9–37

Oida H, Namba T, Sugimoto Y, Ushikubi F, Ohishi H, Ichikawa A, Narumiya S (1995) In situ hybridization studies of prostacyclin receptor mRNA expression in various mouse organs. Br J Pharmacol 116:2828–2837

Ostman JA, Nassar MA, Wood JN, Baker MD (2008) GTP up-regulated persistent Na^+ current and enhanced nociceptor excitability require NaV1.9. J Physiol 586:1077–1087

Parada CA, Yeh JJ, Reichling DB, Levine JD (2003) Transient attenuation of protein kinase Cepsilon can terminate a chronic hyperalgesic state in the rat. Neuroscience 120:219–226

Perl ER (1996) Cutaneous polymodal receptors: characteristics and plasticity. Prog Brain Res 113:21–37

Petho G, Reeh PW (2012) Sensory and signaling mechanisms of bradykinin, eicosanoids, platelet-activating factor, and nitric oxide in peripheral nociceptors. Physiol Rev 92:1699–1775

Petruska JC, Napaporn J, Johnson RD, Gu JG, Cooper BY (2000) Subclassified acutely dissociated cells of rat DRG: histochemistry and patterns of capsaicin-, proton-, and ATP-activated currents. J Neurophysiol 84:2365–2379

Petruska JC, Napaporn J, Johnson RD, Cooper BY (2002) Chemical responsiveness and histochemical phenotype of electrophysiologically classified cells of the adult rat dorsal root ganglion. Neuroscience 115:15–30

Price TJ, Flores CM (2007) Critical evaluation of the colocalization between calcitonin gene-related peptide, substance P, transient receptor potential vanilloid subfamily type 1 immunoreactivities, and isolectin B4 binding in primary afferent neurons of the rat and mouse. J Pain 8:263–272

Priest BT, Murphy BA, Lindia JA, Diaz C, Abbadie C, Ritter AM, Liberator P, Iyer LM, Kash SF, Kohler MG, Kaczorowski GJ, MacIntyre DE, Martin WJ (2005) Contribution of the tetrodotoxin-resistant voltage-gated sodium channel NaV1.9 to sensory transmission and nociceptive behavior. Proc Natl Acad Sci U S A 102:9382–9387

Priestley JV, Michael GJ, Averill S, Liu M, Willmott N (2002) Regulation of nociceptive neurons by nerve growth factor and glial cell line derived neurotrophic factor. Can J Physiol Pharmacol 80:495–505

Qu Y, Rogers J, Tanada T, Scheuer T, Catterall WA (1994) Modulation of cardiac Na^+ channels expressed in a mammalian cell line and in ventricular myocytes by protein kinase C. Proc Natl Acad Sci U S A 91:3289–3293

Raymond CK, Castle J, Garrett-Engele P, Armour CD, Kan Z, Tsinoremas N, Johnson JM (2004) Expression of alternatively spliced sodium channel α-subnit genes: unique splicing patterns are observed in dorsal root ganglia. J Biol Chem 279:46234–46241

Reichling DB, Levine JD (2009) Critical role of nociceptor plasticity in chronic pain. Trends Neurosci 32:611–618

Renganathan M, Cummins TR, Hormuzdiar WN, Waxman SG (2000) alpha-SNS produces the slow TTX-resistant sodium current in large cutaneous afferent DRG neurons. J Neurophysiol 84:710–718

Renganathan M, Cummins TR, Waxman SG (2001) Contribution of Na(v)1.8 sodium channels to action potential electrogenesis in DRG neurons. J Neurophysiol 86:629–640

Ringkamp MMRA (2009) Physiology of nociceptors. In: Basbaum AIBMC (ed) Science of pain. Elsevier, pp 97–114

Rizzo MA, Kocsis JD, Waxman SG (1995) Selective loss of slow and enhancement of fast Na^+ currents in cutaneous afferent dorsal root ganglion neurones following axotomy. Neurobiol Dis 2:87–96

Roy ML, Narahashi T (1992) Differential properties of tetrodotoxin-sensitive and tetrodotoxin-resistant sodium channels in rat dorsal root ganglion neurons. J Neurosci 12:2104–2111

Rush AM, Waxman SG (2004) PGE(2) increases the tetrodotoxin-resistant Na(v)1.9 sodium current in mouse DRG neurons via G-proteins. Brain Res 1023:264–271

Rush AM, Brau ME, Elliott AA, Elliott JR (1998) Electrophysiological properties of sodium current subtypes in small cells from adult rat dorsal root ganglia. J Physiol 511:771–789

Rush AM, Cummins TR, Waxman SG (2007) Multiple sodium channels and their roles in electrogenesis within dorsal root ganglion neurons. J Physiol 579:1–14

Sachs D, Villarreal C, Cunha F, Parada C, Ferreira S (2009) The role of PKA and PKCepsilon pathways in prostaglandin E2-mediated hypernociception. Br J Pharmacol 156:826–834

Sampo B, Tricaud N, Leveque C, Seagar M, Couraud F, Dargent B (2000) Direct interaction between synaptotagmin and the intracellular loop I-II of neuronal voltage-sensitive sodium channels. Proc Natl Acad Sci U S A 97:3666–3671

Sangameswaran L, Delgado SG, Fish LM, Koch BD, Jakeman LB, Stewart GR, Sze P, Hunter JC, Eglen RM, Herman RC (1996) Structure and function of a novel voltage-gated, tetrodotoxin-resistant sodium channel specific to sensory neurons. J Biol Chem 271:5953–5956

Sangameswaran L, Fish LM, Koch BD, Rabert DK, Delgado SG, Ilnicka M, Jakeman LB, Novakovic S, Wong K, Sze P, Tzoumaka E, Stewart GR, Herman RC, Chan H, Eglen RM, Hunter JC (1997) A novel tetrodotoxin-sensitive, voltage-gated sodium channel expressed in rat and human dorsal root ganglia. J Biol Chem 272:14805–14809

Schild JH, Kunze DL (1997) Experimental and modeling study of Na^+ current heterogeneity in rat nodose neurons and its impact on neuronal discharge. J Neurophysiol 78:3198–3209

Schmidt JW, Catterall WA (1986) Biosynthesis and processing of the α subunit of the voltage-sensitive sodium channel in rat brain neurons. Cell 46:437–444

Schreibmayer W, Dascal N, Lotan I, Wallner M, Weigl L (1991) Molecular mechanism of protein kinase C modulation of sodium channel α-subunits expressed in Xenopus oocytes. FEBS Lett 291:341–344

Schreibmayer W, Frohnwieser B, Dascal N, Platzer D, Spreitzer B, Zechner R, Kallen RG, Lester HA (1994) β-adrenergic modulation of currents produced by rat cardiac Na^+ channels expressed in Xenopus laevis oocytes. Receptors Channels 2:339–350

Seger R, Krebs EG (1995) The MAPK signaling cascade. FASEB J 9:726–735

Smith RD, Goldin AL (1992) Protein kinase A phosphorylation enhances sodium channel currents in Xenopus oocytes. Am J Physiol 263:C660–C666

Smith RD, Goldin AL (1996) Phosphorylation of brain sodium channels in the I-II linker modulates channel function in Xenopus oocytes. J Neurosci 16:1965–1974

Smith MR, Goldin AL (1997) Interaction between the sodium channel inactivation linker and domain III S4-S5. Biophys J 73:1885–1895

Smith RD, Goldin AL (2000) Potentiation of rat brain sodium channel currents by PKA in Xenopus oocytes involves the I-II linker. Am J Physiol 278:C638–C645

Snider WD, McMahon SB (1998) Tackling pain at the source: new ideas about nociceptors. Neuron 20:629–632

Spiegel I, Adamsky K, Eshed Y, Milo R, Sabanay H, Sarig-Nadir O, Horresh I, Scherer SS, Rasband MN, Peles E (2007) A central role for Necl4 (SynCAM4) in Schwann cell-axon interaction and myelination. Nat Neurosci 10:861–869

Stamboulian S, Choi JS, Ahn HS, Chang YW, Tyrrell L, Black JA, Waxman SG, Dib-Hajj SD (2010) ERK1/2 mitogen-activated protein kinase phosphorylates sodium channel Na(v)1.7 and alters its gating properties. J Neurosci 30:1637–1647

Stucky CL, Lewin GR (1999) Isolectin B(4)-positive and -negative nociceptors are functionally distinct. J Neurosci 19:6497–6505

Sugimoto Y, Shigemoto R, Namba T, Negishi M, Mizuno N, Narumiya S, Ichikawa A (1994) Distribution of the messenger RNA for the prostaglandin E receptor subtype EP3 in the mouse nervous system. Neuroscience 62:919–928

Tate S, Benn S, Hick C, Trezise D, John V, Mannion RJ, Costigan M, Plumpton C, Grose D, Gladwell Z, Kendall G, Dale K, Bountra C, Woolf CJ (1998) Two sodium channels contribute to the TTX-R sodium current in primary sensory neurons. Nat Neurosci 1:653–655

Toledo-Aral JJ, Moss BL, He ZJ, Koszowski AG, Whisenand T, Levinson SR, Wolf JJ, Silos-Santiago I, Halegoua S, Mandel G (1997) Identification of PN1, a predominant voltage-dependent sodium channel expressed principally in peripheral neurons. Proc Natl Acad Sci U S A 94:1527–1532

Tripathi PK, Trujillo L, Cardenas CA, Cardenas CG, de Armendi AJ, Scroggs RS (2006) Analysis of the variation in use-dependent inactivation of high-threshold tetrodotoxin-resistant sodium currents recorded from rat sensory neurons. Neuroscience 143:923–938

Tyrrell L, Renganathan M, Dib-Hajj SD, Waxman SG (2001) Glycosylation alters steady-state inactivation of sodium channel Nav1.9/NaN in dorsal root ganglion neurons and is developmentally regulated. J Neurosci 21:9629–9637

Vanoye CG, Kunic JD, Ehring GR, George AL Jr (2013) Mechanism of sodium channel NaV1.9 potentiation by G-protein signaling. J Gen Physiol 141:193–202

Vasko MR, Campbell WB, Waite KJ (1994) Prostaglandin E2 enhances bradykinin-stimulated release of neuropeptides from rat sensory neurons in culture. J Neurosci 14:4987–4997

Vijayaragavan K, O'Leary ME, Chahine M (2001) Gating properties of Na(v)1.7 and Na(v)1.8 peripheral nerve sodium channels. J Neurosci 21:7909–7918

Vijayaragavan K, Boutjdir M, Chahine M (2004) Modulation of nav1.7 and nav1.8 peripheral nerve sodium channels by protein kinase a and protein kinase C. J Neurophysiol 91:1556–1569

Villarreal CF, Sachs D, Cunha FQ, Parada CA, Ferreira SH (2005) The role of Na(V)1.8 sodium channel in the maintenance of chronic inflammatory hypernociception. Neurosci Lett 386:72–77

Waddell PJ, Lawson SN (1990) Electrophysiological properties of subpopulations of rat dorsal root ganglion neurons in vitro. Neuroscience 36:811–822

Waxman SG, Kocsis JD, Black JA (1994) Type III sodium channel mRNA is expressed in embryonic but not adult spinal sensory neurons, and is reexpressed following axotomy. J Neurophysiol 72:466–470

West JW, Numann R, Murphy BJ, Scheuer T, Catterall WA (1991) A phosphorylation site in the Na^+ channel required for modulation by protein kinase C. Science 254:866–868

Widmann C, Gibson S, Jarpe MB, Johnson GL (1999) Mitogen-activated protein kinase: conservation of a three-kinase module from yeast to human. Physiol Rev 79:143–180

Wittmack EK, Rush AM, Hudmon A, Waxman SG, Dib-Hajj SD (2005) Voltage-gated sodium channel Nav1.6 is modulated by p38 mitogen-activated protein kinase. J Neurosci 25:6621–6630

Woolf CJ, Costigan M (1999) Transcriptional and posttranslational plasticity and the generation of inflammatory pain. Proc Natl Acad Sci U S A 96:7723–7730

Woolf CJ, Ma Q (2007) Nociceptors–noxious stimulus detectors. Neuron 55:353–364

Wright DE, Snider WD (1996) Focal expression of glial cell line-derived neurotrophic factor in developing mouse limb bud. Cell Tissue Res 286:209–217

Xu JT, Xin WJ, Wei XH, Wu CY, Ge YX, Liu YL, Zang Y, Zhang T, Li YY, Liu XG (2007) p38 activation in uninjured primary afferent neurons and in spinal microglia contributes to the development of neuropathic pain induced by selective motor fiber injury. Exp Neurol 204:355–365

Yoshida S, Matsuda Y (1979) Studies on sensory neurons of the mouse with intracellular-recording and horseradish peroxidase-injection techniques. J Neurophysiol 42:1134–1145

Zelano J, Plantman S, Hailer NP, Cullheim S (2009) Altered expression of nectin-like adhesion molecules in the peripheral nerve after sciatic nerve transection. Neurosci Lett 449:28–33

Zhang H, Cang CL, Kawasaki Y, Liang LL, Zhang YQ, Ji RR, Zhao ZQ (2007) Neurokinin-1 receptor enhances TRPV1 activity in primary sensory neurons via PKCepsilon: a novel pathway for heat hyperalgesia. J Neurosci 27:12067–12077

Zhao J, O'Leary ME, Chahine M (2011) Regulation of $Na_v1.6$ and $Na_v1.8$ peripheral nerve Na^+ channels by auxiliary {beta}-subunits. J Neurophysiol 106:608–619

Zheng T, Kakimura J, Matsutomi T, Nakamoto C, Ogata N (2007) Prostaglandin E2 has no effect on two components of tetrodotoxin-resistant Na^+ current in mouse dorsal root ganglion. J Pharmacol Sci 103:93–102

Zhou J, Yi J, Hu NN, George AL Jr, Murray KT (2000) Activation of protein kinase A modulates trafficking of the human cardiac sodium channel in Xenopus oocytes. Circ Res 87:33–38

Zhou J, Shin HG, Yi J, Shen W, Williams CP, Murray KT (2002) Phosphorylation and putative ER retention signals are required for protein kinase A-mediated potentiation of cardiac sodium current. Circ Res 91:540–546

Zwick M, Davis BM, Woodbury CJ, Burkett JN, Koerber HR, Simpson JF, Albers KM (2002) Glial cell line-derived neurotrophic factor is a survival factor for isolectin B4-positive, but not vanilloid receptor 1-positive, neurons in the mouse. J Neurosci 22:4057–4065

Zylka MJ, Rice FL, Anderson DJ (2005) Topographically distinct epidermal nociceptive circuits revealed by axonal tracers targeted to Mrgprd. Neuron 45:17–25

The Role of Late I_{Na} in Development of Cardiac Arrhythmias

Charles Antzelevitch, Vladislav Nesterenko, John C. Shryock, Sridharan Rajamani, Yejia Song, and Luiz Belardinelli

Contents

Abstract

Late I_{Na} is an integral part of the sodium current, which persists long after the fast-inactivating component. The magnitude of the late I_{Na} is relatively small in all species and in all types of cardiomyocytes as compared with the amplitude of the fast sodium current, but it contributes significantly to the shape and duration of the action potential. This late component had been shown to increase in several acquired or congenital conditions, including hypoxia, oxidative stress, and heart failure, or due to mutations in *SCN5A*, which encodes the α-subunit of

C. Antzelevitch (✉) • V. Nesterenko
Masonic Medical Research Laboratory, 2150 Bleecker Street, Utica, NY 13501, USA
e-mail: ca@mmrl.edu

J.C. Shryock • S. Rajamani • L. Belardinelli
Department of Biology, Cardiovascular Therapeutic Area, Gilead Sciences, Foster City, CA, USA

Y. Song
Division of Cardiology, College of Medicine, University of Florida, Gainesville, FL, USA

P.C. Ruben (ed.), *Voltage Gated Sodium Channels*, Handbook of Experimental Pharmacology 221, DOI 10.1007/978-3-642-41588-3_7,

the sodium channel, as well as in channel-interacting proteins, including multiple β subunits and anchoring proteins. Patients with enhanced late I_{Na} exhibit the type-3 long QT syndrome (LQT3) characterized by high propensity for the life-threatening ventricular arrhythmias, such as Torsade de Pointes (TdP), as well as for atrial fibrillation. There are several distinct mechanisms of arrhythmogenesis due to abnormal late I_{Na}, including abnormal automaticity, early and delayed afterdepolarization-induced triggered activity, and dramatic increase of ventricular dispersion of repolarization. Many local anesthetic and antiarrhythmic agents have a higher potency to block late I_{Na} as compared with fast I_{Na}. Several novel compounds, including ranolazine, GS-458967, and F15845, appear to be the most selective inhibitors of cardiac late I_{Na} reported to date. Selective inhibition of late I_{Na} is expected to be an effective strategy for correcting these acquired and congenital channelopathies.

Keywords
Ion channel currents • Electrophysiology • Long QT syndrome • Sudden cardiac death • Cardiac arrhythmias

Recent years have witnessed a resurgence of interest in the late component of the sodium current (late I_{Na}), particularly its role in development of cardiac arrhythmias and as a pharmacologic target for the prevention of life-threatening arrhythmias and sudden cardiac death. In this review, our principal aim is to discuss the molecular basis for late I_{Na}, its cellular distinctions, and its contribution to the electrophysiological function of the heart in health and disease. We refer the readers to recent reviews dealing with the characteristics of the cardiac late I_{Na} (Belardinelli et al. 2006; Noble and Noble 2006; Saint 2006, 2008; Zaza et al. 2008; Undrovinas and Maltsev 2008a; Maier 2009; Antzelevitch et al. 2011; Shryock et al. 2013) as well as reviews dealing with cardiac sodium channelopathies associated with a gain of function of late I_{Na} and its role in arrhythmogenesis (Zimmer and Surber 2008; Ruan et al. 2009; Amin et al. 2010; Rook et al. 2012).

1 Late I_{Na} and Its Relationship to Peak I_{Na}

Voltage-gated sodium channels mediate excitability of heart, nerve, endocrine, and skeletal muscle tissues. When membrane depolarization achieves threshold potential, the Na^+ channels open, thus giving rise to the "peak" I_{Na} and the rapid upstroke (phase 0) of the action potential (AP).

The sodium channel activates during phase 0 of the AP and largely inactivates within 1 ms at body temperature. Between 0.1 % and 1 % the current inactivates more slowly during the plateau of the action potential (AP) (Patlak and Ortiz 1985) with the time constant being between 75 and 450 ms in humans (Undrovinas et al. 2002; Maltsev and Undrovinas 2006). Amplitude of the late component

being small compared with the peak I_{Na} is large as compared with other ionic currents during AP plateau, e.g., around 0.5 pA/pF in normal human and canine ventricular myocytes (Maltsev and Undrovinas 2006; Undrovinas et al. 2006). Late I_{Na} amplitude varies depending on cell type, species, and conditions of measurement (e.g., holding and test potentials, temperature, duration of test pulse, and intracellular Na^+ concentration). Late I_{Na} amplitude is reported to be around 0.1 % of peak I_{Na} in rat (Patlak and Ortiz 1985) and guinea pig (Kiyosue and Arita 1989), but can reach 1 % in human (Maltsev and Undrovinas 2006) ventricular myocytes. It had been shown that all components of I_{Na} inactivation are due to different modes of gating of the same cardiac variant ($Na_V1.5$) of the sodium channel (Maltsev et al. 2009).

The amplitude of late I_{Na} is largest in M cells (Eddlestone et al. 1996) and in Purkinje fibers and much smaller in epicardial or endocardial cells in the canine heart. The more prominent late I_{Na} contributes to the longer AP and greater rate dependence of AP duration in M cells and Purkinje fibers (Eddlestone et al. 1996; Zygmunt et al. 2001) and thus to transmural dispersion of repolarization. Tetrodotoxin (TTX) is reported to inhibit late I_{Na} and abbreviate APD more in M cells and Purkinje fibers than in epicardial cells in the dog heart (Zygmunt et al. 2001; Coraboeuf et al. 1979), thus reducing the transmural dispersion of repolarization. In the guinea pig heart, however, late I_{Na} has been reported to be smaller in mid-myocardial than in epicardial and endocardial cells (Sakmann et al. 2000). The difference appears to be due to methodological considerations. Experiments involving isolated tissues indicate that the guinea pig heart is similar to that of the dog, containing M and transitional cells in the midmyocardium and cells with much briefer APD, showing little response to I_{Kr} block, in the endocardial and epicardial layers (Sicouri et al. 1996). However, unlike the dog, dissociation of myocytes from smaller hearts is fraught with problems because epicardial and endocardial cells are under-represented (Antzelevitch et al. 1999). Indeed, studies involving dissociation of myocytes from guinea pig hearts have reported cells with electrophysiological and pharmacological profiles of M and transitional cells, but not of endocardial or epicardial cells (Bryant et al. 1998). Rather than lacking M cells, the studies reported by Sakmann et al. (2000) may be lacking in epicardial and endocardial cells.

At the single channel level, late I_{Na} is predominantly due to sodium channel reopenings during the plateau of the AP (Maltsev and Undrovinas 2006), which allow a relatively small but persistent influx of Na^+ into the cell. Such activity may be the result of single or bursts of openings of Na^+ channels (Fig. 1) (Patlak and Ortiz 1985; Undrovinas et al. 2002; Kiyosue and Arita 1989; Liu et al. 1992; Saint et al. 1992; Maltsev et al. 1998). The magnitude of the late I_{Na} is increased when the channel fails to enter the inactivated state after the initial opening. Sodium channel toxins including aconitine, veratridine, and sea anemone toxin II (ATX-II) prevent the sodium channel transition into the inactivated state, thus increasing late reopening of the channel, measured in excised or cell-attached patches during long voltage-clamp pulses (>200 ms).

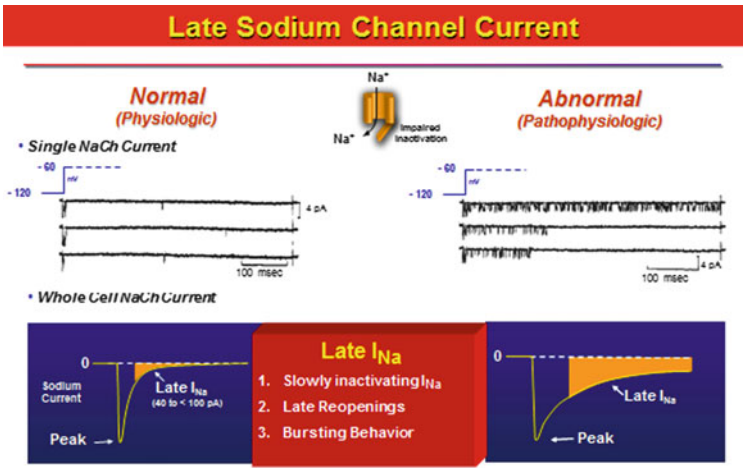

Fig. 1 Late sodium channel current is the current flowing during the plateau of the cardiac action potential and is comprised of slowly inactivating sodium channel current, late re-openings, and bursting behavior of the sodium channels. Modified from Belardinelli et al. (2004), with permission

2 Causes of an Enhanced Late I_{Na}

The magnitude of late I_{Na} in cardiac myocytes increases in several acquired or congenital conditions such as heart failure (Maltsev et al. 2007; Valdivia et al. 2005), hypoxia (Hammarstrom and Gage 2002), inflammation (Ward et al. 2006), and hyperthyroxinemia (Harris et al. 1991), or due to mutations in *SCN5A*, which encodes the α-subunit of the sodium channel (Rivolta et al. 2001), as well as in channel-interacting proteins, including multiple β subunits and anchoring proteins. Such an increase of late I_{Na} can be reproduced experimentally by application of natural and synthetic toxins [see (Honerjager 1982) for review] such as ATX-II, veratridine, and aconitine that bind to various sites on the Na^+ channel (Denac et al. 2000). It is important to make the distinction between toxins that bind near the local anesthetic binding sites (veratridine and aconitine) and those that bind to the sodium channel at unrelated sites (e.g., ATX-II). It had been shown that these compounds can cause arrhythmias when applied to intact or isolated heart preparations. For example, local application of aconitine causes atrial ectopic activity (Scherf et al. 1948) and ventricular tachycardia and fibrillation (Lu and De 1993). Bursting behavior, which results in a larger late I_{Na}, is reported to be increased as a consequence of some LQT3 mutations including ΔKPQ (Hartmann et al. 1994) and Y1795C (Rivolta et al. 2001). Table 1 lists the conditions and agents that are known to increase cardiac late I_{Na}.

Table 1 Conditions and agents that have been demonstrated to increase cardiac late I_{Na}

Conditions/endogenous agents	Drugs and toxins
Activation of CaMKII	Aconitine
Activation of Fyn tyrosine kinase	ATX-II
Activation of PKC	Batrachotoxin
Angiotensin II	DPI 201–106 and analogs
Carbon monoxide	KB130015
2,3-Diphosphoglycerate	Ouabain (indirectly)
Hydrogen peroxide (H_2O_2)	Pyrethroids (e.g., tefluthrin)
Hypoxia, ischemia Hyperthyroxinemia	Veratridine
Lysophosphatidylcholine	
Nitric oxide (NO)	
Palmitoyl-L-carnitine	

Modified from Shryock et al. (2013), with permission

3 Acquired Causes of an Enhanced Late I_{Na}

Ischemia is the most common pathology associated with enhanced late I_{Na}. An increase in late I_{Na} during ischemia contributes to the intracellular Na^+ loading observed in the ischemic heart (Xiao and Allen 1999; Liu et al. 2007; Tang et al. 2012). Simulated-demand ischemia was found to increase oxidative stress, late I_{Na}, and cytosolic Ca^{2+} levels in rabbit isolated myocytes; the rise of intracellular Ca^{2+} was reduced by inhibitors of late I_{Na} and Na^+/Ca^{2+} exchanger (NCX) and by the free radical scavenger Tiron (Zhang et al. 2008). Activity of NCX is markedly increased by reactive oxygen species during re-oxygenation (Eigel et al. 2004). Hydrogen peroxide, nitric oxide, and thrombin are all reported to increase cardiac late I_{Na} (Ward and Giles 1997; Song et al. 2006; Ahern et al. 2000; Pinet et al. 2008). Nitric oxide (Ahern et al. 2000), hydrogen peroxide (Song et al. 2006), hypoxia (Ju et al. 1996), glycolytic metabolites (Kohlhardt et al. 1989), lysophosphatidylcholine (Undrovinas et al. 1992), and heart failure (Maltsev and Undrovinas 2006) also increase the incidence of bursts of Na^+ channel late openings that contribute to late I_{Na}. Protein kinases including CaMKII, PKC, AMPK, and PKA are activated during ischemia. Calcium and reactive oxygen species activate CaMKII and PKC (Erickson et al. 2011; Barnett et al. 2007), lysophosphatidylcholine activates PKC and tyrosine kinase (Murray et al. 1997), loss of ATP and elevation of AMP stimulate AMP-activated protein kinase, and norepinephrine release from cardiac nerve terminals leads to activation of PKA and increased L-type Ca^{2+} current. Each of these kinases, as well as intracellular Ca^{2+}, can modulate Na^+ channel function or expression.

Late I_{Na} is increased in myocytes isolated from failing human and dog hearts (Undrovinas and Maltsev 2008a; Undrovinas et al. 2002; Maltsev et al. 1998, 2007;

Valdivia et al. 2005; Undrovinas et al. 1999), although peak I_{Na} is decreased (Undrovinas et al. 2002; Zicha et al. 2004). I_{Na} inactivates more slowly in cells isolated from failing hearts and the magnitude of late I_{Na} is 2–5 fold greater (Maltsev et al. 2007; Valdivia et al. 2005). Most $Na_V1.5$ channels in ventricular myocytes are localized near the intercalated discs where they interact with βIV-spectrin (Hund et al. 2010) and the rest are in the T-tubules and other areas of the plasma membrane. It is not known whether Na^+ channels located in these different regions of the cell are differentially regulated in terms of their late current in normal and/or diseased hearts.

The final common pathways leading to an increase of late I_{Na} in the failing heart, as in ischemia, may be ROS-induced oxidation and Ca^{2+}-induced kinase activation and phosphorylation of the Na^+ channel and/or channel-interacting proteins (Maltsev et al. 2008; Xie et al. 2009; Gautier et al. 2008). In the hypertrophied and/or failing heart, reduction of repolarizing current contributes to prolongation of AP duration in a nonuniform manner (Keung and Aronson 1981) and to alternans of Ca^{2+} transients and AP duration (Wilson et al. 2009), thus promoting an arrhythmogenic substrate.

4 Congenital Causes of Late I_{Na}

The long QT syndrome type-3 (LQT3) is caused by inherited "gain of function" mutations in the *SCN5A* gene [for reviews, see (Zimmer and Surber 2008; Ruan et al. 2009; Moreno and Clancy 2012; Blaufox et al. 2012)] and by mutations in Na^+ channel-interacting proteins that lead to an increase of late I_{Na} (Abriel 2010). The first description of an inherited LQT3 mutation, a deletion of amino acids 1,505–1,507 (ΔKPQ) in a patient with a prolonged QT interval, was presented in 1995 (Wang et al. 1995). The mutated *SCN5A* channel was heterologously expressed in HEK293 cells and demonstrated to cause an increase of late I_{Na} and of the duration of the action potential (Bennett et al. 1995; Wang et al. 1996). More than 80 different *SCN5A* mutations that increase cardiac ($Na_V1.5$) late I_{Na} have since been described in patients with LQT3. Most LQT3 mutations are missense mutations that cause late current by increasing the probability that the Na^+ channel will either fail to inactivate quickly or will reopen more readily from the closed state. Some of these mutations occur at sites that are also known targets for phosphorylation by protein kinases (Ahern et al. 2005). Sodium channel mutations such as ΔKPQ and Y1795C cause increased bursting activity of the Na^+ channel (Chandra et al. 1998; Clancy and Rudy 1999; Clancy et al. 2002) as do mutations in the IFM motif of the inactivation gate (West et al. 1992).

Four β subunits have been shown to play a critical role in cell surface expression, subcellular localization, as well as biophysical function of the Na^+ channels (Abriel 2010; Maier et al. 2004; Meadows and Isom 2005). Mutations in the Na^+ channel β subunits $Na_{v\beta}$ (β_1–β_4) are reported to be a cause of congenital LQT syndrome, atrial fibrillation, Brugada syndrome, and conduction slowing [reviewed by Abriel (2010)]. Loss of β_1 expression in mice results in increases of both peak and late

I_{Na} and a prolonged QT interval (Lopez-Santiago et al. 2007). Late I_{Na} is increased in cells expressing *SCN5A* with the β_1, but not with the β_2, subunit compared to cells expressing *SCN5A* alone (Maltsev et al. 2009). Mutations in both β_3 and β_4 subunits have been identified in LQT3 and/or sudden infant death syndrome (SIDS) patients and found to cause an increased late I_{Na} when expressed with *SCN5A* in HEK293 cells (Medeiros-Domingo et al. 2007; Tan et al. 2010).

Numerous proteins are known to interact with the cardiac sodium channel (Rook et al. 2012; Abriel 2010; Vatta et al. 2006; Shao et al. 2009). Mutations in scaffolding and/or cytoskeletal "channel interaction proteins" (ChIPs) are recognized causes of LQT syndrome (Ackerman and Mohler 2010). Mutations in caveolin-3 (Vatta et al. 2006), alpha-1 syntrophin (Ueda et al. 2008; Wu et al. 2008a), and β_{IV} spectrin (Hund et al. 2010; Wu et al. 2008a; Sarhan et al. 2009; Vatta and Faulkner 2006) are associated with increased magnitude of late I_{Na} and with LQT and/or SIDS. Proteins such as F-actin, telethonin, α-actinin-2, and Z-band alternatively spliced PDZ-motif (ZASP) that are anchored at the Z-line may participate in the trafficking of ion channels to the T-tubule membrane (Vatta and Faulkner 2006). A mutation in telethonin is reported to increase Na^+ window current (Mazzone et al. 2008), and a missense mutation in ZASP shifts the voltage dependence of Na^+ channel activation (Li et al. 2010). Reduced interaction of the Na^+ channel with ChIPs such as the intercalated disc-associated proteins ankyrin-G and SAP97 may lead to a Na^+ channel loss-of-function phenotype such as conduction slowing or Brugada syndrome (Mohler et al. 2004; Scherer et al. 2008). Silencing of expression of SAP97 reduced peak I_{Na} in rat cardiomyocytes (Petitprez et al. 2011). The last three residues of the $Na_V1.5$ C-terminus associate with dystrophin protein complexes in the lateral membranes of cardiomyocytes, and a deficiency of dystrophin leads to decreased $Na_V1.5$ expression and myocardial Na^+ current (Petitprez et al. 2011; Gavillet et al. 2006).

5 Late I_{Na}-Mediated Arrhythmias

Patients with LQT3 syndrome are at a high risk not only for Torsade de Pointes (TdP) ventricular arrhythmias but also for atrial fibrillation (Benito et al. 2008; Darbar et al. 2008; Zellerhoff et al. 2009). In studies of isolated hearts and myocytes, enhancement of late I_{Na} using ATX-II, veratridine, or aconitine is reported to cause arrhythmic activity in both atrial and ventricular tissues. In both inherited and acquired sodium channelopathies, late I_{Na} may be increased while peak I_{Na} is decreased (Maltsev et al. 2007; Valdivia et al. 2005; Zicha et al. 2004; Makita et al. 2008; Remme et al. 2006) and both can contribute to arrhythmogenesis.

Reduction in repolarization reserve can amplify the effect of an increase in late I_{Na} to delay repolarization, thus enabling the development of arrhythmias (Wu et al. 2004, 2006, 2008b, 2011)

6 Mechanisms Underlying Late I_{Na}-Induced Arrhythmogenesis

6.1 Late I_{Na} and Diastolic Depolarization: Abnormal Automaticity

Spontaneous diastolic depolarization responsible for pacemaking in sinoatrial and compact atrioventricular node cells is driven by ion currents including L- and T-type Ca^{2+} channel currents, "funny" current (HCN channels), and NCX [for reviews see (Chandler et al. 2009; Hoeker et al. 2009)]. Diastolic depolarization of myocytes in atrial and ventricular tissues is rare in the normal intact heart but is often observed in atrial cells and tissues excised from diseased human (Gelband et al. 1972; Escande et al. 1986; Mary-Rabine et al. 1980; Trautwein et al. 1962) and animal (Chen et al. 2000; Cheung 1981; Hogan and Davis 1968; Wit and Cranefield 1977) hearts.

A critical role for late I_{Na} in pacemaking was highlighted by recent studies demonstrating that atrial automaticity can be modulated by late I_{Na} enhancers and inhibitors (Song et al. 2009). Late I_{Na} was found to be present in atrial myocytes that undergo diastolic depolarization (Song et al. 2009). Sea anemone toxin II (ATX-II), a specific enhancer of late I_{Na} (Isenberg and Ravens 1984), accelerates diastolic depolarization and induces rapid firing of APs by atrial myocytes (Song et al. 2009). Reactive oxygen species H_2O_2 increases late I_{Na} and causes diastolic depolarization and rapid AP firing of atrial myocytes, which can be suppressed by block of late I_{Na} using ranolazine (1–5 μmol/L) or TTX (1 μmol/L) (Song et al. 2009). A slowly inactivating TTX-sensitive current, similar to late I_{Na}, was reported to contribute to diastolic depolarization of cardiac Purkinje cells (Carmeliet 1987a; Rota and Vassalle 2003) and of sinoatrial node cells (Baruscotti et al. 2000). In non-pacemaking ventricular myocytes, late I_{Na} was shown to be present at voltages as negative as −70 mV (Sakmann et al. 2000; Saint et al. 1992), well within the voltage range at which spontaneous diastolic depolarization can be observed in these cells (Escande et al. 1986; Mary-Rabine et al. 1980; Trautwein et al. 1962). Sicouri et al. (2012a) recently demonstrated an effect of ranolazine to suppress phase 4 depolarization in superior vena cava sleeves isolated from the canine right atria. These findings suggest that enhancement of late I_{Na} may be a potential cause of atrial arrhythmogenesis.

6.2 Late I_{Na}-Induced Triggered Activity

Early and delayed afterdepolarization (EAD and DAD) are important mechanisms of arrhythmic activity whose occurrence is facilitated when late I_{Na} is enhanced.

Late I_{Na} contributes to AP prolongation (Kiyosue and Arita 1989; Liu et al. 1992; Colatsky 1982). Because the magnitude of late I_{Na} is greater at slow heart rates (Wu et al. 2011; Jia et al. 2011) and the effect of late I_{Na} to increase AP duration is greater in mid-myocardial than in epi- or endocardial myocytes (Zygmunt et al. 2001; Sicouri et al. 1997a; Antzelevitch and Belardinelli 2006),

the role of late I_{Na} to increase dispersion of repolarization and EAD formation is facilitated by heart rate slowing. A role for late I_{Na} in EAD formation is supported by findings that enhancers of late I_{Na} such as ATX-II and anthopleurin-A cause EADs and TdP (Isenberg and Ravens 1984; Ben et al. 2008; Boutjdir and El-Sherif 1991; Song et al. 2004; Ueda et al. 2004; Spencer and Sham 2005; Auerbach et al. 2011). Moreover, inhibitors of late I_{Na} reduce occurrences of EADs and TdP induced by I_{Kr} blockers (Abrahamsson et al. 1996; Shimizu and Antzelevitch 1997a; Orth et al. 2006; Wu et al. 2009a), heart failure (Maltsev et al. 2007; Undrovinas et al. 1999), or left ventricular hypertrophy (Guo et al. 2010).

While a modest increase in late I_{Na} may not cause significant prolongation of AP duration in the normal heart, it can facilitate APD prolongation and EADs induction by I_{Kr} and I_{Ks} blockers. Consistent with this observation, individual susceptibility to drug-induced long QT syndromes has been shown to be linked to *SCN5A* mutations (e.g., L1825P or Y1102) that augment late I_{Na} (Makita et al. 2002; Splawski et al. 2002). Patients with these Na^+ channel gene mutations have normal QT intervals prior to exposure to the drugs, but develop long QT intervals and TdP when given agents such as cisapride or amiodarone (Makita et al. 2002; Splawski et al. 2002). Experimental studies involving isolated hearts, tissues, or myocytes have shown that a small increase of late I_{Na} may facilitate the proarrhythmic effects of I_{Kr} and I_{Ks} blockers (Wu et al. 2006; Song et al. 2004), drugs such as cisapride, amiodarone (Wu et al. 2008c), and quinidine (Wu et al. 2008b), as well as "low-risk" drugs such as moxifloxacin and ziprasidone (Wu et al. 2006). As expected, inhibition of late I_{Na} by ranolazine attenuates the increase of AP duration and EAD induction caused by the combination of ATX-II and I_{Kr}-blocking drugs (Song et al. 2004, 2008). These observations suggest that enhanced late I_{Na} is a major risk factor predisposing cardiac myocytes to development of EADs under both acquired and inherited long QT conditions.

Delayed afterdepolarizations (DADs) have been recognized as a mechanism of digitalis-induced arrhythmogenesis distinct from diastolic phase 4 depolarization, for over 40 years (Ferrier et al. 1973; Wit and Rosen 1983). DADs are observed under conditions in which myocytes are overloaded with Ca^{2+}, causing spontaneous Ca^{2+} release from sarcoplasmic reticulum and Ca^{2+} waves during diastole, leading to aftercontractions (Kass et al. 1978; Kort et al. 1985; Marban et al. 1986; Capogrossi et al. 1987; Stern et al. 1988; Schlotthauer and Bers 2000; Tweedie et al. 2000; Fujiwara et al. 2008). The transient inward current I_{TI} generated by electrogenic Na^+/Ca^{2+} exchange is responsible for these DADs (Kass et al. 1978; Schlotthauer and Bers 2000; Fedida et al. 1987).

Enhancement of late I_{Na}, similarly to inhibition of the sodium–potassium pump by cardiac glycosides, causes Na^+ loading of myocytes. Late I_{Na}-mediated Na^+ loading reduces the driving force for Ca^{2+} efflux from the cell via NCX (Noble and Noble 2006; Shattock and Bers 1989), thereby increasing the diastolic Ca^{2+} concentration and Ca^{2+} uptake by sarcoplasmic reticulum, and reducing the rate and extent of diastolic relaxation (Fig. 2) (Undrovinas et al. 2010; Sossalla et al. 2008). In the normal heart, Na^+ influx during the AP plateau is estimated to account for 30 % of total Na^+ influx at a heart rate of 60/min (Makielski and Farley 2006). Na^+

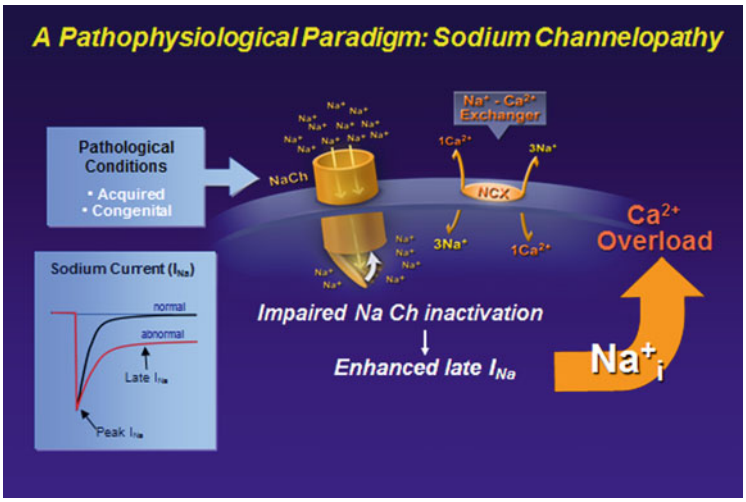

Fig. 2 The pathophysiological paradigm for enhanced late I_{Na}. In both acquired and congenital syndromes, impaired inactivation of the sodium channel leads to enhanced late I_{Na}, causing a rise in intracellular Na concentration, which leads to calcium overload conditions. Modified from Belardinelli et al. (2006), with permission

influx can be increased several-fold when late I_{Na} is enhanced by ischemia, lysophosphatidylcholine, H_2O_2, or *SCN5A* mutations (Makielski and Farley 2006) thus increasing the incidence of DADs (Song et al. 2008; Wu and Corr 1995). Similarly, in myocytes from failing hearts the late I_{Na} is increased by 50 % or more (Valdivia et al. 2005; Undrovinas et al. 2010; Undrovinas and Maltsev 2008b).

DADs induced by cardiac glycosides or other interventions are suppressed by inhibitors of late I_{Na}, including TTX, lidocaine, mexiletine, propafenone, R56865, and ranolazine (Song et al. 2008; Rosen and Danilo 1980; Zeiler et al. 1984; Vollmer et al. 1987; Sawanobori et al. 1987; Inomata and Ishihara 1988; Tsuchida and Otomo 1990; Damiano et al. 1991). Reduction of late I_{Na} by ranolazine and GS-458967, a selective and potent inhibitor of late I_{Na}, has also been shown to reduce the incidence of DADs in experimental studies of pulmonary vein and superior vena cava sleeves (Sicouri et al. 2012a, b, 2013) Blocking late I_{Na} using R 56865, ranolazine, or TTX has been shown to reduce Na^+-dependent Ca^{2+} loading of cardiac myocytes from normal and failing hearts (Song et al. 2006; Undrovinas et al. 2010; Sossalla et al. 2008; Haigney et al. 1994; Fraser et al. 2006). These findings implicate increased Na^+ entry into myocytes via Na^+ channels as a cause of Na^+ and Ca^{2+} loading of myocytes, and arrhythmogenic DADs, while inhibition of late I_{Na} can be used as a means of reducing occurrences of DADs.

6.3 Role of CaMKII Activation in Augmentation of Late I_{Na}

Positive feedback loops have been identified between increases in late I_{Na} and increased expression and activation of CaMKII. These feedback loops appear to contribute to the pathology of Na^+/Ca^{2+} overload in the failing and/or ischemic heart, where late I_{Na} (Saint 2006; Maltsev et al. 2007; Valdivia et al. 2005; Ju et al. 1996; Undrovinas et al. 1999; Le Grand et al. 1995) and expression and activity of CaMKII (Kirchhefer et al. 1999; Hoch et al. 1999) are increased. CaMKII phosphorylates phospholamban to increase Ca^{2+} uptake by sarcoplasmic reticulum (Ji et al. 2003) and RyR2 (Rodriguez et al. 2003) to increase the sensitivity of calcium release channels to Ca^{2+}-induced opening. These two events can lead to increased leak of Ca^{2+} from the sarcoplasmic reticulum during diastole (Maier et al. 2003; Ai et al. 2005; Guo et al. 2006; Sag et al. 2009; Sossalla et al. 2010; Neef et al. 2010) that may elicit regenerative, spontaneous waves of Ca^{2+} release causing aftercontractions, transient inward current (I_{Ti}), and DADs (Fujiwara et al. 2008; Curran et al. 2010). CaMKII expression and activity is increased in the failing heart (Kirchhefer et al. 1999; Hoch et al. 1999; Ai et al. 2005; Sossalla et al. 2010; Anderson et al. 2011). Inhibition of CaMKII activity was shown to abolish isoproterenol-induced spontaneous Ca^{2+} waves and DADs in ventricular myocytes isolated from failing rabbit (Curran et al. 2010) and mouse (Sag et al. 2009) hearts, to decrease I_{Kr}-block-induced EADs in rabbit heart (Anderson et al. 1998), and to improve contractile function and reduce the leak of Ca^{2+} from the sarcoplasmic reticulum in myocytes from failing human hearts (Sossalla et al. 2010). Atrial fibrillation has been associated with increases of both late I_{Na} and CaMKII activity (Benito et al. 2008; Neef et al. 2010; Hove-Madsen et al. 2004).

The positive feedback loop between late I_{Na} and CaMKII activation is completed by a CaMKII-mediated increase of late I_{Na} (Maltsev et al. 2008; Wagner et al. 2006, 2011; Aiba et al. 2010; Ma et al. 2012). CaMKII associates with and phosphorylates the Na^+ channel (Hund et al. 2010; Wagner et al. 2006). Inhibition of CaMKII has been shown to reduce both contractile dysfunction and late I_{Na} in guinea pig isolated hearts and myocytes exposed to ouabain (Hoyer et al. 2011), and inhibition of late I_{Na} was shown to reduce arrhythmic activity and a rapid pacing-induced increase of diastolic tension in papillary muscles isolated from mice overexpressing CaMKIIδ_C (Sossalla et al. 2011). The late I_{Na} inhibitor ranolazine decreases phosphorylation of CaMKII, RyR2, and phospholamban in N1325S mouse hearts (Yao et al. 2011). Thus, the feedback loop between the amplitude of late I_{Na} and CaMKII activity can be interrupted using inhibitors of CaMKII or late I_{Na}, either of which can reduce EADs and DAD incidence, dispersion of repolarization, Ca^{2+} alternans, and diastolic contracture. Finally, during the development of cardiac hypertrophy and failure, CaMKII appears to have an important role in the regulation of cardiac gene transcription (Zhang et al. 2007; Backs et al. 2009). Sodium channel expression is decreased in the failing heart (Undrovinas et al. 2002; Zicha et al. 2004), but evidence linking transcriptional control of *SCN5A* by CaMKII is lacking.

6.4 Role of Late I_{Na} in Dispersion of Repolarization and Related Arrhythmias

Reentrant arrhythmias generally involve unidirectional block and conduction around a circuit long enough to enable recovery of excitability at each point in the circuit before the circus wave of excitation returns (Mines 1914). The length of the circuit must be greater than the distance that an impulse can travel (i.e., the wavelength, a product of conduction velocity, and refractory period) before reaching the same point again. The establishment of unidirectional block is facilitated by an increase in dispersion of repolarization associated with both acquired or congenital conditions that prolong or abbreviate AP duration and the QT interval, thus promoting the substrate for reentry (Di Diego and Antzelevitch 1993; Antzelevitch 2007, 2008; Patel and Antzelevitch 2008a; Galinier et al. 1998; Yan et al. 2001; Sicouri et al. 2010; Benoist et al. 2012). Computational modeling studies also indicate that increased AP dispersion and weaker cell-to-cell coupling is associated with the susceptibility to reentrant arrhythmic activity (Ghanem et al. 2001; Burnes et al. 2001).

Preferential abbreviation of AP duration and refractoriness in epicardium vs. endocardium under short QT and Brugada syndrome conditions can also provide the substrate for reentry, both in atria and ventricles (Antzelevitch 2008; Sicouri et al. 2010; Antzelevitch and Sicouri 2012; Nof et al. 2010; Fish and Antzelevitch 2008; Patel and Antzelevitch 2008b). Acute ischemia also contributes to induction of reentry by causing electrical heterogeneity and conduction block (Vermeulen et al. 1996; Sidorov et al. 2011).

In normal hearts, late I_{Na} is greater in Purkinje fibers and M cells than in endo- or epicardial cells, thereby contributing to the longer duration of the AP in these cells (Zygmunt et al. 2001; Coraboeuf et al. 1979) and to spatial dispersion of AP duration and refractoriness. Block of late I_{Na} reduces AP duration in Purkinje fibers and M cells and is associated with reduction of the transmural dispersion of AP duration. (Sicouri et al. 1997a, b; Shimizu and Antzelevitch 1997b; Antzelevitch and Oliva 2006; Antzelevitch et al. 2006) Augmented late I_{Na} likely contributes to arrhythmogenesis in failing hearts due to increase in dispersion of repolarization and repolarization variability secondary to the increase in late I_{Na} (Maltsev et al. 2007). Reduction of late I_{Na} is effective in abbreviating APD and repolarization variability (Undrovinas et al. 2006). Late I_{Na} enhancers, including anthopleurin-A and veratridine increase the dispersion of AP duration in intact isolated guinea pig and rabbit hearts, respectively (Restivo et al. 2004; Milberg et al. 2005). Augmentation of late I_{Na} with ATX-II has been shown to dramatically increase transmural dispersion of repolarization and refractoriness in canine left ventricular wedge preparations, giving rise to TdP (Shimizu and Antzelevitch 1997a, b).

Inhibition of late I_{Na} whether by mexiletine, ranolazine, or other agents reverses the effect of the late I_{Na} enhancers, effectively reducing spatial dispersion of repolarization and refractoriness, thus suppressing TdP (Wu et al. 2004; Shimizu and Antzelevitch 1997b, 1998, 1999a, b; Wu et al. 2003). Figure 3 illustrates the

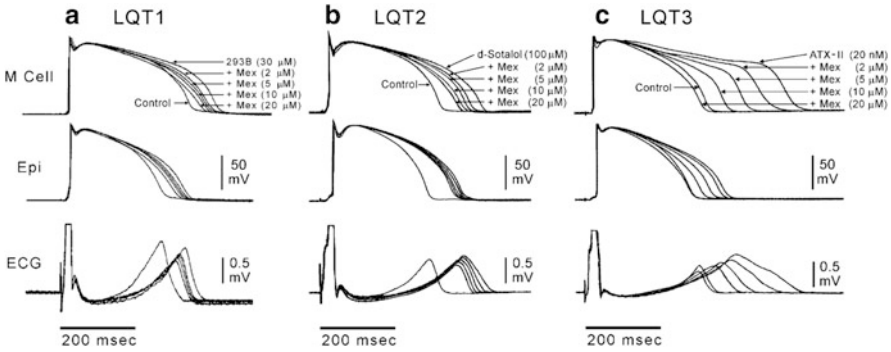

Fig. 3 I_{Kr} and I_{Ks} blockers and Late I_{Na} agonist promote transmural dispersion (TDR) of repolarization and prolonged Tpeak–Tend intervals in the ECG by producing a preferential prolongation of the M cell action potential duration. Block of late I_{Na} with mexiletine reduces TDR in these experimental models of the long QT syndrome. Each panel shows transmembrane action potentials recorded from M and epicardial (Epi) sites in canine left ventricular wedge preparations together with a transmural ECG recorded across the bath (BCL of 2,000 ms). Traces are recorded in the presence of the I_{Ks} blocker, chromanol 293B (LQT1), I_{Kr} blocker D-sotalol (LQT2), and late I_{Na} agonist, ATX-II (LQT3), plus increasing concentrations of mexiletine. Mexiletine produced a greater abbreviation of the M cell vs. epicardial action potential at every concentration, resulting in a reduction in transmural dispersion of repolarization in all three LQTS models. Modified from (Shimizu and Antzelevitch 1997b, 1998) with permission

effect of I_{Kr} and I_{Ks} blockers as well as a late I_{Na} agonist to promote transmural dispersion of repolarization (TDR) and prolonged Tpeak–Tend intervals in the ECG by producing a preferential prolongation of the M cell action potential duration. Block of late I_{Na} with mexiletine reduces TDR in these experimental models of long QT 1, 2, and 3. Reduction of late I_{Na} can also reduce spatial dispersion of repolarization and beat-to-beat variability of repolarization caused by treatment of rabbit isolated hearts with the I_{Kr} blocker, E-4031 (Wu et al. 2009b). Taken together, these results support the view that either reduction of repolarizing K^+ current or enhancement of late I_{Na} results in increased dispersion of repolarization that may lead to arrhythmias and that reduction of late I_{Na} is effective is reversing these proarrhythmic effects (Fig. 4).

6.5 Role of Late I_{Na} in Cardiomyopathy

As discussed above, acquired and congenital defects that augment late I_{Na} do so by varied molecular mechanisms, including sodium channel phosphorylation, mutations of a specific amino acid residue(s) in the α or β subunits, or by alteration of channel-interacting proteins, which may promote varied phenotypes. In addition to congenital and acquired LQTS, an increase in late I_{Na} can result in mechanical dysfunction of the heart. Dilated cardiomyopathy has been reported in patients (McNair et al. 2004) as well as in mice (Zhang et al. 2011) with mutations in *SCN5A*

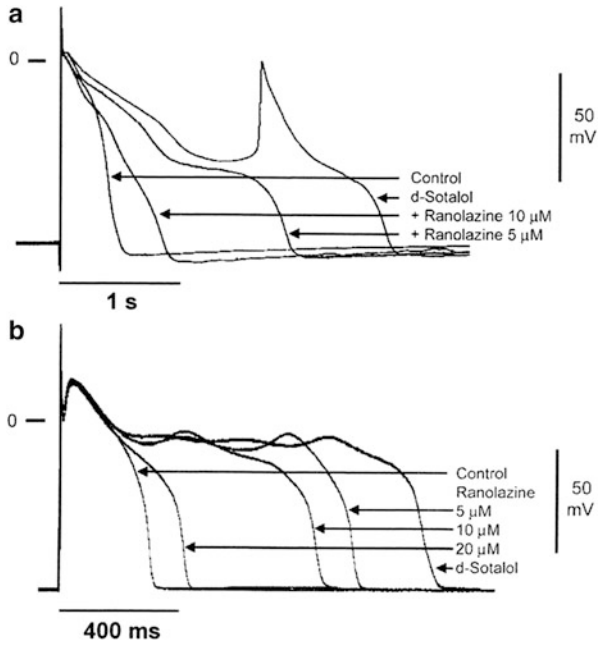

Fig. 4 Effect of ranolazine to suppress D-sotalol-induced action potential prolongation and early afterdepolarizations in Purkinje fiber (**a**) and M cell preparations (**b**). Modified from Antzelevitch et al. (2004)

associated with a gain of function in late I_{Na}. Mechanical dysfunction can result from an increase of intracellular Na^+ to decrease the electrochemical gradient for Ca^{2+} extrusion by Na^+–Ca^{2+} exchange (Belardinelli et al. 2006; Noble and Noble 2006; Sossalla et al. 2008). Slowing of Ca^{2+} extrusion could lead to slowing of diastolic relaxation. It is noteworthy that patients expressing the LQT3-ΔKPQ mutant Na^+ channel are reported to have an impaired diastolic left ventricular relaxation and AP prolongation that were improved after administration of ranolazine (Moss et al. 2008).

Hypertrophic cardiomyopathy (HCM) is the most common monogenic cardiac disorder encountered in the clinic. Recent studies have identified the presence of cells with M cell characteristics in the septum of the human heart, (Barajas-Martinez et al. 2013; Coppini et al. 2013) as has previously been described in the canine heart (Glass et al. 2007; Sicouri et al. 1994) displaying higher levels of late I_{Na}. An ameliorative effect of ranolazine was shown to reduce the augmented late I_{Na} and thus to reduce the prolonged APD in the setting of HCM.

Coppini et al. (2013) showed that in cardiomyocytes isolated from HCM, enhanced CaMKII activity slows ICa inactivation and increases late I_{Na}, thus contributing to APD prolongation and related arrhythmias. Their data also suggested that by altering the function of EC-coupling proteins, CaMKII might

also contribute to the altered Ca^{2+}-transient kinetics and elevation of diastolic [Ca^{2+}]i, which are responsible for the development of delayed afterdepolarizations (DAD). Therapeutic concentrations of ranolazine partially reversed the HCM-related cellular abnormalities via inhibition of late I_{Na}, with negligible effects in myocytes isolated from control hearts.

7 Drugs That Inhibit Cardiac Late I_{Na}

Local anesthetic and antiarrhythmic agents, including mexiletine, lidocaine, ranolazine, amiodarone, propranolol, verapamil, pentobarbital, quinidine, and flecainide, as well as antiepileptic drugs such as phenytoin and riluzole, are known to inhibit late I_{Na} in cardiac myocytes . These drugs lack selectivity for inhibition of late I_{Na} relative to other currents or receptor targets (Table 2). TTX is a selective Na^+ channel blocker (Narahashi 2008) that inhibits late I_{Na} in the heart at concentrations 5–10-fold lower than it inhibits peak I_{Na} (Carmeliet 1987a; Wu et al. 2009a; Le Grand et al. 1995; Josephson and Sperelakis 1989) and it is commonly used in experiments to validate the effects of other late I_{Na} blockers. However, TTX blocks neuronal Na^+ channels at much lower concentrations than those at which cardiac $Na_V1.5$ channels are blocked, accounting for its high toxicity.

The antianginal drug ranolazine (Antzelevitch et al. 2011), GS-458967 (Belardinelli et al. 2013), and the Pierre Fabre experimental compound F15845 (Vacher et al. 2009) appear to be the most selective inhibitors of cardiac late I_{Na} reported to date. Ranolazine has been demonstrated to be safe (Morrow 2007) in patients with non-ST-elevation acute coronary syndromes and angina pectoris. Ranolazine inhibits late I_{Na} and I_{Kr} with potencies of 6 and 12–14 μmol/L, respectively, (Antzelevitch et al. 2004) and slightly prolongs the QT interval in humans (Chaitman 2006). It also blocks both α- and β-adrenergic receptors with low potency (Zhao et al. 2011).

Most drugs that selectively inhibit cardiac late I_{Na} are believed to bind to the local anesthetic site in the $Na_V1.5$ Na^+ channel vestibule, and they cause both use- and voltage-dependent block of the Na^+ current (Zygmunt et al. 2011; Nesterenko et al. 2011). Local anesthetic binding to the Na^+ channel is state dependent, and high-affinity binding depends on the availability of a channel conformation in which certain amino acids are arranged in a specific 3D relationship to form a binding domain (Lipkind and Fozzard 2005). In any different conformation (e.g., the closed state), the same amino acids are present but in different relative 3D positions that do not form a local anesthetic binding site of high affinity. The amino acids that form the putative local anesthetic site in open/inactivated Na^+ channel include F1759 and Y1766 (F1760 and Y1767 in hH1) in DIVS6, but much data indicate that other amino acids contribute to local anesthetic binding, and more than one binding site may be present [for review, see Mike and Lukacs (2010)]. It should be noted that the binding site for batrachotoxin in the Na^+ channel vestibule overlaps that for local anesthetics (however, at a molecular weight of

Table 2 IC_{50} values for drug-induced block of peak and late I_{Na} as well as I_{Kr} by I_{Na} blockers

Drug	MW	IC_{50} value for tonic block (μM)			References
		Late I_{Na}	Peak I_{Na}	hERG (I_{Kr})	
Amiodarone (acute)	645	3.0, 6.7	178, 87	~1	Wu et al. (2008c), Maltsev et al. (2001)
Flecainide	414	1.4	10–15	2.1, 3.9	Liu et al. (2003), Heath et al. (2011)
F15845	376	~1	23 % at 10 μM	15 % at 10 μM	Vacher et al. (2009), Pignier et al. (2010)
GS458967	347	0.2	>10	>10	Sicouri et al. (2012c)
KC12291	413	≤10	~15	No inhibition?	Tamareille et al. (2002), John et al. (2004)
Lidocaine	236	~25	~300	No inhibition	Bean et al. (1983), Grant et al. (1989), Starmer et al. (1991)
Mexiletine	179	3–5	28–253	No inhibition	Yatani and Akaike (1985), Sunami et al. (1993)
Propafenone	341	<1	≤1	0.4–0.8	Schreibmayer and Lindner (1992), Edrich et al. (2005), Witchel et al. (2004)
Propranolol	259	~3	22–28	No inhibition	Wang et al. (2008, 2010)
Quinidine	324	12	11	~1	Colatsky (1982), Grant et al. (1982)
R56865	413	0.2	~5	Probable inhibition	Wilhelm et al. (1991), Verdonck et al. (1991)
Ranolazine	428	7	428	12–14	Antzelevitch et al. (2004), Zygmunt et al. (2011), Undrovinas et al. (2004)
Riluzole	234	2.7–3	100–150		Song et al. (1997), Weiss et al. (2010)
Tetrodotoxin	319	0.53	6.0	No inhibition	Josephson and Sperelakis (1989), Carmeliet (1987b)
Vernakalant	349	~30	107	7–21	Orth et al. (2006), Fedida (2007)

539, batrachotoxin is larger than most local anesthetics) and displacement of its binding has been used to identify potential use-dependent Na^+ channel blockers (Carter et al. 2000; Grauert et al. 2002).

The antiarrhythmic effects of drugs and agents that reduce late I_{Na} have been demonstrated by many investigators using many different cardiac preparations (e.g., (Antzelevitch et al. 2004, 2011; Ruan et al. 2009; Undrovinas et al. 1999; Wu et al. 2004; Sicouri et al. 1997a; Scirica et al. 2007; Antzelevitch and Belardinelli 2006; Song et al. 2004; Sheu and Lederer 1985; Fedida et al. 2006; Burashnikov et al. 2007; Pignier et al. 2010)). In these studies, late I_{Na} is enhanced as a result of disease (e.g., heart failure), ischemia or hypoxia, gain-of-function mutations in *SCN5A*, or application of toxins (e.g., ATX-II, veratridine, aconitine), intermediary metabolites (e.g., palmitoyl-L-carnitine), or H_2O_2. Inhibition of late I_{Na} has been shown to improve function and reduce arrhythmogenic activity in ventricular, atrial, pulmonary vein sleeve, and nodal cardiac tissues. Diastolic depolarization, triggered

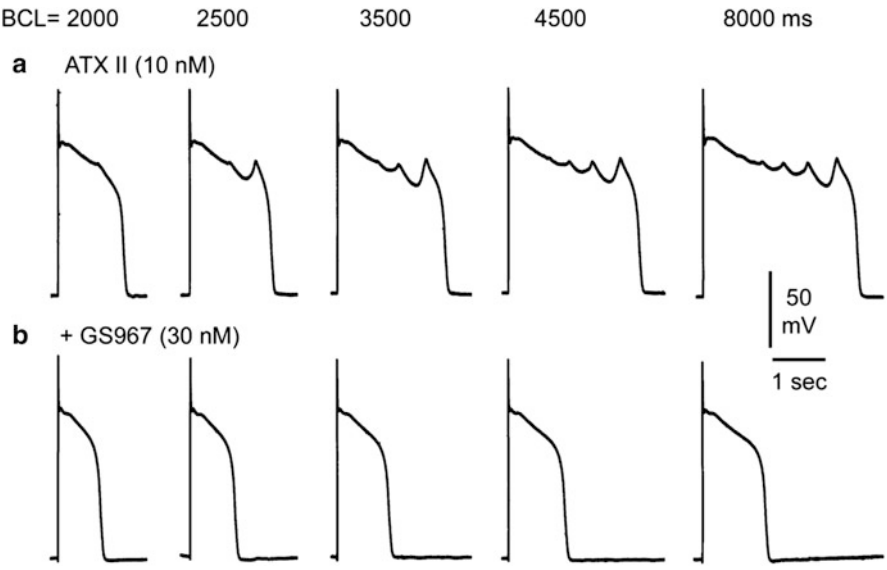

Fig. 5 GS-458967 abolishes early afterdepolarizations (EADs) and EAD-induced triggered activity elicited by exposure to ATX-II in a canine Purkinje fiber. (**a**) ATX-II (10 nM) elicited EADs and EAD-induced triggered activity at basic cycle lengths (BCLs) of 2,000, 2,500, 3,500, 4,500, and 8,000 ms. GS-458967 (30 nM) abolished all EADs and triggered activity. From Sicouri et al. (2013) with permission

activity (EADs, DADs), AP duration and variability, and cytosolic concentrations of Na^+ and Ca^{2+} are reduced following inhibition of a pathologically enhanced late I_{Na}. Reduction of late I_{Na} increases repolarization reserve (shortens AP duration) and attenuates the proarrhythmic effects of I_{Kr} blockers. Spontaneous and pause-triggered arrhythmic activity (i.e., *TdP*) induced by amiodarone, quinidine, moxifloxacin, cisapride, and ziprasidone in the female rabbit isolated heart is reduced by the late I_{Na} inhibitor ranolazine (Wu et al. 2006, 2008b, c). In the dog heart, inhibition of late I_{Na} reduces AP duration more in myocytes with longer AP durations (Purkinje fibers and M cells) than in myocytes with short AP duration (epicardial cells) and thus decreases the transmural dispersion of repolarization (Antzelevitch and Belardinelli 2006; Shimizu and Antzelevitch 1997b). No risks associated with the block of cardiac late I_{Na} have been identified to date.

GS-458967, a recently introduced Gilead Sciences compound, is a selective late I_{Na} inhibitor with an IC_{50} of 200 nM. The compound was shown to cause modest abbreviation of APD and to prevent or abolish both ATX-II and E-4031-induced (i.e., models of LQT3 and LQT2, respectively) ventricular tachycardias in rabbit hearts (Belardinelli et al. 2013). Other recent studies have also demonstrated the effect of GS-458967 to abolish EADs and EAD-induced triggered activity elicited by exposure of canine Purkinje fibers to ATX-II (Fig. 5), increased extracellular calcium, and isoproterenol (Sicouri et al. 2013). GS-458967 may be useful to

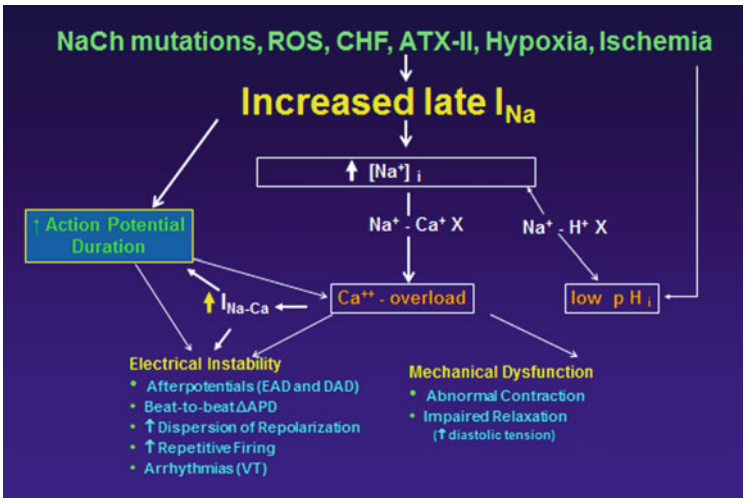

Fig. 6 Mechanisms contributing to electrical instability and mechanical dysfunction in acquired and congenital conditions that enhance late I_{Na}

confirm the pathologic roles of late I_{Na} and to investigate physiologic and pathologic effects of inhibiting late I_{Na} in other excitable tissues.

Conclusion

Evidence implicating enhancement of late I_{Na} in pathophysiological electrical and mechanical instabilities of the heart is steadily increasing (Fig. 6). Selective inhibition of late I_{Na} is expected to be an effective strategy for correcting these channelopathies and cardiomyopathies. Unlike most other antiarrhythmic drugs, selective inhibitors of late I_{Na} do not appear to be proarrhythmic. Future direction focused on development of highly selective late I_{Na} blockers are needed to test this hypothesis in the clinic.

Support Supported by grants HL47678 from NHLBI, NIH (CA), C026424 from NYSTEM (CA), Gilead Sciences, Inc. and the Masons of New York State, Florida, Massachusetts Connecticut, Maryland, Rhode Island, and Wisconsin.

Conflicts of Interest

Dr. Antzelevitch is a consultant to Gilead Sciences and Dr. Belardinelli, Shryock, and Rajamani are employed by Gilead Sciences.

References

Abrahamsson C, Carlsson L, Duker G (1996) Lidocaine and nisoldipine attenuate almokalant-induced dispersion of repolarization and early afterdepolarizations in vitro. J Cardiovasc Electrophysiol 7:1074–1081

Abriel H (2010) Cardiac sodium channel Na(v)1.5 and interacting proteins: physiology and pathophysiology. J Mol Cell Cardiol 48:2–11

Ackerman MJ, Mohler PJ (2010) Defining a new paradigm for human arrhythmia syndromes: phenotypic manifestations of gene mutations in ion channel- and transporter-associated proteins. Circ Res 107:457–465

Ahern GP, Hsu SF, Klyachko VA, Jackson MB (2000) Induction of persistent sodium current by exogenous and endogenous nitric oxide. J Biol Chem 275:28810–28815

Ahern CA, Zhang JF, Wookalis MJ, Horn R (2005) Modulation of the cardiac sodium channel NaV1.5 by Fyn, a Src family tyrosine kinase. Circ Res 96:991–998

Ai X, Curran JW, Shannon TR, Bers DM, Pogwizd SM (2005) Ca2+/calmodulin-dependent protein kinase modulates cardiac ryanodine receptor phosphorylation and sarcoplasmic reticulum Ca2+ leak in heart failure. Circ Res 97:1314–1322

Aiba T, Hesketh GG, Liu T, Carlisle R, Villa-Abrille MC, O'Rourke B, Akar FG, Tomaselli GF (2010) Na+ channel regulation by Ca2+/calmodulin and Ca2+/calmodulin-dependent protein kinase II in guinea-pig ventricular myocytes. Cardiovasc Res 85:454–463

Amin AS, Tan HL, Wilde AAM (2010) Cardiac ion channels in health and disease. Heart Rhythm 7:117–135

Anderson ME, Braun AP, Wu Y, Lu T, Wu Y, Schulman H, Sung RJ (1998) KN-93, an inhibitor of multifunctional Ca++/calmodulin-dependent protein kinase, decreases early afterdepolarizations in rabbit heart. J Pharmacol Exp Ther 287:996–1006

Anderson ME, Brown JH, Bers DM (2011) CaMKII in myocardial hypertrophy and heart failure. J Mol Cell Cardiol 51:468–473

Antzelevitch C (2007) Heterogeneity and cardiac arrhythmias: an overview. Heart Rhythm 4:964–972

Antzelevitch C (2008) Drug-induced spatial dispersion of repolarization. Cardiol J 15:100–121

Antzelevitch C, Belardinelli L (2006) The role of sodium channel current in modulating transmural dispersion of repolarization and arrhythmogenesis. J Cardiovasc Electrophysiol 17(Suppl 1):S79–S85

Antzelevitch C, Oliva A (2006) Amplification of spatial dispersion of repolarization underlies sudden cardiac death associated with catecholaminergic polymorphic VT, long QT, short QT and Brugada syndromes. J Intern Med 259:48–58

Antzelevitch C, Sicouri S (2012) Mechanisms underlying arrhythmogenesis in long QT syndrome. Card Electrophysiol Clin 4:17–27

Antzelevitch C, Shimizu W, Yan GX, Sicouri S, Weissenburger J, Nesterenko VV, Burashnikov A, Di Diego JM, Saffitz J, Thomas GP (1999) The M cell: its contribution to the ECG and to normal and abnormal electrical function of the heart. J Cardiovasc Electrophysiol 10:1124–1152

Antzelevitch C, Belardinelli L, Zygmunt AC, Burashnikov A, Di Diego JM, Fish JM, Cordeiro JM, Thomas GP (2004) Electrophysiologic effects of ranolazine: a novel anti-anginal agent with antiarrhythmic properties. Circulation 110:904–910

Antzelevitch C, Guerchicoff A, Pollevick GD (2006) The role of spatial dispersion of repolarization in sudden cardiac death. ISHNE World Wide Internet Symposium on Sudden Cardiac Death, http://hf2010.ishne.org/vs/scd-2006/lectures/ing_antzelevitch_charles.pdf

Antzelevitch C, Burashnikov A, Sicouri S, Belardinelli L (2011) Electrophysiological basis for the antiarrhythmic actions of ranolazine. Heart Rhythm 8:1281–1290

Auerbach DS, Grzda KR, Furspan PB, Sato PY, Mironov S, Jalife J (2011) Structural heterogeneity promotes triggered activity, reflection and arrhythmogenesis in cardiomyocyte monolayers. J Physiol 589:2363–2381

Backs J, Backs T, Neef S, Kreusser MM, Lehmann LH, Patrick DM, Grueter CE, Qi X, Richardson JA, Hill JA, Katus HA, Bassel-Duby R, Maier LS, Olson EN (2009) The delta isoform of CaM kinase II is required for pathological cardiac hypertrophy and remodeling after pressure overload. Proc Natl Acad Sci U S A 106:2342–2347

Barajas-Martinez H, Hu D, Goodrow RJ Jr, Joyce F, Antzelevitch C (2013) Electrophysiologic characteristics and pharmacologic response of human cardiomyocytes isolated from a patient with hypertrophic cardiomyopathy. Pacing Clin Electrophysiol 36:1512–1515

Barnett ME, Madgwick DK, Takemoto DJ (2007) Protein kinase C as a stress sensor. Cell Signal 19:1820–1829

Baruscotti M, DiFrancesco D, Robinson RB (2000) Na(+) current contribution to the diastolic depolarization in newborn rabbit SA node cells. Am J Physiol Heart Circ Physiol 279:H2303–H2309

Bean BP, Cohen CJ, Tsien RW (1983) Lidocaine block of cardiac sodium channels. J Gen Physiol 81:613–642

Belardinelli L, Antzelevitch C, Fraser H (2004) Inhibition of late (sustained/persistent) sodium current: a potential drug target to reduce intracellular sodium-dependent calcium overload and its detrimental effects on cardiomyocyte function. Eur Heart J Suppl 6:i3–i7

Belardinelli L, Shryock JC, Fraser H (2006) Inhibition of the late sodium current as a potential cardioprotective principle: effects of the late sodium current inhibitor ranolazine. Heart 92 (Suppl 4):iv6–iv14

Belardinelli L, Liu G, Smith-Maxwell C, Wang WQ, El-Bizri N, Hirakawa R, Karpinski S, Kornyeyev D, Li CH, Hu L, Li XJ, Crumb W, Wu L, Koltun D, Zablocki J, Yao L, Dhalla AK, Rajamani S, Shryock J (2013) A novel, potent, and selective inhibitor of cardiac late sodium current suppresses experimental arrhythmias. J Pharmacol Exp Ther 344:23–32

Ben CE, Boutjdir M, Himel HD, El-Sherif N (2008) Role of subendocardial Purkinje network in triggering torsade de pointes arrhythmia in experimental long QT syndrome. Europace 10: 1218–1223

Benito B, Brugada R, Perich RM, Lizotte E, Cinca J, Mont L, Berruezo A, Tolosana JM, Freixa X, Brugada P, Brugada J (2008) A mutation in the sodium channel is responsible for the association of long QT syndrome and familial atrial fibrillation. Heart Rhythm 5:1434–1440

Bennett PB, Yazawa K, Makita N, George AL Jr (1995) Molecular mechanism for an inherited cardiac arrhythmia. Nature 376:683–685

Benoist D, Stones R, Drinkhill MJ, Benson AP, Yang Z, Cassan C, Gilbert SH, Saint DA, Cazorla O, Steele DS, Bernus O, White E (2012) Cardiac arrhythmia mechanisms in rats with heart failure induced by pulmonary hypertension. Am J Physiol Heart Circ Physiol 302: H2381–H2395

Blaufox AD, Tristani-Firouzi M, Seslar S, Sanatani S, Trivedi B, Fischbach P, Paul T, Young ML, Tisma-Dupanovic S, Silva J, Cuneo B, Fournier A, Singh H, Tanel RE, Etheridge SP (2012) Congenital long QT 3 in the pediatric population. Am J Cardiol 109:1459–1465

Boutjdir M, El-Sherif N (1991) Pharmacological evaluation of early afterdepolarisations induced by sea anemone toxin (ATXII) in dog heart. Cardiovasc Res 25:815–819

Bryant SM, Wan X, Shipsey SJ, Hart G (1998) Regional differences in the delayed rectifier current (I_{Kr} and I_{Ks}) contribute to the differences in action potential duration in basal left ventricular myocytes in guinea-pig. Cardiovasc Res 40:322–331

Burashnikov A, Di Diego JM, Zygmunt AC, Belardinelli L, Antzelevitch C (2007) Atrium-selective sodium channel block as a strategy for suppression of atrial fibrillation: differences in sodium channel inactivation between atria and ventricles and the role of ranolazine. Circulation 116:1449–1457

Burnes JE, Ghanem RN, Waldo AL, Rudy Y (2001) Imaging dispersion of myocardial repolarization, I: comparison of body- surface and epicardial measures. Circulation 104:1299–1305

Capogrossi MC, Houser SR, Bahinski A, Lakatta EG (1987) Synchronous occurrence of spontaneous localized calcium release from the sarcoplasmic reticulum generates action potentials in rat cardiac ventricular myocytes at normal resting membrane potential. Circ Res 61:498–503

Carmeliet E (1987a) Slow inactivation of the sodium current in rabbit cardiac Purkinje fibers. Pflugers Arch 408:18–26

Carmeliet E (1987b) Voltage-dependent block by tetrodotoxin of the sodium channel in rabbit cardiac Purkinje fibers. Biophys J 51:109–114

Carter AJ, Grauert M, Pschorn U, Bechtel WD, Bartmann-Lindholm C, Qu Y, Scheuer T, Catterall WA, Weiser T (2000) Potent blockade of sodium channels and protection of brain tissue from ischemia by BIII 890 CL. Proc Natl Acad Sci U S A 97:4944–4949

Chaitman BR (2006) Ranolazine for the treatment of chronic angina and potential use in other cardiovascular conditions. Circulation 113:2462–2472

Chandler NJ, Greener ID, Tellez JO, Inada S, Musa H, Molenaar P, DiFrancesco D, Baruscotti M, Longhi R, Anderson RH, Billeter R, Sharma V, Sigg DC, Boyett MR, Dobrzynski H (2009) Molecular architecture of the human sinus node: insights into the function of the cardiac pacemaker. Circulation 119:1562–1575

Chandra R, Starmer CF, Grant AO (1998) Multiple effects of KPQ deletion mutation on gating of human cardiac Na+ channels expressed in mammalian cells. Am J Physiol 274:H1643–H1654

Chen YJ, Chen SA, Chang MS, Lin CI (2000) Arrhythmogenic activity of cardiac muscle in pulmonary veins of the dog: implication for the genesis of atrial fibrillation. Cardiovasc Res 48:265–273

Cheung DW (1981) Electrical activity of the pulmonary vein and its interaction with the right atrium in the guinea-pig. J Physiol 314:445–456

Clancy CE, Rudy Y (1999) Linking a genetic defect to its cellular phenotype in a cardiac arrhythmia. Nature 400:566–569

Clancy CE, Tateyama M, Kass RS (2002) Insights into the molecular mechanisms of bradycardia-triggered arrhythmias in long QT-3 syndrome. J Clin Invest 110:1251–1262

Colatsky TJ (1982) Mechanisms of action of lidocaine and quinidine on action potential duration in rabbit cardiac Purkinje fibers: an effect on steady-state sodium current? Circ Res 50:17–27

Coppini R, Ferrantini C, Yao L, Fan P, Del LM, Stillitano F, Sartiani L, Tosi B, Suffredini S, Tesi C, Yacoub M, Olivotto I, Belardinelli L, Poggesi C, Cerbai E, Mugelli A (2013) Late sodium current inhibition reverses electromechanical dysfunction in human hypertrophic cardiomyopathy. Circulation 127:575–584

Coraboeuf E, Deroubaix E, Coulombe A (1979) Effect of tetrodotoxin on action potentials of the conducting system in the dog heart. Am J Physiol 236:H561–H567

Curran J, Brown KH, Santiago DJ, Pogwizd S, Bers DM, Shannon TR (2010) Spontaneous Ca waves in ventricular myocytes from failing hearts depend on Ca(2+)-calmodulin-dependent protein kinase II. J Mol Cell Cardiol 49:25–32

Damiano BP, Stump GL, Yagel SK (1991) Investigation of electrophysiologic mechanisms for the antiarrhythmic actions of R 56865 in cardiac glycoside toxicity. J Cardiovasc Pharmacol 18: 415–428

Darbar D, Kannankeril PJ, Donahue BS, Kucera G, Stubblefield T, Haines JL, George AL Jr, Roden DM (2008) Cardiac sodium channel (*SCN5A*) variants associated with atrial fibrillation. Circulation 117:1927–1935

Denac H, Mevissen M, Scholtysik G (2000) Structure, function and pharmacology of voltage-gated sodium channels. Naunyn Schmiedebergs Arch Pharmacol 362:453–479

Di Diego JM, Antzelevitch C (1993) Pinacidil-induced electrical heterogeneity and extrasystolic activity in canine ventricular tissues. Does activation of ATP-regulated potassium current promote phase 2 reentry? Circulation 88:1177–1189

Eddlestone GT, Zygmunt AC, Antzelevitch C, Eddlestone GT, Zygmunt AC, Antzelevitch C (1996) Larger late sodium current contributes to the longer action potential of the M cell in canine ventricular myocardium. Pacing Clin Electrophysiol 19(Pt 2):569, Abstract

Edrich T, Wang SY, Wang GK (2005) State-dependent block of human cardiac hNav1.5 sodium channels by propafenone. J Membr Biol 207:35–43

Eigel BN, Gursahani H, Hadley RW (2004) ROS are required for rapid reactivation of Na+/Ca2+ exchanger in hypoxic reoxygenated guinea pig ventricular myocytes. Am J Physiol Heart Circ Physiol 286:H955–H963

Erickson JR, He BJ, Grumbach IM, Anderson ME (2011) CaMKII in the cardiovascular system: sensing redox states. Physiol Rev 91:889–915

Escande D, Coraboeuf E, Planche C, Lacour-Gayet F (1986) Effects of potassium conductance inhibitors on spontaneous diastolic depolarization and abnormal automaticity in human atrial fibers. Basic Res Cardiol 81:244–257

Fedida D (2007) Vernakalant (RSD1235): a novel, atrial-selective antifibrillatory agent. Expert Opin Investig Drugs 16:519–532

Fedida D, Noble D, Rankin AC, Spindler AJ (1987) The arrhythmogenic transient inward current I_{ti} and related contraction in isolated guinea-pig ventricular myocytes. J Physiol (London) 392:523–542

Fedida D, Orth PM, Hesketh JC, Ezrin AM (2006) The role of late I and antiarrhythmic drugs in EAD formation and termination in Purkinje fibers. J Cardiovasc Electrophysiol 17(Suppl 1): S71–S78

Ferrier GR, Saunders JH, Mendez C (1973) A cellular mechanism for the generation of ventricular arrhythmias by acetylstrophanthidin. Circ Res 32:600–609

Fish JM, Antzelevitch C (2008) Cellular mechanism and arrhythmogenic potential of T-wave alternans in the Brugada syndrome. J Cardiovasc Electrophysiol 19:301–308

Fraser H, Belardinelli L, Wang L, Light PE, McVeigh JJ, Clanachan AS (2006) Ranolazine decreases diastolic calcium accumulation caused by ATX-II or ischemia in rat hearts. J Mol Cell Cardiol 41:1031–1038

Fujiwara K, Tanaka H, Mani H, Nakagami T, Takamatsu T (2008) Burst emergence of intracellular Ca^{2+} waves evokes arrhythmogenic oscillatory depolarization via the Na^{+}-Ca^{2+} exchanger: simultaneous confocal recording of membrane potential and intracellular Ca^{2+} in the heart. Circ Res 103:509–518

Galinier M, Vialette JC, Fourcade J, Cabrol P, Dongay B, Massabuau P, Boveda S, Doazan JP, Fauvel JM, Bounhoure JP (1998) QT interval dispersion as a predictor of arrhythmic events in congestive heart failure. Importance of aetiology. Eur Heart J 19:1054–1062

Gautier M, Zhang H, Fearon IM (2008) Peroxynitrite formation mediates LPC-induced augmentation of cardiac late sodium currents. J Mol Cell Cardiol 44:241–251

Gavillet B, Rougier JS, Domenighetti AA, Behar R, Boixel C, Ruchat P, Lehr HA, Pedrazzini T, Abriel H (2006) Cardiac sodium channel Nav1.5 is regulated by a multiprotein complex composed of syntrophins and dystrophin. Circ Res 99:407–414

Gelband H, Bush HL, Rosen MR, Myerburg RJ, Hoffman BF (1972) Electrophysiologic properties of isolated preparations of human atrial myocardium. Circ Res 30:293–300

Ghanem RN, Burnes JE, Waldo AL, Rudy Y (2001) Imaging dispersion of myocardial repolarization, II: noninvasive reconstruction of epicardial measures. Circulation 104:1306–1312

Glass A, Sicouri S, Antzelevitch C (2007) Development of a coronary-perfused interventricular septal preparation as a model for studying the role of the septum in arrhythmogenesis. J Electrocardiol 40:S142–S144

Grant AO, Trantham JL, Brown KK, Strauss HC (1982) pH-dependent effects of quinidine on the kinetics of dV/dt_{max} in guinea pig ventricular myocardium. Circ Res 50:210–217

Grant AO, Dietz MA, Gilliam FR III, Starmer CF (1989) Blockade of cardiac sodium channels by lidocaine. Single-channel analysis. Circ Res 65:1247–1262

Grauert M, Bechtel WD, Weiser T, Stransky W, Nar H, Carter AJ (2002) Synthesis and structure-activity relationships of 6,7-benzomorphan derivatives as use-dependent sodium channel blockers for the treatment of stroke. J Med Chem 45:3755–3764

Guo T, Zhang T, Mestril R, Bers DM (2006) Ca2+/calmodulin-dependent protein kinase II phosphorylation of ryanodine receptor does affect calcium sparks in mouse ventricular myocytes. Circ Res 99:398–406

Guo D, Young LH, Wu Y, Belardinelli L, Kowey PR, Yan GX (2010) Increased late sodium current in left atrial myocytes of rabbits with left ventricular hypertrophy: its role in the genesis of atrial arrhythmias. Am J Physiol Heart Circ Physiol 298:H1375–H1381

Haigney MC, Lakatta EG, Stern MD, Silverman HS (1994) Sodium channel blockade reduces hypoxic sodium loading and sodium-dependent calcium loading. Circulation 90:391–399

Hammarstrom AK, Gage PW (2002) Hypoxia and persistent sodium current. Eur Biophys J 31: 323–330

Harris DR, Green WL, Craelius W (1991) Acute thyroid hormone promotes slow inactivation of sodium current in neonatal cardiac myocytes. Biochim Biophys Acta 1095:175–181

Hartmann HA, Tiedeman AA, Chen S-F, Brown AM, Kirsch GE (1994) Effects of III-IV linker mutations on human heart Na^+ channel inactivation gating. Circ Res 75:114–122

Heath BM, Cui Y, Worton S, Lawton B, Ward G, Ballini E, Doe CP, Ellis C, Patel BA, McMahon NC (2011) Translation of flecainide- and mexiletine-induced cardiac sodium channel inhibition and ventricular conduction slowing from nonclinical models to clinical. J Pharmacol Toxicol Methods 63:258–268

Hoch B, Meyer R, Hetzer R, Krause EG, Karczewski P (1999) Identification and expression of delta-isoforms of the multifunctional Ca2+/calmodulin-dependent protein kinase in failing and nonfailing human myocardium. Circ Res 84:713–721

Hoeker GS, Katra RP, Wilson LD, Plummer BN, Laurita KR (2009) Spontaneous calcium release in tissue from the failing canine heart. Am J Physiol Heart Circ Physiol 297:H1235–H1242

Hogan PM, Davis LD (1968) Evidence for specialized fibers in the canine right atrium. Circ Res 23:387–396

Honerjager P (1982) Cardioactive substances that prolong the open state of sodium channels. Rev Physiol Biochem Pharmacol 92:1–74

Hove-Madsen L, Llach A, Bayes-Genis A, Roura S, Rodriguez FE, Aris A, Cinca J (2004) Atrial fibrillation is associated with increased spontaneous calcium release from the sarcoplasmic reticulum in human atrial myocytes. Circulation 110:1358–1363

Hoyer K, Song Y, Wang D, Phan D, Balser J, Ingwall JS, Belardinelli L, Shryock JC (2011) Reducing the late sodium current improves cardiac fuction during sodium pump inhibition by ouabain. J Pharmacol Exp Ther 337:513–523

Hund TJ, Koval OM, Li J, Wright PJ, Qian L, Snyder JS, Gudmundsson H, Kline CF, Davidson NP, Cardona N, Rasband MN, Anderson ME, Mohler PJ (2010) A beta(IV)-spectrin/CaMKII signaling complex is essential for membrane excitability in mice. J Clin Invest 120:3508–3519

Inomata N, Ishihara T (1988) Mechanism of inhibition by SUN 1165, a new Na channel blocking antiarrhythmic agent, of cardiac glycoside-induced triggered activity. Eur J Pharmacol 145: 313–322

Isenberg G, Ravens U (1984) The effects of the anemonia sulcata toxin (ATX II) on membrane currents of isolated mammalian myocytes. J Physiol 357:127–149

Ji Y, Li B, Reed TD, Lorenz JN, Kaetzel MA, Dedman JR (2003) Targeted inhibition of Ca2+/calmodulin-dependent protein kinase II in cardiac longitudinal sarcoplasmic reticulum results in decreased phospholamban phosphorylation at threonine 17. J Biol Chem 278:25063–25071

Jia S, Lian J, Guo D, Xue X, Patel C, Yang L, Yuan Z, Ma A, Yan GX (2011) Modulation of the late sodium current by the toxin, ATX-II, and ranolazine affects the reverse use-dependence and proarrhythmic liability of I(Kr) blockade. Br J Pharmacol 164:308–316

John GW, Letienne R, Le GB, Pignier C, Vacher B, Patoiseau JF, Colpaert FC, Coulombe A (2004) KC 12291: an atypical sodium channel blocker with myocardial antiischemic properties. Cardiovasc Drug Rev 22:17–26

Josephson IR, Sperelakis N (1989) Tetrodotoxin differentially blocks peak and steady-state sodium channel currents in early embryonic chick ventricular myocytes. Pflugers Arch 414: 354–359

Ju YK, Saint DA, Gage PW (1996) Hypoxia increases persistent sodium current in rat ventricular myocytes. J Physiol 497(Pt 2):337–347

Kass RS, Lederer WJ, Tsien RW et al (1978) Role of calcium ions in transient inward currents and aftercontractions induced by strophantidin in cardiac Purkinje fibers. J Physiol (London) 281:187–208

Keung ECH, Aronson RS (1981) Transmembrane action potentials and the electrocardiogram in rats with renal hypertension. Cardiovasc Res 15:611–614

Kirchhefer U, Schmitz W, Scholz H, Neumann J (1999) Activity of cAMP-dependent protein kinase and Ca2+/calmodulin-dependent protein kinase in failing and nonfailing human hearts. Cardiovasc Res 42:254–261

Kiyosue T, Arita M (1989) Late sodium current and its contribution to action potential configuration in guinea pig ventricular myocytes. Circ Res 64:389–397

Kohlhardt M, Fichtner H, Frobe U (1989) Metabolites of the glycolytic pathway modulate the activity of single cardiac Na^+ channels. FASEB J 3:1963–1967

Kort AA, Lakatta EG, Marban E, Stern MD, Wier WG (1985) Fluctuations in intracellular calcium concentration and their effect on tonic tension in canine cardiac Purkinje fibres. J Physiol (London) 367:291–308

Le Grand B, Talmant JM, Rieu JP, Patoiseau JF, Colpaert FC, John GW (1995) Investigation of the mechanism by which ketanserin prolongs the duration of the cardiac action potential. J Cardiovasc Pharmacol 26:803–809

Li Z, Ai T, Samani K, Xi Y, Tzeng HP, Xie M, Wu S, Ge S, Taylor MD, Dong JW, Cheng J, Ackerman MJ, Kimura A, Sinagra G, Brunelli L, Faulkner G, Vatta M (2010) A ZASP missense mutation, S196L, leads to cytoskeletal and electrical abnormalities in a mouse model of cardiomyopathy. Circ Arrhythm Electrophysiol 3:646–656

Lipkind GM, Fozzard HA (2005) Molecular modeling of local anesthetic drug binding by voltage-gated sodium channels. Mol Pharmacol 68:1611–1622

Liu Y, DeFelice LJ, Mazzanti M (1992) Na channels that remain open throughout the cardiac action potential plateau. Biophys J 63:654–662

Liu H, Atkins J, Kass RS (2003) Common molecular determinants of flecainide and lidocaine block of heart Na + channels: evidence from experiments with neutral and quaternary flecainide analogues. J Gen Physiol 121:199–214

Liu X, Williams JB, Sumpter BR, Bevensee MO (2007) Inhibition of the Na/bicarbonate cotransporter NBCe1-A by diBAC oxonol dyes relative to niflumic acid and a stilbene. J Membr Biol 215:195–204

Lopez-Santiago LF, Meadows LS, Ernst SJ, Chen C, Malhotra JD, McEwen DP, Speelman A, Noebels JL, Maier SK, Lopatin AN, Isom LL (2007) Sodium channel *Scn1b* null mice exhibit prolonged QT and RR intervals. J Mol Cell Cardiol 43:636–647

Lu HR, De CF (1993) R 56 865, a Na+/Ca(2+)-overload inhibitor, protects against aconitine-induced cardiac arrhythmias in vivo. J Cardiovasc Pharmacol 22:120–125

Ma J, Luo A, Wu L, Wan W, Zhang P, Ren Z, Zhang S, Qian C, Shryock JC, Belardinelli L (2012) Calmodulin kinase II and protein kinase C mediate the effect of increased intracellular calcium to augment late sodium current in rabbit ventricular myocytes. Am J Physiol Cell Physiol 302: C1141–C1151

Maier LS (2009) A novel mechanism for the treatment of angina, arrhythmias, and diastolic dysfunction: inhibition of late I_{Na} using ranolazine. J Cardiovasc Pharmacol 54:279–286

Maier LS, Zhang T, Chen L, DeSantiago J, Brown JH, Bers DM (2003) Transgenic CaMKIIdeltaC overexpression uniquely alters cardiac myocyte Ca2+ handling: reduced SR Ca2+ load and activated SR Ca2+ release. Circ Res 92:904–911

Maier SK, Westenbroek RE, McCormick KA, Curtis R, Scheuer T, Catterall WA (2004) Distinct subcellular localization of different sodium channel a and b subunits in single ventricular myocytes from mouse heart. Circulation 109:1421–1427

Makielski JC, Farley AL (2006) Na(+) current in human ventricle: implications for sodium loading and homeostasis. J Cardiovasc Electrophysiol 17(Suppl 1):S15–S20

Makita N, Horie M, Nakamura T, Ai T, Sasaki K, Yokoi H, Sakurai M, Sakuma I, Otani H, Sawa H, Kitabatake A (2002) Drug-induced long-QT syndrome associated with a subclinical SCN5A mutation. Circulation 106:1269–1274

Makita N, Behr E, Shimizu W, Horie M, Sunami A, Crotti L, Schulze-Bahr E, Fukuhara S, Mochizuki N, Makiyama T, Itoh H, Christiansen M, McKeown P, Miyamoto K, Kamakura S, Tsutsui H, Schwartz PJ, George AL Jr, Roden DM (2008) The E1784K mutation in SCN5A is associated with mixed clinical phenotype of type 3 long QT syndrome. J Clin Invest 118:2219–2229

Maltsev VA, Undrovinas AI (2006) A multi-modal composition of the late Na+ current in human ventricular cardiomyocytes. Cardiovasc Res 69:116–127

Maltsev VA, Sabbah HN, Higgins RS, Silverman N, Lesch M, Undrovinas AI (1998) Novel, ultraslow inactivating sodium current in human ventricular cardiomyocytes. Circulation 98:2545–2552

Maltsev VA, Sabbah HN, Undrovinas AI (2001) Late sodium current is a novel target for amiodarone: studies in failing human myocardium. J Mol Cell Cardiol 33:923–932

Maltsev VA, Silverman N, Sabbah HN, Undrovinas AI (2007) Chronic heart failure slows late sodium current in human and canine ventricular myocytes: implications for repolarization variability. Eur J Heart Fail 9:219–227

Maltsev VA, Reznikov V, Undrovinas NA, Sabbah HN, Undrovinas A (2008) Modulation of late sodium current by Ca^{2+}, calmodulin, and CaMKII in normal and failing dog cardiomyocytes: similarities and differences. Am J Physiol Heart Circ Physiol 294:H1597–H1608

Maltsev VA, Kyle JW, Undrovinas A (2009) Late Na^+ current produced by human cardiac Na^+ channel isoform $Na_v1.5$ is modulated by its b_1 subunit. J Physiol Sci 59:217–225

Marban E, Robinson SW, Wier WG (1986) Mechanism of arrhythmogenic delayed and early afterdepolarizations in ferret muscle. J Clin Invest 78:1185–1192

Mary-Rabine L, Hordof AJ, Danilo P, Malm JR, Rosen MR (1980) Mechanisms for impulse initiation in isolated human atrial fibers. Circ Res 47:267–277

Mazzone A, Strege PR, Tester DJ, Bernard CE, Faulkner G, Degiorgio R, Makielski JC, Stanghellini V, Gibbons SJ, Ackerman MJ, Farrugia G (2008) A mutation in telethonin alters $Na_v1.5$ function. J Biol Chem 283:16537–16544

McNair WP, Ku L, Taylor MR, Fain PR, Dao D, Wolfel E, Mestroni L (2004) SCN5A mutation associated with dilated cardiomyopathy, conduction disorder, and arrhythmia1. Circulation 110:2163–2167

Meadows LS, Isom LL (2005) Sodium channels as macromolecular complexes: implications for inherited arrhythmia syndromes. Cardiovasc Res 67:448–458

Medeiros-Domingo A, Kaku T, Tester DJ, Iturralde-Torres P, Itty A, Ye B, Valdivia C, Ueda K, Canizales-Quinteros S, Tusie-Luna MT, Makielski JC, Ackerman MJ (2007) *SCN4B*-encoded sodium channel b4 subunit in congenital long-QT syndrome. Circulation 116:134–142

Mike A, Lukacs P (2010) The enigmatic drug binding site for sodium channel inhibitors. Curr Mol Pharmacol 3:129–144

Milberg P, Reinsch N, Wasmer K, Monnig G, Stypmann J, Osada N, Breithardt G, Haverkamp W, Eckardt L (2005) Transmural dispersion of repolarization as a key factor of arrhythmogenicity in a novel intact heart model of LQT3. Cardiovasc Res 65:397–404

Mines GR (1914) On circulating excitations in heart muscles and their possible relation to tachycardia and fibrillation. Trans R Soc Can 8:43–52

Mohler PJ, Splawski I, Napolitano C, Bottelli G, Sharpe L, Timothy K, Priori SG, Keating MT, Bennett V (2004) A cardiac arrhythmia syndrome caused by loss of ankyrin-B function. Proc Natl Acad Sci U S A 10:9137–9142

Moreno JD, Clancy CE (2012) Pathophysiology of the cardiac late Na current and its potential as a drug target. J Mol Cell Cardiol 52:608–619

Morrow DA (2007) MERLIN-TIMI-36 (Metabolic Efficiency with Ranolazine for Less Ischemia in NSTE ACS). Clin Cardiol 30:418–419

Moss AJ, Zareba W, Schwarz KQ, Rosero S, McNitt S, Robinson JL (2008) Ranolazine shortens repolarization in patients with sustained inward sodium current due to type-3 long-QT syndrome. J Cardiovasc Electrophysiol 19:1289–1293

Murray KT, Hu NN, Daw JR, Shin HG, Watson MT, Mashburn AB, George AL Jr (1997) Functional effects of protein kinase C activation on the human cardiac Na^+ channel. Circ Res 80:370–376

Narahashi T (2008) Tetrodotoxin: a brief history. Proc Jpn Acad Ser B Phys Biol Sci 84:147–154

Neef S, Dybkova N, Sossalla S, Ort KR, Fluschnik N, Neumann K, Seipelt R, Schondube FA, Hasenfuss G, Maier LS (2010) CaMKII-dependent diastolic SR Ca2+ leak and elevated diastolic Ca2+ levels in right atrial myocardium of patients with atrial fibrillation. Circ Res 106:1134–1144

Nesterenko VV, Zygmunt AC, Rajamani S, Belardinelli L, Antzelevitch C (2011) Mechanisms of atrial-selective block of Na + channels by ranolazine: II. Insights from a mathematical model. Am J Physiol Heart Circ Physiol 301:H1615–H1624

Noble D, Noble PJ (2006) Late sodium current in the pathophysiology of cardiovascular disease: consequences of sodium-calcium overload. Heart 92(Suppl 4):iv1–iv5

Nof E, Burashnikov A, Antzelevitch C (2010) Cellular basis for atrial fibrillation in an experimental model of short QT1: implications for a pharmacological approach to therapy. Heart Rhythm 7:251–257

Orth PM, Hesketh JC, Mak CK, Yang Y, Lin S, Beatch GN, Ezrin AM, Fedida D (2006) RSD1235 blocks late I(Na) and suppresses early afterdepolarizations and torsades de pointes induced by class III agents. Cardiovasc Res 70:486–496

Patel C, Antzelevitch C (2008a) Pharmacological approach to the treatment of long and short QT syndromes. Pharmacol Ther 118:138–151

Patel C, Antzelevitch C (2008b) Cellular basis for arrhythmogenesis in an experimental model of the SQT1 form of the short QT syndrome. Heart Rhythm 5:585–590

Patlak JB, Ortiz M (1985) Slow currents through single sodium channels of the adult rat heart. J Gen Physiol 86:89–104

Petitprez S, Zmoos AF, Ogrodnik J, Balse E, Raad N, El-Haou S, Albesa M, Bittihn P, Luther S, Lehnart SE, Hatem SN, Coulombe A, Abriel H (2011) SAP97 and dystrophin macromolecular complexes determine two pools of cardiac sodium channels Nav1.5 in cardiomyocytes. Circ Res 108:294–304

Pignier C, Rougier JS, Vie B, Culie C, Verscheure Y, Vacher B, Abriel H, Le GB (2010) Selective inhibition of persistent sodium current by F 15845 prevents ischaemia-induced arrhythmias. Br J Pharmacol 161:79–91

Pinet C, Algalarrondo V, Sablayrolles S, Le GB, Pignier C, Cussac D, Perez M, Hatem SN, Coulombe A (2008) Protease-activated receptor-1 mediates thrombin-induced persistent sodium current in human cardiomyocytes. Mol Pharmacol 73:1622–1631

Remme CA, Verkerk AO, Nuyens D, Van Ginneken AC, Belterman CN, Wilders R, van Roon MA, Tan HL, Wilde AA, Carmeliet P, de Bakker JM, Veldkamp MW, Bezzina CR (2006) Overlap syndrome of cardiac sodium channel disease in mice carrying the equivalent mutation of human SCN5A-1795insD. Circulation 114:2584–2594

Restivo M, Caref EB, Kozhevnikov DO, El-Sherif N (2004) Spatial dispersion of repolarization is a key factor in the arrhythmogenicity of long QT syndrome. J Cardiovasc Electrophysiol 15:323–331

Rivolta I, Abriel H, Tateyama M, Liu H, Memmi M, Vardas P, Napolitano C, Priori SG, Kass RS (2001) Inherited Brugada and LQT-3 syndrome mutations of a single residue of the cardiac sodium channel confer distinct channel and clinical phenotypes. J Biol Chem 276:30623–30630

Rodriguez P, Bhogal MS, Colyer J (2003) Stoichiometric phosphorylation of cardiac ryanodine receptor on serine 2809 by calmodulin-dependent kinase II and protein kinase A. J Biol Chem 278:38593–38600

Rook MB, Evers MM, Vos MA, Bierhuizen MF (2012) Biology of cardiac sodium channel Nav1.5 expression. Cardiovasc Res 93:12–23

Rosen MR, Danilo P Jr (1980) Effects of tetrodotoxin, lidocaine, verapamil and AHR-266 on ouabain induced delayed afterdepolarizations in canine Purkinje fibers. Circ Res 46:117–124

Rota M, Vassalle M (2003) Patch-clamp analysis in canine cardiac Purkinje cells of a novel sodium component in the pacemaker range. J Physiol 548:147–165

Ruan Y, Liu N, Priori SG (2009) Sodium channel mutations and arrhythmias. Nat Rev Cardiol 6:337–348

Sag CM, Wadsack DP, Khabbazzadeh S, Abesser M, Grefe C, Neumann K, Opiela MK, Backs J, Olson EN, Brown JH, Neef S, Maier SK, Maier LS (2009) Calcium/calmodulin-dependent protein kinase II contributes to cardiac arrhythmogenesis in heart failure. Circ Heart Fail 2: 664–675

Saint DA (2006) The role of the persistent Na(+) current during cardiac ischemia and hypoxia. J Cardiovasc Electrophysiol 17(Suppl 1):S96–S103
Saint DA (2008) The cardiac persistent sodium current: an appealing therapeutic target? Br J Pharmacol 153:1133–1142
Saint DA, Ju YK, Gage PW (1992) A persistent sodium current in rat ventricular myocytes. J Physiol (London) 453:219–231
Sakmann B, Spindler AJ, Bryant SM, Linz KW, Noble D (2000) Distribution of a persistent sodium current across the ventricular wall in guinea-pigs. Circ Res 87:910–914
Sarhan MF, Van PF, Ahern CA (2009) A double tyrosine motif in the cardiac sodium channel domain III-IV linker couples calcium-dependent calmodulin binding to inactivation gating. J Biol Chem 284:33265–33274
Sawanobori T, Hirano Y, Hiraoka M (1987) Aconitine-induced delayed afterdepolarization in frog atrium and guinea pig papillary muscles in the presence of low concentrations of Ca2+. Jpn J Physiol 37:59–79
Scherer D, von Lowenstern K, Zitron E, Scholz EP, Bloehs R, Kathofer S, Thomas D, Bauer A, Katus HA, Karle CA, Kiesecker C (2008) Inhibition of cardiac hERG potassium channels by tetracyclic antidepressant mianserin. Naunyn Schmiedebergs Arch Pharmacol 378:73–83
Scherf D, Romano FJ, Terranova R (1948) Experimental studies on auricular flutter and auricular fibrillation. Am Heart J 36:241–251
Schlotthauer K, Bers DM (2000) Sarcoplasmic reticulum Ca(2+) release causes myocyte depolarization. Underlying mechanism and threshold for triggered action potentials. Circ Res 87:774–780
Schreibmayer W, Lindner W (1992) Stereoselective interactions of (R)- and (S)-propafenone with the cardiac sodium channel. J Cardiovasc Pharmacol 20:324–331
Scirica BM, Morrow DA, Hod H, Murphy SA, Belardinelli L, Hedgepeth CM, Molhoek P, Verheugt FW, Gersh BJ, McCabe CH, Braunwald E (2007) Effect of ranolazine, an antianginal agent with novel electrophysiological properties, on the incidence of arrhythmias in patients with non ST-segment elevation acute coronary syndrome: results from the metabolic efficiency with ranolazine for less ischemia in non ST-elevation ACUTE CORONARY syndrome thrombolysis in myocardial infarction 36 (MERLIN-TIMI 36) randomized controlled trial. Circulation 116:1647–1652
Shao D, Okuse K, Djamgoz MB (2009) Protein-protein interactions involving voltage-gated sodium channels: post-translational regulation, intracellular trafficking and functional expression. Int J Biochem Cell Biol 41:1471–1481
Shattock MJ, Bers DM (1989) Rat vs. rabbit ventricle: Ca flux and intracellular Na assessed by ion-selective microelectrodes. Am J Physiol 256:C813–C822
Sheu SS, Lederer WJ (1985) Lidocaine's negative inotropic and antiarrhythmic actions: dependence on shortening of action potential duration and reduction of intracellular sodium activity. Circ Res 57:578–590
Shimizu W, Antzelevitch C (1997a) Sodium channel block with mexiletine is effective in reducing dispersion of repolarization and preventing torsade de pointes in LQT2 as well as LQT3 models of the long QT syndrome. Pacing Clin Electrophysiol 20:1234, Abstract
Shimizu W, Antzelevitch C (1997b) Sodium channel block with mexiletine is effective in reducing dispersion of repolarization and preventing torsade de pointes in LQT2 and LQT3 models of the long-QT syndrome. Circulation 96:2038–2047
Shimizu W, Antzelevitch C (1998) Cellular basis for the ECG features of the LQT1 form of the long QT syndrome: effects of b-adrenergic agonists and antagonists and sodium channel blockers on transmural dispersion of repolarization and torsade de pointes. Circulation 98: 2314–2322
Shimizu W, Antzelevitch C (1999a) Spontaneous and stimulation-induced Torsade de Pointes in LQT1, LQT2 and LQT3 models of the long QT syndrome. Circulation 100(II):359, Abstract
Shimizu W, Antzelevitch C (1999b) Cellular basis for long QT, transmural dispersion of repolarization, and Torsade de Pointes in the long QT syndrome. J Electrocardiol 32(Suppl):177–184

Shryock JC, Song Y, Rajamani S, Antzelevitch C, Belardinelli L (2013) The arrhythmogenic consequences of increasing late INa in the cardiomyocyte. Cardiovasc Res 99:600–611

Sicouri S, Fish J, Antzelevitch C (1994) Distribution of M cells in the canine ventricle. J Cardiovasc Electrophysiol 5:824–837

Sicouri S, Quist M, Antzelevitch C (1996) Evidence for the presence of M cells in the guinea pig ventricle. J Cardiovasc Electrophysiol 7:503–511

Sicouri S, Antzelevitch D, Heilmann C, Antzelevitch C (1997a) Effects of sodium channel block with mexiletine to reverse action potential prolongation in in vitro models of the long QT syndrome. J Cardiovasc Electrophysiol 8:1280–1290

Sicouri S, Moro S, Litovsky SH, Elizari MV, Antzelevitch C (1997b) Chronic amiodarone reduces transmural dispersion of repolarization in the canine heart. J Cardiovasc Electrophysiol 8: 1269–1279

Sicouri S, Glass A, Ferreiro M, Antzelevitch C (2010) Transseptal dispersion of repolarization and its role in the development of torsade de pointes arrhythmias. J Cardiovasc Electrophysiol 21: 441–447

Sicouri S, Blazek J, Belardinelli L, Antzelevitch C (2012a) Electrophysiological characteristics of canine superior vena cava sleeve preparations. Effect of ranolazine. Circ Arrhythm Electrophysiol 5:371–379

Sicouri S, Pourrier M, Gibson JK, Lynch JJ, Antzelevitch C (2012b) Comparison of electrophysiological and antiarrhythmic effects of vernakalant, ranolazine, and sotalol in canine pulmonary vein sleeve preparations. Heart Rhythm 9:422–429

Sicouri S, Blazek J, Belardinelli L, Antzelevitch C (2012c) Antiarrhythmic effects of the highly-selective late sodium channel current blocker GS 458967 in canine Purkinje fibers and pulmonary vein sleeve preparations. Heart Rhythm 9:S186, Abstract

Sicouri S, Belardinelli L, Antzelevitch C (2013) Antiarrhythmic effects of the highly-selective late sodium channel current blocker GS-458967. Heart Rhythm 10(7):1036–1043

Sidorov VY, Uzelac I, Wikswo JP (2011) Regional increase of extracellular potassium leads to electrical instability and reentry occurrence through the spatial heterogeneity of APD restitution. Am J Physiol Heart Circ Physiol 301:H209–H220

Song JH, Huang CS, Nagata K, Yeh JZ, Narahashi T (1997) Differential action of riluzole on tetrodotoxin-sensitive and tetrodotoxin-resistant sodium channels. J Pharmacol Exp Ther 282: 707–714

Song Y, Shryock JC, Wu L, Belardinelli L (2004) Antagonism by ranolazine of the pro-arrhythmic effects of increasing late INa in guinea pig ventricular myocytes. J Cardiovasc Pharmacol 44:192–199

Song Y, Shryock J, Wagner S, Maier LS, Belardinelli L (2006) Blocking late sodium current reduces hydrogen peroxide-induced arrhythmogenic activity and contractile dysfunction. J Pharmacol Exp Ther 318:214–222

Song Y, Shryock JC, Belardinelli L (2008) An increase of late sodium current induces delayed afterdepolarizations and sustained triggered activity in atrial myocytes. Am J Physiol Heart Circ Physiol 294:H2031–H2039

Song Y, Shryock JC, Belardinelli L (2009) A slowly inactivating sodium current contributes to spontaneous diastolic depolarization of atrial myocytes. Am J Physiol Heart Circ Physiol 297: H1254–H1262

Sossalla S, Wagner S, Rasenack EC, Ruff H, Weber SL, Schondube FA, Tirilomis T, Tenderich G, Hasenfuss G, Belardinelli L, Maier LS (2008) Ranolazine improves diastolic dysfunction in isolated myocardium from failing human hearts–role of late sodium current and intracellular ion accumulation. J Mol Cell Cardiol 45:32–43

Sossalla S, Kallmeyer B, Wagner S, Mazur M, Maurer U, Toischer K, Schmitto JD, Seipelt R, Schondube FA, Hasenfuss G, Belardinelli L, Maier LS (2010) Altered Na^+ currents in atrial fibrillation: effects of ranolazine on arrhythmias and contractility in human atrial myocardium. J Am Coll Cardiol 55:2330–2342

Sossalla S, Maurer U, Schotola H, Hartmann N, Didie M, Zimmermann WH, Jacobshagen C, Wagner S, Maier LS (2011) Diastolic dysfunction and arrhythmias caused by overexpression of CaMKIIdelta(C) can be reversed by inhibition of late Na(+) current. Basic Res Cardiol 106: 263–272

Spencer CI, Sham JS (2005) Mechanisms underlying the effects of the pyrethroid, tefluthrin, on action potential duration in isolated rat ventricular myocytes 1. J Pharmacol Exp Ther 315:16–23

Splawski I, Timothy KW, Tateyama M, Clancy CE, Malhotra A, Beggs AH, Cappuccio FP, Sagnella GA, Kass RS, Keating MT (2002) Variant of SCN5A sodium channel implicated in risk of cardiac arrhythmia. Science 297:1333–1336

Starmer CF, Nesterenko VV, Undrovinas AI, Grant AO, Rosenshtraukh LV (1991) Lidocaine blockade of continuously and transiently accessible sites in cardiac sodium channels. J Mol Cell Cardiol 23(Suppl I):73–83

Stern MD, Capogrossi MC, Lakatta EG (1988) Spontaneous calcium release from the sarcoplasmic reticulum in myocardial cells: mechanisms and consequences. Cell Calcium 9:247–256

Sunami A, Fan Z, Sawanobori T, Hiraoka M (1993) Use-dependent block of Na + currents by mexiletine at the single channel level in guinea-pig ventricular myocytes. Br J Pharmacol 110:183–192

Tamareille S, Le GB, John GW, Feuvray D, Coulombe A (2002) Anti-ischemic compound KC 12291 prevents diastolic contracture in isolated atria by blockade of voltage-gated sodium channels. J Cardiovasc Pharmacol 40:346–355

Tan BH, Pundi KN, Van Norstrand DW, Valdivia CR, Tester DJ, Medeiros-Domingo A, Makielski JC, Ackerman MJ (2010) Sudden infant death syndrome–associated mutations in the sodium channel beta subunits. Heart Rhythm 7:771–778

Tang L, Joung B, Ogawa M, Chen PS, Lin SF (2012) Intracellular calcium dynamics, shortened action potential duration, and late-phase 3 early after depolarization in langendorff-perfused rabbit ventricles. J Cardiovasc Electrophysiol 23:1364–1371

Trautwein W, Kassebaum DG, Nelson RM, HECHTHH (1962) Electrophysiological study of human heart muscle. Circ Res 10:306–312

Tsuchida K, Otomo S (1990) Electrophysiological effects of Monensin, a sodium ionophore, on cardiac Purkinje fibers. Eur J Pharm 190:313–320

Tweedie D, Harding SE, MacLeod KT (2000) Sarcoplasmic reticulum Ca content, sarcolemmal Ca influx and the genesis of arrhythmias in isolated guinea-pig cardiomyocytes. J Mol Cell Cardiol 32:261–272

Ueda N, Zipes DP, Wu J (2004) Prior ischemia enhances arrhythmogenicity in isolated canine ventricular wedge model of long QT 3. Cardiovasc Res 63:69–76

Ueda K, Valdivia C, Medeiros-Domingo A, Tester DJ, Vatta M, Farrugia G, Ackerman MJ, Makielski JC (2008) Syntrophin mutation associated with long QT syndrome through activation of the nNOS-SCN5A macromolecular complex. Proc Natl Acad Sci U S A 105:9355–9360

Undrovinas A, Maltsev VA (2008a) Late sodium current is a new therapeutic target to improve contractility and rhythm in failing heart. Cardiovasc Hematol Agents Med Chem 6:348–359

Undrovinas A, Maltsev VA (2008b) Late sodium current is a new therapeutic target to improve contractility and rhythm in failing heart. Cardiovasc Hematol Agents Med Chem 6:348–359

Undrovinas AI, Fleidervish IA, Makielski JC (1992) Inward sodium current at resting potentials in single cardiac myocytes induced by the ischemic metabolite lysophosphatidylcholine. Circ Res 71:1231–1241

Undrovinas AI, Maltsev VA, Sabbah HN (1999) Repolarization abnormalities in cardiomyocytes of dogs with chronic heart failure: role of sustained inward current. Cell Mol Life Sci 55:494–505

Undrovinas AI, Maltsev VA, Kyle JW, Silverman N, Sabbah HN (2002) Gating of the late Na+ channel in normal and failing human myocardium. J Mol Cell Cardiol 34:1477–1489

Undrovinas AI, Undrovinas NA, Belardinelli L, Sabbah HN (2004) Ranolazine inhibits late sodium current in isolated left ventricular myocytes of dogs with heart failure. J Am Coll Cardiol 43 (supplA):178A, Abstract

Undrovinas AI, Belardinelli L, Undrovinas NA, Sabbah HN (2006) Ranolazine improves abnormal repolarization and contraction in left ventricular myocytes of dogs with heart failure by inhibiting late sodium current. J Cardiovasc Electrophysiol 17:S161–S177

Undrovinas NA, Maltsev VA, Belardinelli L, Sabbah HN, Undrovinas A (2010) Late sodium current contributes to diastolic cell Ca2+ accumulation in chronic heart failure. J Physiol Sci 60:245–257

Vacher B, Pignier C, Letienne R, Verscheure Y, Le GB (2009) F 15845 inhibits persistent sodium current in the heart and prevents angina in animal models. Br J Pharmacol 156:214–225

Valdivia CR, Chu WW, Pu J, Foell JD, Haworth RA, Wolff MR, Kamp TJ, Makielski JC (2005) Increased late sodium current in myocytes from a canine heart failure model and from failing human heart. J Mol Cell Cardiol 38:475–483

Vatta M, Faulkner G (2006) Cytoskeletal basis of ion channel function in cardiac muscle. Future Cardiol 2:467–476

Vatta M, Ackerman MJ, Ye B, Makielski JC, Ughanze EE, Taylor EW, Tester DJ, Balijepalli RC, Foell JD, Li Z, Kamp TJ, Towbin JA (2006) Mutant caveolin-3 induces persistent late sodium current and is associated with long-QT syndrome. Circulation 114:2104–2112

Verdonck F, Bielen FV, Ver DL (1991) Preferential block of the veratridine-induced, non-inactivating Na + current by R56865 in single cardiac Purkinje cells. Eur J Pharmacol 203:371–378

Vermeulen JT, Tan HL, Rademaker H, Schumacher CA, Loh P, Opthof T, Coronel R, Janse MJ (1996) Electrophysiologic and extracellular ionic changes during acute ischemia in failing and normal rabbit myocardium. J Mol Cell Cardiol 28:123–131

Vollmer B, Meuter C, Janssen PA (1987) R 56865 prevents electrical and mechanical signs of ouabain intoxication in guinea-pig papillary muscle. Eur J Pharmacol 142:137–140

Wagner S, Dybkova N, Rasenack EC, Jacobshagen C, Fabritz L, Kirchhof P, Maier SK, Zhang T, Hasenfuss G, Brown JH, Bers DM, Maier LS (2006) Ca2+/calmodulin-dependent protein kinase II regulates cardiac Na+ channels. J Clin Invest 116:3127–3138

Wagner S, Ruff HM, Weber SL, Bellmann S, Sowa T, Schulte T, Anderson ME, Grandi E, Bers DM, Backs J, Belardinelli L, Maier LS (2011) Reactive oxygen species-activated Ca/calmodulin kinase IIdelta is required for late I(Na) augmentation leading to cellular Na and Ca overload. Circ Res 108:555–565

Wang Q, Shen J, Li Z, Timothy KW, Vincent GM, Priori SG, Schwartz PJ, Keating MT (1995) Cardiac sodium channel mutations in patients with long QT syndrome, an inherited cardiac arrhythmia. Hum Mol Genet 4:1603–1607

Wang DW, Yazawa K, George AL Jr, Bennett PB (1996) Characterization of human cardiac Na^+ channel mutations in the congenital long QT syndrome. Proc Natl Acad Sci U S A 93:13200–13205

Wang DW, Crotti L, Shimizu W, Pedrazzini M, Ikeda T, Schwartz PJ, George AL (2008) Malignant perinatal variant of long-QT syndrome caused by a profoundly dysfunctional cardiac sodium channel. Circ Arrhythm Electrophysiol 1:370–378

Wang DW, Mistry AM, Kahlig KM, Kearney JA, Xiang J, George AL Jr (2010) Propranolol blocks cardiac and neuronal voltage-gated sodium channels. Front Pharmacol 1:144

Ward CA, Giles WR (1997) Ionic mechanism of the effects of hydrogen peroxide in rat ventricular myocytes. J Physiol 500(Pt 3):631–642

Ward CA, Bazzazi H, Clark RB, Nygren A, Giles WR (2006) Actions of emigrated neutrophils on Na(+) and K(+) currents in rat ventricular myocytes. Prog Biophys Mol Biol 90:249–269

Weiss S, Benoist D, White E, Teng W, Saint DA (2010) Riluzole protects against cardiac ischaemia and reperfusion damage via block of the persistent sodium current. Br J Pharmacol 160:1072–1082

West JW, Patton DE, Scheuer T (1992) A cluster of hydrophobic amino acid residues required for fast Na^+ channel inactivation. Proc Natl Acad Sci U S A 89:10910–10914

Wilhelm D, Himmel H, Ravens U, Peters T (1991) Characterization of the interaction of R 56865 with cardiac Na- and L-type Ca channels. Br J Pharmacol 104:483–489

Wilson LD, Jeyaraj D, Wan X, Hoeker GS, Said TH, Gittinger M, Laurita KR, Rosenbaum DS (2009) Heart failure enhances susceptibility to arrhythmogenic cardiac alternans. Heart Rhythm 6:251–259

Wit AL, Cranefield PF (1977) Triggered and automatic activity in the canine coronary sinus. Circ Res 41:435–445

Wit AL, Rosen MR (1983) Pathophysiologic mechanisms of cardiac arrhythmias. Am Heart J 106: 798–811

Witchel HJ, Dempsey CE, Sessions RB, Perry M, Milnes JT, Hancox JC, Mitcheson JS (2004) The low-potency, voltage-dependent HERG blocker propafenone–molecular determinants and drug trapping. Mol Pharmacol 66:1201–1212

Wu J, Corr PB (1995) Palmitoylcarnitine increases [Na+]i and initiates transient inward current in adult ventricular myocytes. Am J Physiol 268:H2405–H2417

Wu L, Song Y, Shryock JC, Li Y, Antzelevitch C, Belardinelli L (2003) Ranolazine attenuates the prolongation of ventricular monophasic action potential and suppresses ventricular tachycardia caused by sea anemone toxin, ATX-II, in guinea pig isolated hearts. PACE 26:1023, Abstract

Wu L, Shryock JC, Song Y, Li Y, Antzelevitch C, Belardinelli L (2004) Antiarrhythmic effects of ranolazine in a guinea pig in vitro model of long-QT syndrome. J Pharmacol Exp Ther 310:599–605

Wu L, Shryock JC, Song Y, Belardinelli L (2006) An increase in late sodium current potentiates the proarrhythmic activities of low-risk QT-prolonging drugs in female rabbit hearts. J Pharmacol Exp Ther 316:718–726

Wu G, Ai T, Kim JJ, Mohapatra B, Xi Y, Li Z, Abbasi S, Purevjav E, Samani K, Ackerman MJ, Qi M, Moss AJ, Shimizu W, Towbin JA, Cheng J, Vatta M (2008a) a-1-syntrophin mutation and the long-QT syndrome: a disease of sodium channel disruption. Circ Arrhythm Electrophysiol 1:193–201

Wu L, Guo D, Li H, Hackett J, Yan GX, Jiao Z, Antzelevitch C, Shryock JC, Belardinelli L (2008b) Role of late sodium current in modulating the proarrhythmic and antiarrhythmic effects of quinidine. Heart Rhythm 5:1726–1734

Wu L, Rajamani S, Shryock JC, Li H, Ruskin J, Antzelevitch C, Belardinelli L (2008c) Augmentation of late sodium current unmasks the proarrhythmic effects of amiodarone. Cardiovasc Res 77:481–488

Wu Y, Song Y, Belardinelli L, Shryock JC (2009a) The late Na^+ current (I_{Na}) inhibitor ranolazine attenuates effects of Palmitoyl-L-Carnitine to increase late I_{Na} and cause ventricular diastolic dysfunction. J Pharmacol Exp Ther 330:550–557

Wu L, Rajamani S, Li H, January CT, Shryock JC, Belardinelli L (2009b) Reduction of repolarization researve unmasks the pro-arrhythmic role of endogenous late sodium current in the heart. Am J Physiol Heart Circ Physiol 297:H1048–H1057

Wu L, Ma J, Li H, Wang C, Grandi E, Zhang P, Luo A, Bers DM, Shryock JC, Belardinelli L (2011) Late sodium current contributes to the reverse rate-dependent effect of IKr inhibition on ventricular repolarization. Circulation 123:1713–1720

Xiao XH, Allen DG (1999) Role of Na(+)/H(+) exchanger during ischemia and preconditioning in the isolated rat heart. Circ Res 85:723–730

Xie LH, Chen F, Karagueuzian HS, Weiss JN (2009) Oxidative-stress-induced after depolarizations and calmodulin kinase II signaling. Circ Res 104:79–86

Yan GX, Wu Y, Liu T, Wang J, Marinchak RA, Kowey PR (2001) Phase 2 early afterdepolarization as a trigger of polymorphic ventricular tachycardia in acquired long-qt syndrome: direct evidence from intracellular recordings in the intact left ventricular wall. Circulation 103:2851–2856

Yao L, Fan P, Jiang Z, Viatchenko-Karpinski S, Wu Y, Kornyeyev D, Hirakawa R, Budas GR, Rajamani S, Shryock JC, Belardinelli L (2011) Nav1.5-dependent persistent Na+ influx

activates CaMKII in rat ventricular myocytes and N1325S mice. Am J Physiol Cell Physiol 301:C577–C586

Yatani A, Akaike N (1985) Blockage of the sodium current in isolated single cells from rat ventricle with mexiletine and disopyramide. J Mol Cell Cardiol 17:467–476

Zaza A, Belardinelli L, Shryock JC (2008) Pathophysiology and pharmacology of the cardiac "late sodium current". Pharmacol Ther 119:326–339

Zeiler RH, Gough WB, El-Sherif N (1984) Electrophysiologic effects of propafenone on canine ischemic cardiac cells. Am J Cardiol 54:424–429

Zellerhoff S, Pistulli R, Monnig G, Hinterseer M, Beckmann BM, Kobe J, Steinbeck G, Kaab S, Haverkamp W, Fabritz L, Gradaus R, Breithardt G, Schulze-Bahr E, Bocker D, Kirchhof P (2009) Atrial arrhythmias in long-QT syndrome under daily life conditions: a nested case control study. J Cardiovasc Electrophysiol 20:401–407

Zhang T, Kohlhaas M, Backs J, Mishra S, Phillips W, Dybkova N, Chang S, Ling H, Bers DM, Maier LS, Olson EN, Brown JH (2007) CaMKIIdelta isoforms differentially affect calcium handling but similarly regulate HDAC/MEF2 transcriptional responses. J Biol Chem 282: 35078–35087

Zhang XQ, Yamada S, Barry WH (2008) Ranolazine inhibits an oxidative stress-induced increase in myocyte sodium and calcium loading during simulated-demand ischemia. J Cardiovasc Pharmacol 51:443–449

Zhang T, Yong SL, Drinko JK, Popovic ZB, Shryock JC, Belardinelli L, Wang QK (2011) LQTS mutation N1325S in cardiac sodium channel gene SCN5A causes cardiomyocyte apoptosis, cardiac fibrosis and contractile dysfunction in mice. Int J Cardiol 147:239–245

Zhao G, Walsh E, Shryock JC, Messina E, Wu Y, Zeng D, Xu X, Ochoa M, Baker SP, Hintze TH, Belardinelli L (2011) Antiadrenergic and hemodynamic effects of ranolazine in conscious dogs. J Cardiovasc Pharmacol 57:639–647

Zicha S, Maltsev VA, Nattel S, Sabbah HN, Undrovinas AI (2004) Post-transcriptional alterations in the expression of cardiac Na+ channel subunits in chronic heart failure1. J Mol Cell Cardiol 37:91–100

Zimmer T, Surber R (2008) *SCN5A* channelopathies - an update on mutations and mechanisms. Prog Biophys Mol Biol 98:120–136

Zygmunt AC, Eddlestone GT, Thomas GP, Nesterenko VV, Antzelevitch C (2001) Larger late sodium conductance in M cells contributes to electrical heterogeneity in canine ventricle. Am J Physiol 281:H689–H697

Zygmunt AC, Nesterenko VV, Rajamani S, Hu D, Barajas-Martinez H, Belardinelli L, Antzelevitch C (2011) Mechanisms of atrial-selective block of sodium channel by ranolazine I. Experimental analysis of the use-dependent block. Am J Physiol Heart Circ Physiol 301: H1606–H1614

Proton Modulation of Cardiac I_{Na}: A Potential Arrhythmogenic Trigger

David K. Jones and Peter C. Ruben

Contents

Abstract

Voltage-gated sodium (Na_V) channels generate the upstroke and mediate duration of the ventricular action potential, thus they play a critical role in mediating cardiac excitability. Cardiac ischemia triggers extracellular pH to drop as low as pH 6.0, within just 10 min of its onset. Heightened proton concentrations reduce sodium conductance and alter the gating parameters of the cardiac-specific voltage-gated sodium channel, $Na_V1.5$. Most notably, acidosis destabilizes fast inactivation, which plays a critical role in regulating action potential duration. The changes in $Na_V1.5$ channel gating contribute to cardiac dysfunction during ischemia that can cause syncope, cardiac arrhythmia, and even sudden cardiac death. Understanding Na_V channel modulation by protons is paramount to treatment and prevention of the deleterious effects of cardiac ischemia and other triggers of cardiac acidosis.

Keywords

Protons • pH • Acidosis • Ischemia • Gating current

D.K. Jones (✉)
University of Wisconsin-Madison, Madison, WI, USA
e-mail: djones9@wisc.edu

P.C. Ruben
Simon Fraser University, Burnaby, BC, Canada
e-mail: pruben@sfu.ca

P.C. Ruben (ed.), *Voltage Gated Sodium Channels*, Handbook of Experimental Pharmacology 221, DOI 10.1007/978-3-642-41588-3_8,

1 Introduction

It is widely known that voltage-gated sodium (Na_V) channel activity contributes to the onset and duration of the cardiac action potential through a delicate balance with voltage-gated potassium and calcium channels. Activation and opening of Na_V channels leads to membrane depolarization and Phase 0 of the ventricular action potential. Na_V channel fast inactivation as well as activation of the transient outward potassium current (I_{to}) contributes to Phase 1, the initial repolarization of the action potential. During Phases 2 and 3, late sodium current works in tandem with L-type calcium channels to slow repolarization by the rapid and slow delayed rectifier potassium currents (I_{Kr} and I_{Ks}, respectively), forming the action potential plateau. Lastly, slow inactivation and closed-state fast inactivation determine Na_V channel availability during Phase 4 and, thus, mediate overall membrane excitability. Mutations and/or extrinsic factors acting on the channel that impart defects in any of the Na_V channel's biophysical states can manifest as an abnormal action potential and prompt cardiac dysfunction. A causal relationship between several such abnormalities, such as modulation by protons, and the panoply of Na_V channel mutations have led to a greater understanding of the molecular underpinnings of cardiac arrhythmias as well as a deeper appreciation for the intricacies of Na_V channel function. Here we will review the fundamental connection between Na_V channel dysfunction and arrhythmia during acidosis.

2 I_{Na} in Ischemic Arrhythmia

Ischemic heart disease is the leading cause of death in the USA, accounting for >600,000 of deaths nationally in 2009 (Kochanek et al. 2009). During ischemia, arterial pH quickly decreases. This cardiac acidosis alters cardiac I_{Na} and initiates a series of events that can trigger arrhythmia, myocardial infarction, and sudden cardiac death (Yatani et al. 1984; Ju et al. 1996; Antzelevitch and Belardinelli 2006; Hale et al. 2008). Although several Na_V channel isoforms are expressed in cardiac tissue, $Na_V1.5$ is by far predominant and the most likely culprit behind altered cardiac I_{Na} during acidosis (Maier et al. 2002, 2004; Haufe et al. 2005a, b; Jones et al. 2011).

pH is a tightly regulated physiological parameter. Intracellular pH (pH_i) and extracellular pH (pH_o) are maintained at pH 7.2 and pH 7.4, respectively. Elevations in proton concentration resulting in a decrease of only pH 0.05 can alter protein function (Bountra and Vaughan-Jones 1989). Changes in pH_o and pH_i affect the cardiac action potential (Leem et al. 1999; Fry and Poole-Wilson 1981). A reduction in pH_i below pH 6.95 is considered beyond the physiologically permissive range, and protein function throughout the cardiomyocyte is altered, including changes to action potential morphology, Ca^{2+} handling, and contractile force generation (Bountra and Vaughan-Jones 1989; Leem et al. 1999).

Acidosis can be caused metabolically or through respiratory dysfunction. Respiratory acidosis is the result of inefficient gas exchange in the lungs leading to elevated pCO_2 in the blood. When pCO_2 becomes elevated, arterial CO_2 is converted to carbonic acid via the reaction:

$$CO_2 + H_2O \leftrightarrow HCO_3^- + H^+$$

This reaction, catalyzed by the enzyme carbonic anhydrase, results in reduced pH_o and pH_i within minutes. Metabolic acidosis occurs when the body produces an excess, or fails to extrude a normal production level, of natural metabolic acids, such as lactic acid (Fry and Poole-Wilson 1981). The most common cause of acidosis is ischemia, where arterial occlusion or collapse results in a decreased delivery of blood relative to demand. In cardiac ischemia, the mechanisms of metabolic and respiratory acidosis work in tandem to rapidly reduce the pH_o and pH_i. pH_o has been measured as low as 5.9 during ischemia (Gebert et al. 1971; Benzing et al. 1971; Carmeliet 1999). Independent of the etiology, altered protein function during and shortly following cardiac acidosis creates an unstable environment that often leads to arrhythmia, myocardial infarction, and even sudden cardiac death (Crampin et al. 2006).

The links between altered cardiac I_{Na}, cardiac arrhythmia, and myocardial infarction during ischemia are relatively well defined. During ischemia pH_i declines as intracellular O_2 and ATP stores are depleted and the cell switches to anaerobic metabolism. Decreased pO_2 and elevated pCO_2 begin to reduce pH_o. The reduced intracellular ATP reduces Na^+/K^+ ATPase activity, while the rise in intracellular protons increases Na^+/H^+ exchanger (NHE) activity. NHE function further elevates extracellular proton concentration while elevating $[Na^+]_i$. $[Na^+]_i$ rise is recognized as a precursor to arrhythmia during myocardial ischemia (Hale et al. 2008). Oxidative stress and reduced pH_o concomitantly augment late I_{Na} while reducing peak I_{Na} (Yatani et al. 1984; Ju et al. 1996; Jones et al. 2011, Murphy et al. 2011). The increased late I_{Na} further increases $[Na^+]_i$, delays repolarization, and increases the heterogeneity of repolarization, whereas reduced peak I_{Na} slows conduction velocity (Antzelevitch and Belardinelli 2006; Makielski and Farley 2006; Liu et al. 1992; Hale et al. 2008; Jones et al. 2013b). Delayed repolarization increases the likelihood of early after depolarization through re-excitation of L-type calcium currents, whereas slowed conduction velocity can generate reentrant loops between ischemic and non-ischemic tissue. Elevated $[Na^+]_i$ slows Na^+/Ca^{2+} exchanger into reverse mode leading to elevated $[Ca^{2+}]_i$. During prolonged ischemia elevated $[Na^+]_i$ eventually forces the Na^+/Ca^{2+} exchanger into reverse mode. As $[Ca^{2+}]_i$ rises, the cardiomyocyte undergoes calcium overload that can lead to arrhythmia as well as the release of cytochrome c (Mattson and Chan 2003), proteases (Clapham 2007; Loetscher et al. 2001), and dehydrogenases (McCormack et al. 1990) from the mitochondria that trigger apoptosis. Reperfusion exacerbates this process by increasing the outward driving force for protons through NHE (Nguyen-Thi et al. 1981). This sequence is summarized in Fig. 1.

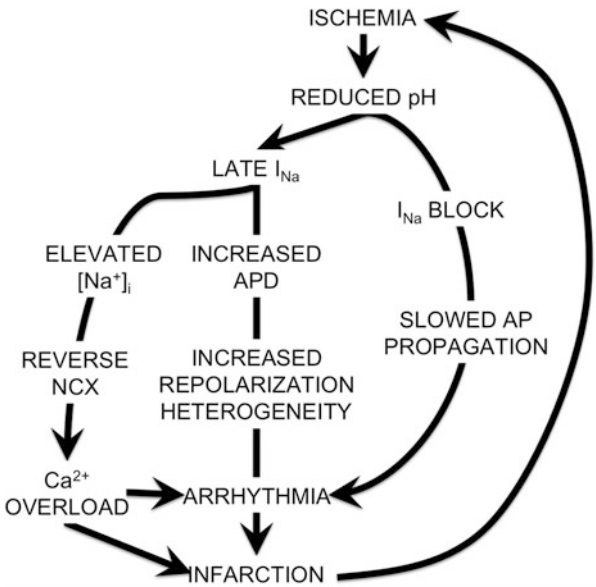

Fig. 1 I_{Na}, contributes to arrhythmia during ischemia. The schematic depicts the relationship between proton modulation of cardiac I_{Na}, arrhythmia, and myocardial infarction

3 Proton Modulation of $Na_V1.5$ Channels

Recordings from intact cardiomyocytes show a reduction in peak I_{Na}, a positive shift of the voltage dependence of activation and steady-state fast inactivation, as well as an increase in persistent I_{Na} in response to hypoxia (Zhang and Siegelbaum 1991; Yatani et al. 1984, Murphy et al. 2012; Saint 2006). $Na_V1.5$ channels, expressed in either HEK or *Xenopus* oocytes, accurately recapitulate proton modulation of cardiac I_{Na} when exposed to reduced pH_o (Khan et al. 2006; Jones et al. 2011, 2013b; Vilin et al. 2012). Heterologous expression systems have thus allowed in-depth study of the molecular aspects of I_{Na} proton modulation without the confounding effects of other ion channel proteins.

3.1 Proton Block

Extracellular protons inhibit sodium conductance in intact cardiomyocytes with a $pK_a \approx 5.5$ (Yatani et al. 1984; Zhang and Siegelbaum 1991). In oocyte systems extracellular acidosis reduces $Na_V1.5$ conductance with a $pK_a \approx$ pH 6.0 and complete block at $\approx$ pH 4.0 (Jones et al. 2011; Khan et al. 2006). The molecular mechanism of this proton block has been well studied. P-loop residues D372, E898, K1419, and A1710 (DEKA), compose the selectivity filter of $Na_V1.5$ channels, and along with a ring of carboxylate residues E375, E901, D1423, and D1714 (EEDD) mediate sodium permeation of $Na_V1.5$ channels (Terlau et al. 1991; Favre et al. 1996; Balser et al. 1996). These residues are conserved across all Na_V isoforms.

Khan et al. (2002) hypothesized that protonation of p-loop residues increases the electrostatic potential within the Na_V channel outer vestibule, thereby repelling Na^+ ions (Khan et al. 2002). Indeed, protonation of EEDD triggers proton block of the majority of Na_V channel isoforms (Khan et al. 2002, 2006; Jones et al. 2013b). C373 protonation blocks $Na_V1.5$ but not other Na_V channel isoforms (Khan et al. 2006; Jones et al. 2013b) and unlike $Na_V1.5$, not all Na_V channel isoforms are fully blocked by protons (Khan et al. 2002, 2006; Jones et al. 2013b). $Na_V1.4$, the skeletal isoform, displays a pH-insensitive current that is roughly ~14 % of maximum conductance (Khan et al. 2002). The homologous residue to C373 in $Na_V1.4$ channels is Y401. Replacement of Y401 with a cysteine abolishes the proton-insensitive current (Khan et al. 2006). Further, replacement of Y401 with a phenylalanine or a serine, the equivalent residues in $Na_V1.2$ and $Na_V1.8$, respectively, does not alter the pH-insensitive current suggesting that $Na_V1.2$ and $Na_V1.8$ would have a similar proton block asymptote as $Na_V1.4$ (Khan et al. 2006; Vilin et al.). In $Na_V1.5$, replacing C373 with a tyrosine, serine, or phenylalanine imparts a proton-insensitive current like that in $Na_V1.4$ (~12 %) (Khan et al. 2006; Jones et al. 2013b). A sixth residue, H880, contributes to proton block, although its role is not completely defined (Jones et al. 2013b). Interestingly, replacing H880 with a glutamine generates a pH-insensitive current that is intermediate to wild-type and C373 mutant $Na_V1.5$ channels (Jones et al. 2013b). C373 is adjacent to the selectivity filter, where the electrostatic potential is the most negative. H880, however, is predicted to be at the top of the Na_V channel P1 helix of domain II. Based on their relative locations it is understandable that the effect of the H880Q mutation would be less dramatic than that observed by the C373F mutation. A similar trend has been observed in proton modulation of slow inactivation (discussed later) (Jones et al. 2013b).

3.2 Proton Modulation of $Na_V1.5$

3.2.1 Activation

When $Na_V1.5$ channels are expressed in either oocytes or HEK cells, reducing pH_o from 7.4 to 6.0 reversibly blocks peak current by ~50 %, depolarizes the $V_{1/2}$ of activation, and increases the time to peak current (Vilin et al.; Jones et al. 2011; Khan et al. 2006).

Classically, shifts in voltage-dependent gating by cations is attributed to the Gouy–Chapman–Stern theory, also known as charge screening, which predicts a reduction in surface potential with increased divalent cation concentration (Hille et al. 1975; Cukierman et al. 1988; Green et al. 1987; Zhang et al. 1999; Hille 1968). As pH_o drops, protons effectively screen the charge across the membrane therefore a greater depolarization is required to gate voltage-dependent proteins. Many aspects of $Na_V1.5$ proton modulation are readily explained by charge screening, particularly proton-dependent shifts in activation and fast inactivation. Surprisingly, the pH-dependent shifts in the $V_{1/2}$ and z of activation display a similar pK_a to that of proton block (Jones et al. 2011). This could be coincidental; however, it

may suggest that similar residues trigger proton block and the changes in activation properties. Further, direct comparison of Hill curves fitted to the change in $V_{1/2}$ and z revealed similar pK_a values but very different slopes. This implies multiple modulatory mechanisms for the depolarized $V_{1/2}$ during acidosis, perhaps through a combination of surface charge titration and direct proton–protein effects (Cukierman et al. 1988). Indeed numerous extracellular $Na_V1.5$ residues are charged and putatively protonatable, particularly at the voltage sensors (Jones et al. 2013b; Khan et al. 2002; Abriel et al. 2001; Tester et al. 2005; Murphy et al.). Protonation of one or more of these residues could alter channel gating (Cukierman et al. 1988; Hoshi and Armstrong 2012; Payandeh et al. 2011).

3.2.2 Fast Inactivation

Reduced pH_o also reversibly destabilizes the fast-inactivated state in $Na_V1.5$, increasing the relative window and persistent I_{Na} (Jones et al. 2011). This is in agreement with analysis from intact cardiomyocytes (Murphy et al. 2011; Zhang and Siegelbaum 1991; Yatani et al. 1984; Saint 2006). Kinetic analysis of fast inactivation demonstrates accelerated recovery and delayed onset of fast inactivation (Jones et al. 2011, 2013b; Vilin et al. 2012). Destabilization of fast inactivation is a well-documented trigger for cardiac arrhythmia (Jones and Ruben 2008). So delicate is the balance between depolarizing and repolarizing currents that the reopening and/or failed closure of just two Na_V channels per cardiomyocyte is believed sufficient to delay repolarization and elevate $[Na^+]_i$ (Noble and Noble 2006; Hale et al. 2008; Antzelevitch and Belardinelli 2006; Zygmunt et al. 2001). Here, the slowed fast inactivation onset slows the initial repolarization of the cardiac AP, whereas increased window current, acting in concert with accelerated recovery and the increased persistent I_{Na} increases the probability of channel re-openings during the AP plateau, further slowing repolarization (Antzelevitch and Belardinelli 2006; Jones et al. 2011; Zygmunt et al. 2001).

3.2.3 Slow Inactivation

Amino acid residues within Na_V channel p-loops largely mediate the stability of the slow-inactivated state. It is no surprise then that altering the electrostatic environment within the pore alters the properties of slow inactivation (Townsend and Horn 1997; Xiong et al. 2003; Kuzmenkin et al. 2002). Townsend and Horn (1997) showed that permeant alkali metal cations inhibit closing of the slow inactivation gate (Townsend and Horn 1997). Similarly, protons accelerate the recovery and slow the onset, but have no effect on the maximum probability of slow inactivation in $Na_V1.5$ channels (Jones et al. 2011, 2013b). The mutual association of protons and slow inactivation at the pore seems sufficient to expect some effect of protons on steady-state slow inactivation. Why pH affected the rates of but not steady-state slow inactivation is unclear.

Perhaps a more accurate measure of the effects of acidosis on slow inactivation has been done through the use of use-dependent analysis. Use-dependent analysis uses sequential depolarizing pulses to frame a more physiologically relevant picture of the dynamic equilibrium between the various channel states. Using a

use-dependent protocol that mimicked a cardiac action potential, Jones et al. (2011) demonstrated that protons inhibit movement into the slow-inactivated state resulting in an increase in channel availability during acidosis (Jones et al. 2011). Mutational analysis later showed that slow inactivation modulation stems from protonation of p-loop residues (Jones et al. 2013b). It was demonstrated that the p-loop mutations C373F or H880Q abolish proton modulation of use-dependent inactivation (UDI) and alter modulation of slow inaction kinetics (Jones et al. 2013b). Overall, the H880Q mutation shows intermediate responses to protons compared to WT and C373F channels. These results led to the suggestion that, like their role in proton block, the relative positions of H880 and C373 may underlie the differential contribution to slow inactivation proton modulation. As slow inactivation is thought to be dependent on the electrostatic characteristics of the p-loop, protonation of C373 might be predicted to have a greater effect on slow inactivation than H880 (Khan et al. 2002; Townsend and Horn 1997). Further, accumulation of positive charge around the $Na_V1.5$ channel pore mediates destabilization of UDI and that C373 protonation represents a "tipping point" of positive charge that induces the reduction in $Na_V1.5$ UDI. Although only C373 and H880 have been specifically identified, it's likely that protonation at the EEDD ring also contributes to proton modulation of slow inactivation (Jones et al. 2013b; Khan et al. 2002, 2006). Lastly, it seems likely that proton block and slow inactivation modulation occur in tandem given the strong overlap in results between the two processes.

3.2.4 Gating Currents

Data describing proton modulation of Na_V channel gating currents, recorded in intact tissues have generated mixed conclusions (Neumcke et al. 1980; Schauf 1983; Rojas 1976; Keynes and Rojas 1974; Wanke et al. 1983; Campbell and Hahin 1984; Campbell 1983). No effect was observed on gating charge between pH 5.0 and pH 8.0 in squid giant axons (Keynes and Rojas 1974); however, Wanke et al. (1983) found that elevated intracellular pH reversibly prevented charge immobilization in squid giant axon (Wanke et al. 1983). Reducing extracellular pH reduced total charge and had no effect on the kinetics of I_{gOFF} in bristle worm axons (Schauf 1983). In frog axons, extracellular protons increased total charge and slowed the kinetics of I_{gOFF} (Neumcke et al. 1980). In frog skeletal muscle fibers, extracellular protons had no effect on total gating charge but depolarized the $V_{1/2}$ of the Q/V relationship, accelerated I_{gOFF} kinetics, reduced charge immobilization, and displayed a multifaceted slowing effect on the kinetics of I_{gON} (Campbell 1983). Tissue-specific proton modulation of gating currents is likely attributable to isoform-specific Na_V channel proton modulation (Vilin et al. 2012). Despite the variability of effects between tissues, a consensus exists on a depolarizing shift in the voltage dependence of gating current in response to reduced extracellular pH.

When $Na_V1.5$ channels are expressed in oocytes, lowering the extracellular pH from 7.4 to 6.0 depolarizes the $V_{1/2}$ of the Q_{ON}/V and Q_{OFF}/V relationships, slows I_{gON} kinetics, and accelerates fast I_{gOFF} kinetics (Jones et al. 2013a). These effects are consistent with a charge screening effect and explain the shifts in the voltage-dependence of ionic current during acidosis (Jones et al. 2013b;

Jones et al. 2011; Cukierman et al. 1988; Vilin et al. 2012; Murphy et al. 2011). Protons also induce a voltage-independent reduction of the slow component of I_{gOFF} decay that coincides with a reduced onset rate and magnitude of charge immobilization during depolarization (Jones et al. 2013a). These effects were not attributable to a charge screening effect. Voltage-independent destabilized charge immobilization implies a direct proton–protein interaction, most likely at the extracellular side of the VSD (Neumcke et al. 1980; Jones et al. 2013a). These data demonstrate that proton-dependent destabilization of fast inactivation and impaired charge immobilization are functionally related events. Whether destabilized fast inactivation reduces immobilization or vice versa has not been definitively shown, although the latter is the most likely explanation given that the majority of charge immobilization precedes and independent of fast inactivation (Groome et al. 2007, 2011; Armstrong and Bezanilla 1977; Bezanilla and Armstrong 1977; Sheets and Hanck 2005). Future studies could explore the causal relationship between charge immobilization and fast inactivation during acidosis.

3.2.5 β-Subunits

Na_V channel β-subunits are found in cardiac tissue (Goldin 1993; McEwen and Isom 2004), but their effects on $Na_V1.5$ gating appear limited (Makita et al. 1996, 2000; Vilin et al. 1999; McCormick et al. 1998, 1999). β subunits appear to augment late I_{Na} in $Na_V1.5$ while stabilizing steady-state fast inactivation (Maltsev et al. 2009; Baroudi et al. 2000; Makita et al. 2000; Tan et al. 2010; Medeiros-Domingo et al. 2007). Although it is evident that β-subunits are required for proper channel Na_V and cardiomyocyte function (Tan et al. 2010; Medeiros-Domingo et al. 2007), a definitive role in proton modulation of cardiac I_{Na} has not been demonstrated (Jones et al. 2011).

3.2.6 Action Potential Morphology

The modulation of voltage-gated ion channels by protons triggers significant changes in action potential morphology during extracellular acidosis. How exactly $Na_V1.5$ proton modulation alters action potential morphology is difficult to interpret. Protons interact with a wide range of cardiac ion channels and the contribution of $Na_V1.5$ modulation is easily confounded. In a computational model of epicardial, mid-myocardial, and endocardial ventricular action potentials, $Na_V1.5$ proton block at pH 6.0 triggered a 60 % reduction in AP upstroke velocity, whereas destabilized fast inactivation preferentially prolonged mid-myocardial action potentials (Jones et al. 2013b). These effects would be predicted to reduce conduction velocity and increase the transmural dispersion of repolarization in the intact myocardium, respectively (Lubinski et al. 1998; Antzelevitch and Belardinelli 2006; Antzelevitch et al. 2004; Murphy et al. 2011; Zygmunt et al. 2001). The time between epicardial and mid-myocardial AP repolarization defines the dispersion of repolarization and any increase would be expected to increase the likelihood of arrhythmia (Lubinski et al. 1998).

Conclusion

Protons are dangerous modifiers of Na_V channel kinetics that interact with $Na_V1.5$ channels directly, triggering dysfunction and thereby contributing to cardiac arrhythmia. Protons block conductance, destabilize fast and slow inactivation, and reduce the rate of onset and total immobilization of gating charge in $Na_V1.5$ channels. Alteration of cardiac I_{Na} is a widely described precursor to cardiac arrhythmia and clearly plays an arrhythmogenic role during ischemia and cardiac acidosis. Molecular data explain how $Na_V1.5$ proton modulation contributes to the changes in cardiac I_{Na} during acidosis and sheds light as to how this contributes to arrhythmia (Jones et al. 2011, 2013b; Murphy et al. 2011; Khan et al. 2006; Khan et al. 2002). Protons augment window as well as persistent I_{Na} in $Na_V1.5$, delaying ventricular repolarization and increasing its heterogeneity. Proton block reduces peak I_{Na}, slowing the maximum action potential upstroke velocity and thereby slowing action potential propagation. Proton block is partially countermanded by reduced slow inactivation; however, loss of current due to proton block is the predominate effect.

Through a combined understanding of the changes in cardiac I_{Na}, from the channel/proton interaction to the level of the functioning heart, future research can develop drug treatments to correct or prevent the deleterious changes in cardiac physiology during cardiac ischemia. Already, drugs have been developed to target specific aspects of Na_V channel function. With the emergence of drugs like amiodarone, ranolazine, and flecainide, late I_{Na} is an increasingly common pharmacological target (Moreno and Clancy 2012). The late I_{Na} blocker, ranolazine, has demonstrated to be an effective treatment for cardiac ischemia, hypoxia, and chronic heart disease presumably by stopping intracellular Ca^{2+} accumulation through inhibition of late I_{Na} (Scirica et al. 2007; Chaitman 2006). Other compounds target other aspects of Na_V channel gating, such as lacosamide, which preferentially stabilizes the slow-inactivated state in neuronal Na_V channels (Errington et al. 2008). By doing so lacosamide reduces channel availability during repeated stimulus, reducing excitability, and proving to be an effective drug in the treatment of various forms of epilepsy (Errington et al. 2008; Zaccara et al. 2013). Lidocaine displays preferential binding of the open- and/or fast-inactivated states (Hille 1977; Ragsdale et al. 1994) and is used as a local anesthetic as well as in cardiac arrhythmia (Allen et al. 2011; Chang et al. 2009). These drugs underscore the importance of understanding Na_V channel biophysics and modulation thereof in order to properly treat disorders of excitability.

References

Abriel H, Cabo C, Wehrens XHT, Rivolta I, Motoike HK, Memmi M, Napolitano C, Priori SG, Kass RS (2001) Novel arrhythmogenic mechanism revealed by a long-QT syndrome mutation in the cardiac Na channel. Circulation Res 88:740

Allen NM, Azam M, Dunne KP, Walsh KP (2011) Idiopathic ventricular tachycardia in a newborn: immediate response to lidocaine. Pediatr Cardiol 32:706–707

Antzelevitch C, Belardinelli L (2006) The role of sodium channel current in modulating transmural dispersion of repolarization and arrhythmogenesis. J Cardiovasc Electrophysiol 17(Suppl 1):S79–S85

Antzelevitch C, Belardinelli L, Zygmunt AC, Burashnikov A, DI Diego JM, Fish JM, Cordeiro JM, Thomas G (2004) Electrophysiological effects of ranolazine, a novel antianginal agent with antiarrhythmic properties. Circulation 110:904–910

Armstrong CM, Bezanilla F (1977) Inactivation of the sodium channel II. Gating current experiments. J Gen Physiol 70:567–590

Balser JR, Nuss HB, Chiamvimonvat N, Perez-Garcia MT, Marban E, Tomaselli GF (1996) External pore residue mediates slow inactivation in mu 1 rat skeletal muscle sodium channels. J Physiol 494(Pt 2):431–442

Baroudi G, Carbonneau E, Pouliot V, Chahine M (2000) SCN5A mutation (T1620M) causing Brugada syndrome exhibits different phenotypes when expressed in Xenopus oocytes and mammalian cells. FEBS Lett 467:12–16

Benzing H, Gebert G, Strohm M (1971) Extracellular acid–base changes in the dog myocardium during hypoxia and local ischemia, measured by means of glass micro-electrodes. Cardiology 56:85–88

Bezanilla F, Armstrong CM (1977) Inactivation of the sodium channel I. Sodium current experiments. J Gen Physiol 70:549–566

Bountra C, Vaughan-Jones RD (1989) Effect of intracellular and extracellular pH on contraction in isolated, mammalian cardiac muscle. J Physiol 418:163–187

Campbell DT (1983) Sodium channel gating currents in frog skeletal muscle. J Gen Physiol 82:679–701

Campbell DT, Hahin R (1984) Altered sodium and gating current kinetics in frog skeletal muscle caused by low external pH. J Gen Physiol 84:771–788

Carmeliet E (1999) Cardiac ionic currents and acute ischemia: from channels to arrhythmias. Physiol Rev 79:917–1017

Chaitman BR (2006) Ranolazine for the treatment of chronic angina and potential use in other cardiovascular conditions. Circulation 113:2462–2472

Chang JH, Weng TI, Fang CC (2009) Long QT syndrome and torsades de pointes induced by acute sulpiride poisoning. Am J Emerg Med 27(1016):e1–e3

Clapham DE (2007) Calcium signaling. Cell 131:1047–1058

Crampin EJ, Smith NP, Langham AE, Clayton RH, Orchard CH (2006) Acidosis in models of cardiac ventricular myocytes. Philos Trans A Math Phys Eng Sci 364:1171–1186

Cukierman S, Zinkand WC, French RJ, Krueger BK (1988) Effects of membrane surface charge and calcium on the gating of rat brain sodium channels in planar bilayers. J Gen Physiol 92:431–447

Errington AC, Stohr T, Heers C, Lees G (2008) The investigational anticonvulsant lacosamide selectively enhances slow inactivation of voltage-gated sodium channels. Mol Pharmacol 73:157–169

Favre I, MOCZYDLOWSKI E, SCHILD L (1996) On the structural basis for ionic selectivity among Na+, K+, and Ca2+ in the voltage-gated sodium channel. Biophys J 71:3110–3125

Fry CH, Poole-Wilson PA (1981) Effects of acid–base changes on excitation–contraction coupling in guinea-pig and rabbit cardiac ventricular muscle. J Physiol 313:141–160

Gebert G, Benzing H, Strohm M (1971) Changes in the interstitial pH of dog myocardium in response to local ischemia, hypoxia, hyper- and hypocapnia, measured continuously by means of glass microelectrodes. Pflugers Arch 329:72–81

Goldin AL (1993) Accessory subunits and sodium channel inactivation. Curr Opin Neurobiol 3:272–277

Green WN, Weiss LB, Andersen OS (1987) Batrachotoxin-modified sodium channels in planar lipid bilayers. Characterization of saxitoxin- and tetrodotoxin-induced channel closures. J Gen Physiol 89:873–903

Groome JR, Dice MC, Fujimoto E, Ruben PC (2007) Charge immobilization of skeletal muscle Na + channels: role of residues in the inactivation linker. Biophys J 93:1519–1533

Groome J, Lehmann-Horn F, Holzherr B (2011) Open- and closed-state fast inactivation in sodium channels: differential effects of a site-3 anemone toxin. Channels (Austin) 5:65–78

Hale SL, Shryock JC, Belardinelli L, Sweeney M, Kloner RA (2008) Late sodium current inhibition as a new cardioprotective approach. J Mol Cell Cardiol 44:954–967

Haufe V, Camacho JA, Dumaine R, Gunther B, Bollensdorff C, Von Banchet GS, Benndorf K, Zimmer T (2005a) Expression pattern of neuronal and skeletal muscle voltage-gated Na + channels in the developing mouse heart. J Physiol 564:683–696

Haufe V, Cordeiro JM, Zimmer T, Wu YS, Schiccitano S, Benndorf K, Dumaine R (2005b) Contribution of neuronal sodium channels to the cardiac fast sodium current INa is greater in dog heart Purkinje fibers than in ventricles. Cardiovasc Res 65:117–127

Hille B (1968) Charges and potentials at the nerve surface. J Gen Physiol 51:221

Hille B (1977) Local anesthetics: hydrophilic and hydrophobic pathways for the drug-receptor reaction. J Gen Physiol 69:497–515

Hille B, Woodhull AM, Shapiro BI (1975) Negative surface charge near sodium channels of nerve: divalent ions, monovalent ions, and pH. Philos Trans R Soc Lond B Biol Sci 270:301–318

Hoshi T, Armstrong CM (2012) Initial steps in the opening of a Shaker potassium channel. Proc Natl Acad Sci U S A 109:12800–12804

Jones DK, Ruben PC (2008) Biophysical defects in voltage-gated sodium channels associated with long QT and Brugada syndromes. Channels (Austin) 2:70–80

Jones DK, Peters CH, Tolhurst SA, Claydon TW, Ruben PC (2011) Extracellular proton modulation of the cardiac voltage-gated sodium channel, NaV.15. Biophysical 101:2147–2156

Jones DK, Claydon TW, Ruben PC (2013a) Extracellular protons inhibit charge immobilization in the cardiac voltage-gated sodium channel. Biophysical 105:101–107

Jones DK, Peters CH, Allard CR, Claydon TW, Ruben PC (2013b) Proton sensors in the pore domain of the cardiac voltage-gated sodium channel. J Biol Chem 288:4782–4791

Ju YK, Saint DA, Gage PW (1996) Hypoxia increases persistent sodium current in rat ventricular myocytes. J Physiol 497(Pt 2):337–347

Keynes RD, Rojas E (1974) Kinetics and steady-state properties of the charged system controlling sodium conductance in the squid giant axon. J Physiol 239:393–434

Khan A, Romantseva L, Lam A, Lipkind G, Fozzard HA (2002) Role of outer ring carboxylates of the rat skeletal muscle sodium channel pore in proton block. J Physiol 543:71

Khan A, Kyle JW, Hanck DA, Lipkind GM, Fozzard HA (2006) Isoform-dependent interaction of voltage-gated sodium channels with protons. J Physiol 576:493

Kochanek KD, Kirmeyer SE, Martin JA, Strobino DM, Guyer B (2009) Annual summary of vital statistics. Pediatrics 129:338–348

Kuzmenkin A, Muncan V, Jurkat-Rott K, Hang C, Lerche H, Lehmann-Horn F, Mitrovic N (2002) Enhanced inactivation and pH sensitivity of Na(+) channel mutations causing hypokalaemic periodic paralysis type II. Brain 125:835–843

Leem CH, Lagadic-Gossmann D, Vaughan-Jones RD (1999) Characterization of intracellular pH regulation in the guinea-pig ventricular myocyte. J Physiol 517(Pt 1):159–180

Liu YM, Defelice LJ, Mazzanti M (1992) Na channels that remain open throughout the cardiac action potential plateau. Biophys J 63:654–662

Loetscher H, Niederhauser O, Kemp J, Gill R (2001) Is caspase-3 inhibition a valid therapeutic strategy in cerebral ischemia? Drug Discov Today 6:671–680

Lubinski A, Lewicka-Nowak E, Kempa M, Baczynska AM, Romanowska I, Swiatecka G (1998) New insight into repolarization abnormalities in patients with congenital long QT syndrome: the increased transmural dispersion of repolarization. Pacing Clin Electrophysiol 21:172–175

Maier SK, Westenbroek RE, Schenkman KA, Feigl EO, Scheuer T, Catterall WA (2002) An unexpected role for brain-type sodium channels in coupling of cell surface depolarization to contraction in the heart. Proc Natl Acad Sci U S A 99:4073–4078

Maier SK, Westenbroek RE, Mccormick KA, Curtis R, Scheuer T, Catterall WA (2004) Distinct subcellular localization of different sodium channel alpha and beta subunits in single ventricular myocytes from mouse heart. Circulation 109:1421–1427

Makielski JC, Farley AL (2006) Na(+) current in human ventricle: implications for sodium loading and homeostasis. J Cardiovasc Electrophysiol 17(Suppl 1):S15–S20

Makita N, Bennett PB, George AL (1996) Molecular determinants of B1 subunit-induced gating modulation in voltage-dependent Na + channels. J Neurosci 16:7117–7127

Makita N, Shirai N, Wang DW, Sasaki K, George AL, Kanno M, Kitabatake A (2000) Cardiac Na + channel dysfunction Brugada syndrome is aggravated by B1-subunit. Circulation 101:54–60

Maltsev VA, Kyle JW, Undrovinas A (2009) Late Na + current produced by human cardiac Na + channel isoform Nav1.5 is modulated by its beta1 subunit. J Physiol Sci 59:217–225

Mattson MP, Chan SL (2003) Calcium orchestrates apoptosis. Nat Cell Biol 5:1041–1043

Mccormack JG, Halestrap AP, Denton RM (1990) Role of calcium ions in regulation of mammalian intramitochondrial metabolism. Physiol Rev 70:391–425

Mccormick KA, Isom LI, Ragsdales D, Smith D, Scheuer T, Catterall W (1998) Molecular determinants of Na + channel function in the extracellular domain of b1 sununit. J Biol Chem 273:3954–3962

Mccormick KA, Srinivasan J, White K, Scheuer T (1999) The extracellular domain of the b1 subunit is both necessary and sufficient for b1- like modulation of sodium channel gating. J Biol Chem 274:32638–32646

Mcewen DP, Isom LL (2004) Heterophilic interactions of sodium channel {beta}1 subunits with axonal and glial cell adhesion molecules. J Biol Chem 279:52744–52752

Medeiros-Domingo A, Kaku T, Tester DJ, Iturralde-Torres P, Itty A, Ye B, Valdivia C, Ueda K, Canizales-Quinteros S, Tusie-Luna MT, Makielski JC, Ackerman MJ (2007) SCN4B-encoded sodium channel beta4 subunit in congenital long-QT syndrome. Circulation 116:134–142

Moreno JD, Clancy CE (2012) Pathophysiology of the cardiac late Na current and its potential as a drug target. J Mol Cell Cardiol 52:608–619

Murphy L, Renodin D, Antzelevitch C, Di Diego JM, Cordeiro JM (2011) Extracellular proton depression of peak and late Na(+) current in the canine left ventricle. Am J Physiol Heart Circ Physiol 301:H936–H944

Murphy LL, Moon-Grady AJ, Cuneo BF, Wakai RT, Yu S, Kunic JD, Benson DW, George AL Jr (2012) Developmentally regulated SCN5A splice variant potentiates dysfunction of a novel mutation associated with severe fetal arrhythmia. Heart Rhythm 9:590–597

Neumcke B, Schwarz W, Stampfli R (1980) Increased charge displacement in the membrane of myelinated nerve at reduced extracellular pH. Biophys J 31:325–331

Nguyen-Thi A, Ruiz-Ceretti E, Schanne OF (1981) Electrophysiologic effects and electrolyte changes in total myocardial ischemia. Can J Physiol Pharmacol 59:876–883

Noble D, Noble PJ (2006) Late sodium current in the pathophysiology of cardiovascular disease: consequences of sodium-calcium overload. Heart 92(Suppl 4):iv1–iv5

Payandeh J, Scheuer T, Zheng N, Catterall WA (2011) The crystal structure of a voltage-gated sodium channel. Nature 475:353–358

Ragsdale DS, Mcphee JC, Scheuer T, Catterall WA (1994) Molecular determinants of state-dependent block of Na + channels by local anesthetics. Science 265:1724–1728

Rojas E (1976) Gating mechanism for the activation of the sodium conductance in nerve membranes. Cold Spring Harb Symp Quant Biol 40:305–320

Saint DA (2006) The role of the persistent Na(+) current during cardiac ischemia and hypoxia. J Cardiovasc Electrophysiol 17(Suppl 1):S96–S103

Schauf CL (1983) Evidence for negative gating charges in Myxicola axons. Biophys J 42:225–231

Scirica BM, Morrow DA, Hod H, Murphy SA, Belardinelli L, Hedgepeth CM, Molhoek P, Verheugt FW, Gersh BJ, Mccabe CH, Braunwald E (2007) Effect of ranolazine, an antianginal agent with novel electrophysiological properties, on the incidence of arrhythmias in patients with non ST-segment elevation acute coronary syndrome: results from the Metabolic Efficiency With Ranolazine for Less Ischemia in Non ST-Elevation Acute Coronary Syndrome Thrombolysis in Myocardial Infarction 36 (MERLIN-TIMI 36) randomized controlled trial. Circulation 116:1647–1652

Sheets MF, Hanck DA (2005) Charge immobilization of the voltage sensor in domain IV is independent of sodium current inactivation. J Physiol 563:83–93

Tan BH, Pundi KN, Van Norstrand DW, Valdivia CR, Tester DJ, Medeiros-Domingo A, Makielski JC, Ackerman MJ (2010) Sudden infant death syndrome-associated mutations in the sodium channel beta subunits. Heart Rhythm 7:771–778

Terlau H, Heinemann SH, Stuhmer W, Pusch M, Conti F, Imoto K, Numa S (1991) Mapping the site of block by tetrodotoxin and saxitoxin of sodium channel II. FEBS Lett 293:93–96

Tester DJ, Will ML, Haglund CM, Ackerman MJ (2005) Compendium of cardiac channel mutations in 541 consecutive unrelated patients referred for long QT syndrome genetic testing. Heart Rhythm 2:507–517

Townsend C, Horn R (1997) Effect of alkali metal cations on slow inactivation of cardiac Na + channels. J Gen Physiol 110:23–33

Vilin YY, Makita N, George AL, Ruben PC (1999) Structural determinants of slow inactivation in human cardiac and skeletal muscle sodium channels. Biophys J 77:1384–1393

Vilin YY, Peters CH, Ruben PC (2012) Acidosis differentially modulates inactivation in na(v)1.2, na(v)1.4, and na(v)1.5 channels. Front Pharmacol 3:109

Wanke E, Testa PL, Prestipino G, Carbone E (1983) High intracellular pH reversibly prevents gating-charge immobilization in squid axons. Biophys J 44:281–284

Xiong W, Li RA, Tian Y, Tomaselli GF (2003) Molecular motions of the outer ring of charge of the sodium channel: do they couple to slow inactivation? J Gen Physiol 122:323–332

Yatani A, Brown AM, Akaike N (1984) Effect of extracellular pH on sodium current in isolated, single rat ventricular cells. J Membr Biol 78:163–168

Zaccara G, Perucca P, Loiacono G, Giovannelli F, Verrotti A (2013) The adverse event profile of lacosamide: a systematic review and meta-analysis of randomized controlled trials. Epilepsia 54:66–74

Zhang JF, Siegelbaum SA (1991) Effects of external protons on single cardiac sodium channels from guinea pig ventricular myocytes. J Gen Physiol 98:1065–1083

Zhang Y, Hartmann HA, Satin J (1999) Glycosylation influences voltage-dependent gating of cardiac and skeletal muscle sodium channels. J Membr Biol 171:195–207

Zygmunt AC, Eddlestone GT, Thomas GP, Nesterenko VV, Antzelevitch C (2001) Larger late sodium conductance in M cells contributes to electrical heterogeneity in canine ventricle. Am J Physiol Heart Circ Physiol 281:H689–H697

Probing Gating Mechanisms of Sodium Channels Using Pore Blockers

Marcel P. Goldschen-Ohm and Baron Chanda

Contents

Abstract

Several classes of small molecules and peptides bind at the central pore of voltage-gated sodium channels either from the extracellular or intracellular side of the membrane and block ion conduction through the pore. Biophysical studies that shed light on the chemical nature, accessibility, and kinetics of binding of these naturally occurring and synthetic compounds reveal a wealth of information about how these channels gate. Here, we discuss insights into the structural underpinnings of gating of the channel pore and its coupling to the voltage sensors obtained from pore blockers including site 1 neurotoxins and local anesthetics.

M.P. Goldschen-Ohm • B. Chanda (✉)
Department of Neuroscience, University of Wisconsin, Madison, WI, USA
e-mail: Baron.chanda@gmail.com

P.C. Ruben (ed.), *Voltage Gated Sodium Channels*, Handbook of Experimental Pharmacology 221, DOI 10.1007/978-3-642-41588-3_9,

Keywords
Neurotoxin • Local anesthetic • State-dependent blocker • Sodium channel • Gating

1 Introduction

Activation of voltage-gated sodium channels underlies the initiation of action potentials in a variety of excitable cells in both cardiac and skeletal muscle tissues and throughout the nervous system (Hodgkin and Huxley 1952). The function of these channels is critical for normal signaling in these cellular networks. Their importance is highlighted by inherited genetic mutations that confer aberrant channel behavior causing serious human diseases including muscular dysfunction (Chahine et al. 1994; Cannon 1996; Jurkat-Rott et al. 2010), cardiac arrhythmias (Wang et al. 1995; Ackerman 1998; Kambouris et al. 1998), and epilepsy (Wallace et al. 1998).

In addition to genetic manipulations, sodium channels are targets for a variety of small molecules and peptides which upon binding modulate the channel's behavior. Several classes of these agents act by blocking ion conduction through the channel's central pore. Of these, local anesthetics have found widespread clinical use for various disorders including as analgesics by blocking pain-related signaling and as treatments for cardiac arrhythmias and epilepsy due to the antiarrhythmic properties conferred by the use dependence of their blocking action.

Structurally, eukaryotic voltage-gated sodium channels are comprised of a single α subunit with four homologous but nonidentical domains DI–IV (Bezanilla 2000; Catterall 2010). Each domain contains six transmembrane helices S1–6, where S1–4 contain the voltage sensors for each domain and S5–6 from all four domains combine to form the channel's central pore (Fig. 1a). The outer pore region and selectivity filter is formed largely by a membrane-reentrant loop between S5 and S6 which forms the selectivity filter, and the inner pore is lined by the S6 helices. An important distinction between these channels and both their bacterial homologues and eukaryotic potassium channels is that the latter are composed of four identical subunits, whereas the nonidentical domains in eukaryotic sodium channels have distinct functional roles (Chahine et al. 1994; Chen et al. 1996; Lerche et al. 1997; McPhee et al. 1998; Sheets et al. 1999; Chanda and Bezanilla 2002; Bosmans et al. 2008).

One of the major challenges to developing better disease therapies in the form of novel sodium channel modulators is that the detailed molecular mechanisms underlying the functional effects of perturbations such as disease-related mutations or local anesthetic binding remain only poorly understood. In particular, it is imperative to develop more comprehensive physical models of channel behavior that can account for how perturbations in the pore are transmitted to other channel domains such as the voltage sensors. Here, we describe how pore blockers have been used as biophysical tools to gain fundamental insights into sodium channel gating.

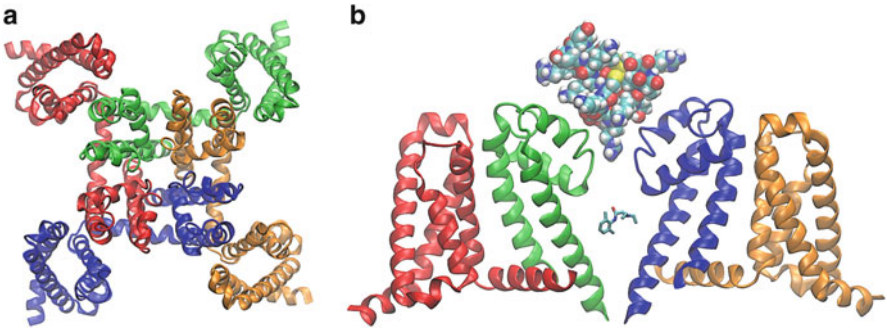

Fig. 1 (**a**) Crystal structure of the bacterial voltage-gated sodium channel NavAb from Payandeh et al. (2011). View is from the extracellular side of the membrane looking down through the channel. Each domain is represented by a different color. (**b**) View from within the plane of the membrane perpendicular to the plane bisecting the channel from the upper left to lower right corner as shown in (**a**). Only the pore segments from two domains and voltage sensors from the remaining two domains are shown. The pore blockers μ-CTX GIIIA (*van der waals representation*) and lidocaine (*licorice representation*) are shown in the proximity of their respective binding sites merely as a visual guide (i.e., these are not docked configurations). The ability of lidocaine to access its binding site in the inner pore is enhanced upon opening of an intracellular pore gate near the bottom of the S6 helices

2 Extracellular Pore Blockers

2.1 Site 1 Neurotoxins and Nonpermeant Cations

The central ion-conducting pore of the sodium channel is subject to block from the extracellular side of the membrane by several potent neurotoxins which bind to the outer mouth of the pore in a region known as site 1 and completely block ion conduction in single channels (French et al. 1984; Catterall et al. 2007) (Fig. 1b). Site 1 pore-blocking toxins include both small hydrophilic compounds containing a charged guanidinium group such as tetrodotoxin (TTX) and saxitoxin (STX) and larger peptide toxins such as μ-conotoxin (μ-CTX). Various subtypes of μ-CTX exist including GIIIA, GIIIB, KIIIA, SIIIA, PIIIA, and MrVIB. As potent blockers of sodium channels, these toxins were originally isolated from the venom of several animal species. For example, μ-CTX is found in the venom of marine cone snails (Terlau and Olivera 2004), whereas TTX has been found in a variety of toxic species including the pufferfish, although it is now known that TTX is actually produced by bacteria carried in these animals (Lee and Ruben 2008; Moczydlowski 2013). Several other toxins such as the spider toxins hainantoxin-IV and huwentoxin-IV also bind at site 1 and block the channel (Peng et al. 2002; Liu et al. 2003).

A hallmark of site 1 neurotoxins is their high affinity and specificity for sodium channels, the combination of which has made them useful biophysical tools for the

specific elimination of sodium currents in a variety of preparations. Application of nanomolar to micromolar quantities is usually sufficient to insure that nearly all channels have bound toxin. The ability to specifically block sodium currents apart from that of other ion channels has been invaluable in elucidating the role of sodium channels in the function of excitable cellular networks.

Although toxins such as TTX block all sodium channel subtypes, their affinity depends on critical residues which can vary between channel isoforms. For example, the lower micromolar affinity of TTX for cardiac Nav1.5 channels is largely due to the presence of a cysteine residue in a homologous position to that of an aromatic in more TTX-sensitive channels such as Nav1.4 from skeletal muscle or Nav1.2 from neuronal tissue (Backx et al. 1992; Heinemann et al. 1992; Favre et al. 1995; Santarelli et al. 2007; Lee and Ruben 2008).

Sodium channels are also sensitive to block from extracellular divalent cations such as calcium, as well as by protons, which compete for the same binding sites as the guanidinium toxins TTX and STX (Woodhull 1973; Hille 1975; Henderson et al. 1974; Weigele and Barchi 1978; Barchi and Weigele 1979; Yamamoto et al. 1984; Sheets and Hanck 1992; Doyle et al. 1993). Furthermore, binding of TTX and STX is inhibited by increasing concentrations of extracellular permeant ions to a degree that reflects the rank order of channel selectivity for the competing ion (Reed and Raftery 1976; Weigele and Barchi 1978; Barchi and Weigele 1979; Doyle et al. 1993). These data as well as single channel studies suggest that both guanidinium toxins and divalent cations compete for one-to-one binding to channel carboxyl groups involved in permeation (Woodhull 1973; Hille 1975; Moczydlowski et al. 1984; Worley et al. 1986; Green et al. 1987; Schild and Moczydlowski 1991). In contrast, μ-CTX does not compete with sodium ion for binding (Li et al. 2003), likely due to the different nature by which the larger peptide toxins bind to the outer pore (see below).

2.2 Mapping the Structure of the Outer Pore with Neurotoxins

The high affinity and specificity of TTX and STX for sodium channels has been exploited to purify sodium channel α and β subunits from preparations such as the eel electric organ (Agnew et al. 1978). However, there are currently no crystal structures of a eukaryotic voltage-gated sodium channel. Thus, structural information has come largely from mutagenesis in conjunction with crystal structures of homologous voltage-gated potassium channels (Long et al. 2005; Banerjee et al. 2013) and bacterial voltage-gated sodium channels (Payandeh et al. 2011; McCusker et al. 2012). However, the bacterial sodium channels, like potassium channels are comprised of four identical subunits and thus do not provide a clear picture of how nonidentical domains in the eukaryotic channels give rise to domain-specific functions.

Given the lack of direct structural information, functional data that can constrain homology models is crucial for developing a realistic view of eukaryotic sodium channel structure. To this end, site 1 neurotoxins represent well-defined spatial

probes around which their receptor sites can be accurately modeled once the interactions between the toxin and the channel are known. This lock-and-key analysis has been utilized to obtain detailed models of the outer pore structure.

Mutagenesis, photoaffinity labeling, and channel chimeras have localized the binding site for site 1 neurotoxins to the extracellular mouth of the channel pore (Li et al. 1997; Xue et al. 2003; Zhang et al. 2007; McArthur et al. 2011). In addition, specific interactions between aspects of the toxin and channel residues have been identified using mutant cycle analysis (Chang et al. 1998). In brief, the individual effects on binding/blocking affinity of either single mutations in the channel or perturbations in the toxin are assessed. These are then compared to the pair-wise effects of simultaneous perturbations in the channel and toxin. If a given pair-wise perturbation is not equivalent to the sum of the effects of its individual perturbations, then an interaction between the perturbed sites on the channel and toxin is presumed.

Using the interacting pairs between toxin and channel residues elucidated from mutagenesis as structural constraints, several groups have generated homology models of the outer pore around docked toxin molecules (Choudhary et al. 2007; Fozzard and Lipkind 2010; Tikhonov and Zhorov 2012). These models provide a detailed view of the outer pore structure given the stringent constraints imposed by maintaining interactions for known binding partners between the channel and much smaller and less flexible toxins. In addition to the molecular details these models provide, toxin-binding interactions have also revealed that the nonidentical domains in eukaryotic sodium channels adopt a clockwise arrangement from DI to DIV as viewed from the extracellular side of the membrane (Dudley et al. 2000; Li et al. 2001).

Typically, site 1 toxins compete with each other for their binding site such that only one toxin is bound at any given time. However, although the binding sites for site 1 toxins overlap, they are not identical. Toxins containing a charged guanidinium group such as TTX bind tightly to the mouth of the pore in close proximity to the selectivity filter where they form a steric occlusion of the outer pore entrance (Hille 1975). In contrast, the larger peptide μ-conotoxins interact with residues slightly more extracellular from all four domains, and their ability to completely block ion conduction depends critically on a single positively charged arginine residue which represents an electrostatic barrier to ions entering the pore in addition to any steric occlusion of the permeation pathway (Hui et al. 2002). Indeed, mutating this arginine residue results in conotoxins that only partially block the pore, as evidenced by a reduction, but not complete block of single channel currents (Becker et al. 1992). It is also now known that the μ-conotoxin derivative KIIIA can bind simultaneously with TTX, with bound μ-CTX KIIIA inhibiting both binding and unbinding of TTX, consistent with a more extracellular position of μ-CTX relative to that of TTX (Zhang et al. 2009).

2.3 Resolving Closed-State Transitions Using Gating Currents

Since elucidating that voltage-dependent current responses arise through the opening and closing of discrete ion channels, it was postulated that these channels must

contain charged residues that moved within the membrane electric field in order to confer voltage-dependent activity. However, the onset of ionic currents through the channel pore in macroscopic preparations overlaps the time course during which the gating charges are moving. Thus, resolving the gating current alone requires blocking ion conduction through the pore, which is typically achieved by extracellular application of a saturating concentration of an outer pore neurotoxin such as TTX or μ-CTX, often in conjunction with the removal of permeant ions from the bath solution.

In practice, accurate measurement of gating currents requires not only a complete block of ionic conduction through the central pore but also a rapid voltage clamp of the channel containing membrane with good capacitance compensation to accurately resolve the kinetics of the gating charge movement. Finally, robust channel expression is usually required to obtain sufficient current density to resolve the movement of the 6–12 electronic charges contributed per channel (Hirschberg et al. 1995; Gamal El-Din et al. 2008). For these reasons, measurements of gating currents have largely been confined to preparations such as squid giant axons and cut-open oocytes (Stefani and Bezanilla 1998).

Kinetic models have become an important tool for understanding the mechanisms of protein function. However, for ion channels a fundamental challenge to constructing realistic kinetic models is that typically only a small subset of the states which a channel adopts during gating conduct ions via an open pore. Thus, measurements of open channel ionic currents probe only a subset of conformational states.

To differentiate between the often numerous possible models, constraints on transitions among closed states are crucial. The ability to measure gating currents represents the observation of channel conformational changes other than pore opening/closing and provides an important constraint on a model's transitions among closed states. Indeed, utilizing gating current responses in conjunction with ionic pore currents has yielded several detailed models of both sodium and potassium channel function (Vandenberg and Bezanilla 1991; Zagotta et al. 1994; Schoppa and Sigworth 1998).

2.4 Asynchronous Movement of Distinct Voltage Sensors

Gating current kinetics exhibit at least two components: a fast component with a time constant on the order of a few 100 μs and a slow component with a time constant on the order of a few milliseconds. In macroscopic recordings the fast component largely precedes the onset of pore current, whereas the slow component overlaps the time course of channel activation. Multiple kinetic phases of gating charge movement could reflect multiple kinetic steps in each voltage sensor. However, serial mutagenesis of the primary gating charges in each domain has revealed that fast and slow gating charge movement is at least partially due to differential rates of charge movement in distinct domains (Sheets et al. 1999). For example, neutralization of the S4 arginines in domain IV greatly reduces the slow

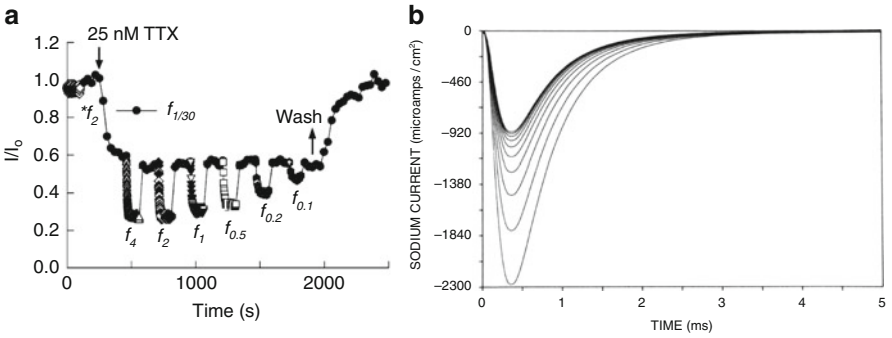

Fig. 2 Use-dependent block by both guanidinium toxins and local anesthetics. (**a**) Peak current block induced upon application of 25 nM TTX is increased during 50 s trains of 10 ms pulses from −120 to −10 mV to a degree depending on the frequency of the pulse trains (4–0.1 Hz) (from Huang et al. 2012). (**b**) Progressive reduction in peak current amplitude in the presence of 200 μM QX-314 for subsequent pulses from −120 to 0 mV delivered at a frequency of 5 Hz (from Starmer et al. 1984)

component of gating currents, suggesting that domain IV activates more slowly than domains I–III.

These observations are corroborated by measurements of voltage sensor movement in individual domains with site-specific fluorescent probes (Chanda and Bezanilla 2002; Goldschen-Ohm et al. 2013). Fluorescence changes from labels at the N-terminal end of each individual S4 segment in domains I–III indicate that these regions undergo conformational changes that similarly correlate with the fast component of the gating current. In contrast, conformational changes at the analogous region of the domain IV S4 segment appear to occur more slowly and correlate with the slow component of the gating current. Thus, membrane depolarization initiates distinct movements in specific asymmetric domains of eukaryotic voltage-gated sodium channels.

2.5 Interactions Between Gating Machinery and Outer Pore Blockers

Both TTX and STX exhibit use-dependent block, wherein the toxin-blocking efficiency is increased up to about threefold during a train of repetitive depolarizing voltage steps from a hyperpolarized holding potential (Cohen et al. 1981; Makielski et al. 1993) (Fig. 2a). The full increase in use-dependent toxin block can be achieved with only a single brief depolarizing pre-pulse less than 1 ms in duration, which is sufficient to observe activation of the voltage sensors, but shorter than required to achieve robust ionic current due to opening of the channel pore (Salgado et al. 1986; Lönnendonker 1989). This suggests that the mechanism of use dependence involves a conformational change associated with a closed state or states

having one or more voltage sensors at least partially activated, but yet prior to pore opening. Consistent with such an idea, the amount of use-dependent block observed with TTX is reduced at more depolarizing holding potentials where the voltage sensors may be semi-activated, and mutations affecting voltage sensor activation have analogous effects (i.e., in the same direction) on TTX use dependence (Patton and Goldin 1991). In contrast, removal of fast inactivation does not affect TTX use dependence (Patton and Goldin 1991; Dumaine and Hartmann 1996). Although an alternative explanation for use-dependent block by site 1 toxins incorporates electrostatic effects due to ions trapped within the permeation pathway (Salgado et al. 1986), this idea is not supported by observations that TTX use dependence is unaffected by mutations altering either toxin affinity, sodium versus potassium selectivity, or calcium permeability, all of which might be expected to alter the profile of ions in the pore (Santarelli et al. 2007; Huang et al. 2012).

The first direct evidence that site 1 toxins interact with one of the channel's voltage sensors came from a recent study of a series of mutant channels exhibiting omega currents through each specific voltage sensor (Capes et al. 2012). To assay the position of each individual voltage sensor, we mutated several of the gating charges such that at hyperpolarized potentials an aqueous ion-conducting channel is formed through the voltage sensors themselves. Because these currents arise at potentials more hyperpolarized than those where the channel's central pore opens, we can directly compare the omega current through each individual mutant voltage sensor both without and with toxin bound to site 1 in the outer pore. We found that whereas gating pore currents through the DI–III voltage sensors were unaffected by either TTX or μ-CTX binding, TTX binding produced a conformational change in the DIV voltage sensor resulting in a decrease in current through the DIV gating pore. This interaction appears to be specific to pore sites near the selectivity filter where TTX binds, as μ-CTX which binds slightly more extracellularly did not confer a similar change in DIV gating pore current. Consistent with a specific interaction between the TTX-binding site and the channel's voltage sensors, TTX reduced the magnitude of OFF gating currents, whereas μ-CTX had no effect (Capes et al. 2012). The lack of an effect of μ-CTX binding on the conformational change at the TTX site next to the selectivity filter may explain why μ-CTX does not exhibit use dependence (Huang et al. 2012).

Given that C-type inactivation in voltage-gated potassium channels involves conformational changes in the selectivity filter (López-Barneo et al. 1993; Cordero-Morales et al. 2006; Cuello et al. 2010), it seems plausible that the functionally similar slow inactivation in sodium channels may be due to a similar mechanism. Consistent with this idea, both outer pore mutations as well as the concentration of permeant ions affect slow inactivation (Balser et al. 1996; Townsend and Horn 1997; Bénitah et al. 1999; Todt et al. 1999; Ong et al. 2000; Xiong et al. 2003, 2006; Zarrabi et al. 2010), and TTX inhibits entry into ultraslow-inactivated states (Todt et al. 1999). Given that the DIV voltage sensor is specifically associated with inactivation, it is interesting to surmise that DIV voltage sensor movement might contribute not only to entry into fast inactivation via an occlusion of the pore on the cytoplasmic side but also by inducement of structural changes at the selectivity

filter. In any event, these data show that the pore region near the selectivity filter is coupled to movement of the DIV voltage sensor specifically.

3 Intracellular Pore Blockers and Channel Gating

3.1 Local Anesthetics, Polyamines, and Associated β Subunits

In addition to block by neurotoxins and divalent cations at the extracellular pore entrance, voltage-gated sodium channels are subject to block at the intracellular side of the pore by local anesthetics such as lidocaine as well as similar charged polyamines such as the tetraalkylammonium molecule QX-314 (Fig. 1b). Local anesthetics exhibit several mechanisms of channel block involving at least two distinct binding sites. At depolarized voltages where channels are active, local anesthetics occupy their high-affinity site at the intracellular mouth of the pore where they completely block ion conduction through single channels (Fozzard et al. 2011). At hyperpolarized potentials these compounds also block the channel in its resting state, albeit with lower affinity. The mechanism of resting state block and its binding site remain unclear, whereas the high-affinity site has been both well localized and better studied. One complication in elucidating the pathway for resting state block is that local anesthetics have pK_as such that they can adopt either charged or neutral forms over a physiological range of pH (Strichartz 1981). Indeed, entry into the cytoplasmic pore cavity via portals buried in the membrane has been posited as a possible route for uncharged molecules such as local anesthetics based on a crystal structure of a bacterial sodium channel (Payandeh et al. 2011), although functional evidence supporting this idea is lacking.

In addition to charged amines, sodium channels have been shown to be blocked from the intracellular side by the hydrophobic tail of the associated β_4 subunit. This hydrophobic tail competes with the fast inactivation motif for binding to the open channel and prevents the pore from closing once bound (Raman and Bean 2001; Grieco et al. 2005). Upon repolarization, unbinding of the β_4 tail results in a transient resurgent current prior to pore closure. Although similar pore block by associated subunits has been observed in other channels such as the BK potassium channel (Gonzalez-Perez et al. 2012), the in vivo role of such a pore-blocking mechanism remains unclear for sodium channels.

3.2 Modulated vs. Guarded Receptor Hypotheses

Similar to TTX and STX at the extracellular pore, local anesthetics and quaternary amines exhibit a use-dependent block at their high-affinity site in response to trains of repetitive depolarizing voltage pulses from a hyperpolarized holding potential (Strichartz 1973) (Fig. 2b). There are two mechanisms that can explain the functional features of this use dependence, both of which postulate that local anesthetics bind in a state-dependent manner. The guarded receptor hypothesis suggests that

local anesthetics can only access their high-affinity binding site when the intracellular channel gate is open, but are physically prevented from reaching it at hyperpolarized potentials where the channel is closed (Strichartz 1973). In contrast, the modulated receptor hypothesis explains the state dependence of local anesthetic binding using an allosteric model where local anesthetic binding stabilizes open or inactivated states, which in turn bind local anesthetics with higher affinity than resting closed states (Hille 1977). In both cases, use dependence reflects the accumulation of blocked channels due to a preference for binding to open/inactivated states which are populated upon channel activation. Although both the modulated and guarded receptor hypotheses can largely explain the functional observations of use-dependent block, they posit two distinct structural mechanisms for these phenomena. This highlights the need for a more detailed understanding of the molecular conformational changes that regulate local anesthetic binding.

Use dependence was originally attributed to preferential binding to inactivated states based on observations that removal of fast inactivation using pronase abolished use-dependent block by QX-314 in squid axons (Cahalan 1978; Yeh 1978). However, removing inactivation using either chloramine-T or modification of an introduced cysteine in the IFM motif failed to eliminate use-dependent block in subsequent studies (Wang et al. 1987; Vedantham and Cannon 1999), raising doubts about the requirement for inactivated states. Indeed, a triple mutant that lacks fast inactivation exhibits similar affinity for lidocaine to that of normally inactivating Nav1.4 wild-type channels, suggesting that open states are sufficient to mediate high-affinity local anesthetic binding (Wang et al. 2004). Interestingly, we have recently shown that this mutant adopts multiple distinct open pore conformations which are kinetically correlated with the movement of individual voltage sensors in wild-type channels, suggesting that these pore conformations reflect channel gating normally occluded by fast inactivation (Goldschen-Ohm et al. 2013). Thus, an intriguing idea is that preferential binding to particular pore conformations driven by voltage sensor gating rather than direct entry into inactivated states may underlie high-affinity binding of local anesthetics.

3.3 A Structural Model of the Inner Pore

The critical residues for high-affinity local anesthetic binding have largely been explored using mutagenesis, which has localized the binding site to the intracellular S6 helices of domains III and IV (Ragsdale et al. 1994; Wright et al. 1998; Wang et al. 2000; Yarov-Yarovoy et al. 2001). Of these, a phenylalanine in domain IV (F1579 in Nav1.4) is critical for high-affinity use-dependent block (Ahern et al. 2008). This residue does not affect resting state block, however, consistent with a separate binding site for the two blocking mechanisms.

Upon binding to their high-affinity site, local anesthetics block ion conduction by both electrostatic repulsion and steric occlusion of the pore. Structural models of bound local anesthetics based on homology models of the inner pore and functional observations of important binding interactions with channel residues suggest that

occupation of their binding site introduces a steric barrier to pore closure (Lipkind and Fozzard 2005), similar to previous observations that quaternary ammonium compounds prevent pore closure in voltage-gated ion channels (Armstrong 1971). Thus, intracellular pore block appears to involve a foot-in-the-door mechanism wherein the pore is held in at least a partially open conformation.

3.4 Interactions Between Inner Pore Blockers and Voltage Sensors

In addition to blocking the pore, local anesthetics and other charged quaternary amine derivatives such as QX-314 modulate the behavior of the voltage sensors. Understanding the mechanisms underlying these interactions is of fundamental importance to determining how the pore and voltage sensors are coupled. The first evidence that local anesthetics were able to influence the movement of the voltage sensors came from gating current studies which found that the binding of local anesthetics such as lidocaine reduced the overall gating charge moved by about one-third (Keynes and Rojas 1974; Peganov and Khodorov 1977; Cahalan 1978; Cahalan and Almers 1979; Tanguy and Yeh 1989; Hanck et al. 1994), similar to tetraethylammonium block of voltage-gated potassium channels (Bezanilla et al. 1991). Subsequent mutagenesis showed that the fraction of immobilized charge was reduced upon neutralization of gating charges specifically in domains III and IV, suggesting that local anesthetics primarily immobilized the voltage sensors for these two domains (Sheets and Hanck 2003; Fozzard et al. 2011). The immobilization of the DIII voltage sensor by local anesthetics is abolished along with high-affinity binding upon mutation of F1579 in the DIV S6 of Nav1.4, indicating that resting state block does not involve immobilization of the gating charges (Muroi and Chanda 2009).

To determine the domain-specific effects of local anesthetic binding on individual voltage sensors, we monitored the movement of each specific voltage-sensing domain with a site-specific fluorescent probe on the N-terminal end of the S4 segment (Muroi and Chanda 2009). These labeling sites have previously been shown to track voltage sensor movement in that they display kinetics correlated with those of gating currents (Chanda and Bezanilla 2002). Consistent with previous gating current studies, lidocaine shifted the fluorescence–voltage (F–V) curve to more hyperpolarized voltages for DIII, with no obvious effect on DI or DII (Muroi and Chanda 2009). QX-314 also shifted the F–V more than 50 mV in the hyperpolarizing direction, with a smaller hyperpolarizing shift observed for DIV. These data corroborate previous mutagenesis results and further suggest that the reduction in gating charge movement for domains III and IV is due to their being held in an activated or semi-activated conformation upon local anesthetic binding. Given the binding site between the S6 helices of DIII and DIV, we suggest that local anesthetic binding prevents the DIII and DIV S6 pore helices from fully closing, which in turn stabilizes the voltage sensors from these domains in at least a partially activated conformation. A cartoon illustrating such a mechanism for lidocaine

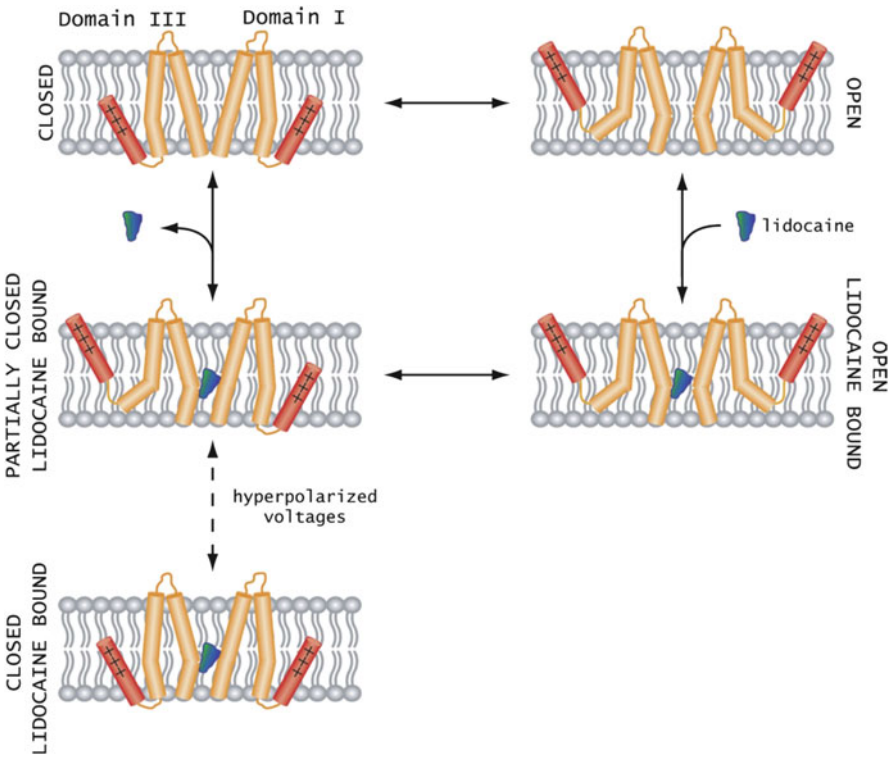

Fig. 3 Cartoon depicting a plausible structural mechanism of local anesthetic binding to voltage-gated sodium channels (from Arcisio-Miranda et al. 2010). For clarity, only domains I and III are shown. Here, lidocaine binding is associated with opening of the DIII pore segment specifically, which stabilizes the DIII voltage sensor in an activated conformation

binding is shown in Fig. 3. Interestingly, QX-314 binding had only small effects on the DIV voltage sensor as compared to that of DIII, despite earlier suggestions that local anesthetics bound preferentially to inactivated states for which DIV voltage sensor activation specifically is important.

To address the molecular details of how lidocaine binding in the pore holds the domain III voltage sensor in its activated conformation, we performed tryptophan scanning mutagenesis along the pore and S4–5 linker regions of domain III in conjunction with site-specific fluorescent measurements from a fluorophore on the N-terminal end of the DIII S4 segment. We identified several mutations in the S4 and S5 and S6 helices that had little effect on pore block by lidocaine, but reduced the stabilization of the outer portion of the domain III voltage sensor (Arcisio-Miranda et al. 2010). Thus, these mutations functionally uncoupled lidocaine binding from outward stabilization of the DIII voltage sensor. The simplest explanation for these results is that these residues are involved specifically in mediating local anesthetic binding to immobilization of the DIII voltage sensor and more generally in coupling between voltage sensor activation and pore opening. The

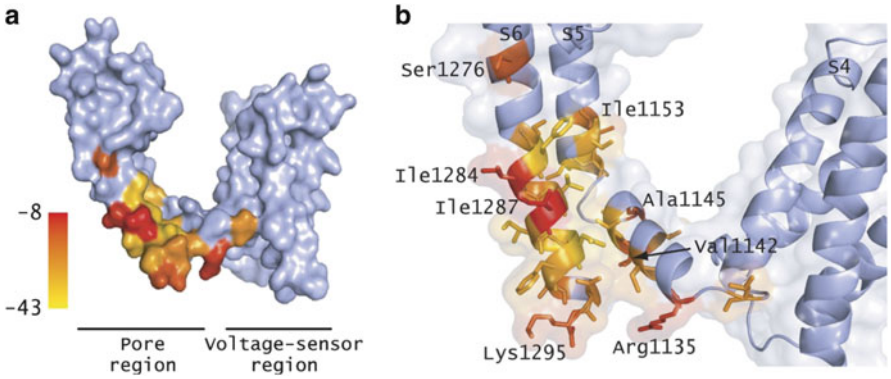

Fig. 4 Residues involved in mediating interactions between the pore and voltage sensor of domain III mapped to the hinge regions of the S4–5 linker and S5/6 pore helices in a homology model (from Arcisio-Miranda et al. 2010). (**a**) Domain III shown in surface representation with residues involved in transmitting local anesthetic binding to immobilization of the voltage sensor colored from *yellow to red* according to the shift in the voltage dependence of fluorescence from a probe on the N-terminal end of the DIII voltage sensor. (**b**) Same as in (**a**) with transparent surface representation and important residues shown in licorice representation

identified residues fall in regions where fairly rigid alpha helices bend or kink in a homology model of the channel (Fig. 4), suggesting that voltage sensor movement may be coupled to the pore via the rigid helices connected by elastic hinges.

4 Future Directions

Although functional studies with pore blockers have revealed a wealth of information regarding the nature of the gating mechanisms coupling voltage sensing to pore opening, very little is known about their structural underpinnings. At present we do not have a structure of a eukaryotic voltage-gated sodium channel. Such structures coupled with detailed functional studies of transitions between various conformations will help refine our ideas of how these channels work.

In particular, there is an emerging understanding that outer pore blockers are intimately coupled with at least one of the voltage sensors (domain IV) as well as gating conformational changes such as those involved in slow inactivation, From a clinical perspective, this suggests that these blockers or derivatives thereof may have therapeutic relevance as novel sodium channel gating modulators.

References

Ackerman MJ (1998) The long QT syndrome: ion channel diseases of the heart. Mayo Clin Proc Mayo Clinic 73:250–269. doi:10.1016/S0025-6196(11)64469-8

Agnew WS, Levinson SR, Brabson JS, Raftery MA (1978) Purification of the tetrodotoxin-binding component associated with the voltage-sensitive sodium channel from Electrophorus electricus electroplax membranes. Proc Natl Acad Sci USA 75(6):2606–2610

Ahern CA, Eastwood AL, Dougherty DA, Horn R (2008) Electrostatic contributions of aromatic residues in the local anesthetic receptor of voltage-gated sodium channels. Circ Res 102:86–94. doi:10.1161/CIRCRESAHA.107.160663

Arcisio-Miranda M, Muroi Y, Chowdhury S, Chanda B (2010) Molecular mechanism of allosteric modification of voltage-dependent sodium channels by local anesthetics. J Gen Physiol 136:541–554. doi:10.1085/jgp.201010438

Armstrong CM (1971) Interaction of tetraethylammonium ion derivatives with the potassium channels of giant axons. J Gen Physiol 58:413–437

Backx PH, Yue DT, Lawrence JH, Marban E, Tomaselli GF (1992) Molecular localization of an ion-binding site within the pore of mammalian sodium channels. Science 257:248–251

Balser JR, Nuss HB, Chiamvimonvat N, Pérez-García MT, Marban E, Tomaselli GF (1996) External pore residue mediates slow inactivation in mu 1 rat skeletal muscle sodium channels. J Physiol 494(Pt 2):431–442

Banerjee A, Lee A, Campbell E, MacKinnon R (2013) Structure of a pore-blocking toxin in complex with a eukaryotic voltage-dependent K + channel. eLife 2:e00594–e00594. doi:10.7554/eLife.00594

Barchi RL, Weigele JB (1979) Characteristics of saxitoxin binding to the sodium channel of sarcolemma isolated from rat skeletal muscle. J Physiol 295:383–396

Becker S, Prusak-Sochaczewski E, Zamponi G, Beck-Sickinger AG, Gordon RD, French RJ (1992) Action of derivatives of mu-conotoxin GIIIA on sodium channels. Single amino acid substitutions in the toxin separately affect association and dissociation rates. Biochemistry 31:8229–8238

Bénitah JP, Chen Z, Balser JR, Tomaselli GF, Marbán E (1999) Molecular dynamics of the sodium channel pore vary with gating: interactions between P-segment motions and inactivation. J Neurosci 19:1577–1585

Bezanilla F (2000) The voltage sensor in voltage-dependent ion channels. Physiol Rev 80:555–592

Bezanilla F, Perozo E, Papazian DM, Stefani E (1991) Molecular basis of gating charge immobilization in Shaker potassium channels. Science (New York, NY) 254:679–683

Bosmans F, Martin-Eauclaire M-F, Swartz KJ (2008) Deconstructing voltage sensor function and pharmacology in sodium channels. Nature 456:202–208. doi:10.1038/nature07473

Cahalan MD (1978) Local anesthetic block of sodium channels in normal and pronase-treated squid giant axons. Biophys J 23:285–311. doi:10.1016/S0006-3495(78)85449-6

Cahalan MD, Almers W (1979) Interactions between quaternary lidocaine, the sodium channel gates, and tetrodotoxin. Biophys J 27:39–55. doi:10.1016/S0006-3495(79)85201-7

Cannon SC (1996) Sodium channel defects in myotonia and periodic paralysis. Annu Rev Neurosci 19:141–164. doi:10.1146/annurev.ne.19.030196.001041

Capes DL, Arcisio-Miranda M, Jarecki BW, French RJ, Chanda B (2012) Gating transitions in the selectivity filter region of a sodium channel are coupled to the domain IV voltage sensor. Proc Natl Acad Sci U S A 109:2648–2653. doi:10.1073/pnas.1115575109

Catterall WA (2010) Ion channel voltage sensors: structure, function, and pathophysiology. Neuron 67:915–928. doi:10.1016/j.neuron.2010.08.021

Catterall WA, Cestèle S, Yarov-Yarovoy V, Yu FH, Konoki K, Scheuer T (2007) Voltage-gated ion channels and gating modifier toxins. Toxicon 49:124–141. doi:10.1016/j.toxicon.2006.09.022

Chahine M, George AL, Zhou M, Ji S, Sun W, Barchi RL, Horn R (1994) Sodium channel mutations in paramyotonia congenita uncouple inactivation from activation. Neuron 12:281–294

Chanda B, Bezanilla F (2002) Tracking voltage-dependent conformational changes in skeletal muscle sodium channel during activation. J Gen Physiol 120:629–645

Chang NS, French RJ, Lipkind GM, Fozzard HA, Dudley S (1998) Predominant interactions between mu-conotoxin Arg-13 and the skeletal muscle Na + channel localized by mutant cycle analysis. Biochemistry 37:4407–4419. doi:10.1021/bi9724927

Chen LQ, Santarelli V, Horn R, Kallen RG (1996) A unique role for the S4 segment of domain 4 in the inactivation of sodium channels. J Gen Physiol 108:549–556

Choudhary G, Aliste MP, Tieleman DP, French RJ, Dudley SC (2007) Docking of mu-conotoxin GIIIA in the sodium channel outer vestibule. Channels (Austin, Tex) 1:344–52

Cohen CJ, Bean BP, Colatsky TJ, Tsien RW (1981) Tetrodotoxin block of sodium channels in rabbit Purkinje fibers. Interactions between toxin binding and channel gating. J Gen Physiol 78:383–411

Cordero-Morales JF, Cuello LG, Perozo E (2006) Voltage-dependent gating at the KcsA selectivity filter. Nat Struct Mol Biol 13:319–322. doi:10.1038/nsmb1070

Cuello LG, Jogini V, Cortes DM, Perozo E (2010) Structural mechanism of C-type inactivation in K(+) channels. Nature 466:203–208. doi:10.1038/nature09153

Doyle DD, Guo Y, Lustig SL, Satin J, Rogart RB, Fozzard HA (1993) Divalent cation competition with [3H]saxitoxin binding to tetrodotoxin-resistant and -sensitive sodium channels. A two-site structural model of ion/toxin interaction. J Gen Physiol 101:153–182

Dudley SC, Chang N, Hall J, Lipkind G, Fozzard HA, French RJ (2000) mu-conotoxin GIIIA interactions with the voltage-gated Na(+) channel predict a clockwise arrangement of the domains. J Gen Physiol 116:679–690

Dumaine R, Hartmann HA (1996) Two conformational states involved in the use-dependent TTX blockade of human cardiac Na + channel. Am J Physiol 270:H2029–H2037

Favre I, Moczydlowski E, Schild L (1995) Specificity for block by saxitoxin and divalent cations at a residue which determines sensitivity of sodium channel subtypes to guanidinium toxins. J Gen Physiol 106:203–229

Fozzard HA, Lipkind GM (2010) The tetrodotoxin binding site is within the outer vestibule of the sodium channel. Marine Drugs 8:219–234. doi:10.3390/md8020219

Fozzard HA, Sheets MF, Hanck DA (2011) The sodium channel as a target for local anesthetic drugs. Front Pharmacol 2:68. doi:10.3389/fphar.2011.00068

French RJ, Worley JF, Krueger BK (1984) Voltage-dependent block by saxitoxin of sodium channels incorporated into planar lipid bilayers. Biophys J 45:301–310. doi:10.1016/S0006-3495(84)84156-9

Gamal El-Din TM, Grögler D, Lehmann C, Heldstab H, Greeff NG (2008) More gating charges are needed to open a Shaker K + channel than are needed to open an rBIIA Na + channel. Biophys J 95:1165–1175. doi:10.1529/biophysj.108.130765

Goldschen-Ohm MP, Capes DL, Oelstrom KM, Chanda B (2013) Multiple pore conformations driven by asynchronous movements of voltage sensors in a eukaryotic sodium channel. Nat Commun 4:1350. doi:10.1038/ncomms2356

Gonzalez-Perez V, Zeng X-H, Henzler-Wildman K, Lingle CJ (2012) Stereospecific binding of a disordered peptide segment mediates BK channel inactivation. Nature 485:133–136. doi:10.1038/nature10994

Green WN, Weiss LB, Andersen OS (1987) Batrachotoxin-modified sodium channels in planar lipid bilayers. Characterization of saxitoxin- and tetrodotoxin-induced channel closures. J Gen Physiol 89:873–903

Grieco TM, Malhotra JD, Chen C, Isom LL, Raman IM (2005) Open-channel block by the cytoplasmic tail of sodium channel beta4 as a mechanism for resurgent sodium current. Neuron 45:233–244. doi:10.1016/j.neuron.2004.12.035

Hanck DA, Makielski JC, Sheets MF (1994) Kinetic effects of quaternary lidocaine block of cardiac sodium channels: a gating current study. J Gen Physiol 103:19–43

Heinemann SH, Terlau H, Imoto K (1992) Molecular basis for pharmacological differences between brain and cardiac sodium channels. Pflugers Archiv European. J Physiol 422:90–92

Henderson R, Ritchie JM, Strichartz GR (1974) Evidence that tetrodotoxin and saxitoxin act at a metal cation binding site in the sodium channels of nerve membrane. Proc Natl Acad Sci U S A 71:3936–3940

Hille B (1975) The receptor for tetrodotoxin and saxitoxin. A structural hypothesis. Biophys J 15:615–619. doi:10.1016/S0006-3495(75)85842-5

Hille B (1977) Local anesthetics: hydrophilic and hydrophobic pathways for the drug-receptor reaction. J Gen Physiol 69:497–515

Hirschberg B, Rovner A, Lieberman M, Patlak J (1995) Transfer of twelve charges is needed to open skeletal muscle Na + channels. J Gen Physiol 106:1053–1068

Hodgkin AL, Huxley AF (1952) A quantitative description of membrane current and its application to conduction and excitation in nerve. J Physiol 117:500–544

Huang C-J, Schild L, Moczydlowski EG (2012) Use-dependent block of the voltage-gated Na(+) channel by tetrodotoxin and saxitoxin: effect of pore mutations that change ionic selectivity. J Gen Physiol 140:435–454. doi:10.1085/jgp.201210853

Hui K, Lipkind G, Fozzard HA, French RJ (2002) Electrostatic and steric contributions to block of the skeletal muscle sodium channel by mu-conotoxin. J Gen Physiol 119:45–54

Jurkat-Rott K, Holzherr B, Fauler M, Lehmann-Horn F (2010) Sodium channelopathies of skeletal muscle result from gain or loss of function. Pflügers Archiv 460:239–248. doi:10.1007/s00424-010-0814-4

Kambouris NG, Nuss HB, Johns DC, Tomaselli GF, Marban E, Balser JR (1998) Phenotypic characterization of a novel long-QT syndrome mutation (R1623Q) in the cardiac sodium channel. Circulation 97:640–644

Keynes RD, Rojas E (1974) Kinetics and steady-state properties of the charged system controlling sodium conductance in the squid giant axon. J Physiol 239:393–434

Lee CH, Ruben PC (2008) Interaction between voltage-gated sodium channels and the neurotoxin, tetrodotoxin. Channels (Austin, Tex) 2:407–412

Lerche H, Peter W, Fleischhauer R, Pika-Hartlaub U, Malina T, Mitrovic N, Lehmann-Horn F (1997) Role in fast inactivation of the IV/S4-S5 loop of the human muscle Na + channel probed by cysteine mutagenesis. J Physiol 505(Pt 2):345–352

Li RA, Tsushima RG, Kallen RG, Backx PH (1997) Pore residues critical for mu-CTX binding to rat skeletal muscle Na+ channels revealed by cysteine mutagenesis. Biophys J 73:1874–1884. doi:10.1016/S0006-3495(97)78218-3

Li RA, Ennis IL, French RJ, Dudley SC, Tomaselli GF, Marbán E (2001) Clockwise domain arrangement of the sodium channel revealed by (mu)-conotoxin (GIIIA) docking orientation. J Biol Chem 276:11072–11077. doi:10.1074/jbc.M010862200

Li RA, Hui K, French RJ, Sato K, Henrikson CA, Tomaselli GF, Marbán E (2003) Dependence of mu-conotoxin block of sodium channels on ionic strength but not on the permeating [Na+]: implications for the distinctive mechanistic interactions between Na + and K + channel pore-blocking toxins and their molecular targets. J Biol Chem 278:30912–30919. doi:10.1074/jbc.M301039200

Lipkind GM, Fozzard HA (2005) Molecular modeling of local anesthetic drug binding by voltage-gated sodium channels. Mol Pharmacol 68:1611–1622. doi:10.1124/mol.105.014803

Liu Z, Dai J, Chen Z, Hu W, Xiao Y, Liang S (2003) Isolation and characterization of hainantoxin-IV, a novel antagonist of tetrodotoxin-sensitive sodium channels from the Chinese bird spider Selenocosmia hainana. CMLS 60:972–978. doi:10.1007/s00018-003-2354-x

Long SB, Campbell EB, Mackinnon R (2005) Crystal structure of a mammalian voltage-dependent Shaker family K+ channel. Science (New York, NY) 309:897–903. doi:doi:10.1126/science.1116269

Lönnendonker U (1989) Use-dependent block of sodium channels in frog myelinated nerve by tetrodotoxin and saxitoxin at negative holding potentials. Biochim Biophys Acta 985:153–160

López-Barneo J, Hoshi T, Heinemann SH, Aldrich RW (1993) Effects of external cations and mutations in the pore region on C-type inactivation of Shaker potassium channels. Receptors Channels 1:61–71

Makielski JC, Satin J, Fan Z (1993) Post-repolarization block of cardiac sodium channels by saxitoxin. Biophys J 65:790–798. doi:10.1016/S0006-3495(93)81102-0

McArthur JR, Ostroumov V, Al-Sabi A, McMaster D, French RJ (2011) Multiple, distributed interactions of μ-conotoxin PIIIA associated with broad targeting among voltage-gated sodium channels. Biochemistry 50:116–124. doi:10.1021/bi101316y

McCusker EC, Bagnéris C, Naylor CE, Cole AR, D'Avanzo N, Nichols CG, Wallace BA (2012) Structure of a bacterial voltage-gated sodium channel pore reveals mechanisms of opening and closing. Nat Commun 3:1102. doi:10.1038/ncomms2077

McPhee JC, Ragsdale DS, Scheuer T, Catterall WA (1998) A critical role for the S4-S5 intracellular loop in domain IV of the sodium channel alpha-subunit in fast inactivation. J Biol Chem 273:1121–1129

Moczydlowski EG (2013) The molecular mystique of tetrodotoxin. Toxicon 63:165–183. doi:10.1016/j.toxicon.2012.11.026

Moczydlowski E, Garber SS, Miller C (1984) Batrachotoxin-activated Na + channels in planar lipid bilayers. Competition of tetrodotoxin block by Na+. J Gen Physiol 84:665–686

Muroi Y, Chanda B (2009) Local anesthetics disrupt energetic coupling between the voltage-sensing segments of a sodium channel. J Gen Physiol 133:1–15. doi:10.1085/jgp.200810103

Ong BH, Tomaselli GF, Balser JR (2000) A structural rearrangement in the sodium channel pore linked to slow inactivation and use dependence. J Gen Physiol 116:653–662

Patton DE, Goldin AL (1991) A voltage-dependent gating transition induces use-dependent block by tetrodotoxin of rat IIA sodium channels expressed in Xenopus oocytes. Neuron 7:637–647

Payandeh J, Scheuer T, Zheng N, Catterall WA (2011) The crystal structure of a voltage-gated sodium channel. Nature 475:353–358. doi:10.1038/nature10238

Peganov EM, Khodorov BI (1977) Gating current in the membrane of nodes of Ranvier under conditions of linear alteration of the membrane potential. Biulleten' eksperimental'noĭ biologii i meditsiny 84:515–518

Peng K, Shu Q, Liu Z, Liang S (2002) Function and solution structure of huwentoxin-IV, a potent neuronal tetrodotoxin (TTX)-sensitive sodium channel antagonist from Chinese bird spider Selenocosmia huwena. J Biol Chem 277:47564–47571. doi:10.1074/jbc.M204063200

Ragsdale DS, McPhee JC, Scheuer T, Catterall WA (1994) Molecular determinants of state-dependent block of Na + channels by local anesthetics. Science (New York, NY) 265:1724–1728

Raman IM, Bean BP (2001) Inactivation and recovery of sodium currents in cerebellar Purkinje neurons: evidence for two mechanisms. Biophys J 80:729–737. doi:10.1016/S0006-3495(01)76052-3

Reed JK, Raftery MA (1976) Properties of the tetrodotoxin binding component in plasma membranes isolated from Electrophorus electricus. Biochemistry 15:944–953

Salgado VL, Yeh JZ, Narahashi T (1986) Use- and voltage-dependent block of the sodium channel by saxitoxin. Ann N Y Acad Sci 479:84–95. doi:10.1111/j.1749-6632.1986.tb15563.x

Santarelli VP, Eastwood AL, Dougherty DA, Ahern CA, Horn R (2007) Calcium block of single sodium channels: role of a pore-lining aromatic residue. Biophys J 93:2341–2349. doi:10.1529/biophysj.107.106856

Schild L, Moczydlowski E (1991) Competitive binding interaction between Zn2+ and saxitoxin in cardiac Na + channels. Evidence for a sulfhydryl group in the Zn2+/saxitoxin binding site. Biophys J 59:523–537. doi:10.1016/S0006-3495(91)82269-X

Schoppa NE, Sigworth FJ (1998) Activation of shaker potassium channels. I. Characterization of voltage-dependent transitions. J Gen Physiol 111:271–294

Sheets MF, Hanck DA (1992) Mechanisms of extracellular divalent and trivalent cation block of the sodium current in canine cardiac Purkinje cells. J Physiology 454:299–320

Sheets MF, Hanck DA (2003) Molecular action of lidocaine on the voltage sensors of sodium channels. J Gen Physiol 121:163–175

Sheets MF, Kyle JW, Kallen RG, Hanck DA (1999) The Na channel voltage sensor associated with inactivation is localized to the external charged residues of domain IV, S4. Biophys J 77:747–757. doi:10.1016/S0006-3495(99)76929-8

Starmer CF, Grant AO, Strauss HC (1984) Mechanisms of use-dependent block of sodium channels in excitable membranes by local anesthetics. Biophys J 46:15–27. doi:10.1016/S0006-3495(84)83994-6

Stefani E, Bezanilla F (1998) Cut-open oocyte voltage-clamp technique. Meth Enzymol 293:300–318

Strichartz GR (1973) The inhibition of sodium currents in myelinated nerve by quaternary derivatives of lidocaine. J Gen Physiol 62:37–57

Strichartz GR (1981) Current concepts of the mechanism of action of local anesthetics. J Dent Res 60:1460–1467. doi:10.1177/00220345810600080904

Tanguy J, Yeh JZ (1989) QX-314 restores gating charge immobilization abolished by chloramine-T treatment in squid giant axons. Biophys J 56:421–427. doi:10.1016/S0006-3495(89)82688-8

Terlau H, Olivera BM (2004) Conus venoms: a rich source of novel ion channel-targeted peptides. Physiol Rev 84:41–68. doi:10.1152/physrev.00020.2003

Tikhonov DB, Zhorov BS (2012) Architecture and pore block of eukaryotic voltage-gated sodium channels in view of NavAb bacterial sodium channel structure. Mol Pharmacol 82:97–104. doi:10.1124/mol.112.078212

Todt H, Dudley SC, Kyle JW, French RJ, Fozzard HA (1999) Ultra-slow inactivation in mu1 Na + channels is produced by a structural rearrangement of the outer vestibule. Biophys J 76:1335–1345. doi:10.1016/S0006-3495(99)77296-6

Townsend C, Horn R (1997) Effect of alkali metal cations on slow inactivation of cardiac Na + channels. J Gen Physiol 110:23–33

Vandenberg CA, Bezanilla F (1991) A sodium channel gating model based on single channel, macroscopic ionic, and gating currents in the squid giant axon. Biophys J 60:1511–1533. doi:10.1016/S0006-3495(91)82186-5

Vedantham V, Cannon SC (1999) The position of the fast-inactivation gate during lidocaine block of voltage-gated Na + channels. J Gen Physiol 113:7–16

Wallace RH, Wang DW, Singh R, Scheffer IE, George AL, Phillips HA, Saar K, Reis A, Johnson EW, Sutherland GR, Berkovic SF, Mulley JC (1998) Febrile seizures and generalized epilepsy associated with a mutation in the Na + -channel beta1 subunit gene SCN1B. Nat Genet 19:366–370. doi:10.1038/1252

Wang GK, Brodwick MS, Eaton DC, Strichartz GR (1987) Inhibition of sodium currents by local anesthetics in chloramine-T-treated squid axons. The role of channel activation. J Gen Physiol 89:645–667

Wang Q, Shen J, Splawski I, Atkinson D, Li Z, Robinson JL, Moss AJ, Towbin JA, Keating MT (1995) SCN5A mutations associated with an inherited cardiac arrhythmia, long QT syndrome. Cell 80:805–811

Wang SY, Nau C, Wang GK (2000) Residues in Na(+) channel D3-S6 segment modulate both batrachotoxin and local anesthetic affinities. Biophys J 79:1379–1387. doi:10.1016/S0006-3495(00)76390-9

Wang S-Y, Mitchell J, Moczydlowski E, Wang GK (2004) Block of inactivation-deficient Na + channels by local anesthetics in stably transfected mammalian cells: evidence for drug binding along the activation pathway. J Gen Physiol 124:691–701. doi:10.1085/jgp.200409128

Weigele JB, Barchi RL (1978) Saxitoxin binding to the mammalian sodium channel. Competition by monovalent and divalent cations. FEBS Lett 95:49–53

Woodhull AM (1973) Ionic blockage of sodium channels in nerve. J Gen Physiol 61:687–708

Worley JF, French RJ, Krueger BK (1986) Trimethyloxonium modification of single batrachotoxin-activated sodium channels in planar bilayers. Changes in unit conductance and in block by saxitoxin and calcium. J Gen Physiol 87:327–349

Wright SN, Wang SY, Wang GK (1998) Lysine point mutations in Na + channel D4-S6 reduce inactivated channel block by local anesthetics. Mol Pharmacol 54:733–739

Xiong W, Li RA, Tian Y, Tomaselli GF (2003) Molecular motions of the outer ring of charge of the sodium channel: do they couple to slow inactivation? J Gen Physiol 122:323–332. doi:10.1085/jgp.200308881

Xiong W, Farukhi YZ, Tian Y, Disilvestre D, Li RA, Tomaselli GF (2006) A conserved ring of charge in mammalian Na + channels: a molecular regulator of the outer pore conformation during slow inactivation. J Physiol 576:739–754. doi:10.1113/jphysiol.2006.115105

Xue T, Ennis IL, Sato K, French RJ, Li RA (2003) Novel interactions identified between micro -Conotoxin and the Na + channel domain I P-loop: implications for toxin-pore binding geometry. Biophys J 85:2299–2310

Yamamoto D, Yeh JZ, Narahashi T (1984) Voltage-dependent calcium block of normal and tetramethrin-modified single sodium channels. Biophys J 45:337–344. doi:10.1016/S0006-3495(84)84159-4

Yarov-Yarovoy V, Brown J, Sharp EM, Clare JJ, Scheuer T, Catterall WA (2001) Molecular determinants of voltage-dependent gating and binding of pore-blocking drugs in transmembrane segment IIIS6 of the Na(+) channel alpha subunit. J Biol Chem 276:20–27. doi:10.1074/jbc.M006992200

Yeh JZ (1978) Sodium inactivation mechanism modulates QX-314 block of sodium channels in squid axons. Biophys J 24:569–574. doi:10.1016/S0006-3495(78)85403-4

Zagotta WN, Hoshi T, Aldrich RW (1994) Shaker potassium channel gating. III: Evaluation of kinetic models for activation. J Gen Physiol 103:321–362

Zarrabi T, Cervenka R, Sandtner W, Lukacs P, Koenig X, Hilber K, Mille M, Lipkind GM, Fozzard HA, Todt H (2010) A molecular switch between the outer and the inner vestibules of the voltage-gated Na + channel. J Biol Chem 285:39458–39470. doi:10.1074/jbc.M110.132886

Zhang M-M, Green BR, Catlin P, Fiedler B, Azam L, Chadwick A, Terlau H, McArthur JR, French RJ, Gulyas J, Rivier JE, Smith BJ, Norton RS, Olivera BM, Yoshikami D, Bulaj G (2007) Structure/function characterization of micro-conotoxin KIIIA, an analgesic, nearly irreversible blocker of mammalian neuronal sodium channels. J Biol Chem 282:30699–30706. doi:10.1074/jbc.M704616200

Zhang M-M, McArthur JR, Azam L, Bulaj G, Olivera BM, French RJ, Yoshikami D (2009) Synergistic and antagonistic interactions between tetrodotoxin and mu-conotoxin in blocking voltage-gated sodium channels. Channels 3:32–38

Animal Toxins Influence Voltage-Gated Sodium Channel Function

John Gilchrist, Baldomero M. Olivera, and Frank Bosmans

Contents

Abstract

Voltage-gated sodium (Nav) channels are essential contributors to neuronal excitability, making them the most commonly targeted ion channel family by toxins found in animal venoms. These molecules can be used to probe the functional aspects of Nav channels on a molecular level and to explore their physiological role in normal and diseased tissues. This chapter summarizes our existing knowledge of the mechanisms by which animal toxins influence Nav channels as well as their potential application in designing therapeutic drugs.

J. Gilchrist
Department of Physiology, Johns Hopkins University, School of Medicine, Baltimore, MD 21205, USA

B.M. Olivera (✉)
Department of Biology, University of Utah, Salt Lake City, UT 84112, USA
e-mail: olivera@biology.utah.edu

F. Bosmans (✉)
Department of Physiology, Johns Hopkins University, School of Medicine, Baltimore, MD 21205, USA

Department of Neuroscience, Solomon H. Snyder, Johns Hopkins University, School of Medicine, Baltimore, MD 21205, USA
e-mail: frankbosmans@jhmi.edu

P.C. Ruben (ed.), *Voltage Gated Sodium Channels*, Handbook of Experimental Pharmacology 221, DOI 10.1007/978-3-642-41588-3_10,

Keywords
Sodium channel • Animal toxin • Pore-blocker • Gating-modifier • Venom

1 Introduction

Voltage-gated sodium (Nav) channels regulate the Na^+ permeability of the cell membrane, thereby generating electrical signals that encode and propagate vital information across long distances (Catterall 2000; Hille 2001; Hodgkin and Huxley 1952; Ashcroft 1999). Venomous animals and poisonous plants readily exploit this excitatory role by producing toxins that modify Nav channel opening or closing (e.g., gating) with the goal of incapacitating prey or as defense against predators (Bosmans and Swartz 2010; Catterall et al. 2007; Billen et al. 2008; Smith and Blumenthal 2007; Mebs 2002; Escoubas et al. 2002; de la Vega et al. 2005). Historically, toxins from spider, scorpion, sea anemone, cone snail, insect venoms, and plant extracts have been used to describe diverse receptor sites in particular regions of the nine Nav channel isoforms that have been identified in various mammalian tissues (Nav1.1–Nav1.9) (Catterall 1980; Martin-Eauclaire and Couraud 1992; Catterall et al. 2005; Terlau and Olivera 2004; Honma and Shiomi 2006; Hanck and Sheets 2007). Based on their primary amino acid sequence, all Nav channel isoforms seem to be similarly configured and consist of four domains (I–IV) that each contains a voltage sensor and a portion of the structure that forms the Na^+-selective pore which can open upon activation of the four voltage sensors in response to changes in membrane potential (Catterall 2000; Bosmans et al. 2008; Cha et al. 1999; Chanda and Bezanilla 2002; Horn et al. 2000; Sheets et al. 1999, 2000). The voltage sensors in domains I–III are essential for channel opening, whereas domain IV movement is crucial for terminating the Na^+ flux after the channel has opened by initiating fast inactivation (Billen et al. 2008; Cha et al. 1999; Chanda and Bezanilla 2002; Horn et al. 2000; Sheets et al. 1999, 2000; Campos et al. 2008; Capes et al. 2012). Similar to voltage-activated potassium (Kv) channels (Bosmans et al. 2008; Alabi et al. 2007; Jiang et al. 2003; Long et al. 2007; Phillips et al. 2005; Ruta and MacKinnon 2004; Swartz 2007; Swartz and MacKinnon 1997a, b; Xu et al. 2013), each Nav channel voltage sensor possesses a conserved S3b-S4 motif, or paddle motif, which drives activation of the voltage sensor in each domain and opening of the pore (Billen et al. 2008; Bosmans et al. 2011; Xiao et al. 2008; Campos et al. 2007, 2008). As is the case with Kv channels, each of the four Nav channel paddle motifs is a key pharmacological target for a range of animal toxins (Bosmans and Swartz 2010; Bosmans et al. 2008, 2011; Xiao et al. 2008; Rogers et al. 1996).

Overall, toxins that influence Nav channel function do so through two distinct mechanisms. Pore-blocking toxins inhibit the flow of Na^+ by binding to the outer vestibule or inside the ion conduction pore (Hille 2001; Terlau and Olivera 2004) whereas gating-modifier toxins interact with a region of the channel that changes conformation during channel opening to alter the gating mechanism (Cahalan 1975; Koppenhofer and Schmidt 1968a, b). Although certain gating-modifier toxins interact

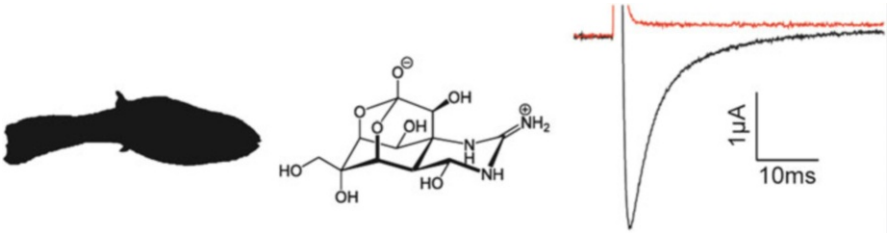

Fig. 1 Tetrodotoxin inhibits Nav channel opening. TTX is found in the Japanese puffer fish (silhouette of *Takifugu rupripes* on the *left*) and has a complex molecular structure (*middle*). At 10 nM, TTX inhibits rNav1.2a currents evoked from a holding potential of −90 mV to a voltage of −20 mV when expressed in *Xenopus* oocytes. *Black* is control and *red* is after addition of 10 nM TTX (*right*)

with the voltage-sensing domains as well as the pore region (Quandt and Narahashi 1982), their subsequent effect on Nav channel gating can usually be associated with their ability to stabilize a voltage sensor in a particular state. As such, in the next sections we will refer to the interaction site of animal toxins within mammalian Nav channels as either the voltage-sensing domains or the pore region and we will further refine this division using the primary functional effects of toxins on channel gating.

2 Toxins Influencing Nav Channel Function by Interacting with the Pore Region

2.1 Non-Peptidic Toxins

2.1.1 Tetrodotoxin and Saxitoxin

The naturally occurring marine toxins tetrodotoxin (TTX) and saxitoxin (STX) interact strongly with the Nav channel pore region to occlude the Na^+ permeation pathway (Fig. 1) (Hille 1975). Both toxins are of great historical and medical value and were originally isolated more than five decades ago from the Japanese Puffer fish (TTX) and marine dinoflagellates (STX) (Furukawa et al. 1959; Moore et al. 1967; Narahashi 1974; Narahashi et al. 1964). STX is perhaps most notorious for its role in paralytic shellfish poisoning, caused by the consumption of toxic shellfish such as clams and mussels. TTX and STX have been used extensively in studying the structural and functional properties of Nav channels. Early work by Narahashi and others revealed that TTX affects neuronal Na^+ currents only when applied to the extracellular surface of the cell and not when perfused inside axons (Narahashi et al. 1964, 1967). After resolving the crystal structure of TTX in 1964 (Woodward 1964) and STX in 1975 (Schantz et al. 1975), this information was used by Hille to predict the diameter of the Nav channel pore (Hille 1975), thereby providing unique insights into the molecular structure of this ion channel family that resonate until this day (Payandeh et al. 2011, 2012; Zhang et al. 2012; McCusker et al. 2012). Later, the low-nanomolar affinity of $^{[3H]}$TTX contributed to the isolation of the Nav channel pore-forming subunit from the electroplaque organ of the electric eel, *Electrophorus*

electricus (Miller et al. 1983; Agnew et al. 1978). Similarly, $^{[3H]}$STX played a vital role in the purification of the neuronal Nav channel from rat brain (Hartshorne and Catterall 1981) and skeletal muscle (Barchi et al. 1980), thereby also revealing the existence of two associated auxiliary subunits (Hartshorne et al. 1982). Nowadays, TTX sensitivity is extensively used to divide the Nav channel family into two groups; TTX-sensitive channels (Nav1.1–Nav1.4, Nav1.6–Nav1.7) are inhibited by nanomolar amounts (Fig. 1), whereas Nav1.8 and Nav1.9 require millimolar quantities to be fully blocked (Catterall 2000). Although Nav1.5 inhibition requires an intermediate micromolar concentration, TTX response can be markedly increased by substituting a cysteine in the domain I S5–S6 loop with a hydrophobic or aromatic residue such as a tryptophan of phenylalanine (Lipkind and Fozzard 1994; Leffler et al. 2005; Sivilotti et al. 1997). The latter amino acids support nanomolar blockade through the formation of a cation–pi interaction with TTX, possibly via an interaction with the charged guanidinium groups within the toxin (Lipkind and Fozzard 1994). These cationic groups also interact with anionic residues within the pore region of the channel to prevent Na^+ conductance. As such, experiments geared toward finding residues that diminished Nav channel TTX sensitivity aided in the discovery of amino acids that create the Nav channel selectivity filter (Terlau et al. 1991), namely an aspartate (DI S5–S6 loop), glutamate (DII S5–S6 loop), lysine (DIII S5–S6 loop), and alanine (DIV S5–S6 loop) (Lipkind and Fozzard 2008). Even though this region of the selectivity filter plays a role in STX interaction as well, other important extracellular residues have now been implicated in forming the STX receptor site (Fozzard and Lipkind 2010), most likely due to supplementary interactions with the additional guanidinium group present within the toxin.

Despite its potential toxicity, clinical trials in which TTX was used to treat various pain disorders have been conducted (Nieto et al. 2012). However, the results are ambiguous and further research is essential. Of note is the peculiar protein saxiphilin, a transferrin-like molecule that binds STX with nanomolar affinity (Morabito and Moczydlowski 1994). Saxiphilin is found across a variety of aquatic and terrestrial species, including fish, reptiles, amphibians, and even arthropods. Notwithstanding its ancient character and global distribution, the physiological role of saxiphilin is not fully understood. A possible contribution to neutralizing dietary or environmental STX seems most obvious, but many animals expressing saxiphilin do not occupy biomes in which they will encounter STX (Llewellyn et al. 1997). Regardless, saxiphilin may still find use as an alternative to animal testing or be incorporated into more efficient STX assays (Llewellyn et al. 1998).

2.1.2 Ciguatoxin and Brevetoxin

Aside from TTX and STX, the cyclic polyether ciguatoxins (Michio et al. 1989) and brevetoxins (Yong-Yeng et al. 1981) found in algae can also cause seafood poisoning. Produced by the dinoflagellates *Gambierdiscus toxicus* (Bagnis et al. 1980) and *Karenia brevis* (Yong-Yeng et al. 1981), *respectively*, these molecules can accumulate in the food chain in fish that are consumed by humans or marine mammals in which they disrupt Nav channel function (Lewis et al. 1991). Although ciguatoxins research has been hindered by the small quantities available from marine fauna (Legrand et al. 1989), this hurdle was recently overcome by Hirama et al. (2001)

when they synthesized CTX3C, thereby permitting easier access to large quantities of purified toxin. Initial forays into algaetoxin pharmacology indicated that ciguatoxin (Bidard et al. 1984) as well as brevetoxin (Lombet et al. 1987), albeit with a much lower affinity (Lombet et al. 1987), can potentiate opening of multiple Nav channel isoforms in addition to altering their Na^+ permeability. As a result, both molecules are capable of inducing spontaneous firing in neurons which eventually leads to paralysis (Benoit et al. 1986). Interestingly, the Nav1.8 isoform found in the periphery seems particularly susceptible to CTX3C, resulting in the appearance of a large persistent current upon toxin exposure, an observation that may in part explain some of the neurological sequelae seen in ciguatera victims (Yamaoka et al. 2009). Although the exact working mechanism is unclear, photolabeling experiments on Nav channels indicate that the S6 segment within domain I and the S5 segment of domain IV are involved in brevetoxin binding (Trainer et al. 1994). Moreover, a study utilizing chimeric Nav1.4 and Nav1.8 channels in combination with CTX3C suggest an interaction site of this toxin within domains I and II (Yamaoka et al. 2009). Finally, it has been suggested that these ladder-like polyether toxins may partition in the membrane to complement a structural motif within the Nav channel (e.g., α-helix) by means of a hydrogen bond network, which may lead to their biological activity (Ujihara et al. 2008).

2.1.3 Batrachotoxin

Well known in popular culture is the image of the jungle cannibal dispatching his prey with poison-tipped darts launched from a blowgun. The poison used here is often found in the secretions of "poison dart frogs" (family *Dendrobatidae*) endemic to Central and South America. While all members of the *Dendrobatidae* secrete toxins, only the *Phyllobates* genus is known to produce batrachotoxin (BTX), a potent Nav channel toxin with an unusual steroidal alkaloid structure (Fig. 2) (Tokuyama et al. 1969). Frogs reared in captivity are not toxic, leading to the conclusion that they acquire and concentrate the toxin from their environment. Similarly, select species of birds from New Guinea (*Ifrita kowaldi* and members of the *Pitohui* genus) are found to secrete BTX onto their skin and feathers (Dumbacher et al. 2000). Dumbacher and coworkers propose that Melyrid beetles may be the dietary source of BTX for both poison-dart frogs and *Pitohui* birds; *Choresine* beetles are known to be rich sources of BTX alkaloids and related species are found in the New World (Dumbacher et al. 2004).

Although the exact working mechanism has yet to be elucidated, the Nav channel receptor site for BTX has been shown to involve a cluster of residues located in the S6 pore-segments of domains I (Wang and Wang 1998), III (Wang et al. 2000; Du et al. 2011), and IV (Linford et al. 1998) and may partially overlap with the binding site of local anesthetics (Wang et al. 1998). Unlike lidocaine, which blocks Na^+ currents, BTX may partially occlude the ion permeation pathway, thereby leaving room for a fraction of Na^+ to pass through the pore. Although BTX may bind within the pore region, the toxin also (1) abolishes fast and slow inactivation (Huang et al. 1982) (Fig. 2) and (2) shifts Nav channel opening to voltages where it is normally closed (Quandt and Narahashi 1982; Bosmans et al. 2004), thereby leading to repeated depolarizations in vivo and eventual paralysis as

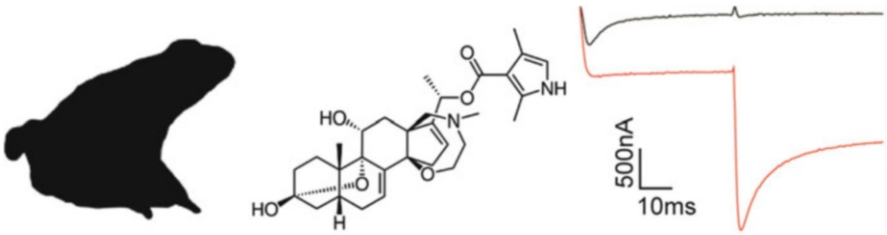

Fig. 2 Batrachotoxin disrupts Nav channel gating. BTX is found in particular frog species (silhouette of *Phyllobates bicolor* on the *left*) and has a complex molecular structure (*middle*). At 5 μM, BTX completely inhibits fast inactivation of rNav1.8 currents evoked from a holding potential of −90 mV to a voltage of 20 mV when expressed in *Xenopus* oocytes. During the second voltage step to −30 mV, channels normally close; however, BTX-bound channels are still deactivating. *Black* is control and *red* is after addition of TTX (*right*)

muscles become insensitive to neuronal signals (Wang and Wang 1998; Linford et al. 1998; Bosmans et al. 2004; Wasserstrom et al. 1993; Catterall 1975).

Even though BTX is unsuitable for drug design, radioactive BTX has been used extensively for Nav channel identification in tissues and vesicles and in screening potential therapeutics (Cooper et al. 1987; Gill et al. 2003). A functional relative of BTX is veratridine, an alkaloid toxin found in *Liliaceae* plants, which causes persistent opening of Nav channels while reducing single-channel conductance (Ulbricht 1998). Although veratridine is thought to interact with the pore-forming S6 segments in open Nav channels, the exact mechanism by which the toxin causes persistent Nav channel opening remains uncertain. Nevertheless, due to its ability to open Nav channels, veratridine is used extensively in drug screening essays for which controlling the membrane voltage is impractical (Felix et al. 2004).

2.2 Peptidic Toxins

2.2.1 Cone Snail Toxins

The pore-blocking μ-conotoxin peptides found in cone snail venom are among the best-characterized Nav channel antagonists. Identifying cone snail venoms likely to contain novel Nav channel pore-blocking peptide toxins was made possible by using the molecular phylogeny framework established for the 700 species of cone snails (Fig. 3). The biological rationale for the presence of these toxins in the venom of a specific subset of *Conus* species is presented here.

Cone snails (Fig. 4) are venomous predatory marine gastropods that are slow moving, unable to swim, and have little in the way of mechanical weaponry for catching their prey. As such, their successful adaptive radiation throughout tropical marine environments required the evolution of venoms that provide the only effective arsenal for capturing their victims. All pore-blocking Nav channel targeting conopeptides characterized to date are found in the venom of cone snail species that specialize in hunting fish as their primary prey (approximately 100 different species of

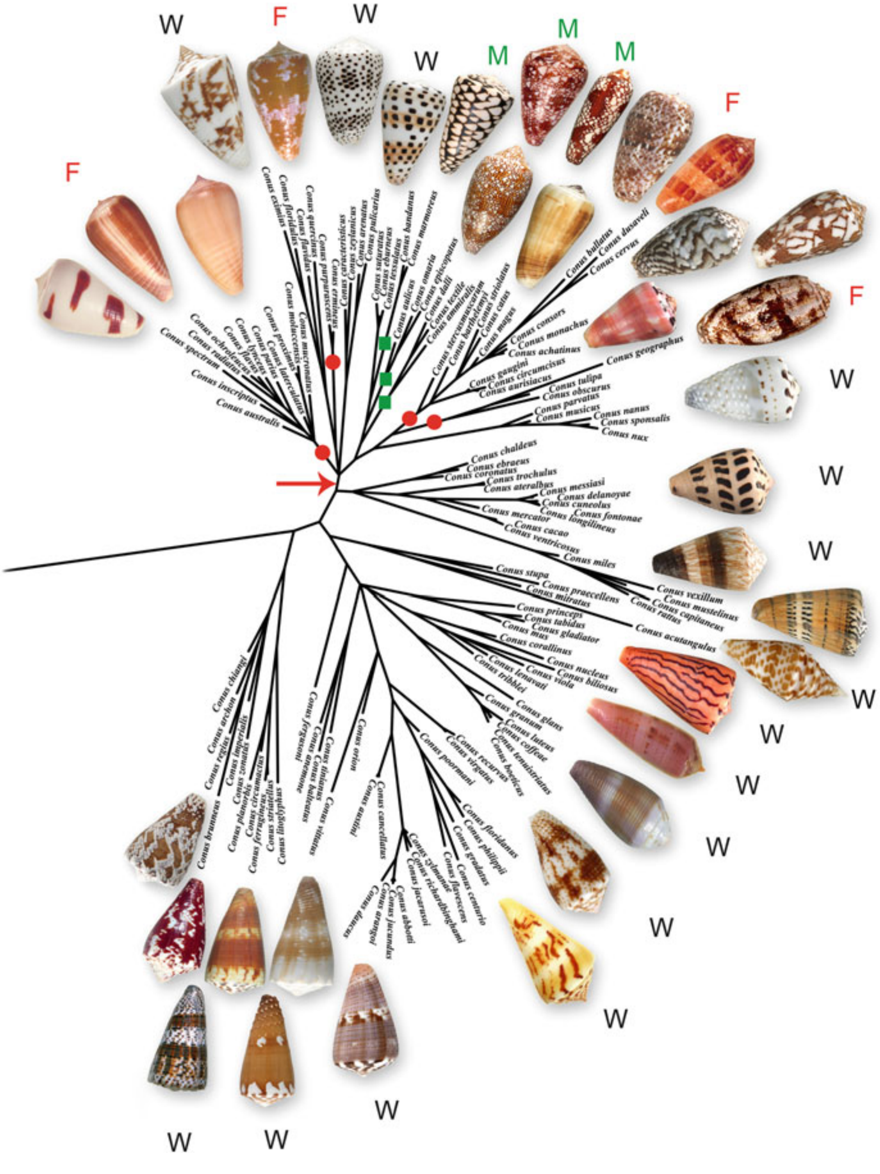

Fig. 3 Phylogenetic tree of a variety of *Conus* species. Fish-hunting clades are labeled with a red dot, mollusc-hunting clades with a green square; others are labeled "W" and are believed to be worm-hunting *Conus*. μ-conotoxins are derived from venoms of fish-hunting clades, whereas the μO-conotoxins are from the venom of a snail-hunting species. The tree is based on 12S mitochondrial rRNA markers; data generated by M. Watkins; tree constructed by J. P. Ownby

Fig. 4 *Conus* shells are remarkably diverse. Shells of fish-hunting *Conus* species listed in Table 1. *Top row*, left to right: *C. consors*; *C. magus*; *C. tulipa*; *C. aurisiacus*; *C. geographus*; and *C. striatus*. *Bottom row*, left to right: *C. bullatus*; *C. stercusmuscarum*; *C. purpurascens*; and *C. striolatus*. Different clades of fish-hunting *Conus* are represented. *Conus purpurascens* belongs to the subgenus *Textilia*, *Conus tulipa* and *Conus geographus* to the subgenus *Gastridium*, and all other species shown to the subgenus *Pionoconus*. Figure prepared by My Hyunh

cone snails are believed to be fish-hunting) (Olivera 1997). In order to block neuromuscular transmission, cone snails evolved groups of peptides that act coordinately (called "cabals") but each on a different molecular target. Among those are the functionally linked signal components of the neuromuscular transmission circuitry, i.e., the nicotinic receptor at the postsynaptic terminus, the presynaptic voltage-gated calcium channels that control neurotransmitter release, and Nav channels that mediate action potential transmission on the muscle membrane (Terlau and Olivera 2004). The most abundantly expressed pore-blocking toxins within cone snail venoms, the μ-conotoxins, primarily interact with Nav1.4, a Nav channel isoform found in skeletal muscle. Nonetheless, the affinity of each peptide for other Nav channel subtypes can vary considerably. By systematically investigating μ-conotoxins from diverse clades of fish-hunting cone snails [see (Baldomero et al. 2014) for a discussion of different lineages of fish-hunting cone snails], a series of peptides with varying neuronal Nav channel selectivity profiles has been obtained. To summarize this work, μ-conotoxins from *Conus* species in five lineages are shown in Table 1 (Wilson et al. 2011) which demonstrates the striking affinity differences of a range of peptides for neuronal Nav channel subtypes.

The importance of μ-conotoxins for the Nav channel field stems from the fact that at the present time, a sufficient diversity of toxins have been characterized to assemble a pharmacological kit for distinguishing various Nav channel isoforms. This toolkit takes advantage of individual μ-conotoxin selectivity for the various neuronal Nav channel subtypes shown in Table 1 (Wilson et al. 2011; Bulaj et al. 2005; Leipold et al. 2011; Zhang et al. 2006). For example, μ-conotoxin SxIIIA is highly selective for Nav1.4 while having at least a 50-fold lower affinity

Table 1 Affinities of μ-conopeptides (μM) for Nav channel subtypes

Peptide	*Conus* species (Fish-hunting clade)	1.1	1.2	1.3	1.4	1.5	1.6	1.7	1.8	
SmIIIA	*C. stercusmuscarum* (1)	0.0038	0.0013	0.035	0.00022	1.3[aa]	0.16[a]	1.3[a]	>100[a]	West et al. (2002)
KIIIA	*C. kinoshitai* (2)	0.29	0.005	8[a]	0.09[a]	287[a]	0.24[a]	0.29	>100[a]	Bulaj et al. (2005)
SIIIA	*C. striatus* (1)	11[a]	0.05	11[a]	0.13[a]	251[a]	0.76[a]	65[a]	>100[a]	Bulaj et al. (2005)
CnIIIA	*C. consors* (1)	14.2[a]	0.25	11[a]	0.27[a]	7.4[a]	7.1[a]	>100[a]	>100[a]	Zhang et al. (2006)
MIIIA	*C. magus* (1)	22.6[a]	0.45	7.7	0.33	>100[a]	21.6[a]	97[a]	>100[a]	Zhang et al. (2006)
GIIIA	*C. geographus* (3)	0.26	17.8[a]	>100[a]	0.019[a]	>100[a]	0.68[a]	>100[a]	>100[a]	Cruz et al. (1985)
PIIIA	*C. purpurascens* (4)	0.12[a]	0.62[a]	3.2[a]	0.036[a]	>100[a]	0.1[a]	>100[a]	>100[a]	Shon et al. (1998)
SxIIIA	*C. striolatus* (1)	0.37[a]	1[a]	>100[a]	0.007[a]	>100[a]	0.57[a]	>100[a]	>100[a]	Walewska et al. (2008)
BuIIIA	*C. bullatus* (5)	0.35	0.012	0.35	0.013	13.8[a]	4.4[a]	>100[a]	>100[a]	Holford et al. (2009)
BuIIIB	*C. bullatus* (5)	0.36	0.013	0.2	0.0036	9[a]	1.8[a]	>100[a]	>100[a]	Kuang et al. (2013)
TIIIA	*C. tulipa* (2)	0.9[a]	0.045	7.9[a]	0.005	>100[a]	25[a]	>100[a]	>100[a]	Lewis et al. (2007)

Fish-hunting clades: (1) *Pionoconus*; (2) *Alfonsoconus*; (3) *Gastridium*; (4) *Chelyconus*; (5) *Textilia*

[a]IC_{50} values; all other values are K_Ds. All Nav channel clones were from rat except Nav1.6, which is from mouse

Table 2 μ-Conopeptide activity matrix: peptides that best discriminate between given pairs of Nav1-isoforms, as revealed by their discrimination index (DI) values

Nav	1.1	1.2	1.3	1.4	1.5	1.6	1.7
1.1		SIIIA	MIIIA	TIIIA	CnIIIA	SIIIA	KIIIA
		2.3	0.5	2.3	0.3	1.2	0.0
1.2	GIIIA		PIIIA	GIIIA	GIIIA	GIIIA	GIIIA
	1.8		−0.7	3.0	−0.8	1.4	−0.8
1.3	GIIIA	KIIIA		SxIIIA	CnIIIA	SxIIIA	KIIIA
	2.6	3.2		4.2	0.2	2.2	1.4
1.4	KIIIA	KIIIA	MIIIA		CnIIIA	KIIIA	KIIIA
	−0.5	1.3	−1.4		−1.4	−0.4	−0.5
1.5	KIIIA	KIIIA	BuIIIB	TIIIA		KIIIA	KIIIA
	3.0	4.8	1.7	4.3		3.1	3.0
1.6	SmIIIA	TIIIA	BuIIIA	TIIIA	CnIIIA		KIIIA
	1.6	2.7	1.1	3.7	0.0		−0.1
1.7	PIIIA	BuIIIB	BuIIIB	BuIIIB	CnIIIA	PIIIA	
	2.9	3.9	2.7	4.4	1.1	3.0	

for all other subtypes, whereas μ-conotoxin KIIIA and CnIIIA predominantly interact with neuronal Nav channel isoforms. Structure–function studies on KIIIA analogs (Bulaj et al. 2005; McArthur et al. 2011; Van Der Haegen et al. 2011; Zhang et al. 2007, 2009, 2010) demonstrate that the binding sites of the μ-conotoxin and TTX overlap but not coincidence. Consequently, it was shown that KIIIA interacts with additional amino acid residues within the pore vestibule (McArthur et al. 2011; Van Der Haegen et al. 2011; Zhang et al. 2007). Thus, different μ-conotoxins presumably interact with a particular subset of residues within the pore, thereby accounting for the diverse targeting selectivity for the various neuronal Nav channel isoforms. This diversity makes it possible to list which μ-conotoxins are most effective for discriminating between any pair of Nav channel isoforms (see Table 2). Zhang et al. (2013a) employed μ-conotoxins to identify particular Nav channel isoforms in native neuronal cell preparations and demonstrated that a combination of three μ-conotoxins is sufficient to determine which TTX-sensitive Nav channel isoform contributes to the Na^+ current in the different neuronal subclasses present in the dorsal root ganglion. As such, the standard Nav channel classification into TTX-sensitive and TTX-resistant classes can be more finely parsed into the individual subtypes, using the appropriate combination of different μ-conotoxins. Zhang and coworkers (Zhang et al. 2013b) also found that auxiliary β-subunits can influence the kinetics of toxin block thereby raising the possibility of employing μ-conotoxins to discriminate different combinations of α- and β-subunits present in native neurons.

2.2.2 Spider Toxins

Although a few spider toxins have been shown to inhibit Na^+ flux without altering channel gating, the mechanism through which they act remains elusive. For

example, the binding site of Tx1 from the *Phoneutria nigriventer* spider may overlap with that of the μ-conotoxin GIIIA, but not that of TTX (Silva et al. 2012). However, additional experiments are needed to clarify the state-dependent binding of Tx1, an observation that suggests an interaction with one or more Nav channel voltage-sensing domains. An additional example is Hainantoxin-I from the *Selenocosmia hainana* tarantula (Li et al. 2003), a toxin that weakly inhibits mammalian Nav channel currents without affecting channel opening or fast inactivation. However, a potential competition with cone snail toxins, TTX, or an interaction with the Nav channel pore region or its voltage sensors has not yet been investigated.

3 Toxins Influencing Nav Channel Gating by Interacting with the Voltage Sensors

3.1 Sea Anemone Toxins

Sea anemones are primitive aquatic animals that possess tentacles containing cells bearing a specialized structure called the nematocyst which, when triggered, injects a mix of toxins into the target. While this venom contains a diversity of chemical components, it is primarily the peptides that have been of great interest to neuroscientists. The majority of peptide toxins that target mammalian Nav channels have been isolated from the venom of the genii *Anemonia*, *Anthopleura*, and *Heteractis* (Kem et al. 1989). Despite this seemingly limited distribution, there are untold numbers of anemone species whose toxic components have not yet been explored, leaving open the possibility of many more bioactive peptides remaining to be discovered (Honma and Shiomi 2006). Sea anemone toxins that act on mammalian Nav channels are typically basic proteins, sharing a conserved arginine at position 14 (Khera and Blumenthal 1996) and a lysine residue around position 37 (Benzinger et al. 1998). The lysine is considered to be crucial for mammalian toxicity (Gallagher and Blumenthal 1994; Norton 2009; Barhanin et al. 1981) and flexibility of the loop containing this residue is important for Nav channel isoform discrimination by the toxin (Gooley et al. 1984; Seibert et al. 2003).

Due to their intimate interaction with the paddle motif in the domain IV voltage sensor (Rogers et al. 1996), sea anemone toxins can (1) inhibit Nav channel fast inactivation at nanomolar concentrations (Fig. 5) (Alsen et al. 1981; Romey et al. 1976; Catterall and Beress 1978), albeit with exceptionally slow on- and off-rates; and (2) enhance recovery from inactivation without affecting Nav channel activation, deactivation, or closed-state inactivation (Hanck and Sheets 2007; Sherif et al. 1992; Richard Benzinger 1999). Although careful studies on various Nav channel isoforms with ATX-II and Ap-B (Fig. 5) reveal that sea anemone toxins exert their effect by delaying domain IV voltage sensor activation, Oliveira and colleagues observed that ATX-II is more potent on Nav1.2 when compared to Nav1.6 (Oliveira et al. 2004). Since the domain IV paddle motif in these two channel isoforms is very similar, their results suggest that ATX-II may interact

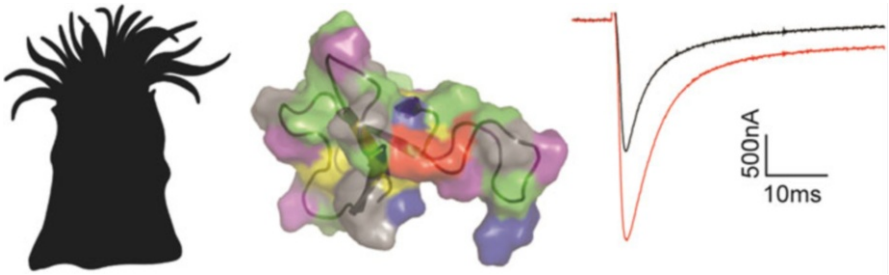

Fig. 5 ATX-II inhibits Nav channel fast inactivation. ATX-II is found in the *Anemonia sulcata* sea anemone and amino acids important to toxin functionality have been identified throughout the related peptide Ap-a (*middle figure*: protein backbone is shown together with the electrostatic surface of the protein. *Blue* are basic residues, *red* acidic, *green* hydrophobic, *yellow* cysteine, and *purple* polar.). At 500 nM, ATX-II inhibits fast inactivation of rNav1.2a currents evoked from a holding potential of −90 mV to a voltage of −20 mV when expressed in *Xenopus* oocytes. *Black* is control and *red* is after addition of 500 nM ATX-II (*right*)

with regions other than the domain IV voltage sensor. In contrast to Kv channels and acid-sensing ion channels for which sea anemone venoms have proven to be a valuable source of therapeutic leads (Chandy et al. 2004; Baron et al. 2013), a molecule with similar potential that targets Nav channels has yet to emerge.

3.2 Scorpion Toxins

Throughout some 400 million years of evolution, scorpions have perfected peptide toxins to specifically and potently target mammalian or insect ion channel families. As such, classic studies on scorpion venom recognized the presence of toxins capable of interfering with Nav channel voltage sensor function (Martin-Eauclaire and Couraud 1992; Cahalan 1975; Koppenhofer and Schmidt 1968a, b). In general, scorpion toxins interact with extracellular loops between S3 and S4 to stabilize the voltage sensors of Nav channels in particular states. Based on their functional effects, two classes of Nav channel scorpion toxins have been defined (Couraud et al. 1982).

First, α-scorpion toxins act on Nav channels in a manner similar to sea anemone toxins and as such were found to compete for binding at the same location in the domain IV voltage sensor (Fig. 6) (Jover et al. 1978). Nonetheless, early antibody and photo-affinity-labeling studies indicated an interaction of LqTX (isolated from *Leiurus quinquestriatus* venom) with the S5–S6 loops of domains I (Tejedor and Catterall 1988) and IV (Thomsen and Catterall 1989) in rat neuronal Nav channels. Later, mutagenesis experiments revealed a strong interaction with the S3–S4 paddle motif within domain IV (Rogers et al. 1996), as well as with the domain I S5–S6 loop and domain IV S1–S2 loop (Wang et al. 2011). This secondary binding site in domain I may help to position the α-scorpion toxin in such a way that the crucial hydrophobic residues within the toxin are positioned correctly for their interaction

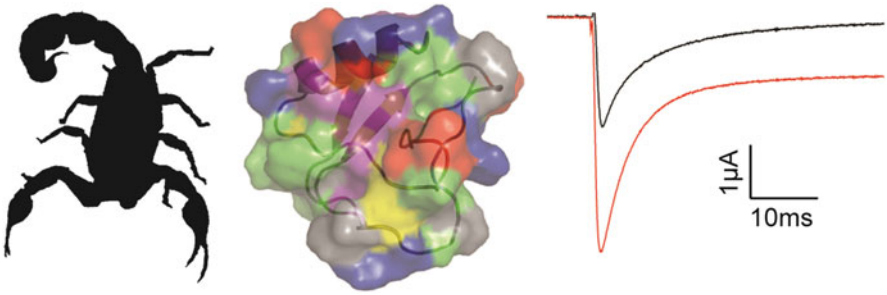

Fig. 6 α-scorpion toxins hamper Nav channel fast inactivation. The α-scorpion toxin AaHII is produced by the *Androctonus australis* Hector scorpion (silhouette on the *left*) and amino acids important to toxin functionality have been identified in both the hydrophobic patch as well as charged residues surrounding it (*middle figure*: protein backbone is shown together with the electrostatic surface of the protein). At 100 nM, AaHII inhibits fast inactivation of rNav1.2a currents evoked from a holding potential of −90 mV to a voltage of −20 mV when expressed in *Xenopus* oocytes. *Black* is control and *red* is after addition of 100 nM AaHII (*right*)

with the domain IV voltage sensor. Recently, a study by Campos et al. (2004) used Ts3 from *Tityus serrulatus* in concert with fluorescently labeled voltage-sensing domains demonstrating an inhibitory effect on voltage-sensing domain IV movement resulting in the inhibition of fast inactivation as well as speeding recovery from fast inactivation. Interestingly, Ts3 also affected the voltage-dependent gating of domain I suggesting the notion of an allosteric coupling between the adjacent domains I and IV.

A second class of Nav channel toxins present in scorpion venom are the β-scorpion toxins which promote subthreshold channel opening by shifting the voltage dependence of activation to more negative membrane potentials (Fig. 7). Distinct from α-scorpion toxins and sea anemone toxins, β-scorpion toxins are thought to primarily target the paddle motif within the domain II voltage sensor and trap it in an activated state (Cestèle et al. 1998, 2006). With the voltage sensor trapped, further depolarizations require the transition of fewer voltage-sensing domains, resulting in the hyperpolarized voltage-dependent activation observed in toxin-bound channels (Fig. 7). A common practice to examine the functional effects of β-scorpion toxins is to apply a short depolarizing pre-pulse in order to initiate their effect on Nav channel gating (Cestèle et al. 1998; Leipold et al. 2012). Although it is conceivable that this pre-pulse facilitates an interaction with the activated domain II voltage sensor, not every β-scorpion toxin requires this additional depolarization. For example, TsVII from *Tityus serrulatus* (Marcotte et al. 1997) and Tz1 from the *Tityus zulianus* scorpion (Leipold et al. 2006) do not need such a pulse to influence Nav channel gating, possibly because these toxins are capable of influencing regions other than the one in domain II (Bosmans et al. 2008).

Despite the tedious nature of purifying scorpion toxins from complex venom mixtures, researchers have been successful in identifying peptides that show

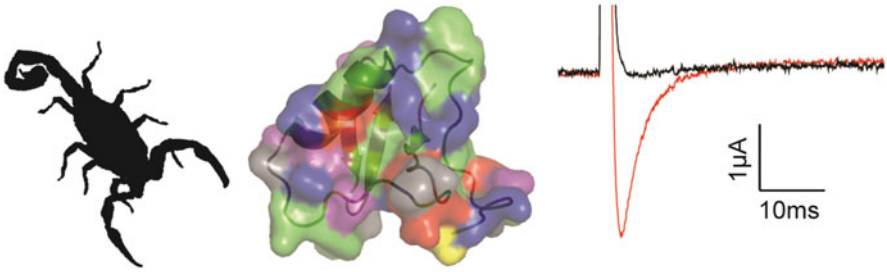

Fig. 7 β-scorpion toxins promote Nav channel opening. The β-scorpion toxin CssIV is found in the venom of the *Centruroides suffusus* suffusus scorpion (silhouette on the *left*) and amino acids important to toxin functionality have been identified in both the hydrophobic region and a ring of charged residues a (*middle figure*: protein backbone of the related β-scorpion toxin TsVII is shown together with the electrostatic surface of the protein). At 1 μM, CssIV opens rNav1.2a at voltages where the channel is normally closed. Current trace shown was evoked from a holding potential of −90 mV to a voltage of −40 mV when expressed in *Xenopus* oocytes. *Black* is control and *red* is after addition of 1 μM CssIV (*right*)

promise for designing drugs to treat disorders such as erectile dysfunction (Nunes et al. 2013), autoimmune diseases (Norton et al. 2004), and cancer (Stroud et al. 2011). The advent of advanced recombinant (Vita et al. 1995) and synthetic production techniques (M'Barek et al. 2004) in combination with genetic approaches may soon yield Nav channel drug leads as well.

3.3 Spider Toxins

In contrast to toxins from sea anemone, scorpion, and cone snail venoms, the exploration of the mechanism by which spider toxins interact with mammalian Nav channel voltage sensors has only recently begun. Structure–function studies on Magi 5 from the hexathelid spider *Macrothele gigas* with Nav channels (Corzo et al. 2007) and the Kv channel toxin SGTx1 from the *Scodra griseipes* tarantula (Lee et al. 2004) reveal the functional importance of a hydrophobic residue cluster surrounded by charged amino acids. As a result of this ubiquitous amphipathic character, spider toxins may access their receptor site within Nav channel and Kv channel voltage-sensing domains after partitioning into the membrane (Bosmans and Swartz 2010; Milescu et al. 2007, 2009; Swartz 2008). Depending on which voltage sensors are targeted and how they couple to the overall Nav channel-gating process, spider toxins can have three diverse effects on Nav channel function. The most commonly observed is for the toxin to inhibit channel opening in response to membrane depolarization (Fig. 8) (Bosmans et al. 2008; Edgerton et al. 2008; Middleton et al. 2002; Smith et al. 2005, 2007; Sokolov et al. 2008). Another outcome is for the toxin to delay fast inactivation by impairing domain IV movement (Wang et al. 2008). Finally, as uniquely observed with Magi 5, the toxin can facilitate channel opening by shifting the activation voltage to more hyperpolarized

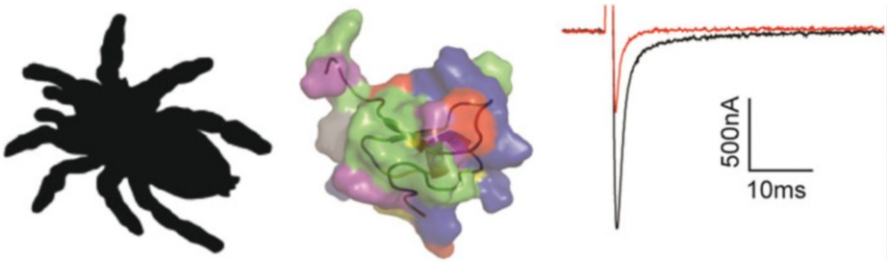

Fig. 8 Hanatoxin is a tarantula toxin that inhibits Nav channel opening. HaTx is found in the venom of the Chilean Rose tarantula (*Grammostola spatulata*) (silhouette of the related tarantula *Brachypelma smithi* is shown on the *left*) and amino acids important to toxin functionality have been identified in both the hydrophobic dimple as well as the ring of charged residues surrounding it (*middle*: protein backbone is shown together with the electrostatic surface of the protein). At 100 nM, HaTx inhibits rNav1.2a opening when currents are evoked from a holding potential of −90 mV to a voltage of −20 mV when expressed in *Xenopus* oocytes. *Black* is control and *red* is after addition of 100 nM HaTx (*right*)

values (Corzo et al. 2007). Recently, the identification of an S3b–S4 paddle motif within each of the four Nav channel voltage sensors significantly contributed to our understanding of the multifaceted working mechanism of spider toxins. As a result of this discovery, it was demonstrated that the paddle motif in each of the four Nav channel voltage sensors can interact with spider toxins and that multiple paddle motifs are often targeted by a single toxin (Bosmans et al. 2008). These novel insights also led to the identification of the first tarantula toxin (ProTx-I) active on Nav1.9, a Nav channel isoform predominantly expressed in nociceptive DRG neurons (Bosmans et al. 2011; Cummins et al. 1999). Interestingly, ProTx-I potentiates Nav1.9-mediated currents in rat DRG neurons, whereas the other TTX-resistant channel Nav1.8 is inhibited (Bosmans et al. 2011). The related tarantula toxin ProTx-II selectively targets Nav1.7, a Nav channel isoform implicated in various pain syndromes, with an affinity that is at least 100-fold higher when compared to other Nav channel isoforms that were examined (Schmalhofer et al. 2008). Although C-fiber compound action potential in de-sheathed cutaneous nerves can be completely inhibited, ProTx-II is not efficacious in rodent models of acute or inflammatory pain. As is the case with HWTX-IV from the Chinese bird spider *Selenocosmia huwena*, ProTx-II preferentially targets the Nav1.7 domain II voltage sensor (Xiao et al. 2010). Yet, ProTx-II also binds to the paddle motif in domain IV of this particular isoform, thereby resulting in a noticeable slowing of fast inactivation, a phenomenon that is not visible with Nav1.2 (Fig. 8) (Bosmans et al. 2008; Xiao et al. 2011). Several tarantula toxins have also been shown to possess a certain degree of selectivity toward Nav1.5, a Nav channel isoform known to be involved in cardiovascular function. For example, CcoTx3, JzTx-I, and JzTx-III modulate cardiac Na^+ currents; however, the isoform specificity of JzTX-I and JzTx-III has not yet been examined (Bosmans et al. 2006, 2009; Liao et al. 2007; Xiao et al. 2005). Overall, toxins isolated from spider venom have proven to be valuable tools to probe the structure and functional

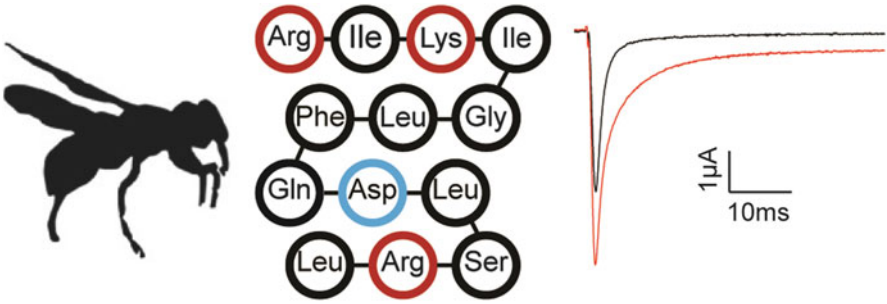

Fig. 9 Pompilidotoxins inhibit Nav channel fast inactivation. β-pompilidotoxin from *Batozonellus maculifrons* (silhouette of related wasp *Vespula germanica* on the *left*—peptide sequence in the *middle*) inhibits rNav1.2a fast inactivation when currents are evoked from a holding potential of −90 mV to a voltage of −20 mV when expressed in *Xenopus* oocytes. *Black* is control and *red* is after addition of 1 μM toxin (*right*)

mechanisms of Nav channels. As such, future opportunities may arise for using these peptides as therapeutic drugs.

3.4 Wasp Toxins

The two wasp toxins that have been thoroughly examined so far, α-pompilidotoxin from *Anoplius samariensis* and β-pompilidotoxin from *Batozonellus maculifrons* (Konno et al. 1998), are short peptides with no disulfide bonds or homology to toxins isolated from other organisms (Sahara et al. 2000). Both peptides slow fast inactivation of neuronal Nav channels but not Nav1.4 and Nav1.5, doing so in a manner similar to α-scorpion and sea anemone toxins (Fig. 9). Single amino acid mutagenesis of Nav1.2 has revealed an important role for a glutamate residue in the paddle motif of the domain IV voltage sensor in forming the toxin receptor site (Kinoshita et al. 2001). Moreover, similar to α-scorpion and sea anemone toxins, cationic residues within these peptides were found to be critical for toxin activity (Konno et al. 2000). Mandaratoxin, a 19 kDa protein isolated from the hornet *Vespa mandarinia* venom, irreversibly reduces Na^+ current (Abe et al. 1982). Little else is known about this toxin, yet it serves as a reminder that many toxins in nature remain to be discovered, some of which with novel mechanisms of action that may be exploited for therapeutic or research use.

3.5 Cone Snail Toxins

Several distinct groups of cone snail toxins are thought to influence Nav channel gating by interacting with the voltage-sensing domains. The biological backdrop resulting in the evolution of these peptides is different from that of the cone snail pore-blocking toxins. In a number of fish-hunting cone snail clades, the ability to

rapidly elicit muscle paralysis was insufficient for success. As a result, these snails have evolved to make prey capture even more efficient through a mechanism that is functionally equivalent to electrocuting their victims. In essence, at the venom injection site, a combination of peptides that block Kv channels but keep Nav channels open, elicits a massive depolarization of the axons first encountered by the venom. This causes the affected axons to fire action potentials uncontrollably, analogous to applying a Taser at the point of injection. The result is an almost immediate tetanic paralysis after a successful strike by the cone snail. The group of toxins that cause this very rapid prey immobilization is called the "lighting strike cabal." The first characterized group of Nav channel targeting cone snail toxins that belong to this lightning strike cabal are called δ-conopeptides and inhibit channel fast inactivation (Terlau et al. 1996) resulting in a continuous entry of Na^+ into the affected axons followed by a massive depolarization of the targeted plasma membranes. Consistent with their effect on Nav channel fast inactivation, it was shown that δ-conotoxins target the paddle motif in the domain IV voltage sensor (Leipold et al. 2005). δ-conotoxins are expressed in a wide range of cone snail venoms and are typically between 25 and 35 amino acids in length. Despite the fact that they are ubiquitous in cone snail venoms, the hydrophobic character of these peptides makes them a challenge to synthesize chemically thereby rendering them a less well-characterized family when compared to the μ-conotoxins (Figs. 3 and 4). δ-conotoxins belong to the O-superfamily, are genetically unrelated to the pore-blocking μ-conotoxins (which belong to the M-superfamily), and are primarily found in several clades of fish-hunting cone snails (Barbier et al. 2004; Bulaj et al. 2001; West et al. 2005; Fainzilber et al. 1995; Shon et al. 1995), and in at least one clade of mollusc-hunting snails (Hasson et al. 1993; Hillyard et al. 1989; Shon et al. 1994; Sudarslal et al. 2003). Interestingly, the first δ-conotoxin was discovered in the molluscivorous species *Conus textile* and was called the King Kong peptide because injection of the toxin into lobsters caused the animal to continuously assume a dominant posture (Hillyard et al. 1989).

A second group of cone snail toxins that contribute to the lightning strike cabal are the ι-conotoxins, which shift Nav channel activation to more hyperpolarized potentials thereby causing these channels to open at voltages where they are normally closed. These peptides differ from the μ-conotoxins and the δ-conotoxins in their mechanism of action, the gene superfamily to which they belong, and the presence of unusual posttranslational modifications. So far, these peptides have been found in only one species of fish-hunting cone snail, *Conus radiatus*, and belong to the I_1 gene superfamily which is typically defined by four disulfide crosslinks and a length of about 40–50 amino acids. A most unusual feature of many native ι-conotoxins is the presence of a single posttranslationally modified D-amino acid toward the C-terminal end. The first biochemically characterized ι-conotoxin, r11a was found to contain a single D-Phe44 (Buczek et al. 2005a). The NMR structure of this peptide revealed that three of the disulfide linkages are consistent with an inhibitory cysteine knot (ICK) motif, with one additional disulfide linkage. The modified D-Phe residue is present beyond the last disulfide crosslink in the C-terminal region, and the NMR structure suggests

that this region of the peptide is disordered in solution. Functionally, r11a target selectivity with respect to Nav channel isoforms expressed in *Xenopus* oocytes is Nav1.6 > Nav1.2 > Nav1.7, whereas other channel subtypes tested are insensitive to the toxin (Fiedler et al. 2008). Substitution of L-Phe for D-Phe has two major functional consequences: (1) a twofold lower affinity and twofold faster off-rate can be observed for the Nav1.6 subtype and (2) the L-Phe analog is inactive on Nav1.2. So far, four ι-toxins have been purified from *Conus radiatus* and chemically synthesized, whereas only one peptide (r11a) has been identified and characterized from the worm-hunting cone snail, *Conus arenatus* (Buczek et al. 2005a, b, 2008; Jimenez et al. 2003). While all of the ι-conotoxins from the fish-hunting species *Conus radiatus* cause severe excitotoxic symptoms when injected into mice, the *Conus arenatus* ι-conotoxin only causes mild symptoms even at high doses. Furthermore, it was demonstrated that three of the peptides from *Conus radiatus* (r11a, r11b, and r11c) have a posttranslationally modified amino acid at the predicted site as opposed to only one peptide from *Conus radiatus* (r11d) and one from *Conus arenatus* (r11a) in which all amino acids are in the L configuration. Despite their unique characteristics, the receptor site to which ι-conotoxins bind remains to be determined, yet it seems likely that one of the three voltage sensors involved in channel opening may be stabilized in an activated state.

Similar to a variety of other polypeptide toxins, the μO-conotoxins target Nav channel voltage sensors, yet they have distinctive properties (Daly et al. 2004; Leipold et al. 2007; Zorn et al. 2006). Unlike other conotoxins, the μO-conotoxins have not been found in fish-hunting cone snails. Instead, they were discovered in the molliscivorous *Conus marmoreus*. After this *Conus* species stings other snails, their envenomated prey become progressively more flaccid; thus, like fish-hunting cone snails, some molluscivorous *Conus* may have the equivalent of a "motor cabal" to block neuromuscular transmission and would likely have evolved Nav channel antagonists. In contrast to the μ-conotoxins that physically occlude the pore region, the μO-conotoxins are gating modifiers capable of antagonizing Nav channel opening (Leipold et al. 2007; Zorn et al. 2006). It has been hypothesized that they inhibit conductance by preventing the domain II voltage sensor from activating, a feature known to prevent channel opening. The two μO-conotoxins that have been characterized thus far, μO-MrVIA and MrVIB (Fainzilber et al. 1995; Daly et al. 2004; McIntosh et al. 1995),were shown to inhibit Na channel conductance without competing with the pore-blocking μ-conotoxins (Terlau et al. 1996). The analysis carried out by Heinemann and collaborators (Leipold et al. 2007; Zorn et al. 2006) demonstrates that the peptide interacts with both domains II and III, and competition with the β-scorpion toxin Ts1 suggests that the receptor site of μO-conotoxins may overlap with that of β-scorpion toxins (Leipold et al. 2006). Part of the intense interest in μO-conotoxins (Bulaj et al. 2006; Ekberg et al. 2006) stems from their ability to inhibit TTX-resistant Nav channel isoforms, some of which are thought to be involved in nociception (Gilchrist et al. 2012; Knapp et al. 2012). Subsequently, μO-conotoxins have been assessed for analgesic activity and were shown to be anti-nociceptive in various animal models of pain (Teichert et al. 2012).

Conclusions

Notwithstanding their limited availability, animal toxins have been successfully employed for many decades to investigate Nav channel function. Now more than ever, the ability to construct cDNA libraries from animal venom glands in concert with recombinant and synthetic production techniques will allow researchers to fully exploit animal peptides and probe the functional aspects of various Nav channel isoforms on a molecular level as well as investigate their physiological role in healthy and diseased tissues. Moreover, novel synthetic methods such as minimization, cyclization, and the use of diselenide bridges (Bulaj 2008) can address the challenges that may exist between the initial drug discovery phase and the clinical application of animal toxins, which will expand the use of these peptides as therapeutic drugs.

Acknowledgements We would like to thank Kenton J Swartz and Marie-France Martin-Eauclaire for hanatoxin, and AaHII/CssIV, respectively, and Thomas Gilchrist for making silhouettes that were adapted from photographs of Takifugu rupripes (Emőke Dénes/CC-BY-SA 2.5), Phyllobates bicolor (Luis Miguel Bugallo Sánchez/CC-BY-SA 3.0), Brachypelma smithi (Fir0002/CC-BY-SA 3.0), Centruroides suffusus (Pedro Sánchez/CC-BY-SA 3.0), Androctonus australis (Kmo5ap/CC-BY-SA 3.0), Vespula germanica (Richard Bartz/CC-BY-SA 2.5), and a diagram of an anemone (Hans Hillewaert/CC-BY-SA 3.0). TTX and β-pompilidotoxin were acquired from Alomone labs, ATX-II from Sigma Aldrich, and BTX was obtained from Latoxan through Fisher Scientific.

References

Abe T, Kawai N, Niwa A (1982) Purification and properties of a presynaptically acting neurotoxin, mandaratoxin, from hornet (Vespa mandarinia). Biochemistry 21(7):1693–1697

Agnew WS et al (1978) Purification of the tetrodotoxin-binding component associated with the voltage-sensitive sodium channel from Electrophorus electricus electroplax membranes. Proc Natl Acad Sci U S A 75(6):2606–10

Alabi AA et al (2007) Portability of paddle motif function and pharmacology in voltage sensors. Nature 450(7168):370–5

Alsen C, Harris J, Tesseraux I (1981) Mechanical and electrophysiological effects of sea anemone (Anemonia sulcata) toxins on rat innervated and denervated skeletal muscle. Br J Pharmacol 74 (1):61–71

Ashcroft F (1999) Ion channels and disease, vol 1. Elsevier, Amsterdam, p 481

Bagnis R et al (1980) Origins of ciguatera fish poisoning: a new dinoflagellate, Gambierdiscus toxicus Adachi and Fukuyo, definitively involved as a causal agent. Toxicon 18(2):199–208

Baldomero MO, Patrice SC, Maren W, Alexander F (2014) Biodiversity of cone snails and other venomous marine gastropods: evolutionary success through neuropharmacology. Annu Rev Anim Biosci 2:487–513

Barbier J et al (2004) A d-conotoxin from Conus ermineus venom inhibits inactivation in vertebrate neuronal Na^+ channels but not in skeletal and cardiac muscles. J Biol Chem 279:4680–4685

Barchi R, Cohen S, Murphy L (1980) Purification from rat sarcolemma of the saxitoxin-binding component of the excitable membrane sodium channel. Proc Natl Acad Sci U S A 77(3):1306–1310

Barhanin J et al (1981) Structure-function relationships of sea anemone toxin II from Anemonia sulcata. J Biol Chem 256(11):5764–5769

Baron A et al (2013) Venom toxins in the exploration of molecular, physiological and pathophysiological functions of acid-sensing ion channels. Toxicon 75:187–204
Benoit E, Legrand A, Dubois J (1986) Effects of ciguatoxin on current and voltage clamped frog myelinated nerve fibre. Toxicon 24(4):357–364
Benzinger G et al (1998) A specific interaction between the cardiac sodium channel and site-3 toxin anthopleurin B. J Biol Chem 273(1):80–84
Bidard J et al (1984) Ciguatoxin is a novel type of Na+ channel toxin. J Biol Chem 259(13):8353–8357
Billen B, Bosmans F, Tytgat J (2008) Animal peptides targeting voltage-activated sodium channels. Curr Pharm Des 14(24):2492–502
Bosmans F, Escoubas P, Nicholson GM (2009) Animal toxins: state of the art. In: De Lima ME (ed) Perspectives in health and biotechnology. Editora UFMG, Belo Horizonte
Bosmans F, Swartz KJ (2010) Targeting voltage sensors in sodium channels with spider toxins. Trends Pharmacol Sci 31(4):175–182
Bosmans F et al (2004) The poison Dart frog's batrachotoxin modulates Nav1.8. FEBS Lett 577 (1–2):245–8
Bosmans F et al (2006) Four novel tarantula toxins as selective modulators of voltage-gated sodium channel subtypes. Mol Pharmacol 69(2):419–29
Bosmans F, Martin-Eauclaire MF, Swartz KJ (2008) Deconstructing voltage sensor function and pharmacology in sodium channels. Nature 456(7219):202–8
Bosmans F et al (2011) Functional properties and toxin pharmacology of a dorsal root ganglion sodium channel viewed through its voltage sensors. J Gen Physiol 138(1):59–72
Buczek O et al (2005a) Characterization of D-amino-acid-containing excitatory conotoxins and redefinition of the I-conotoxin superfamily. FEBS J 272(16):4178–88
Buczek O, Bulaj G, Olivera BM (2005b) Conotoxins and the posttranslational modification of secreted gene products. CMLS 62(24):3067–79
Buczek O et al (2008) I(1)-superfamily conotoxins and prediction of single D-amino acid occurrence. Toxicon 51(2):218–29
Bulaj G (2008) Integrating the discovery pipeline for novel compounds targeting ion channels. Curr Opin Chem Biol 12(4):441–7
Bulaj G et al (2001) d-Conotoxin structure/function through a cladistic analysis. Biochemistry 40:13201–13208
Bulaj G et al (2005) Novel conotoxins from Conus striatus and Conus kinoshitai selectively block TTX-resistant sodium channels. Biochemistry 44:7259–7265
Bulaj G et al (2006) Synthetic μO-conotoxin MrVIB blocks TTX-resistant sodium channel Nav1.8 and has a long-lasting analgesic activity. Biochemistry 45:7404–7414
Cahalan MD (1975) Modification of sodium channel gating in frog myelinated nerve fibres by Centruroides sculpturatus scorpion venom. J Physiol 244(2):511–34
Campos F, Coronas F, Beirão P (2004) Voltage-dependent displacement of the scorpion toxin Ts3 from sodium channels and its implication on the control of inactivation. Br J Pharmacol 142 (7):1115–1122
Campos FV et al (2007) beta-Scorpion toxin modifies gating transitions in all four voltage sensors of the sodium channel. J Gen Physiol 130(3):257–68
Campos FV et al (2008) Alpha-scorpion toxin impairs a conformational change that leads to fast inactivation of muscle sodium channels. J Gen Physiol 132(2):251–63
Capes DL et al (2012) Gating transitions in the selectivity filter region of a sodium channel are coupled to the domain IV voltage sensor. Proc Natl Acad Sci U S A 109(7):2648–53
Catterall W (1975) Activation of the action potential Na+ ionophore of cultured neuroblastoma cells by veratridine and batrachotoxin. J Biol Chem 250(11):4053–4059
Catterall WA (1980) Neurotoxins that act on voltage-sensitive sodium channels in excitable membranes. Annu Rev Pharmacol Toxicol 20:15–43
Catterall WA (2000) From ionic currents to molecular mechanisms: the structure and function of voltage-gated sodium channels. Neuron 26(1):13–25

Catterall W, Beress L (1978) Sea anemone toxin and scorpion toxin share a common receptor site associated with the action potential sodium ionophore. J Biol Chem 253(20):7393–7396
Catterall WA, Goldin AL, Waxman SG (2005) International Union of Pharmacology XLVII. Nomenclature and structure-function relationships of voltage-gated sodium channels. Pharmacol Rev 57(4):397–409
Catterall WA et al (2007) Voltage-gated ion channels and gating modifier toxins. Toxicon 49 (2):124–41
Cestèle S et al (1998) Voltage sensor-trapping: enhanced activation of sodium channels by beta-scorpion toxin bound to the S3-S4 loop in domain II. Neuron 21(4):919–931
Cestèle S et al (2006) Structure and function of the voltage sensor of sodium channels probed by a beta-scorpion toxin. J Biol Chem 281(30):21332–21344
Cha A et al (1999) Voltage sensors in domains III and IV, but not I and II, are immobilized by Na+ channel fast inactivation. Neuron 22(1):73–87
Chanda B, Bezanilla F (2002) Tracking voltage-dependent conformational changes in skeletal muscle sodium channel during activation. J Gen Physiol 120(5):629–45
Chandy KG et al (2004) K+ channels as targets for specific immunomodulation. Trends Pharmacol Sci 25(5):280–9
Cooper EC, Tomiko SA, Agnew WS (1987) Reconstituted voltage-sensitive sodium channel from Electrophorus electricus: chemical modifications that alter regulation of ion permeability. Proc Natl Acad Sci U S A 84(17):6282–6
Corzo G et al (2007) Solution structure and alanine scan of a spider toxin that affects the activation of mammalian voltage-gated sodium channels. J Biol Chem 282(7):4643–52
Couraud F et al (1982) Two types of scorpion receptor sites, one related to the activation, the other to the inactivation of the action potential sodium channel. Toxicon 20(1):9–16
Cruz LJ et al (1985) Conus geographus toxins that discriminate between neuronal and muscle sodium channels. J Biol Chem 260:9280–9288
Cummins TR et al (1999) A novel persistent tetrodotoxin-resistant sodium current in SNS-null and wild-type small primary sensory neurons. J Neurosci 19(24):RC43
Daly NL et al (2004) Structures of muO-conotoxins from Conus marmoreus. I nhibitors of tetrodotoxin (TTX)-sensitive and TTX-resistant sodium channels in mammalian sensory neurons. J Biol Chem 279(24):25774–82
de la Vega R, Vega RC, Possani LD (2005) Overview of scorpion toxins specific for Na+ channels and related peptides: biodiversity, structure-function relationships and evolution. Toxicon 46 (8):831–44
Du Y et al (2011) Identification of new batrachotoxin-sensing residues in segment IIIS6 of the sodium channel. J Biol Chem 286(15):13151–60
Dumbacher J, Spande T, Daly J (2000) Batrachotoxin alkaloids from passerine birds: a second toxic bird genus (Ifrita kowaldi) from New Guinea. Proc Natl Acad Sci U S A 97(24):12970–12975
Dumbacher J et al (2004) Melyrid beetles (Choresine): a putative source for the batrachotoxin alkaloids found in poison-dart frogs and toxic passerine birds. Proc Natl Acad Sci U S A 101 (45):15857–15860
Edgerton GB, Blumenthal KM, Hanck DA (2008) Evidence for multiple effects of ProTxII on activation gating in Na(V)1.5. Toxicon 52(3):489–500
Ekberg J et al (2006) muO-conotoxin MrVIB selectively blocks Nav1.8 sensory neuron specific sodium channels and chronic pain behavior without motor deficits. Proc Natl Acad Sci U S A 103(45):17030–5
Escoubas P et al (2002) Novel tarantula toxins for subtypes of voltage-dependent potassium channels in the Kv2 and Kv4 subfamilies. Mol Pharmacol 62(1):48–57
Fainzilber M et al (1995) New sodium channel blocking conotoxins also affect calcium currents in Lymnaea neurons. Biochemistry 34:5364–5371
Felix JP et al (2004) Functional assay of voltage-gated sodium channels using membrane potential-sensitive dyes. Assay Drug Dev Technol 2(3):260–8

Fiedler B et al (2008) Specificity, affinity and efficacy of iota-conotoxin RXIA, an agonist of voltage-gated sodium channels Na(V)1.2, 1.6 and 1.7. Biochem Pharmacol 75(12):2334–44
Fozzard HA, Lipkind GM (2010) The tetrodotoxin binding site is within the outer vestibule of the sodium channel. Marine Drugs 8(2):219–34
Furukawa T, Sasaoka T, Hosoya Y (1959) Effects of tetrodotoxin on the neuromuscular junction. Jpn J Physiol 9(2):143–52
Gallagher M, Blumenthal K (1994) Importance of the unique cationic residues arginine 12 and lysine 49 in the activity of the cardiotonic polypeptide anthopleurin B. J Biol Chem 269 (1):254–259
Gilchrist J, Bosmans F (2012) Animal toxins can alter the function of Nav1.8 and Nav1.9. Toxins 4 (8):620–32
Gill S et al (2003) Flux assays in high throughput screening of ion channels in drug discovery. Assay Drug Dev Technol 1(5):709–17
Gooley P, Blunt J, Norton R (1984) Conformational heterogeneity in polypeptide cardiac stimulants from sea anemones. FEBS Lett 174(1):15–19
Hanck D, Sheets M (2007) Site-3 toxins and cardiac sodium channels. Toxicon 49(2):181–193
Hartshorne R, Catterall W (1981) Purification of the saxitoxin receptor of the sodium channel from rat brain. Proc Natl Acad Sci U S A 78(7):4620–4624
Hartshorne R et al (1982) The saxitoxin receptor of the sodium channel from rat brain. Evidence for two nonidentical beta subunits. J Biol Chem 257(23):13888–13891
Hasson A et al (1993) Alteration of sodium currents by new peptide toxins from the venom of a molluscivorous Conus snail. Eur J Neurosci 5(1):56–64
Hille B (1975) The receptor for tetrodotoxin and saxitoxin. A structural hypothesis. Biophys J 15 (6):615–619
Hille B (2001) Ion channels of excitable membranes, vol 1, 3rd edn. Sinauer Associates, Sunderland, MA, p 814
Hillyard DR et al (1989) A molluscivorous Conus toxin: conserved frameworks in conotoxins. Biochemistry 28(1):358–61
Hirama M et al (2001) Total synthesis of ciguatoxin CTX3C. Science (New York, NY) 294 (5548):1904–1907
Hodgkin AL, Huxley AF (1952) Propagation of electrical signals along giant nerve fibers. Proc R Soc Lond B Biol Sci 140(899):177–83
Holford M et al (2009) Pruning nature: Biodiversity-derived discovery of novel sodium channel blocking conotoxins from Conus bullatus. Toxicon 53(1):90–8
Honma T, Shiomi K (2006) Peptide toxins in sea anemones: structural and functional aspects. Marine Biotechnol 8(1):1–10
Horn R, Ding S, Gruber HJ (2000) Immobilizing the moving parts of voltage-gated ion channels. J Gen Physiol 116(3):461–76
Huang L, Moran N, Ehrenstein G (1982) Batrachotoxin modifies the gating kinetics of sodium channels in internally perfused neuroblastoma cells. Proc Natl Acad Sci U S A 79(6):2082–2085
Jiang Y et al (2003) X-ray structure of a voltage-dependent K+ channel. Nature 423(6935):33–41
Jimenez EC et al (2003) Novel excitatory Conus peptides define a new conotoxin superfamily. J Neurochem 85(3):610–21
Jover E et al (1978) Scorpion toxin: specific binding to rat synaptosomes. Biochem Biophys Res Commun 85(1):377–382
Kem W et al (1989) Isolation, characterization, and amino acid sequence of a polypeptide neurotoxin occurring in the sea anemone Stichodactyla helianthus. Biochemistry 28 (8):3483–3489
Khera P, Blumenthal K (1996) Importance of highly conserved anionic residues and electrostatic interactions in the activity and structure of the cardiotonic polypeptide anthopleurin B. Biochemistry 35(11):3503–3507

Kinoshita E et al (2001) Novel wasp toxin discriminates between neuronal and cardiac sodium channels. Molecular pharmacology 59(6):1457–1463
Knapp O, McArthur JR, Adams DJ (2012) Conotoxins targeting neuronal voltage-gated sodium channel subtypes: potential analgesics? Toxins 4(11):1236–60
Konno K et al (1998) Isolation and structure of pompilidotoxins, novel peptide neurotoxins in solitary wasp venoms. Biochem Biophys Res Commun 250(3):612–616
Konno K et al (2000) Molecular determinants of binding of a wasp toxin (PMTXs) and its analogs in the Na+ channels proteins. Neurosci Lett 285(1):29–32
Koppenhofer E, Schmidt H (1968a) Effect of scorpion venom on ionic currents of the node of Ranvier. I. The permeabilities PNa and PK. Pflugers Arch 303(2):133–49
Koppenhofer E, Schmidt H (1968b) Effect of scorpion venom on ionic currents of the node of Ranvier. II. Incomplete sodium inactivation. Pflugers Arch 303(2):150–61
Kuang Z, Zhang M-M, Gupta K, Gajewiak J, Gulyas J, Balaram P, Rivier JE, Olivera BM, Yoshikami D, Bulaj G, Norton RS (2013) Mammalian neuronal sodium channel blocker μ-conotoxin BuIIIB has a structured N-terminus that influences potency. ACS Chem Biol 8 (6):1344–1351
Lee CW et al (2004) Solution structure and functional characterization of SGTx1, a modifier of Kv2.1 channel gating. Biochemistry 43(4):890–7
Leffler A et al (2005) Pharmacological properties of neuronal TTX-resistant sodium channels and the role of a critical serine pore residue. Pflugers Archiv 451(3):454–63
Legrand AM et al (1989) Isolation and some properties of ciguatoxin. J Appl Phycol 1:183–188
Leipold E et al (2005) Molecular interaction of delta-conotoxins with voltage-gated sodium channels. FEBS Lett 579(18):3881–4
Leipold E et al (2006) Subtype specificity of scorpion beta-toxin Tz1 interaction with voltage-gated sodium channels is determined by the pore loop of domain 3. Mol Pharmacol 70(1):340–347
Leipold E et al (2007) μO conotoxins inhibit NaV channels by interfering with their voltage sensors in domain-2. Channels (Austin) 1(4):253–62
Leipold E et al (2011) Molecular determinants for the subtype specificity of mu-conotoxin SIIIA targeting neuronal voltage-gated sodium channels. Neuropharmacology 61(1–2):105–11
Leipold E, Borges A, Heinemann SH (2012) Scorpion beta-toxin interference with NaV channel voltage sensor gives rise to excitatory and depressant modes. J Gen Physiol 139(4):305–19
Lewis R et al (1991) Purification and characterization of ciguatoxins from moray eel (Lycodontis javanicus, Muraenidae). Toxicon 29(9):1115–1127
Lewis RJ et al (2007) Isolation and structure-activity of mu-conotoxin TIIIA, a potent inhibitor of tetrodotoxin-sensitive voltage-gated sodium channels. Mol Pharmacol 71(3):676–85
Li D et al (2003) Function and solution structure of hainantoxin-I, a novel insect sodium channel inhibitor from the Chinese bird spider Selenocosmia hainana. FEBS Lett 555(3):616–22
Liao Z et al (2007) Solution structure of Jingzhaotoxin-III, a peptide toxin inhibiting both Nav1.5 and Kv2.1 channels. Toxicon 50(1):135–43
Linford N et al (1998) Interaction of batrachotoxin with the local anesthetic receptor site in transmembrane segment IVS6 of the voltage-gated sodium channel. Proc Natl Acad Sci U S A 95(23):13947–13952
Lipkind G, Fozzard H (1994) A structural model of the tetrodotoxin and saxitoxin binding site of the Na+ channel. Biophys J 66(1):1–13
Lipkind GM, Fozzard HA (2008) Voltage-gated Na channel selectivity: the role of the conserved domain III lysine residue. J Gen Physiol 131(6):523–9
Llewellyn L, Bell P, Moczydlowski E (1997) Phylogenetic survey of soluble saxitoxin-binding activity in pursuit of the function and molecular evolution of saxiphilin, a relative of transferrin. Proc R Soc 264(1383):891–902
Llewellyn L, Doyle J, Negri A (1998) A high-throughput, microtiter plate assay for paralytic shellfish poisons using the saxitoxin-specific receptor, saxiphilin. Anal Biochem 261(1):51–56

Lombet A, Bidard J, Lazdunski M (1987) Ciguatoxin and brevetoxins share a common receptor site on the neuronal voltage-dependent Na+ channel. FEBS Lett 219(2):355–359
Long SB et al (2007) Atomic structure of a voltage-dependent K+ channel in a lipid membrane-like environment. Nature 450(7168):376–82
Marcotte P et al (1997) Effects of Tityus serrulatus scorpion toxin gamma on voltage-gated Na+ channels. Circ Res 80(3):363–9
Martin-Eauclaire MF, Couraud F (1992) Scorpion neurotoxins: effects and mechanisms. In: Chang LW, Dyer RS (eds) Handk. neurotoxicology. Marcel-Dekker, New York, NY
M'Barek S et al (2004) First chemical synthesis of a scorpion alpha-toxin affecting sodium channels: the Aah I toxin of Androctonus australis hector. J Peptide Sci 10(11):666–677
McArthur JR et al (2011) Interactions of key charged residues contributing to selective block of neuronal sodium channels by mu-conotoxin KIIIA. Mol Pharmacol 80(4):573–84
McCusker EC et al (2012) Structure of a bacterial voltage-gated sodium channel pore reveals mechanisms of opening and closing. Nat Commun 3:1102
McIntosh JM et al (1995) A new family of conotoxins that blocks voltage-gated sodium channels. J Biol Chem 270:16796–16802
Mebs D (2002) Venomous and poisonous animals: a handbook for biologists, toxicologists and toxinologists, physicians and pharmacists, 1st edn. Medpharm, Lyttelton, New Zealand, p 360
Michio M et al (1989) Structures of ciguatoxin and its congener. J Am Chem Soc 111:8289–8931
Middleton RE et al (2002) Two tarantula peptides inhibit activation of multiple sodium channels. Biochemistry 41(50):14734–47
Milescu M et al (2007) Tarantula toxins interact with voltage sensors within lipid membranes. J Gen Physiol 130(5):497–511
Milescu M et al (2009) Interactions between lipids and voltage sensor paddles detected with tarantula toxins. Nat Struct Mol Biol 16(10):1080–1085
Miller J, Agnew W, Levinson S (1983) Principal glycopeptide of the tetrodotoxin/saxitoxin binding protein from electrophorus electricus: isolation and partial chemical and physical characterization. Biochemistry 22(2):462–470
Moore JW et al (1967) Basis of tetrodotoxin's selectivity in blockage of squid axons. J Gen Physiol 50(5):1401–11
Morabito M, Moczydlowski E (1994) Molecular cloning of bullfrog saxiphilin: a unique relative of the transferrin family that binds saxitoxin. Proc Natl Acad Sci U S A 91(7):2478–2482
Narahashi T (1974) Chemicals as tools in the study of excitable membranes. Physiol Rev 54 (4):813–89
Narahashi T, Moore JW, Scott WR (1964) Tetrodotoxin blockage of sodium conductance increase in lobster giant axons. J Gen Physiol 47:965–74
Narahashi T, Anderson N, Moore J (1967) Comparison of tetrodotoxin and procaine in internally perfused squid giant axons. J Gen Physiol 50(5):1413–1428
Nieto FR et al (2012) Tetrodotoxin (TTX) as a therapeutic agent for pain. Marine Drugs 10 (2):281–305
Norton R (2009) Structures of sea anemone toxins. Toxicon 54(8):1075–1088
Norton RS, Pennington MW, Wulff H (2004) Potassium channel blockade by the sea anemone toxin ShK for the treatment of multiple sclerosis and other autoimmune diseases. Curr Med Chem 11(23):3041–52
Nunes KP et al (2013) New insights on arthropod toxins that potentiate erectile function. Toxicon 69:152–9
Oliveira J et al (2004) Binding specificity of sea anemone toxins to Nav 1.1-1.6 sodium channels: unexpected contributions from differences in the IV/S3-S4 outer loop. J Biol Chem 279 (32):33323–33335
Olivera BM (1997) Conus venom peptides, receptor and ion channel targets and drug design: 50 million years of neuropharmacology (E.E. Just Lecture, 1996). Mol Biol Cell 8:2101–2109
Payandeh J et al (2011) The crystal structure of a voltage-gated sodium channel. Nature 475 (7356):353–8

Payandeh J et al (2012) Crystal structure of a voltage-gated sodium channel in two potentially inactivated states. Nature 486(7401):135–9
Phillips LR et al (2005) Voltage-sensor activation with a tarantula toxin as cargo. Nature 436 (7052):857–60
Quandt F, Narahashi T (1982) Modification of single Na+ channels by batrachotoxin. Proc Natl Acad Sci U S A 79(21):6732–6736
Richard Benzinger G (1999) G. Tonkovich, and D. Hanck, *Augmentation of recovery from inactivation by site-3 Na channel toxins. A single-channel and whole-cell study of persistent currents*. J Gen Physiol 113(2):333–346
Rogers J et al (1996) Molecular determinants of high affinity binding of alpha-scorpion toxin and sea anemone toxin in the S3-S4 extracellular loop in domain IV of the Na+ channel alpha subunit. J Biol Chem 271(27):15950–15962
Romey G et al (1976) Sea anemone toxin:a tool to study molecular mechanisms of nerve conduction and excitation-secretion coupling. Proc Natl Acad Sci U S A 73(11):4055–4059
Ruta V, MacKinnon R (2004) Localization of the voltage-sensor toxin receptor on KvAP. Biochemistry 43(31):10071–9
Sahara Y et al (2000) A new class of neurotoxin from wasp venom slows inactivation of sodium current. Eur J Neurosci 12(6):1961–1970
Schantz E et al (1975) Letter: The structure of saxitoxin. J Am Chem Soc 97(5):1238
Schmalhofer WA et al (2008) ProTx-II, a selective inhibitor of NaV1.7 sodium channels, blocks action potential propagation in nociceptors. Mol Pharmacol 74(5):1476–84
Seibert A et al (2003) Arg-14 loop of site 3 anemone toxins: effects of glycine replacement on toxin affinity. Biochemistry 42(49):14515–14521
Sheets MF et al (1999) The Na channel voltage sensor associated with inactivation is localized to the external charged residues of domain IV, S4. Biophys J 77(2):747–57
Sheets MF, Kyle JW, Hanck DA (2000) The role of the putative inactivation lid in sodium channel gating current immobilization. J Gen Physiol 115(5):609–20
Sherif N, Fozzard H, Hanck D (1992) Dose-dependent modulation of the cardiac sodium channel by sea anemone toxin ATXII. Circul Res 70(2):285–301
Shon KJ et al (1994) Delta-conotoxin GmVIA, a novel peptide from the venom of Conus gloriamaris. Biochemistry 33(38):11420–5
Shon K et al (1995) Purification, characterization and cloning of the lockjaw peptide from Conus purpurascens venom. Biochemistry 34:4913–4918
Shon K (1998) et al., μ-Conotoxin PIIIA, a new peptide for discriminating among tetrodotoxin-sensitive Na channel subtypes. J. Neurosci 18:473–4481
Silva AO et al (2012) Inhibitory effect of the recombinant Phoneutria nigriventer Tx1 toxin on voltage-gated sodium channels. Biochimie 94(12):2756–63
Sivilotti L et al (1997) A single serine residue confers tetrodotoxin insensitivity on the rat sensory-neuron-specific sodium channel SNS. FEBS Lett 409(1):49–52
Smith JJ, Blumenthal KM (2007) Site-3 sea anemone toxins: molecular probes of gating mechanisms in voltage-dependent sodium channels. Toxicon 49(2):159–70
Smith JJ et al (2005) Differential phospholipid binding by site 3 and site 4 toxins. Implications for structural variability between voltage-sensitive sodium channel domains. J Biol Chem 280 (12):11127–33
Smith JJ et al (2007) Molecular interactions of the gating modifier toxin ProTx-II with NaV 1.5: implied existence of a novel toxin binding site coupled to activation. J Biol Chem 282 (17):12687–97
Sokolov S et al (2008) Inhibition of sodium channel gating by trapping the domain II voltage sensor with protoxin II. Mol Pharmacol 73(3):1020–8
Stroud MR, Hansen SJ, Olson JM (2011) In vivo bio-imaging using chlorotoxin-based conjugates. Curr Pharmaceut Design 17(38):4362–71
Sudarslal S et al (2003) Sodium channel modulating activity in a delta-conotoxin from an Indian marine snail. FEBS letters 553(1–2):209–12

Swartz KJ (2007) Tarantula toxins interacting with voltage sensors in potassium channels. Toxicon 49(2):213–30
Swartz KJ (2008) Sensing voltage across lipid membranes. Nature 456(7224):891–7
Swartz KJ, MacKinnon R (1997a) Hanatoxin modifies the gating of a voltage-dependent K+ channel through multiple binding sites. Neuron 18(4):665–73
Swartz KJ, MacKinnon R (1997b) Mapping the receptor site for hanatoxin, a gating modifier of voltage-dependent K+ channels. Neuron 18(4):675–82
Teichert RW, et al (2012) Characterization of two neuronal subclasses through constellation pharmacology. In: Proceedings of the National Academy of Sciences. PNAS Early Edition: p. Published ahead of print, July 9
Tejedor F, Catterall W (1988) Site of covalent attachment of alpha-scorpion toxin derivatives in domain I of the sodium channel alpha subunit. Proc Natl Acad Sci U S A 85(22):8742–8746
Terlau H, Olivera BM (2004) Conus venoms: a rich source of novel ion channel-targeted peptides. Physiol Rev 84(1):41–68
Terlau H et al (1991) Mapping the site of block by tetrodotoxin and saxitoxin of sodium channel II. FEBS Lett 293(1–2):93–96
Terlau H et al (1996) Strategy for rapid immobilization of prey by a fish-hunting cone snail. Nature 381:148–151
Thomsen W, Catterall W (1989) Localization of the receptor site for alpha-scorpion toxins by antibody mapping: implications for sodium channel topology. Proc Natl Acad Sci U S A 86 (24):10161–10165
Tokuyama T, Daly J, Witkop B (1969) The structure of batrachotoxin, a steroidal alkaloid from the Colombian arrow poison frog, Phyllobates aurotaenia, and partial synthesis of batrachotoxin and its analogs and homologs. J Am Chem Soc 91(14):3931–3938
Trainer V, Baden D, Catterall W (1994) Identification of peptide components of the brevetoxin receptor site of rat brain sodium channels. J Biol Chem 269(31):19904–19909
Ujihara S et al (2008) Interaction of ladder-shaped polyethers with transmembrane alpha-helix of glycophorin A as evidenced by saturation transfer difference NMR and surface plasmon resonance. Bioorg Med Chem Lett 18(23):6115–8
Ulbricht W (1998) Effects of veratridine on sodium currents and fluxes. Rev Physiol Biochem Pharmacol 133:1–54
Van Der Haegen A, Peigneur S, Tytgat J (2011) Importance of position 8 in μ-conotoxin KIIIA for voltage-gated sodium channel selectivity. FEBS J 278:3408–3418
Vita C et al (1995) Scorpion toxins as natural scaffolds for protein engineering. Proc Natl Acad Sci U S A 92(14):6404–6408
Walewska A et al (2008) NMR-based mapping of disulfide bridges in cysteine-rich peptides: application to the mu-conotoxin SxIIIA. J Am Chem Soc 130(43):14280–6
Wang S, Wang G (1998) Point mutations in segment I-S6 render voltage-gated Na+ channels resistant to batrachotoxin. Proc Natl Acad Sci U S A 95(5):2653–2658
Wang GK, Quan C, Wang SY (1998) Local anesthetic block of batrachotoxin-resistant muscle Na + channels. Mol Pharmacol 54(2):389–96
Wang S, Nau C, Wang G (2000) Residues in Na(+) channel D3-S6 segment modulate both batrachotoxin and local anesthetic affinities. Biophys J 79(3):1379–1387
Wang M et al (2008) JZTX-IV, a unique acidic sodium channel toxin isolated from the spider Chilobrachys jingzhao. Toxicon 52(8):871–80
Wang J et al (2011) Mapping the receptor site for alpha-scorpion toxins on a Na+ channel voltage sensor. Proc Natl Acad Sci U S A 108(37):15426–15431
Wasserstrom J et al (1993) Modification of cardiac Na+ channels by batrachotoxin: effects on gating, kinetics, and local anesthetic binding. Biophys J 65(1):386–395
West PJ et al (2002) μ-Conotoxin SmIIIA, a potent inhibitor of TTX-resistant sodium channels in amphibian sympathetic and sensory neurons. Biochemistry 41:15388–15393
West PJ, Bulaj G, Yoshikami D (2005) Effects of delta-conotoxins PVIA and SVIE on sodium channels in the amphibian sympathetic nervous system. J Neurophysiol 94(6):3916–24

Wilson MJ et al (2011) μ-conotoxins that differentially block sodium channels NaV1.1 through 1.8 identify those responsible for action potentials in sciatic nerve. Proc Natl Acad Sci U S A 108 (25):10302–7

Woodward R (1964) The structure of tetrodotoxin. Pure Appl Chem 9:49–74

Xiao Y et al (2005) Jingzhaotoxin-I, a novel spider neurotoxin preferentially inhibiting cardiac sodium channel inactivation. J Biol Chem 280(13):12069–76

Xiao Y et al (2008) Tarantula huwentoxin-IV inhibits neuronal sodium channels by binding to receptor site 4 and trapping the domain ii voltage sensor in the closed configuration. J Biol Chem 283(40):27300–13

Xiao Y et al (2010) The tarantula toxins ProTx-II and huwentoxin-IV differentially interact with human Nav1.7 voltage sensors to inhibit channel activation and inactivation. Mol Pharmacol 78(6):1124–34

Xiao Y et al (2011) Common molecular determinants of tarantula huwentoxin-IV inhibition of Na + channel voltage sensors in domains II and IV. J Biol Chem 286(31):27301–10

Xu Y et al (2013) Energetic role of the paddle motif in voltage gating of Shaker K(+) channels. Nat Struct Mol Biol 20(5):574–81

Yamaoka K et al (2009) Synthetic ciguatoxins selectively activate Nav1.8-derived chimeric sodium channels expressed in HEK293 cells. J Biol Chem 284(12):7597–7605

Yong-Yeng L et al (1981) Isolation and structure of brevetoxin B from the "red tide" dinoflagellate Ptychodiscus brevis (Gymnodinium breve). J Am Chem Soc 103:6773–6776

Zhang MM et al (2006) Structural and functional diversities among mu-conotoxins targeting TTX-resistant sodium channels. Biochemistry 45(11):3723–32

Zhang MM et al (2007) Structure/function characterization of micro-conotoxin KIIIA, an analgesic, nearly irreversible blocker of mammalian neuronal sodium channels. J Biol Chem 282 (42):30699–706

Zhang MM et al (2009) Synergistic and antagonistic interactions between tetrodotoxin and mu-conotoxin in blocking voltage-gated sodium channels. Channels (Austin) 3(1):32–8

Zhang MM et al (2010) Cooccupancy of the outer vestibule of voltage-gated sodium channels by micro-conotoxin KIIIA and saxitoxin or tetrodotoxin. J Neurophysiol 104:88–97

Zhang X et al (2012) Crystal structure of an orthologue of the NaChBac voltage-gated sodium channel. Nature 486(7401):130–4

Zhang MM et al (2013a) Co-expression of Na(V) beta-subunits alters the kinetics of inhibition of voltage-gated sodium channels by pore-blocking mu-conotoxins. Br J Pharmacol 168:1597–1610

Zhang MM, Wilson MJ, Gajewiak J, Rivier JE, Bulaj G, Olivera BM, Yoshikami D (2013) Pharmacological fractionation of tetrodotoxin-sensitive sodium currents in rat dorsal root ganglion neurons by μ-conotoxins. Br J Pharmacol 169(1):102–14

Zorn S et al. (2006) The muO-conotoxin MrVIA inhibits voltage-gated sodium channels by associating with domain-3. FEBS Lett 580(5):1360–4.

Ubiquitylation of Voltage-Gated Sodium Channels

Cédric J. Laedermann, Isabelle Decosterd, and Hugues Abriel

Contents

C.J. Laedermann
Department of Clinical Research, University of Bern, Murtenstrasse, 35, 3010 Bern, Switzerland

Department of Fundamental Neuroscience, University of Lausanne, Lausanne, Switzerland

Pain Center, Department of Anesthesiology, University Hospital Center (CHUV) and University of Lausanne, Av. Bugnon 46, 1011 Lausanne, Switzerland
e-mail: Cedric.Laedermann@unil.ch

I. Decosterd
Department of Fundamental Neuroscience, University of Lausanne, Lausanne, Switzerland

Pain Center, Department of Anesthesiology, University Hospital Center (CHUV) and University of Lausanne, Av. Bugnon 46, 1011 Lausanne, Switzerland
e-mail: Isabelle.Decosterd@chuv.ch

H. Abriel (✉)
Department of Clinical Research, University of Bern, Murtenstrasse, 35, 3010 Bern, Switzerland
e-mail: Hugues.Abriel@dkf.unibe.ch

P.C. Ruben (ed.), *Voltage Gated Sodium Channels*, Handbook of Experimental Pharmacology 221, DOI 10.1007/978-3-642-41588-3_11,

Abstract

Ion channel proteins are regulated by different types of posttranslational modifications. The focus of this review is the regulation of voltage-gated sodium channels (Na_vs) upon their ubiquitylation. The amiloride-sensitive epithelial sodium channel (ENaC) was the first ion channel shown to be regulated upon ubiquitylation. This modification results from the binding of ubiquitin ligase from the Nedd4 family to a protein–protein interaction domain, known as the PY motif, in the ENaC subunits. Many of the Na_vs have similar PY motifs, which have been demonstrated to be targets of Nedd4-dependent ubiquitylation, tagging them for internalization from the cell surface. The role of Nedd4-dependent regulation of the Na_v membrane density in physiology and disease remains poorly understood. Two recent studies have provided evidence that Nedd4-2 is downregulated in dorsal root ganglion (DRG) neurons in both rat and mouse models of nerve injury-induced neuropathic pain. Using two different mouse models, one with a specific knockout of Nedd4-2 in sensory neurons and another where Nedd4-2 was overexpressed with the use of viral vectors, it was demonstrated that the neuropathy-linked neuronal hyperexcitability was the result of $Na_v1.7$ and $Na_v1.8$ overexpression due to Nedd4-2 downregulation. These studies provided the first in vivo evidence of the role of Nedd4-2-dependent regulation of Na_v channels in a disease state. This ubiquitylation pathway may be involved in the development of symptoms and diseases linked to Na_v-dependent hyperexcitability, such as pain, cardiac arrhythmias, epilepsy, migraine, and myotonias.

Keywords

Ubquitin • Nedd4 ubiquitin ligases • PY motif • Neuropathic pain

1 Introduction

As with other membrane proteins, the pore-forming subunits of voltage-gated sodium channels (Na_v) are modified by several well-known posttranslational modifications, i.e., glycosylation (Catterall 2000; Cohen and Levitt 1993; Waechter et al. 1983), palmitoylation, sulfation (Schmidt and Catterall 1987), and the phosphorylation of serine, threonine, and tyrosine residues (Catterall 2000). The methylation of arginine residues (Beltran-Alvarez et al. 2011) and the nitrosylation of $Na_v1.5$ (Ueda et al. 2008), as well as the methylglyoxal modification of $Na_v1.8$ (Bierhaus et al. 2012), have also been recently reported.

The aim of this chapter is to review the most recent findings demonstrating that Na_v channels can be ubiquitylated (covalently bound to ubiquitin and ubiquitin chains) and to summarize the roles of the ubiquitylation process known to date. The main focus will be on the regulation of Na_vs by the ubiquitin ligases of the Nedd4/Nedd4-like family, since most Na_vs have a conserved motif in their C-terminus which binds these enzymes.

2 Ubiquitylation of Membrane Proteins

Ubiquitylation is a well-recognized posttranslational process that regulates the number of many different plasma membrane proteins at the cell surface (Staub and Rotin 2006). Most ubiquitylated membrane proteins are internalized and then either degraded or recycled (Abriel and Staub 2005). Ubiquitin is a small and highly conserved polypeptide of 76 amino acids that was first reported to be an adenylate cyclase stimulator (Schlesinger and Goldstein 1975; Schlesinger et al. 1975; Schlesinger et al. 1978). In the early 1980s, Hershko, Rose, and Ciechanover identified the polypeptide heat-sensitive ATP-dependent proteolysis factor 1 (APF-1), which was shown to be implicated in non-lysosomal proteolysis. They reported that APF-1, later identified as ubiquitin, covalently attaches to the target protein via an isopeptide link and is involved in proteolysis in an ATP- and Mg^{2+}-dependent manner (Ciechanover et al. 1980; Hershko et al. 1979, 1980; Wilkinson et al. 1980). Interest in the study of ubiquitin has steadily grown and multiple other functions have since been identified. In 2004, Hershko, Rose, and Ciechanover were awarded the Nobel Prize in chemistry for their discovery. For supplemental information regarding the discovery of this pathway, refer to the article by Kresge et al. (2006).

Ubiquitylation of proteins requires three successive enzymatic steps (Fig. 3) (Ciechanover 2005). Ubiquitin is first bound and activated by an ubiquitin-activating enzyme (E1). The interaction involves the ATP-dependent formation of a thioester bond between the lateral chain of an E1 active cysteine residue and the C-terminus of ubiquitin. Ubiquitin is then transferred to a ubiquitin-conjugating enzyme (E2), again via a thioester bond. This complex further interacts with a ubiquitin–protein ligase (E3) that eventually ubiquitylates the substrate protein. E3 enzymes provide the specificity of the cascade as they bind to a recognition motif on the target protein, usually a ε-NH2 group of a lysine residue (Schwarz et al. 1998). There are at least 1,000 different E3 enzymes encoded by the human genome (Hicke et al. 2005), further highlighting the specific roles of E3 (i.e., ~10 different genes encode for E1 and ~100 for E2) and attesting that this process likely plays an important role in cellular regulation. Several authors have extensively reviewed this pathway (Hershko and Ciechanover 1998; Metzger et al. 2012; Pickart 2001). The ubiquitin molecule possesses seven lysine residues (K6, K11, K27, K29, K33, K48, and K63) that enable the formation of polyubiquitin chains (Xu et al. 2009). The fate of ubiquitylated proteins depends on the pattern of ubiquitylation. Polyubiquitylated proteins (generally lysine K48 chains, but potentially other lysines) are generally degraded by the proteasomes found in the cytoplasm, in the nucleus, or at the level of the endoplasmic reticulum (Xu et al. 2009). The proteasome is a macromolecular complex of proteases with a regulatory ring that binds to polyubiquitin and a catalytic cylinder. The mono-ubiquitylation (or di-ubiquitylation, generally on lysine K63) of a membrane protein leads to its internalization, followed by either its lysosomal degradation by a complex endosomal sorting system (ESCRT—endosomal sorting complex required for transport) or to it being recycled (Ciechanover 2005; Hurley and Emr 2006; Shih et al. 2000).

3 Nedd4/Nedd4-Like Ubiquitin Ligase Family

There are two major classes of E3 ubiquitin ligases: the RING finger (really interesting new gene) E3s dependent on Zn^{2+} binding (Joazeiro and Weissman 2000) and the HECT (homologous to E6-AP COOH terminal) E3s (Metzger et al. 2012). The latter contain a HECT domain, the catalytic site responsible for the ubiquitylation of the target protein (Huibregtse et al. 1995; Scheffner et al. 1995). The Nedd4/Nedd4-like (neuronal precursor cell-expressed developmentally downregulated gene 4) ubiquitin–protein ligases (Ingham et al. 2004) are important members of the HECT E3 ligases, and their involvement in the ubiquitylation of membrane proteins has been well described (Rotin et al. 2000). In addition to a catalytic HECT domain, they have both a NH2-terminal C2 domain (calcium-dependent lipid binding domain) (Rizo and Sudhof 1998) responsible for substrate localisation and a variable number (two to four) of WW domains (protein–protein interaction) (Staub and Rotin 1996) responsible for substrate recognition. There are nine members in the Nedd4 family in humans: *NEDD4*, *NEDD4-2*, *SMURF1*, *SMURF2*, *WWP1*, *WWP2*, *NEDL1*, *NEDL2*, and *ITCH* (Harvey and Kumar 1999; Ingham et al. 2004). Nedd4 is presumably the ancestral member of the family, whereas Nedd4-2 emerged later in the evolution process (Yang and Kumar 2009). Nedd4 was first identified as part of a set of genes strongly downregulated in the developing mouse brain (Sazuka et al. 1992). Nedd4 and Nedd4-2 are closely related to each other and are widely expressed in different tissues in the body, such as the heart, kidney, and nervous system (Yang and Kumar 2009). The WW domains play an important role in the interaction with the substrate proteins. The C2 domain, in addition to enabling Nedd4 to bind to the phospholipid of membranes, can also participate in this interaction (Plant et al. 2000). WW motifs (also called WWP motifs due to the presence of a conserved proline) consist of 35–40 amino acids, and received their name due to the presence of two conserved tryptophan residues (W) separated by 20–22 amino acids (Bork and Sudol 1994; Sudol 1996). These motifs fold into a triple stranded antiparallel β-sheet (Macias et al. 1996) that surrounds a hydrophobic core. The WW motifs of the Nedd4 protein family bind to a short, proline-rich, and conserved motif (Chen and Sudol 1995; Sudol and Hunter 2000), known as the PY motif consisting of a L/PPxY sequence in which x corresponds to any kind of amino acid (Kanelis et al. 2001; Lu et al. 1999). Because these domains have different affinities for PY motifs (Fotia et al. 2003; Harvey et al. 1999; Harvey and Kumar 1999; Kanelis et al. 2001), and given the different combinations of these domains in Nedd4 an Nedd4-2 (Harvey and Kumar 1999; Itani et al. 2003), they can interact with numerous different substrates with variable strengths. Many different membrane transporters possess such PY motifs (Fig. 1).

4 Nedd4 Family and Epithelial Sodium Channel ENaC

The amiloride-sensitive epithelial sodium channel (ENaC) was the first, and remains probably the best, described ion channel found to be regulated by the ubiquitin-mediated trafficking pathways (Rossier et al. 2002). ENaC plays an important role in sodium homeostasis. In 1994, a mutation leading to a truncated ENaC was identified. It

Gene	access Number	first residue	extended PY-motif sequence
$Na_v1.1$	P35498	1978	S T A C C **P P S Y** D R V T K
$Na_v1.2$	Q99250	1967	P S T T S **P P S Y** D S V T K
$Na_v1.3$	Q9NY46	1962	S S T T S **P P S Y** D S V T K
$Na_v1.5$	Q14524	1969	S S T S F **P P S Y** D S V T R
$Na_v1.6$	Q9UQD0	1939	P S T A S **L P S Y** D S V T K
$Na_v1.7$	Q15858	1950	S S T T S **P P S Y** D S V T K
$Na_v1.8$	Q9Y5Y9	1913	S A T S F **P P S Y** D S V T R
αENaC	P37088	636	A L T A P **P P A Y** A T L G P
βENaC	P51168	612	I P G T P **P P N Y** D S L R L
γENaC	P51170	619	V P G T P **P P K Y** N T L R L
TrkA	P04629	783	A L A Q A **P P V Y** L D V L G
$K_v7.1$	P51787	654	L P S N T **L P T Y** E Q L T V
$K_v7.2$	O43526	662	K E P E P A **P P Y** H S P E D
$K_v7.3$	O43525	689	E T G P P E **P P Y** S F H Q V
$K_v11.1$	Q12809	1070	Q M T L V **P P A Y** S A V T T
SGK1	O00141	290	M L Y G L **P P F Y** S R N T A
SGK2	Q9HBY8	287	M L H G L **P P F Y** S Q D V S
SGK3	Q96BR1	354	M L Y G L **P P F Y** C R D V A

Fig. 1 Alignment of the amino acid sequences bearing a PY motif found in membrane proteins (except SGKs that are cytosolic). UniProtKB/Swiss-Prot accession number and the first residue of the sequence position are shown

was associated with an autosomal dominant hypertensive disease known as Liddle's syndrome (Shimkets et al. 1994; Hansson et al. 1995). ENaC consists of three subunits, α, β, and γ, all of which possess a PY motif in their C-terminal domain (Schild et al. 1996; Staub et al. 2000) (Fig. 1). Further studies demonstrated that mutating the PY motif of ENaC was sufficient for generating this hereditary form of arterial hypertension (Schild et al. 1996) and led to an increased expression of functional ENaC at the cell membrane (Firsov et al. 1996). Other groups confirmed the importance of the PY motif (Fotia et al. 2003; Harvey et al. 1999; Henry et al. 2003) and have implicated the Nedd4 family in its regulation. In vitro studies demonstrated that Nedd4-2 (Abriel et al. 1999; Kamynina et al. 2001), and to a lesser extent Nedd4 (Henry et al. 2003), downregulated ENaC cell surface expression. A functional effect of Nedd4-2 in vivo was recently shown using knocking out Nedd4-2 expression in the kidney, which caused salt-sensitive hypertension, presumably mediated by increased ENaC activity (Shi et al. 2008) and subsequent increased Na^+ reabsorption.

5 Nedd4 Family Ubiquitin Ligases Regulate Na_vs

With the exception of $Na_v1.4$ and $Na_v1.9$, every Na_vs isoform has a conserved PY motif at the α-subunit C-terminal, making them potential targets for the Nedd4 ubiquitin ligase family (Fig. 1). Nedd4 was demonstrated to downregulate membrane $Na_v1.5$ in *Xenopus* oocytes, a process that was dependent on both an intact

PY motif and a functional catalytic site (Abriel et al. 2000). This provided the first evidence that E3 ligase can negatively regulate Na_vs in cell expression systems. Nedd4-2 regulation of Na_vs, in particular $Na_v1.5$, has been extensively investigated in HEK293 cells, with the following results: (1) a decrease in current density upon Nedd4-2 co-expression, (2) which was dependent on the PY motif, (3) concomitant with the ubiquitylation of the sodium channel, (4) which relied on an intact catalytic site of Nedd4-2, (5) and finally implicating an interaction between the two proteins (van Bemmelen et al. 2004). These results were further transposed to other neuronal isoforms, namely $Na_v1.2$ and $Na_v1.3$, in the same cellular expression systems (Rougier et al. 2005) and more recently were also observed for $Na_v1.7$ (Laedermann et al. 2013). Nedd4-2 was also shown to downregulate $Na_v1.2$, $Na_v1.7$ and $Na_v1.8$ in *Xenopus oocytes* (Fotia et al. 2004). The molecular determinants of the PY motif of Na_v channels were studied by several groups. Notably, the first proline of the PPxY motif can be substituted by a leucine, a motif found in $Na_v1.6$, without notable loss of affinity (Kasanov et al. 2001; Rougier et al. 2005). This helps explain why Nedd4-2 was also reported to decrease $Na_v1.6$ in vitro (Gasser et al. 2010), despite the absence of the strict PPxY motif in this isoform.

Despite the increasing evidence that Na_vs are negatively regulated by Nedd4-2 in vitro (Rotin and Staub 2011), its functional significance for regulating Na_vs in vivo was only recently investigated. Using the spared nerve injury model of neuropathic pain (SNI) (Decosterd and Woolf 2000), Laedermann et al. (2013) observed a reduction of Nedd4-2 expression in primary sensory neurons with a concomitant increase in the expression and function of $Na_v1.7$ and $Na_v1.8$. Since Nedd4-2 has a negative regulatory effect, it was hypothesized that the two observations were causally linked. To further validate this hypothesis and study the role of Nedd4-2 in pain pathophysiology, a nociceptive neuron-specific knock-out of Nedd4-2 was generated. Dysregulation of $Na_v1.7$ and $Na_v1.8$ expression, as that observed after SNI, was found. The mice also showed an altered nociceptive pain phenotype. This study is the first demonstration that Nedd4-2 regulates Na_vs in vivo, and that altering this regulation leads to erratic Na_vs trafficking, which can be responsible for the hyperexcitability and hypersensitivity in mice.

6 PY Motif and Other Motifs as Binding Sites for Nedd4 Ligases

The hydrophobic core, surrounded by β-sheets of WW domains, interacts with the canonical sequence (L/P)PxY (Kasanov et al. 2001) via a polyproline type II helix. The importance of the PY motif in the Nedd4-2 regulation of Na_vs was demonstrated when proline or tyrosine residues in this motif were mutated into an alanine in $Na_v1.5$ (van Bemmelen et al. 2004), $Na_v1.7$ (Laedermann et al. 2013), and $Na_v1.8$ (Fotia et al. 2004), which led to the loss of the Nedd4-2 downregulatory effect. A hydrophobic residue in position +3 after the tyrosine of the PY motif (Tyr +3, Fig. 1) is involved in the binding to the WW-domain pocket, providing additional binding energy. It is referred to as “the extended PY motif” (Henry

et al. 2003; Kanelis et al. 2001), as previously described for ENaC. Interestingly, the consensus sequence P/LPxYxxV is observed in every Na_vs with a PY motif (Fig. 1). A mutation in this extended PY motif in Tyr +3 did not alter the affinity between the $Na_v1.5$ or $Na_v1.7$ PY motif and Nedd4-2 (Laedermann et al. 2013; Rougier et al. 2005). Furthermore, the downregulatory effect of Nedd4-2 on these two mutant isoforms, although reduced, was still present (Laedermann et al. 2013; Rougier et al. 2005). These findings suggest that unlike ENaC, the extended PY motif is not essential for the Nedd4-2 downregulation of Na_vs.

As aforementioned, PY motif mutations in ENaC cause arterial hypertension in humans. The importance of this motif in both cardiac and neuronal Na_vs isoforms (Fotia et al. 2004; Laedermann et al. 2013; Rougier et al. 2005) suggests that mutations in this sequence may underlie other types of disorders. For example, the mutation p.Y1977N of the $Na_v1.5$ PY motif has been proposed to cause congenital long QT syndrome (Kapa et al. 2009; Rougier et al. 2012).

The conserved PY motif in the C-terminus of Na_vs plays a key role, but the WW domains can also bind to alternative motifs (Sudol and Hunter 2000), such as phosphorylated Px(pS/T)P (Lu et al. 1999), PPLP (Bedford et al. 1997), and PR (Bedford et al. 1998) motifs. A recent study (Gasser et al. 2010) demonstrated that a conserved PGSP motif in the intracellular loop L1 of $Na_v1.6$ was phosphorylated by phospho-p38 (activated stress-induced p38 MAPK), which converted this motif into a Px(pS)P Nedd4-2 binding motif (Fig. 3). It was reported that both the LPxY motif in the C-terminus and the Px(pS)P in L1 were necessary for Nedd4-2 to downregulate $Na_v1.6$ (Gasser et al. 2010).

Thus far, the necessity of an intact PY motif in Na_vs for Nedd4-dependent regulation has been demonstrated for every isoform tested. However, the effect of Nedd4-2 on other proteins, such as $K_v7.3$, is not altered upon mutation of the PY motif (Ekberg et al. 2007). Nedd4-2 can downregulate $K_v1.3$ (Henke et al. 2004), which is devoid of a PY motif. This provides further evidence that Nedd4-2 may have the ability to bind to other sequences. These findings, however, could also result from mechanisms involving adaptor proteins, such as those of the NDFIP family (NEDD4 family-interacting proteins) (Mund and Pelham 2009). Nedd4-2 may also regulate $K_v1.3$ through chaperones and accessory proteins such as KChAP, which do have a PY motif (Kuryshev et al. 2001).

7 Cellular Fate of Ubiquitylated Na_vs

The decrease of the $Na_v1.5$ and $Na_v1.7$-mediated current was demonstrated to be concomitant with increased ubiquitylation in HEK293 cells, suggesting that it is the addition of ubiquitin moieties that enables Nedd4-2 to decrease the number of functional channels at the cell surface (Laedermann et al. 2013; Rougier et al. 2005). The evidence that ubiquitylation led to the internalization of Na_vs was first demonstrated using $Na_v1.5$-YFP fusion proteins (van Bemmelen et al. 2004). Under control conditions, $Na_v1.5$ was predominantly located at the plasma membrane (Fig. 2a), but the distribution of this isoform was homogenously redistributed

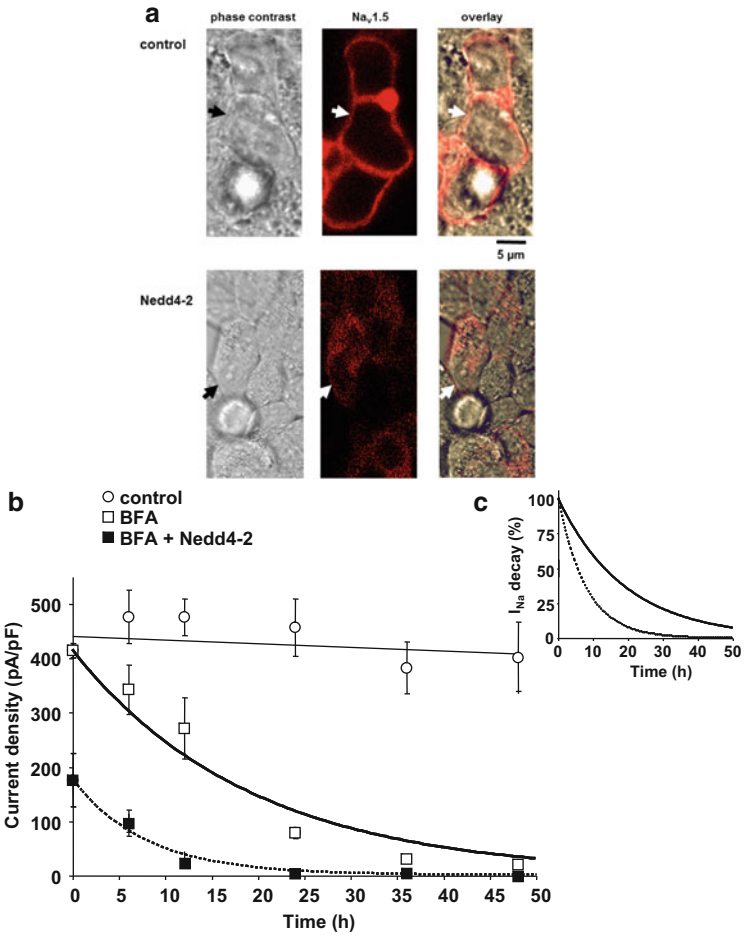

Fig. 2 Nedd4-2 internalizes Na$_v$1.5 in vitro. (**a**) HEK293 cells transiently transfected with Na$_v$1.5 YFP fusion protein and co-expressed with Nedd4-2. The peripheral localization of the Na$_v$1.5-YFP was reduced upon Nedd4-2 cotransfection. (**b**) Time course of peak current densities of HEK293 cells stably expressing Na$_v$1.5 in three experimental conditions: control (*open circle*), cells treated with 50 ng/ml brefeldin A (BFA) (*open square*), and transiently transfected 24 h earlier with Nedd4-2 and treated with BFA ($t = 0$) (*closed circle*). The *bold* and *dotted* curves are monoexponential fits of the I_{Na} decays. (**c**) Normalization of the fitted I_{Na} decays shown in (**b**) after BFA suggests that Nedd4-2 increases the internalization rate of Na$_v$1.5 (*bold line*, BFA alone; *dotted line*, BFA + Nedd4-2). Modified from van Bemmelen et al. (2004) and Rougier et al. (2005)

throughout the cytosol upon Nedd4-2 co-expression, suggesting that the channel was internalized. To confirm that Nedd4-2 increases the internalization rate, brefeldin A (BFA), a fungal metabolite that blocks the trafficking of newly synthesized channels to the plasma membrane, was used (Rougier et al. 2005). The use of BFA in a cell line stably expressing Na$_v$1.5 led to the demonstration that the half-life of Na$_v$1.5 expressed at the membrane was approximately 13 h (Fig. 2b, c). Upon Nedd4-

2 cotransfection, the $Na_v1.5$ half-life was decreased to 6 h (Fig. 2b, c), providing further evidence that Nedd4-2 increases the internalization rate of $Na_v1.5$.

The pattern of ubiquitylation and the fate of Na_vs upon Nedd4-2 ubiquitylation have yet to be studied in detail. The finding of the diffuse band of ubiquitylated $Na_v1.5$ in HEK293 cells (Rougier et al. 2005) suggests that Nedd4-2 polyubiquitylates Na_vs in cell expression systems. The same diffuse ubiquitylation band was also observed for $Na_v1.7$ in HEK293 cells (Laedermann et al. 2013) upon Nedd4-2 co-expression. If $Na_v1.5$ and $Na_v1.7$ are polyubiquitylated, they are most likely to be subject to proteasomal degradation (Xu et al. 2009). However, in the two aforementioned studies, even though the I_{Na} mediated by $Na_v1.5$ and $Na_v1.7$ was decreased, the global expression of these proteins in the total lysate was not decreased upon Nedd4-2 co-expression. This suggests that Na_vs are not subject to proteolysis in HEK293 cells after internalization. The identification of the lysine residues involved in the Nedd4 family ubiquitylation, as well as the pattern of ubiquitylation, remains to be determined.

In vivo ubiquitylation has to our knowledge only been observed for $Na_v1.5$ expressed in cardiac tissue (van Bemmelen et al. 2004), and the band of ubiquitylated $Na_v1.5$ was less diffuse than the one observed in HEK293 cells. This suggests that Nedd4-2 may promote mono- or oligo-ubiquitylation of Na_vs in vivo. The in vivo fate of ubiquitylated Na_vs has only been sparsely investigated. A study using sensory-specific Nedd4-2 knockout mice (Laedermann et al. 2013) reported that $Na_v1.7$ total lysate expression is not modified in sensory neurons despite the strong increase in the $Na_v1.7$-mediated current, suggesting that the channels are not degraded after internalization. This observation is consistent with Na_vs expression being more subject to mono-ubiquitylation in native tissues. The results obtained for $Na_v1.8$ suggest an internalization process followed by degradation, as the wild-type mice show less amounts of functional $Na_v1.8$ when compared to knockout mice (Laedermann et al. 2013), and there is a complete loss of signal in the total lysate fraction. This suggests that the ubiquitylation of each Na_vs isoform depends on the identity of the sodium channel, as well as the ubiquitin ligase involved. Further experiments are required to unravel the exact mechanisms proceeding internalization of Na_vs both in vitro and in vivo.

8 Posttranslational Regulation of Nedd4-2

The regulation of Nedd4-2 at the posttranslational level was largely studied in the kidney, which demonstrated the central role of Nedd4-2 phosphorylation (Fig. 3). The mineralocorticoid hormone aldosterone induces the transcription of serum and glucocorticoid-induced kinase type 1 (SGK1) (Snyder 2009), which binds (via a WW motif), phosphorylates, and prevents Nedd4-2 activity by provoking an increase of ENaC function (Debonneville et al. 2001). A similar role is shared by the two other isoforms, SGK2 and SGK3 (Friedrich et al. 2003). Conversely, the hormone vasopressin activates adenylate cyclase, leading to an increase in cAMP and the subsequent activation of protein kinase A (PKA) (Snyder et al. 2004). These two kinases phosphorylate the same consensus sequence

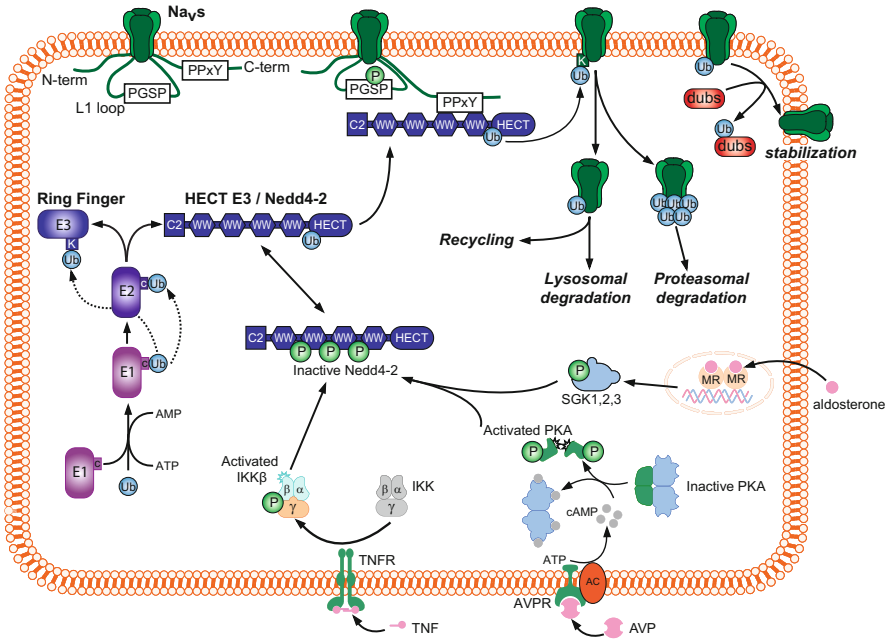

Fig. 3 Schematic representation of the roles of Na_v channel ubiquitylation and its regulatory pathways. *Ub* ubiquitin, *E1* Ubiquitin-activating enzyme, *E2* Ubiquitin-conjugating enzyme, *E3* Ubiquitin ligase, *C* cysteine residue, *L*: lysine residue, *ATP* adenosine triphosphate, *AMP* adenosine monophosphate, *cAMP* cyclic adenosine monophosphate, *RING* really interesting new gene ubiquitin ligases family, *HECT* Homologous to E6-AP carboxyl-terminus ubiquitin ligases family, *C2* calcium-dependent lipid binding domain domain, *dubs* deubiquitylating enzymes, *P* phosphate group, *MR* mineralocorticoid receptor, *AVP* vasopressin, *AVPR* vasopressin receptor, *TNF* tumor necrosis factor, *TNFR* TNF receptor, *SGK* serum glucocorticoid kinase, *PKA* protein kinase A, *IKK* IκB ([inhibitor of nuclear factor κB (NF-κB)]) kinase, *IKKβ* IκB kinase β-subunit. Note that PGSP motif is specific to $Na_v1.6$, whereas PPxY motif is found in every Na_v isoform except $Na_v1.4$ and $Na_v1.9$

RxRxx(S/T) at three different sites (Ser 221, Thr 246, and Ser 327) and reduce Nedd4-2 s ability to bind to ENaC, rendering this motif a convergent point for different regulatory pathways.

In inflammatory processes, cytokines are implicated in a complex pathway leading to NF-κB activation. Cytokines activate IκB [inhibitor of nuclear factor κB (NF-κB)] kinase (IKK) via phosphorylation, which in turn phosphorylates and inactivates IκB inhibitory proteins. The transcription factor NF-κB is disinhibited and its anti-apoptotic functions are triggered (Delhase et al. 1999). A subunit of IKK, IKKβ, was recently reported to phosphorylate Ser327 of Nedd4-2 (Edinger et al. 2009), resulting in enhanced ENaC function in the kidney. IKK is enriched in unmyelinated nerves and could possibly act as a negative regulator of Nedd4-2 in these neurons following inflammation. Nevertheless, the fact that the conditional sensory-specific knockout of this protein leads to increased mechanical, cold and

noxious heat sensitivity (Bockhart et al. 2009), as well as an increase in TRP channel activity is in conflict with this hypothesis.

Nedd4-2 also regulates its own stability (Bruce et al. 2008). This ubiquitin ligase possesses a LPxY motif, and binding of its own WW motifs to its own PY motifs prevents Nedd4-2 from self-ubiquitylation. This interaction is disrupted upon substrate binding, which permits Nedd4-2 ubiquitylation and its subsequent degradation.

The activity of ubiquitin ligases are counterbalanced by the action of deubiquitylating (DUB) enzymes (Amerik and Hochstrasser 2004), which allows for the removal of ubiquitin from targeted proteins (Fig. 3). One study (Fakitsas et al. 2007) showed that the deubiquitylating enzyme Usp2-45 can increase ENaC function by deubiquitylation of the channel. In another study the Nedd4-2-downregulatory effect on $K_v7.1$ was counteracted when Usp2 was co-expressed in cell expression systems (Krzystanek et al. 2012). Whether similar mechanisms could be involved in Na_vs regulation remains to be investigated.

A strategy for modulating the activity of enzymes of the ubiquitin system was recently proposed (Ernst et al. 2013). Even though initially developed for inhibiting DUBs enzymes by using massively diverse combinatorial libraries of ubiquitin variants, the authors also reported that these ubiquitin variants could enhance both E2 and E3 enzymes activity.

Another mechanism by which Nedd4-2 is regulated is through direct competition of binding to its substrate. For instance, even though WWP2 and Nedd4-2 can both downregulate $Na_v1.5$, their co-expression no longer decreased $Na_v1.5$ due to competitive mechanisms (Rougier et al. 2005). The reason for this competition was unclear, but probably is only partially related to the competitive binding on the PY motif. PY-binding competition has been demonstrated in HEK293 cells (Rougier et al. 2005) and *Xenopus* (Abriel et al. 2000), where an inactive Nedd4-2 CS mutant increased $Na_v1.5$-mediated current. It was proposed that this effect could be due to competition with endogenous Nedd4-2. Silencing Nedd4-2 in HEK293 cells led to a similar increase of the $Na_v1.7$-mediated I_{Na} (Laedermann et al. 2013). This implied that Nedd4-2 is expressed in HEK293 cells, as has been previously demonstrated (unpublished data).

9 Splice Variants and Alternative Regulation of Nedd4-2

Nedd4-2 is present as a single gene, which spans over 400 kb, and contains more than 40 exons. The human Nedd4-2 gene has a complex structure with variable promoters, differential internal splicing, and alternative polyadenylation signal sequences. It has up to 136 different splice variants encoding for at least 24 proteins variants (Itani et al. 2003), as documented with cDNA libraries from human cell lines. These variants may be expressed in either a spatial or temporal specific manner in developing organs.

The role of these splice variants has been functionally investigated with ENaC. The aforementioned role of WW motifs and their differential affinity illustrate that these

splice variants, expressing different combinations of WW motifs, can lead to different Nedd4-2 functions (Itani et al. 2005). Furthermore, there are splice variants that can predict differences in the number of SGK1 phosphorylation sites (Itani et al. 2003). These splice variants could also be devoid of C2 domain, and for instance, despite its presence in human, this domain is not present in mouse Nedd4-2 (Kamynina et al. 2001). There are also Nedd4 splice variants with distinct functions (Chen et al. 2001). Even though the C2 domain does not affect Nedd4 activity, Nedd4 is a more potent inhibitor of ENaC when the C2 domain is deleted (Snyder et al. 2001), highlighting the importance of the presence or absence of these motifs.

Whether these multiple protein variants differentially associate and regulate Na_vs, as they do with ENaC, remains to be investigated.

10 Role of Nedd4-2 in Human Disorders

The potent downregulatory role of the Nedd4 family on Na_vs has uncovered new mechanisms of regulating cellular excitability. The Nedd4 family is involved in animal growth (Cao et al. 2008), immunity (Yang et al. 2008), heart development (Fouladkou et al. 2010), and neurite development (Kawabe et al. 2010). The pathophysiological functions of Nedd4-2 on the control of ion channel surface expression have been demonstrated for ENaC and recently for Na_vs.

Because of these evidences in animal models, researchers started to look for variants in the gene encoding Nedd4-2 in humans. In the light of ENaC regulation, no mutations of Nedd4-2 were identified, but several polymorphisms have been linked to hypertensive diseases (Araki et al. 2008; Dunn et al. 2002; Fouladkou et al. 2004; Luo et al. 2009). One of these naturally occurring Nedd4-2 variants was reported to impair downregulatory activity in vitro (Fouladkou et al. 2004).

A role for Nedd4-2 in photosensitive generalized epilepsy (IGE) has been proposed (Dibbens et al. 2007). In a study involving the screening of more than 250 families, the authors identified three rare Nedd4-2 gene variants: one missense mutation, one intronic mutation, and one substitution mutation. These mutations were all located in the WW motif of Nedd4-2. However, there was no loss of efficiency of Nedd4-2 downregulation of $Na_v1.2$ in *Xenopus oocytes*. Whether these mutants have intact downregulatory effects on other Na_vs is of great interest, as $Na_v1.1$ was reported to be of importance in epilepsy (Catterall et al. 2010).

The human metastatic breast cancer MDA-MB-231 cells have more Nedd4-2 mRNA than the weakly/non-metastatic MCF-7 cells (Kuratomi et al. 2005). The metastatic potential in cells lines is correlated with altered Na_v expression, such as $Na_v1.5$ for example (Fraser et al. 2005; Gillet et al. 2009), even though a relation between the two has yet to be demonstrated. The modulation of Nedd4-2 expression in these cell lines in order to study Na_vs expression and metastatic potential has yet to be done.

Because of their role in cellular excitability, Na_vs have been the target for the development new drugs with the potential to enhance or inhibit their function. One of the goals has been to find Na_v isoform-specific drugs. To date only a few drugs

have been successfully developed as the structures and sequences of the different isoforms are very similar, and blocking a specific isoform is challenging. As a result most of drugs proposed have significant side effects. Targeting the mechanisms of Na_vs regulation, rather than Na_vs themselves, could be a way to avoid this problem. Highlighting this possibility, rescuing Nedd4-2 expression, using a viral vector approach, after the SNI-mediated decrease of this ubiquitin ligase led to a decrease in Na_vs expression and to the attenuation of pain hypersensitivity (Laedermann et al. 2013). The overexpression of Nedd4-2 in naïve animals did not modify Na_vs expression and only affected basal pain sensitivity to a minor extent, representing an obvious therapeutic advantage. Interestingly, intrathecal injection of a proteasome inhibitor also led to the attenuation of pain hypersensitivity after nerve injury (Moss et al. 2002; Ossipov et al. 2007). The authors hypothesized that this effect may be due to the inhibition of the upregulation of ubiquitin C-terminal hydrolase in the dorsal horn of the spinal cord, which enhances proteasome activity. A recent study that treated dystrophin-deficient mice, in which $Na_v1.5$ cardiac expression is decreased, with the proteasome inhibitor MG132, rescued both the reduced protein expression and the sodium current of myocytes (Rougier et al. 2013).

However, the specificity of targeting ubiquitin ligases might also prove problematic since they are widely expressed and act on numerous targets, increasing the likelihood of side effects. Nedd4-2 regulates other voltage-gated ion channels, such as potassium (K_vs and KCNQs) and choride (ClCs) channels, which modulate electrical excitability in neurons (Bongiorno et al. 2011). Nedd4-2 regulation is not restricted to voltage-gated ion channels, but includes interactions with amino acids, dopamine transporters, glutamate transporters, adaptor proteins, and kinases (Yang and Kumar 2009).

Conclusions

Ion channel activity can be regulated at many different levels (Rosati and McKinnon 2004) and can be influenced by a myriad of drugs. With the advances of more specific and sensitive biochemical technologies, it is becoming apparent that posttranslational modifications of the pore-forming subunit of ion channels represent crucial steps in which one can modify their function following biosynthesis. Over the past 15 years, several groups have demonstrated that ion channels can be ubiquitylated and that this modification can be a way to mark channels at the plasma membrane for internalization. Since most Na_v channels have conserved PY motifs in their C-terminus that serve as binding motifs of ubiquitin ligases of the Nedd4 family, it seems logical that this pathway is important for the control of the number of Na_v channels at the cell surface of excitable cells. Thus far, most of the experimental data addressing the role of this pathway were obtained in cellular expression systems. Two recent studies using rat and mouse models of neuropathic pain (Cachemaille et al. 2012; Laedermann et al. 2013) suggested that sensory neuronal hyperexcitability may result from altered ubiquitylation-dependent Na_v regulation. These studies have provided the first in vivo evidence of the role of Nedd4-2-dependent regulation of Na_v

channels in disease. This ubiquitylation pathway may be a target for the pharmacological treatment of symptoms and diseases linked to Na_v-dependent hyperexcitability, such as chronic pain, epilepsy, migraine, myotonia, and cardiac arrhythmias.

Acknowledgments The studies described in this chapter were supported by grants from the Swiss National Science Foundation (31003A-124996 to I.D. and 310030B- 135693 to H.A.), the Synapsis Foundation (to I.D. and H.A.), the European Society of Anesthesiology (to I.D. and H.A.), and the Lemanic Neuroscience Doctoral School Ph.D. Fellowship (to C.J.L.). We thank Dr. A. Felley and Dr. J.S. Rougier for their comments on the manuscript of this chapter.

References

Abriel H, Staub O (2005) Ubiquitylation of ion channels. Physiology (Bethesda) 20:398–407. doi:10.1152/physiol.00033.2005

Abriel H, Loffing J, Rebhun JF, Pratt JH, Schild L, Horisberger JD, Rotin D, Staub O (1999) Defective regulation of the epithelial Na + channel by Nedd4 in Liddle's syndrome. J Clin Invest 103:667–673. doi:10.1172/JCI5713

Abriel H, Kamynina E, Horisberger JD, Staub O (2000) Regulation of the cardiac voltage-gated Na + channel (H1) by the ubiquitin-protein ligase Nedd4. FEBS Lett 466:377–380. doi:10.1016/S0014-5793(00)01098-X

Amerik AY, Hochstrasser M (2004) Mechanism and function of deubiquitinating enzymes. Biochim Biophys Acta 1695:189–207. doi:10.1016/j.bbamcr.2004.10.003

Araki N, Umemura M, Miyagi Y, Yabana M, Miki Y, Tamura K, Uchino K, Aoki R, Goshima Y, Umemura S, Ishigami T (2008) Expression, transcription, and possible antagonistic interaction of the human Nedd4L gene variant: implications for essential hypertension. Hypertension 51:773–777. doi:10.1161/HYPERTENSIONAHA.107.102061

Bedford MT, Chan DC, Leder P (1997) FBP WW domains and the Abl SH3 domain bind to a specific class of proline-rich ligands. EMBO J 16:2376–2383. doi:10.1093/emboj/16.9.2376

Bedford MT, Reed R, Leder P (1998) WW domain-mediated interactions reveal a spliceosome-associated protein that binds a third class of proline-rich motif: The proline glycine and methionine-rich motif. Proc Natl Acad Sci U S A 95:10602–10607. doi:10.1073/pnas.95.18.10602

Beltran-Alvarez P, Pagans S, Brugada R (2011) The cardiac sodium channel is post-translationally modified by arginine methylation. J Proteome Res 10:3712–3719. doi:10.1021/pr200339n

Bierhaus A, Fleming T, Stoyanov S, Leffler A, Babes A, Neacsu C, Sauer SK, Eberhardt M, Schnolzer M, Lasitschka F, Neuhuber WL, Kichko TI, Konrade I, Elvert R, Mier W, Pirags V, Lukic IK, Morcos M, Dehmer T, Rabbani N, Thornalley PJ, Edelstein D, Nau C, Forbes J, Humpert PM, Schwaninger M, Ziegler D, Stern DM, Cooper ME, Haberkorn U, Brownlee M, Reeh PW, Nawroth PP (2012) Methylglyoxal modification of Nav1.8 facilitates nociceptive neuron firing and causes hyperalgesia in diabetic neuropathy. Nat Med 18:926–933. doi:10.1038/nm.2750

Bork P, Sudol M (1994) The WW domain: a signalling site in dystrophin? Trends Biochem Sci 19:531–533. doi:10.1016/0968-0004(94)90053-1

Bockhart V, Constantin CE, Häussler A, Wijnvoord N, Kanngiesser M, Myrczek T, Pickert G, Popp L, JrM S, Pasparakis M, Kuner R, Geisslinger G, Schultz C, Kress M, Tegeder I (2009) Inhibitor κB kinase β deficiency in primary nociceptive neurons increases TRP channel sensitivity. J Neurosci 29:12919–12929. doi:10.1523/JNEUROSCI.1496-09.2009

Bongiorno D, Schuetz F, Poronnik P, Adams DJ (2011) Regulation of voltage-gated ion channels in excitable cells by the ubiquitin ligases Nedd4 and Nedd4-2. Channels (Austin) 5:79–88

Bruce MC, Kanelis V, Fouladkou F, Debonneville A, Staub O, Rotin D (2008) Regulation of Nedd4-2 self-ubiquitination and stability by a PY motif located within its HECT-domain. Biochem J 415:155–163. doi:10.1042/BJ20071708

Cachemaille M, Laedermann CJ, Pertin M, Abriel H, Gosselin RD, Decosterd I (2012) Neuronal expression of the ubiquitin ligase Nedd4-2 in rat dorsal root ganglia: modulation in the spared nerve injury model of neuropathic pain. Neuroscience 227:370–380. doi:10.1016/j.neuroscience.2012.09.044

Cao XR, Lill NL, Boase N, Shi PP, Croucher DR, Shan H, Qu J, Sweezer EM, Place T, Kirby PA, Daly RJ, Kumar S, Yang B (2008) Nedd4 controls animal growth by regulating IGF-1 signaling. Sci Signal 1:ra5. doi:10.1126/scisignal.1160940

Catterall WA (2000) From ionic currents to molecular mechanisms: the structure and function of voltage-gated sodium channels. Neuron 26:13–25. doi:10.1016/s0896-6273(00)81133-2

Catterall WA, Kalume F, Oakley JC (2010) NaV1.1 channels and epilepsy. J Physiol 588:1849–1859. doi:10.1113/jphysiol.2010.187484

Chen HI, Sudol M (1995) The Ww domain of yes-associated protein binds a proline-rich ligand that differs from the consensus established for Src homology 3-binding modules. Proc Natl Acad Sci U S A 92:7819–7823. doi:10.1073/pnas.92.17.7819

Chen H, Ross CA, Wang N, Huo Y, MacKinnon DF, Potash JB, Simpson SG, McMahon FJ, DePaulo JR Jr, McInnis MG (2001) NEDD4L on human chromosome 18q21 has multiple forms of transcripts and is a homologue of the mouse Nedd4-2 gene. Eur J Hum Genet 9:922–930. doi:10.1038/sj.ejhg.5200747

Ciechanover A (2005) Proteolysis: from the lysosome to ubiquitin and the proteasome. Nat Rev Mol Cell Biol 6:79–87. doi:10.1038/nrm1552

Ciechanover A, Heller H, Elias S, Haas AL, Hershko A (1980) ATP-dependent conjugation of reticulocyte proteins with the polypeptide required for protein degradation. Proc Natl Acad Sci U S A 77:1365–1368

Cohen SA, Levitt LK (1993) Partial characterization of the Rh1 sodium-channel protein from rat-heart using subtype-specific antibodies. Circ Res 73:735–742. doi:10.1161/01.res.73.4.735

Debonneville C, Flores SY, Kamynina E, Plant PJ, Tauxe C, Thomas MA, Munster C, Chraibi A, Pratt JH, Horisberger JD, Pearce D, Loffing J, Staub O (2001) Phosphorylation of Nedd4-2 by Sgk1 regulates epithelial Na(+) channel cell surface expression. EMBO J 20:7052–7059. doi:10.1093/emboj/20.24.7052

Decosterd I, Woolf CJ (2000) Spared nerve injury: an animal model of persistent peripheral neuropathic pain. Pain 87:149–158. doi:10.1016/s0304-3959(00)00276-1

Delhase M, Hayakawa M, Chen Y, Karin M (1999) Positive and negative regulation of IκB kinase activity through IKKβ subunit phosphorylation. Science 284:309–313

Dibbens LM, Ekberg J, Taylor I, Hodgson BL, Conroy SJ, Lensink IL, Kumar S, Zielinski MA, Harkin LA, Sutherland GR, Adams DJ, Berkovic SF, Scheffer IE, Mulley JC, Poronnik P (2007) NEDD4-2 as a potential candidate susceptibility gene for epileptic photosensitivity. Genes Brain Behav 6:750–755. doi:10.1111/j.1601-183X.2007.00305.x

Dunn DM, Ishigami T, Pankow J, von Niederhausern A, Alder J, Hunt SC, Leppert MF, Lalouel J-M, Weiss RB (2002) Common variant of human NEDD4L activates a cryptic splice site to form a frameshifted transcript. J Hum Genet 47:665–676

Edinger RS, Lebowitz J, Li H, Alzamora R, Wang H, Johnson JP, Hallows KR (2009) Functional regulation of the epithelial Na+ channel by IκB kinase-β occurs via phosphorylation of the ubiquitin ligase Nedd4-2. J Biol Chem 284:150–157. doi:10.1074/jbc.M807358200

Ekberg J, Schuetz F, Boase NA, Conroy SJ, Manning J, Kumar S, Poronnik P, Adams DJ (2007) Regulation of the voltage-gated K(+) channels KCNQ2/3 and KCNQ3/5 by ubiquitination. Novel role for Nedd4-2. J Biol Chem 282:12135–12142. doi:10.1074/jbc.M609385200

Ernst A, Avvakumov G, Tong J, Fan Y, Zhao Y, Alberts P, Persaud A, Walker JR, Neculai AM, Neculai D, Vorobyov A, Garg P, Beatty L, Chan PK, Juang YC, Landry MC, Yeh C, Zeqiraj E, Karamboulas K, Allali-Hassani A, Vedadi M, Tyers M, Moffat J, Sicheri F, Pelletier L, Durocher D, Raught B, Rotin D, Yang J, Moran MF, Dhe-Paganon S, Sidhu SS (2013)

A strategy for modulation of enzymes in the ubiquitin system. Science 339:590–595. doi:10.1126/science.1230161

Fakitsas P, Adam G, Daidie D, van Bemmelen MX, Fouladkou F, Patrignani A, Wagner U, Warth R, Camargo SM, Staub O, Verrey F (2007) Early aldosterone-induced gene product regulates the epithelial sodium channel by deubiquitylation. J Am Soc Nephrol 18:1084–1092. doi:10.1681/ASN.2006080902

Firsov D, Schild L, Gautschi I, Mérillat AM, Schneeberger E, Rossier BC (1996) Cell surface expression of the epithelial Na channel and a mutant causing Liddle syndrome: a quantitative approach. Proc Natl Acad Sci U S A 93:15370–15375

Fotia AB, Dinudom A, Shearwin KE, Koch JP, Korbmacher C, Cook DI, Kumar S (2003) The role of individual Nedd4-2 (KIAA0439) WW domains in binding and regulating epithelial sodium channels. FASEB J 17:70–72. doi:10.1096/fj.02-0497fje

Fotia AB, Ekberg J, Adams DJ, Cook DI, Poronnik P, Kumar S (2004) Regulation of neuronal voltage-gated sodium channels by the ubiquitin-protein ligases Nedd4 and Nedd4-2. J Biol Chem 279:28930–28935. doi:10.1074/jbc.M402820200

Fouladkou F, Alikhani-Koopaei R, Vogt B, Flores SY, Malbert-Colas L, Lecomte MC, Loffing J, Frey FJ, Frey BM, Staub O (2004) A naturally occurring human Nedd4-2 variant displays impaired ENaC regulation in Xenopus laevis oocytes. Am J Physiol Renal Physiol 287:F550–F561. doi:10.1152/ajprenal.00353.2003

Fouladkou F, Lu C, Jiang C, Zhou L, She Y, Walls JR, Kawabe H, Brose N, Henkelman RM, Huang A, Bruneau BG, Rotin D (2010) The ubiquitin ligase Nedd4-1 is required for heart development and is a suppressor of thrombospondin-1. J Biol Chem 285:6770–6780. doi:10.1074/jbc.M109.082347

Fraser SP, Diss JK, Chioni AM, Mycielska ME, Pan H, Yamaci RF, Pani F, Siwy Z, Krasowska M, Grzywna Z, Brackenbury WJ, Theodorou D, Koyuturk M, Kaya H, Battaloglu E, De Bella MT, Slade MJ, Tolhurst R, Palmieri C, Jiang J, Latchman DS, Coombes RC, Djamgoz MB (2005) Voltage-gated sodium channel expression and potentiation of human breast cancer metastasis. Clin Cancer Res 11:5381–5389. doi:10.1158/1078-0432.CCR-05-0327

Friedrich B, Feng Y, Cohen P, Risler T, Vandewalle A, Broer S, Wang J, Pearce D, Lang F (2003) The serine/threonine kinases SGK2 and SGK3 are potent stimulators of the epithelial Na + channel alpha, beta, gamma-ENaC. Pflugers Arch 445:693–696. doi:10.1007/s00424-002-0993-8

Gasser A, Cheng X, Gilmore ES, Tyrrell L, Waxman SG, Dib-Hajj SD (2010) Two Nedd4-binding motifs underlie modulation of sodium channel Nav1.6 by p38 MAPK. J Biol Chem 285:26149–26161. doi:10.1074/jbc.M109.098681

Gillet L, Roger S, Besson P, Lecaille F, Gore J, Bougnoux P, Lalmanach G, Le Guennec JY (2009) Voltage-gated sodium channel activity promotes cysteine cathepsin-dependent invasiveness and colony growth of human cancer cells. J Biol Chem 284:8680–8691. doi:10.1074/jbc.M806891200

Hansson JH, Nelson-Williams C, Suzuki H, Schild L, Shimkets R, Lu Y, Canessa C, Iwasaki T, Rossier B, Lifton RP (1995) Hypertension caused by a truncated epithelial sodium channel gamma subunit: genetic heterogeneity of Liddle syndrome. Nat Genet 11:76–82. doi:10.1038/ng0995-76

Harvey KF, Kumar S (1999) Nedd4-like proteins: an emerging family of ubiquitin-protein ligases implicated in diverse cellular functions. Trends Cell Biol 9:166–169. doi:10.1016/S0962-8924(99)01541-X

Harvey KF, Dinudom A, Komwatana P, Jolliffe CN, Day ML, Parasivam G, Cook DI, Kumar S (1999) All three WW domains of murine Nedd4 are involved in the regulation of epithelial sodium channels by intracellular Na+. J Biol Chem 274:12525–12530. doi:10.1074/jbc.274.18.12525

Henke G, Maier G, Wallisch S, Boehmer C, Lang F (2004) Regulation of the voltage gated K + channel Kv1.3 by the ubiquitin ligase Nedd4-2 and the serum and glucocorticoid inducible kinase SGK1. J Cell Physiol 199:194–199. doi:10.1002/jcp.10430

Henry PC, Kanelis V, O'Brien MC, Kim B, Gautschi I, Forman-Kay J, Schild L, Rotin D (2003) Affinity and specificity of interactions between Nedd4 isoforms and the epithelial Na + channel. J Biol Chem 278:20019–20028. doi:10.1074/jbc.M211153200

Hershko A, Ciechanover A (1998) The ubiquitin system. Annu Rev Biochem 67:425–479. doi:10.1146/annurev.biochem.67.1.425

Hershko A, Aharon C, Rose IA (1979) Resolution of the ATP-dependent proteolytic system from reticulocytes: a component that Interacts with ATP. Proc Natl Acad Sci U S A 76:3107–3110. doi:10.2307/69938

Hershko A, Ciechanover A, Heller H, Haas AL, Rose IA (1980) Proposed role of ATP in protein breakdown: conjugation of protein with multiple chains of the polypeptide of ATP-dependent proteolysis. Proc Natl Acad Sci U S A 77:1783–1786

Hicke L, Schubert HL, Hill CP (2005) Ubiquitin-binding domains. Nat Rev Mol Cell Biol 6:610–621. doi:10.1038/nrm1701

Huibregtse JM, Scheffner M, Beaudenon S, Howley PM (1995) A family of proteins structurally and functionally related to the E6-AP ubiquitin-protein ligase. Proc Natl Acad Sci U S A 92:5249

Hurley JH, Emr SD (2006) The ESCRT complexes: structure and mechanism of a membrane-trafficking network. Annu Rev Biophys Biomol Struct 35:277–298. doi:10.1146/annurev.biophys.35.040405.102126

Ingham RJ, Gish G, Pawson T (2004) The Nedd4 family of E3 ubiquitin ligases: functional diversity within a common modular architecture. Oncogene 23:1972–1984. doi:10.1038/sj.onc.1207436

Itani OA, Campbell JR, Herrero J, Snyder PM, Thomas CP (2003) Alternate promoters and variable splicing lead to hNedd4-2 isoforms with a C2 domain and varying number of WW domains. Am J Physiol Renal Physiol 285:F916–F929. doi:10.1152/ajprenal.00203.2003

Itani OA, Stokes JB, Thomas CP (2005) Nedd4-2 isoforms differentially associate with ENaC and regulate its activity. Am J Physiol Renal Physiol 289:F334–F346. doi:10.1152/ajprenal.00394.2004

Joazeiro CA, Weissman AM (2000) RING finger proteins: mediators of ubiquitin ligase activity. Cell 102:549–552. doi:10.1016/S0092-8674(00)00077-5

Kamynina E, Debonneville C, Bens M, Vandewalle A, Staub O (2001) A novel mouse Nedd4 protein suppresses the activity of the epithelial Na + channel. FASEB J 15:204–214. doi:10.1096/fj.00-0191com

Kanelis V, Rotin D, Forman-Kay JD (2001) Solution structure of a Nedd4 WW domain-ENaC peptide complex. Nat Struct Biol 8:407–412. doi:10.1038/87562

Kapa S, Tester DJ, Salisbury BA, Harris-Kerr C, Pungliya MS, Alders M, Wilde AA, Ackerman MJ (2009) Genetic testing for long-QT syndrome: distinguishing pathogenic mutations from benign variants. Circulation 120:1752–1760. doi:10.1161/CIRCULATIONAHA.109.863076

Kasanov J, Pirozzi G, Uveges AJ, Kay BK (2001) Characterizing class I WW domains defines key specificity determinants and generates mutant domains with novel specificities. Chem Biol 8:231–241

Kawabe H, Neeb A, Dimova K, Young SM Jr, Takeda M, Katsurabayashi S, Mitkovski M, Malakhova OA, Zhang DE, Umikawa M, Kariya K, Goebbels S, Nave KA, Rosenmund C, Jahn O, Rhee J, Brose N (2010) Regulation of Rap2A by the ubiquitin ligase Nedd4-1 controls neurite development. Neuron 65:358–372. doi:10.1016/j.neuron.2010.01.007

Kresge N, Simoni RD, Hill RL (2006) The discovery of ubiquitin-mediated proteolysis by Aaron Ciechanover, Avram Hershko, and Irwin Rose. J Biol Chem 281:e32

Krzystanek K, Rasmussen HB, Grunnet M, Staub O, Olesen SP, Abriel H, Jespersen T (2012) Deubiquitylating enzyme USP2 counteracts Nedd4-2-mediated downregulation of KCNQ1 potassium channels. Heart Rhythm 9:440–448. doi:10.1016/j.hrthm.2011.10.026

Kuratomi G, Komuro A, Goto K, Shinozaki M, Miyazawa K, Miyazono K, Imamura T (2005) NEDD4-2 (neural precursor cell expressed, developmentally down-regulated 4-2) negatively regulates TGF-beta (transforming growth factor-beta) signalling by inducing ubiquitin-mediated

degradation of Smad2 and TGF-beta type I receptor. Biochemical J 386:461–470. doi:10.1042/BJ20040738

Kuryshev YA, Wible BA, Gudz TI, Ramirez AN, Brown AM (2001) KChAP/Kvβ1.2 interactions and their effects on cardiac Kv channel expression. Am J Physiol Cell Physiol 281:C290–C299

Laedermann CJ, Cachemaille M, Kirschmann G, Pertin M, Gosselin RD, Chang I, Albesa M, Towne C, Schneider BL, Kellenberger S, Abriel H, Decosterd I (2013) Dysregulation of voltage-gated sodium channels by ubiquitin-ligase NEDD4-2 in neuropathic pain. J Clin Investig 123:3002–3013. doi:10.1172/JCI68996

Lu P-J, Zhou XZ, Shen M, Lu KP (1999) Function of WW domains as phosphoserine- or phosphothreonine-binding modules. Science 283:1325–1328. doi:10.1126/science.283.5406.1325

Luo F, Wang YB, Wang XJ, Sun K, Zhou XL, Hui RT (2009) A functional variant of NEDD4L is associated with hypertension, antihypertensive response, and orthostatic hypotension. Hypertension 54:796–801. doi:10.1161/Hypertensionaha.109.135103

Macias MJ, Hyvonen M, Baraldi E, Schultz J, Sudol M, Saraste M, Oschkinat H (1996) Structure of the WW domain of a kinase-associated protein complexed with a proline-rich peptide. Nature 382:646–649. doi:10.1038/382646a0

Metzger MB, Hristova VA, Weissman AM (2012) HECT and RING finger families of E3 ubiquitin ligases at a glance. J Cell Sci 125:531–537. doi:10.1242/jcs.091777

Moss A, Blackburn-Munro G, Garry EM, Blakemore JA, Dickinson T, Rosie R, Mitchell R, Fleetwood-Walker SM (2002) A role of the ubiquitin-proteasome system in neuropathic pain. J Neurosci 22:1363–1372

Mund T, Pelham HR (2009) Control of the activity of WW-HECT domain E3 ubiquitin ligases by NDFIP proteins. EMBO Rep 10:501–507. doi:10.1038/embor.2009.30

Ossipov MH, Bazov I, Gardell LR, Kowal J, Yakovleva T, Usynin I, Ekstrom TJ, Porreca F, Bakalkin G (2007) Control of chronic pain by the ubiquitin proteasome system in the spinal cord. J Neurosci 27:8226–8237

Pickart CM (2001) Mechanisms underlying ubiquitination. Annu Rev Biochem 70:503–533. doi:10.1146/annurev.biochem.70.1.503

Plant PJ, Lafont F, Lecat S, Verkade P, Simons K, Rotin D (2000) Apical membrane targeting of Nedd4 is mediated by an association of its C2 domain with annexin XIIIb. J Cell Biol 149:1473–1483. doi:10.1083/jcb.149.7.1473

Rizo J, Sudhof TC (1998) C2-domains, structure and function of a universal Ca2 + -binding domain. J Biol Chem 273:15879–15882. doi:10.1074/jbc.273.26.15879

Rosati B, McKinnon D (2004) Regulation of ion channel expression. Circ Res 94:874–883. doi:10.1161/01.RES.0000124921.81025.1F

Rossier BC, Pradervand S, Schild L, Hummler E (2002) Epithelial sodium channel and the control of sodium balance: interaction between genetic and environmental factors. Annu Rev Physiol 64:877–897. doi:10.1146/annurev.physiol.64.082101.143243

Rotin D, Staub O (2011) Role of the ubiquitin system in regulating ion transport. Pflugers Arch 461:1–21. doi:10.1007/s00424-010-0893-2

Rotin D, Staub O, Haguenauer-Tsapis R (2000) Ubiquitination and endocytosis of plasma membrane proteins: role of Nedd4/Rsp5p family of ubiquitin-protein ligases. J Membr Biol 176:1–17

Rougier JS, van Bemmelen MX, Bruce MC, Jespersen T, Gavillet B, Apotheloz F, Cordonier S, Staub O, Rotin D, Abriel H (2005) Molecular determinants of voltage-gated sodium channel regulation by the Nedd4/Nedd4-like proteins. Am J Physiol Cell Physiol 288:C692–C701. doi:10.1152/ajpcell.00460.2004

Rougier JS, Albesa M, Remme CA, Ogrodnik J, Petitprez S, Bankston J, Kass RS, Bezzina CR, Chung W, Abriel H (2012) Long QT syndrome type 3 caused by a PY-motif mutation leading to altered ubiquitylation and increased expression of Nav1.5 in knock-in mice. FASEB J 26

Rougier JS, Gavillet B, Abriel H (2013) Proteasome inhibitor (MG132) rescues Nav1.5 protein content and the cardiac sodium current in dystrophin-deficient mdx (5cv) mice. Front Physiol 4:51. doi:10.3389/fphys.2013.00051

Sazuka T, Tomooka Y, Kathju S, Ikawa Y, Noda M, Kumar S (1992) Identification of a developmentally regulated gene in the mouse central-nervous-system which encodes a novel proline rich protein. Biochim Biophys Acta 1132:240–248. doi:10.1016/0167-4781(92)90156-T

Scheffner M, Nuber U, Huibregtse JM (1995) Protein ubiquitination involving an E1-E2-E3 enzyme ubiquitin thioester cascade. Nature 373:81–83. doi:10.1038/373081a0

Schild L, Lu Y, Gautschi I, Schneeberger E, Lifton RP, Rossier BC (1996) Identification of a PY motif in the epithelial Na channel subunits as a target sequence for mutations causing channel activation found in Liddle syndrome. EMBO J 15:2381–2387

Schlesinger DH, Goldstein G (1975) Molecular conservation of 74 amino-acid sequence of ubiquitin between cattle and man. Nature 255:423–424. doi:10.1038/255423a0

Schlesinger DH, Goldstein G, Niall HD (1975) The complete amino acid sequence of ubiquitin, an adenylate cyclase stimulating polypeptide probably universal in living cells. Biochemistry 14: 2214–2218. doi:10.1021/bi00681a026

Schlesinger DH, Goldstein G, Scheid MP, Bitensky M (1978) Chemical synthesis of a hexadecapeptide segment of ubiquitin that activates adenylate-cyclase and induces lymphocytes to differentiate. Experientia 34:703–704. doi:10.1007/Bf01947269

Schmidt JW, Catterall WA (1987) Palmitylation, sulfation, and glycosylation of the alpha subunit of the sodium channel. Role of post-translational modifications in channel assembly. J Biol Chem 262:13713–13723

Schwarz SE, Rosa JL, Scheffner M (1998) Characterization of human hect domain family members and their interaction with UbcH5 and UbcH7. J Biol Chem 273:12148–12154. doi:10.1074/jbc.273.20.12148

Shi PP, Cao XR, Sweezer EM, Kinney TS, Williams NR, Husted RF, Nair R, Weiss RM, Williamson RA, Sigmund CD, Snyder PM, Staub O, Stokes JB, Yang B (2008) Salt-sensitive hypertension and cardiac hypertrophy in mice deficient in the ubiquitin ligase Nedd4-2. Am J Physiol Renal Physiol 295:F462–F470. doi:10.1152/ajprenal.90300.2008

Shih SC, Sloper-Mould KE, Hicke L (2000) Monoubiquitin carries a novel internalization signal that is appended to activated receptors. EMBO J 19:187–198. doi:10.1093/emboj/19.2.187

Shimkets RA, Warnock DG, Bositis CM, Nelson-Williams C, Hansson JH, Schambelan M, Gill JR Jr, Ulick S, Milora RV, Findling JW et al (1994) Liddle's syndrome: heritable human hypertension caused by mutations in the beta subunit of the epithelial sodium channel. Cell 79:407–414. doi:10.1016/0092-8674(94)90250-x

Snyder PM, Olson DR, McDonald FJ, Bucher DB (2001) Multiple WW domains, but not the C2 domain, are required for inhibition of the epithelial Na + channel by human Nedd4. J Biol Chem 276:28321–28326. doi:10.1074/jbc.M011487200

Snyder PM, Olson DR, Kadra R, Zhou R, Steines JC (2004) cAMP and serum and glucocorticoid-inducible kinase (SGK) regulate the epithelial Na(+) channel through convergent phosphorylation of Nedd4–2. J Biol Chem 279:45753–45758. doi:10.1074/jbc.M407858200.

Snyder PM (2009) Down-regulating destruction: phosphorylation regulates the E3 ubiquitin ligase Nedd4-2. Sci Signal 2:pe41. doi:10.1126/scisignal.279pe41

Staub O, Rotin D (1996) WW domains. Structure 4:495–499. doi:10.1016/S0969-2126(96)00054-8

Staub O, Rotin D (2006) Role of ubiquitylation in cellular membrane transport. Physiol Rev 86:669–707. doi:10.1152/physrev.00020.2005

Staub O, Abriel H, Plant P, Ishikawa T, Kanelis V, Saleki R, Horisberger JD, Schild L, Rotin D (2000) Regulation of the epithelial Na + channel by Nedd4 and ubiquitination. Kidney Int 57:809–815. doi:10.1046/j.1523-1755.2000.00919.x

Sudol M (1996) Structure and function of the WW domain. Prog Biophys Mol Biol 65:113–132. doi:10.1016/S0079-6107(96)00008-9

Sudol M, Hunter T (2000) NeW wrinkles for an old domain. Cell 103:1001–1004. doi:10.1016/s0092-8674(00)00203-8

Ueda K, Valdivia C, Medeiros-Domingo A, Tester DJ, Vatta M, Farrugia G, Ackerman MJ, Makielski JC (2008) Syntrophin mutation associated with long QT syndrome through activation

of the nNOS-SCN5A macromolecular complex. Proc Natl Acad Sci U S A 105:9355–9360. doi:10.1073/pnas.0801294105

van Bemmelen MX, Rougier JS, Gavillet B, Apotheloz F, Daidie D, Tateyama M, Rivolta I, Thomas MA, Kass RS, Staub O, Abriel H (2004) Cardiac voltage-gated sodium channel Nav1.5 is regulated by Nedd4-2 mediated ubiquitination. Circ Res 95:284–291

Waechter CJ, Schmidt JW, Catterall WA (1983) Glycosylation is required for maintenance of functional sodium channels in neuroblastoma cells. J Biol Chem 258:5117–5123

Wilkinson KD, Urban MK, Haas AL (1980) Ubiquitin is the ATP-dependent proteolysis factor I of rabbit reticulocytes. J Biol Chem 255:7529–7532

Xu P, Duong DM, Seyfried NT, Cheng D, Xie Y, Robert J, Rush J, Hochstrasser M, Finley D, Peng J (2009) Quantitative proteomics reveals the function of unconventional ubiquitin chains in proteasomal degradation. Cell 137:133–145. doi:10.1016/j.cell.2009.01.041

Yang B, Kumar S (2009) Nedd4 and Nedd4-2: closely related ubiquitin-protein ligases with distinct physiological functions. Cell Death Differ 17:68–77

Yang B, Gay DL, MacLeod MK, Cao X, Hala T, Sweezer EM, Kappler J, Marrack P, Oliver PM (2008) Nedd4 augments the adaptive immune response by promoting ubiquitin-mediated degradation of Cbl-b in activated T cells. Nat Immunol 9:1356–1363. doi:10.1038/ni.1670

Pharmacological Insights and Quirks of Bacterial Sodium Channels

Ben Corry, Sora Lee, and Christopher A. Ahern

Contents

Abstract

The pedigree of voltage-gated sodium channels spans the millennia from eukaryotic members that initiate the action potential firing in excitable tissues to primordial ancestors that act as enviro-protective complexes in bacterial extremophiles. Eukaryotic sodium channels (eNavs) are central to electrical signaling throughout the cardiovascular and nervous systems in animals and are established clinical targets for the therapeutic management of epilepsy, cardiac arrhythmia, and painful syndromes as they are inhibited by local anesthetic compounds. Alternatively, bacterial voltage-gated sodium channels (bNavs) likely regulate the survival response against extreme pH conditions, electrophiles, and hypo-osmotic shock and may represent a founder of the voltage-gated cation channel family. Despite apparent differences between eNav and bNav channel physiology, gating, and gene structure, the discovery that bNavs are amenable to crystallographic study opens the door for the possibility of structure-guided rational design of the next generation of therapeutics that target eNavs. Here we summarize the gating behavior of these

B. Corry
Research School of Biology, The Australian National University, Canberra, ACT, Australia

S. Lee • C.A. Ahern (✉)
The Department of Molecular Physiology and Biophysics, The University of Iowa, Iowa City, IA, USA
e-mail: christopher-ahern@uiowa.edu

P.C. Ruben (ed.), *Voltage Gated Sodium Channels*, Handbook of Experimental Pharmacology 221, DOI 10.1007/978-3-642-41588-3_12,

disparate channel members and discuss mechanisms of local anesthetic inhibition in light of the growing number of bNav structures.

Keywords
Bacteria • pH homeostasis • Pharmacology • Modulation

1 Eukaryotic Sodium Channel Gating and Pharmacology

Eukaryotic voltage-gated sodium channels (eNavs) display ultrarapid, sub-millisecond activation and strong sodium ion selectivity, properties which endow them with the responsibility of initiating fast action potential firing in the vast majority of electrical signaling pathways in eukaryotes. Inherited mutations in human eNav channels result in debilitating and lethal phenotypes in the cardiovascular and central and peripheral nervous systems. These large macromolecular complexes have four heterologous domains (DI–DIV) each of which have six transmembrane (TM) α-helical segments (S1–S6) with S1–S4 comprising the voltage sensor and S5, S6, and a reentrant p-loop forming the pore domain (Fig. 1a). Both the selectivity filter and the internal end of the S6 helix ("activation gate") are believed to serve as putative voltage-sensitive gates for the Na^+ ion permeation pathway, with the selectivity filter contributing to the process of "slow inactivation." These channels are highly evolved to perform the complex task of integrating electrical signaling with metabolic and cell stress information in the form of transient phosphorylation, oxidation, palmitylation, sulfation glycosylation, and nitrosylation (Costa and Catterall 1984; Scheuer 2011; Renganathan et al. 2002; Ahern et al. 2000, 2005; Kassmann et al. 2008; Schmidt and Catterall 1987) in addition to modulation by extracellular protons (Mozhayeva et al. 1984; Hille 1968), intracellular Ca^{2+}/calmodulin (Tan et al. 2002; Van Petegem et al. 2012), fibroblast growth factor homologous factor 1B (Liu et al. 2003), and auxiliary beta subunits (Isom et al. 1992).

Antiepileptic, analgesic, and antiarrhythmic agents reduce electrical firing by blocking the ion-conducting pathway eNav channels, thus reducing sodium influx and their contribution to membrane depolarization. These molecules, known largely as "local anesthetics," are organic cations with pK_a values in the physiological range and thus have charged and neutral populations and are known to be able to block eNavs in at least two ways. It is widely believed that the neutral form elicits channel blockade after accessing the internal blocking site through a hydrophobic pathway defined by the membrane core and/or a proteinaceous passage (Hille 1977a, b). This is evidenced by the ability of such compounds to block the channel even when the intracellular gate has not been open or by relief of blocked channels during periods in which the channel remains closed (Hille 1977a). This low-affinity "tonic" inhibition of resting channels displays affinities in the upper micromolar to millimolar range and is enlisted in clinical local anesthetic applications where the aim is to eliminate electrical signaling entirely.

However, a finer touch is required for antiarrhythmic and antiepileptic drugs which aim to only modestly reduce the contributions of overactive sodium channels to action

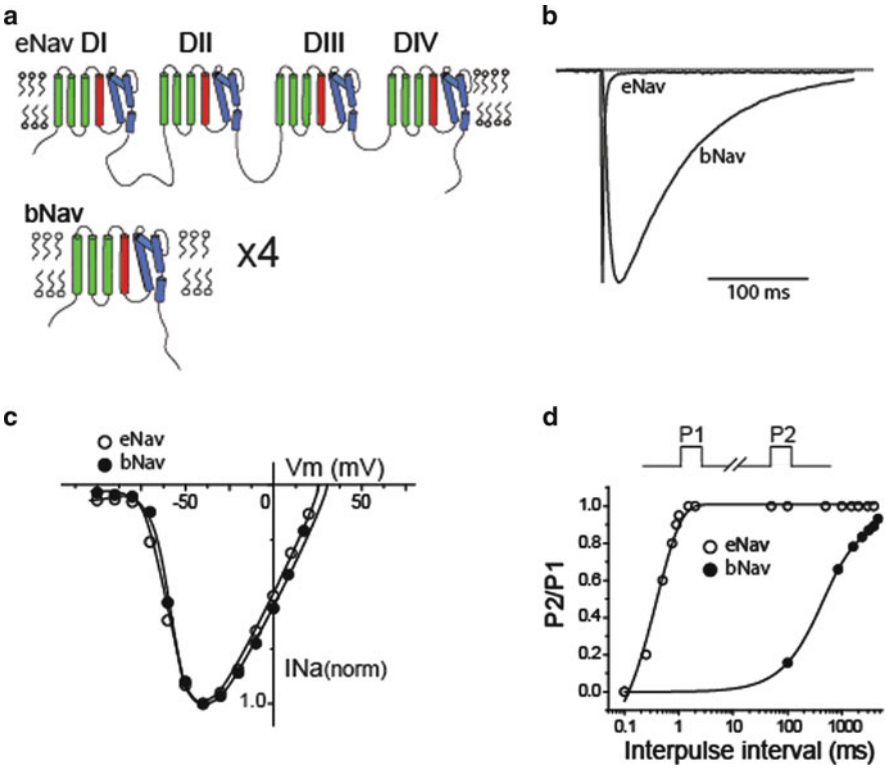

Fig. 1 Topological and gating comparisons of bNav and eNav channels. (**a**) Predicted membrane topology of eukaryotic (eNav) and bacterial (bNav) voltage-gated sodium channels. Above, eNavs are heterotetrametric channels comprised of a single polypeptide with four similar domains (DI–DIV) connected by three cytoplasmic linkers with low conservation between eNav channels and a ~250 aa carboxyl-terminus (CT) which contains conserved Ca^{2+}-sensing and CaM-binding elements. Below, bNav channels are homotetramers with an unconserved CT domain. Both channel families are comprised of four domains, each with six transmembrane segments (S1–S6) with a voltage-sensing domain (S1–S4), *green* and *red* cylinders and pore-domain (S5–S6) shown in *blue*. (**b**) Activation and inactivation gating of eNav and the bNav channel, NaChBac. In each case, inward sodium currents we evoked under patch-clamp from a holding potential of −120 mV with a single depolarizing pulse to −20 mV. Note the slow activation and inactivation kinetics of the NaChBac. Scale bar is equal to 100 ms. (**c**) current–voltage relationships for eNav and bNav channels demonstrate similarities in the voltage dependence of peak INa. (**d**) Recovery from inactivation at −120 mV induced by a 20 ms or 750 ms depolarizing pulse for eNav and bNav channels, respectively. *X*-axis represents inter pulse interval and indicates that eNav channels recover in ~1 ms, while NaChBac recovery takes 3–5 s for full recovery

potential firing in the cardiovascular and nervous systems. These compounds are valuable tools to manage excessive electrical signaling because they display low micromolar affinity block of open and inactivated eNav states, channel conformations which predominate in hyperexcitable neuronal and cardiac tissue. Furthermore, unbinding from a cytoplasmic blocking site and recovery from inactivation is required

before the channel can contribute to action potential firing and this unique pharmacological behavior gives rise to the phenomenon of "use-dependent block" (UDB), where receptor affinity is positively correlated with channel activation. Also, circulating levels of these compounds at therapeutically effective concentrations has little or no affinity for, or effect on, resting channels. Despite the large difference in binding affinities, tonic and UDB sites are apparently overlapping and are both near the cytoplasmic entrance to the selectivity filter, deep within the inner vestibule of the channel (McNulty et al. 2007; Gingrich et al. 1993; Kimbrough and Gingrich 2000; Zamponi et al. 1993). However, different residues contribute to tonic and use-dependent inhibition (Ragsdale et al. 1994a), consistent with the possibility of a local conformational change in the inner vestibule associated with channel opening and inactivation, and these motions allow for an activity dependent change in drug-binding affinity. Additionally, a highly conserved pair of aromatic side chains in the DIVS6 segment support use-dependent inhibition (Ragsdale et al. 1994a), with the upper residue employing a cation–pi interaction with cationic local anesthetics, and this chemical interaction helps to define the class 1b antiarrhythmic drug family (Ahern et al. 2008; Pless et al. 2011). Despite the relative functional and molecular clarity of the mechanisms of eukaryotic sodium channel inhibition, no eNav structural data yet exists that would facilitate the design of the next generation of sodium channel drugs. Therefore the discovery of a bacterial gene family which encodes for a sodium selective voltage-gated ion channel has led to the general anticipation that these channels could serve as structural homologues to their eukaryotic cousins and simultaneously provide a functionally simpler model sodium channel prototype.

2 Bacterial Sodium Channels

Since the initial discovery of the bacterial channel NaChBac (Takami and Horikoshi 1999), 9 channels out of more than 40 phylogenetically identified bacterial sodium channel homologues (Irie et al. 2010) have been expressed for structural and biochemical studies including Na_vSP, Na_vPZ (Koishi et al. 2004), Na_vBP (Ito et al. 2004), Na_vRosD, Na_vSheP, Na_vBacL (Irie et al. 2010), Na_vAb (Payandeh et al. 2011), Na_vMS (McCusker et al. 2012; Ulmschneider et al. 2013), and electrophysiological approaches, NaChBac (Ren et al. 2001; Lee et al. 2012a; Lee et al. 2012b; Payandeh et al. 2012a), (Table 1). These genes encode for voltage-gated sodium selective ion channels that are comprised of four homotetramers, where each monomer is comprised of six transmembrane domains, with S1–S4 forming a voltage-sensing domain and S5–p-loop–S6 comprising the pore, akin to the arrangement of each eNav domain (Fig. 1a).

A paucity of functional data is available for the greater family of bNavs given their general aversion to expression and subsequent electrophysiological study in conventional eukaryotic systems. However, NaChBac appears to be unique among bNavs and is readily in eukaryotic cell lines (HEK, tSA-201, CHO) (Ren et al. 2001; Lee et al. 2012a; Waters et al. 2006) or via injection of cRNA into *Xenopus laevis* oocytes (Lee et al. 2012a). While modulatory mechanisms important to eNav

Table 1 Bacterial sodium channel homologues

bNav channel name	Species	Source of isolation
NaChBac	*Bacillus halodurans*	Soil (Takami and Horikoshi 1999)
NavRosD	*Roseobacter denitrificans*	Marine algae (Shiba 1991)
NavSp	*Silicibacter pomeroyi*	Marine environment (González et al. 2003)
NavPz	*Paracoccus zeaxanthinifaciens*	Seaweed from the African Red Sea (Berry et al. 2003)
NavSheP	*Shewanella putrefaciens*	Marine environment, anaerobic sandstone (Fredrickson et al. 1998)
NavBacL	*Bacillus licheniformis*	Soil, bird feathers (Rey et al. 2004)
NavBp	*Bacillus pseudofirmus*	Soil, animal manure (Nielsen et al. 1995)
NavAb	*Arcobacter butzleri*	Human and animal pathogens (Miller et al. 2007; Payandeh et al. 2011)
NavMs	*Magnetococcus sp.*	Sea water (Blakemore 1975; McCusker et al. 2012)

functions, such as phosphorylation and glycosylation can take place in bacteria (Deutscher and Saier 2005; Abu-Qarn et al. 2008), it is not yet known if such transient modifications are used to fine-tune bNav gating and expression. Interestingly, however, it has been recently shown that NaChBac can be positively regulated by auxiliary eukaryotic sodium channel beta subunits in an isoform-specific manner, suggesting that some form of receptive architecture exists within the bNav pore domain (in submission). In terms of functionality of expressed channels, eNav and bNav channels display voltage-dependent activation and inactivation, Fig. 1b, c, yet NaChBac shows significantly slowed voltage- and state-dependent gating transitions compared to eNavs. This is manifest in a slower activation (time course of channel opening) in response to changes in depolarizing membrane potentials, and inactivation, the process that describes the spontaneous entry into nonconducting channel states despite a continuous depolarizing voltage step. The mechanism by which bNavs inactivate is not known but could evoke conformational changes near the selectivity filter in a process similar to slow inactivation in potassium channels (Pavlov et al. 2005; Choi et al. 1991) or slippage/reclosure of the S6 gate (Shin et al. 2004) or through a novel conformational pathway that has yet to be described. The basis for the voltage-gated activation and inactivation mechanisms employed by bacterial sodium channels remains poorly understood, although the voltage-sensing domain with the S4 segment and its basic Arg and Lys residues play a role similar to eNav channels (Blanchet and Chahine 2007; Blanchet et al. 2007). However, while the molecular role that bNav channels support in the bacterial context remains to be elucidated, knowing such information may be helpful in determining how they may inform on eNav pharmacology and gating.

It has been hypothesized that bacterial ion channels could be crucial in mediating mechanisms of protection against extreme pH conditions, electrophiles, and hypo-osmotic shock (Booth 1985). Their role in the maintenance of the transmembrane membrane potential in bacteria is not well known, however, use of a genetically

encoded in vivo fluorescent voltage-sensitive protein in *Escherichia coli* has revealed unexpected and complex fluctuations in bacterial transmembrane potential and the electrically regulated conductance of both anions and cations through the membrane of an intact bacterium (Kralj et al. 2011). NaChBac, was isolated from *Bacillus Halodurans C-125*, a facultative alkaliphilic bacteria strain that is known to be aerobic, spore-forming, gram-positive, and motile (Takami and Horikoshi 1999). These extremophiles grow in high temperature (55°C), in high pH (between pH 9.0 and pH 11.5), and in high salt concentration [12 % NaCl (1.5 M)] (Krulwich and Guffanti 1989; Takami and Horikoshi 1999) and it has been speculated that voltage-gated sodium channels in alkaliphilic bacteria support proton motive force-dependent flagellar motion and pH homeostasis (Ito et al. 2004; Kralj et al. 2011). Further, facultative alkaliphilic bacteria maintain a slightly more acidic cytoplasmic pH than the external environment (Mandel et al. 1980), yet it is not known how they maintain cytoplasmic pH that is 2 pH units lower than the external condition (Krulwich et al. 1997). However, pH homeostasis of alkaliphilic bacteria is regulated by both passive and active mechanisms (Krulwich et al. 1997), with the former serving as protection against internal alkalization that is mediated by substantial presence of two acidic polymers found in cell walls, teichuronic acid and gluatamate-rich teichuronopeptide, as a protection of hydroxide ion entry to the cytoplasm (Krulwich et al. 1997). Alternatively, active mechanisms for pH regulation involve Na^+/H^+ anti-porter activity to counter the accumulation of protons in exchange for Na^+ efflux to maintain cytoplasmic pH homeostasis (Ito et al. 2004; Mager et al. 2011; Mandel et al. 1980). Lastly, intracellular Na^+ translocation via NaChBac, along with other solute transporters (Na^+/solute symporters, pH-sensitive Na^+ channels) might be an important route of sodium cycling for the consequent Na^+/H^+ antiporter activity to maintain pH homeostasis of facultative alkaliphilic bacteria (Dimroth and Cook 2004; McLaggan et al. 1984; Sugiyama 1995). One interesting possibility is that if indeed bNavs play essential role(s) in bacterial function and viability they might be novel antibacterial targets.

In terms of pharmacology, it is known that bNavs can be blocked by cadmium and lanthanum as well as dihydropyridines similar to eukaryotic Ca^{2+} channels (Ren et al. 2001), but their interaction with local anesthetics and thus their possible use as eNav pharmacological models has only begun to be explored. Local anesthetic compounds can elicit an instantaneous low affinity blockade of both eNav and bNav sodium channels (Lee et al. 2012a). Permanently charged compounds (QX-314) can only block the channel when applied from the intracellular side of the membrane from where they can enter the channel once open. Also, similar to eNav behavior, neutral species, such as benzocaine, display tonic block, indicative of a hydrophobic entrance route and binding mechanism that is common to both families.

But, while bNavs share some pharmacological aspects of eNav channels such as a cytoplasmic blocking site and sensitivity to local anesthetic molecules, there are differences that are worth considering. First, given the slow recovery from bNav inactivation, the frequent depolarizations required to investigate use-dependent drug block are not experimentally feasible, Fig. 1d. Further, eNav pharmacology is intricately linked to the process of fast inactivation, yet bNav channels lack key

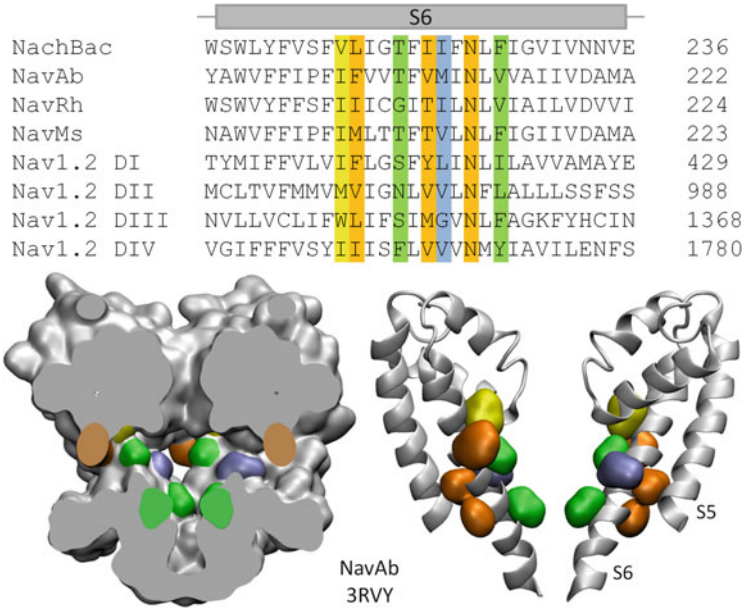

Fig. 2 Sequence alignment and structure of bNavs. The sequences of the S6 helices of the four channels for which structures have been obtained are aligned to the S6 helix from the four domains of the eukaryotic channel Nav1.2. Residues implicated in LA binding are indicated in *green*, those implicated in drug binding in Cav's in *blue*, that influence tonic block in *orange*, and that allow extracellular entry of charged drugs in *yellow*. The structure of the pore domain of NavAb in the pre-open state (PDB accession 3RVY) is shown below with the same residues colored. On the *left* a cut through of the protein surface is shown indicating the shape of the pore and fenestrations, while two of the four subunits are indicated on the *right*

domains that support inactivation in eNavs, such as the cytoplasmic DIII–DIV linker in eNav channels (West et al. 1992). One crucial manifestation of local anesthetic inhibition of eNavs is that inhibition by these drugs delays the recovery from inactivated states after a depolarizing stimulus. And, if the next pulse is delivered within the recovery interval, then fewer channels will be available to open, resulting in a loss of current with each additional pulse and the phenomenon of use dependence. However, lidocaine, benzocaine, or ranolazine produce rapid, reversible, and robust block of expressed NaChBac channels *without* affecting the recovery from inactivation, suggesting a limited or transient interaction between local anesthetics and bNav-inactivated conformations (Lee et al. 2012b). Second, key residues, including conserved pore-lining aromatics, known to support eNav interactions with local anesthetics during use-dependent inhibition are poorly conserved in bNav channels, Fig. 2a. However, side-chain chemistry is but one trait that contributes to a binding site and it is possible the bNav inner vestibule superficially resembles the architecture of the eNav family, despite having low sequence homology. Third, local anesthetics are notoriously polymodal in their interaction with other channel types. For instance, the block of NaChBac by

lidocaine, kd = 260 μM, is similar to the blocking affinity of a myriad of channels, including, but not limited to K_{ATP} (Olschewski et al. 1996), K2P (Kindler et al. 2003), Kv (Trellakis et al. 2006), hERG (Paul et al. 2002), voltage-gated Ca^{2+} (Josephson 1988), in addition to nicotinic acetylcholine (Alberola-Die et al. 2011) and GABA receptors (Sugimoto et al. 2000). Thus, while it is clear that the data support the notion that eNav and bNav channel families share common traits of selectivity and voltage sensitivity, many differences persist that might serve to complicate the use of bNav channels as pharmacological models of eNav isoforms. However, one compelling similarity exists: the presence of hydrophobic routes for possible drug entry from the membrane core that could facilitate closed state blockade.

3 Structural Analysis of Bacterial Sodium Channels

The growing list of high-resolution of bNav structures has provided a physical basis from which to understand the pharmacology and gating mechanisms of bNav and, potentially, eNav channels. The crystal structure of NavAb depicted a channel with a similar overall topography to the family of voltage-gated potassium channels (Fig. 2), where the four subunits arrange symmetrically with the S6 helices forming an inverted teepee that lines the inner half of the pore and a reentrant loop forming the narrow outer part of the pore known from mutation experiments to be responsible for ion selectivity (Payandeh et al. 2011). The pore lining S6 helices of bNavs have sequence similarity to S6 from domain IV of eNavs (Fig. 2), but there is much greater sequence diversity in this region of the bNavs than in the eukaryotic counterparts.

From the point of view of channel pharmacology, one of the most interesting aspects of this and subsequent structures is the presence of lateral lipid filled access routes, aka fenestrations, between adjacent subunits that extend from the center of the pore to the membrane as indicated in the cross section shown in Fig. 2. It was immediately recognized that these fenestrations could provide the route of entry for small neutral or hydrophobic drugs associated with tonic block (Payandeh et al. 2011). The first structure determined is proposed to be in a "pre-open" state with a closed activation gate but with an activated (outward leaning) conformation of voltage sensor. Subsequent structures have been obtained which are suggested to represent inactivated (corresponding to the eNav slow-inactivated) (Payandeh et al. 2012a; Zhang et al. 2012b) and open (McCusker et al. 2012) states of the channel. A comparison of these putative conformations allows for some of the pharmacological implications of the fenestrations to be investigated.

Are such fenestrations actually wide enough to allow for the passage of neutral drugs such as benzocaine, lidocaine, or phenytoin? In Fig. 3 cut-through images of a number of the bNav structures compare the size and shape of the pore and fenestrations for comparison. In addition, the minimum radius of the fenestrations is plotted in Fig. 4 for each of the structures as a function of distance from the central pore axis. In nearly all cases, the narrowest radius is larger than 2 Å, and it is possible that flexibility of the side chains could widen the fenestrations further.

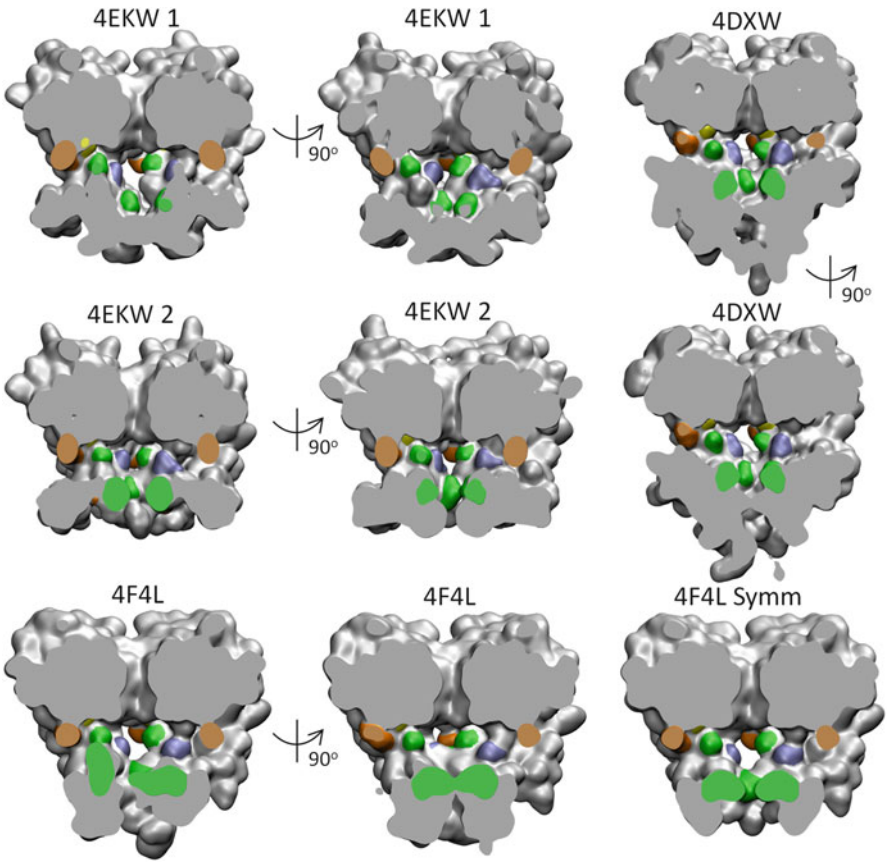

Fig. 3 Cut-through images showing the size and shape of the pore and fenestrations for each bNav structure. Colors are as for Fig. 2, nonsymmetric structures are shown in two orientations, and a symmetric model based on the 4F4L structure is also shown. PDB accession numbers for each structure are shown and correspond to NavAB [3RVY (Payandeh et al. 2011), 4EKW (Payandeh et al. 2012b)], NavRh [4DXW (Zhang et al. 2012a)], and NavMs [4F4L (McCusker et al. 2012)]

Given that the nonsymmetrical shape of the passage would allow molecular dimensions slightly larger than this to pass, the fenestrations are almost certainly sufficient to fit a single phenyl ring (~4.4 Å diameter), and one would suspect that planar molecules such as benzocaine should be able to pass provided they can displace lipids. Bulkier molecules such as the antiepileptic phenytoin may require more distortion of the protein or drug.

How much do the fenestrations differ among the available structures, and in particular, are they unique to certain bNav conformations or a general feature of transmembrane ion channel proteins? While the initial pre-open structure is symmetric and all four fenestrations are identical, the proposed inactivated structures involve two subunits moving toward the pore axis and two moving apart to create a

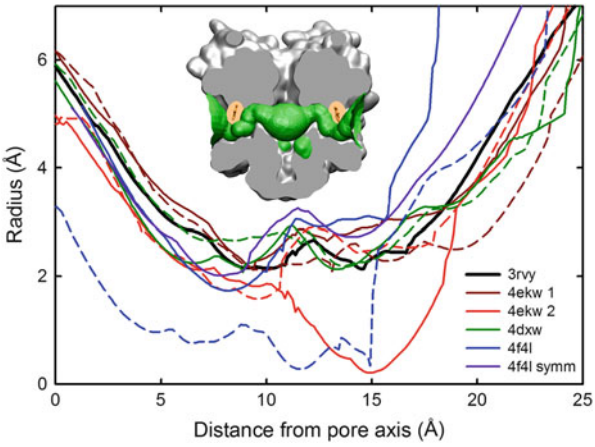

Fig. 4 Fenestration radius as a function of distance from the pore axis. Plots are shown for each bNav structure and for two fenestrations for each nonsymmetric structure (the second fenestration indicated by *dotted lines*). All radii are calculated using the program HOLE, and an indication of the fenestration shape found by this method is shown for 3RVY in the inset

dimer-of-dimers configuration (Payandeh et al. 2012a; Zhang et al. 2012b). As a consequence, two of the fenestrations narrow slightly, while two are actually enlarged. It has been suggested that this change may yield differential access of drugs to the different states of the channel (Payandeh et al. 2012a) as postulated by the modulated receptor hypothesis (Hille 1977a). A comparison of the sizes of the fenestrations (Fig. 4) shows that the change in diameter to the wider fenestration is relatively small (<1 Å), although the shape of the passageway does change (Payandeh et al. 2012a), but it is important to test if this is sufficient to yield significant differences in drug access. Experimental-binding studies in which the channel state is carefully controlled or simulations that can account for the flexibility of the fenestration lining may be the best way to provide a definitive answer. In contrast, one of the narrowed fenestration configurations in the inactivated state is significantly slimmer, and the loss of half the possible exits from the channel in this inactivated state could reduce the ability of drugs to exit the channel in this state.

The most recently determined structure has been interpreted as representing an open conformation of the channel (McCusker et al. 2012). In this case the fenestrations are larger than those in the pre-open state of NavAb and it has been suggested that this difference could be exploited in the design of drugs that stabilize the open state (McCusker et al. 2012). Figures 3 and 4 show the widening of the outer portion of the fenestration, and drugs that reside here may lock this widened configuration and stabilize this state. However, the inner entrance to the cavity (near the residues implicated in LA binding) is of similar size to that seen for the other states and thus there may not be differential state-dependent access to the cavity. One minor complicating factor in the analysis of this structure is the uncertainty as to its functional state, where in particular, the structure is nonsymmetrical, with each subunit in a slightly different conformation. Although the internal end of the S6 helix differs slightly in position from that in the pre-open NavAb, the structure appears to have an occluded activation gate (Fig. 3). A symmetric model generated from the most open subunits creates a wider pore

proposed as the open state by McCusker et al., shown in Fig. 3, but the lack of resolution of critical side chains and residues in the region the activation gate, and the fact that the pore does not remain open without restraints in simulations (Ulmschneider et al. 2013) leaves some doubt as to the functional state captured in the X-ray structure.

Nonetheless, if the fenestrations provide the entry route for drugs involved in tonic block of Navs then we might expect that mutations that influence tonic block will cluster around these pathways. One such residue (I1761 in Nav1.2 or F203 in NavAb) does appear to play a critical role in modifying the size of the fenestrations. The structures from NavAb show the side chain of F203 partially obstructing the fenestrations (Fig. 2), but in eNavs as well as NaChBac, Na_vRh, and Na_vMs, the equivalent sequence position is occupied by less bulky nonaromatic residues which may subtly change the profile of which drugs can use this route to enter the channel. Indeed, some of the widening seen in the proposed open structure can be attributed to the smaller residue in this position. Modifications at this sequence position in eNavs have also been shown to alter the properties of tonic block where the I1761A mutation enhances tonic block at a given drug LA concentration, (Ragsdale et al. 1994b) which is consistent if this widens the fenestration and aids drug entry in the resting state. The two mutations V1766A and N1769A also enhance tonic inhibition by etidocaine in Nav1.2. These positions sit just behind the cavity lining residues and just below the fenestration in bNavs (Fig. 2), and while it is possible that they could widen the fenestration, the exact mechanisms by which these enhance tonic block is less clear.

An important, but expected result captured in the recent structures is the location of residues at the same sequence position as those implicated in LA binding in eNavs. The mutations F1764A and Y1771A have been shown to greatly reduce the affinity of Nav1.2 for etidocaine, lidocaine, and phenytoin, while smaller reductions in affinity were seen for drugs known to preferentially bind to open channels (Ragsdale et al. 1994b, 1996). Residues at equivalent positions in the bNav structures are highlighted in green in Figs. 2 and 3 and can be seen to line the central pore cavity. An additional residue known to be important in small molecule block of voltage-gated calcium channels (Hockerman et al. 1997) is indicted in blue. Sodium channel inhibitors share the common features of a phenyl ring attached to a basic nitrogen with a range of appendages (Nardi et al. 2012). In eNavs, the residues implicated in drug binding would define a largely aromatic surface to which the aromatic portions of the LA can bind. In bNavs most of the aromatic character is removed, as can be seen in the sequence alignment (Fig. 2), and a less-specific hydrophobic binding is likely. The importance of the basic nitrogen in Nav inhibitors is beginning to be clarified and studies using unnatural amino acids have suggested the involvement of the positively charged hydrogen atoms attached to the nitrogen in specific cation-α interactions with the conserved phenylalanine residue (F1764 in Nav1.2) for both a range of LAs and class 1 antiarrhythmic compounds (Ahern et al. 2008; Pless et al. 2011). This interaction has also been suggested in molecular models (Lipkind and Fozzard 2010) and would explain why mutations of this residue virtually abolish drug inhibition and

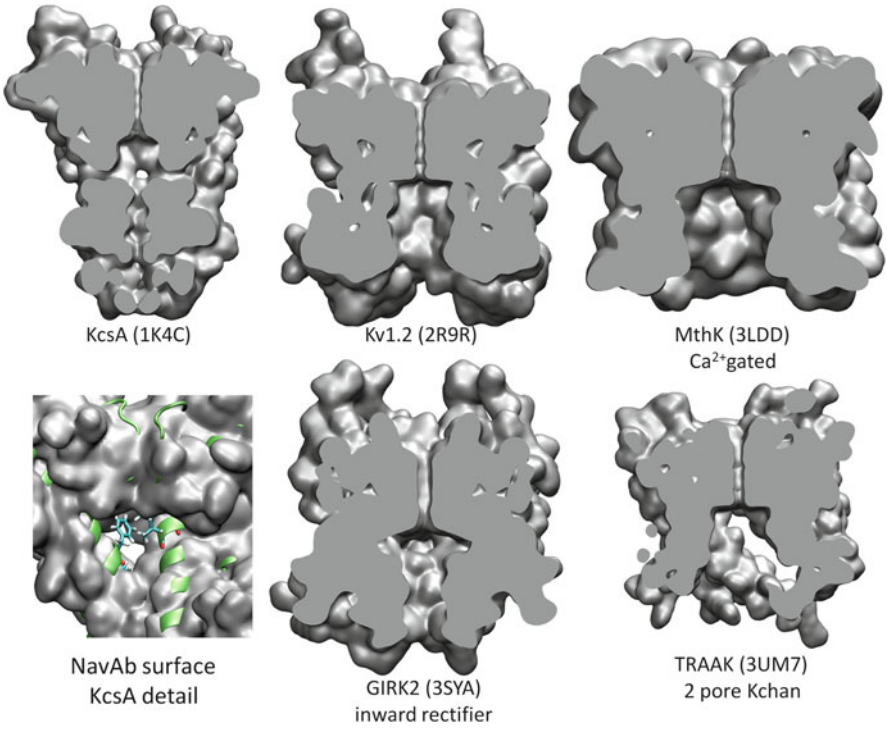

Fig. 5 Comparison of pore architecture and fenestrations in voltage-gated potassium channels. At the bottom left the surface of NavAb is shown looking from the through one of the fenestrations with the aligned protein backbone of KcsA superimposed. Residues I100 and F103 from KcsA that block the potential fenestration are highlighted. PDB data corresponds to accession codes IK4C (Zhou et al. 2001), 2R9R (Long et al. 2007), 3LDD (Trellakis et al. 2006), 3SYA (Whorton and MacKinnon 2011), and 3UM7 (Brohawn et al. 2012)

why this chemical moiety is common to Nav inhibitors. The absence of this aromatic residue in bNavs would remove this specific interaction which could explain the generally lower affinity of LAs to bNavs than eNavs (Lee et al. 2012a). A single mutation I1760A at the position shown in yellow in Fig. 2 has also been shown to allow for the entry of the charged inhibitor QX314 from the extracellular side (Ragsdale et al. 1994b); however, the bNav structures do not provide an obvious explanation for this unexpected pharmacological trait.

Lastly, local anesthetic molecules have been shown to also block a variety of potassium selective pores, as outlined above, and given the large number of structures that are available for potassium channels, it is instructive to see if fenestrations similar to those found in bNavs are present. Figure 5 shows a cut-through image of the protein surface for a number of potassium channels, oriented to highlight the presence of any fenestrations. KcsA does contain small fenestrations, however, they would appear to be too narrow to allow for the entry of typical LAs; however, small structural perturbations might allow small molecules

to enter through this pathway. Many of the other channels pictured have a more robust structure, with no obvious fenestration. The exception to this is the two-pore channel TRAAK, which has two very large fenestrations running from the pore into the membrane, and it is possible that similarities exist with TASK-2 which is known to be blocked by LAs.

Notably, the presence or absence of fenestration in potassium channels does not appear to be related to the backbone positions. Rather, it is largely dictated by the nature and position of the amino acid side chains on S6. To illustrate this, we align and overlay the backbone of KcsA on the NavAb protein surface in the bottom left picture in Fig. 5. The S6 backbone positions, indicated by the green cartoon representation, lies largely within the protein volume of NavAb indicating that roughly the same size gap exists between the S6 helices in each case. However, in KcsA, the side chains of two residues (I100 and F103) occlude the fenestration. A similar situation exists for Kv1.2 and MthK: the gap between the S6 helices is blocked by large side chains. That some channels in the voltage-gated cation channel superfamily have evolved robust pore walls, while others are exposed to the lipid by the lateral fenestrations, raises the interesting questions as to what the physiological role of these pathways might be.

4 Closing Considerations

The data show that bNav channels display local anesthetic-binding affinities similar to the resting state of eukaryotic channels, and structures depict suitable hydrophobic pathways through closed channels to a central blocking site. However, the slow-gating characteristics of the available bNavs have barred the application of more advanced electrophysiological protocols needed to study use-dependent block, and many such bNav channels lack key residues shown to support open and inactivated state inhibition in eNavs. However, bNav protein structures would likely adopt a depolarized conformation, making them potentially useful as models of open/inactivated eNav channels. Thus, additional structural, biochemical, and functional studies are required to determine if bNav channels are fair therapeutic models of eNavs, and if so, which pharmacological states these bacterial channels best represent. Ultimately, the determination of high-resolution structures of eNav channels in combination with the growing variety chemical techniques for probing drug interactions with channels and conformational motions in vivo and in vitro will provide the eventual insights required to make such comparisons.

References

Abu-Qarn M, Eichler J, Sharon N (2008) Not just for Eukarya anymore: protein glycosylation in Bacteria and Archaea. Curr Opin Struct Biol 18:544–550

AHERN GP, Hsu SF, Klyachko VA, Jackson MB (2000) Induction of persistent sodium current by exogenous and endogenous nitric oxide. J Biol Chem 275:28810–28815

Ahern CA, Zhang JF, Wookalis MJ, Horn R (2005) Modulation of the cardiac sodium channel NaV1.5 by Fyn, a Src family tyrosine kinase. Circ Res 96:991–998
Ahern CA, Eastwood AL, Dougherty DA, Horn R (2008) Electrostatic contributions of aromatic residues in the local anesthetic receptor of voltage-gated sodium channels. Circ Res 102:86–94
Alberola-Die A, Martinez-Pinna J, Gonzalez-Ros JM, Vorra I, Morales A (2011) Multiple inhibitory actions of lidocaine on Torpedo nicotinic acetylcholine receptors transplanted to Xenopus oocytes. J Neurochem 117:1009–1019
Berry A, Janssens D, Hümbelin M, Jore JPM, Hoste B, Cleenwerck I, Vancanneyt M, Bretzel W, Mayer AF, Lopez-Ulibarri R et al (2003) Paracoccus zeaxanthinifaciens sp. nov., a zeaxanthin-producing bacterium. Int J Syst Evol Microbiol 53:231–238
Blakemore R (1975) Magnetotactic bacteria. Science 190:377–379
Blanchet J, Chahine M (2007) Accessibility of four arginine residues on the S4 segment of the Bacillus halodurans sodium channel. J Membr Biol 215:169–180
Blanchet J, Pilote S, Chahine M (2007) Acidic residues on the voltage-sensor domain determine the activation of the NaChBac sodium channel. Biophys J 92:3513–3523
Booth IR (1985) Regulation of cytoplasmic pH in bacteria. Microbiol Rev 49:359–378
Brohawn SG, Del Marmol J, Mackinnon R (2012) Crystal structure of the human K2P TRAAK, a lipid- and mechano-sensitive K + ion channel. Science 335:436–441
Choi KL, Aldrich RW, Yellen G (1991) Tetraethylammonium blockade distinguishes two inactivation mechanisms in voltage-activated K + channels. Proc Natl Acad Sci U S A 88:5092–5095
Costa MR, Catterall WA (1984) Cyclic AMP-dependent phosphorylation of the alpha subunit of the sodium channel in synaptic nerve ending particles. J Biol Chem 259:8210–8218
Deutscher J, Jr Saier MH (2005) Ser/Thr/Tyr protein phosphorylation in bacteria - for long time neglected, now well established. J Mol Microbiol Biotechnol 9:125–131
Dimroth P, Cook GM (2004) Bacterial Na+- or H+-coupled ATP synthases operating at low electrochemical potential. Adv Microb Physiol 49:175–218
Fredrickson JK, Zachara JM, Kennedy DW, Dong H, Onstott TC, Hinman NW, Li S (1998) Biogenic iron mineralization accompanying the dissimilatory reduction of hydrous ferric oxide by a groundwater bacterium. Geochim Cosmochim Acta 62:3239–3257
Gingrich KJ, Beardsley D, Yue DT (1993) Ultra-deep blockade of Na + channels by a quaternary ammonium ion: catalysis by a transition-intermediate state? J Physiol 471:319–341
González JM, Covert JS, Whitman WB, Henriksen JR, Mayer F, Scharf B, Schmitt R, Buchan A, Fuhrman JA, Kiene RP et al (2003) Silicibacter pomeroyi sp. nov. and Roseovarius nubinhibens sp. nov., dimethylsulfoniopropionate-demethylating bacteria from marine environments. Int J Syst Evol Microbiol 53:1261–1269
Hille B (1968) Charges and potentials at the nerve surface. Divalent ions and pH. J Gen Physiol 51:221–236
Hille B (1977a) Local anesthetics: hydrophilic and hydrophobic pathways for the drug-receptor reaction. J Gen Physiol 69:497–515
Hille B (1977b) The pH-dependent rate of action of local anesthetics on the node of Ranvier. J Gen Physiol 69:475–496
Hockerman GH, PETERSON BZ, Johnson BD, Catterall WA (1997) Molecular determinants of drug binding and action on L-type calcium channels. Annu Rev Pharmacol Toxicol 37: 361–396
Irie K, Kitagawa K, Nagura H, Imai T, Shimomura T, Fujiyoshi Y (2010) Comparative study of the gating motif and C-type inactivation in prokaryotic voltage-gated sodium channels. J Biol Chem 285:3685–3694
Ito M, Xu H, Guffanti AA, Wei Y, Zvi L, Clapham DE, Krulwich TA (2004) The voltage-gated Na+ channel NaVBP has a role in motility, chemotaxis, and pH homeostasis of an alkaliphilic Bacillus. Proc Natl Acad Sci USA 101:10566–10571
Isom LL, DE Jongh KS, Patton DE, Reber BF, Offord J, Charbonneau H, Walsh K, Goldin AL, Catterall WA (1992) Primary structure and functional expression of the beta 1 subunit of the rat brain sodium channel. Science 256:839–842

Josephson IR (1988) Lidocaine blocks Na, Ca and K currents of chick ventricular myocytes. J Mol Cell Cardiol 20:593–604

Kassmann M, Hansel A, Leipold E, Birkenbeil J, Lu S, Hoshi T, Heinemann SH (2008) Oxidation of multiple methionine residues impairs rapid sodium channel inactivation. Pflugers Arch 456:1085–1095

Kimbrough JT, Gingrich KJ (2000) Quaternary ammonium block of mutant Na + channels lacking inactivation: features of a transition-intermediate mechanism. J Physiol 529(Pt 1):93–106

Kindler CH, Paul M, Zou H, Liu C, Winegar BD, Gray AT, Yost CS (2003) Amide local anesthetics potently inhibit the human tandem pore domain background K + channel TASK-2 (KCNK5). J Pharmacol Exp Ther 306:84–92

Koishi R, Xu H, Ren D, Navarro B, Spiller BW, Shi Q, Clapham DE (2004) A superfamily of voltage-gated sodium channels in bacteria. J Biol Chem 279:9532–9538

Kralj JM, Hochbaum DR, Douglass AD, Cohen AE (2011) Electrical spiking in Escherichia coli probed with a fluorescent voltage-indicating protein. Science 333:345–348

Krulwich TA, Guffanti AA (1989) Alkalophilic bacteria. Annu Rev Microbiol 43:435–463

Krulwich TA, Ito M, Gilmour R, Guffanti AA (1997) Mechanisms of cytoplasmic pH regulation in alkaliphilic strains of Bacillus. Extremophiles 1:163–169

Lee S, Goodchild SJ, Ahern CA (2012a) Local anesthetic inhibition of a bacterial sodium channel. J Gen Physiol 139:507–516

Lee S, Goodchild SJ, Ahern CA (2012b) Molecular and functional determinants of local anesthetic inhibition of NaChBac. Channels 6:403–406

Lipkind GM, Fozzard HA (2010) Molecular model of anticonvulsant drug binding to the voltage-gated sodium channel inner pore. Mol Pharmacol 78:631–638

Liu CJ, Dib-Hajj SD, Renganathan M, Cummins TR, Waxman SG (2003) Modulation of the cardiac sodium channel Nav1.5 by fibroblast growth factor homologous factor 1B. J Biol Chem 278:1029–1036

Long SB, Tao X, Campbell EB, Mackinnon R (2007) Atomic structure of a voltage-dependent K + channel in a lipid membrane-like environment. Nature 450:376–382

Mager T, Rimon A, Padan E, Fendler K (2011) Transport mechanism and pH regulation of the Na+/H+ antiporter NhaA from Escherichia coli. J Biol Chem 286:23570–23581

Mandel KG, Guffanti AA, Krulwich TA (1980) Monovalent cation/proton antiporters in membrane vesicles from Bacillus alcalophilus. J Biol Chem 255:7391–7396

McCusker EC, Bagnéris C, Naylor CE, Cole AR, D'Avanzo N, Nichols CG, Wallace BA (2012) Structure of a bacterial voltage-gated sodium channel pore reveals mechanisms of opening and closing. Nat Commun 3:1102

McLaggan D, Selwyn MJ, Dawson AP (1984) Dependence on Na+ of control of cytoplasmic pH in a facultative alkalophile. FEBS Lett 165:254–258

Mcnulty MM, Edgerton GB, Shah RD, Hanck DA, Fozzard HA, Lipkind GM (2007) Charge at the lidocaine binding site residue Phe-1759 affects permeation in human cardiac voltage-gated sodium channels. J Physiol 581:741–755

Miller WG, Parker CT, Rubenfield M, Mendz GL, Wosten MMSM, Ussery DW, Stolz JF, Binnewies TT, Hallin PF, Wang G et al (2007) The complete genome sequence and analysis of the epsilonproteobacterium Arcobacter butzleri. PLoS One 2:e1358

Mozhayeva GN, Naumov AP, Nosyreva ED (1984) A study on the potential-dependence of proton block of sodium channels. Biochim Biophys Acta 775:435–440

Nardi A, Damann N, Hertrampf T, Kless A (2012) Advances in targeting voltage-gated sodium channels with small molecules. ChemMedChem 7:1712–1740

Nielsen P, Fritze D, Priest FG (1995) Phenetic diversity of alkaliphilic Bacillus strains: proposal for nine new species. Microbiology 141:1745–1761

Olschewski A, Brau ME, Olschewski H, Hempelmann G, Vogel W (1996) ATP-dependent potassium channel in rat cardiomyocytes is blocked by lidocaine. Possible impact on the antiarrhythmic action of lidocaine. Circulation 93:656–659

Paul AA, Witchel HJ, Hancox JC (2002) Inhibition of the current of heterologously expressed HERG potassium channels by flecainide and comparison with quinidine, propafenone and lignocaine. Br J Pharmacol 136:717–729

Pavlov E, Bladen C, Winkfein R, Diao C, Dhaliwal P, French RJ (2005) The pore, not cytoplasmic domains, underlies inactivation in a prokaryotic sodium channel. Biophys J 89:232–242

Payandeh J, Scheuer T, Zheng N, Catterall WA (2011) The crystal structure of a voltage-gated sodium channel. Nature 475:353–358

Payandeh J, El-Din TMG, Scheuer T, Zheng N, Catterall WA (2012a) Crystal structure of a voltage-gated sodium channel in two potentially inactivated states. Nature 486:135–U166

Payandeh J, Gamal El-Din TM, Scheuer T, Zheng N, Catterall WA (2012b) Crystal structure of a voltage-gated sodium channel in two potentially inactivated states. Nature 486:135–139

Pless SA, Galpin JD, Frankel A, Ahern CA (2011) Molecular basis for class Ib anti-arrhythmic inhibition of cardiac sodium channels. Nat Commun 2:351

Ragsdale DS, Mcphee JC, Scheuer T, Catterall WA (1994a) Molecular determinants of state-dependent block of Na + channels by local anesthetics. Science 265:1724–1728

Ragsdale DS, Mcphee JC, Scheuer T, Catterall WA (1994b) Molecular determinants of state-dependent block of Na + channels by local-anesthetics. Science 265:1724–1728

Ragsdale DS, Mcphee JC, Scheuer T, Catterall WA (1996) Common molecular determinants of local anesthetic, antiarrhythmic, and anticonvulsant block of voltage-gated Na + channels. Proc Natl Acad Sci U S A 93:9270–9275

Ren D, Navarro B, Xu H, Yue L, Shi Q, Clapham DE (2001) A prokaryotic voltage-gated sodium channel. Science 294:2372–2375

Renganathan M, Cummins TR, Waxman SG (2002) Nitric oxide blocks fast, slow, and persistent Na + channels in C-type DRG neurons by S-nitrosylation. J Neurophysiol 87:761–775

Rey MW, Ramaiya P, Nelson BA, Brody-Karpin SD, Zaretsky EJ, Tang M, de Leon AL, Xiang H, Gusti V, Clausen IG et al (2004) Complete genome sequence of the industrial bacterium Bacillus licheniformis and comparisons with closely related Bacillus species. Genome Biol 5: r77

Scheuer T (2011) Regulation of sodium channel activity by phosphorylation. Semin Cell Dev Biol 22:160–165

Schmidt JW, Catterall WA (1987) Palmitylation, sulfation, and glycosylation of the alpha subunit of the sodium channel. Role of post-translational modifications in channel assembly. J Biol Chem 262:13713–13723

Shiba T (1991) Roseobacter litoralis gen. nov., sp. nov., and Roseobacter denitrificans sp. nov., aerobic pink-pigmented bacteria which contain bacteriochlorophyll a. Syst Appl Microbiol 14:140–145

Shin KS, Maertens C, Proenza C, Rothberg BS, Yellen G (2004) Inactivation in HCN channels results from reclosure of the activation gate: desensitization to voltage. Neuron 41:737–744

Sugimoto M, Uchida I, Fukami S, Takenoshita M, Mashimo T, Yoshiya I (2000) The alpha and gamma subunit-dependent effects of local anesthetics on recombinant GABA(A) receptors. Eur J Pharmacol 401:329–337

Sugiyama S (1995) Na+ driven flagellar motors as a likely Na+ re-entry pathway in alkaliphilic bacteria. Mol Microbiol 15:592

Tan HL, Kupershmidt S, Zhang R, Stepanovic S, Roden DM, Wilde AA, Anderson ME, Balser JR (2002) A calcium sensor in the sodium channel modulates cardiac excitability. Nature 415:442–447

Takami H, Nogi Y, Horikoshi K (1999) Reidentification of the keratinase-producing facultatively alkaliphilic Bacillus sp. AH-101 as Bacillus halodurans. Extremophiles 3:293–296

Trellakis S, Benzenberg D, Urban BW, Friederich P (2006) Differential lidocaine sensitivity of human voltage-gated potassium channels relevant to the auditory system. Otol Neurotol 27:117–123

Ulmschneider MB, Bagnéris C, McCusker EC, DeCaen PG, Delling M, Clapham DE, Ulmschneider JP, Wallace BA (2013) Molecular dynamics of ion transport through the open conformation of a bacterial voltage-gated sodium channel. Proc Natl Acad Sci USA 110:6364–6369

Van Petegem F, Lobo PA, Ahern CA (2012) Seeing the forest through the trees: towards a unified view on physiological calcium regulation of voltage-gated sodium channels. Biophys J 103:2243–2251

Waters MF, Minassian NA, Stevanin G, Figueroa KP, Bannister JP, Nolte D, Mock AF, Evidente VG, Fee DB, Muller U, Durr A, Brice A, Papazian DM, Pulst SM (2006) Mutations in voltage-gated potassium channel KCNC3 cause degenerative and developmental central nervous system phenotypes. Nat Genet 38:447–451

West JW, Patton DE, Scheuer T, Wang Y, Goldin AL, Catterall WA (1992) A cluster of hydrophobic amino acid residues required for fast Na(+)-channel inactivation. Proc Natl Acad Sci U S A 89:10910–10914

Whorton MR, Mackinnon R (2011) Crystal structure of the mammalian GIRK2 K + channel and gating regulation by G proteins, PIP2, and sodium. Cell 147:199–208

Zamponi GW, Doyle DD, French RJ (1993) Fast lidocaine block of cardiac and skeletal muscle sodium channels: one site with two routes of access. Biophys J 65:80–90

Zhang X, Ren W, Decaen P, Yan C, Tao X, Tang L, Wang J, Hasegawa K, Kumasaka T, HE J, Clapham DE, Yan N (2012a) Crystal structure of an orthologue of the NaChBac voltage-gated sodium channel. Nature 486:130–134

Zhang X, Ren WL, Decaen P, Yan CY, Tao X, Tang L, Wang JJ, Hasegawa K, Kumasaka T, He JH, Wang JW, Clapham DE, Yan N (2012b) Crystal structure of an orthologue of the NaChBac voltage-gated sodium channel. Nature 486:130–U160

Zhou Y, Morais-Cabral JH, Kaufman A, Mackinnon R (2001) Chemistry of ion coordination and hydration revealed by a K+ channel-Fab complex at 2.0 A resolution. Nature 414:43–48

Bacterial Sodium Channels: Models for Eukaryotic Sodium and Calcium Channels

Todd Scheuer

Contents

Abstract

Eukaryotic sodium and calcium channels are made up of four linked homologous but different transmembrane domains. Bacteria express sodium channels comprised of four identical subunits, each being analogous to a single

T. Scheuer (✉)
Department of Pharmacology, University of Washington School of Medicine, Seattle, WA, USA
e-mail: scheuer@u.washington.edu

P.C. Ruben (ed.), *Voltage Gated Sodium Channels*, Handbook of Experimental Pharmacology 221, DOI 10.1007/978-3-642-41588-3_13,

homologous domain of their eukaryotic counterparts. Key elements of primary structure are conserved between bacterial and eukaryotic sodium and calcium channels. The simple protein structure of the bacterial channels has allowed extensive structure–function probes of key regions as well as allowing determination of several X-ray crystallographic structures of these channels. The structures have revealed novel features of sodium and calcium channel pores and elucidated the structural importance of many of the conserved features of primary sequence. The structural information has also formed the basis for computational studies probing the basis for sodium and calcium selectivity and gating.

Keywords

Sodium channels • Calcium channels • Structure • Bacterial proteins • Structure–activity relationship • Channel permeation • Channel gating • Ion transport

1 A Family of Bacterial Sodium Channels

The era of bacterial sodium channels began with the identification and description of NaChBac (Catterall 2001; Ren et al. 2001). At that time the known sodium and calcium channels were composed of four homologous but different domains of specialized structure and function that were linked as a single molecule (Fig. 1). These four linked domains of a single molecule fold to form the core of the functional sodium or calcium channel. NaChBac and similar bacterial sodium channels that have been identified since consist of a single domain analogous to one homologous domain of the vertebrate channels; four identical domains come together to form the functional channel, as occurs for voltage-gated potassium channels. The most basic attribute of ion channels is their ability to selectively conduct a particular ion while excluding others. In NaChBac the key residue at the selectivity filter is Glu. This contrasts with most vertebrate sodium channels which have a selectivity filter containing four key residues, Asp (D), Glu (E), Lys (K), and Ala (A), one donated by the pore of each homologous domain. Instead vertebrate calcium channels resemble NaChBac in that each homologous domain contributes 1 Glu. Since NaChBac had a selectivity filter formed by 4 Glus, it was predicted to be selective for calcium. Surprisingly, physiological studies showed that NaChBac instead selected sodium over calcium (Ren et al. 2001); this has been true for other NaChBac-like channels where selectivity has been tested (Koishi et al. 2004; Payandeh et al. 2011; Ren et al. 2001; Shaya et al. 2011; Tang et al. 2014; Zhang et al. 2012). Despite their simple structure and a huge evolutionary distance from vertebrate channels, bacterial sodium channels share major features with their sodium and calcium channel eukaryotic counterparts and thus have become important models for studying the structural basis underlying eukaryotic sodium and calcium channel function.

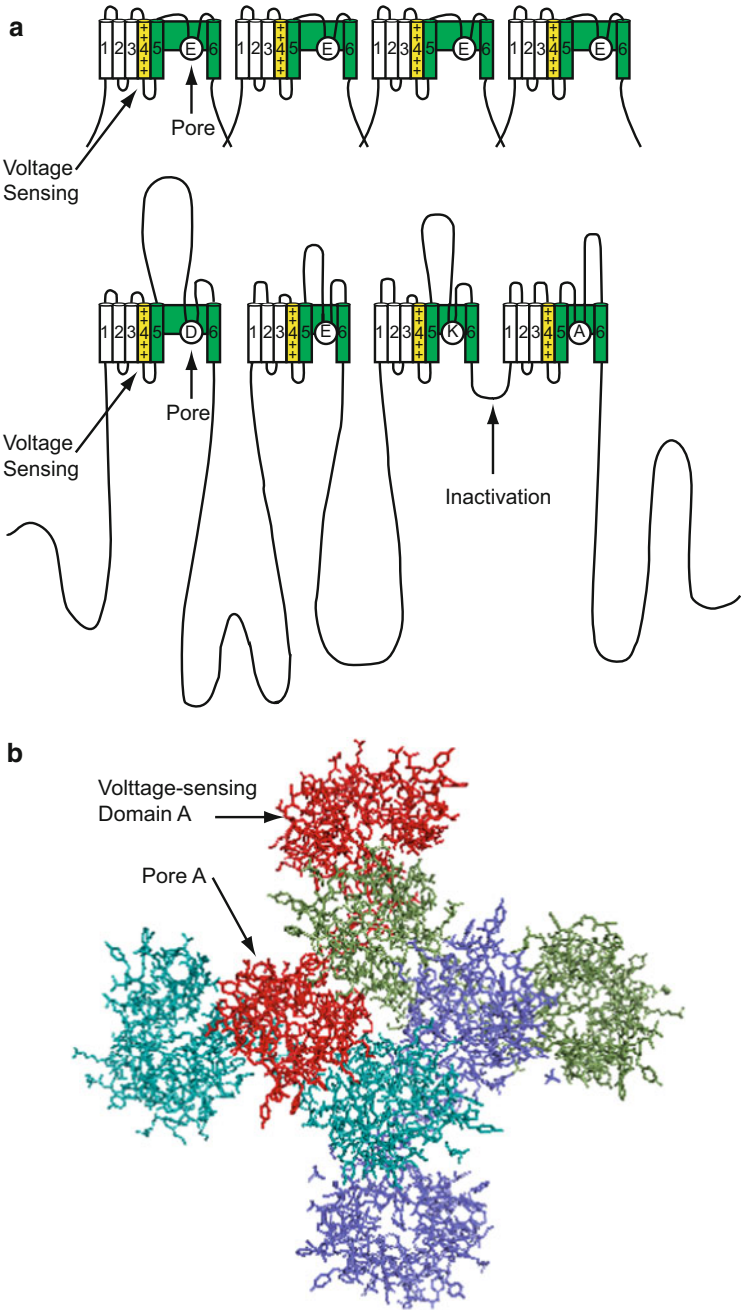

Fig. 1 Overview of sodium channel structure. (**a**) Bacterial sodium channel (*top*) formed by four identical subunits. The voltage-sensing domain contains four transmembrane segments (S1–S4) with the S4 containing four positive charges. The pore module consists of transmembrane segments S5 and S6 connected by a loop that forms the two pore helices of the selectivity filter. The pore loop of each subunit contributes a key glutamate (E) to the selectivity filter. Eukaryotic

The single domain bacterial sodium channel and each homologous but different domain of eukaryotic sodium and calcium channels are similar. However, the vertebrate channels have developed large intracellular loops and N- and C-terminal extensions whose functions are only partially known. Also, extracellular loops within homologous domains have been expanded. Despite these specializations, the core of each homologous domain conserves important structural and functional features that are the trademark of voltage-gated ion channels.

Each homologous domain of eukaryotic sodium and calcium channels or subunit of bacterial sodium channels consists of six alpha helices that are divided between two distinct structural and functional modules (Fig. 1). Transmembrane segments S1, S2, S3, and S4 form the voltage-sensing module. Like other voltage-gated channels, the fourth transmembrane segment is characterized by having a positively charged Arg or Lys every third amino acid that are thought to be the charges responsible for sensing transmembrane voltage. This module is connected via an S4–S5 segment to a pore-forming module composed of transmembrane segment S5, a selectivity filter-containing pore domain and transmembrane segment S6. The S6 segments line the inner aspect of the ion conducting pore and their intracellular ends come together to form the activation gate.

The voltage-sensing modules of both bacterial and vertebrate sodium/calcium channels are similar to each other and quite reminiscent of other voltage-gated channels. All must respond to voltage and that response must be linked to channel gating. In contrast, the selectivity filter regions of sodium- and calcium-selective channels differ from those of potassium and related channels reflecting the requirement that they differentiate between these ions. Conversely, the key features of bacterial sodium channel pores are surprisingly conserved in pore modules of each homologous domain of eukaryotic sodium and calcium channels and differ from those of potassium channels. Thus, bacterial sodium channels are valuable tools for structure/function studies defining key principles underlying function of vertebrate sodium and calcium channels. The simplicity of the channels has allowed solving several X-ray crystallographic structures and the key structural elements that support selective ion permeation.

These structures have shown that bacterial sodium channels are formed of four homologous domains. The pore-forming domains surround a central pore with an extracellularly disposed selectivity filter and a large central cavity closed at its intracellular end by the pore-lining S6 segments. The pore-forming domains are surrounded by voltage-sensing domains. The extracellular aspect of each voltage-sensing domain interacts with the pore domain of the adjacent subunit in the

Fig. 1 (continued) sodium channel (*bottom*) formed by four different but homologous domains, each resembling a subunit of the bacterial sodium channel. The key selectivity residues of pore loops I–IV are aspartate (D), glutamate (E), lysine (K) and alanine (A). Intrasegment and intradomain loops as well as N- and C-termini are large. (**b**) Extracellular view of the crystal structure of the bacterial sodium channel NavAb showing that the voltage-sensing domain of subunit (**a**) interacting with the pore domain of the next subunit in the clockwise direction (Reprinted from Payandeh et al. 2011).

clockwise direction when viewed from the extracellular side (Fig. 1b). As the intracellular end of the voltage-sensing domain is linked to its own pore domain via the S4–S5 linker and the extracellular end to the pore domain of an adjacent subunit, this organization links the four homologous domains of the molecule together. This overall structure is similar in broad strokes to the structure of a voltage-gated potassium channel (Long et al. 2005, 2007).

2 Comparative Primary Structure of Bacterial Sodium Channels and Vertebrate Sodium and Calcium Channels

As the number of bacterial genomes that have been sequenced grows, an increasingly large number are recognizable as bacterial sodium/calcium channels. Although many aspects of these proteins are highly divergent in sequence, key residues in the core functional domains of the proteins are conserved. These same key elements are maintained in the sequences of eukaryotic sodium and calcium channels (Fig. 2)[1]. These constant elements provide the basis for connecting bacterial sodium channel sequences and structures with their eukaryotic counterparts. These similarities of these signature elements between the best-studied bacterial sodium channels and vertebrate sodium and calcium channels are highlighted below.

2.1 The Voltage-Sensing Domain

The voltage-sensing domains of NaChBac and other voltage-gated bacterial sodium channels are readily recognized as the voltage-sensing domain of a voltage-gated channel (Fig. 2). The S4 segments themselves are highly conserved between bacterial sodium channels and eukaryotic sodium channels as well as with other voltage-gated channels. A quartet of positively charged residues is characteristic of S4 voltage sensors of bacterial sodium channels and this motif is extended to up to eight positively charged arginines and lysines in S4 segments of vertebrate sodium and calcium channels. The differing number of positively charged residues between homologous domains in eukaryotic channels presumably reflects differing functions and interactions of the gating residues. Physiological studies showing that these residues are mechanistically important are reviewed in subsequent sections.

The S1, S2, and S3 helices of voltage-sensing domains surround the S4 in voltage sensor structures (Payandeh et al. 2011, 2012) and also contain conserved functionally critical elements. The S1 helix contains a series of residues that are conserved between bacterial sodium channels and eukaryotic sodium and calcium

[1] For the discussion of comparative sequences, residue numbers refer to the NaChBac sequence. Sequence numbers for other constructs are provided in Fig. 2.

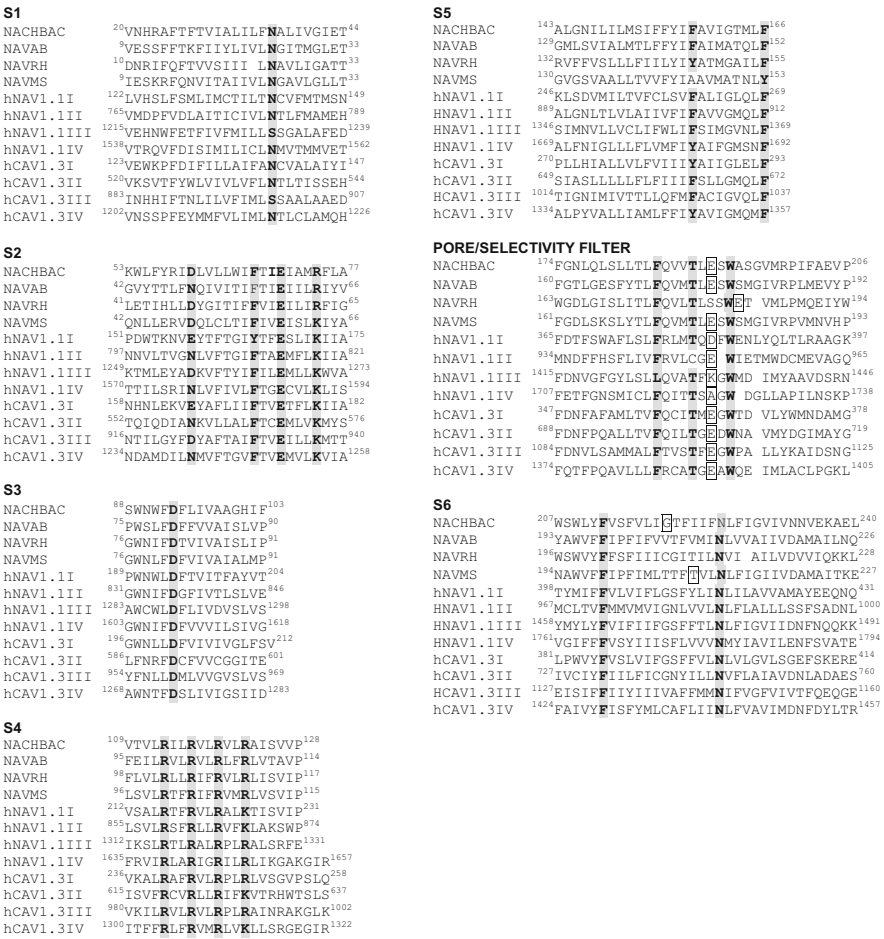

Fig. 2 Sequence alignment of bacterial sodium channels and each domain of representative eukaryotic sodium and calcium channels

channels. Most prominent among these is a highly conserved Asn (N36 in NaChBac). Also present is an extracellular glutamate that is found in some but not all domains of eukaryotic voltage-gated sodium and calcium channels (E43 in NaChBac).

The S2 segment contains highly conserved negatively charged or polar elements arranged ten residues apart along the S2 helix. At the intracellular end is E70. This Glu is conserved between bacterial and eukaryotic sodium and calcium channels. Ten residues toward the extracellular N-terminal end of S2 is a position that always is a Glu, Asp, or Asn in the same channels (Asp60 in NaChBac). Four residues intracellular to E70 is a conserved Arg or Lys (R74 in NaChBac). Between the two and three residues extracellular to E70 is a conserved Phe or a Tyr in both bacterial

and eukaryotic sodium and calcium channels and that is thought to form part of the hydrophobic barrier separating the extracellular and intracellular solutions in voltage-gated cation channels. Charge transfer across the analogous Phe has been extensively studied in voltage-gated potassium channels (Cheng et al. 2013; Lacroix and Bezanilla 2011; Long et al. 2005; Tao et al. 2010). This series of conserved charged and hydrophobic residues are key players in voltage sensor function. The S3 segment too contains a conserved negatively charged residue (D93 in NaChBac). This negatively charged residue sits intracellular to a conserved hydrophobic region and makes key gating charge interactions in voltage sensor structures (Payandeh et al. 2011; Yarov-Yarovoy et al. 2012; Zhang et al. 2012). The intracellular ends of the helices of the voltage-sensing domain are characterized by a series of variable positively and negatively charged residues in both eukaryotic and bacterial sodium channels. The conservation of each of these features of voltage-sensing domains from bacterial to vertebrate channels suggests a critical functional role in voltage gating that has been maintained as channels evolved.

2.2 The Selectivity Filter

The selectivity filters of vertebrate sodium, calcium, and potassium channels were identified in early studies as the region between transmembrane segments S5 and S6 of each subunit for potassium channels (MacKinnon 1991) or each homologous domain for eukaryotic sodium (Heinemann et al. 1992; Terlau et al. 1991) and calcium channels (Kim et al. 1993; Tang et al. 1993; Yang et al. 1993; Yatani et al. 1994). Even though located in a common region of the primary sequence, the key amino acids differed between potassium channels and sodium and calcium channels.

The DEKA motif of the selectivity filter of eukaryotic sodium channels is highly asymmetric in structure. Mutation of the positively charged Lys in the third homologous domain or the Ala in the fourth homologous domain to Glu, or mutation of all four selectivity residues to Glu, resulted in conversion of the channel from being selective for sodium to being selective for calcium (Heinemann et al. 1992). Vertebrate calcium channels have a Glu or Asp residue in the analogous position of each homologous domain. However, extensive mutational analysis has shown that, although all are necessary, glutamates in different domains play asymmetrical roles in conferring selectivity (Sather and McCleskey 2003; Yang et al. 1993). This asymmetry is presumably conferred by the surrounding structures that differ between the homologous domains.

As the selectivity filter of bacterial sodium channels is formed of four identical domains, its primary structure is symmetrical. Despite this inherent difference between the vertebrate channels and their bacterial counterparts, important elements of primary and secondary structure are conserved. Key among these is a conserved Trp (NaChBac W193) that is conserved in bacterial sodium channels as well as in each domain of vertebrate sodium and calcium channels. Also largely

conserved is a Thr (NaChBac T189) located four residues N-terminal to the Trp. These residues play a central structural role that will be discussed below. The residues of the selectivity-conferring DEKA ring in vertebrate sodium channels and of the ring of glutamates or glutamates and aspartates in vertebrate calcium channels are located two residues N-terminal to the Trp. Most bacterial sodium channel sequences contain a glutamate in the analogous selectivity-conferring position. The conservation of the Trp suggests that it and its interacting residues are absolutely necessary for the structure and function of the selectivity filter in eukaryotic sodium and calcium channels as well as of bacterial sodium channels.

2.3 The S5 and S6 Segments

The central cavity of the pore is scaffolded by the S5 segments and lined by the S6 segments. The S6 segment is generally hydrophobic in character and contains residues that influence the binding of hydrophobic pore-blocking drugs. The most-conserved residue in the S6 segments is an Asn that is conserved in bacterial sodium channels (NaChBac N225) as well as in each domain of eukaryotic sodium and calcium channels. Mutagenesis of this residue in each domain of vertebrate sodium channels identifies this as a high impact residue with strong effects on activation and inactivation gating as well as on slow inactivation (Chen et al. 2006; Wang and Wang 1997; Yarov-Yarovoy et al. 2002). Also conserved in both bacterial and eukaryotic channels is a Phe (F212 in NaChBac) near the extracellular end of this segment. This residue too occupies a key position in bacterial sodium channel structure. Also conserved between bacterial and eukaryotic sodium and calcium channels are a Phe at the extracellular end of S5 (NaChBac F166) and a position eight residues N-terminal to it (NaChBac F158) where Phe or Tyr is present. These conserved residues also appear to make key interactions in sodium channel structures.

2.4 Similarities and Dissimilarities in Primary Structure

While certain features of bacterial channels have been conserved and provide models for these core elements, linking of the four homologous domains in eukaryotic channels has permitted specialization of each domain. These are particularly evident in the larger extracellular loops connecting transmembrane segments in eukaryotic channels. In addition, intracellular loops connecting the domains have been specialized for novel forms of interaction and regulation that are impossible in the bacterial sodium channels that lack these sequences. These structural elements and their functions therefore must be explored in a eukaryotic context.

3 Overview of Physiology

Most detail concerning the function of bacterial sodium channels has come from studies of NaChBac. Recordings from other related channels highlight the similarities and variability within this family of channels with similar overall primary sequence. Of particular interest are the three sodium channels for which structural information is also available: the sodium channel from *Arcobacter butzleri*, NavAb (Gamal El-Din et al. 2013; Payandeh et al. 2011, 2012); from *Rickettsiales sp. HIMB114*, NavRh (Zhang et al. 2012, 2013); and from *Magnetococcus sp.*, NavMs (Ulmschneider et al. 2013). Sodium channels from NavPz and NavPs have also been studied in some detail (Koishi et al. 2004). The selectivity of the pore of a sodium channel used for structural studies has also been studied in detail (Shaya et al. 2011).

3.1 Selectivity and Permeation

The finding that the selectivity filter of NaChBac contained glutamates arrayed around the selectivity filter suggested that this channel would be selective for calcium. Surprisingly, the expressed channel had a permeability ratio for P_{Ca}/P_{Na} of .15 (Yue et al. 2002). The ratio P_{Na}/P_{K} was 171 (Ren et al. 2001). As for NaChBac, other bacterial sodium channels that have been studied also select Na over both Ca^{2+} and/or K^{+} (Koishi et al. 2004; Payandeh et al. 2011; Shaya et al. 2011; Ulmschneider et al. 2013; Zhang et al. 2012). Thus, like eukaryotic sodium channels and despite their eukaryotic calcium-channel-like pore sequences, bacterial sodium channels are strongly selective for sodium over potassium.

3.2 Gating

Bacterial sodium channels show a broad range of gating properties. Activation and inactivation are generally slower than for mammalian sodium channels, but rates vary over a broad range in the sodium channels that have been studied (Table 1). Voltage dependence, too, is highly variable with half activation voltages varying from −98 mV for NavAb to +21 mV for NavSp (Table 1). In addition to normal closed state inactivation and inactivation during depolarizations, NavAb is characterized by an additional form of slow inactivation that is highly persistent and has been termed late slow inactivation (Gamal El-Din et al. 2013; Payandeh et al. 2012). The highly divergent gating properties of bacterial sodium channels are likely to reflect their diverse and largely unknown physiological functions. The structural basis for the differences in gating between different bacterial sodium channels as well as the differences between bacterial sodium channels and eukaryotic sodium and calcium channels also remains largely unknown.

Table 1 Kinetic properties of bacterial sodium channels

	Activation		Inactivation	
Channel	Tau (ms)	$V_{1/2}$ (mV)	Tau (ms)	$V_{1/2}$ (mV)
NaChBac	13	−24	166	−40
NavPz	21.5	−9.5	102	−35
NavSp	3.4	21	35	−22
NavAb	–	−98	11	−119
NavMs	–	−93	9	−123

Data are from NaChBac (Ren et al. 2001), NavPz and NavSp (Koishi et al. 2004), NavAb (Payandeh et al. 2012), NavMs (Ulmschneider et al. 2013)

4 Structure–Function Studies of Bacterial Sodium Channels and Relationship to Vertebrate Sodium and Calcium Channels

Bacterial sodium channels immediately became targets for structure–function study after they were described. The small size facilitated mutagenesis. The fact that the channel was formed by four subunits meant that mutants potentially had higher impact than those in four domain eukaryotic sodium and calcium channels. Most studies have targeted the NaChBac sodium channel. They have probed the nature of voltage gating, the inactivation process, selectivity, and the process of channel opening and closing. Structure–function studies have also examined drug binding. These studies have outlined some of the functionally important residues of these channels.

4.1 Probes of Voltage Sensor Structure and Function

NaChBac was generally tolerant when voltage sensor residues were replaced by other amino acids and effects of substitution on channel gating have been extensively studied (Blanchet and Chahine 2007; Blanchet et al. 2007; Chahine et al. 2004; DeCaen et al. 2008, 2009, 2011; Paldi and Gurevitz 2010; Yarov-Yarovoy et al. 2012). Studies in eukaryotic sodium and potassium channels have shown that the extracellular portion of the S4 segment resides in an aqueous cleft contiguous with the extracellular medium. Similarly, the intracellular portion resides in an aqueous environment contiguous with the cytoplasm. Studies examining the aqueous accessibility of cysteines substituted for S4 Arg residues to modification by methanethiosulfonate reagents showed that R1C was accessible to extracellular modification, though in a somewhat occluded space; R3C and R4C were accessible intracellularly. R2C could be modified from both the intracellular and extracellular side of the membrane in the resting channel (Blanchet and Chahine 2007; Chahine et al. 2004). R2C could also be modified from the extracellular side in the activated channel. These studies confirmed that, like other channels,

the S4 segment of NaChBac had largely aqueous exposure both intracellularly and extracellularly and that R2 might transit through the hydrophobic gating pore in the resting channel. NaChBac is unusual in its tolerance for mutations of negatively charged residues in the S1, S2, and S3 segments. Such substitutions, like substitutions of the S4 gating charges, had pronounced effects on channel gating (Blanchet and Chahine 2007; DeCaen et al. 2008, 2011; Yarov-Yarovoy et al. 2012; Zhao et al. 2004a). These negatively charged residues are thought to catalyze the movement of the positively charged S4 arginines as they move across the membrane (Papazian et al. 1995; Tiwari-Woodruff et al. 1997).

To further probe the motion of the NaChBac S4 segment relative to other transmembrane segments of the voltage-sensing domain, DeCaen and colleagues used cross-linking of pairs of substituted cysteines (DeCaen et al. 2008, 2009, 2011; Yarov-Yarovoy et al. 2012). In the resting channel disulfide cross-linking between E43C near the extracellular N-terminal end of S1 (E43C) formed disulfide cross-links with R1C and Thr110 located three residues N-terminal to R1. Likewise, resting interactions were observed between D60C in S2 extracellular to the HCS and V109C and L112C near the extracellular end of S4. These interactions show positions visited by the extracellular end of the S4 segment at hyperpolarized potentials.

A different set of extracellular interactions were observed upon depolarization. E43C did not interact with R2C, R3C, or R4C at rest; D60C did not interact with R3C or R4C at rest. However, in response to activating the channel with a single depolarization, R2C and R3C, but not R4C, formed spontaneous disulfide cross-links with E43C. Likewise, R3C and R4C interacted with D60C upon depolarization. Each of these interactions occurred on the ms timescale of channel activation (DeCaen et al. 2009, 2011).

In contrast to E43 and D60, E70 is situated intracellular to the HFS. However, no interactions between R3C or R4C and E70C were observed at rest. Instead, with depolarization, R3C or R4C cross-linked rapidly with E70C. Thus, cysteines substituted for R3 and R4 are not stabilized by the INC at rest but move rapidly into or through the INC upon depolarization. Each of the interactions that require depolarization defines positions of S4 side chains that are not visited at rest but are visited within ms of depolarization. The sum of these interactions in conjunction with other biophysical data allowed the modeling of a series of conformations of the NaChBac voltage sensor as it transitioned from the fully resting to the fully activated state (Yarov-Yarovoy et al. 2012). These features suggest that voltage-dependent gating in bacterial sodium channels is much like that of other voltage-gated ion channels that have been extensively studied.

The gating transitions of NaChBac produce robust gating currents (Kuzmenkin et al. 2004) due to movement of fixed charges in the S4 and elsewhere relative to the transmembrane electric field. The channels were found to move ~6 elementary charges per channel. The voltage dependence of charge movement was negative to that of channel opening as expected of a channel where activation of multiple voltage sensor had to occur before the channel could open. As in other voltage-gated channels, prolonged depolarization of NaChBac resulted in the charge becoming immobilized and its voltage dependence shifting to more negative potentials (Gamal El-Din et al. 2013; Kuzmenkin et al. 2004).

4.2 Pore/Selectivity

Yue et al. explored the nature of pore sodium selectivity by mutagenesis in an elegant series of experiments. Replacing a series of NaChBac selectivity filter residues with Asp transformed the channel from being sodium selective to being calcium selective (Yue et al. 2002). The resulting channel had most hallmarks of eukaryotic calcium channels. The mutant NaChBac channels passed sodium current when calcium was absent, but the sodium current was blocked by low concentrations of calcium. Increasing calcium further resulted in Ca-selective permeation (Yue et al. 2002). This biphasic behavior as function of calcium concentration is termed anomalous mole fraction behavior and is a characteristic of eukaryotic calcium channels (Almers and McCleskey 1984; Hess and Tsien 1984). The ability to transform a sodium-permeable channel into a calcium-permeable one with a few simple mutations is consistent with the idea that the basic structural architecture underlying sodium-selective permeation and calcium-selective permeation is likely to be similar. The structural basis for the transformation from Na to Ca permeation has recently been elucidated (Tang et al. 2014).

4.3 Structural Basis for Inactivation

The rapid inactivation that occurs upon depolarization in eukaryotic sodium channels requires sequences in the intracellular loop between homologous domains III and IV of those channels (Catterall 2000). Bacterial sodium channels such as NaChBac lack such intracellular sequences. Therefore, inactivation was likely to occur by different mechanisms. Pavlov et al. (2005) demonstrated directly that alterations in a pore Ser 4 positions C-terminal to the selectivity-conferring glutamate residues altered the rate of channel inactivation, much as pore residues affect rates of slow inactivation in vertebrate sodium channels (Capes et al. 2012; Xiong et al. 2006; Zarrabi et al. 2010). This suggested that inactivation in NaChBac was mechanistically similar to slow inactivation in eukaryotic sodium channels. Interestingly, Lee et al. (2012) identified mutation T220A in the S6 segment that virtually abolished inactivation during depolarization of NaChBac. Thus, residues in both the pore and the S6 segments are likely to collaborate in the inactivation process of bacterial sodium channels much as residues in both regions affect inactivation in vertebrate sodium channels.

The late slow inactivation of NavAb is likely to have a different genesis than the inactivation that occurs during single depolarizations (Gamal El-Din et al. 2013; Payandeh et al. 2012). That persistent form of slow inactivation was blocked when either the conserved S2 Asn (NavAb N49) was replaced by Lys or when R3 of the S4 segment was replaced by Cys, indicating that this aspect of slow inactivation required interaction between these residues (Gamal El-Din et al. 2013). However, inactivation during depolarization like that of other bacterial sodium channels such as NaChBac remained in the presence of these mutations, indicating that late slow inactivation was mechanistically distinct and separable from the remaining inactivation processes.

4.4 S6 Segment Function

Activation gates of many ion channels are formed by the sealing of crossed pore-lining helices (S6 segments in voltage-gated channels) at their intracellular ends (Doyle et al. 1998), and channel opening was proposed to occur by bending of S6 segments at a Gly found in the middle of that segment (Jiang et al. 2002). Zhao et al. (2004a, b) probed the importance of a putative bend in the S6 helix of NaChBac at the position of such a Gly hinge. Substitution of a P for the native glycine resulted in channels that opened at very negative potentials, closed very slowly, and virtually lacked inactivation (Zhao et al. 2004b). Proline substitutions at other positions had varied effects, but proline substitutions at three positions on the same face of the helix as G219 reversed the voltage dependence of channel opening (Zhao et al. 2004a). Now when the voltage sensor was at rest, the channel was open, and when it moved outward in response to depolarization, the channel closed. Altering the structure of the S6 segment at key positions has truly dramatic effects on channel opening, presumably by changing the conformational change in the S6 segments that occur in response to depolarization.

Although altering the structure of S6 by substitution of Pro and other amino acids greatly impacts many aspects of NaChBac function, Gly residues are absent from S6 segments of most bacterial sodium channels and thus cannot be necessary for gating. Interestingly, comparison of the structures of NavMs and NavAb indicated that gating of the S6 segments could be hinged by a simple angular change at the position of a Thr located 1 helical turn C-terminal to G219 (McCusker et al. 2011). This provided the attractive hypothesis that channel opening and closing could occur by simple rotation around a single bond or small subset of bonds at this position.

5 Structures of Bacterial Sodium Channels

Although NaChBac was described in 2001, determination of a structure of a bacterial sodium channel proved extremely challenging. It was not until 10 years later in 2011 that the structure of a NaChBac homolog, NavAb, was described (Payandeh et al. 2011). This was followed by structures of two other channels (D'Avanzo et al. 2013; McCusker et al. 2012; Zhang et al. 2012) as well as a structure of new states of NavAb (Payandeh et al. 2012). Each provides a fascinating snapshot of a channel in one potentially physiological state.

5.1 Bacterial Sodium Channel Structure

The first NavAb structure introduced the hallmarks that differentiate bacterial sodium channel structures from previous structures of potassium channels (Payandeh et al. 2011). The overall structure was reminiscent of a voltage-gated potassium channel with a central pore and four peripherally situated voltage sensor

domains. The extracellular end of each voltage sensor domain was adjacent to the pore domain of the next subunit in the clockwise direction when viewed from the extracellular side (Fig. 1b). However, the pore domain and particularly the selectivity filter were strikingly different from those of potassium channels.

5.2 Selectivity Filter

Classical biophysical studies showed that the selectivity filter of vertebrate sodium channels had a large cross section and was likely to transport sodium in a partially hydrated state (Hille 1975, 2001). This contrasts with potassium channels that transport fully dehydrated potassium in a single file through a narrow pore (Hille 2001). The structure of NavAb outlined the key architectural features of the selectivity filter and ion conduction pathway of these bacterial sodium channels (Fig. 3a; Payandeh et al. 2011). The outer aspect of the pore forms a wide, electronegative funnel. Ions then pass through a selectivity filter that is considerably wider and shorter than that of voltage-gated potassium channels (Fig. 3a). The inner portion of the ion conduction pathway is a large central cavity. The intracellular mouth of the NavAb pore is closed by the S6 segments at the level of M221.[2] The selectivity filter of NavAb is formed by two α helices connected by a loop (Fig. 3a). The N-terminal and more intracellular of these helices is analogous to the pore helix of potassium channels. Its C-terminus is pointed toward the central cavity with an induced dipole that could stabilize cations in the central cavity. This is followed by a turn that exposes the backbone carbonyls of T175 and L176 (NavAb numbering) to the pore lumen (Fig. 3a, b). The negatively charged side chains of the 4 Glu 177 residues point upward and inward toward the outer mouth of the filter to stabilize cations that arrive from the extracellular side of the channel. The turn is followed by a second (P2) α helix that is not found in potassium channels (Fig. 3a). The P2 helix is amphipathic in nature. It exposes negatively charged residues on its aqueous exposed extracellular surface and forms the electronegative entrance funnel to the core of the selectivity filter. The conserved Trp (W179 in NavAb; Fig. 3c) is found at the extracellular transition between the turn and the P2 helix. It reaches down and interacts with the side chain of T175 of the adjacent subunit, the residue at the turn between the P1 helix and the selectivity loop, and ties the selectivity filter loops of adjacent subunits together. The Trp and Thr are conserved in most domains of vertebrate channels (Fig. 2). In others the Thr is replaced by Cys or Ser, which might also interact with Trp in these channels.

The selectivity filter formed by this unique structure differs from that of potassium channels. It is far wider and shorter. The extracellular glutamates define an extracellular high field strength site ($Site_{HFS}$) with an opening of 4.6 × 4.6 Å (Fig. 3b, c). This is large enough to allow passage of a partially hydrated sodium

[2] For the discussion of channel structures, residue numbers refer to the NavAb sequence. Sequence numbers for other constructs are provided in Fig. 2.

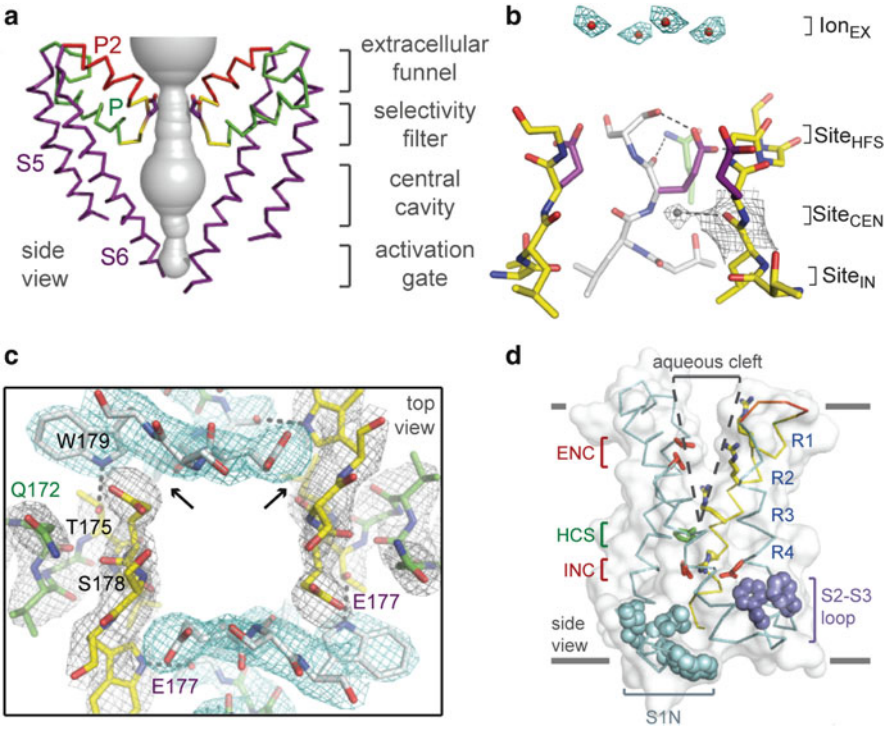

Fig. 3 Structural features of bacterial sodium channels. (**a**) Side view of the backbone of two opposite pore domain subunits showing the P and P2 helices. The side chain of Glu 177 at the extracellular entrance to the selectivity filter is shown. (**b**) Expanded view of the loops between the P and P2 helices from three subunits. The loop from the foreground subunit has been omitted. Putative ion binding sites, Site HFS formed by the Glu 177 side chains, and Site CEN and Site IN formed by the backbone carbonyls of Leu 176 and Thr 175 are indicated. (**c**) *Top view* of the selectivity filter entrance showing the key hydrogen bond between Trp (W) 179 and Thr (T) 175 of the adjacent subunit. (**d**) *Side view* of the NavAb voltage sensor showing the extracellular negatively charged cluster (ENC), the hydrophobic constriction site (HCS), and the intracellular negatively charged cluster (INC). Side chains of S4 arginines R1–R4 are shown. Modified from Payandeh et al. (2011)

ion. The backbone carbonyls of Leu176 and Thr175 define a central site ($Site_{CEN}$) and an intracellular site ($Site_{IN}$), respectively. The channel is wide at these positions and can accommodate a square array of water molecules surrounding a central sodium ion.

5.3 The S6 Segment and Fenestrations

The S6 segments lining the central cavity of bacterial sodium channels also have maintained strong homology to mammalian sodium and calcium channels. Each S6 segment of bacterial sodium channels contains a Phe at the level of the selectivity

filter that is highly conserved in bacterial and eukaryotic sodium channels and a conserved Asn that is virtually invariant.

The Phe is part of a network of interacting residues linking the extracellular aspect of the pore helices to S6 that was identified by comparison of the original pre-open structure of NavAb (Payandeh et al. 2011) with inactivated structures (Payandeh et al. 2012). Presumably, this conserved Phe plays the same structural role in eukaryotic sodium and calcium channels. Interestingly, mutations of residues in this network in S6 and the pore domain affect slow inactivation (Vilin et al. 2001; Zarrabi et al. 2010). Conservation of these residues between bacterial sodium channels and vertebrate sodium channels indicates a key functional role of these residues in linking conformational changes between the S6 segments and the pore helices.

The universal conservation of Asn 211 suggests that it too is critically important (Fig. 2). Conformational changes in the voltage-sensing domains of voltage-gated channels are thought to be transmitted to the pore domain via an interaction between the S4–S5 linkers and the S6 segments of the adjacent subunit or homologous domain. Asn is found near the S4–S5 linker in all structures (Payandeh et al. 2011, 2012; Zhang et al. 2012). In the inactivated structure of NavAb WT, Asn 211 actually interacts with a backbone carbonyl of Leu 123 in the S4–S5 linker of the adjacent domain (Payandeh et al. 2012). In the inactivated conformation that was crystallized, this interaction is only observed in two of the four domain pairs; in the other two pairs, Asn 211 is distant from the S4–S5 linker as dictated by the flattened shape of the inactivated state structure. Interestingly, mutations of the analogous Asn have much greater effects on slow inactivation in domains I and III than in domains II and IV of mammalian Nav1.2 sodium channels (Chen et al. 2006). While the patent structural link observed in this inactivated channel is not observed in the original NavAb structure or in the NavRh structure, the strict conservation of this residue indicates a critical functional and structural role that will be further defined as future structures become available.

The S6 segments of domains III and IV of mammalian sodium and calcium channels contain central cavity-lining residues affecting the action of local anesthetics, antiarrhythmics, and anticonvulsants (sodium channels) and calcium channels antagonists such as phenylalkylamines (e.g., verapamil), dihydropyridines (e.g., nifedipine), and benzothiazepines (e.g., diltiazem). Tertiary members of these drug families affect closed channels suggesting that they can reach binding sites in the pore even though the intracellular mouth of the channel is tightly closed. A novel feature of the structure of the NavAb sodium channel is the presence of openings in the walls of the central cavity, even though the pore is closed. These openings or fenestrations measured 8×10 Å in the original structure and were threaded by fatty acyl lipid tails. Interestingly, the shape and size of the fenestrations may be altered in a state-dependent fashion as they differed in the inactivated structure of WT NavAb (Payandeh et al. 2012). A recent structure of only the pore domain of a bacterial sodium channel with high homology to NavAb, NavMs, was found to have an open activation gate and provided the view of channel activation gating discussed earlier (McCusker et al. 2012). Fenestrations

were also present in this open structure but were enlarged relative to those in the closed NavAb structure (McCusker et al. 2012).

5.4 Voltage-Sensing Domain

The voltage-sensing domain of NavAb pre-open state structure (Payandeh et al. 2011), the WT NavAb inactivated structures (Payandeh et al. 2012), and the structure of NavRh (Zhang et al. 2012) are generally similar (and similar to those of potassium channels) but differ in detail. Voltage-sensing domains are characterized by an extracellular negatively charged cluster (ENC) and intracellular charged cluster (INC) separated by a hydrophobic constriction site (HCS) (Fig. 3d). The extracellular aspect of the voltage-sensing domain is characterized by an aqueous cleft extending approximately 10 Å into the sensor. This aqueous extension makes it likely that the voltage field is highly focused across the HCS. Arg side chains interact with either the INC or the ENC as they move past the HCS. Thus charge movement across the membrane is thought to occur when positively charged side chains of the S4 voltage sensor move across the HCS. In all NavAb structures R1, R2, and R3 are extracellular to the HCS. R4 is intracellular to the HCS and stabilized by the charges of the INC formed of E59, the conserved negatively charged residue in S2 and D80, the conserved negatively charged residue in S3 (Payandeh et al. 2011, 2012). In the structure of NavRh, R1–R4 side chains are extracellular to the HCS (Zhang et al. 2012). Since 3 or 4 of the S4 positive charges are extracellular to the HCS in each of these structures, these are considered to be activated conformations of the voltage sensor (Zhang et al. 2012).

Each of the voltage-sensing domain structures have an S4 segment containing a stretch of 3_{10} helix. Such a structure differs from an α helix in that it places each of the Arg residues of the S4 in register and would allow them to move linearly past the INC, HCS, and the ENC of the voltage sensor domain. All NavAb structures contain a stretch of 3_{10} helix running from R1 through R4 of the S4 segment (Payandeh et al. 2011, 2012). In the structure of NavRh, only the region between the R3 and the R4 gating charges forms a 3_{10} helix; the more extracellular portion of the S4 segment is α helical (Zhang et al. 2012). The difference in structure between the more inward voltage sensors of NavAb containing a longer stretch of 3_{10} helix and the more outward voltage sensor of NavRh where the 3_{10} helix is shorter could be the structural correlate of a helical relaxation that accompanies S4 movement to a more activated state as has been proposed for activation of NaChBac from mutagenesis, cross-linking, and modeling studies (Yarov-Yarovoy et al. 2012).

The pore domain structure and the positioning of the entire voltage-sensing domain relative to the pore is dramatically different between each of the published structures. For the NavAb pre-open state and inactivated state structures, the intradomain structure of the voltage-sensing domain remains relatively unchanged from S1 through the S4–S5 linker (Payandeh et al. 2011, 2012). Despite this similarity, the entire voltage-sensing domain has moved relative to the pore domain with hinging occurring at the base of the S5 segment (Payandeh et al. 2012).

Likewise, when comparing the NavRh structure to the NavAb structure, similarly large changes in relationship of the pore domains and the voltage-sensing domains have occurred (Zhang et al. 2012). These different structures are due largely to substantial rigid body displacements of whole domains with only minor intradomain changes may represent different functional states of the channel(s).

6 Computational Studies of Bacterial Sodium Channel Permeation

The availability of structures of bacterial sodium channels has made them the subject of computational studies of ion occupancy, permeation, and selectivity of ever-increasing complexity and computational power (Carnevale et al. 2011; Chakrabarti et al. 2013; Corry 2013; Corry and Thomas 2011; Furini and Domene 2012; Ke et al. 2013; Qiu et al. 2012; Stock et al. 2013; Ulmschneider et al. 2013; Zhang et al. 2013). The theoretical basis for sodium versus calcium or potassium selectivity in these channels has also been explored (Dudev and Lim 2010, 2012). Some computational studies have explored the basis for sodium versus potassium selectivity (Corry and Thomas 2011; Furini and Domene 2012; Ulmschneider et al. 2013). Others have examined the basis of sodium versus calcium selectivity (Zhang et al. 2013).

While a detailed comparison of these studies is beyond the scope of this article, some general themes can be emphasized. The most recent studies utilize either a modeled open structure of NavAb (Stock et al. 2013), the open crystal structure of NavMs (Ulmschneider et al. 2013), or the closed crystal structure of NavAb (Chakrabarti et al. 2013) as their substrates. Model conditions differ for each study, but each emphasizes the multi-ion occupancy of the pore. A common finding is that partially dehydrated sodium ions may prefer to reside asymmetrically in the pore away from the central axis and stabilized by direct interaction with the carboxyl groups of 1 or more glutamates and by hydrogen bonding via waters of hydration with the remaining carboxyl residues. A similar asymmetric arrangement at the level of the backbone carbonyls of L176 (site CEN) has also been described (Chakrabarti et al. 2013; Stock et al. 2013; Ulmschneider et al. 2013).

The study based on the open structure of NavMs (Ulmschneider et al. 2013) found that the pore was occupied most often by 2 Na^+ ions with 1 off axis at the HFS near the glutamates and one on axis at Site CEN or Site IN corresponding to the levels of the backbone carbonyls of T175 and L176 (T51 and L52 in NavMs). The Na^+ ions spend a considerable amount of time in the inner cavity before exiting through the cytoplasmic mouth of the pore. These authors also considered the difference between permeation by Na^+ and permeation by K^+. Potassium ions arriving from outside do not move readily beyond site HFS at the level of the glutamates, indicating that they encounter a large energy barrier at this point. Water conductance through the pore was bidirectional and largely independent of ion flux

through the pore. The fenestrations in the side of the pore were occupied by lipids tails from the inner membrane leaflet that exchanged rapidly without blocking the pore.

An all-atom simulation based on closed NavAb studied at 0 mV (Chakrabarti et al. 2013) showed Na^+ transfer rates from the extracellular milieu to the central cavity of $>6 \times 10^6$ ions per second, consistent with the single channel conductance through open sodium channels. The pore was populated by 2–4 sodium ions at any one time. Sodium ions bound at three sites as well as moving into the central cavity. The first site was stabilized by the Glu177 side chains. A second site was found between E177 and L176. Three ions occupied the selectivity filter 23 % of the time, but two of them were accommodated near each other at $Site_{CEN}$. Intriguingly, the selectivity filter was remarkably dynamic with the side chains of glutamate 177 changing conformation from a position pointing outward toward the extracellular medium to one pointing inward toward the selectivity filter. The inward or "dunked" conformation appeared to be favored when a sodium ion was present in the filter. Furthermore, the conformation of ions, water, and side chains in the selectivity filter were highly degenerate with multiple conformations of nearly equal energy. Thus, sodium ions were solvated by an ever-changing mixture of carboxyl and carbonyl side chains and water. This degenerate stabilization pattern resulted in an exceedingly flat energy landscape for ion permeation (Chakrabarti et al. 2013).

A study of NavRh emphasized the differences in ion transport imparted by the different sequence of the selectivity filter in this channel and the block of ion conductance by calcium and its asymmetry (Zhang et al. 2013). The selectivity filter of NavRh is unusual in containing a Ser at the position where Glu is found in the other bacterial sodium channels discussed here; a Glu is found in NavRh but two residues further extracellular. Thus, the Glu-based high field strength site is displaced outward relative to the narrow part of the pore which is formed by Ser (Zhang et al. 2012). Ca^{2+} blocks NavRh and other sodium channels in physiological experiments. Extracellular Ca^{2+} was found to block near the extracellularly shifted HFS site but did not readily access more intracellular sites within the selectivity filter. This was surprising because the NavRh structure had contained a Ca^{2+} ion near the level of the Leu carbonyl (Site CEN) (Zhang et al. 2012). Simulating Ca^{2+} block in the MD experiment by adding Ca^{2+} from the intracellular side resulted in binding at Site CEN near where Ca^{2+} had been observed in the crystal structure. Thus, Ca^{2+} block appeared highly asymmetrical. Interestingly, physiological studies showed asymmetrical block of Na^+ current by Ca^{2+} depending on whether Ca^{2+} was added intra- or extracellularly (Zhang et al. 2013).

Conclusion

Studies of bacterial sodium channels reveal how their more complicated eukaryotic sodium and calcium channel counterparts might function if stripped of the complexity imparted by their differing subunits and the accretion of intracellular and extracellular modulatory sequences. These channels maintain sodium selectivity and relatively rapid voltage-dependent gating but lack the fast inactivation

that is so prominent for vertebrate sodium channels. They can be altered to behave as calcium channels. The interface between these simple models for functional studies and the structures that can reveal so much is likely to continue to yield many further insights in the future.

References

Almers W, McCleskey EW (1984) Non-selective conductance in calcium channels of frog muscle: calcium selectivity in a single-file pore. J Physiol 353:585–608

Blanchet J, Chahine M (2007) Accessibility of four arginine residues on the S4 segment of the Bacillus halodurans sodium channel. J Membr Biol 215:169–180

Blanchet J, Pilote S, Chahine M (2007) Acidic residues on the voltage-sensor domain determine the activation of the NaChBac sodium channel. Biophys J 92:3513–3523

Capes DL, Arcisio-Miranda M, Jarecki BW, French RJ, Chanda B (2012) Gating transitions in the selectivity filter region of a sodium channel are coupled to the domain IV voltage sensor. Proc Natl Acad Sci U S A 109:2648–2653

Carnevale V, Treptow W, Klein ML (2011) Sodium ion binding sites and hydration in the lumen of a bacterial ion channel from molecular dynamics simulations. J Phys Chem Lett 2:2504–2508

Catterall WA (2000) From ionic currents to molecular mechanisms: the structure and function of voltage-gated sodium channels. Neuron 26:13–25

Catterall WA (2001) Physiology. A one-domain voltage-gated sodium channel in bacteria. Science 294:2306–2308

Chahine M, Pilote S, Pouliot V, Takami H, Sato C (2004) Role of arginine residues on the S4 segment of the Bacillus halodurans Na^+ channel in voltage-sensing. J Membr Biol 201:9–24

Chakrabarti N, Ing C, Payandeh J, Zheng N, Catterall WA, Pomes R (2013) Catalysis of Na^+ permeation in the bacterial sodium channel Na_VAb. Proc Natl Acad Sci U S A 110:11331–11336

Chen Y, Yu FH, Surmeier DJ, Scheuer T, Catterall WA (2006) Neuromodulation of Na^+ channel slow inactivation via cAMP-dependent protein kinase and protein kinase C. Neuron 49:409–420

Cheng YM, Hull CM, Niven CM, Qi J, Allard CR, Claydon TW (2013) Functional interactions of voltage sensor charges with an S2 hydrophobic plug in hERG channels. J Gen Physiol 142:289–303

Corry B (2013) Na^+)/Ca^{2+} selectivity in the bacterial voltage-gated sodium channel NavAb. Peer J 1:e16

Corry B, Thomas M (2011) Mechanism of ion permeation and selectivity in a voltage gated sodium channel. J Am Chem Soc 134:1840–1846

D'Avanzo N, McCusker EC, Powl AM, Miles AJ, Nichols CG, Wallace BA (2013) Differential lipid dependence of the function of bacterial sodium channels. PLoS One 8:e61216

DeCaen PG, Yarov-Yarovoy V, Zhao Y, Scheuer T, Catterall WA (2008) Disulfide locking a sodium channel voltage sensor reveals ion pair formation during activation. Proc Natl Acad Sci U S A 105:10542–10547

DeCaen PG, Yarov-Yarovoy V, Sharp EM, Scheuer T, Catterall WA (2009) Sequential formation of ion pairs during activation of a sodium channel voltage sensor. Proc Natl Acad Sci U S A 106:22498–22503

DeCaen PG, Yarov-Yarovoy V, Scheuer T, Catterall WA (2011) Gating charge interactions with the S1 segment during activation of a Na^+ channel voltage sensor. Proc Natl Acad Sci U S A 108:18825–18830

Doyle DA, Cabral JM, Pfuetzner RA, Kuo AL, Gulbis JM, Cohen SL, Chait BT, MacKinnon R (1998) The structure of the potassium channel: molecular basis of K^+ conduction and selectivity. Science 280:69–77

Dudev T, Lim C (2010) Factors governing the N^+ vs K^+ selectivity in sodium ion channels. J Am Chem Soc 132:2321–2332

Dudev T, Lim C (2012) Why voltage-gated Ca^{2+} and bacterial Na^+ channels with the same EEEE motif in their selectivity filters confer opposite metal selectivity. Phys Chem Chem Phys 14:12451–12456

Furini S, Domene C (2012) On conduction in a bacterial sodium channel. PLoS Comput Biol 8: e1002476

Gamal El-Din TM, Martinez GQ, Payandeh J, Scheuer T, Catterall WA (2013) A gating charge interaction required for late slow inactivation in the bacterial sodium channel Na_VAb. J Gen Physiol 142:181–190

Heinemann SH, Terlau H, Stuhmer W, Imoto K, Numa S (1992) Calcium channel characteristics conferred on the sodium channel by single mutations. Nature 356:441–443

Hess P, Tsien RW (1984) Mechanism of ion permeation through calcium channels. Nature 309:453–456

Hille B (1975) Ionic selectivity, saturation, and block in sodium channels. A four-barrier model. J Gen Physiol 66:535–560

Hille B (2001) Ionic channels of excitable membranes. Sinauer Associates, Sunderland, MA

Jiang Y, Lee A, Chen J, Cadene M, Chait BT, MacKinnon R (2002) The open pore conformation of potassium channels. Nature 417:523–526

Ke S, Zangerl EM, Stary-Weinzinger A (2013) Distinct interactions of Na^+ and Ca^{2+} ions with the selectivity filter of the bacterial sodium channel Na_VAb. Biochem Biophys Res Commun 430:1272–1276

Kim MS, Morii T, Sun LX, Imoto K, Mori Y (1993) Structural determinants of ion selectivity in brain calcium channel. FEBS Lett 318:145–148

Koishi R, Xu H, Ren D, Navarro B, Spiller BW, Shi Q, Clapham DE (2004) A superfamily of voltage-gated sodium channels in bacteria. J Biol Chem 279:9532–9538

Kuzmenkin A, Bezanilla F, Correa AM (2004) Gating of the bacterial sodium channel, NaChBac: voltage-dependent charge movement and gating currents. J Gen Physiol 124:349–356

Lacroix JJ, Bezanilla F (2011) Control of a final gating charge transition by a hydrophobic residue in the S2 segment of a K^+ channel voltage sensor. Proc Natl Acad Sci U S A 108:6444–6449

Lee S, Goodchild SJ, Ahern CA (2012) Local anesthetic inhibition of a bacterial sodium channel. J Gen Physiol 139:507–516

Long SB, Campbell EB, Mackinnon R (2005) Crystal structure of a mammalian voltage-dependent Shaker family K^+ channel. Science 309:897–903

Long SB, Tao X, Campbell EB, MacKinnon R (2007) Atomic structure of a voltage-dependent K^+ channel in a lipid membrane-like environment. Nature 450:376–382

MacKinnon R (1991) New insights into the structure and function of potassium channels. Curr Opin Neurobiol 1:14–19

McCusker EC, D'Avanzo N, Nichols CG, Wallace BA (2011) Simplified bacterial "pore" channel provides insight into the assembly, stability, and structure of sodium channels. J Biol Chem 286:16386–16391

McCusker EC, Bagneris C, Naylor CE, Cole AR, D'Avanzo N, Nichols CG, Wallace BA (2012) Structure of a bacterial voltage-gated sodium channel pore reveals mechanisms of opening and closing. Nat Commun 3:1102

Paldi T, Gurevitz M (2010) Coupling between residues on S4 and S1 defines the voltage-sensor resting conformation in NaChBac. Biophys J 99:456–463

Papazian DM, Shao XM, Seoh SA, Mock AF, Huang Y, Wainstock DH (1995) Electrostatic interactions of S4 voltage sensor in Shaker K^+ channel. Neuron 14:1293–1301

Pavlov E, Bladen C, Winkfein R, Diao C, Dhaliwal P, French RJ (2005) The pore, not cytoplasmic domains, underlies inactivation in a prokaryotic sodium channel. Biophys J 89:232–242

Payandeh J, Scheuer T, Zheng N, Catterall WA (2011) The crystal structure of a voltage-gated sodium channel. Nature 475:353–358

Payandeh J, Gamal El-Din TM, Scheuer T, Zheng N, Catterall WA (2012) Crystal structure of a voltage-gated sodium channel in two potentially inactivated states. Nature 486:135–139

Qiu H, Shen R, Guo W (2012) Ion solvation and structural stability in a sodium channel investigated by molecular dynamics calculations. Biochim Biophys Acta 1818:2529–2535

Ren D, Navarro B, Xu H, Yue L, Shi Q, Clapham DE (2001) A prokaryotic voltage-gated sodium channel. Science 294:2372–2375

Sather WA, McCleskey EW (2003) Permeation and selectivity in calcium channels. Annu Rev Physiol 65:133–159

Shaya D, Kreir M, Robbins RA, Wong S, Hammon J, Bruggemann A, Minor DL Jr (2011) Voltage-gated sodium channel (NaV) protein dissection creates a set of functional pore-only proteins. Proc Natl Acad Sci U S A 108:12313–12318

Stock L, Delemotte L, Carnevale V, Treptow W, Klein ML (2013) Conduction in a biological sodium selective channel. J Phys Chem B 117:3782–3789

Tang S, Mikala G, Bahinski A, Yatani A, Varadi G, Schwartz A (1993) Molecular localization of ion selectivity sites within the pore of a human L-type cardiac calcium channel. J Biol Chem 268:13026–13029

Tang L, Gamal El-Din TM, Payandeh J, Martinez GQ, Heard TM, Scheuer T, Zheng N, Catterall WA (2014) Structural basis for Ca 723 2+ selectivity of a voltage gated calcium channel. Nature 505:56–61

Tao X, Lee A, Limapichat W, Dougherty DA, MacKinnon R (2010) A gating charge transfer center in voltage sensors. Science 328:67–73

Terlau H, Heinemann SH, Stuhmer W, Pusch M, Conti F, Imoto K, Numa S (1991) Mapping the site of block by tetrodotoxin and saxitoxin of sodium channel II. FEBS Lett 293:93–96

Tiwari-Woodruff SK, Schulteis CT, Mock AF, Papazian DM (1997) Electrostatic interactions between transmembrane segments mediate folding of Shaker K^+ channel subunits. Biophys J 72:1489–1500

Ulmschneider MB, Bagneris C, McCusker EC, Decaen PG, Delling M, Clapham DE, Ulmschneider JP, Wallace BA (2013) Molecular dynamics of ion transport through the open conformation of a bacterial voltage-gated sodium channel. Proc Natl Acad Sci U S A 110:6364–6369

Vilin YY, Fujimoto E, Ruben PC (2001) A single residue differentiates between human cardiac and skeletal muscle Na^+ channel slow inactivation. Biophys J 80:2221–2230

Wang SY, Wang GK (1997) A mutation in segment I-S6 alters slow inactivation of sodium channels. Biophys J 72:1633–1640

Xiong W, Farukhi YZ, Tian Y, Disilvestre D, Li RA, Tomaselli GF (2006) A conserved ring of charge in mammalian Na^+ channels: a molecular regulator of the outer pore conformation during slow inactivation. J Physiol 576:739–754

Yang J, Ellinor PT, Sather WA, Zhang JF, Tsien RW (1993) Molecular determinants of Ca^{2+} selectivity and ion permeation in L-type Ca^{2+} channels. Nature 366:158–161

Yarov-Yarovoy V, McPhee JC, Idsvoog D, Pate C, Scheuer T, Catterall WA (2002) Role of amino acid residues in transmembrane segments IS6 and IIS6 of the Na^+ channel α subunit in voltage-dependent gating and drug block. J Biol Chem 277:35393–35401

Yarov-Yarovoy V, DeCaen PG, Westenbroek RE, Pan CY, Scheuer T, Baker D, Catterall WA (2012) Structural basis for gating charge movement in the voltage sensor of a sodium channel. Proc Natl Acad Sci U S A 109:E93–E102

Yatani A, Bahinski A, Mikala G, Yamamoto S, Schwartz A (1994) Single amino acid substitutions within the ion permeation pathway alter single-channel conductance of the human L-type cardiac Ca^{2+} channel. Circ Res 75:315–323

Yue L, Navarro B, Ren D, Ramos A, Clapham DE (2002) The cation selectivity filter of the bacterial sodium channel, NaChBac. J Gen Physiol 120:845–853

Zarrabi T, Cervenka R, Sandtner W, Lukacs P, Koenig X, Hilber K, Mille M, Lipkind GM, Fozzard HA, Todt H (2010) A molecular switch between the outer and the inner vestibules of the voltage-gated Na^+ channel. J Biol Chem 285:39458–39470

Zhang X, Ren W, DeCaen P, Yan C, Tao X, Tang L, Wang J, Hasegawa K, Kumasaka T, He J, Wang J, Clapham DE, Yan N (2012) Crystal structure of an orthologue of the NaChBac voltage-gated sodium channel. Nature 486:130–134

Zhang X, Xia M, Li Y, Liu H, Jiang X, Ren W, Wu J, DeCaen P, Yu F, Huang S, He J, Clapham DE, Yan N, Gong H (2013) Analysis of the selectivity filter of the voltage-gated sodium channel Na_VRh. Cell Res 23:409–422

Zhao Y, Scheuer T, Catterall WA (2004a) Reversed voltage-dependent gating of a bacterial sodium channel with proline substitutions in the S6 transmembrane segment. Proc Natl Acad Sci U S A 101:17873–17878

Zhao Y, Yarov-Yarovoy V, Scheuer T, Catterall WA (2004b) A gating hinge in Na^+ channels; a molecular switch for electrical signaling. Neuron 41:859–865

Index

P.C. Ruben (ed.), *Voltage Gated Sodium Channels*, Handbook of Experimental Pharmacology 221, DOI 10.1007/978-3-642-41588-3,